C55.2:C61/2

Proceedings of the Second Annual NOAA Climate Diagnostics Workshop

Scripps Institution of Oceanography
La Jolla, California
October 18-20, 1977

PENNSYLVA [illegible]
FEB
DOCUMENTS

U.S. DEPARTMENT OF COMMERCE
National Oceanic and Atmospheric Administration

U.S. DEPARTMENT OF COMMERCE
Juanita M. Kreps, Secretary

NATIONAL OCEANIC AND ATMOSPHERIC ADMINISTRATION
Richard A. Frank, Administrator

PROCEEDINGS OF THE SECOND ANNUAL CLIMATE DIAGNOSTICS WORKSHOP

Held at the
Scripps Institution of Oceanography
La Jolla, California

October 18-20, 1977

U. S. Depositor

Digitized by the Internet Archive
in 2012 with funding from
LYRASIS Members and Sloan Foundation

http://archive.org/details/proceedingso00clim

Foreword

Interest in climate and climate change has continued to grow over the last year. This may be what one should expect after such a record-breaking winter. However, as climatologists, we recognize that hardly a year goes by when there are no anomalous conditions that would serve equally well the need to learn more about climate fluctuations. The thing that is significantly different now from a year ago is that the interest in climate is beginning to produce some action. There have been some important events. One of these has been the publication of A United States Climate Program Plan, containing a foreword written by Dr. Frank Press, Director of the White House Office of Science and Technology Policy. This plan provides a framework for a wide range of national activities to enable the nation and the world to respond more effectively to climate-induced problems.

In Congress, the House of Representatives passed a bill, H.R. 6669, the National Climate Program Act of 1977, whose implementation would substantially augment our national efforts to cope with climate. Comparable bills have been introduced in the Senate and are under active consideration. The Congress and the Administration are working together to orchestrate the country's response to what are now clearly identified needs relating to climate. Also worthy of note is the recent publication by the Geophysics Research Board of the National Research Council of their studies Energy and Climate, and Climate, Climatic Change, and Water Supply. The conclusions, in particular those that pertain to the possible climatic threat of increasing atmospheric CO_2, come as no surprise to climatologists, but do serve to reemphasize the importance of being able to deal with climate problems.

This then is the setting for our second Climate Diagnostics Workshop. It is an optimistic one. We must be pleased that it is not only the climatologists, but also the mathematicians and the solar physicists, the palynologists, geochemists, and oceanographers who are thinking about climate and seeking to contribute their talents and their knowledge to this very substantial problem. In this setting we sit together and try to tell each other what we have seen and what we have learned about how the climate machine has been working. We share not only our knowledge and our insights but also our methods and approaches so that we can all go away to another fruitful year of investigation. I trust that this series of meetings will be increasingly productive as we intensify our efforts to understand how the climate operates.

I must acknowledge my gratitude to Dr. William Nierenberg, Director of the Scripps Institution of Oceanography, and to Dr. Jerome Namias of Scripps' Climate Research Group for their kind assistance in hosting and helping to organize the Workshop. I would also commend those who gave formal presentations for their excellent contributions. As Jerry Namias stated so succinctly at the close of the meeting, "No one fell asleep!" I should think that if the quality of workmanship and spirit of cooperation shown by the members of this group become prevailing characteristics of the entire U.S. Climate Program, then we have indeed made a good beginning.

Edward S. Epstein

Preface

This Workshop brought together several views of the previous year's climate -- many of which centered on the unusual characteristics of the Northern Hemisphere winter of 1976-77. A synopsis of these views, to be found in the collection of papers that follow, is given by Wagner and Krueger (page S-1). Lofgren and Fritts help to put the winter of 1976-77 into some perspective by examining long-term records derived from tree-ring analyses; Potter and Ellsaeser, Curran, and Wu comment on specific factors (deserts, clouds and ozone) that may influence or become components of climate variation. The ocean as an element of climate is discussed by several participants including Strong, Miller, Quinn, Kraus, McLain, Levitus, and Murakami.

The Workshop also afforded an opportunity to examine, in some depth, the use of the empirical orthogonal function in diagnostic studies of climate. An overview of these presentations is given by Preisendorfer (page S-6).

While it is not the intention of the Workshop to dwell on climate predictions, the work that is discussed provides insight into the prediction problem and lays a foundation upon which forecast techniques may be developed. Some papers in these proceedings address prediction issues directly. For example, Miyakoda, et al present an attempt at using a general circulation model developed at the Geophysical Fluid Dynamics Laboratory for a one-month (January 1977) forecast, Harnack presents statistically based predictions of winter temperature, and Bryson, et al report on a model for climate forecasts which introduces such factors as volcanic and anthropogenic inputs and pole tides generated by Chandler motion of the earth's rotational axis. A short panel discussion on verification of climate forecasts was held at the close of the Workshop and is summarized by Laurmann in paper 34.

William A. Sprigg
October 1977

List of Participants
Climate Diagnostics Workshop
October 18-20, 1977

Roderick S. Quiroz	NOAA/NMC
Douglas R. McLain	NOAA/NMFS/PEG
Sus Tabata	Marine Sciences Directorate/Canada
William Quinn	Oregon State University
Michael Matson	NOAA/NESS/ESG
Robert Harnack	Rutgers-University of New Jersey
David Halpern	NOAA/ERL/PMEL
Joseph C.K. Huang	NOAA/GLERL
Donald L. Gilman	NOAA/NWS/LRPG
Otto W. Thiele	NASA/GSFC
R. Curran	NASA/GSFC
Mao-Fou Wu	ERT, Inc.
T. R. Allsopp	Atmospheric Environment Service/Canada
J. S. Winston	NOAA/NESS/MSL
Richard D. Rosen	ERT, Inc.
Harry Van Loon	NCAR
Robert R. Dickson	NOAA/NWS/NMC
A. James Wagner	NOAA/NWS/NMC
D. James Baker	NOAA/ERL/PMEL
Kent L. Groninger	NOAA/ERL
Uwe Radok	CIRES, University of Colorado
Arthur D. Belmont	Control Data Corporation
R. Preisendorfer	NOAA/ERL/PMEL
Daniel Cayan	Scripps/University of California
Forrest R. Miller	NOAA/NMFS
E. Paul McClain	NOAA/NESS/ESG
J. Lockwood Chamberlin	Atlantic Environmental Laboratory
William A. Sprigg	NOAA/R&D
James P. McGuirk	Texas A&M University
John O. Roads	Scripps/University of California
Steven Esbensen	Oregon State University
Gerald L. Potter	Laurence Livermore Laboratory
Eric B. Kraus	University of Miami
Tim P. Barnett	Scripps/University of California
Charles K. Stidd	Scripps/University of California
A. M. Tubbs	Scripps/University of California
T. T. Saur	Scripps/University of California
Michitaka Uda	Tokai University/Japan
William Patzert	Scripps/University of California
Gerhard Leipold	Scripps/University of California
Arthur F. Krueger	NOAA/NESS
Edward S. Epstein	NOAA/R&D
William Nierenberg	Scripps/University of California

Brian C. Weare	MIT
Gerald J. Dittberner	USAF/ETAC
Malcolm Reid	NOAA/EDS
Jerome Namias	Scripps/ University of California
Reid A. Bryson	University of Wisconsin
Paul F. Krumpe	Department of State/AID
B. W. Boville	Atmospheric Environment Service/Canada
Robert M. Born	Scripps/University of California
K. Miyakoda	NOAA/GFDL
Takio Murakami	University of Hawaii
C. P. Chang	U.S. Naval Post Graduate School
Joseph O. Fletcher	NOAA/ERL
Robert F. Devereux	Ocean Data Systems
G. R. Lofgren	University of Arizona
John A. Laurmann	Stanford University
Gunter R. Seckel	NOAA/NMFS/PEG
Robert Etkins	NOAA/R&D
David Cutchin	National Science Foundation
Stephan Hastenrath	University of Wisconsin
Sidney Levitus	NOAA/GFDL
Elmar R. Reiter	Colorado State University
Robert G. Quayle	NOAA/EDS/NCC
Eugene M. Rasmusson	NOAA/EDS/CEDDA
William A. Arvola	Department of Water Resources/California
A. Christie	Atmospheric Environmental Service/Canada
Thor Jakobsson	Atmospheric Environmental Service/Canada
H. P. Sleeper, Jr.	Kentron-Hawaii, Ltd.

TABLE OF CONTENTS

Page

Foreword i

Preface ii

List of Participants iii

Summary Reports:

The Climate of 1976-1977, A Summary of Papers Given at October 1977 Climate Diagnostics Workshop at La Jolla, California — A.J. Wagner, A.F. Krueger — S-1

Empirical Orthogonal Functions in the Diagnosis and Prediction of Climate Fluctuations — R. Preisendorfer — S-6

Contributed Papers:

The Circulation and Weather of Fall 1976 and Winter 1976-77: Persistence of Record Cold over the East and Drought over the West — A.J. Wagner — 1-1

Circulation and Weather, Spring and Summer 1977 — D.L. Gilman — 2-1

A Review of the Unusual Climatic Events of 1976-77 in Canada — T.R. Allsopp — 3-1

A Comparison of Three Operational Drought Programs — M.Reid — 4-1

A Comparative Analysis of the 1976-77 Winter in the Contiguous United States — R.G. Quayle, H.F. Diaz — 5-1

Economic Implications of the Temerature Anomalies of January 1977 — E.R. Reiter — 6-1

Winter 1976-77, A Comparison of Circulation Characteristics with Other Winters — R.R. Dickson — 7-1

The Winter of 1976-77 in a Biennial Context — R.S. Quiroz — 8-1

TABLE OF CONTENTS
(Continued)

		Page
Stratospheric Sudden Warming and January 1977 Weather	J.P. McGuirk	9-1
The Satellite Snowcover Record: Status, Trends, and Relationships	M. Matson	10-1
Comparison of the Last Two Winter Season Monthly Zonal Cloud Fractions as Derived from Nimbus-6 ERB Data	R. Curran	11-1
Multiple Causes of the North American Abnormal Winter 1976-1977	J. Namias	12-1
Past Occurrences of Winters Similar to 1976-1977 as Reconstructed from the Tree-Ring Record	G.R. Lofgren H.C. Fritts	13-1
An Attempt at One-Month Forecast of the Event 1976-77	K. Miyakoda	14-1
Circulation Over the Tropics During 1976-77 as Related to that at Middle Latitudes	A.F. Krueger	15-1
Global Patterns of Earth Radiation Budget Components in 1976-77 as Contrasted with the Preceding Year	J.S. Winston	16-1
Comments on Albedo of Deserts and Drought	G.L. Potter H.W. Ellsaeser	17-1
The Total Ozone Variation and Atmospheric General Circulation	M.F. Wu	18-1
Monthly Mean Satellite-Derived Sea Surface Temperatures	A.E. Strong	19-1
The El Nino of 1976-77 in the Southeast Pacific	F.R. Miller	20-1
Diagnosis of the 1976-77 El Nino	W.H. Quinn	21-1
Response of North Atlantic to Anomalous Atmospheric Forces in Spring 1977	E.B. Kraus A. Leetmaa C. Rooth	22-1

TABLE OF CONTENTS
(Continued)

		Page
Fluctuations of Sea Surface Temperature and Density at Coastal Stations During 1976	D.R. McLain	23-1
Present Status of Climate Data in Oceanography	S. Levitus	24-1
Relationship between Monsoon Activity over Southeast Asia and the Changes in Upper Flows over the Equatorial Pacific	T. Murakami	25-1
Teleconnections at Middle and High Latitudes in Winter	H.Van Loon J. Rogers	26-1
On Modes of Tropical Circulation and Climate Anomalies	S. Hastenrath	27-1
Power Spectral Analysis of the Dominant Empirical Orthogonal Functions of Pacific SST and Global Free Air Temperatures	B.C. Weare	28-1
Principal Component Analysis of United States Surface Temperature Data	E.M. Rasmusson P. Arkin J. Jalickee	29-1
Use of Empirical Orthogonal Functions in Diagnosing and Predicting Climate Fluctuations	R.W. Preisendorfer	30-1
Applicability of Analog Methods to Diagnosis of Climate Fluctuations	T.P. Barnett	31-1
Objective Winter Temperature Predictions	R.P. Harnack	32-1
An Experimental Climate Forecasting Model and its Performance	R.A. Bryson E.W. Wahl T.B. Starr	33-1
Commentary Based on: Panel Discussion on Verification of Climate Forecasts	J. Laurmann	34-1

The Climate of 1976-1977,
A Summary of Papers Given at October 1977
Climate Diagnostics Workshop at La Jolla, CA.

A.J. Wagner and A.F. Krueger

The principal characteristics of the seasonal mean 700 mb circulation patterns over the Northern Hemisphere during the past year were reviewed in papers by Wagner and Gilman. A remarkably persistent and highly amplified pattern consisting of a deep mean low south of the Aleutians, a strong ridge near the west coast of North America extending north to the Arctic, and a deep trough over eastern North America was the key to a nearly unbroken siege of cold weather during the fall and winter over southeastern Canada and the eastern half of the United States.

In a paper not formally presented at the Workshop but included in these Proceedings, Namias showed that many of the fall and winter mean 700 mb height anomaly centers exceeded three standard deviations from the mean. Monthly mean temperature records for cold were broken in some area of the eastern United States from October through January, which was the coldest month on record in the Ohio Valley. This pattern, which lasted from late September 1976 until mid-February 1977, essentially reversed itself over North America during the next few weeks. A strong ridge developed over the eastern Pacific, with a deeper than normal trough over the western United States and an unusually strong ridge over east-central North America. Unseasonably mild temperatures prevailed in most areas east of the Continental Divide as a result of the highly persistent spring pattern. Gilman pointed out that usually at least one month of past mild springs was cool or near normal, but the three consecutive months of above normal temperature led to the warmest spring since available records began in 1881, averaging three standard deviations above the current 1941-70 normal west of the Great Lakes.

Summer was also predominantly warmer than normal over much of the country, except for the northern border from the Great Plains to parts of the Northeast. Droughts plagued the northern Great Plains and much of the Southeast.

Allsopp presented data showing the unusual circulation pattern's effect on extremes of weather in Canada. The fall and winter both had record and near-record warmth over portions of the Yukon Territory, Mackenzie District, British Columbia and Alberta. It was the third warmest winter in nearly a century in Alberta.

Record dryness with less than 1/3 normal total accumulated precipitation in some areas, prevailed over much of the southern Canadian Prairies throughout the fall, winter, and well into the spring. Not until May, when this same area had as much as four times its normal rainfall, was the drought decisively broken. The long spell of mild and dry weather over Southwestern Canada led to unusually low snowpack in the coastal and Rocky Mountains. Much of the southern Prairies had no snowpack by the end of winter.

west coast of Mexico. Perhaps this convection contributed towards maintaining the stronger subtropical jetstream across southern United States during the winter.

It is interesting, that with the intrusion of strong westerlies into lower latitudes from both hemispheres the eddy kinetic energy over the tropics decreased. This was accompanied by a filling of the Southern Hemisphere's high level mid-Pacific trough and a shift of the westerlies off the equator, or a weakening of the Walker circulation. The Hadley circulation in turn may have been stronger. Increased cloudiness and temperatures over the tropics suggest this.

The 1976-77 winter appears extremely complex and only a few parts of the puzzle have been considered here. In fact, very few of the fundamental processes involved have even been measured. The oceans, for example, supply a large amount of energy to the atmosphere during winter. Dickson's figure 3, with cold air located over the eastern part of the continents and adjacent warm ocean currents, suggests that during this past winter this oceanic heat flux was even larger than usual. How much larger? The major ocean gyres in turn receive energy from the winds. These were very strong over the North Pacific so that the dissipation probably was also large. How did the North Pacific gyre respond to this input of energy? These are some of the processes that need to be measured for an effective monitoring of the atmosphere and oceans.

The relationships found during and preceding the winter of 1976-77 among various tropospheric, stratospheric and oceanic parameters by many of the workshop contributors suggest that the extreme severity of the past winter may have been due to a coincidence of several partially independent, but to some degree related, effects. The five seasons selected by Dickson as typical of cold winters over the eastern United States contained two biennial pairs, four years suggestive of an El Nino at low latitudes, four seasons with extensive cold water over the north central Pacific, and two winters with a major sudden stratospheric warming. Namias found that during El Nino years sea-level pressure anomalies over much of the North Pacific were similar to last winter, which was in turn similar to a hemisphere-wide sea level teleconnection pattern found by Van Loon and Rogers to be typical of cold winters in Europe and mild winters in Greenland. The intriguing possibility exists that extreme climatic events such as winter 1976-77 may be due to an additive and quite likely synergistic effect of several factors, none of which by itself explains a large amount of atmospheric variance, operating together in such a way as to force the circulation and the attendant weather events into a record-producing anomalous pattern.

water at the beginning of the season could lead to more intense cyclogenesis and greater moisture advection into the continent for subsequent snowfalls later in the fall. These statistical results should be regarded as tentative due to the small number of years' data.

Processes occurring over the tropics and Southern Hemisphere should also be considered and may have been important in establishing the highly anomalous Northern Hemisphere circulation during the 1976-77 winter. What, in fact, was going on over the tropics that was relevant prior to as well as during the winter? Also, how did the Northern Hemisphere wintertime circulation interact with that at low latitudes? Several of the papers presented at this workshop addressed themselves to these questions.

One of the most remarkable variations the large-scale atmospheric circulation over the tropics undergoes is the "Southern Oscillation". Characterized by a period that is of the order of years, it essentially involves a redistribution of mass over the tropical South Pacific between the Easter Island anticyclone and the Indonesian low presure area. It is accompanied by fluctuations in the tradewinds, sea surface temperatures and tropical rainfall. Bjerknes suggested that this complex air-sea interaction influences the subtropical jetstream and accordingly the middle latitude circulation over both hemispheres. Perhaps it also plays a role in coupling the Southern Hemisphere's circulation with that of the Northern.

Quinn has devised several rather simple indices that are useful for monitoring this variation and discusses them here. Note that again this past year, as in 1972, we have experienced a major decline in the Southern Oscillation Index as monitored by the Easter minus Darwin pressure difference. A similar decline in his Ship N minus Darwin difference suggests that the influence also spread into the North Pacific.

Miller notes that this decline began during late Southern autumn of 1976 with a weakening of the pressure gradient over the Peru current and an intrusion of the South Pacific storm track into lower latitudes. He further indicates that this was accompanied by increases in sea surface temperatures over most of the eastern tropical Pacific. This combination of weakened tradewind flow and warm ocean temperatures continued through the 1976 Southern winter. Responses in tropical rainfall were apparently not far behind.

Winston's analysis, using satellite-derived measurements of albedo and longwave cooling, suggests increased convection and rainfall during summer 1976 (Southern winter) over much of the equatorial Pacific. Interestingly, the Indian monsoon was somewhat weaker this season -- it started late and receded early. This decrease in rainfall over Southeast Asia and probably increase over the equatorial Pacific represents a major longitudinal displacement in tropical rainfall and condensation heating. Over the tropical Pacific this pattern continued through fall into the 1976-77 winter. In fact, during this winter the Northern ITCZ over the eastern Pacific became even more active -- possibly in response to the warm ocean surface off the

McGuirk noted that tropospheric circulation changes such as occurred during the record cold January 1977 are typically associated with stratospheric sudden warmings. In several recent cases, strong blocking ridges formed over the Aleutians, and sometimes the north Atlantic, often long before the stratospheric warming began. Intensified northward eddy heat flux, primarily by the long waves, warmed the Arctic while the mid-latitude continents cooled rapidly. The zonal winds decreased at middle and high latitudes (where easterlies often appeared) and the subtropical jet stream increased slightly. Temperatures over the United States east of the Continental Divide dropped substantially below normal, while west of the Rockies either very mild or very cold temperatures were observed during the months with sudden stratospheric warmings, depending upon whether the Arctic air spilled west of the Divide.

Quiroz noted that planetary zonal means of temperature, pressure height, and zonal wind were significantly different during the winters of 1975-76 and 1976-77, and that these changes fitted into a biennial cycle in evidence since 1971. Temperature anomalies at middle and high latitudes were negatively correlated in both winters, as was the height of the 100-mb surface. Wave number 2 at 500 mb was noticeably stronger in winter 1976-77, as was the northward eddy heat transport at 850 mb. An extraordinary polar anticyclone which developed in January 1977, together with a strongly amplified wave number 3 pattern at lower latitudes, was seen as the main factor in the severe cold affecting the United States during winter 1976-77.

Van Loon and Rogers described the tendency for winter temperatures over Greenland and northern Europe to be negatively correlated. This regional "seesaw" was found to be related to characteristic anomalous sea level pressure patterns over the entire Northern Hemisphere, giving further evidence that extreme winters such as 1976-77, or their opposite, are related to events over a wide area of the globe. The sea-level pressure anomalies and their related teleconnection patterns found by Van Loon and Rogers were consistent with 700 mb patterns shown by Namias and Dickson for cold winters over the U.S., and their converse for the mild winters as the early 70's shown by Wagner. The amplitude of the regional North Atlantic "seesaw" appeared to change from decade to decade, with some periods when the entire region would tend to be mild or cold, rather than have negatively correlated temperature between Europe and Greenland. The statistical behavior of climatic anomalies has been found to vary with time in several previous investigations.

Matson presented the results of a decade of satellite snow cover measurements. Little trend was noted over North America, but the extent of winter snow cover has tended to increase over Eurasia. Regression analyses indicated that Eurasian snow cover in the later winter months was usually positively correlated with snow cover earlier in the season. Due to the predominance of the larger Eurasian land mass, similar relationships held for the Northern Hemisphere as a whole, though not for North America alone. An additional statistical relationship showing a marked negative correlation between September sea ice cover in the 0° - 90° E Sector and subsequent winter snow cover extent over Eurasia was presented, suggesting that open

Most of Canada experienced a warm spring, and the south central part shared with the north central United States the core of the warm anomaly which marked the warmest spring on record in that area.

Several contributors presented data placing the unusual 1976-77 seasons, particularly winter, in a historical and climatological context. Diaz and Quayle found that January 1977, winter 1976-77 and the winter half-year (September through March) were all generally the coldest in an 85-year period of record over the eastern United States. Their analyses of monthly and seasonal areally weighted regional average temperatures disclosed some of the other unusually cold past winters in 1903-04, 1904-05, 1911-12, 1917-18, 1935-36, 1939-40, 1962-63, and 1969-70. Wagner showed geographical temperature anomaly patterns for several of these seasons and Allsopp indicated that the winters of 1903-04, 1917-18, and 1933-34 were the coldest on record in Canada.

Diaz and Quayle fitted third order polynomials to their regional temperature analyses and in most cases there was a suggestion that winters were mildest in the 1930's and 1940's with a pronounced cooling trend beginning in the 1950's and continuing through the present.

A number of papers dealt with factors which may have contributed to the severity of the 1976-77 winter, and its possible predictability. Namias pointed out the mean circulation pattern may have been unusually persistent since it represented an amplification of the troughs and ridges in their normal climatological winter positions. He hypothesized that the amplified pattern may have been initially set up and reinforced by an unusually large pre-existing area of colder than normal sea surface temperatures in the north central Pacific Ocean. Atmospheric feedback effects may have also contributed to the record-breaking weather over North America. The general nature, although not the record severity, of the winter was predictable from the November Pacific sea-surface temperature anomaly pattern.

Dickson found several winters since good upper level data became available with mean height anomaly patterns similar to winter 1976-77 over most of the Northern Hemisphere. A significant factor all had in common was a strong continental blocking ridge over western Asia contributing to a deep cold trough near the east coast of Asia. This pattern was already in existence in the preceding November, along with characteristic sea-surface temperature anomaly patterns. A stronger than normal subtropical jet stream was in evidence across southern Asia to the central Pacific, and may have been associated with an enhanced meridional circulation over the South China Sea. The excess kinetic energy in the subtropical jet stream may have led to hydrodynamic instability and the breakdown of the circulation into an amplified wave pattern eastward from the central Pacific, as suggested by Ramage in earlier work.

Empirical Orthogonal Functions In The Diagnosis and Prediction of Climate Fluctuations

R. Preisendorfer

The concepts of the empirical orthogonal function (or principal component) analysis, despite their introduction into meteorology by Lorenz nearly twenty-five years ago (1956), are only now becoming widely used in meteorology, oceanography, and related fields. In their early applications, around 1933, EOF's were directed by such workers as Hotelling toward problems of educational psychology wherein the learning abilities of the mind in many diverse areas of human activity were being sorted out. Compaction of large sets of data were possible by use of EOF's. Now geophysicists are trying to use EOF's to compactify data and to sort out regions in space and time where important variabilities and possible causal connections exist for temperature, presure and other physical fields. As in the case of psychological data, physical data can be tied together by EOF's only in preliminary and more or less suggestive ways; the exact relations (if any) among the data must eventually be elicited by appeal to fundamental underlying laws of behavior or of physics, as the case may be. Thus EOF analysis is a tool by which first cuts at phenomena are made, hopefully to lay bare indications of underlying substance.

When they are better understood, the ideas of EOF analysis may be turned with perhaps increasing incisiveness, to data filtering, data interpolation, and data extrapolation, and even to the indication of common causal relations among geophysical fields. Before this can be done, however, several problems centering on the use of EOF's must be resolved: the matter of physical interpretations, the problem of degenerate eigenvalues, tests for statistical significance of the eigenvectors and eigenvalues arising in EOF analyses, and finally the matter of separation of signal from noise in EOF analysis of physical phenomena. These problems were reviewed by Preisendorfer and the current state of their solutions were discussed. He exhibited some new Monte Carlo and some new analytic approaches to the statistical significance problem.

The papers dealing with EOF's in the workshop represent a good cross section of the potential uses of the tool. Hastenrath's paper on the modes of tropical circulation and climate anomalies combines examinations of EOF's and correlation analysis to indicate e.g. possible interesting causal connections between sea surface temperatures off Peru and the inverse SLP anomalies over the Pacific and Atlantic along with large amplitudes over the Southern Oceans. In Weare's paper, the amplitude functions of the Pacific SST and temperature EOF's are of central interest and are Fourier analyzed for indications of strong spectral peaks and coherence. Van Loon and Rogers use the variance-detection ability of the EOF to see the famous temperature "seesaw" effect between northern Europe and Greenland as part of larger well defined pressure correlations between Ireland, the North Pacific, North Atlantic and other regions. Barnett, in using not a single field but several (SST, 800 mb ht, thickness, precipitation), lumped into one grand 'climate state vector' was able to show contemporaneous teleconnections of the kind studied by Namias between Pacific lows and high pressure ridges over the U.S. west coast and subsequent lower than normal presure over southeastern U.S. There is even a clear indication in the first EOF of the climate vector of Van Loon and Rogers' "seesaw" effect. Finally, Harnack showed, in a particularly careful and illuminating use of EOF's as regressive predictors, how they may be used to make predictions of winter temperatures over the U.S. mainland.

All in all the papers of this EOF session are representative of the current state of the art. Yet it must be noted (with the exception of Weare's paper and certain remarks from the audience) that conspicuously absent from the discussions was any substantive statistical analysis of the individual results. This indicates perhaps most directly the outstanding remaining practical problem in the use of EOF analysis.

THE CIRCULATION AND WEATHER OF FALL 1976 AND WINTER 1976-77: PERSISTENCE OF RECORD COLD OVER THE EAST AND DROUGHT OVER THE WEST

A. JAMES WAGNER
Long Range Prediction Group, National Meteorological Center
National Weather Service, NOAA, Washington, DC 20233

The persistence of a strongly amplified circulation pattern over the Pacific and North American sectors from the last week of September 1976 through the third week of February 1977 set the stage for record-breaking cold temperatures over much of the eastern United States from October to early February. This same pattern led to a severe drought in the West, where a 2-season precipitation deficit of more than 2 feet of rainfall was observed along the Pacific Northwest Coast.

A couplet consisting of a negative monthly mean anomaly center south of the Aleutians and a positive monthly mean anomaly center over British Columbia was quasi-stationary from October through February, while a more mobile negative anomaly center moved within southeastern Canada and New England during this same period.

These and some of the other key anomaly centers in the Northern Hemispheric circulation can be traced back with generally unambiguous continuity to summer 1976, which was characterized by fast zonal flow across the northern Pacific, a strong polar vortex, and mid-latitude blocking over southern Canada and the British Isles, which had the worst drought in over 200 years.

The fall 1976 pattern was such as to deflect moisture-bearing storms that normally strike the Pacific Coast northward to Alaska, where some places had record wet weather. Strong northerly anomalous flow extended from Canada into the United States, which was colder than normal everywhere east of the Rockies. Many cities in the Midwest and South experienced record cold weather in October and November. The early onset of a winter-type pattern in October helped produce an active Gulf-Atlantic Coast storm track, and precipitation was heavier than normal over much of the South and East. Rainfall from tropical storms in September also contributed to the heavier than normal totals over the Southwest and Southeast.

Further amplification of the same basic pattern during much of the winter led to extreme cold over the eastern half of the United States, and persistent drought in the West. Continued deflection of Pacific storms northward to Alaska led to an unusually mild and wet winter there. The large quantity of cold dry air over the mainland and stronger than normal flow with a continental component pushed much of the moisture which normally penetrates inland from the Gulf and South Atlantic back over the water, resulting in drier than normal conditions over much of the central and eastern portion of the country as well.

The cold weather reached its peak during January, which set cold records over a wide area east of the Mississippi River, averaging as much as 19°F below normal at Cincinnati. It was the coldest month on record over much of the Ohio Valley.

January's extreme cold may have been contributed to by a major index cycle (southward expansion of the westerlies and penetration of Arctic air to lower latitudes) associated with the advection of mild maritime air northward at high latitudes and the buildup of a record high pressure at all levels of the atmosphere over the Arctic. The extreme circulation patterns of winter and January 1977 stand in sharp contrast to the 5-year mean 700 mb circulation and its anomaly for the generally mild winters of 1971-72 through 1975-76, representing a sudden reversal of climatic anomalies.

The winters of 1976-77 and 1917-18 were very similar as to degree and extent of cold, with 1976-77 the coldest winter of the 20th Century over much of the Ohio Valley and Southeast, while 1917-18 was the coldest winter in the middle Atlantic and New England States. Other severe winters over the eastern United States during this Century occurred in 1904-05, 1911-12, 1935-36, and 1962-63.

Comparison of daily mean temperatures at New York City and Cincinnati further illustrate the similarity of the two coldest winters of this Century. A persistently cold fall in 1917, indications of a buildup of high pressure over Greenland and the Canadian Arctic in late December 1917, and similar sea-surface temperature anomaly patterns over the north Pacific in fall 1917 and 1976 suggest that similar interactions with preceding atmospheric states, the earth's surface, and the higher atmosphere, may have affected and contributed to the severity of both cold winters.

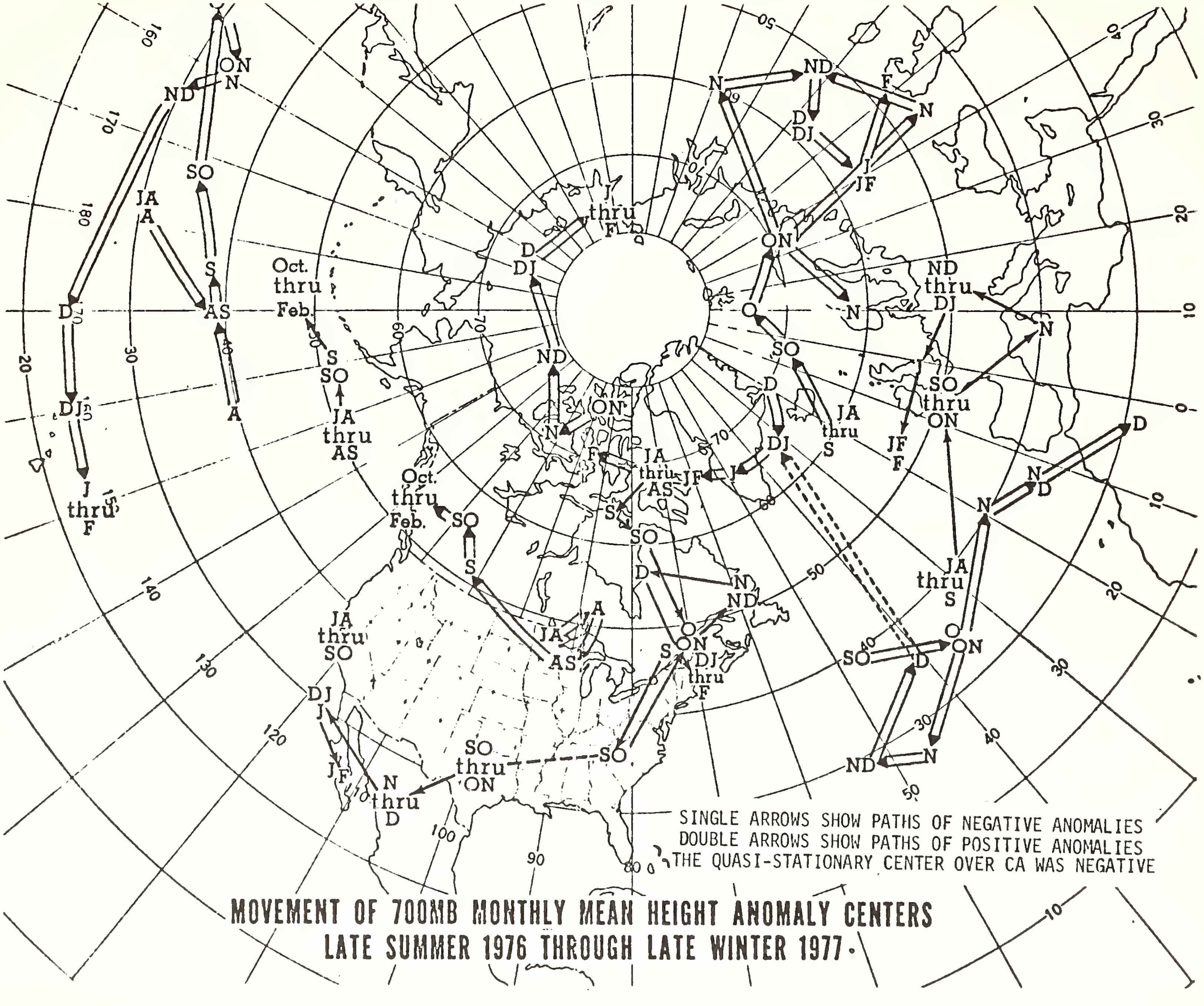

SINGLE ARROWS SHOW PATHS OF NEGATIVE ANOMALIES
DOUBLE ARROWS SHOW PATHS OF POSITIVE ANOMALIES
THE QUASI-STATIONARY CENTER OVER CA WAS NEGATIVE

MOVEMENT OF 700MB MONTHLY MEAN HEIGHT ANOMALY CENTERS
LATE SUMMER 1976 THROUGH LATE WINTER 1977.

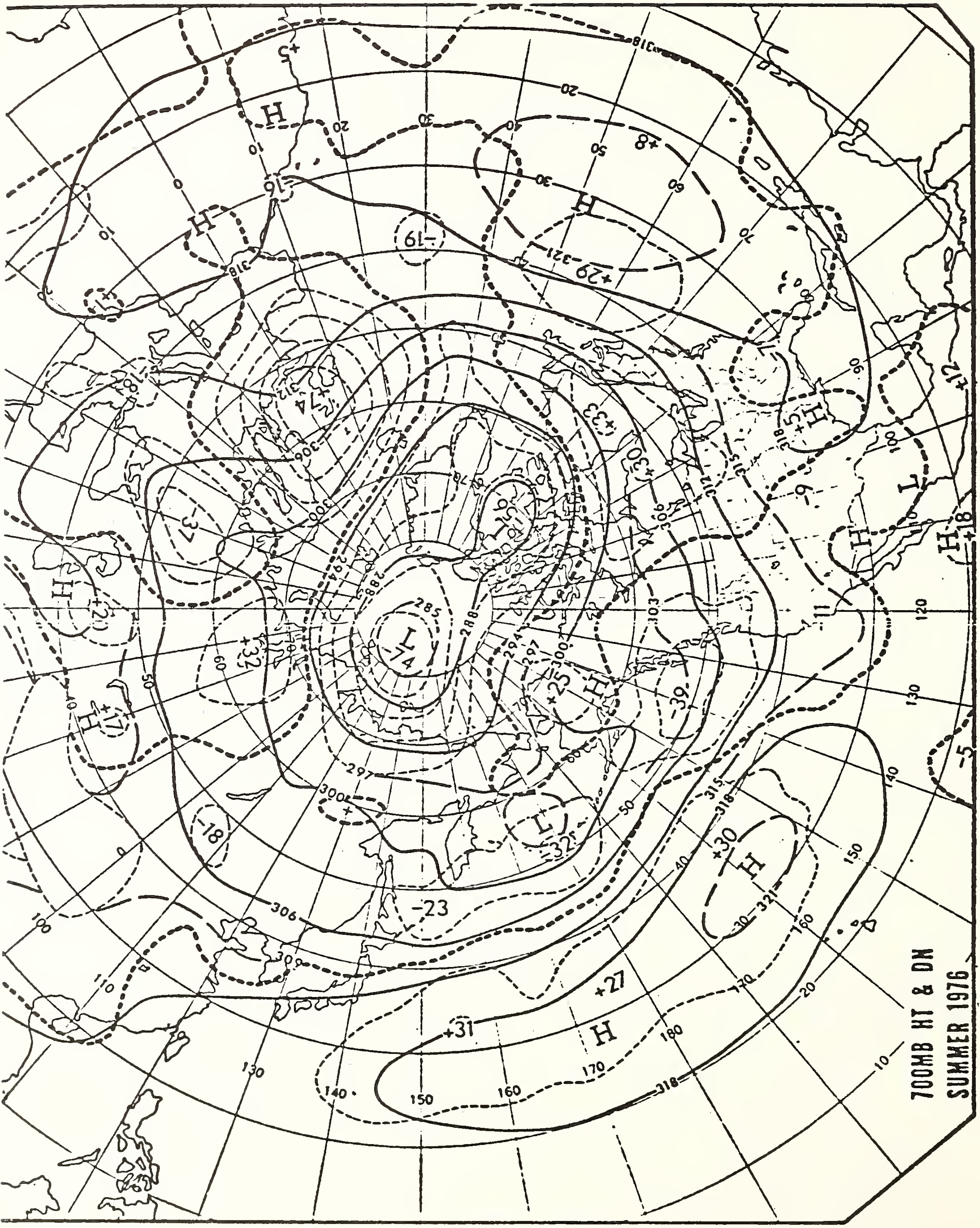

700MB HT & DN
SUMMER 1976

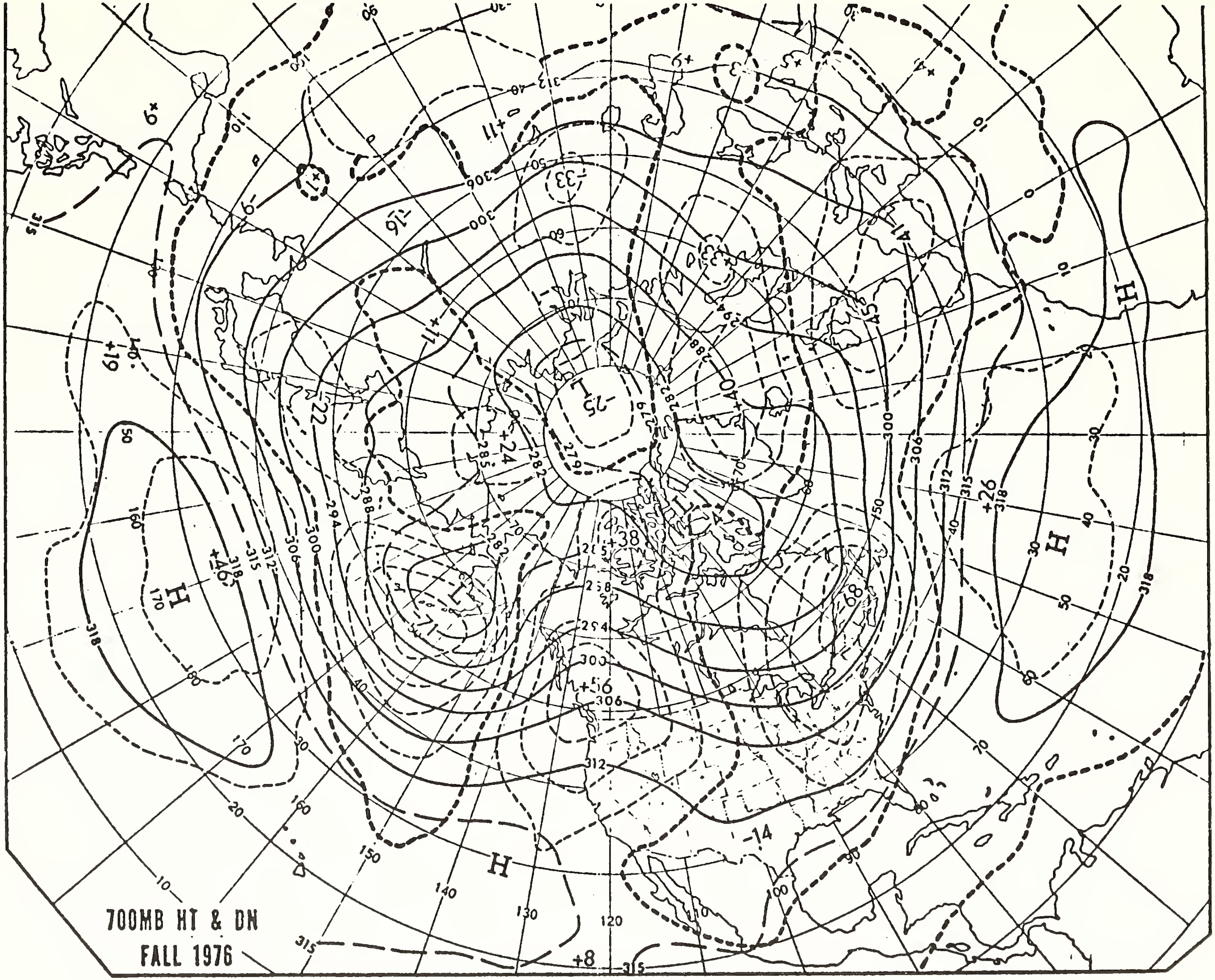

700MB HT & DN
FALL 1976

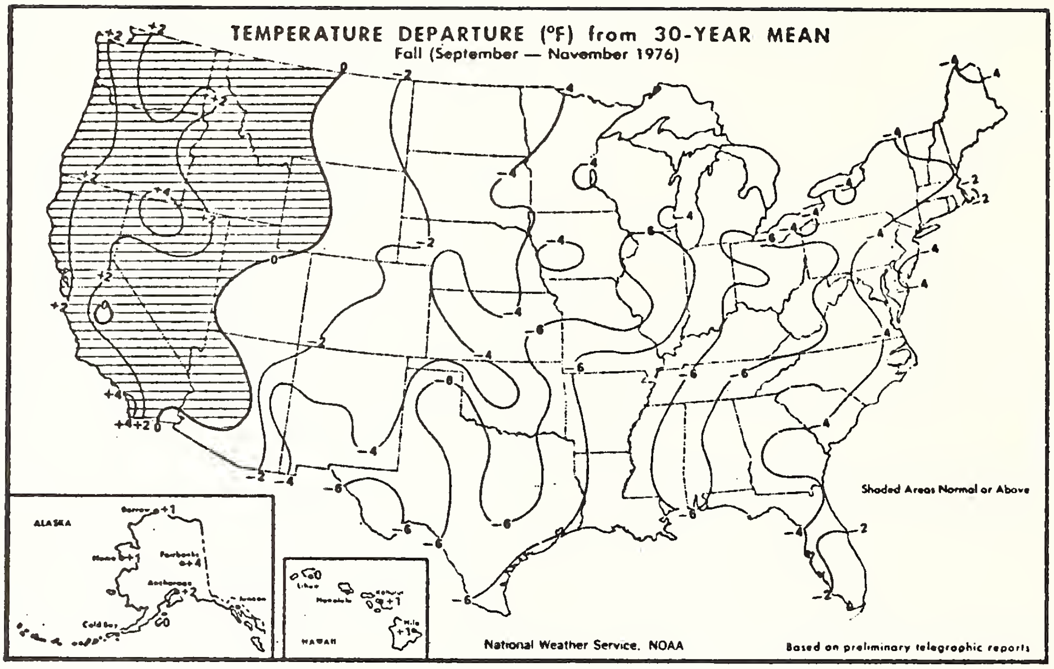

TEMPERATURE DEPARTURE (°F) from 30-YEAR MEAN

Fall (September — November 1976)

Shaded Areas Normal or Above

National Weather Service, NOAA

Based on preliminary telegraphic reports

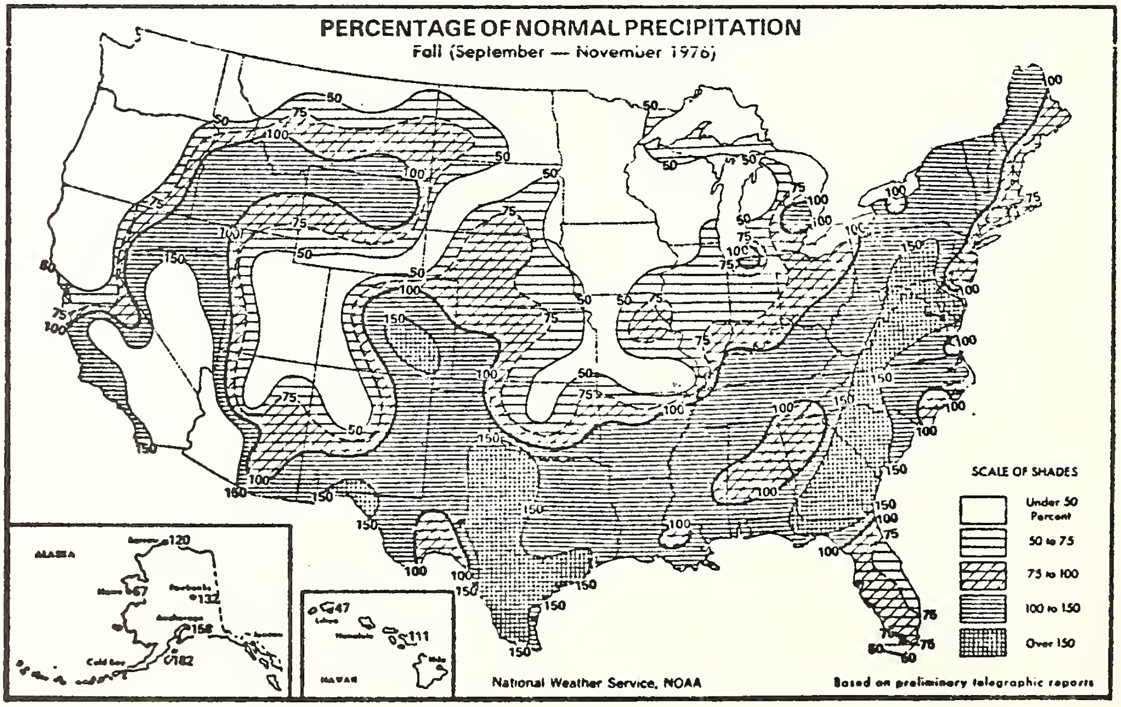

PERCENTAGE OF NORMAL PRECIPITATION

Fall (September — November 1976)

National Weather Service, NOAA

Based on preliminary telegraphic reports

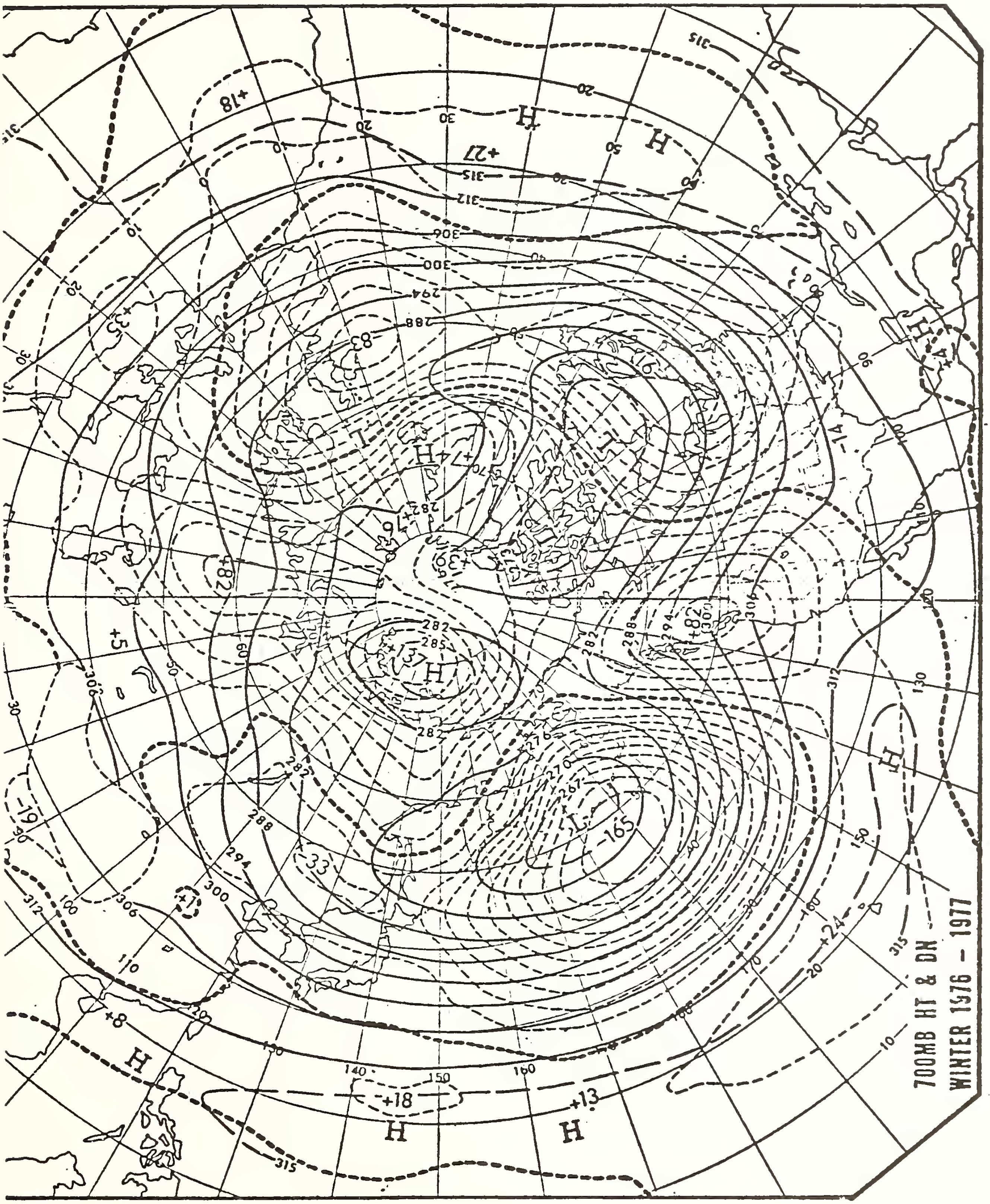
700MB HT & DN
WINTER 1976 - 1977
H
L
-165
+137
+82
+74
+76
+18
+27
+35
+5
-19
-33
+8
+13
+24
-14
-83
315
312
306
300
294
288
282
285
276
267

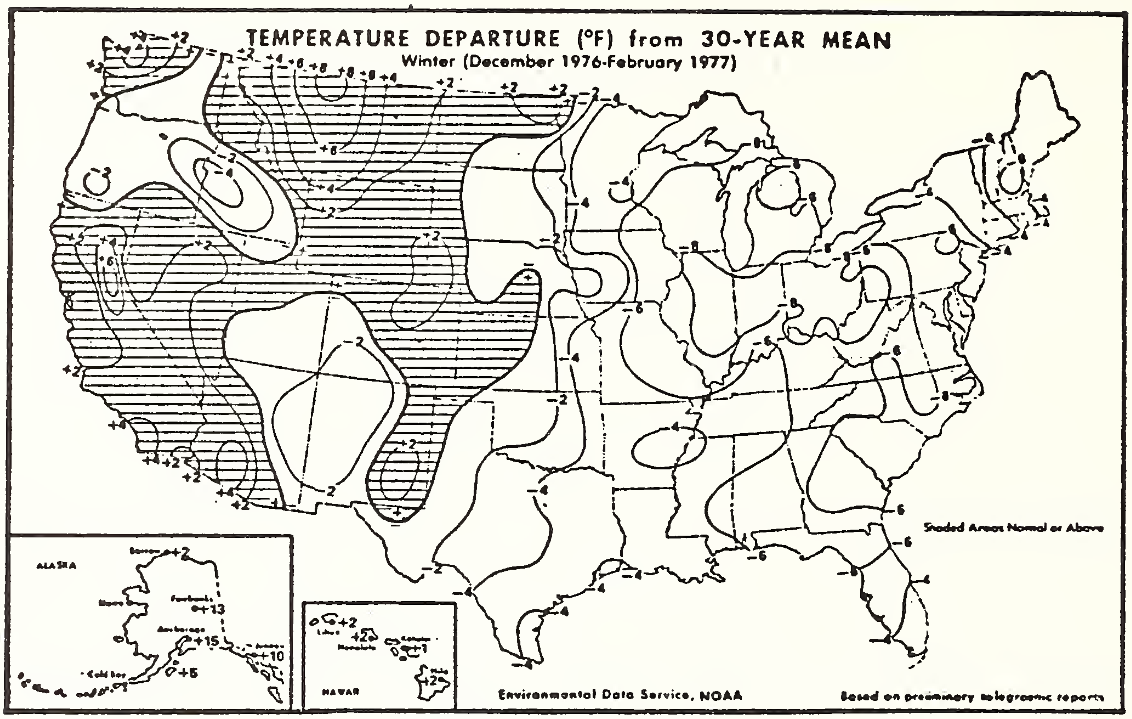
TEMPERATURE DEPARTURE (°F) from 30-YEAR MEAN
Winter (December 1976-February 1977)
Shaded Areas Normal or Above
ALASKA
Barrow +2
Fairbanks +13
Anchorage +15
Cold Bay +6
Juneau +10
HAWAII
Lihue +2
Honolulu +2
Kahului +1
Hilo +2
Environmental Data Service, NOAA
Based on preliminary telegraphic reports

Winter Weather Review

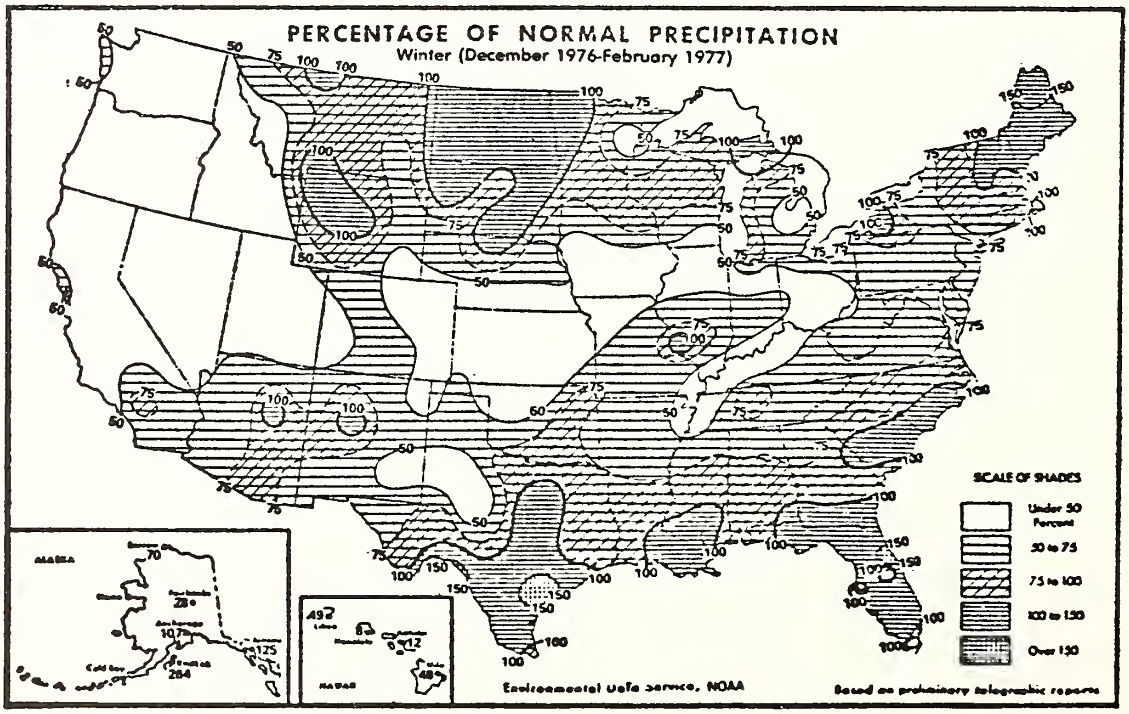

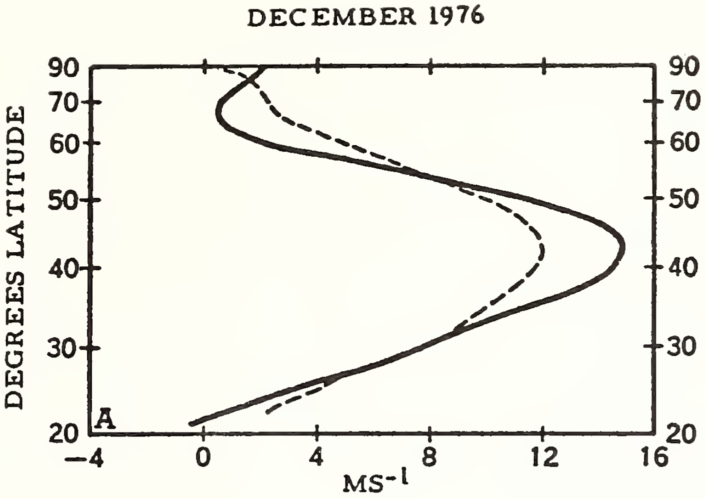
DECEMBER 1976

WESTERN HEMISPHERE 700 MB ZONAL WIND PROFILES

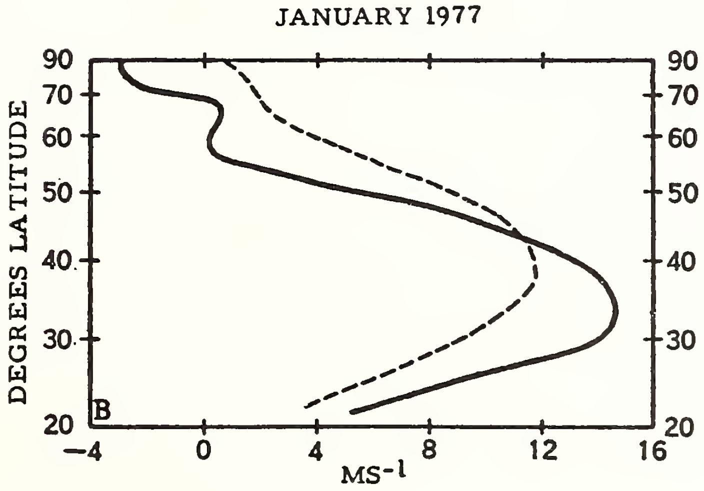
JANUARY 1977

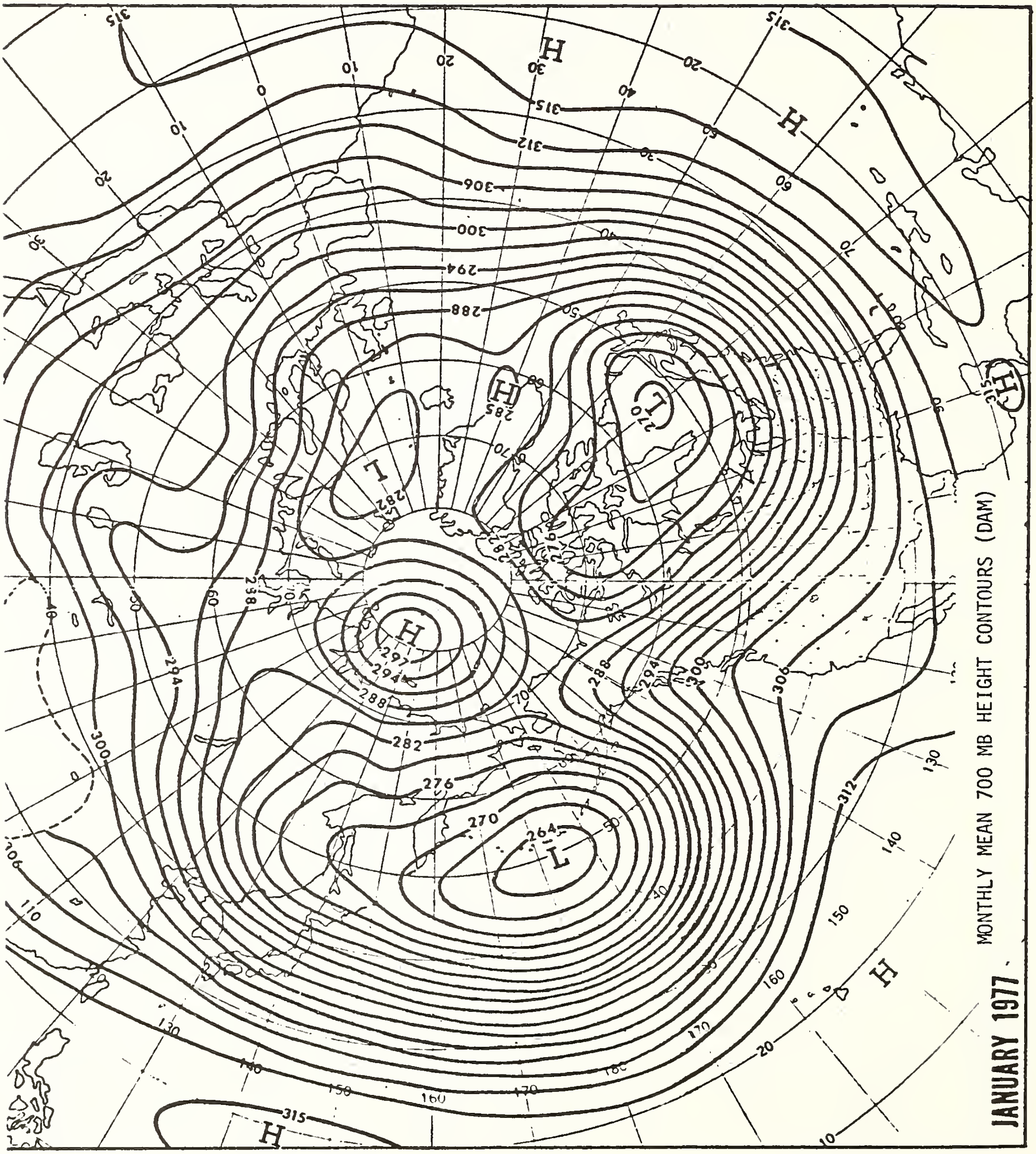

JANUARY 1977 MONTHLY MEAN 700 MB HEIGHT CONTOURS (DAM)

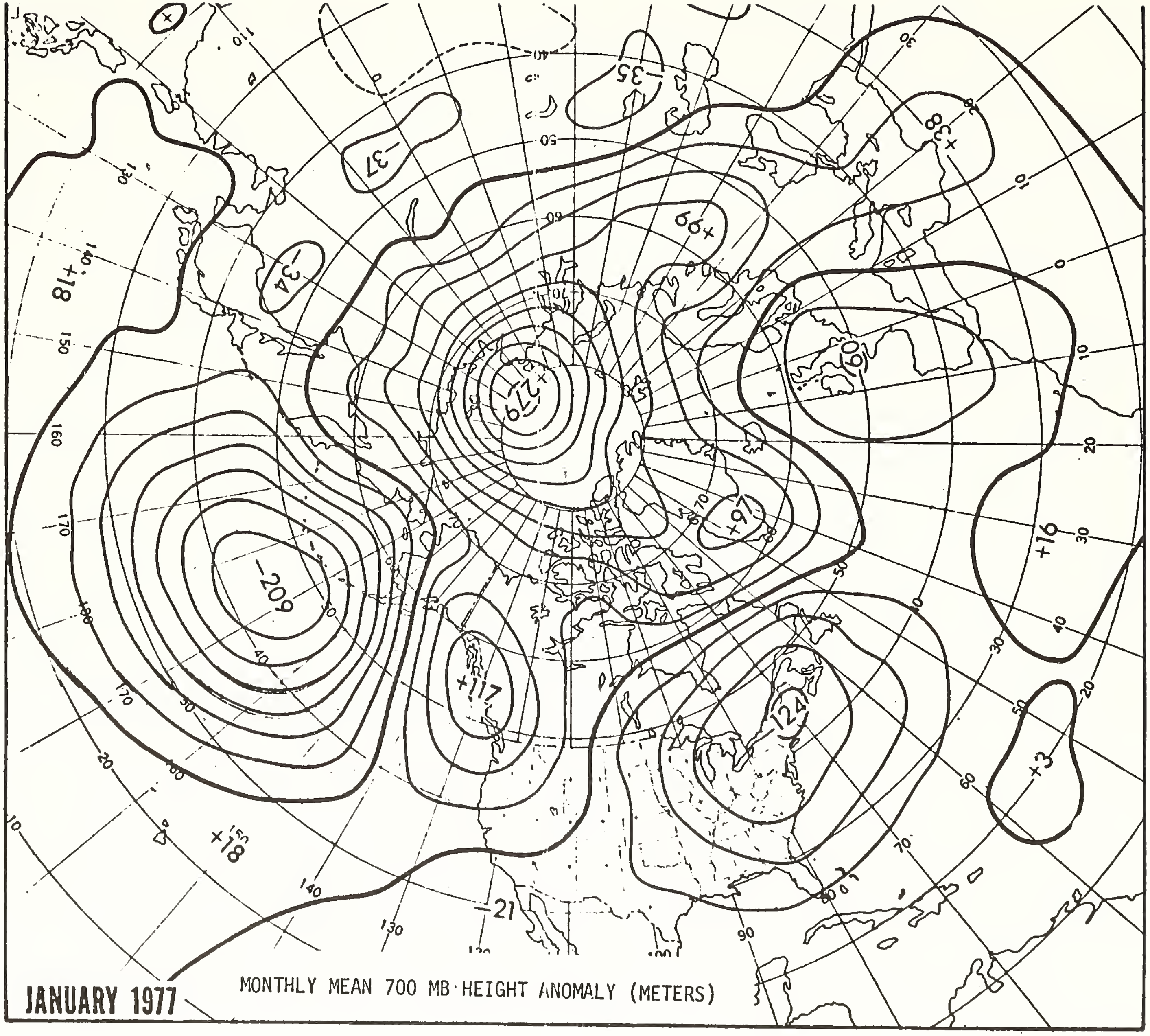

JANUARY 1977 MONTHLY MEAN 700 MB·HEIGHT ANOMALY (METERS)

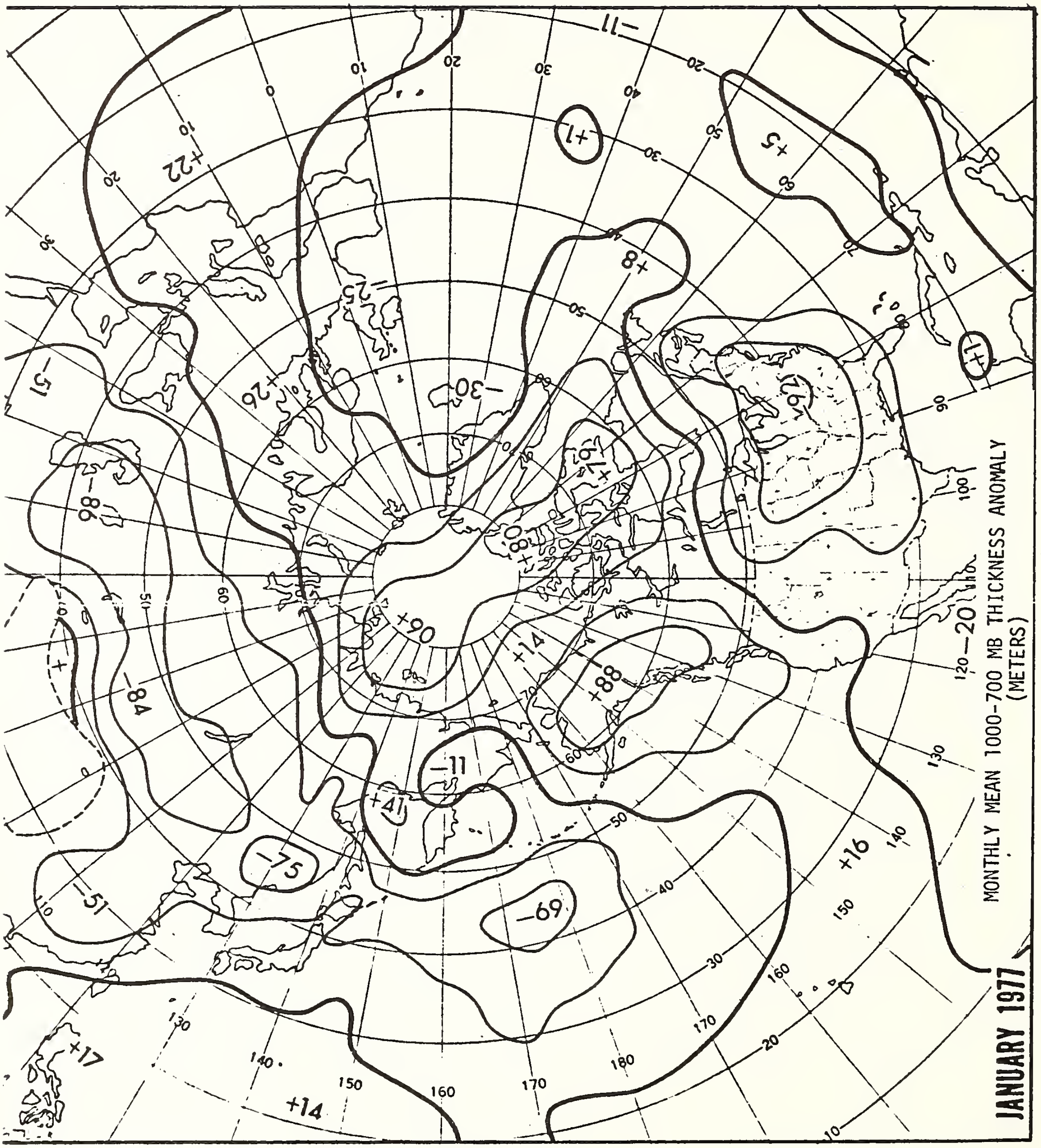

MONTHLY MEAN 1000-700 MB THICKNESS ANOMALY (METERS)

JANUARY 1977

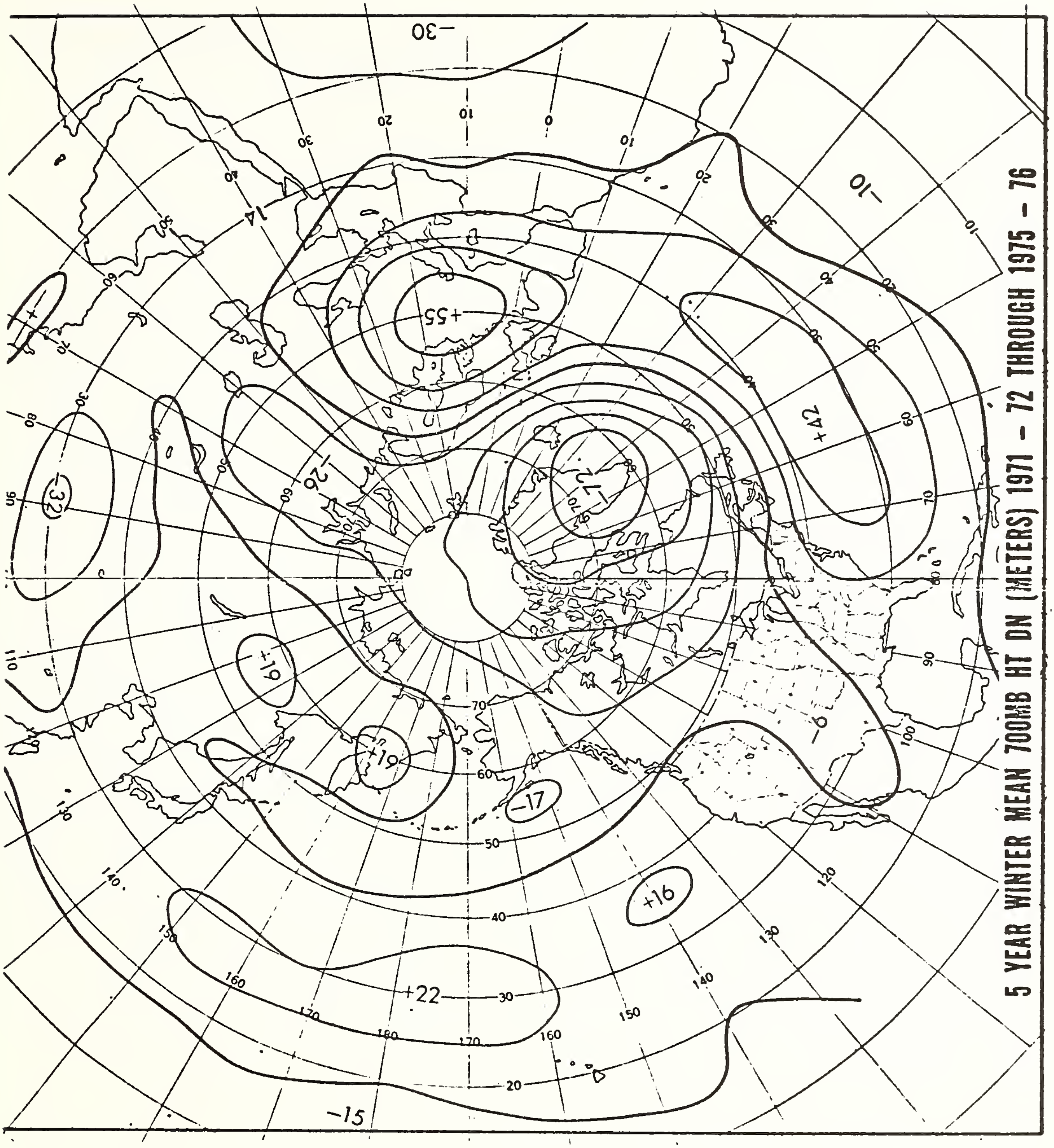

5 YEAR WINTER MEAN 700MB HT DN (METERS) 1971 - 72 THROUGH 1975 - 76

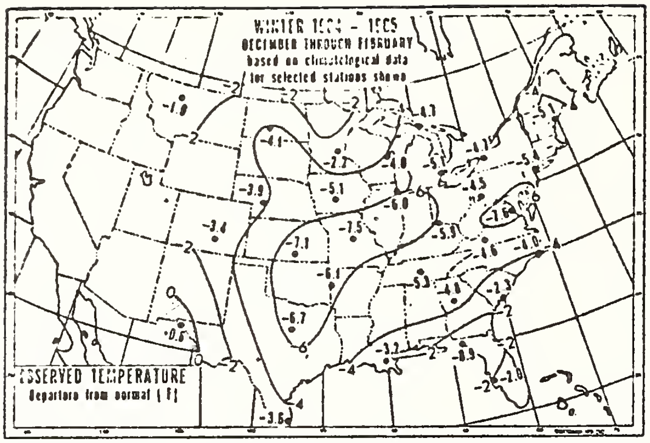
WINTER 1904 - 1905
DECEMBER THROUGH FEBRUARY
based on climatological data
for selected stations shown
OBSERVED TEMPERATURE
Departure from normal (F)

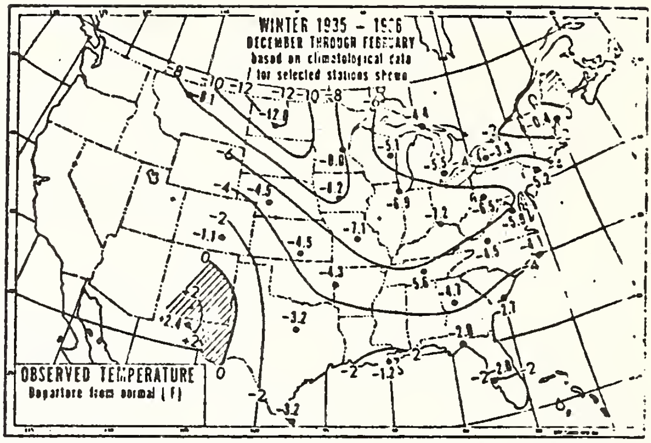
WINTER 1935 - 1936
DECEMBER THROUGH FEBRUARY
based on climatological data
for selected stations shown
OBSERVED TEMPERATURE
Departure from normal (F)

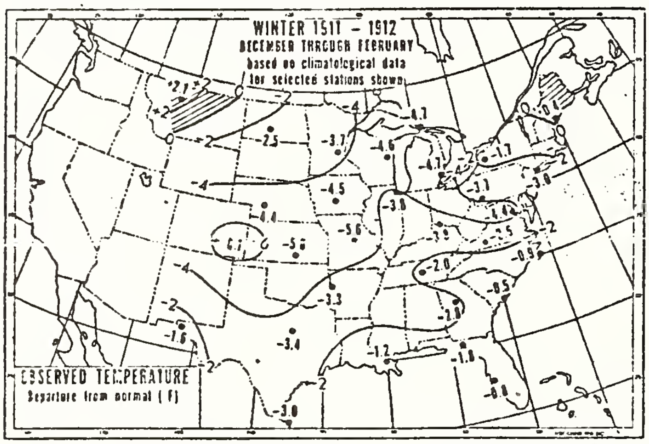
WINTER 1911 - 1912
DECEMBER THROUGH FEBRUARY
based on climatological data
for selected stations shown
OBSERVED TEMPERATURE
Departure from normal (F)

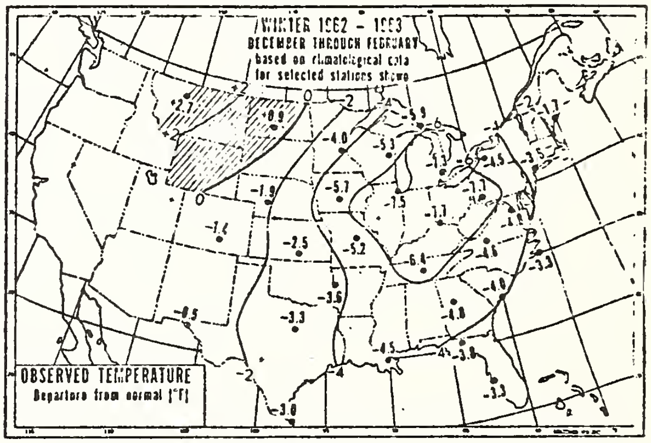
WINTER 1962 - 1963
DECEMBER THROUGH FEBRUARY
based on climatological data
for selected stations shown
OBSERVED TEMPERATURE
Departure from normal (°F)

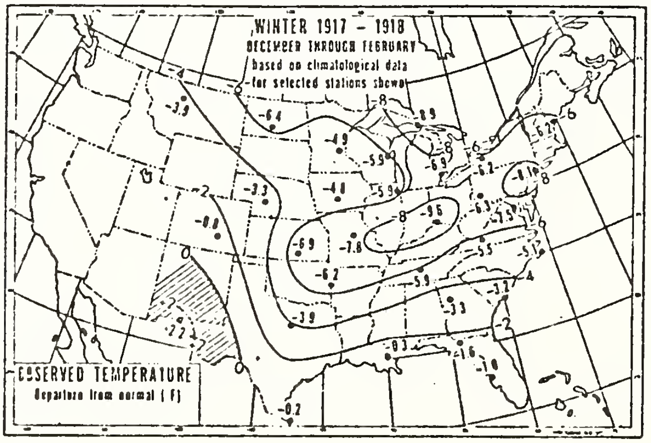
WINTER 1917 - 1918
DECEMBER THROUGH FEBRUARY
based on climatological data
for selected stations shown
OBSERVED TEMPERATURE
Departure from normal (F)

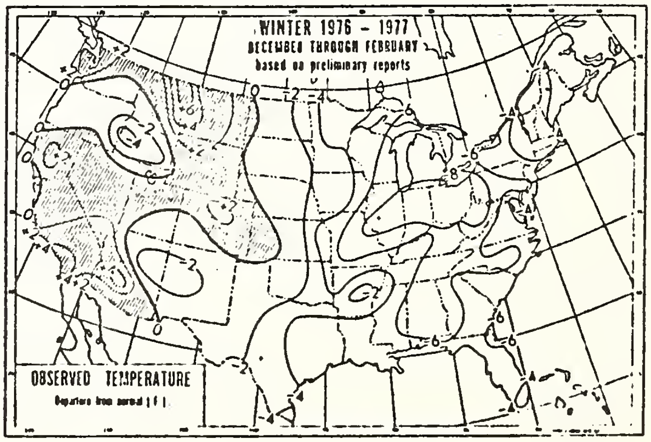
WINTER 1976 - 1977
DECEMBER THROUGH FEBRUARY
based on preliminary reports
OBSERVED TEMPERATURE
Departure from normal (F)

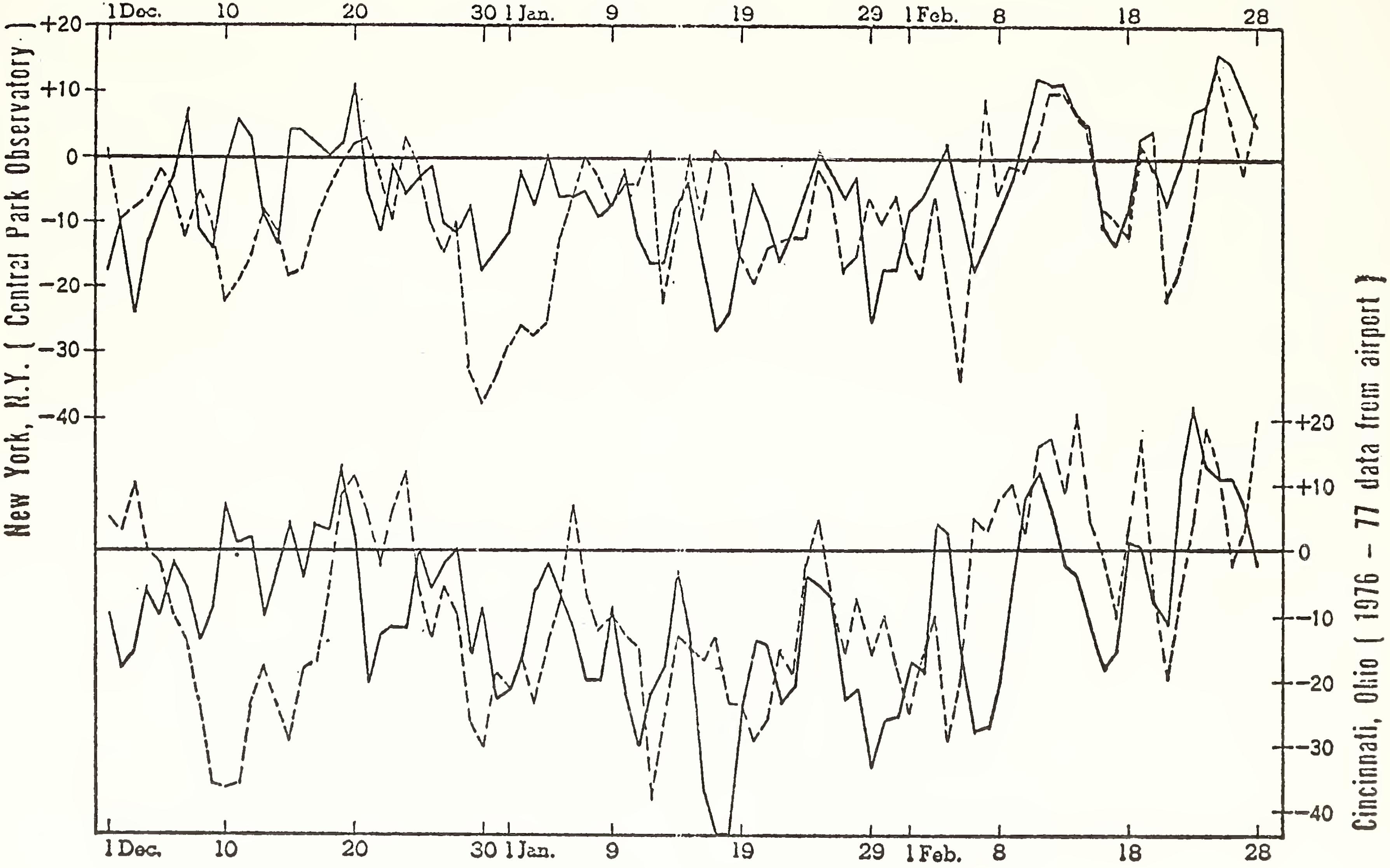

COMPARATIVE DAILY MEAN TEMPERATURE ANOMALIES(°F) FOR NEW YORK CITY & CINCINNATI. DATA FOR 1917-18 ARE SHOWN BY DASHED LINES AND 1976-77 BY SOLID LINES.

CIRCULATION AND WEATHER, SPRING AND SUMMER 1977

Donald L. Gilman
Long Range Prediction Group, NMC
NOAA, National Weather Service

The exceptional character of last year's weather and circulation anomalies did not end when Winter broke in February 1977. The warm Spring (Fig. 1) that prevailed nearly everywhere east of the Rockies, but not in the far West, had not appeared in this configuration since 1946. The magnitude of the temperature anomalies, as large as 8 or 9 degrees F west of the Great Lakes, appears to be without precedent in the period for which we have charts, beginning in 1881. The largest anomalies depart from the 1941-70 normals by about 3 standard deviations. Most Springs of similar type have contained one cool or normal month; that of 1977 was unusually warm throughout, with a rash of broken station records in May.

The average 700 mb circulation pattern for Spring (Fig. 2) was well suited to produce such a striking temperature field: the very strong westerlies crossing the North Pacific underwent a marked split over western North America, allowing a trough to oscillate between the far West and Mexico, then rejoined at unusually high latitudes east of the 100th Meridian. The strength of the height anomalies and the shortening of the flow's wavelength over North America favored the south winds that brought both record warmth and extra rainfall to the central states (Fig. 3).

Summer temperatures over the U.S. were less predominantly warm than those of Spring and set fewer records (Fig. 4). Cold air entered first the Northeast, then the far Northwest, and finally — in strength— the North Central states. The varying frontal activity brought rain to most areas that would usually be dry when high temperatures spread from coast to coast, as in several of the drought summers of the 1930's and 1950's. Only the Southeast and extreme northern Great Plains were left dry in 1977. This rarer combination of temperatures and rainfall was last seen in 1959.

The most striking anomaly of the 700 mb circulation occurred north of Alaska, where a ridge of heights 3 standard deviations above the current normals was anchored through the Summer. Such a ridge location ordinarily implies a cool summer for the far West and much of the Great Plains. This time the polar westerlies (55°-70°) were unusually weak, wavelengths were short, and the mean trough that would have been expected over the Bering Sea — southwest of the ridge— almost entered the Gulf of Alaska instead.

Downstream, height anomalies apparently responded barotropically, positive over the far West and strongly negative around Hudson's Bay. This anomaly configuration will typically yield a temperature pattern over the U.S. very similar to that of 1977.

Figures

Figure 1: Mean temperature anomalies of Spring (March-April-May) 1977. Banded area (A) is Above Normal, dotted area (B) is Below Normal, and blank area (N) is Near Normal. Each category occurs naturally 1/3 of the time. Normals are 1941-70.

Figure 2: Mean 700 mb heights and anomalies of Spring 1977, in meters. Normals are 1948-70.

Figure 3: Total precipitation for Spring 1977. Banded area (H) is Heavy, dotted area (L) is Light, and blank area (M) is Moderate. Each category occurs naturally 1/3 of the time. Category limits from 1948-70 data, gamma function fit.

Figure 4: Mean temperature anomalies of Summer 1977. Format as in Fig. 1.

Figure 5: Total precipitation for Summer 1977. Format as in Fig. 3.

Figure 6: Mean 700 mb heights and anomalies of Summer 1977. Format as in Fig. 2.

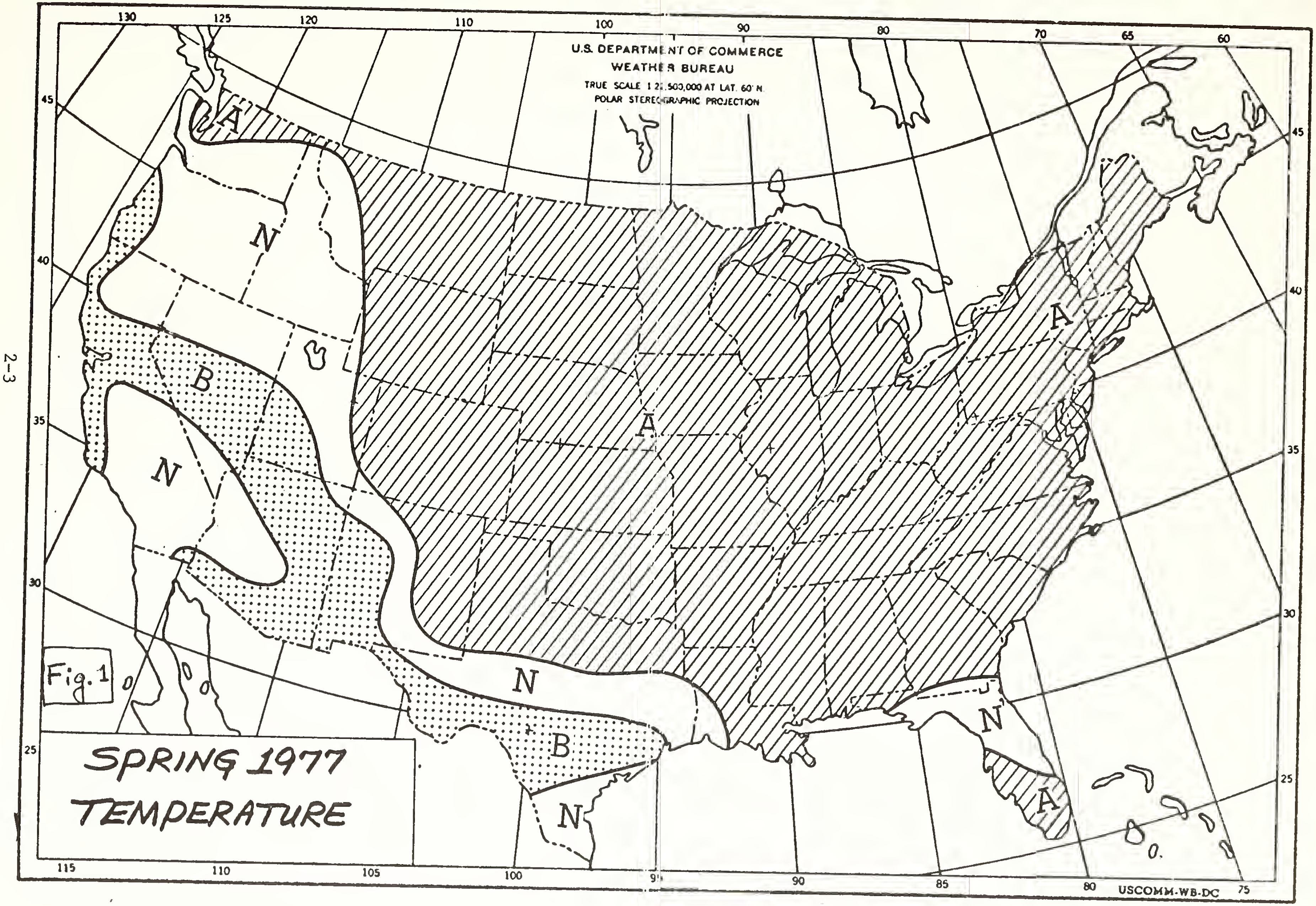

U.S. DEPARTMENT OF COMMERCE
WEATHER BUREAU
TRUE SCALE 1:20,500,000 AT LAT. 60° N.
POLAR STEREOGRAPHIC PROJECTION
130
125
120
110
100
90
80
70
65
60
45
40
35
30
25
115
105
85
75
A
N
B
USCOMM-WB-DC

Fig. 1

SPRING 1977
TEMPERATURE

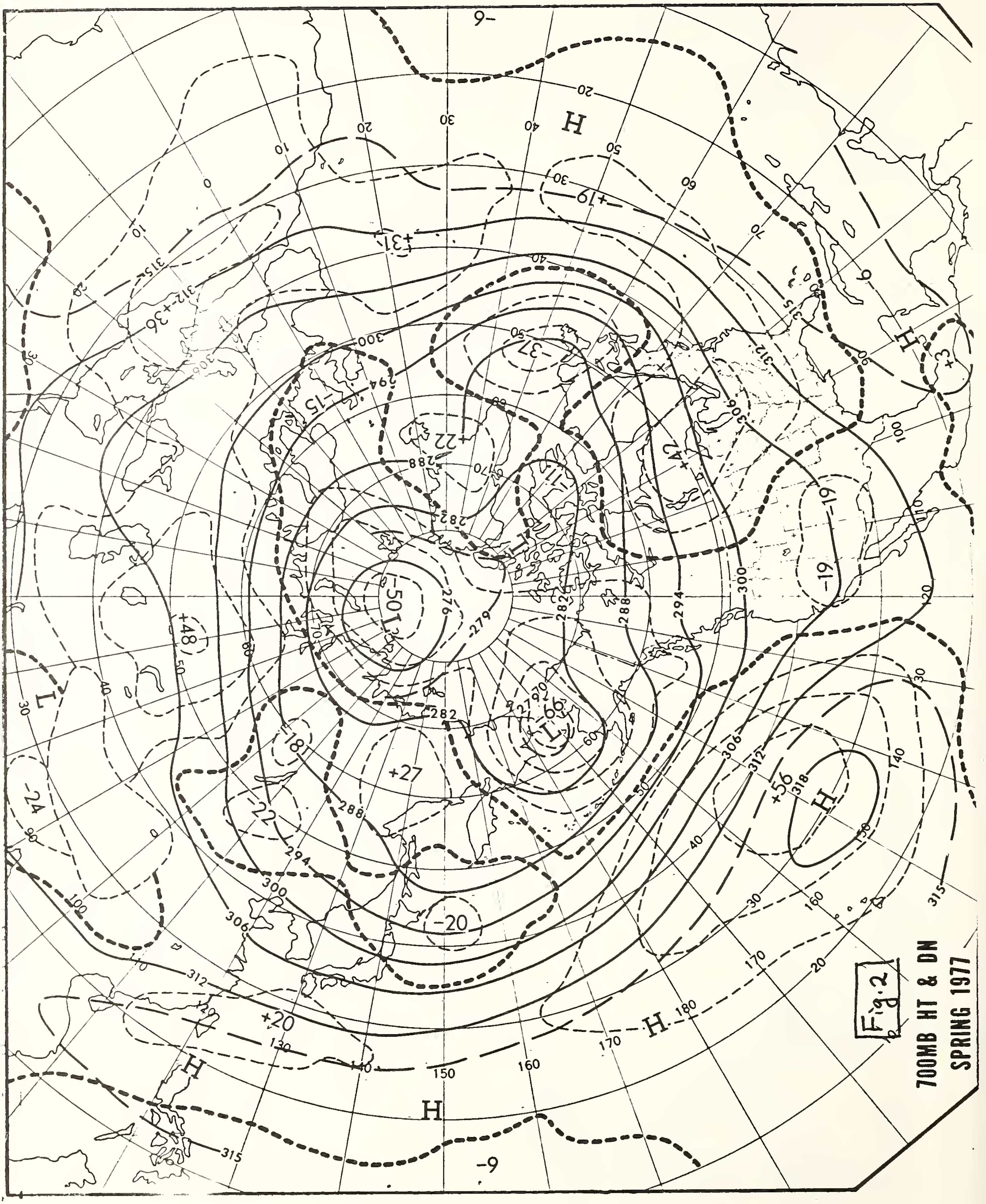

Fig.2

700MB HT & DN
SPRING 1977

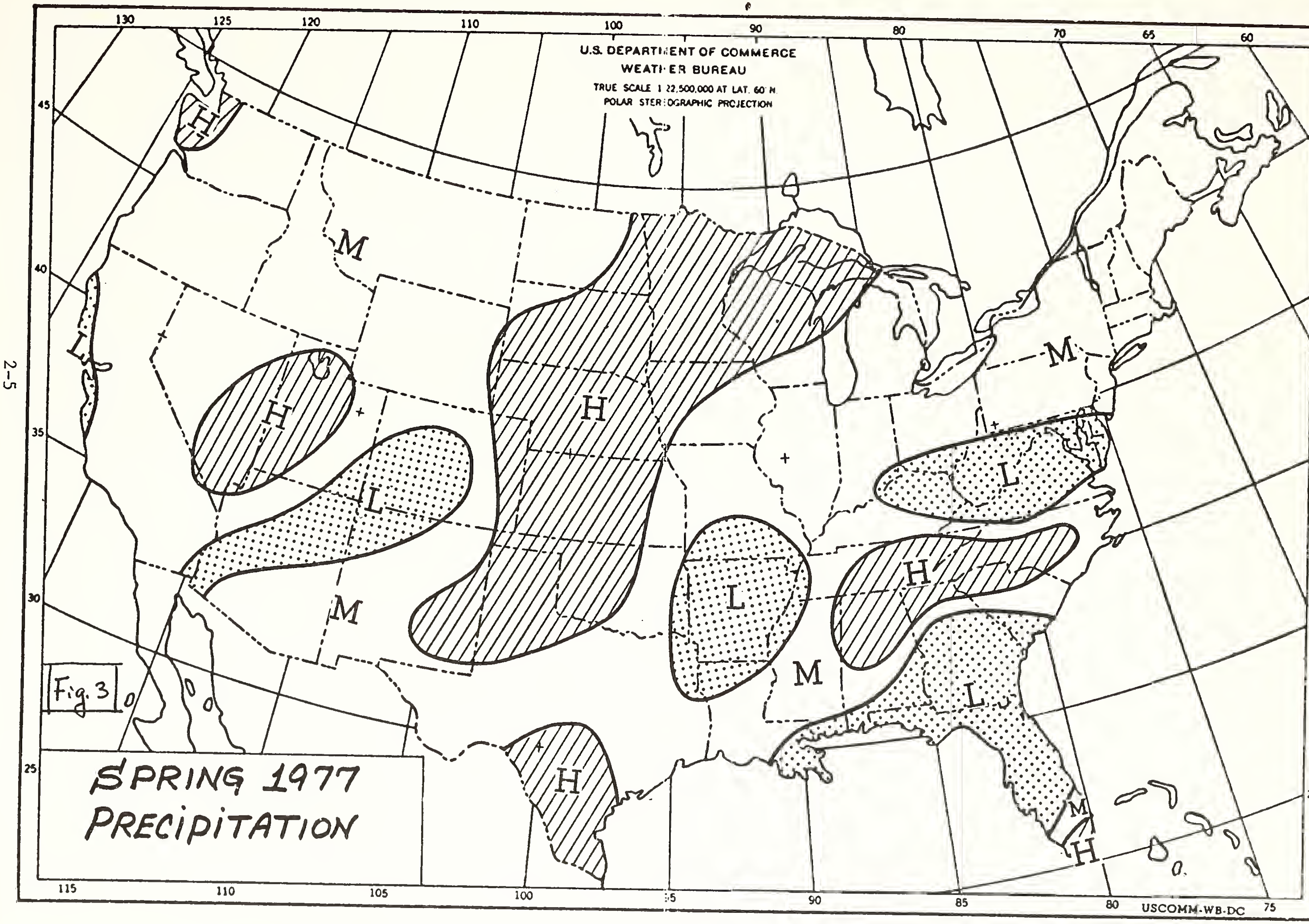
U.S. DEPARTMENT OF COMMERCE
WEATHER BUREAU
TRUE SCALE 1:22,500,000 AT LAT. 60° N
POLAR STEREOGRAPHIC PROJECTION
130
125
120
110
100
90
80
70
65
60
45
40
35
30
25
115
105
95
85
75
H
L
M
USCOMM-WB-DC

Fig. 3

SPRING 1977
PRECIPITATION

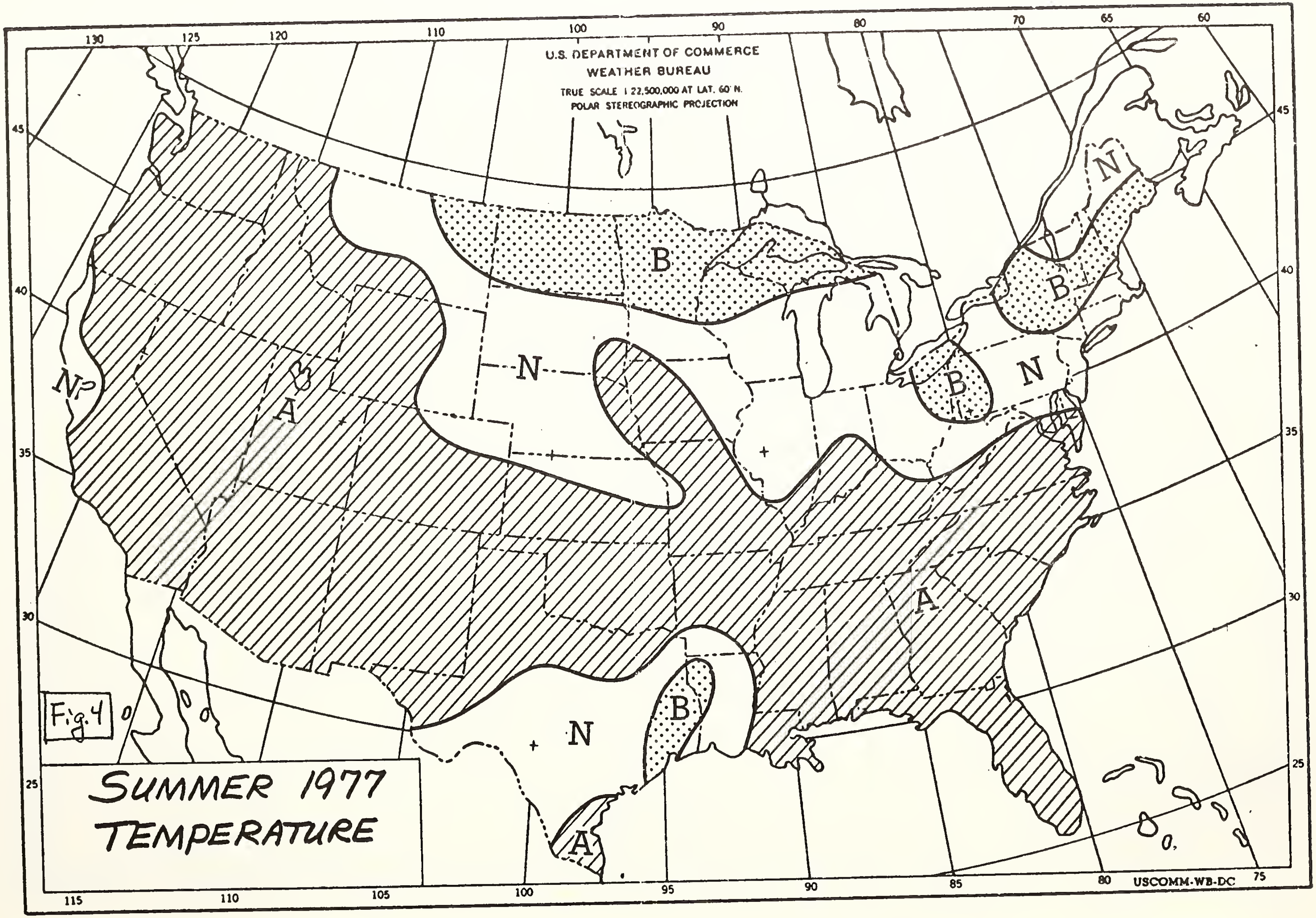
U.S. DEPARTMENT OF COMMERCE
WEATHER BUREAU
TRUE SCALE 1:22,500,000 AT LAT. 60° N.
POLAR STEREOGRAPHIC PROJECTION
130
125
120
110
100
90
80
70
65
60
45
40
35
30
25
115
110
105
100
95
90
85
80
75
N
B
N
B
N
B
N
A
N
B
A
A
USCOMM-WB-DC

Fig. 4

SUMMER 1977
TEMPERATURE

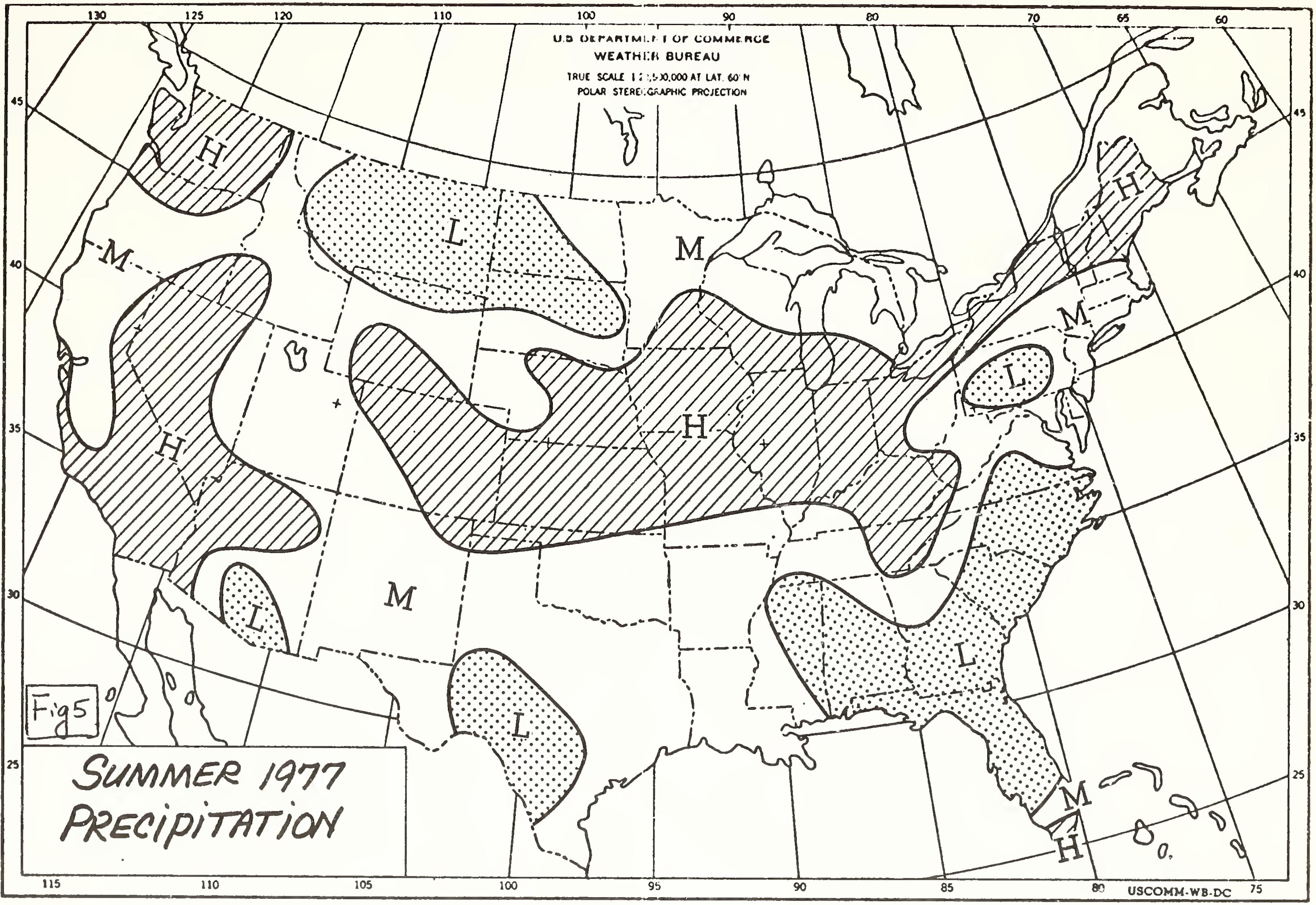

U.S DEPARTMENT OF COMMERCE
WEATHER BUREAU
TRUE SCALE 1:[illegible]500,000 AT LAT. 60°N
POLAR STEREOGRAPHIC PROJECTION
130
125
120
110
100
90
80
70
65
60
45
40
35
30
25
115
105
95
85
75
H
L
M
H
M
H
L
L
M
L
H
M
L
M
H
L
USCOMM-WB-DC

Fig5

SUMMER 1977 PRECIPITATION

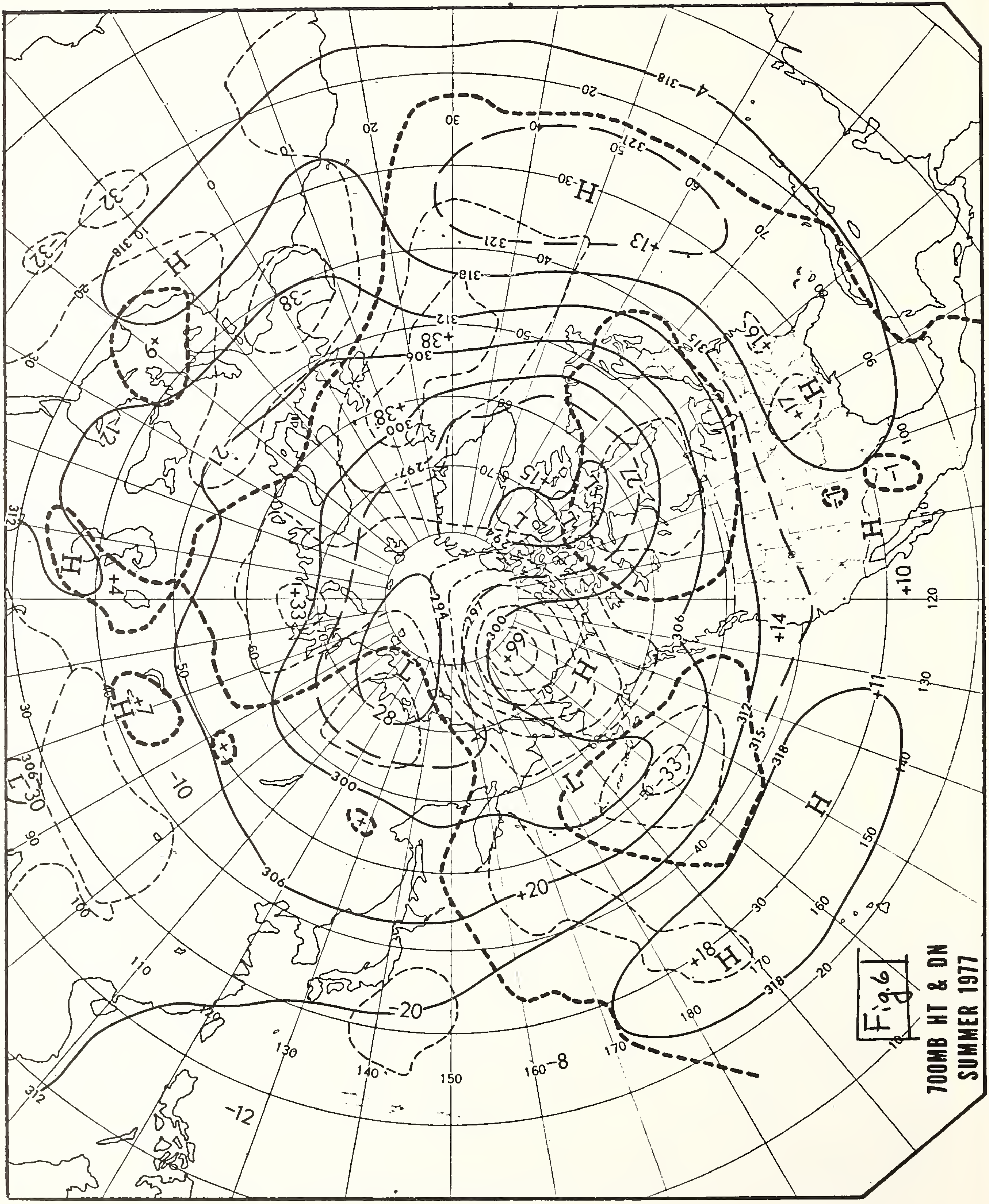

Fig. 6

700MB HT & DN
SUMMER 1977

A Review of the Unusual Climatic Events of 1976-77 in Canada

by T.R. Allsopp, Atmospheric Environment Service, Canada

The extremes of climate which Canada has experienced in the past year accentuate the hypothesis that global climate has entered a period of increased variability. Not since the 1930's has such a spectrum of temperatures and precipitation occurred.

In western Canada drought and anomalously mild weather which began in the fall of 1976 and reached its zenith in the spring of 1977 crippled ski operations, caused low water levels in reservoirs supplied by spring run-off, threatened the 1977 crop season with failure and had provincial fire control centres on the alert for severe forest fire activity.

Extremely cold weather in eastern Canada during the fall and winter seasons added further to heating fuel requirements, increased provincial and municipal winter maintenance costs, hampered shipping on the Great Lakes, although it did stimulate the growing winter recreation industry which had recently experienced poor years.

1. Fall 1976 (September - October - November)

During September a well amplified warm ridge over western North America and a cold trough over eastern North America became established. This mean circulation pattern was to remain quasi-stationary for a remarkable six months. In the vicinity of the warm ridge over British Columbia and Alberta and in the northwesterly flow which extended eastward into northwestern Ontario precipitation was well below normal (figure 1). Some locations, particularly in southern Saskatchewan and southern Manitoba measured record low monthly amounts on the order of 1 mm. Regina, Saskatchewan received a record low 17.5 mm precipitation (14% of normal) in the period August 1 to November 30. From October 8 to November 24 Winnipeg, Manitoba received no measurable precipitation. The situation was similar across the Canadian prairies. At the end of November it was the fifth consecutive month of below normal precipitation in northwestern Ontario.

Near record fall temperature departures of +3°C to +5°C from the 1941-70 normal were centred in the Yukon Territory and District of Mackenzie and the northern fringes of British Columbia and Alberta (figure 2).

Through November, Ontario and Quebec continued to have below normal temperatures for the fifth consecutive month. Departures of -2°C to -3°C from the fall normal occurred over most of Ontario and western Quebec. The cold reached near record proportions for the 20th century. In general, the autumns of 1917, 1933 and 1936 were of similar severity.

2. Winter 1976-77 (December - January - February)

The mean long wave pattern increased in amplitude during this period until the west coast ridge deteriorated in late February. The result was a temperature and precipitation pattern very similar to the fall period. From southern British Columbia across the prairies to northwestern Ontario record low amounts of monthly precipitation were measured. The snowpack in the Coastal and Rocky Mountains was very low. By the end of the period virtually no snowpack was evident over much of Saskatchewan and southern Alberta.

It was the warmest winter on record at many short term Yukon and northern British Columbia localities (figure 3, table 1). In Alberta it was the warmest winter since 1930-31 and in general the third warmest on record at stations taking observations for nearly 100 years. Monthly temperature anomalies ranged as high as +11°C to 13°C in the core of the warm sector.

To the east, Ontario and Quebec continued to experience well below normal temperatures. Temperature departures from normal ranged from -3°C to -9°C over Ontario and Quebec during December and ranged from -5°C to -7°C in southern Ontario during January. It was the coldest January on record at some long term southern Ontario localities (London, Guelph). At Toronto City, no above freezing temperatures occurred during the month of January, a record at a station that originated in 1840. By early February considerable ice had formed on all of the Great Lakes.

Temperature departures ranged as high as -4°C from normal for the winter in southern Ontario. It was perhaps the fourth coldest winter in the 20th century in this part of Canada. Perusal of historical data indicates the winters of 1903-04, 1917-18, 1933-34 were colder. The occurrence of several near normal or warm winters immediately prior to 1976-77 heightened the effect in Ontario.

3. Spring 1977 (March - April - May)

Spring was exceptionally warm over most of Canada with the exception of the coastal regions. Temperature departures ranged as high as +5°C from normal from southeastern Saskatchewan to northwestern Ontario (figure 4), the warmest spring on record. In fact, at some localities in the core of the warm sector the temperatures were 2°C warmer than the previous record.

By April 30 the very dry weather, which had begun in western Canada in late summer 1976, reached its culminating point. The core of the drought area extended from southern British Columbia into southern Alberta and eastward through Saskatchewan and southern Manitoba into northwestern Ontario (figure 5). Precipitation was as low as 31% at Regina and 33% normal at Winnipeg for the period September 1 through April 30. It was the driest on record for that particular period from central Saskatchewan to northwestern Ontario (table 2). By late April dust storms frequently occurred across the prairies. Forest fires raged in the parklands of Saskatchewan and lake districts of Manitoba.

A significant transition in the precipitation pattern took place in May. A mid continental ridge became established over North America. To the west of the ridge record amounts of precipitation fell at many Canadian prairie localities. A band of precipitation greater than four times the normal ran from central Alberta into southern Manitoba (figure 6). Most localities from central Alberta to northwestern Ontario received at least 100 mm of precipitation thus breaking the agricultural drought in those regions. To the east of the ridge it was the driest May on record in central and northeastern Ontario and western Quebec.

4. Summary

This past summer and early fall in Canada have been far from uneventful. Heat waves have occurred from British Columbia to the Canadian Maritimes. Although drought remains in some parts of southern Alberta and southern Saskatchewan cool damp weather has had an adverse affect on harvesting in the eastern prairies. In fact, the cold on the prairies reached record proportions in August, particularly in Manitoba. Further east the record heavy precipitation of the past few months in the lower Great Lakes region of Ontario has reduced agricultural land to a quagmire. In summary, these events and the events of the preceding months clearly indicate that Canada has experienced one of the most unusual climatic years in decades.

ACCUMULATED MONTHLY PRECIPITATION IN MILLIMETRES
NORMAL 1941-70(—)
ACTUAL 1976-77(--)

VANCOUVER INT'L A , B.C.

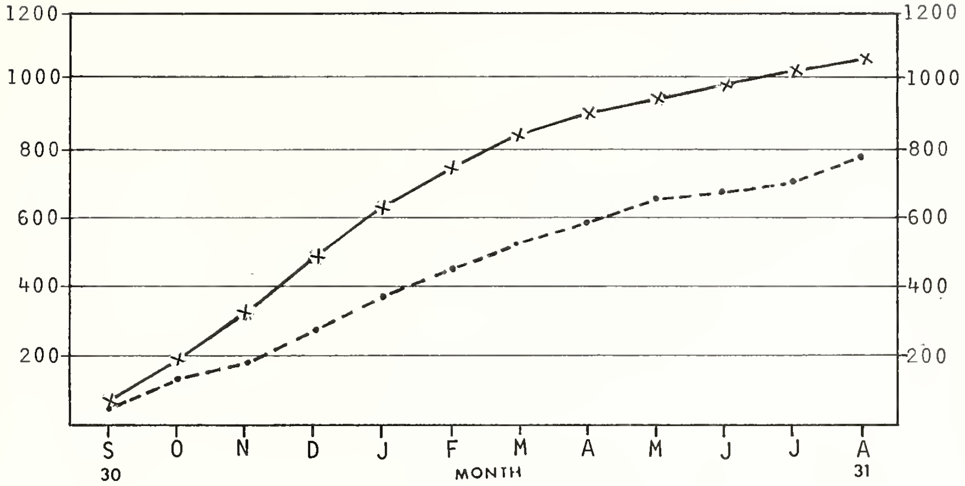

EDMONTON INT'L A , ALTA.

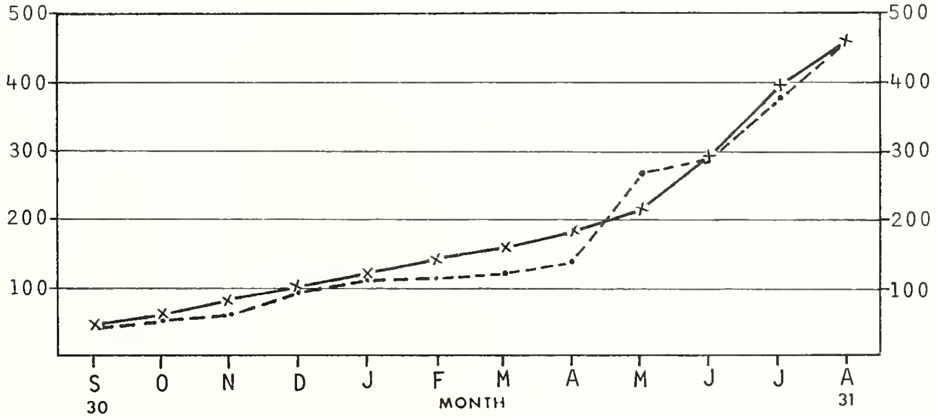

KINDERSLEY , SASK.

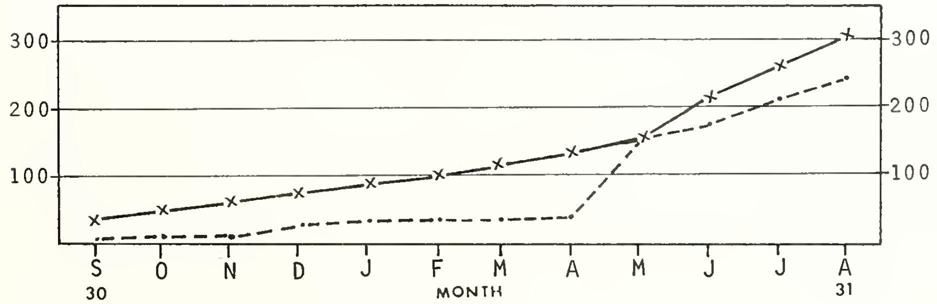

figure 1A

ACCUMULATED MONTHLY PRECIPITATION IN MILLIMETRES
NORMAL 1941-70(—)
ACTUAL 1976-77(--)

REGINA A, SASK.

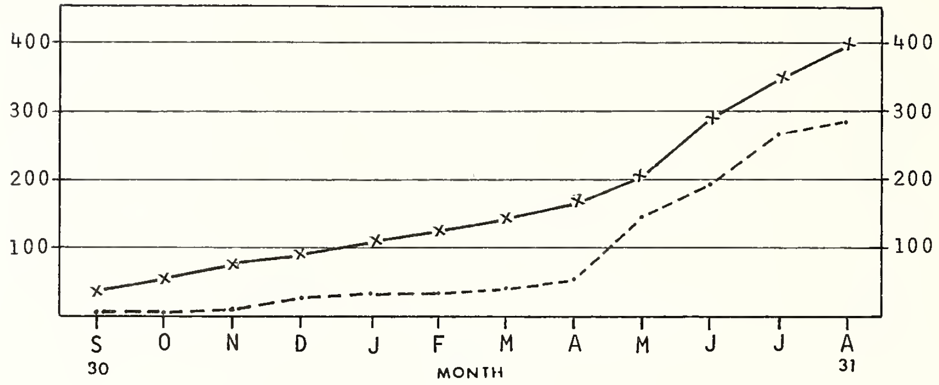

WINNIPEG INT'L A, MAN.

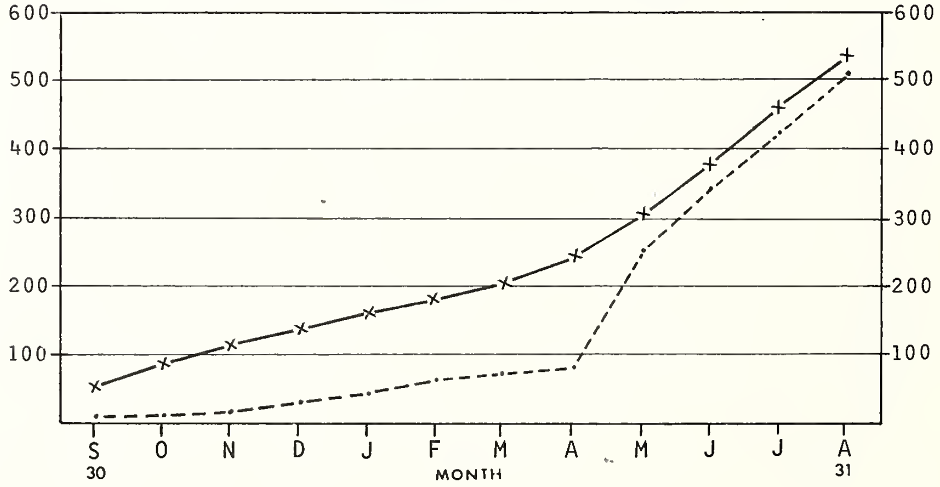

THUNDER BAY A, ONT.

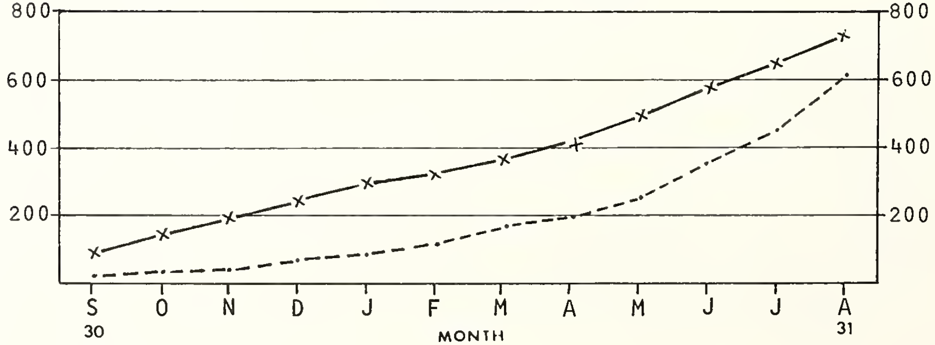

figure 1B

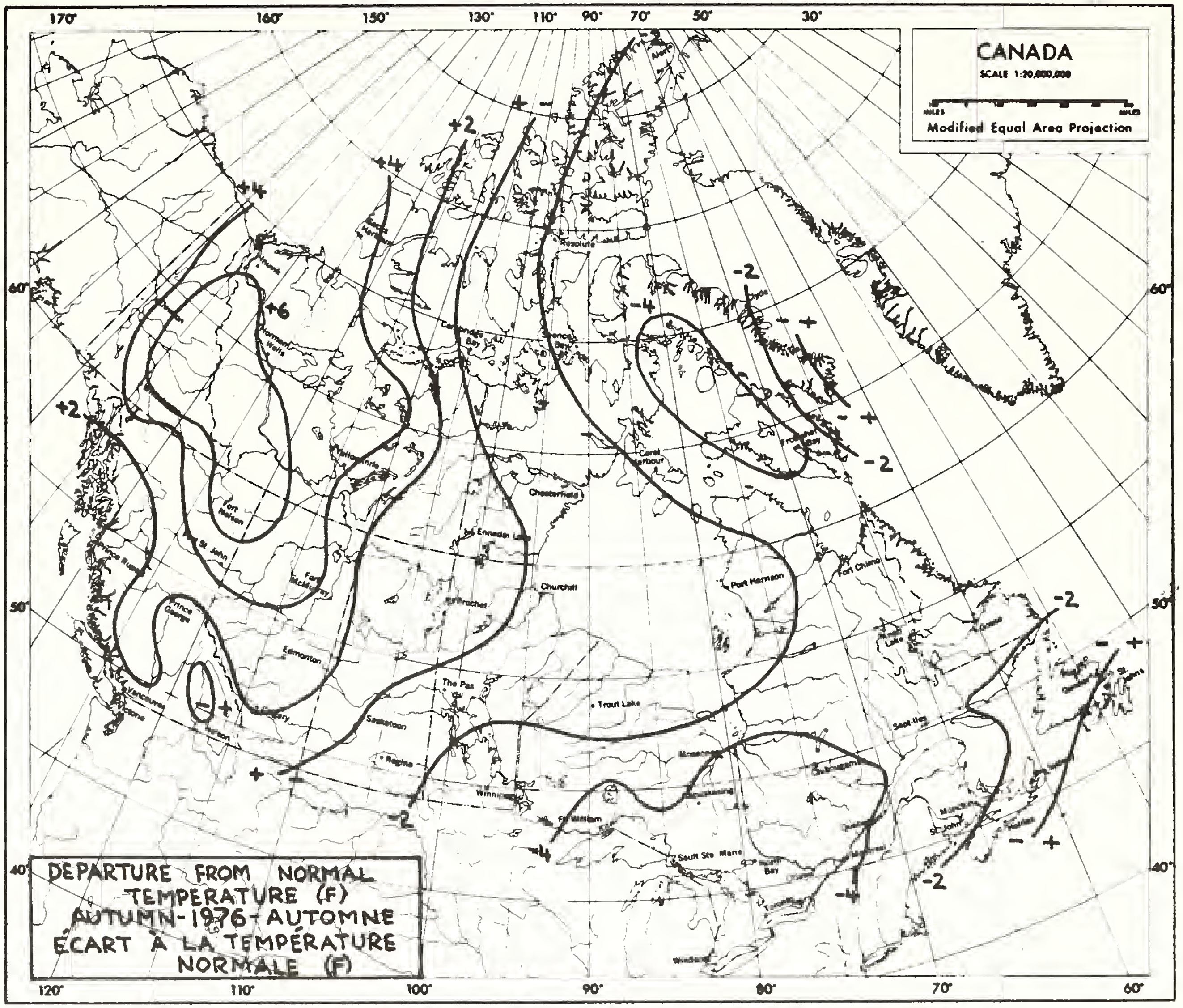
CANADA
SCALE 1:20,000,000
MILES
Modified Equal Area Projection
DEPARTURE FROM NORMAL TEMPERATURE (F)
AUTUMN-1976-AUTOMNE
ÉCART À LA TEMPÉRATURE NORMALE (F)
+6
+4
+2
-2
-4
+
-
Resolute
Cambridge Bay
Spence Bay
Coral Harbour
Chesterfield
Churchill
Port Harrison
Fort Chimo
Norman Wells
Yellowknife
Fort Nelson
St. John
Fort McMurray
Prince George
Edmonton
Vancouver
Victoria
Calgary
Saskatoon
Regina
The Pas
Winnipeg
Trout Lake
Ft. William
Moosonee
Sault Ste Marie
North Bay
Windsor
Sept-Iles
St. John's
Halifax
170°
160°
150°
130°
110°
90°
70°
50°
30°
120°
100°
80°
60°
40°

figure 2

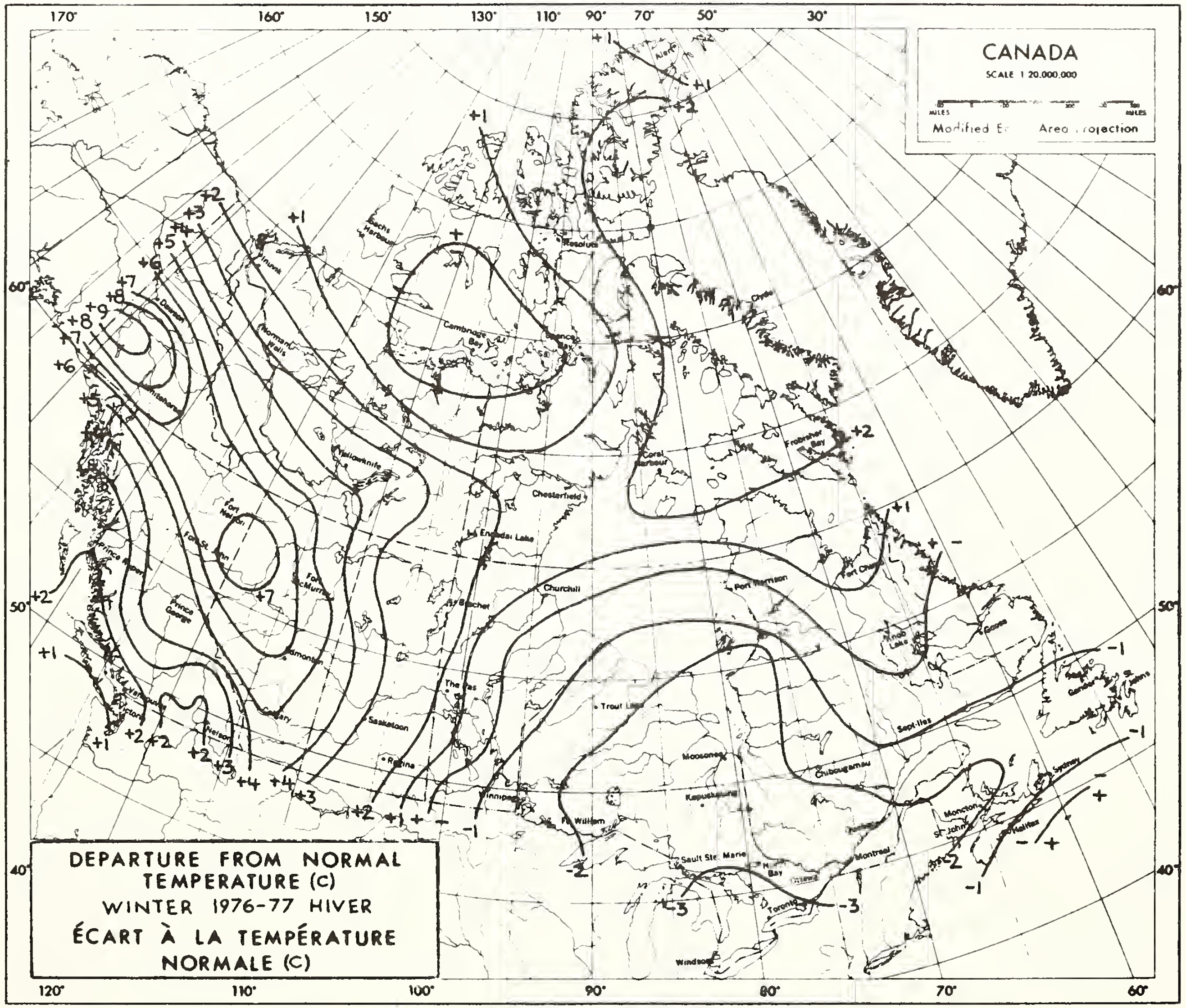

DEPARTURE FROM NORMAL TEMPERATURE (C)
WINTER 1976-77 HIVER
ÉCART À LA TEMPÉRATURE NORMALE (C)

figure 3

TABLE 1 **COMPARATIVE WINTER SEASON (DECEMBER - JANUARY - FEBRUARY) TEMPERATURES (°C)**

LOCATION	RECORDS SINCE	1976-77 TEMP.	DEPARTURE FROM 1941-70 NORMAL	DEPARTURE FROM 1970-76 AVE.	1976-77 RANK	COLDEST YEAR	COLDEST TEMP	WARMEST YEAR	WARMEST TEMP
Beaverlodge CDA, Alta.	1915	-6.4	+5.8	+6.2	4th warmest	1968-69	-20.1	1930-31	+0.8
Calgary, Atla.	1885	-3.4	+5.3	+5.4	3rd warmest	1968-69	-16.9	1930-31	-0.1
Dawson, Yukon	1900	-15.0	+10.7	+13.3	1st warmest	1964-65	-33.7	1976-77	-15.0
Edmonton, Alta.	1880	-5.9	+6.0	+5.4	3rd warmest	1886-87	-20.0	1930-31	-2.9
Fort Nelson, B.C.	1937	-13.1	+7.2	+7.6	1st warmest	1968-69	-25.7	1976-77	-13.1
Fort Vermilion CDA, Alta.	1908	-13.9	+6.6	+6.4	2nd warmest	1917-18	-28.2	1930-31	-12.8
Mayo, Yukon	1925	-13.8	+9.4	+11.8	1st warmest	1964-65	-30.9	1976-77	-13.8
Medicine Hat, Alta.	1884	-5.2	+4.1	+3.9	10th warmest	1886-87	-17.9	1930-31	+0.6
Prince George, B.C.	1942	-3.4	+5.2	+5.3	1st warmest	1949-50) 1968-68)	-15.1	1976-77	-3.4
Watson Lake, Yukon	1938	-13.6	+8.5	+9.7	1st warmest	1968-69	-30.9	1976-77	-13.6
Whitehorse, Yukon	1942	-7.3	+8.6	+10.8	2nd warmest	1968-69	-24.0	1943-44	-7.2
Beatrice, Ontario	1878	-12.1	-3.2	-2.9	8th coldest	1903-04	-13.8	1931-32	-4.8
Harrow CDA, Ontario	1917	-6.9	-4.0	-3.9	4th coldest	1917-18	-7.4	1931-32	+2.7
London, Ontario	1878	-8.7	-3.6	-3.5	3rd coldest	1903-04	-8.9	1889-90	-0.2
Ottawa CDA, Ontario	1890	-11.0	-1.6	-1.5	21st coldest	1933-34	-15.9	1952-53	-5.4
Peterborough, Ontario	1892	-10.2	-2.9	-2.5	8th coldest	1903-04	-12.3	1931-32	-2.7
Southampton, Ontario	1874	-7.8	-2.9	-3.4	9th coldest	1917-18	-9.8	1931-32	-1.0
Thunder Bay, Ontario	1877	-15.0	-2.2	-1.9	15th coldest	1884-85	-17.6	1877-78	-5.3
Toronto, Ontario	1840	-5.9	-2.6	-2.9	21st coldest	1874-75	-8.5	1931-32	0.4
Woodstock, Ontario	1873	-8.2	-3.1	-3.3	9th coldest	1903-04	-9.7	1931-32	-0.2

TABLE 2 **ACCUMULATED PRECIPITATION (MM) FOR THE PERIOD SETPEMBER 1 TO APRIL 30**

LOCATION	RECORDS SINCE	1976-77 TOTAL	1941-70 NORMAL	1976-77 (% OF NORMAL)	1970-76 AVE.	1977 RANK (IN TERMS OF DRIEST)
Medicine Hat, A Alta.	1890	63.1	168.1	38	147.2	4th
Prince Albert, A Alta.	1889	68.4	178.6	38	167.6	1st
Saskatoon, A Sask.	1908	68.5	162.9	42	158.5	1st
Swift Current, A Sask.	1886	75.3	178.0	42	186.1	2nd
Regina, A Sask.	1890	52.1	166.7	31	175.2	1st
Brandon, CDA Man.	1890	67.1*	194.8*	34	247.6	1st
Winnipeg, A Man.	1878	79.9	243.7	33	235.0	1st
Kenora A, Ontario	1916	135.0	321.3	42	337.7	1st
Thunder Bay, A Ontario	1875	196.8	422.0	47	437.3	5th

* total recorded at Brandon A

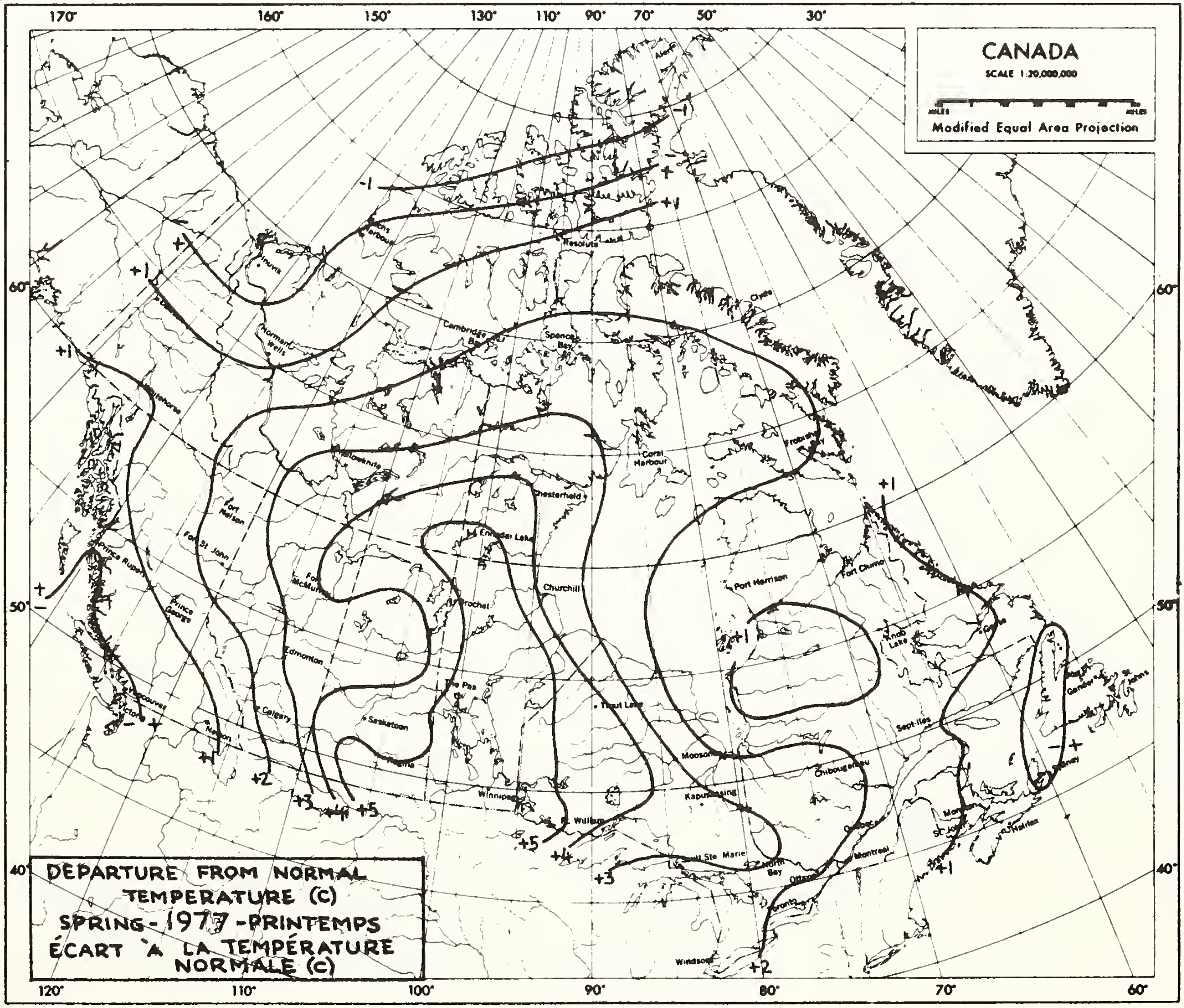
CANADA
SCALE 1:20,000,000
MILES
Modified Equal Area Projection
DEPARTURE FROM NORMAL TEMPERATURE (C)
SPRING - 1977 - PRINTEMPS
ÉCART À LA TEMPÉRATURE NORMALE (C)
170°
160°
150°
130°
110°
90°
70°
50°
30°
60°
50°
40°
120°
110°
100°
90°
80°
70°
60°
-1
+1
+
-
+2
+3
+4
+5
Alert
Resolute
Clyde
Inuvik
Norman Wells
Cambridge Bay
Spence Bay
Coral Harbour
Frobisher Bay
Whitehorse
Yellowknife
Chesterfield
Fort Nelson
Fort St John
Fort McMurray
Ennadai Lake
Churchill
Brochet
Port Harrison
Fort Chimo
Prince Rupert
Prince George
Edmonton
Knob Lake
Goose
Gander
St Johns
Sept-Iles
Vancouver
Victoria
Calgary
Saskatoon
Regina
The Pas
Trout Lake
Moosonee
Chibougamau
Kapuskasing
Winnipeg
Ft William
Nelson
Sault Ste Marie
North Bay
Ottawa
Quebec
Montreal
Moncton
Saint John
Halifax
Sydney
Toronto
Windsor

figure 4

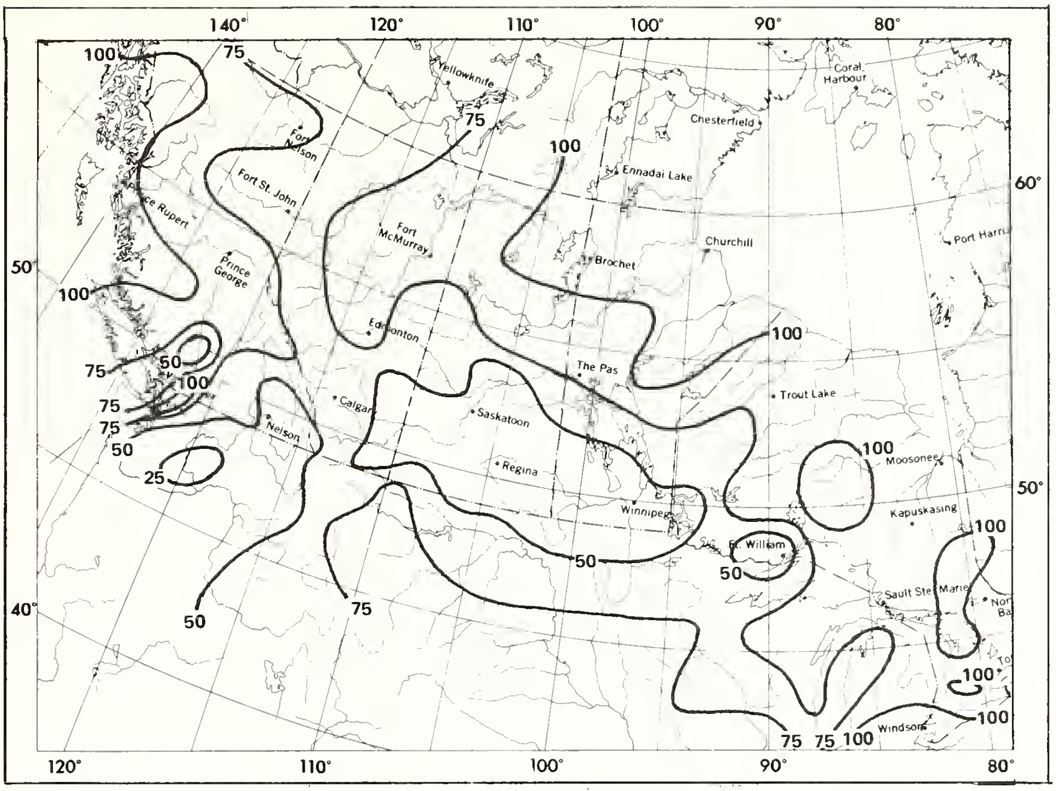

PERCENTAGE NORMAL PRECIPITATION SEPT.1, 1976 TO APRIL 30, 1977

figure 5A

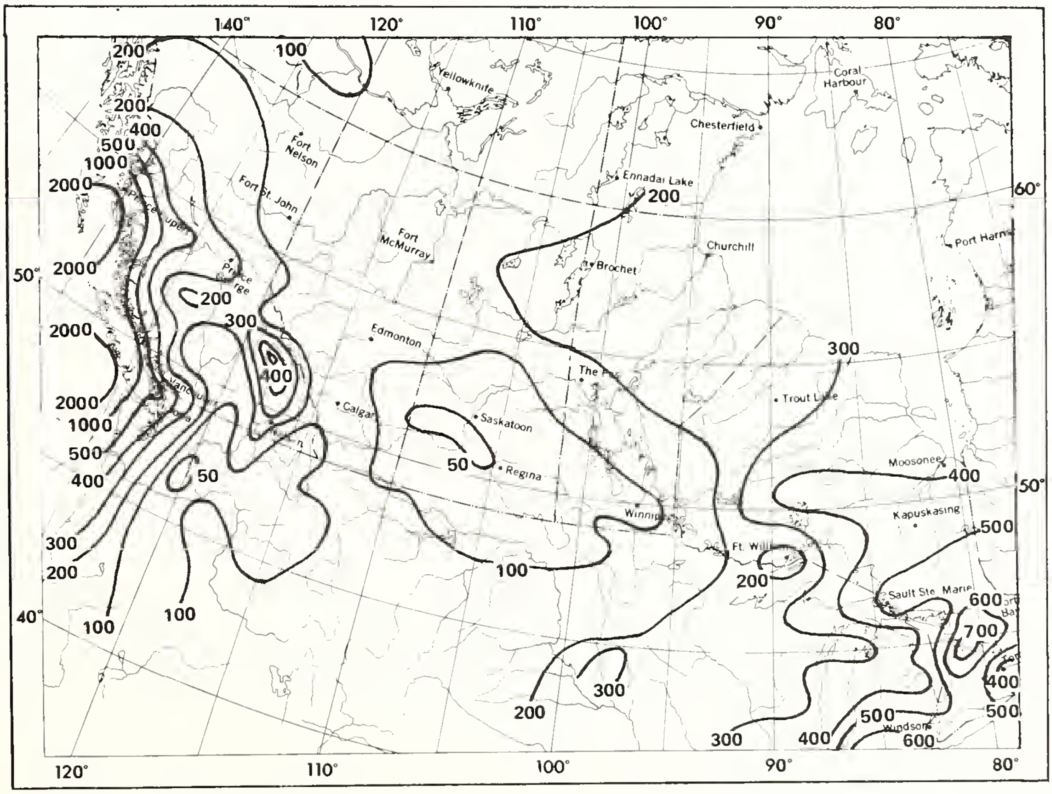

TOTAL PRECIPITATION (mm) SEPT.1, 1976 TO APRIL 30, 1977

figure 5B

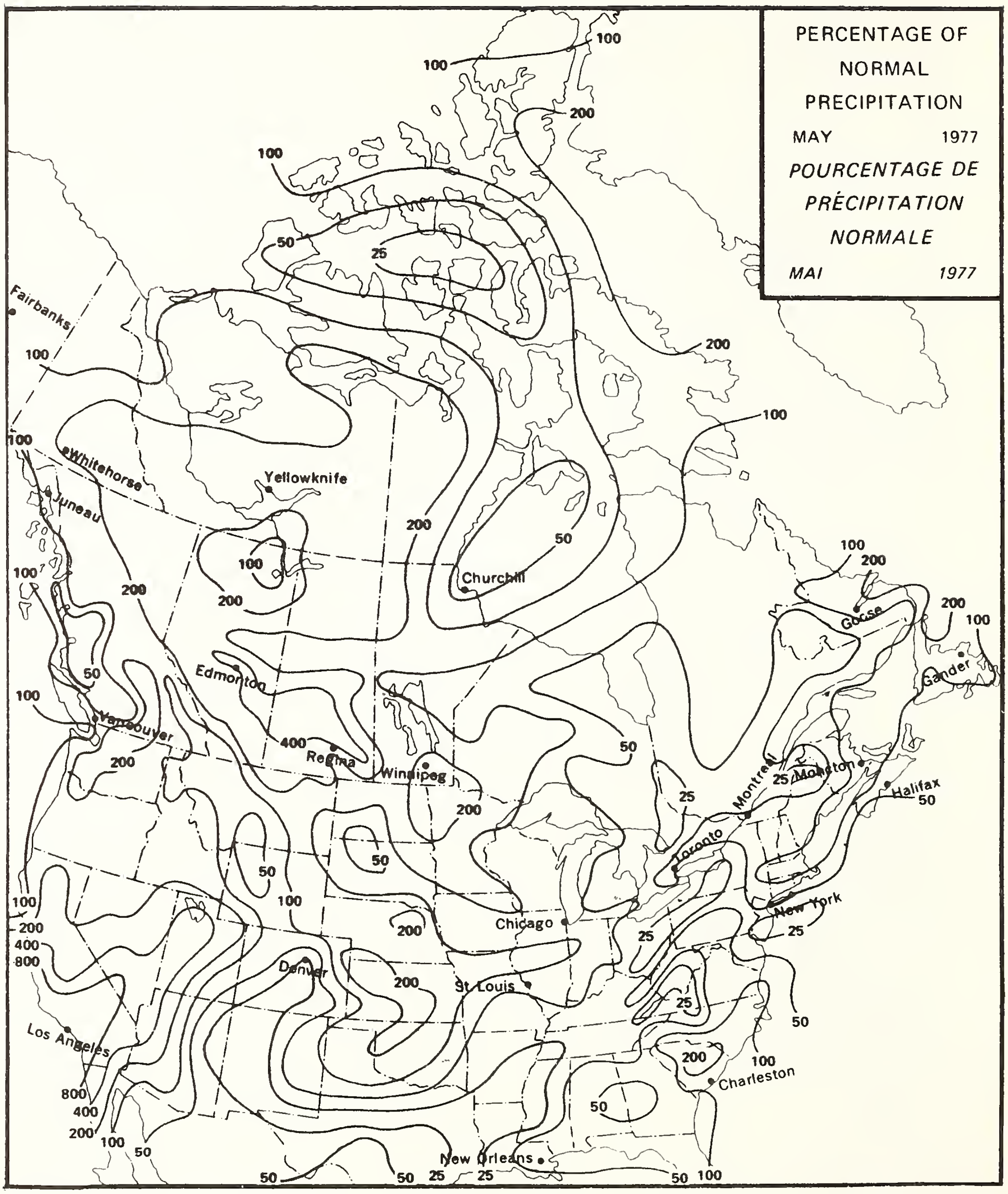
PERCENTAGE OF NORMAL PRECIPITATION
MAY 1977
POURCENTAGE DE PRÉCIPITATION NORMALE
MAI 1977
Fairbanks
Whitehorse
Juneau
Yellowknife
Churchill
Edmonton
Vancouver
Regina
Winnipeg
Goose
Gander
Montreal
Moncton
Halifax
Toronto
New York
Chicago
Denver
St Louis
Los Angeles
Charleston
New Orleans
25
50
100
200
400
800

figure 6

A Comparison of Three Operational Drought Programs

Malcolm Reid
EDS Center for Climatic and Environmental Assessment
Room 416, Page Bldg. 1
Washington, DC 20235

The Environmental Data Service's Center for Climatic and Environmental Assessment (CCEA) has a global mission to relate weather and climate to agriculture and other basic societal activities. A number of meteorological phenomena can directly or indirectly damage or destroy crops: flooding, high winds, freezes, hailstorms, high humidity and related diseases or insect infestation, etc.; however, one phenomenon, moisture deficiency, accounts for more crop loss than do all the other abnormal meteorological occurrences combined. Precipitation amount is normally the most significant meteorological parameter in determining crop yields and, with our present aviation oriented weather observation codes, is one of the most difficult to obtain worldwide. There have been a number of attempts to define drought; and while universal agreement on what the term describes has not been achieved, the farmer, federal "drought" relief programs and the lay public all normally visualize "drought" as indicating crop loss due to moisture deficiency.

A recently developed agricultural drought system suitable for worldwide application is now operational at the Environmental Data Service's Center for Climatic and Environmental Assessment (CCEA). This system, referred to as the "Cumulative Precipitation" program, is designed to produce both a monthly, global depiction of drought and a drought projection, using the surface observational data from the entire NMC data base filtered through CCEA's precipitation summarization program. The Cumulative Precipitation program was evaluated with two other currently operational drought systems -- the Palmer Index and the Crop Moisture Index using USDA's monthly "Pasture and Range Feed Condition Chart" as validation. The main points in this evaluation follow:

1. The Cumulative Precipitation program utilizes both climatological and current values of a single meteorological parameter -- precipitation amount.

2. The Palmer and Crop Moisture Indexes are much more intricate; such non-meteorological terms as water capacity of the soil and evapotranspiration are considered. These programs appear too involved for easy worldwide application.

3. The evaluation considered 43 data points over the U.S. for a five month period -- March through July 1977.

4. The Cumulative Precipitation and Palmer Index initial test results suggest that they are both effective in detecting the drought areas indicated in the Pasture and Range Feed Condition Charts. The Crop Moisture Index appeared to be less sensitive.

5. Cumulative Precipitation and, to a greater extent, the Palmer Index appears to accentuate drought while the Crop Moisture Index appears biased toward absence of drought.

6. Cumulative Precipitation apparent advantages:

   a. simplest of the three programs and at least as reliable an indicator of agricultural drought

   b. simplest to program, worldwide, using the NMC data base

   c. simplest to project using either forecast or normal precipitation data

   d. easiest to adapt to different climate regions and different crops by adjusting the drought criteria

7. Cumulative Precipitation apparent disadvantages:

   a. does not directly consider temperature, ground water and evapotranspiration, all of which are known to influence crop growth

   b. adds another drought program to an already confusing situation

   c. supported by a very limited test sampling

8. Follow on work:

   a. complete testing of the three programs using the USDA crop condition data

   b. analysis of Cumulative Precipitation program to determine optimum drought threshold values

A COMPARISON OF THREE OPERATIONAL DROUGHT PROGRAMS

CCEA/EDS

AUGUST 1977

DROUGHT MEASUREMENT PROGRAMS

(P) - Palmer Index; a mathematical representation of "Meteorological Drought" for evaluating the scope, severity and frequency of prolonged periods of abnormal weather. Terms include: available water capacity of the soil, evapo transpiration, moisture loss from surface and underlying soil layers, average and normal precipitation and temperature, and runoff.

(M) - Crop Moisture Index; a modified Palmer Index for "Agricultural Drought" is a procedure that responds rapidly to changes in those aspects of soil moisture which affect vegetation and field operations.

(C) - Cumulative Precipitation; a simple procedure for equating "Meteorological" and "Agricultural" Drought by relating drought stages to percentage of normal cumulative precipitation. The only terms considered are actual and normal monthly precipitation.

U.S. Drought as of September 30, 1977

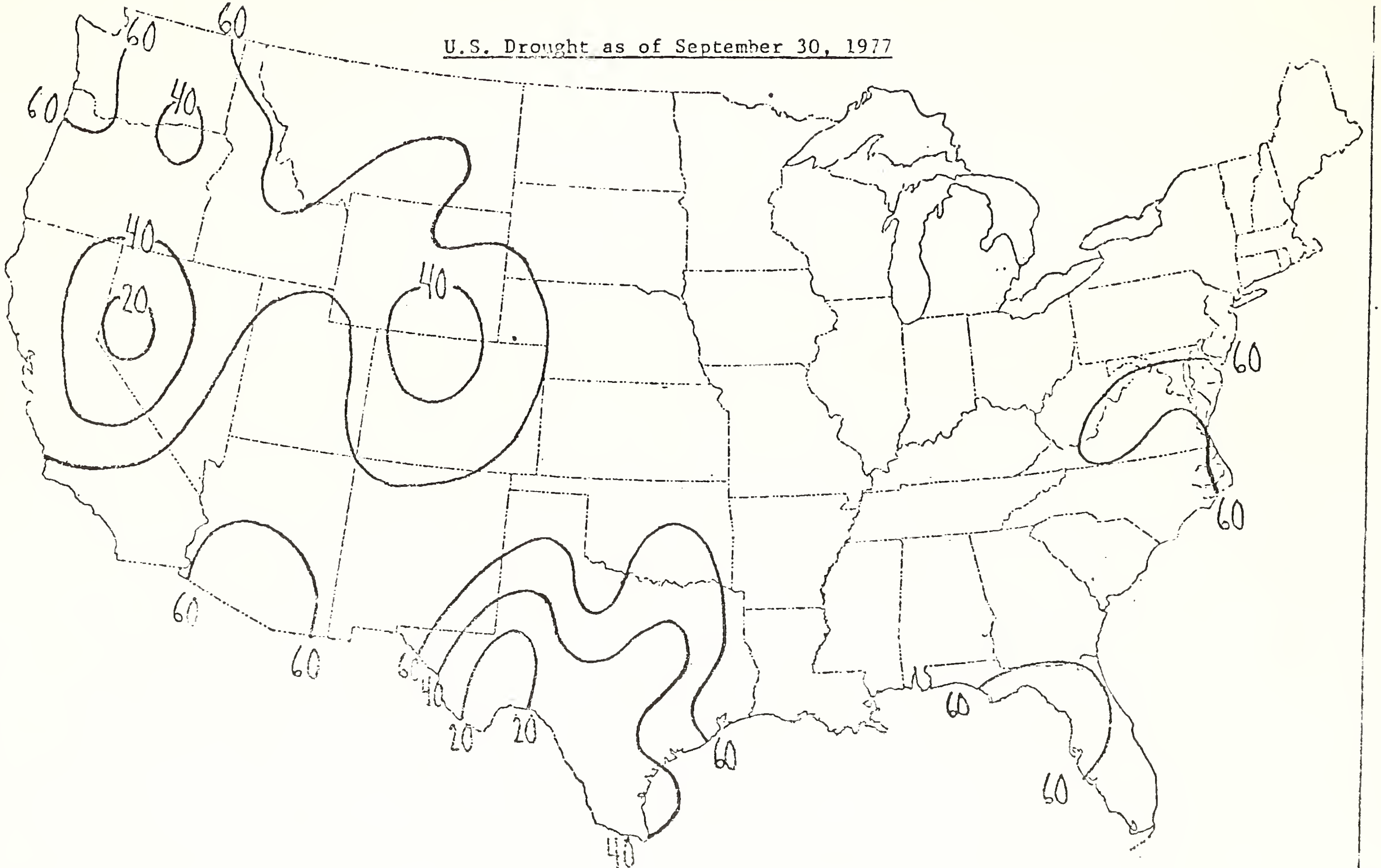

Marginal Drought (less than 60% of normal cumulative precipitation)
Drought (less than 40% of normal cumulative precipitation)
Severe Drought (less than 20% of normal cumulative precipitation)

Drought Projection - Number of Months Required to Alleviate the Drought
Assuming Normal Precipitation beginning Oct. 1, 1977

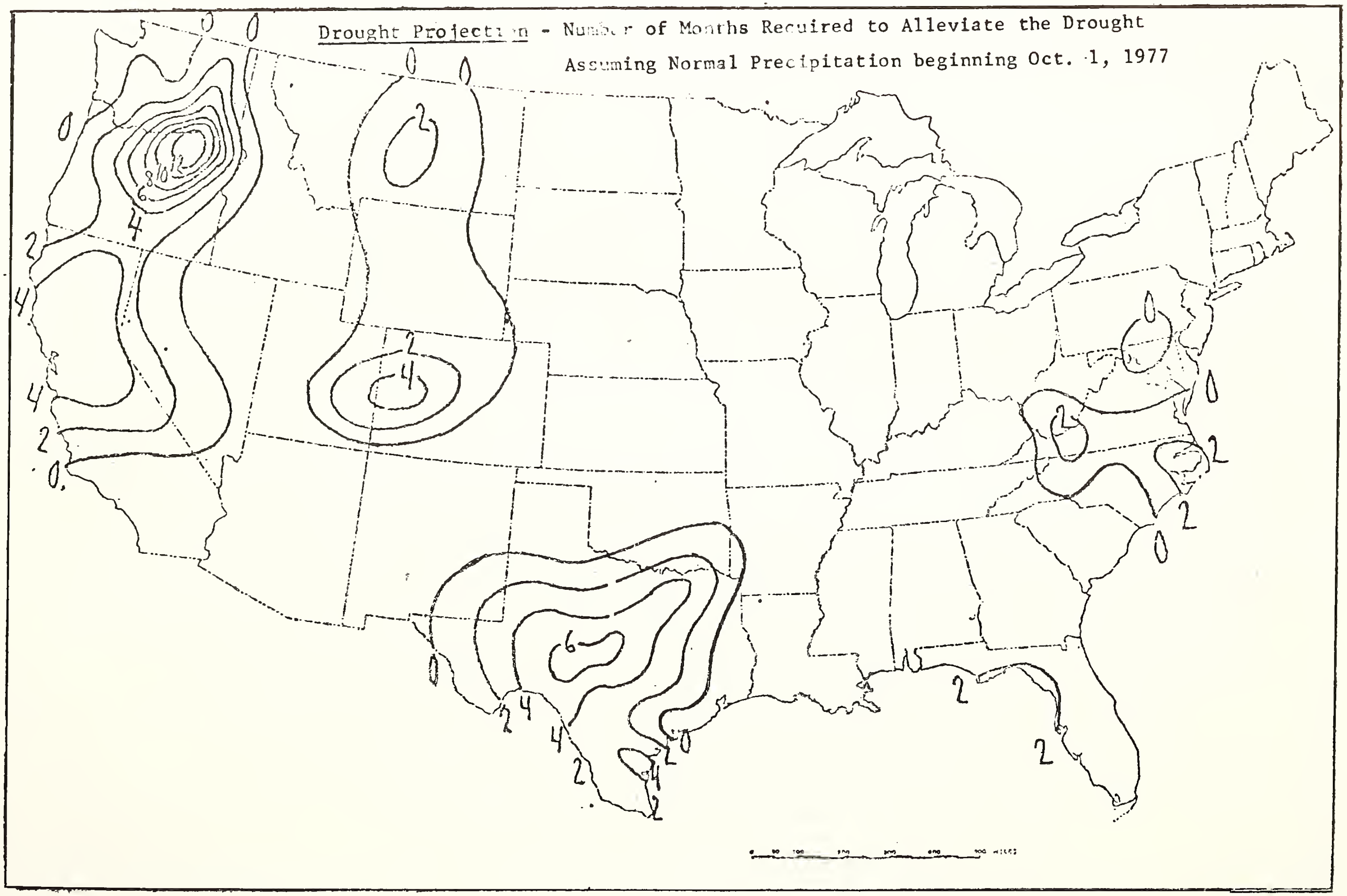

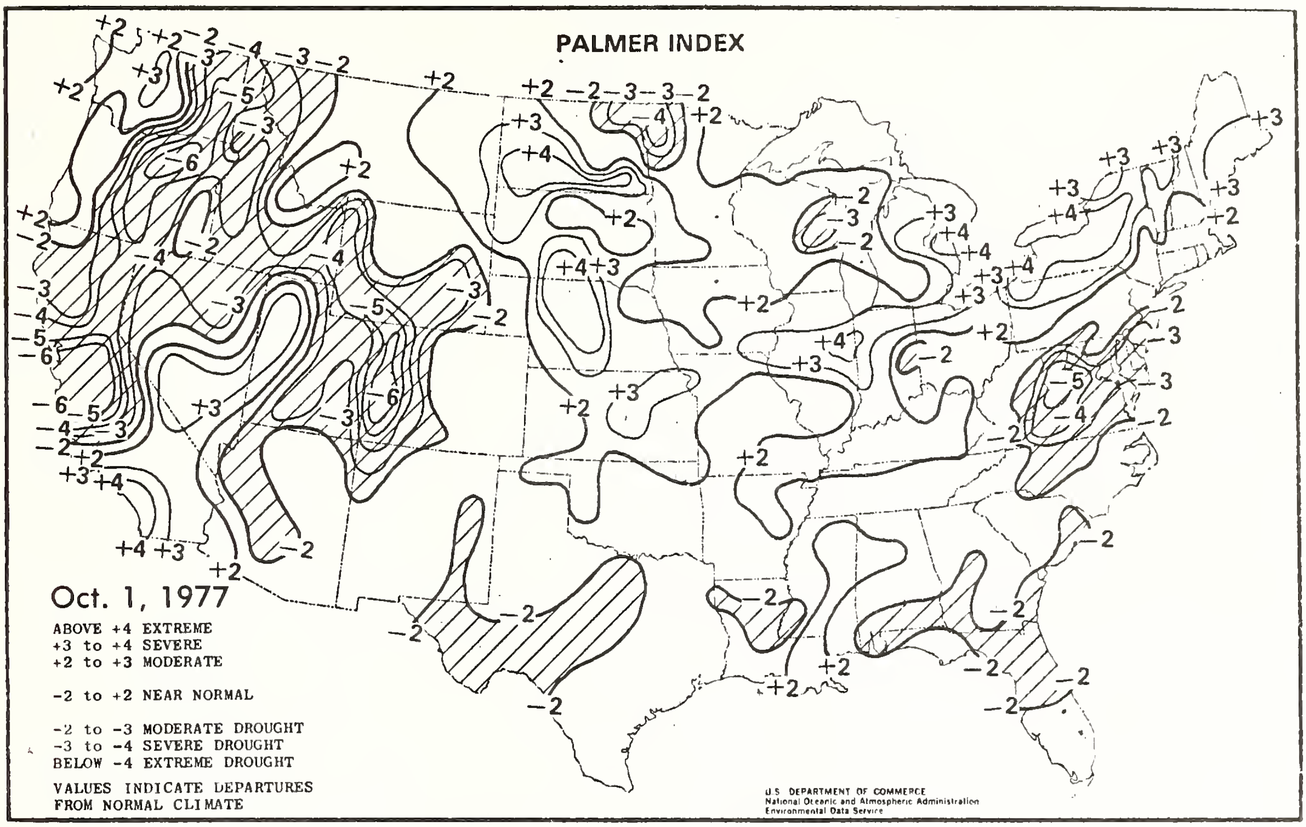
PALMER INDEX
Oct. 1, 1977
ABOVE +4 EXTREME
+3 to +4 SEVERE
+2 to +3 MODERATE
-2 to +2 NEAR NORMAL
-2 to -3 MODERATE DROUGHT
-3 to -4 SEVERE DROUGHT
BELOW -4 EXTREME DROUGHT
VALUES INDICATE DEPARTURES FROM NORMAL CLIMATE
U.S. DEPARTMENT OF COMMERCE
National Oceanic and Atmospheric Administration
Environmental Data Service

The Palmer Index was designed to evaluate the scope, severity, and frequency of prolonged periods of abnormally wet or dry weather. For this purpose it works reasonably well. However, it does not provide a measure of the current status of agricultural drought; i.e. the effects of short periods of very dry weather. For this reason the Crop Moisture Index was developed to respond rapidly to changes in the soil moisture situation and take into account only those moisture aspects which affect vegetation and field operations.

If one is interested in the overall soil moisture situation, which will integrate the effects of the past weather over weeks and even months, the Palmer Index provides the best evaluation. However, if one is interested in the availability of moisture to meet current demands, the Crop Moisture Index is the most useful. For example, a recent rain might have replenished the soil sufficiently to meet the current demands. However, if the Palmer Index is highly negative, one can interpret this to mean that the overall soil moisture situation is very poor.

A negative CMI value means that the demand for moisture, or the potential evapotranspiration, has been greater than available supplies so that actual transpiration has been reduced. On the other hand, positive CMI values mean that either actual evapotranspiration exceeded the expected amount, or recent rainfall exceeded the moisture requirements of the crops and the additional moisture was added to the soil or was regarded as runoff.

Negative Palmer Index values imply negative abnormalities of either evapotranspiration, the amount of moisture stored in or added to the soil, or of runoff, or a combination of all these types of moisture shortages. In other words, negative PI values simply indicate that the weather has been abnormally dry, and do not specify the exact nature of the effects of the dry weather.

However, positive PI values indicate that the moisture supply either from current or antecedent rainfall exceeded the amount required to sustain soil moisture levels that would be considered as normal and appropriate for the climate of the area.

In brief summary, Palmer Index values are based on all aspects of the moisture situation, but the Crop Moisture values refer only to the crop moisture situation. In addition, the PI values are highly dependent upon antecedent moisture conditions, whereas CMI values are much more responsive to weekly or current rainfall, or the lack of it.

The CMI map will appear each week in the Bulletin during the season from now through October. The Palmer Index will be published only in the first issue of each month during the same period.

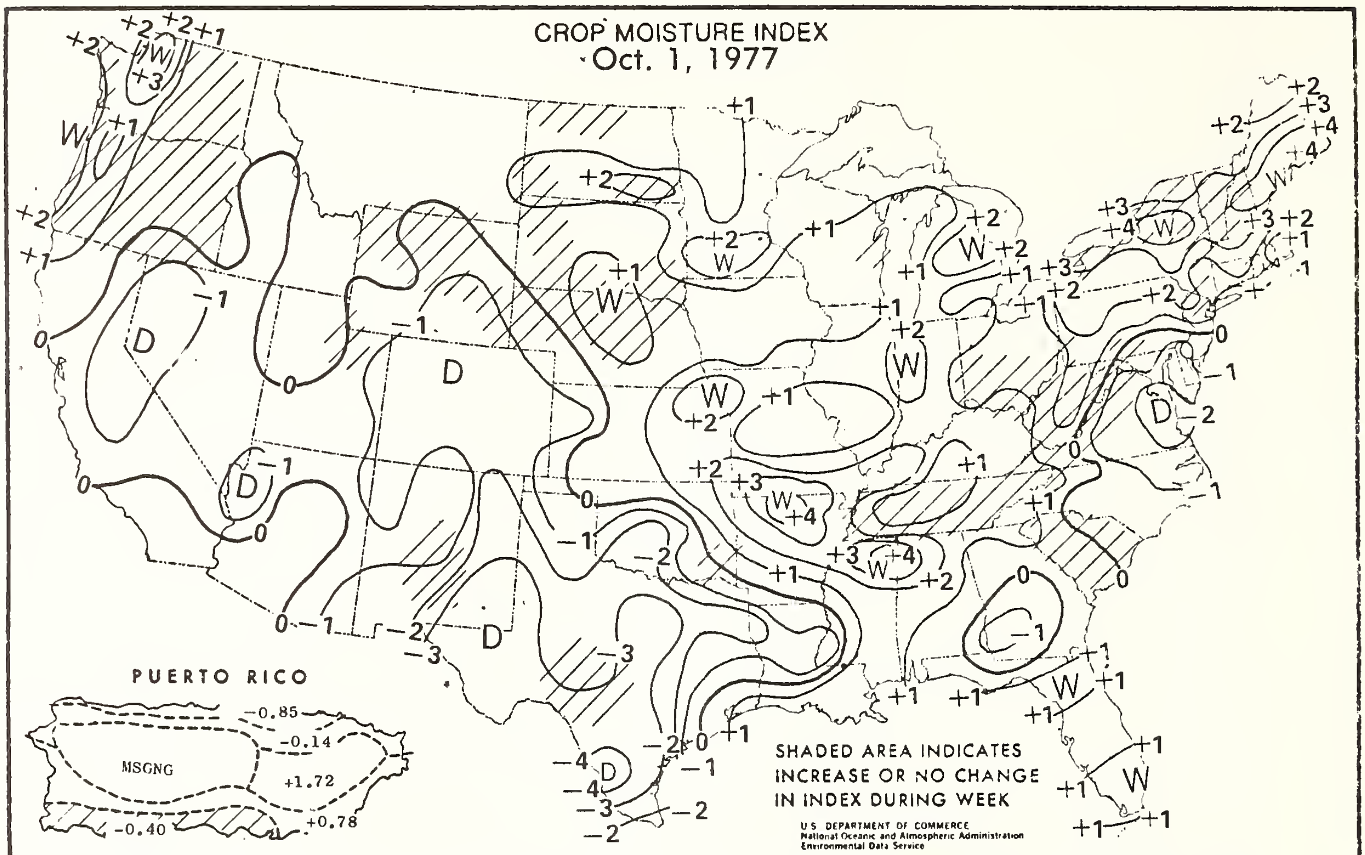

CROP MOISTURE INDEX
Oct. 1, 1977

SHADED AREA INDICATES INCREASE OR NO CHANGE IN INDEX DURING WEEK

U S DEPARTMENT OF COMMERCE
National Oceanic and Atmospheric Administration
Environmental Data Service

The Crop Moisture Index measures the degree to which moisture requirements of growing crops were met during the previous week. The index is computed from average weekly values of temperature and precipitation These values are used to calculate the potential moisture demand. Taking into account the previous soil moisture condition and current rainfall, the actual moisture loss is determined.

If the potential moisture demand, or potential evapotranspiration, exceeds available moisture supplies, actual evapotranspiration is reduced and the CMI gives a negative value. However, if moisture meets or exceeds demand the index is positive

Shaded areas indicate the index was unchanged or increased from the previous week's value; soils dried in the unshaded areas. Centers of positive and negative areas are identified by W for wet and D for dry.

Local moisture conditions may vary because of differences in rainfall distribution or soil types. The type of agriculture and stage of crop development must be considered when assessing the impact of moisture conditions based on the Crop Moisture Index. Some general guidelines follow.

UNSHADED AREAS:			INDEX DECREASED
ABOVE		3.0	SOME DRYING BUT STILL EXCESSIVELY WET
2.0	to	3.0	MORE DRY WEATHER NEEDED, WORK DELAYED
1.0	to	2.0	FAVORABLE, EXCEPT STILL TOO WET IN SPOTS
0	to	1.0	FAVORABLE FOR NORMAL GROWTH AND FIELDWORK
0	to	-1.0	TOPSOIL MOISTURE SHORT GERMINATION SLOW
-1.0	to	-2.0	ABNORMALLY DRY, PROSPECTS DETERIORATING
-2.0	to	-3.0	TOO DRY, YIELD PROSPECTS REDUCED
-3.0	to	-4.0	POTENTIAL YIELDS SEVERELY CUT BY DROUGHT
BELOW		-4.0	EXTREMELY DRY, MOST CROPS RUINED

SHADED AREA:			INDEX INCREASED OR DID NOT CHANGE
ABOVE		3.0	EXCESSIVELY WET, SOME FIELDS FLOODED
2.0	to	3.0	TOO WET, SOME STANDING WATER
1.0	to	2.0	PROSPECTS ABOVE NORMAL, SOME FIELDS TOO WET
0	to	1.0	MOISTURE ADEQUATE FOR PRESENT NEEDS
0	to	-1.0	PROSPECTS IMPROVED BUT RAIN STILL NEEDED
-1.0	to	-2.0	SOME IMPROVEMENT BUT STILL TOO DRY
-2.0	to	-3.0	DROUGHT EASED BUT STILL SERIOUS
-3.0	to	-4.0	DROUGHT CONTINUES, RAIN URGENTLY NEEDED
BELOW		-4.0	NOT ENOUGH RAIN, STILL EXTREMELY DRY

PASTURE AND RANGE FEED CONDITIONS*

September 1, 1977

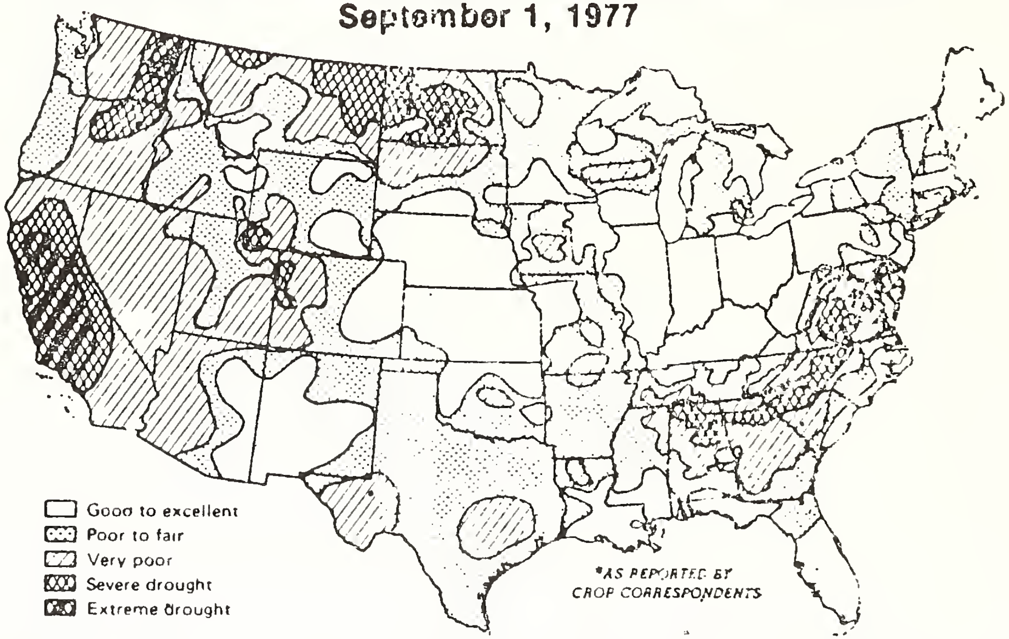

*INDICATES CURRENT SUPPLY OF PASTURE FEED FOR GRAZING ON NON-IRRIGATED PASTURES AND RANGES RELATIVE TO THAT EXPECTED FROM EXISTING STANDS UNDER VERY FAVORABLE WEATHER CONDITIONS.

U.S. DEPARTMENT OF AGRICULTURE NEG. SRS 74 77(9) STATISTICAL REPORTING SERVICE

COMPARISON OF CUMULATIVE PRECIPITATION (C), CROP MOISTURE INDEX (M), AND PALMER INDEX (P) RELATIONSHIPS TO "PASTURE AND RANGE FEED CONDITIONS (R)

MARCH - JULY 1977

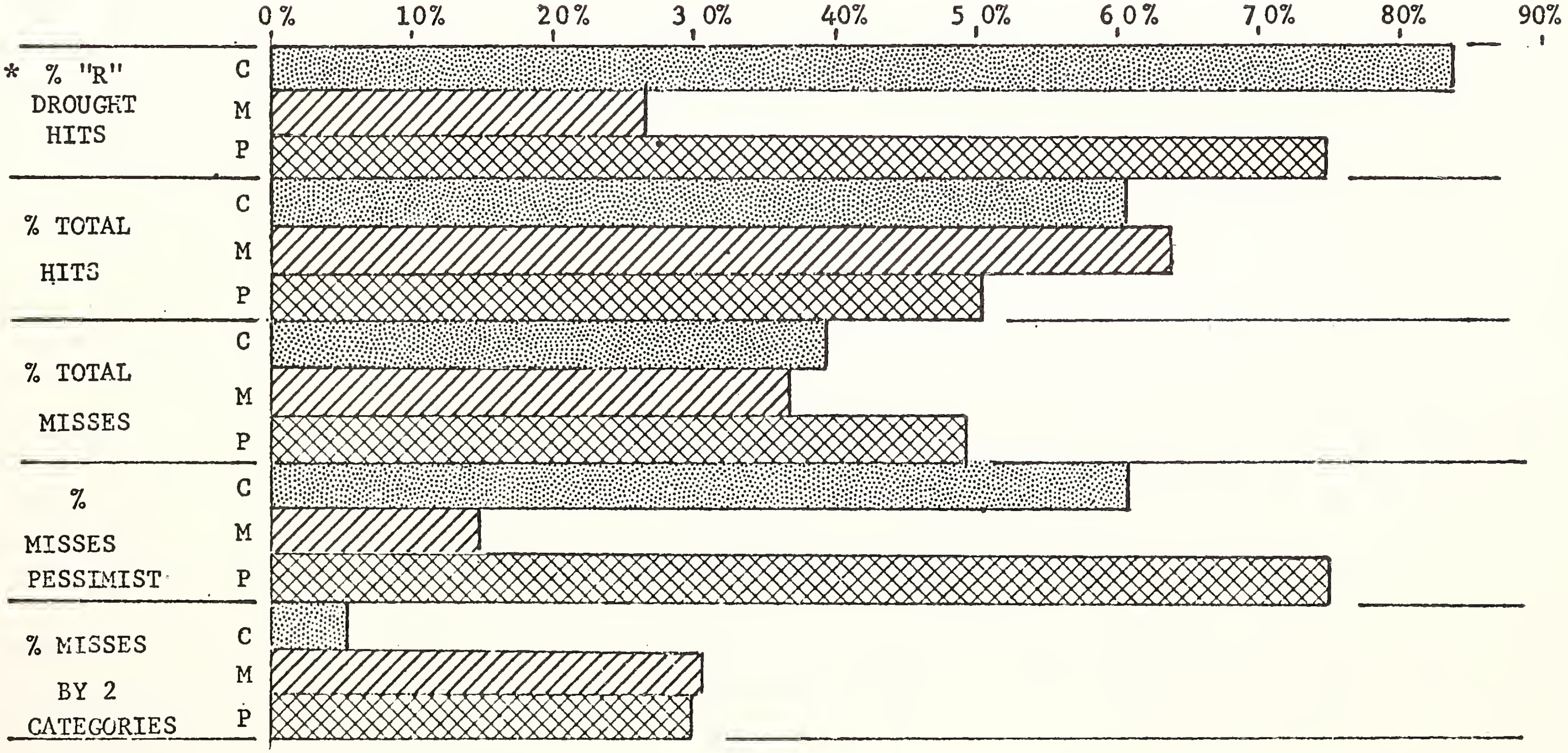

* % R Drought Hits - % of reported Range Drought Conditions (R_2 and R_3) correctly identified by $C2 + C_3$, $M_2 + M_3$ and $P_2 + P_3$

TENTATIVE CONCLUSIONS

1. Cumulative Precipitation and Palmer Index test results suggest they are both effective in detecting drought areas (as indicated on the Pasture and Range Charts). The Crop Moisture Index appeared to be considerably less sensitive.

2. Palmer and Cumulative Precipitation appears to accentuate drought while the Crop Moisture Index accentuates the absence of drought.

3. Cumulative Precipitation apparent advantages:

   a. simplest of the three programs and appears to be at least as reliable an indicator of agricultural drought

   b. simplest to program, worldwide, using the NMC data base

   c. simplest to project using either forecast or normal precipitation data

   d. easiest to adapt to different climate regions and different crops by adjusting the drought criteria

4. Cumulative Precipitation apparent disadvantages:

   a. very limited test sampling -- only five months of one year and only 43 data points

   b. provides an additional program to an already confusing situation

   c. does not attempt to consider temperature, ground water, and evapotranspiration -- all of which are known to influence crop growth

Contribution to the October 1977 Climate Diagnostics Workshop

A Comparative Analysis of The 1976-77 Winter in the Contiguous United States

Henry F. Diaz and Robert G. Quayle
National Climatic Center
Asheville, NC 28801
October 12, 1977

A comparative analysis of the 1976-77 winter temperatures over the contiguous United States is being performed using long-period station records and areally weighted regional averages. The following are the principal findings from this study to date:

1. East of the Mississippi River, with the exception of the New England region, January 1977 was the coldest month on record, probably for a period well in excess of a century. The core of the cold anomaly was centered over the mid-western states from Illinois to Ohio where areally averaged monthly mean temperatures were more than 8°C colder than the 85-year mean for that area.

2. Over much of the eastern U.S. winter temperatures (December-February) were also the coldest on record. Over an area stretching from the Great Lakes to the Atlantic and Gulf coasts, areally weighted temperatures averaged 4°C below the 85-year mean.

3. The persistent nature of the anomalously cold weather experienced during the 1976-77 winter half-year is underscored by the fact that the October-March areally weighted means over much of the aforementioned areas were the coldest of record over the 85-year period; more than 3°C colder than the long-term mean.

Some inferences can be drawn from a few stations having very long-term records (some like Philadelphia, going back into the 1700's). This can be done because of the apparent spatial and temporal coherence of extreme anomalies; i.e., a very extreme event at a single location for a short period of time is often a manifestation of some larger scale phenomenon.

The inverse relationship of anomalies in the eastern U.S. and in the West is well documented, resulting from the size of the continent, the oceanic areas flanking on either side, and the wavelength of Rossby waves. In 1976-77, however, the anomaly in the east was matched by near-normal temperatures in the west, giving some rather striking National winter temperature averages.

With respect to potential fuel consumption, 1976-77 indeed set new records, but at present our data base only goes back to 1931 for population weighted heating degree days (1970 census figures).

Recommendations

Much more work is required if the 1976-77 winter is to be evaluated in a quantitative probabilistic sense relative to the past one to two hundred years.

1. Extend degree day data back in time (studies underway).
2. Verify long term records with regard to urban influence and general homogeneity of records.
3. Perform state and regional analyses for distribution to individual states and planning commissions.
4. Seek out key features in the historical record which may be of dynamic significance and may have predictive value.
5. Investigate climatic reference networks that may have the capability of accurately assessing the significance of anomalous situations in near-real-time, when key resource management decisions must be made. It presently takes a few months to process the thousands of substations required for final results.

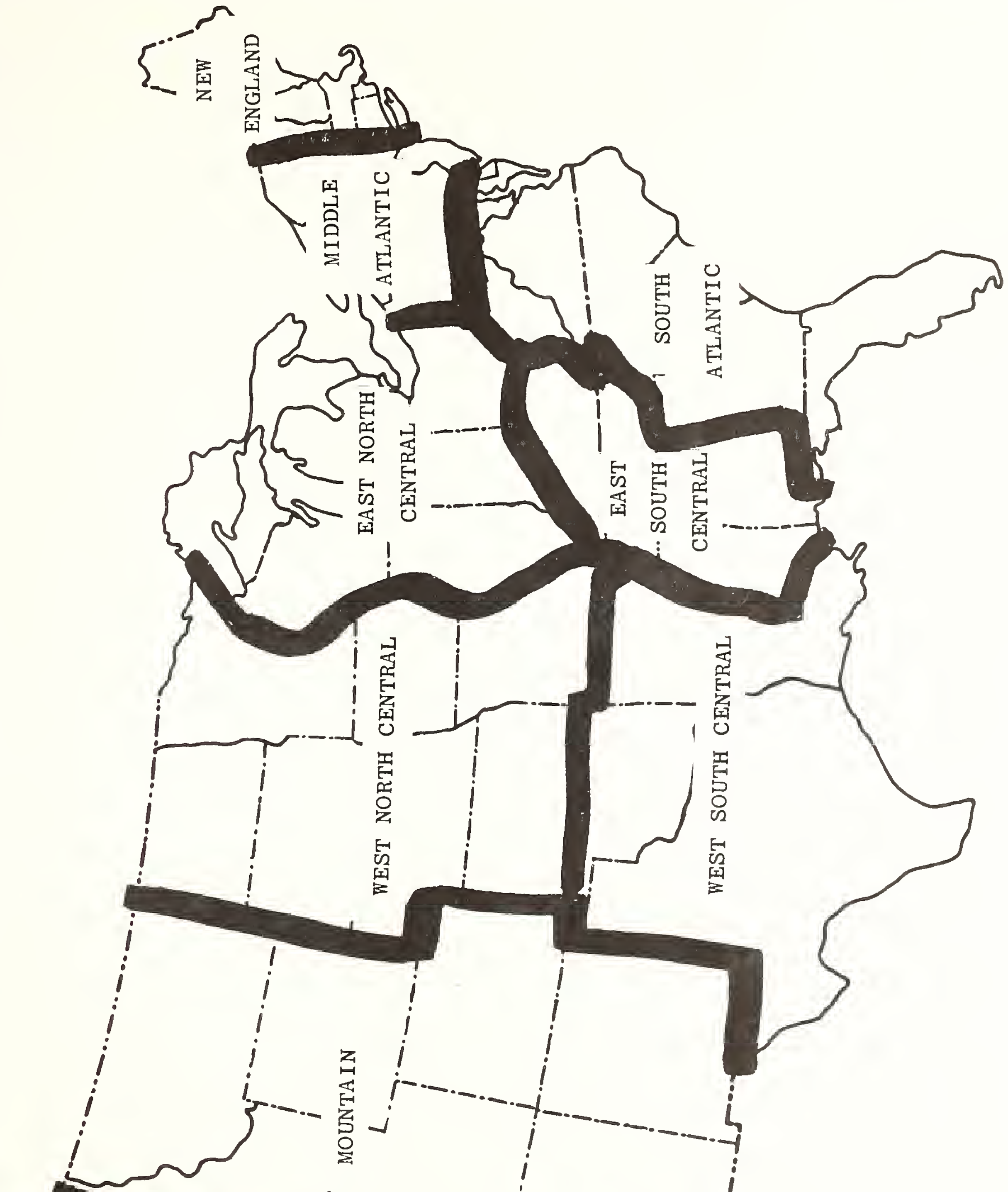
PACIFIC
MOUNTAIN
WEST NORTH CENTRAL
WEST SOUTH CENTRAL
EAST NORTH CENTRAL
EAST SOUTH CENTRAL
NEW ENGLAND
MIDDLE ATLANTIC
SOUTH ATLANTIC

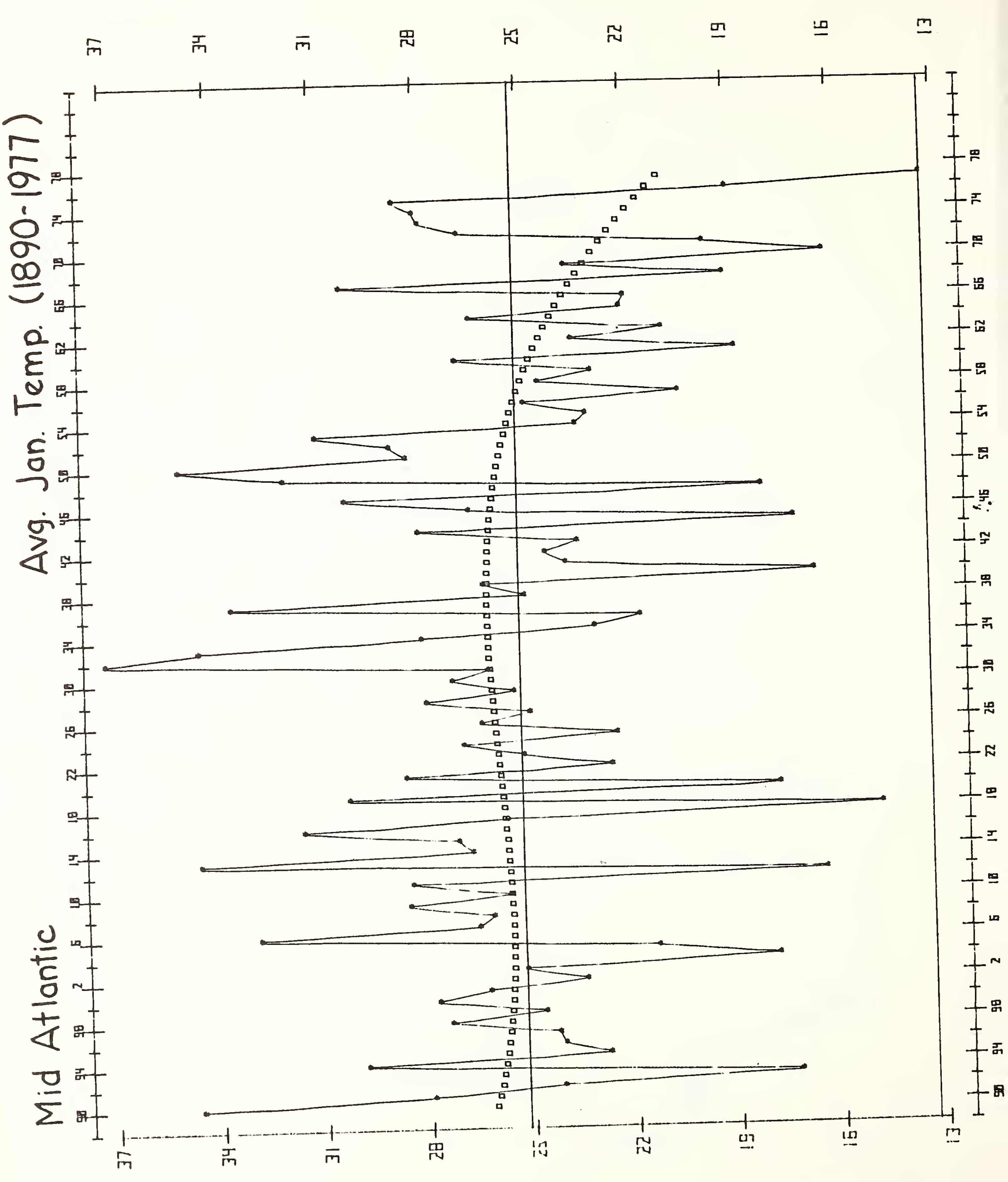
Mid Atlantic
Avg. Jan. Temp. (1890-1977)
37
34
31
28
25
22
19
16
13
90
94
98
2
6
10
14
18
22
26
30
34
38
42
46
50
54
58
62
66
70
74
78

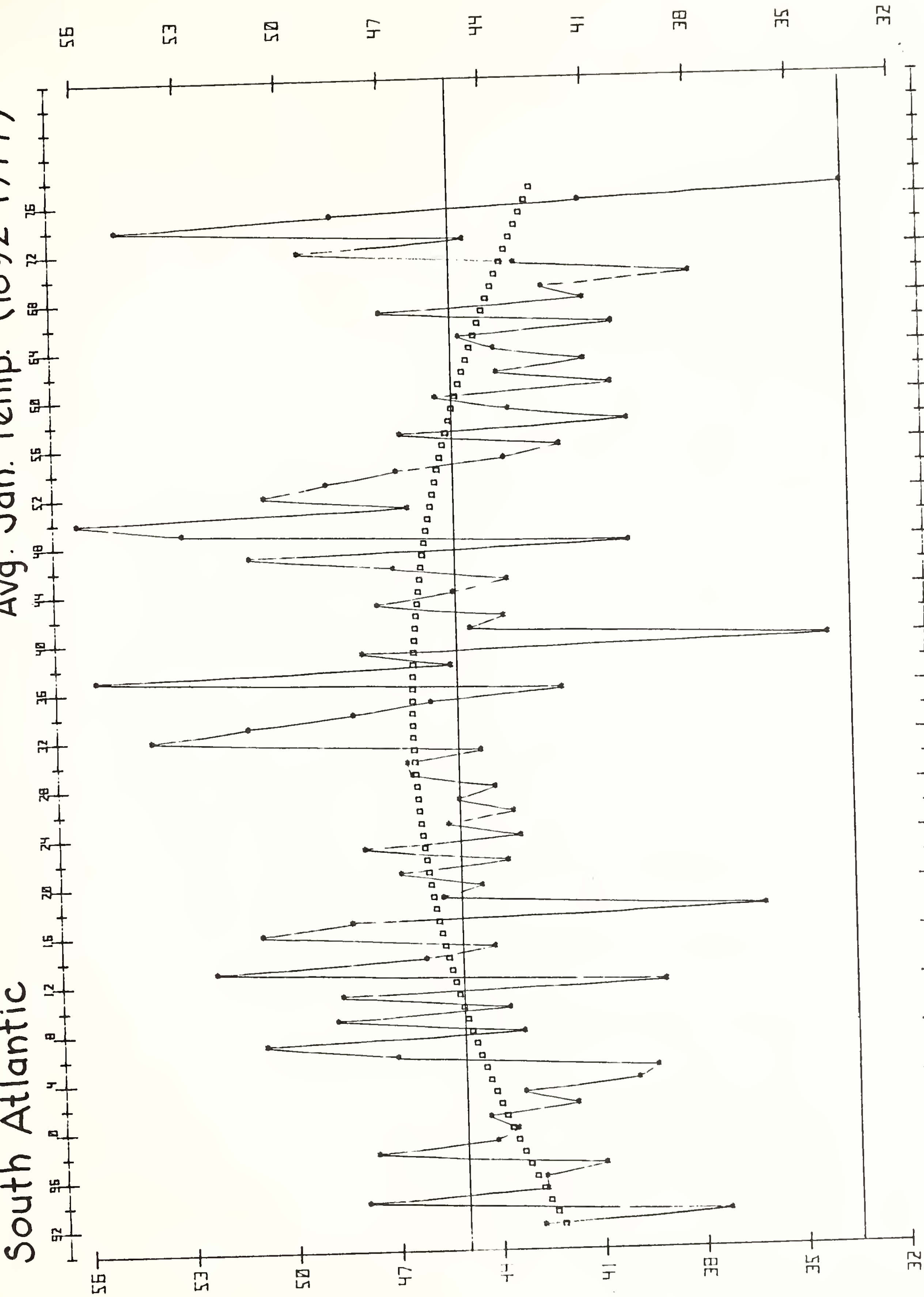
South Atlantic
Avg. Jan. Temp. (1892-1977)
56
53
50
47
44
41
38
35
32
92
96
0
4
8
12
16
20
24
28
32
36
40
44
48
52
56
60
64
68
72
76

East South Central Avg. Jan. Temp. (1889-1977)

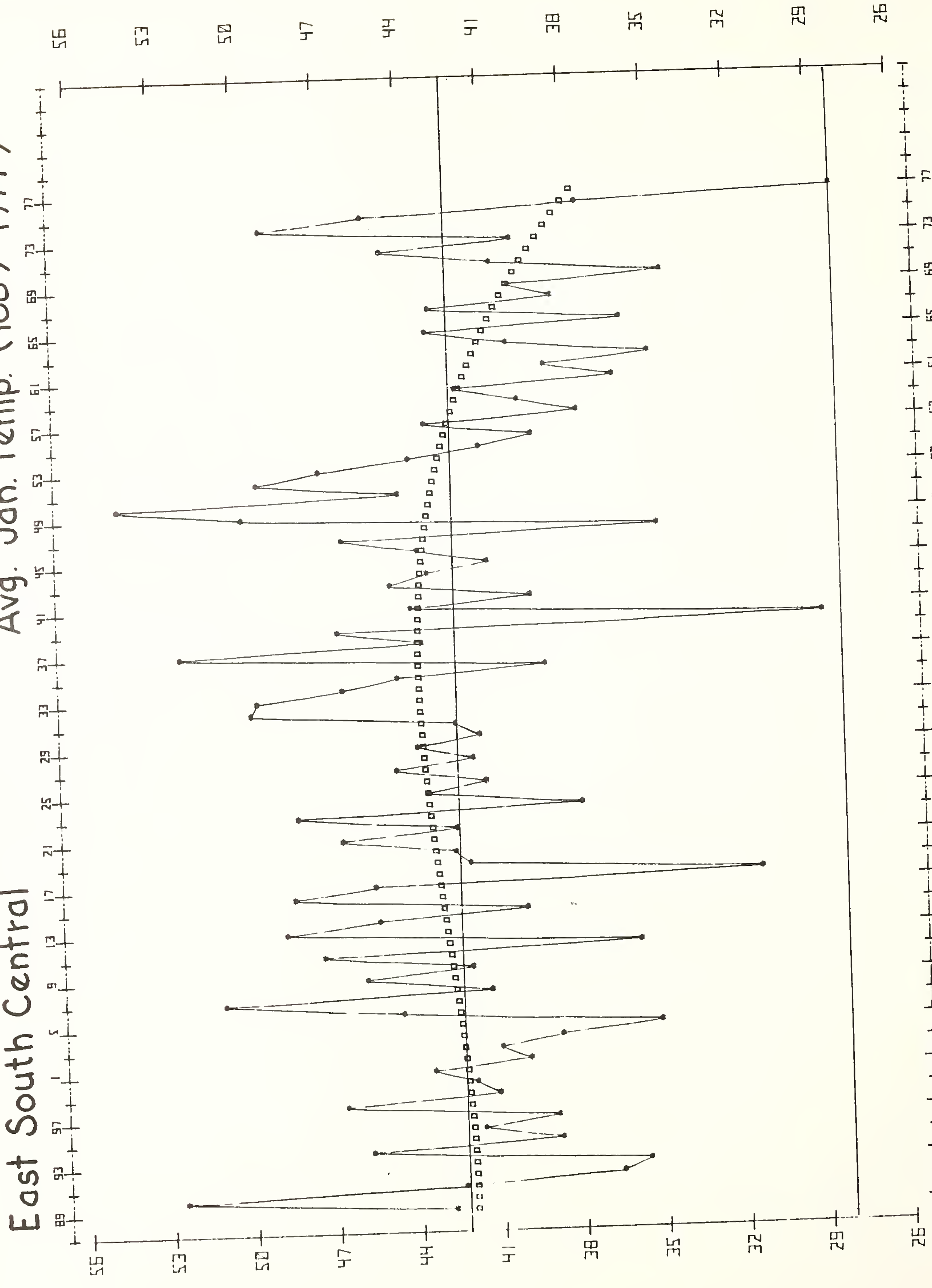

East North Central Avg. Jan. Temp. (1891 - 1977)

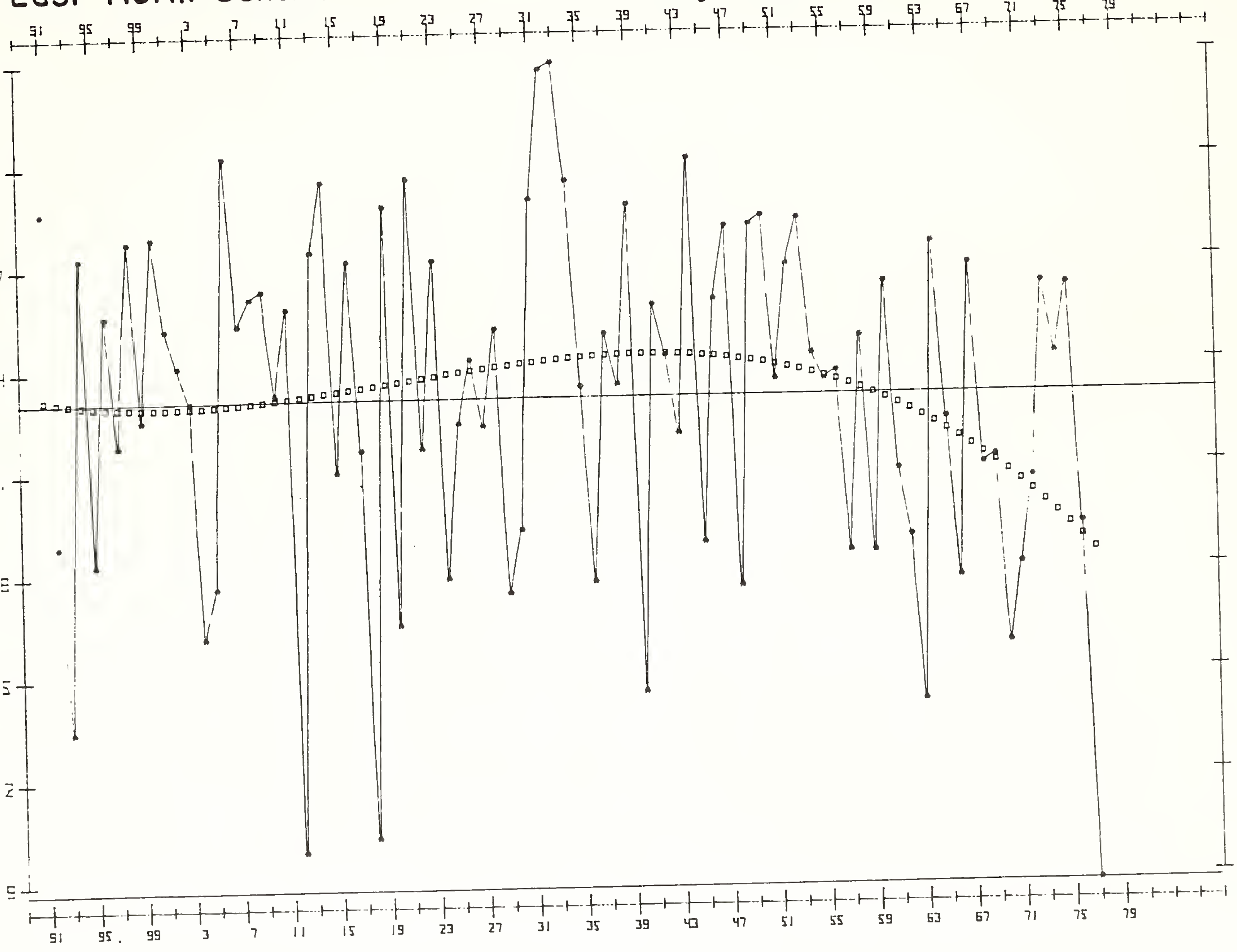

South Atlantic Avg. Winter Temp. (1892-93 - 1976-77)

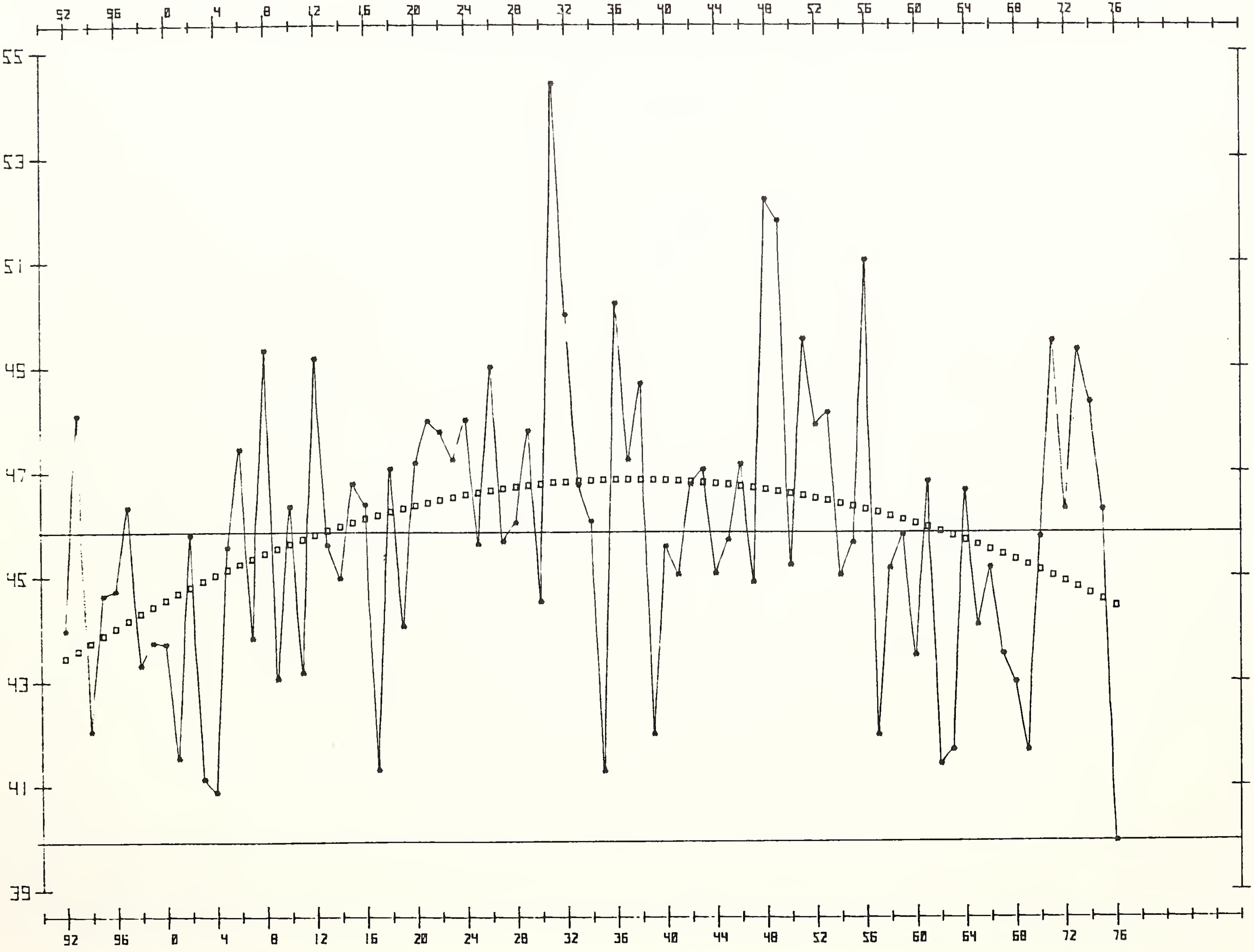

East South Central

Avg. Winter Temp. (1889-90 -1976-77)

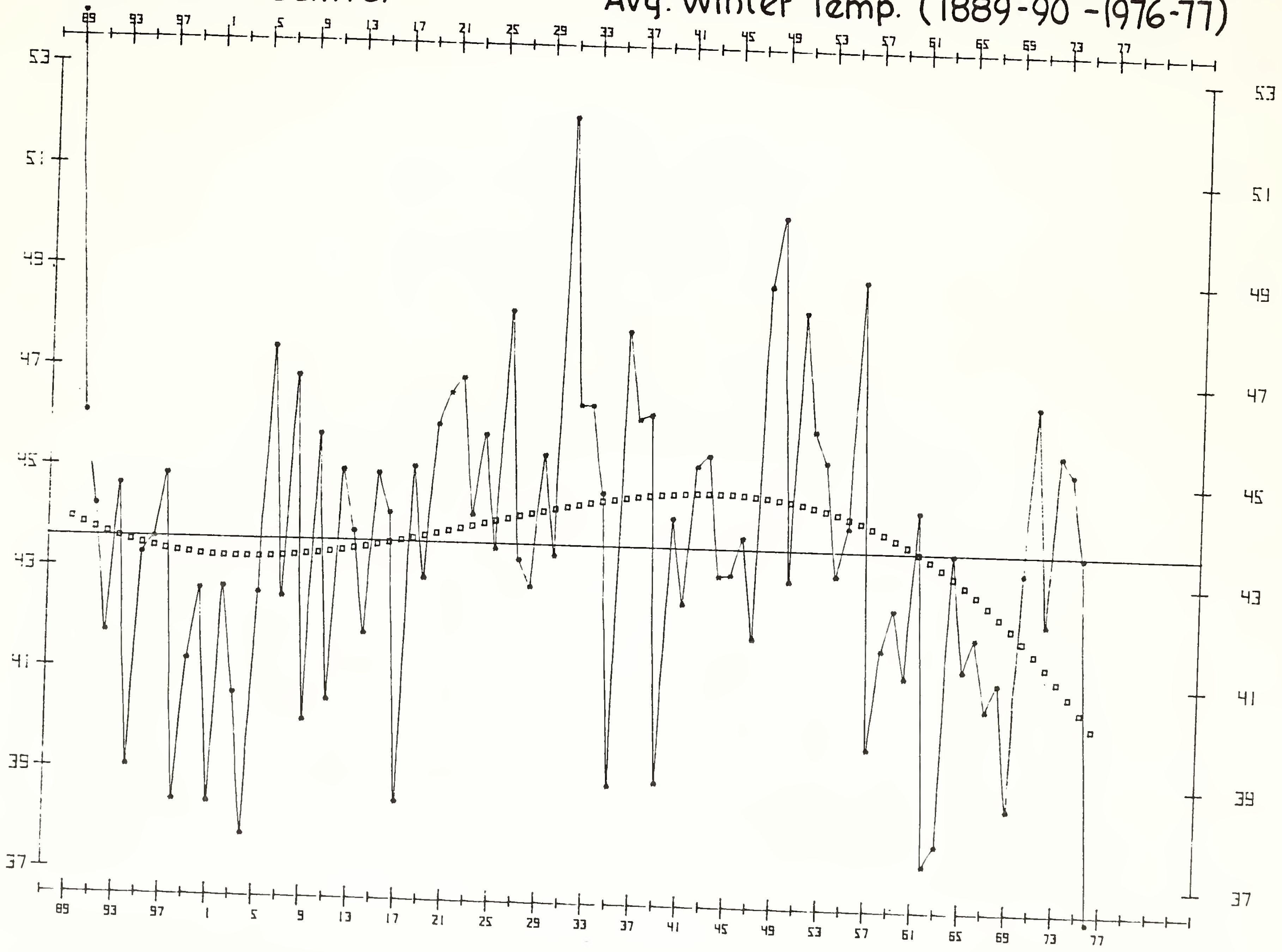

East North Central Avg. Winter Temp.(1891-92 - 1976-77)

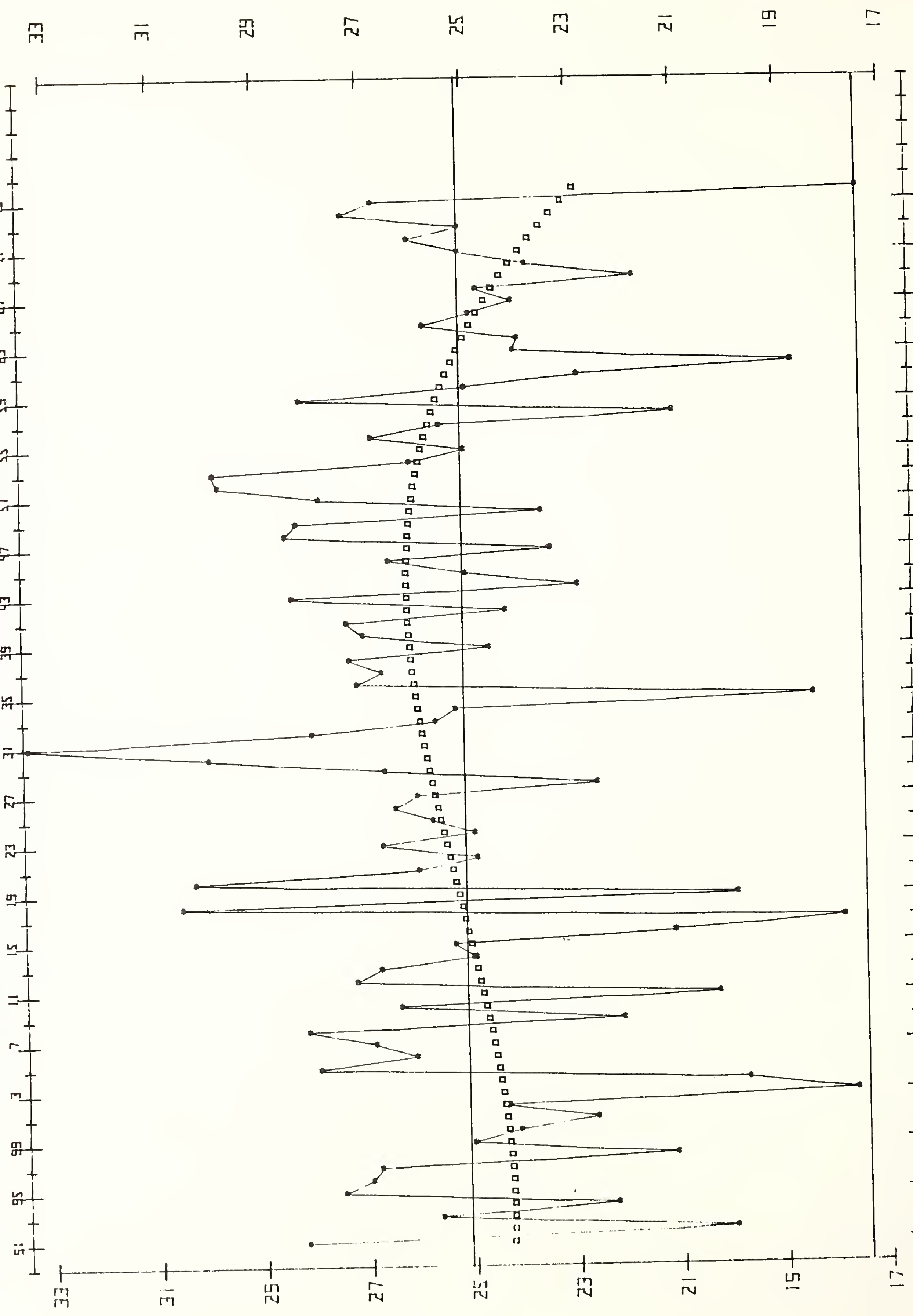

South Atlantic Avg. Oct.-March Temp. (1892-1977)

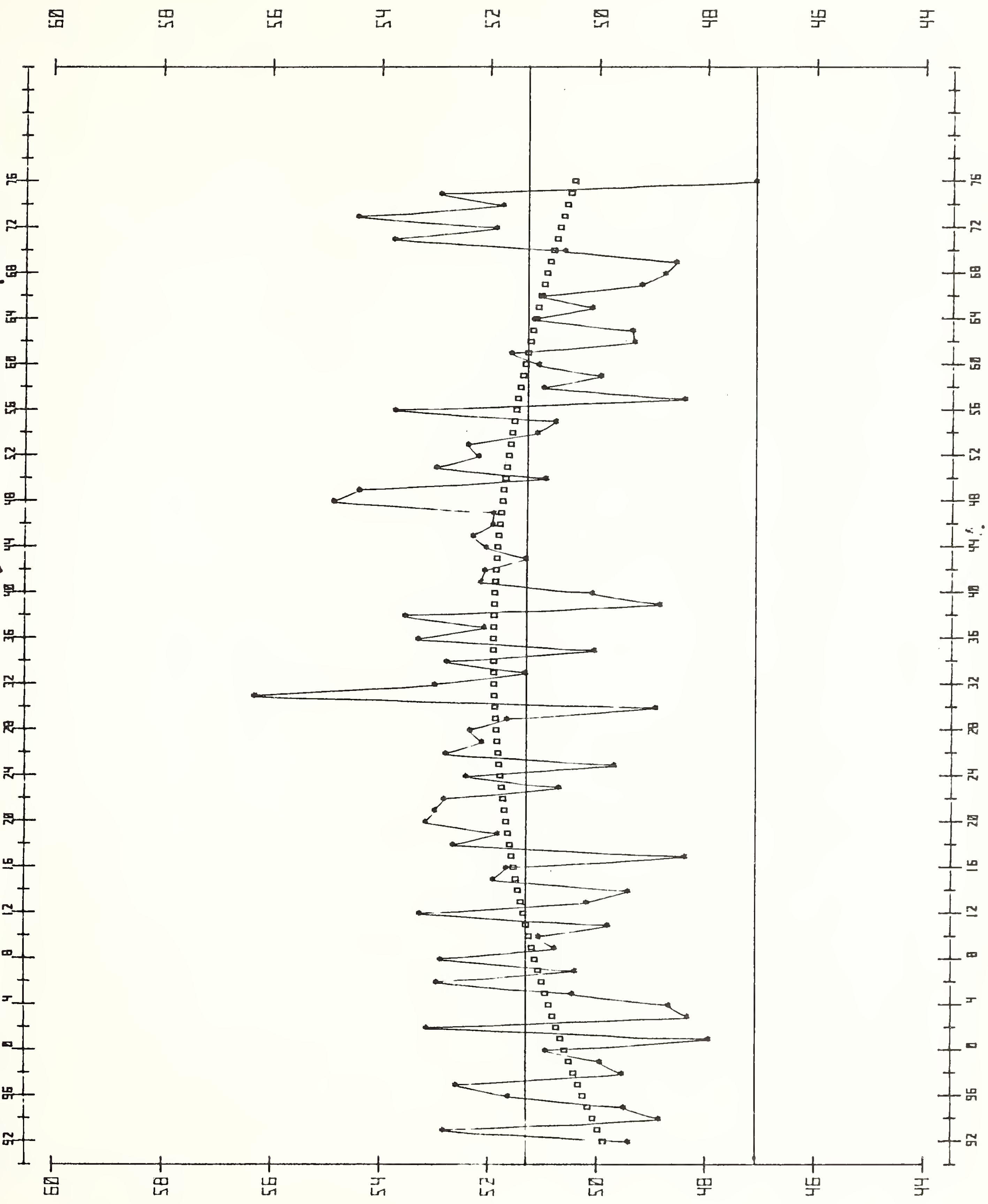

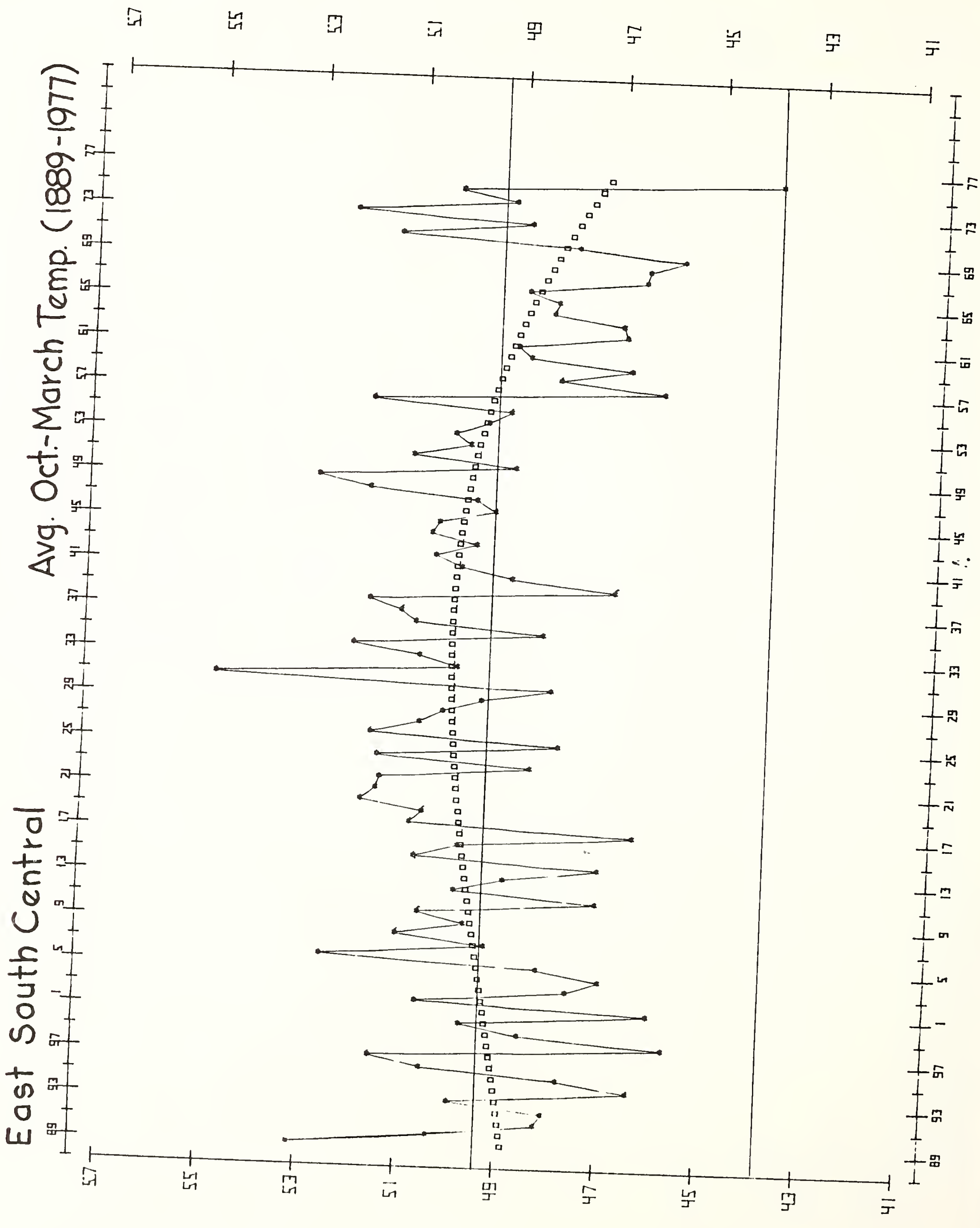

East South Central Avg. Oct.-March Temp. (1889-1977)

East North Central Avg. Oct.-March Temp. (1891-1977)

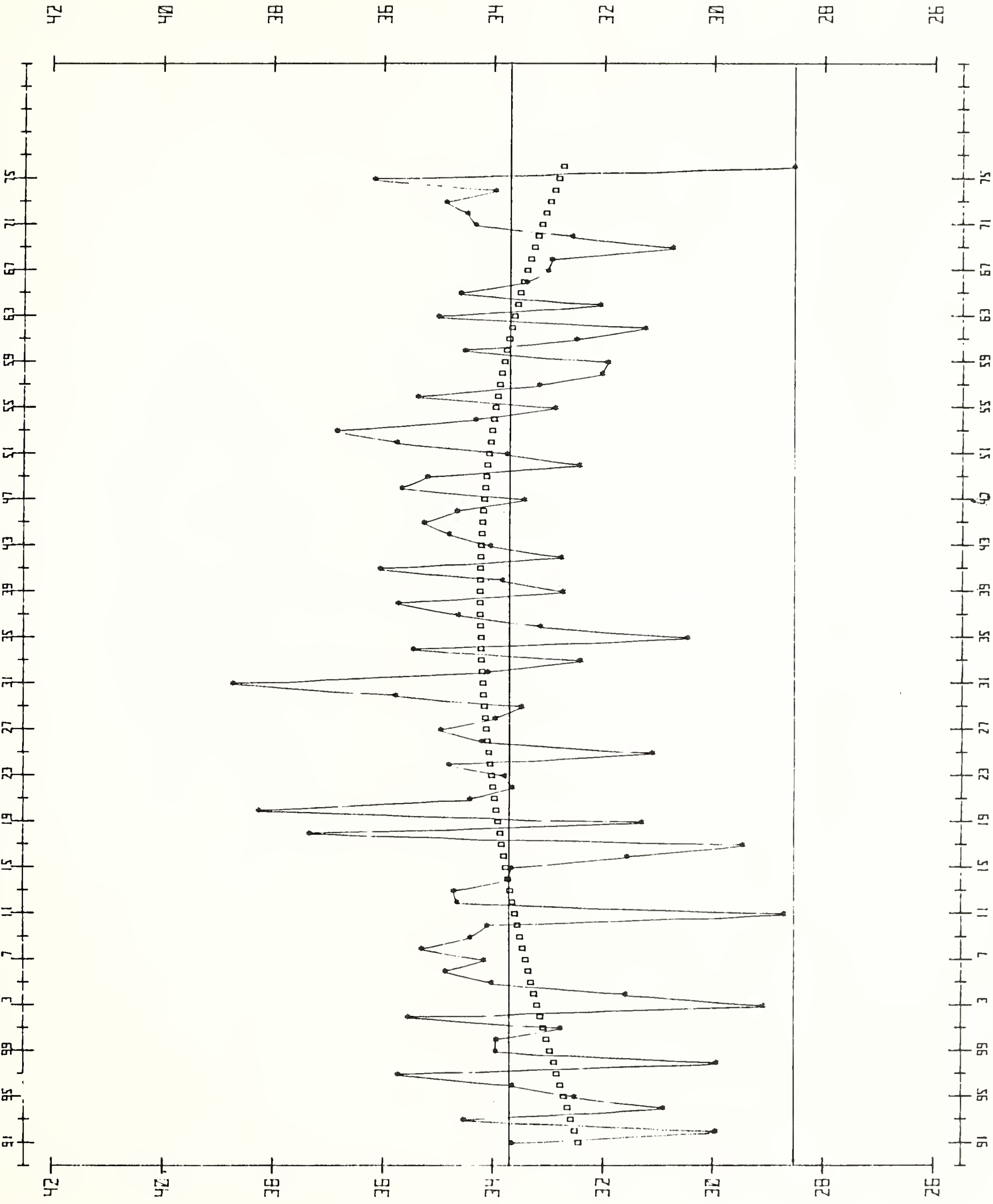

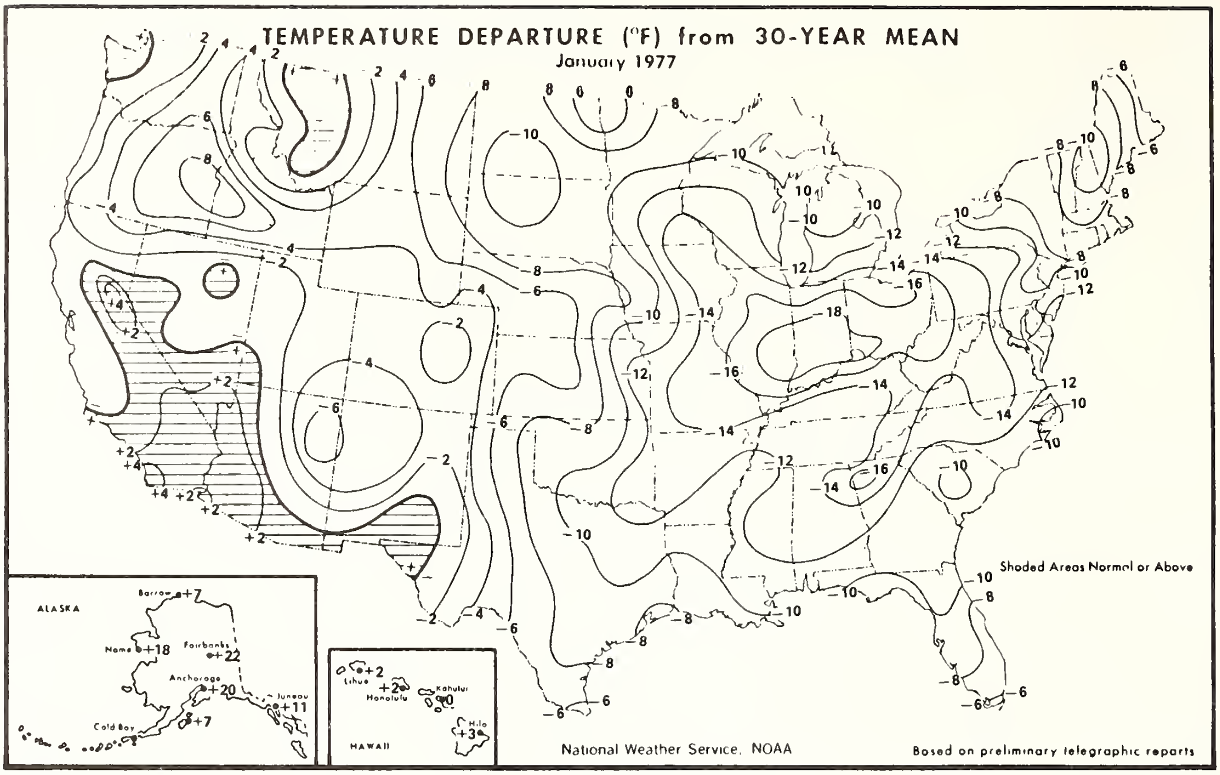
TEMPERATURE DEPARTURE (°F) from 30-YEAR MEAN

January 1977

Shaded Areas Normal or Above

National Weather Service, NOAA

Based on preliminary telegraphic reports

January 1977 departures from normal temperature.

U. S. AVERAGE JANUARY TEMPERATURES

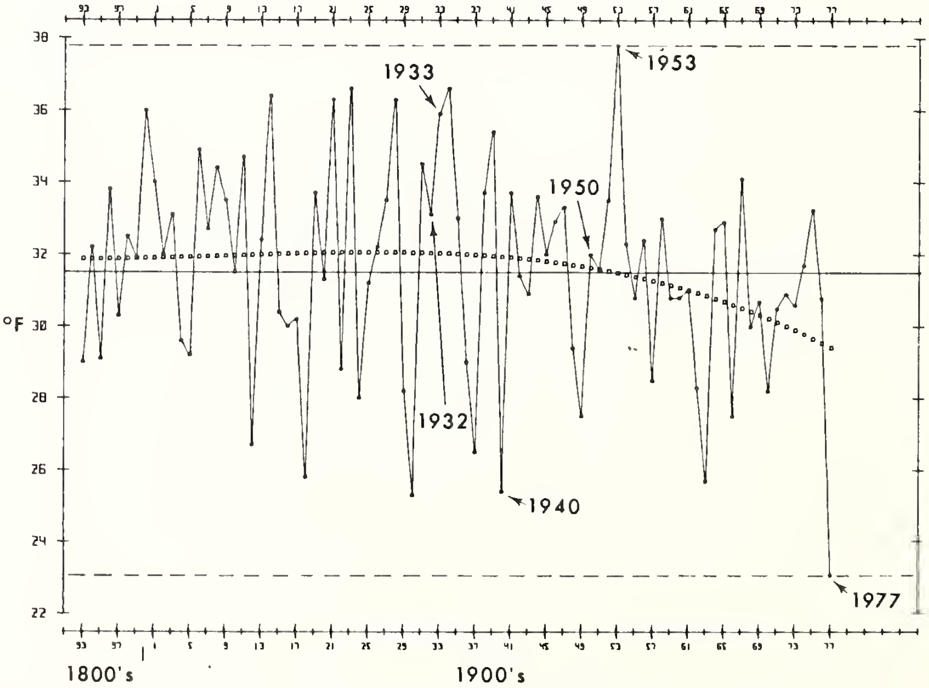

The trend line is a 3rd order polynomial of best fit.

U.S. average January temperature by year, 1893-1977. The trend line is a third order polynomial regression. Data are for the contiguous 48 states.

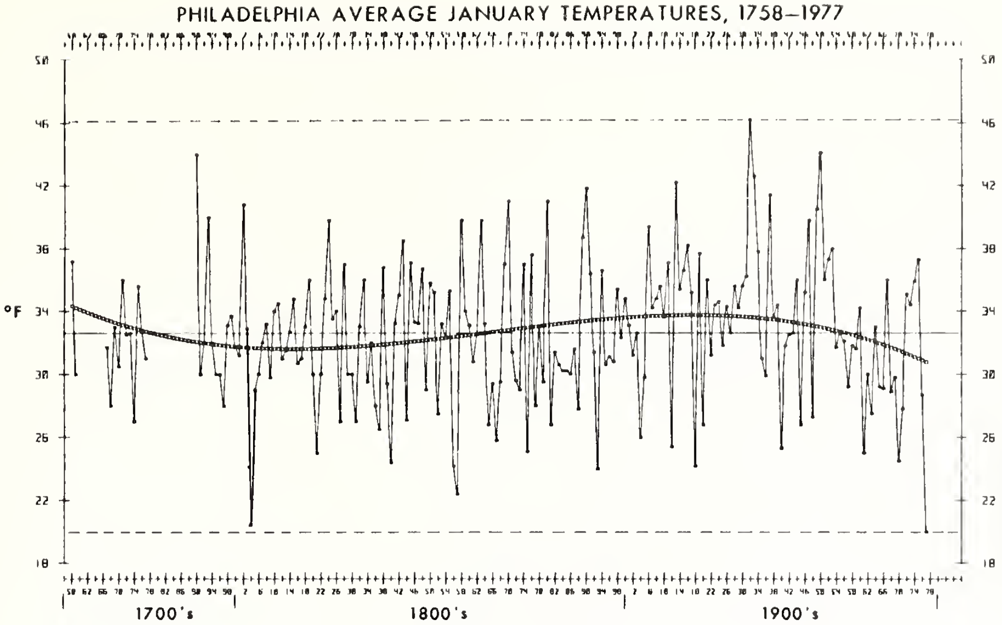

The smooth trend line is a 3rd order polynomial least-squares fit. Does it show a quasi-bicentennial oscillation?

Philadelphia average January temperature by year, 1758-1977. The trend line is a third order polynomial regression.

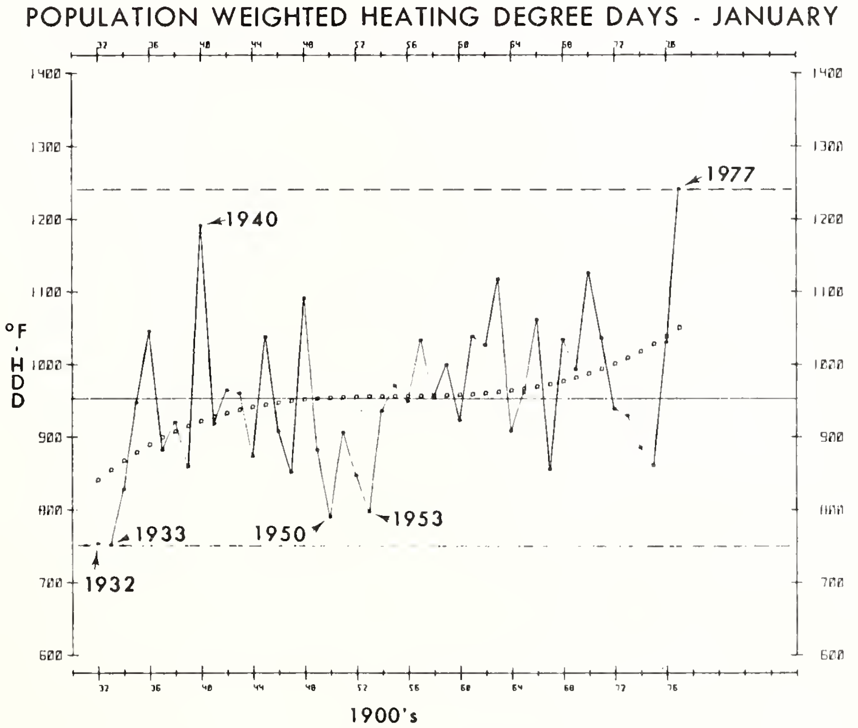

U.S. total January population-weighted heating degree days (1970 census) by year, 1932-1977. The trend line is a third order polynomial regression. Data are for the contiguous 48 states.

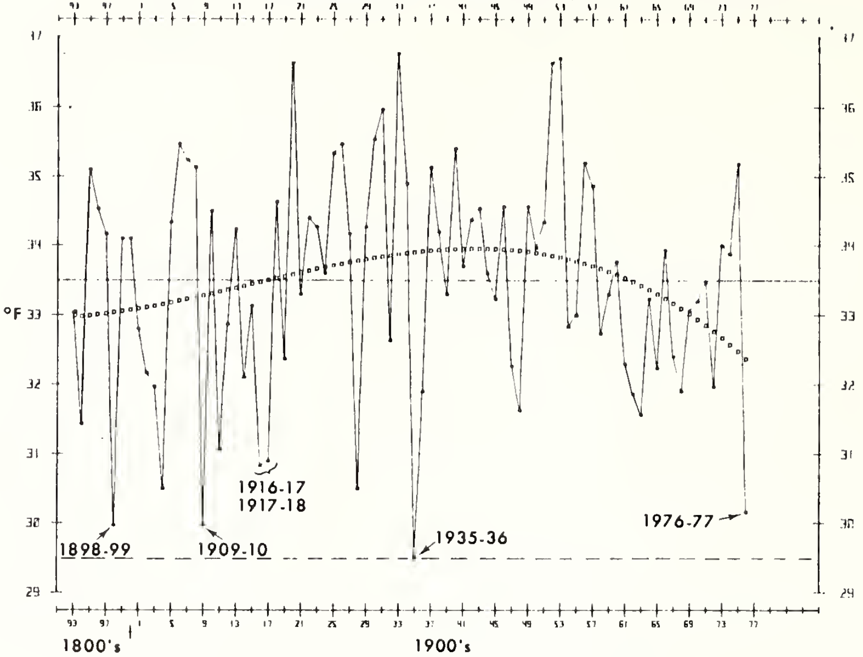

DECEMBER—FEBRUARY SEASONAL AVERAGE TEMPERATURES FOR THE U. S. (1893-1977)

The trend line is a 3rd order polynomial of best fit.

U.S. average December-January-February temperature by season, 1893-94 thru 1976-77 seasons. The trend line is a third order polynomial regression. Data are for the contiguous 48 states.

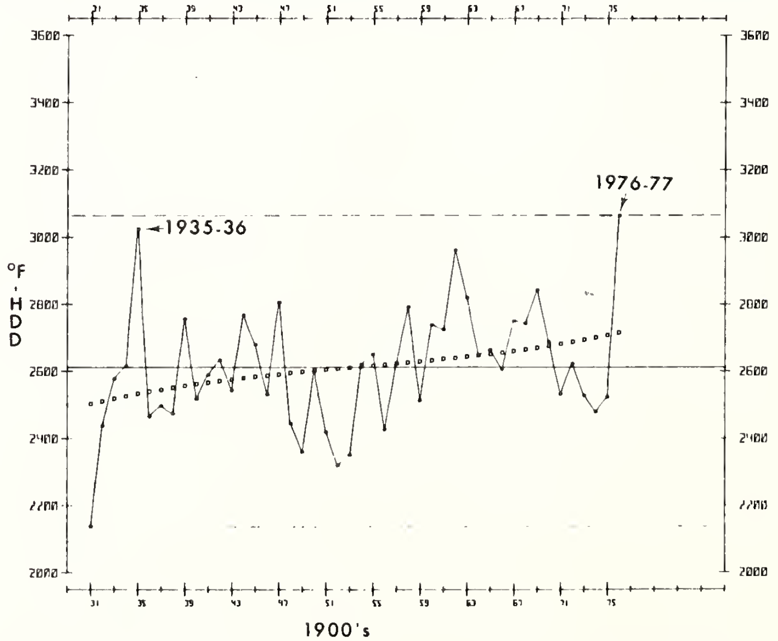

POPULATION WEIGHTED HEATING DEGREE DAYS - WINTER

U.S. total December-January-February population-weighted heating degree days (1970 census) by season, 1931-32 thru 1976-77 seasons. The trend line is a third order polynomial regression. Data are for the contiguous 48 states.

OCTOBER—MARCH SEASONAL AVERAGE TEMPERATURES FOR THE U. S. (1893-1977)

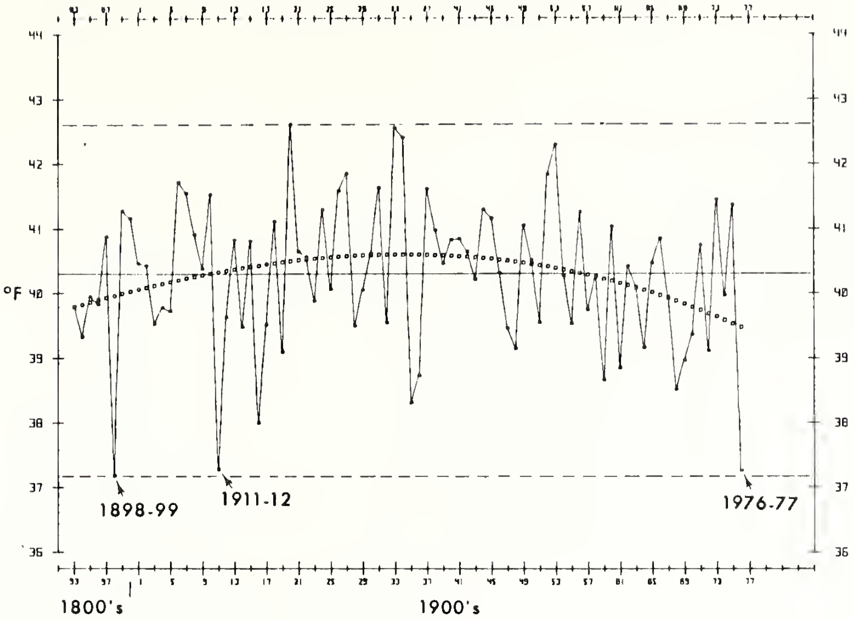

The trend line is a 3rd order polynomial of best fit.

U.S. average October-March temperature by season, 1893-94 thru 1976-77 seasons. The trend line is a third order polynomial regression. Data are for the contiguous 48 states.

POPULATION WEIGHTED HEATING DEGREE DAYS OCTOBER—MARCH

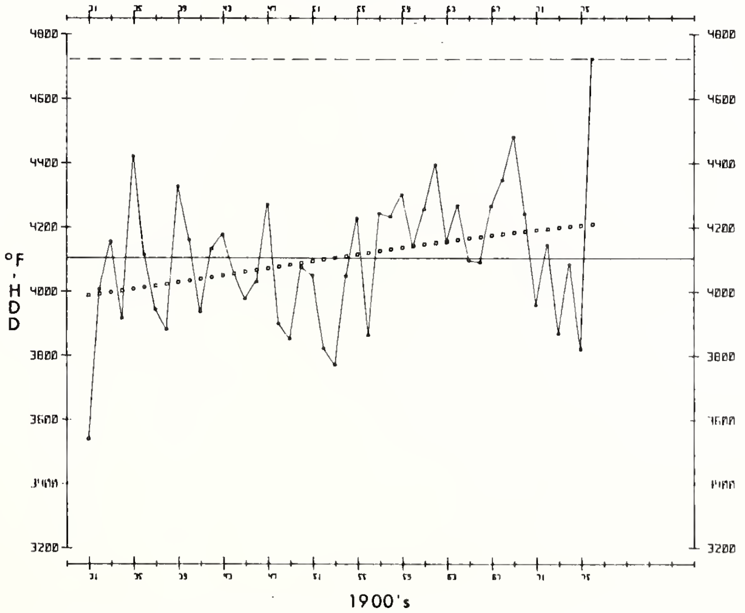

U.S. total October-March population-weighted heating degree days (1970 census) by season, 1931-32 thru 1976-77 seasons. The trend line is a third order polynomial regression. Data are for the contiguous 48 states.

ECONOMIC IMPLICATIONS OF THE TEMPERATURE ANOMALIES OF JANUARY 1977

by

Elmar R. Reiter
Colorado State University
Atmospheric Science Department
Fort Collins, Colorado

We used the temperature anomalies reported by Wagner*(1977) to estimate the excessive energy demands for space heating over the eastern United States. These estimates were based upon accurate (within 1.1%) model predictions of natural gas use for space-heating in Greeley, Colorado during winter. Model output was translated into B.T.U. consumption per capita in Greeley as a function of heating degree days. The following result was obtained for Greeley, Colorado.

$$B = (65 - \overline{T}) \times 4153 + 199479 \text{ (in BTU)} \qquad (1)$$

The temperature-invariant term constitutes the per capita use of energy for industrial purposes.

Figure 1 shows the heating degree days in January 1977, inferred from Wagner's data. Figure 2 shows the percent anomaly of the degree days given in Fig. 1.

We applied the BTU-use coefficient of the temperature-dependent term in eq. 1 to the 1972 census data of population which we have interpolated for 1° latitude x 1° longitude squares. Using the degree-day data of Fig. 1 and the gridded 1972 population data, we arrive at the BTU demand for space-heating only, shown in Fig. 3. It should be emphasized that the underlying assumptions in these calculations are that the per capita allocation of heated building areas (residential, commercial and industrial) measured in Greeley, Colorado, is typical also for the eastern United States. We realize that this assumption in incorrect, but we feel that the computational results are not too far off from reality.

Figure 4 finally shows the "excess" demand of BTU's for space-heating during January 1977 over a normal month of January. (Note that 1 $ft.^3$ of natural gas contains approximately 10^3BTU.) The metropolitan areas of Chicago and New York are clearly evident in Figs. 3 and 4.

---

*Wagner, A.J., 1977: Weather and Circulation of January 1977. The Coldest Month on Record in the Ohio Valley. Mon. Wea. Rev., 105(4):553-560.

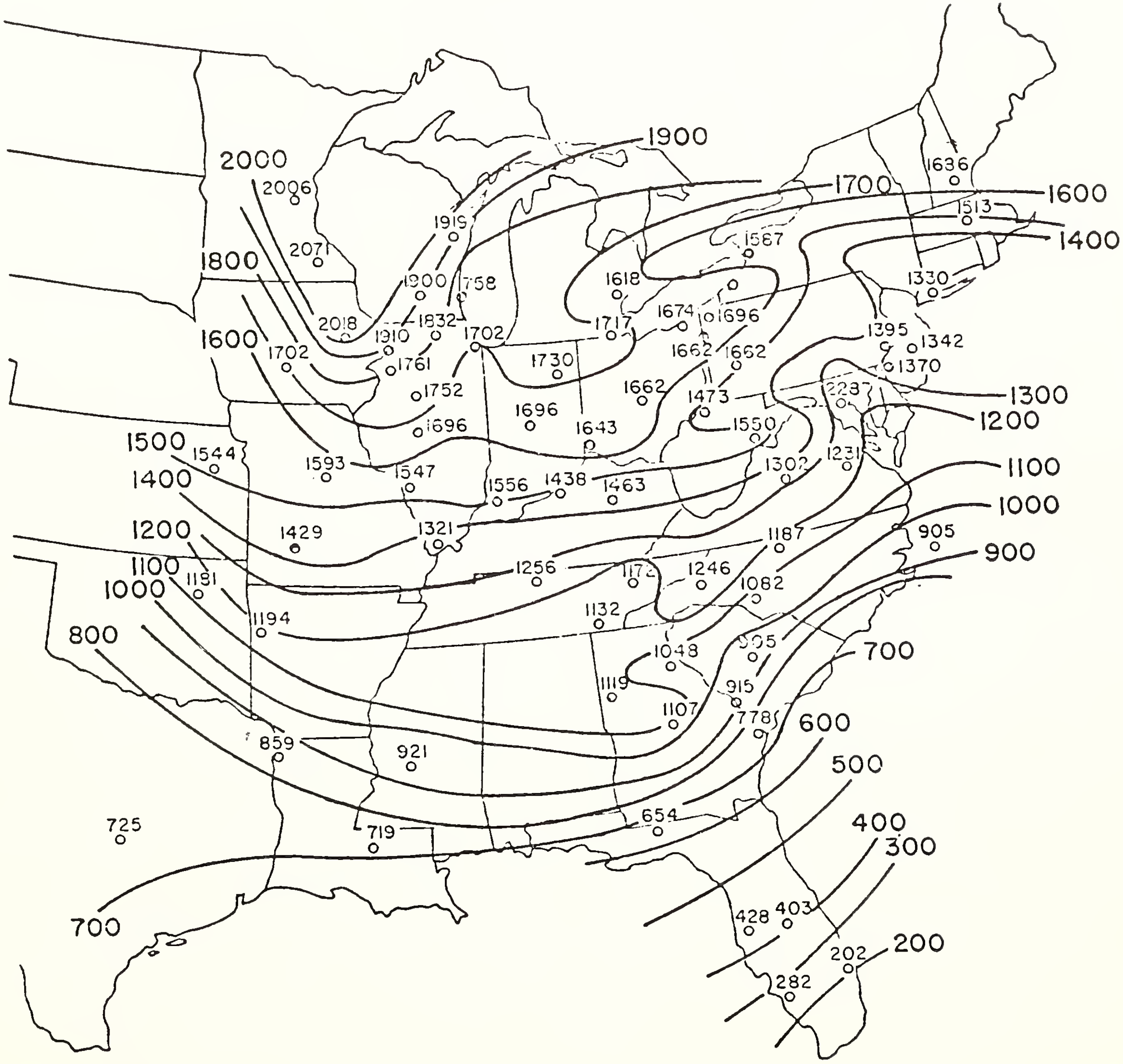

Figure 1. Oil heating degree days for January 1977 in terms of departures from normal (data from Wagner, 1977).

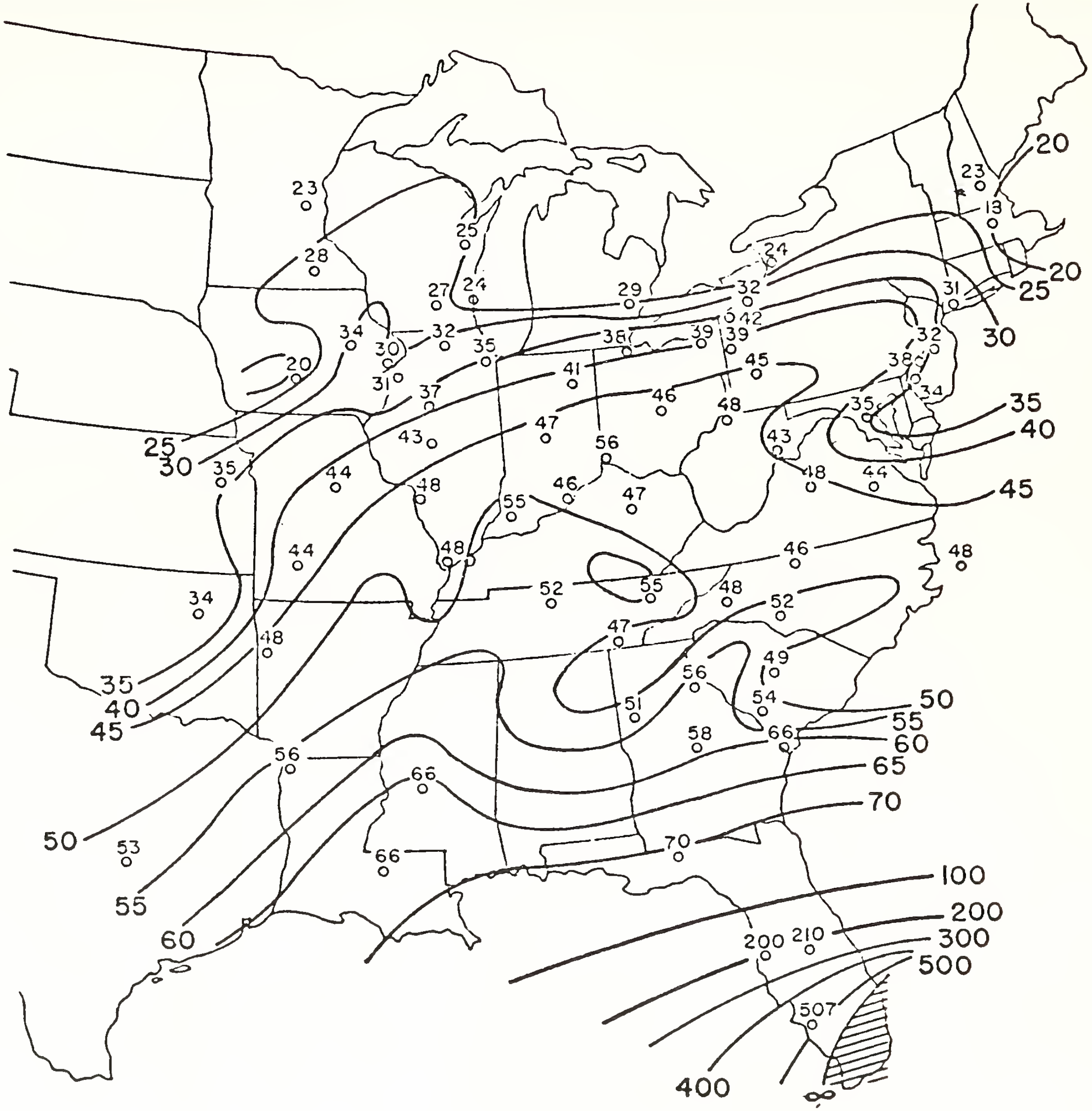

Figure 2. Percent departures of January 1977 heating degree days from normal.

Figure 3. The weather-dependent part of energy demand (Eq. 1) extrapolated to 1970 census data on population.

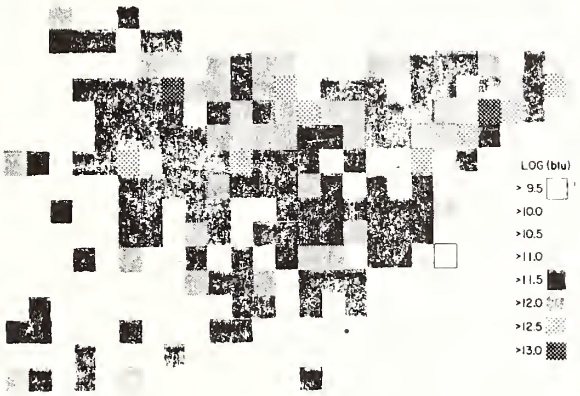

Figure 4. Energy consumption - difference from normal January (log base 10 total BTU).

Winter 1976-77, A Comparison of Circulation Characteristics With Other Winters

Robert R. Dickson
National Weather Service, NOAA

The winter of 1976-77 was extreme with respect to both the temperature anomaly over the United States and also the amplification of the seasonal mean mid-tropospheric circulation pattern in the vicinity of North America. However, examination of comparable maps for the period of good hemispheric upper level data coverage (through winter 1947-48), reveals that winter 1976-77 was but one of a class of cold winters over the eastern half of the United States (fig. 1) having deep mean troughs south of the Aleutians and along the east coast of the United States and a strong mean ridge extending from the northwest coast of the United States to the Canada-Alaska border (fig. 2). Other members of this class were the winters of 1960-61, 1962-63, 1967-68, and 1969-70. It is the intent of this study to focus attention upon the features which these winters and their antecedant Novembers had in common, with the implication that these should include the crucial factors involved.

In addition to the highly amplified wave pattern near North America, the class winters all had blocking ridges over western Asia which diverted both cold air and vorticity maxima to southern Asia and provided a strong baroclinic field and a deep trough along the east coast of Asia (figs. 2 and 3). The associated 200 mb jetstream was unusually strong from south of the Caspian Sea across southern China to the central Pacific (fig. 4). The amplified winter flow pattern transported cold air to extensive areas at middle and low latitudes and warm air to high latitudes (figs. 3 and 5) with a consequent southward dislocation of the baroclinic zone and the mean westerlies (fig. 5). Areas of consistently anomalous sea surface temperature (fig. 6) were well correlated with patterns of both mean height and thickness anomalies.

Ramage (1968) in contrasting conditions during January 1963 (a class winter month of the present study) with the following January concluded that unimpeded flow of cold air to low latitudes off the southeast Asia coast in winter leads to evaporation of large amounts of water from the ocean, heavy rains over the island continent of Indonesia, and the establishment of a meridional circulation which transports heat at high levels from this source to an area south of the west Pacific jetstream, contributing to the baroclinic field and the jetstream strength. He further speculated that hydrodynamic instability on the south side of the jetstream may have led to the formation of the intense blocking ridge extending southward from Alaska in January 1963. In the present study the South China Sea (110° W to 120° W) was the only 10 degree longitudinal span along 15°N (in the area of fig. 4) which had mean south to north 200 mb geostrophic flow in excess of the long term mean in each of the three Januaries of figure 4. Together with the previously described southward flow of cold air at low levels, this suggests the existence in the class winters of the meridional circulation described by Ramage. Thus, it appears that these winters had a strong jetstream emerging from southern Asia to encounter a west Pacific baroclinic field enhanced by both outbreaks of cold air from Asia and this type of meridional circulation. Energy conversions along this intense baroclinic field led to an acceleration of the already strong jetstream, presumably leading to sporadic episodes of hydrodynamical instability and a breakdown of the westerlies into the highly amplified wave pattern found over the central and east Pacific.

In each of the five Novembers preceding the class winters a strong blocking ridge was already extant northeast of the Caspian Sea, bringing cold air to much of south and east Asia (figs. 7 and 8). Diversion of vorticity maxima south of the blocking ridge is most apparent at 200 mb (fig. 9) where a deep mean trough and associated fast westerlies were observed south of the Caspian Sea. Each of the Novembers also displayed a strong andwarm subtropical ridge southeast of Japan. This warm ridge was positioned to provide an enhanced early winter baroclinic zone as the very cold air overlying east Asia (fig. 8) moved eastward. This must have provided an early-winter surge of kinetic energy to the developing Pacific jetstream in the class winters. Other 700 mb features found in each of the antecedant Novembers were deep mean lows over the Bering Sea and north of Hudson Bay. Both lows were associated with quite cold air--available for southward transport when the winter amplification began. As was the case in winter, areas of consistent November sea surface temperature anomalies generally coincided with similar-sign anomalies of height and thickness (figs. 10, 8, and 7). An exception, however, was the cooler than normal water southeast of Japan, which may have contributed to the transience of the overlying November ridge as winter began.

In summary, the mean winter circulation anomaly distribution characteristic of winter 1976-77 was quite similar over much of the Northern Hemisphere to that of four other winters of the past thirty years. Key factors in the Novembers preceding these winters were a blocking ridge over western Asia, a strong subtropical ridge southeast of Japan, and a reservoir of unusually cold air over the Bering Sea and north of Hudson Bay. These factors appear important as contributors to a subsequent anomalous acceleration of the hemispheric subtropical jetstream, especially over the western Pacific upstream from the area where the westerlies broke down into a highly amplified wave pattern.

Reference

Ramage, C.S., "Role of a Tropical Maritime Continent in the Atmospheric Circulation," Monthly Weather Review, vol. 96, No. 1, June 1968, 365-370.

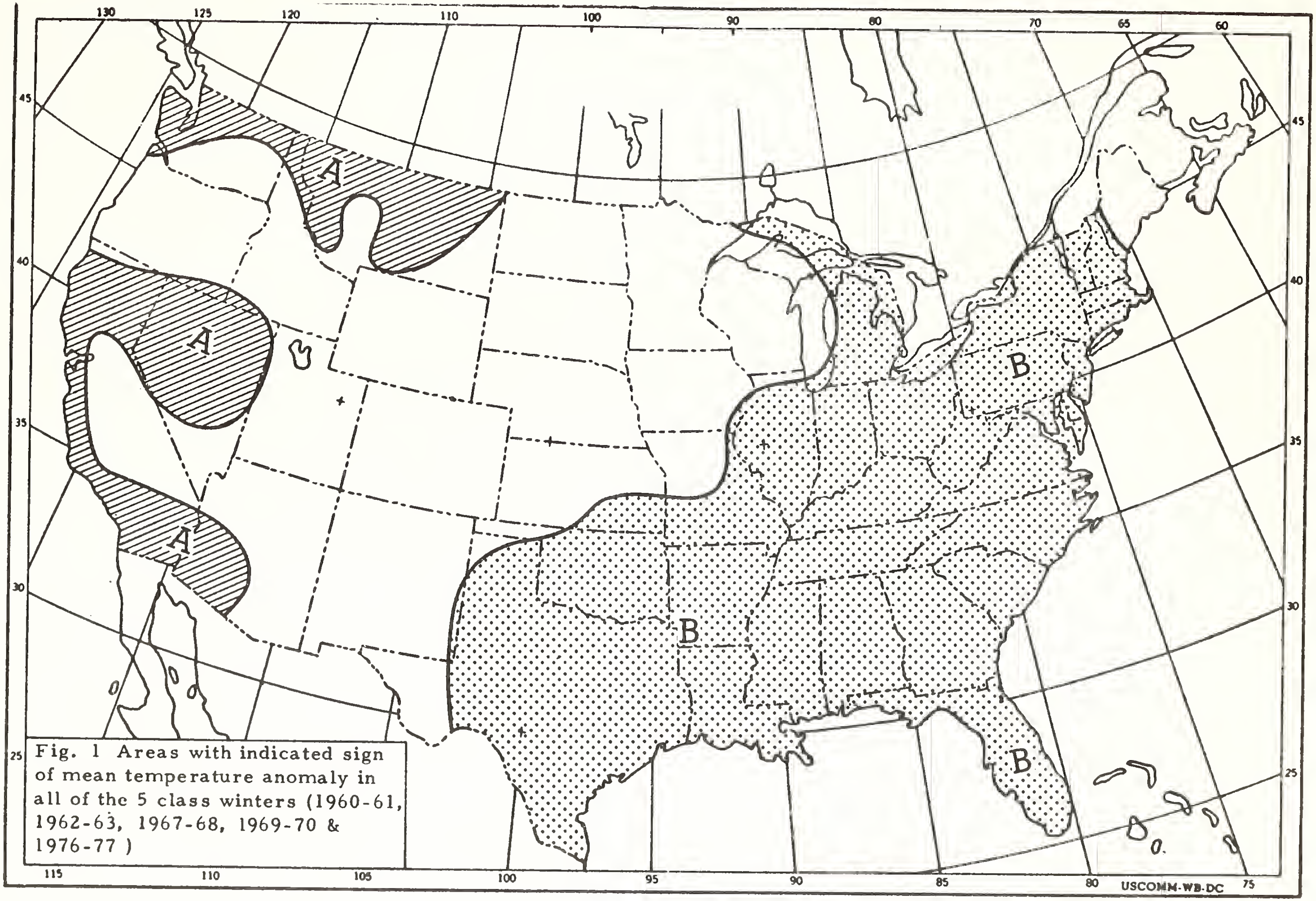

Fig. 1 Areas with indicated sign of mean temperature anomaly in all of the 5 class winters (1960-61, 1962-63, 1967-68, 1969-70 & 1976-77)

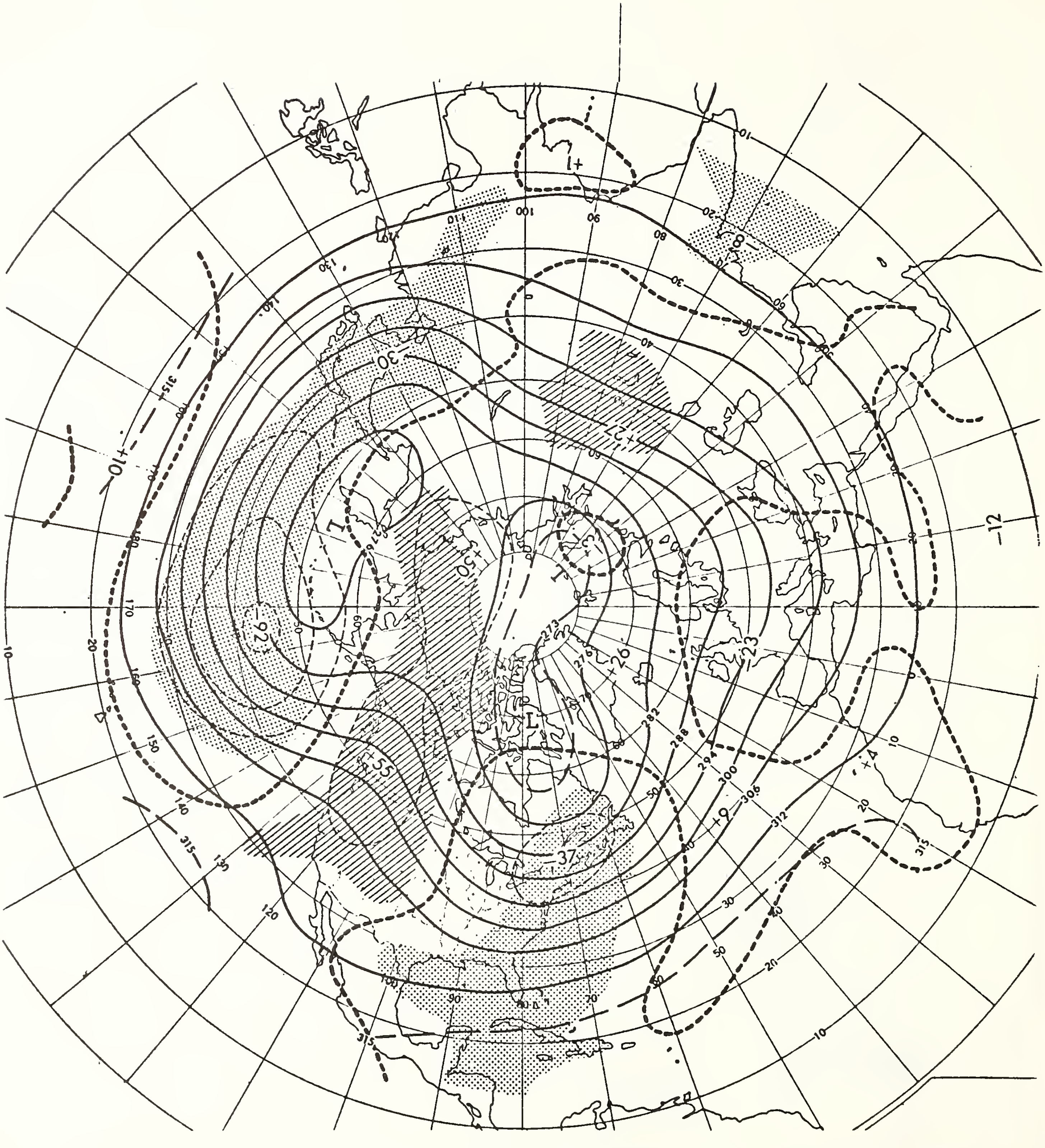

Fig. 2 Mean 700 mb height contours (dam) and departure from normal (m, dashed) for the 5 class winters. Shaded areas had same DN sign in all years.

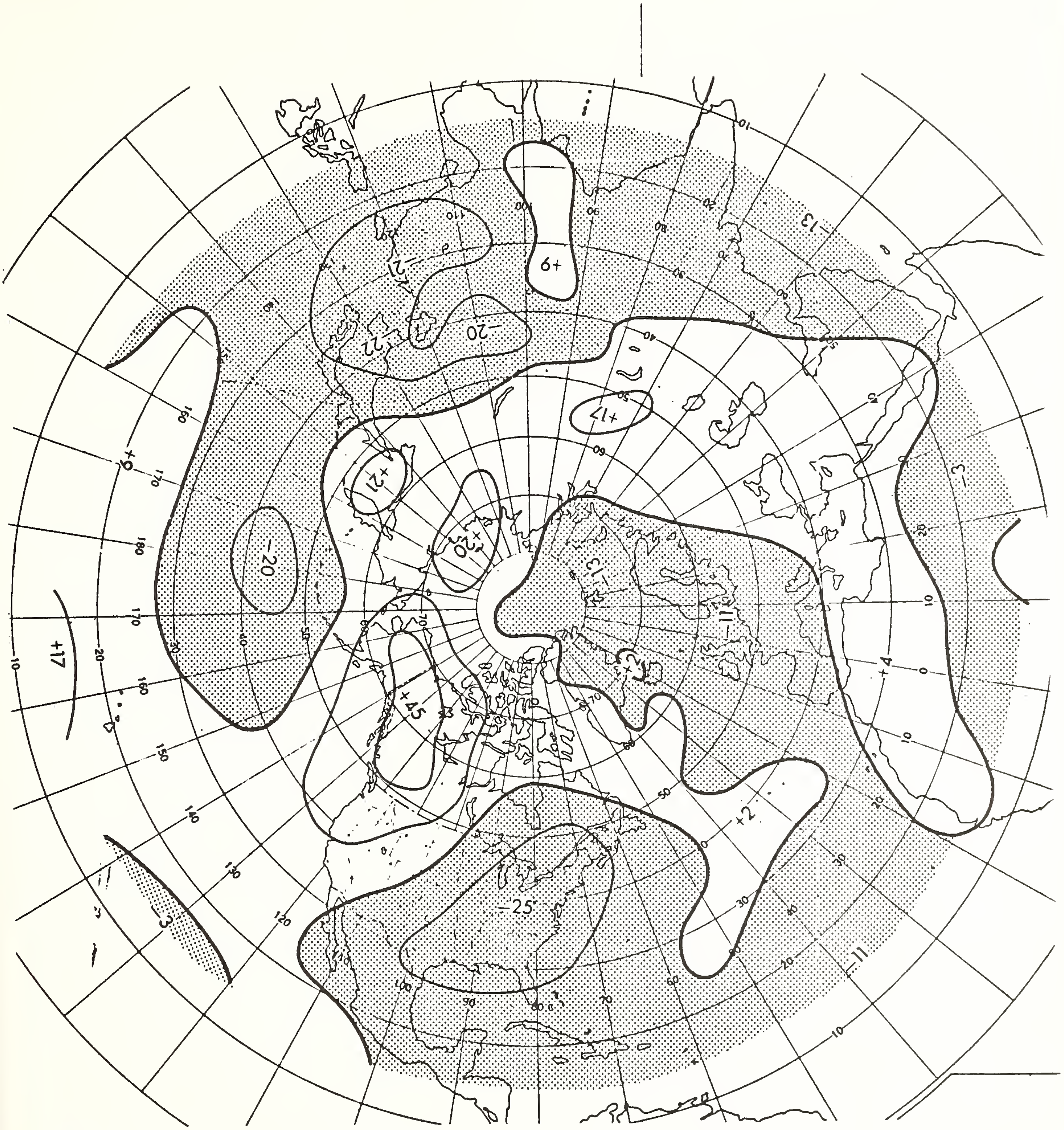

Fig. 3 Departure from normal of mean 1000 to 700 mb thickness (m) for the five class winters.

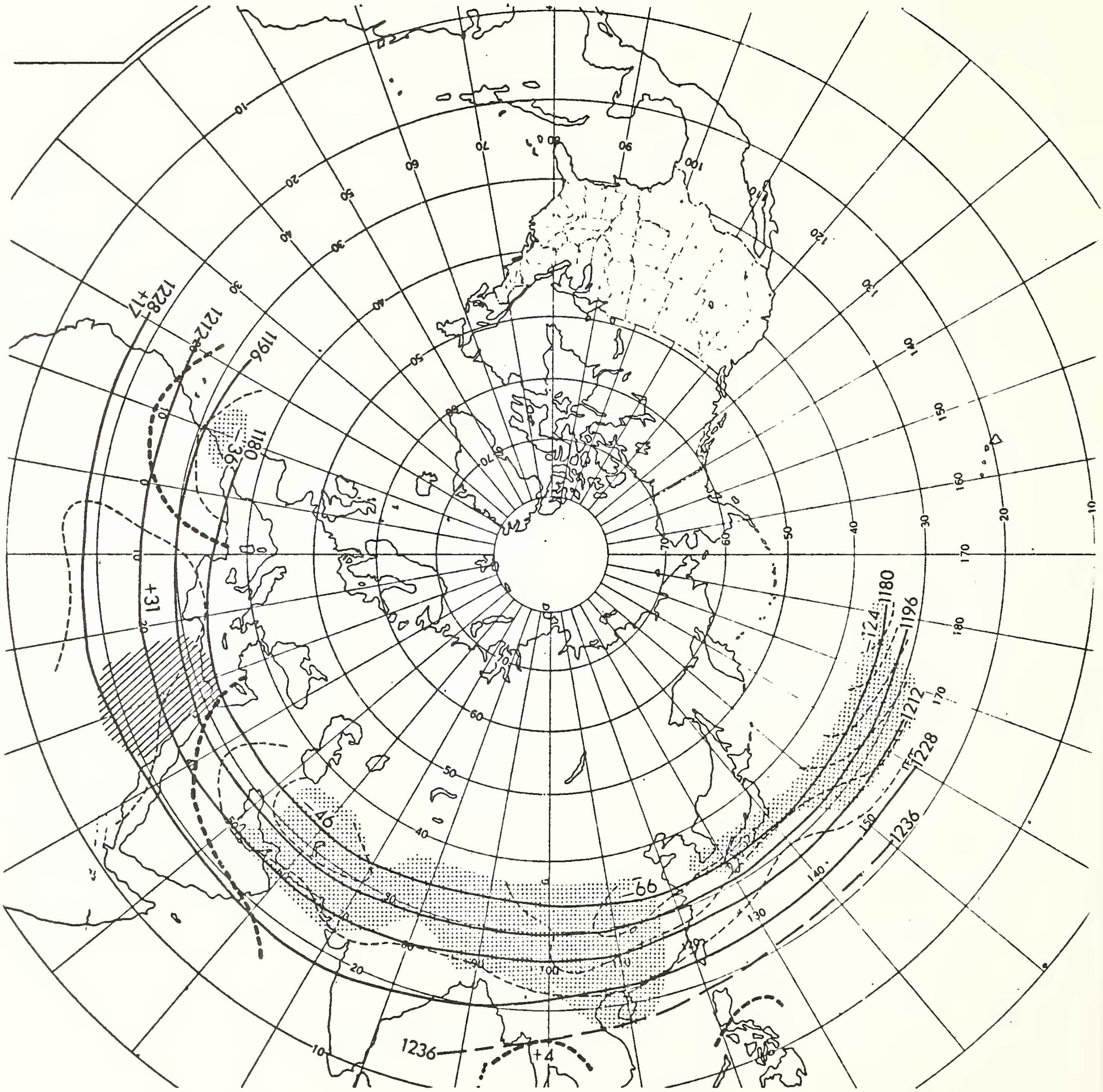

Fig. 4 Mean 200 mb height contours (dam) and departure from the 1967-76 mean (m, dashed) for January 1968, 1970, & 1977. Shaded areas had same sign of departure in all years.

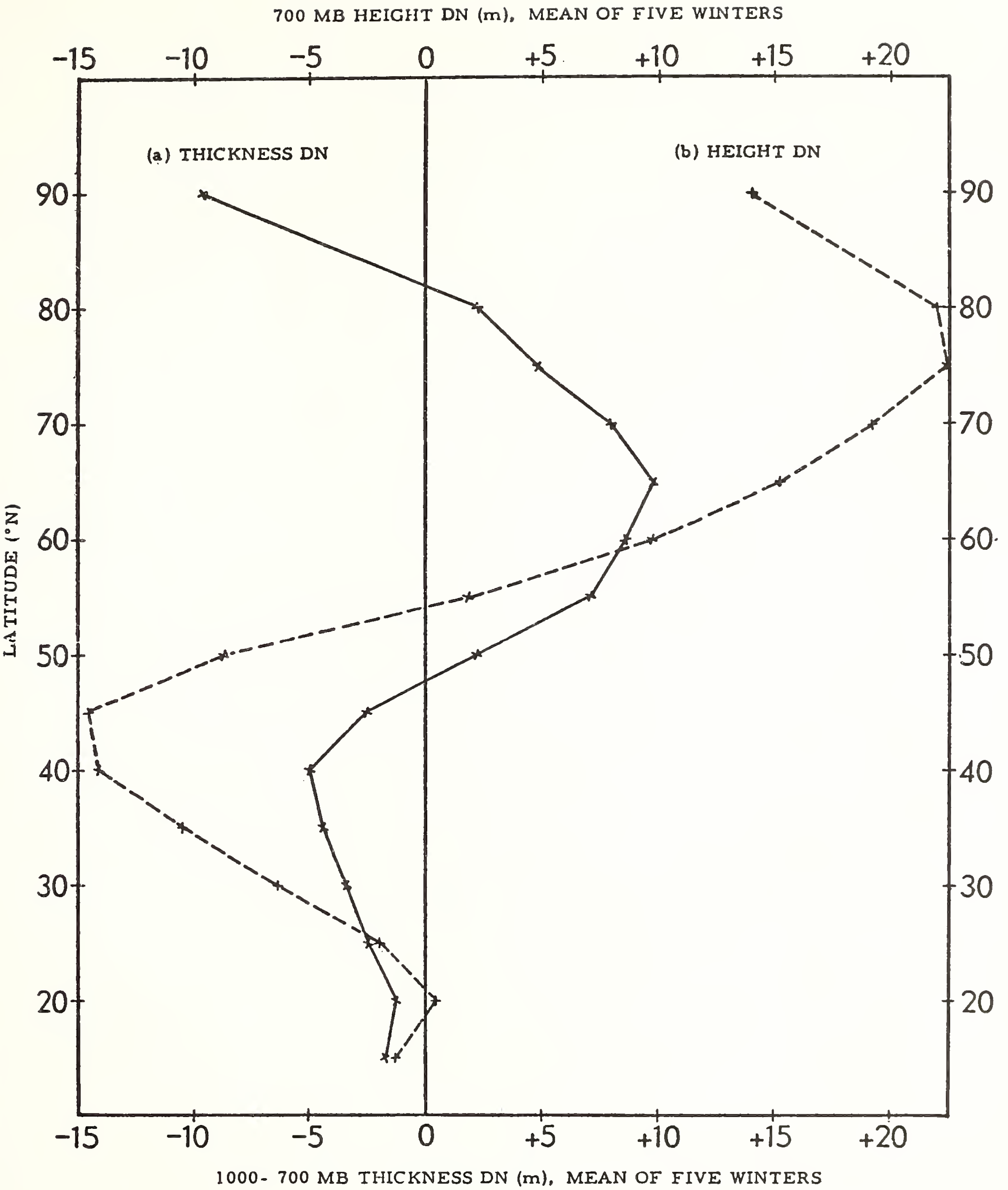

Fig. 5 Profiles of mean departures from normal of (a) 1000 to 700 mb thickness, and (b) 700 mb height; for the five class winters.

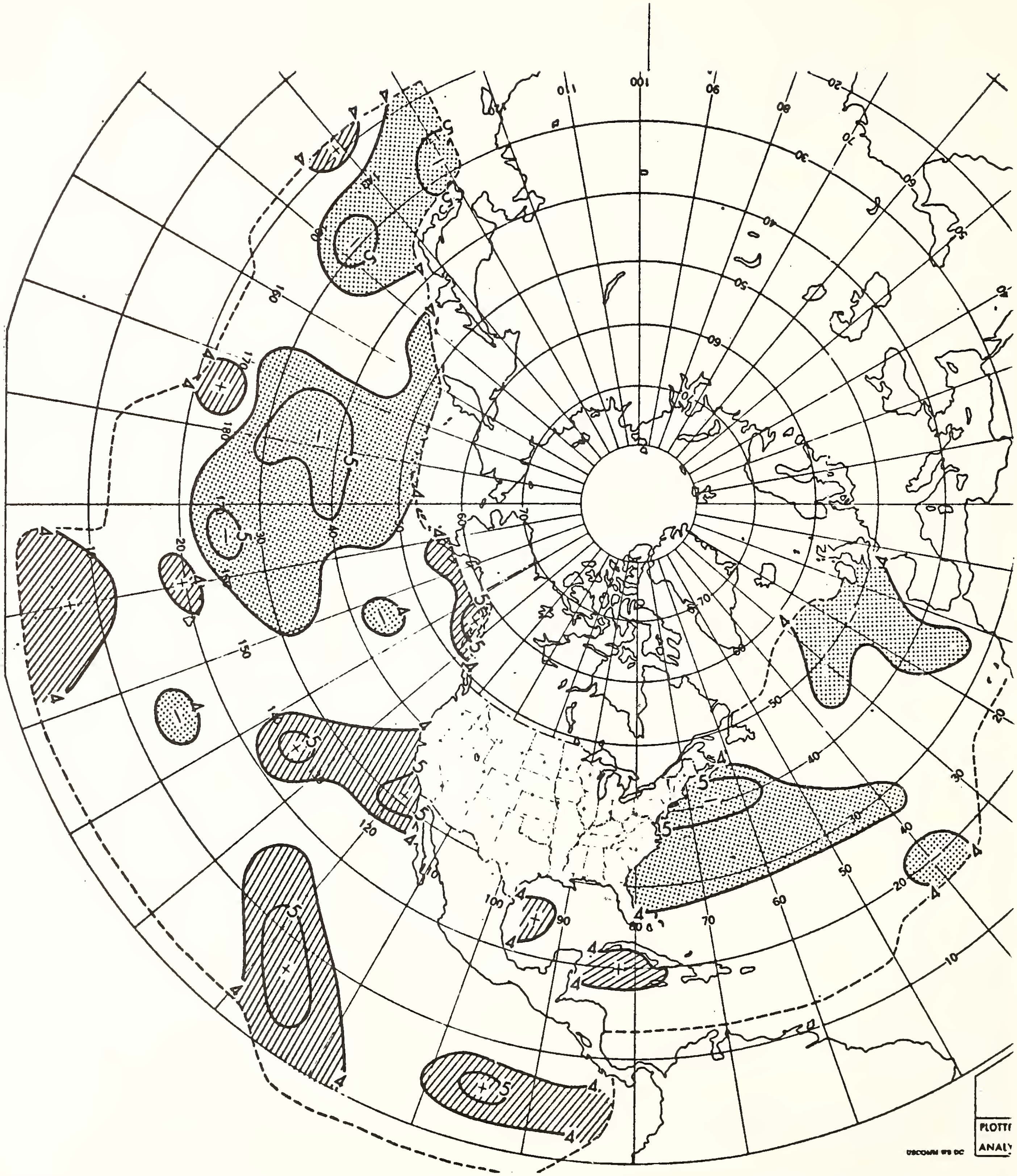

Fig. 6 Areas with indicated sign of mean sea surface temperature anomaly in 4 or 5 Januaries of the class winters.

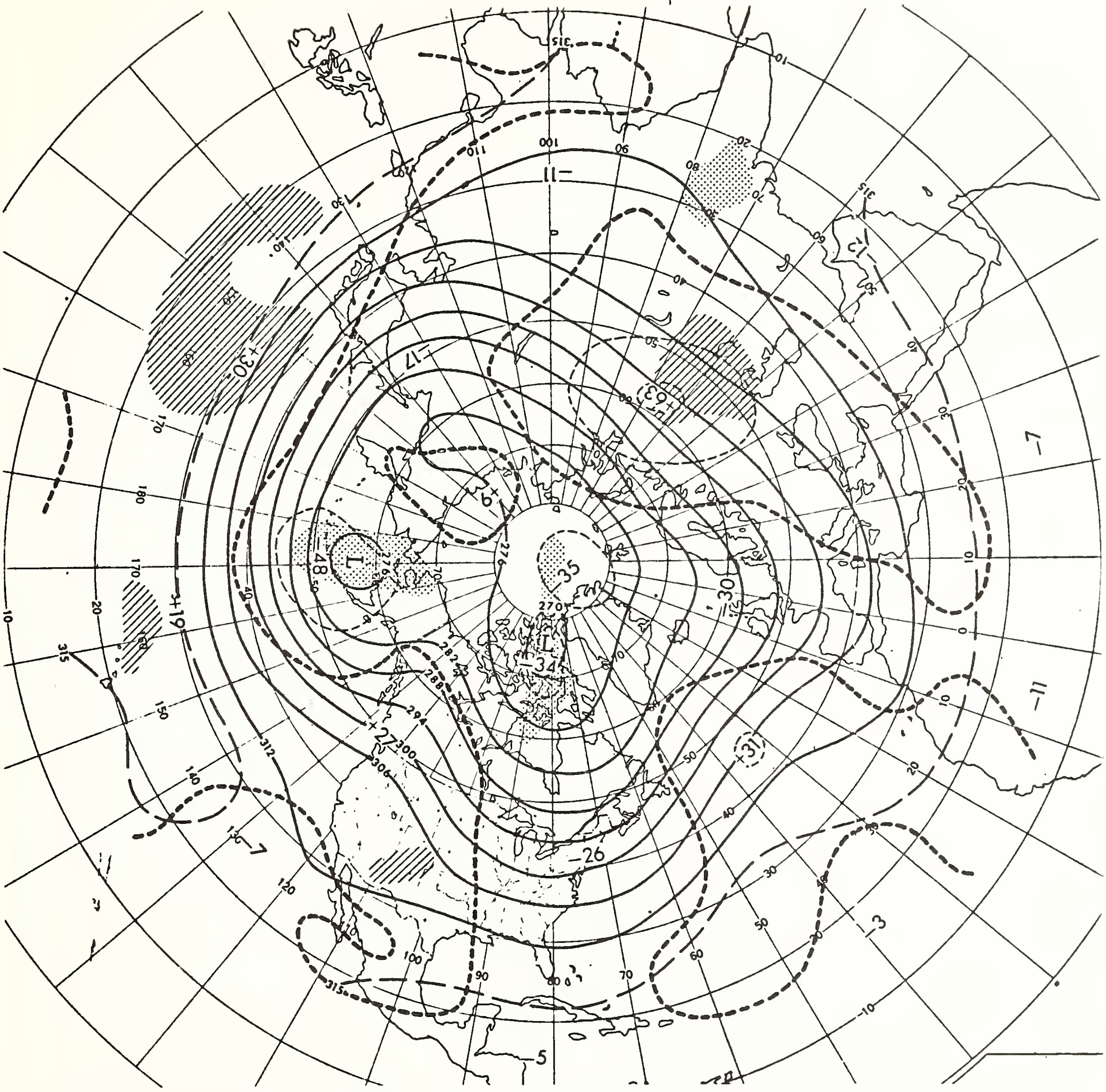

Fig. 7 Mean 700 mb height contours (dam) and departure from normal (m, dashed) for Novembers preceding class winters. Shaded areas had same sign of departure in all years.

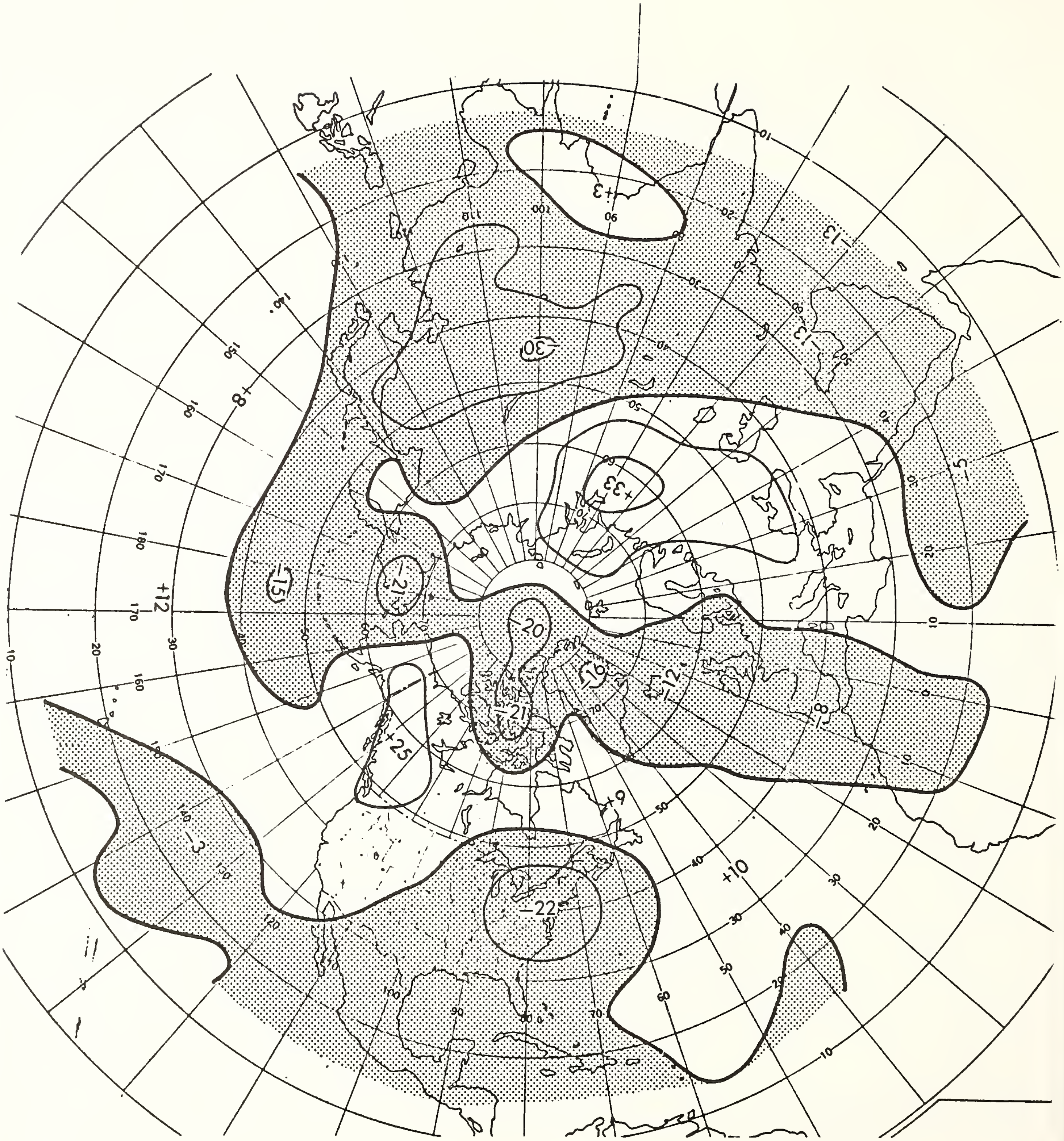

Fig. 8 Departure from normal of mean 1000 to 700 mb thickness (m) for Novembers preceding class winters.

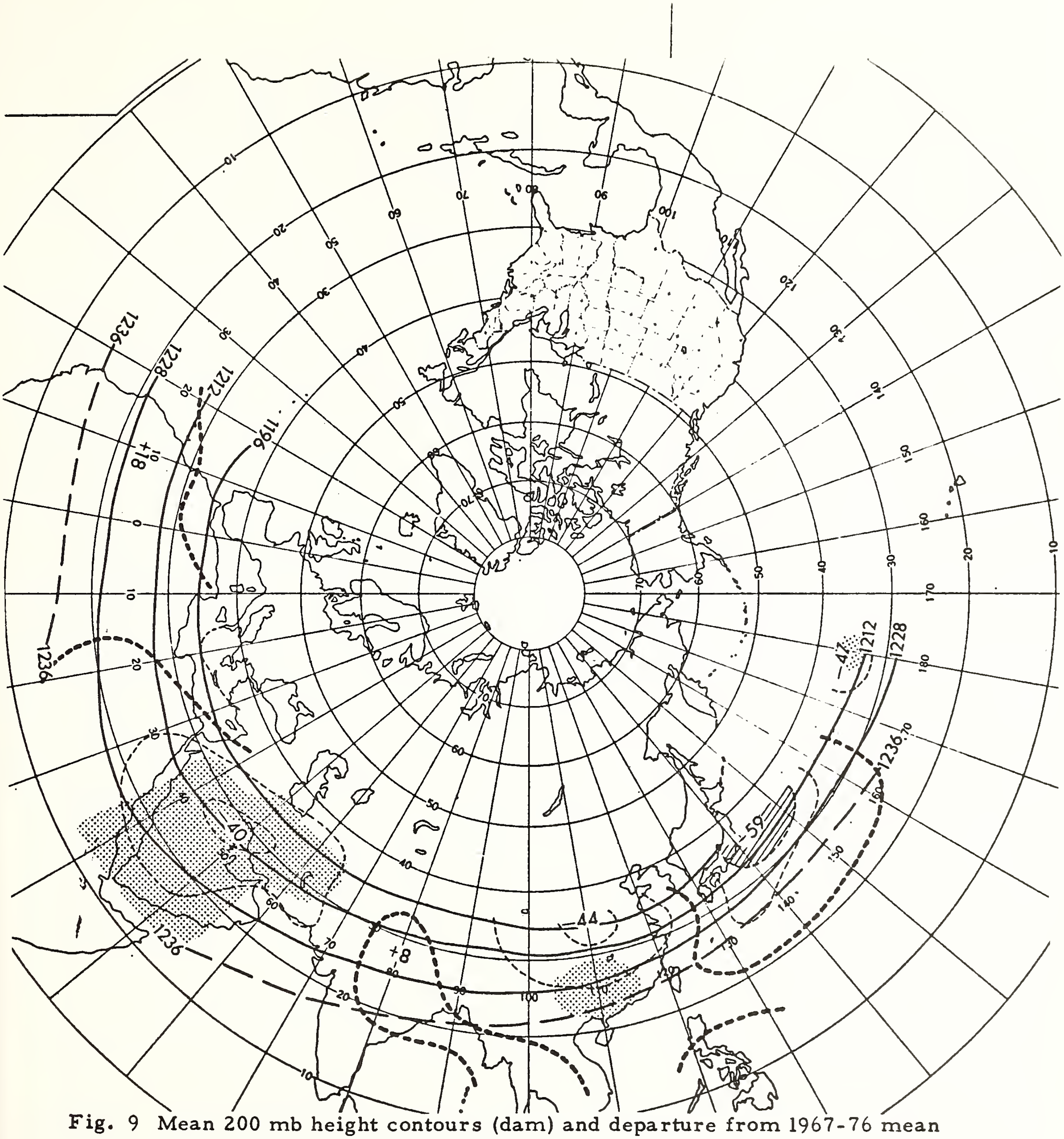

Fig. 9 Mean 200 mb height contours (dam) and departure from 1967-76 mean (m, dashed) for November 1967, 1969, &1976. Shaded areas had same sign of departure in all years.

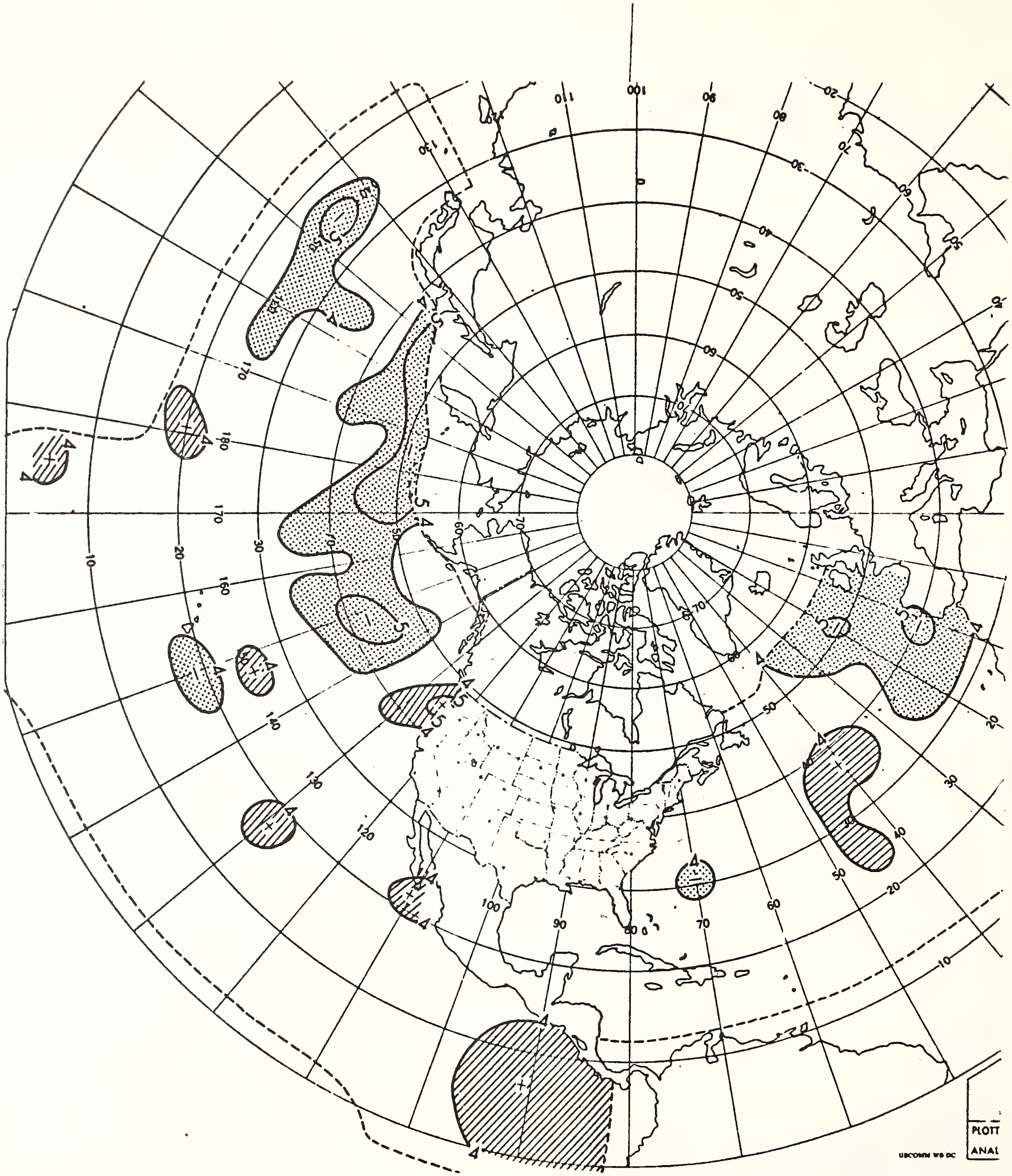

Fig. 10 Areas with indicated sign of mean sea surface temperature anomaly in 4 or 5 Novembers preceding class winters.

THE WINTER OF 1976-77 IN A BIENNIAL CONTEXT*

R. S. Quiroz
National Meteorological Center, NWS, NOAA
Washington, DC 20233

Large changes from the winter 1975-76 to the winter 1976-77 are depicted: (1) in planetary zonal means of temperature, pressure height, and zonal wind (Figs. 1-4, 7); and (2) in amplitudes of the long planetary waves (mainly wave 2) (Figs. 8, 9). These changes are shown to be embedded in an apparent quasi-biennial cycle of tropospheric kinetic energy. The change in long-wave activity appears to bear a relationship to the changing pattern of Pacific Ocean sea surface temperature from 1975 to 1976.

Specific observations include:

(1) Negative temperature anomaly in the winter 1976-77 is shown in the planetary zonal means for latitudes south of 50-60°N; the anomaly was most pronounced in late December and January (Fig. 6). (Positive anomaly prevailed in mid-winter 1975-76).
(2) In high latitudes, anomalies were typically of opposite sense. (Arctic warming in the troposphere in mid-winter 76-77 was also coupled with intense stratospheric warming.)
(3) Correlations near -0.8 were found in 100-mb pressure surface height, between heights at 80 and 40N (Fig. 7).
(4) Although the interannual change in several parameters was greatest from mid-winter to mid-winter, the pattern of change is shown to have begun months earlier (Figs. 3, 4).
(5) In January 1977, the tropospheric jet stream circulation was very significantly stronger than in January 1976 and was some 10 m s^{-1} stronger (at the core) than normal (Fig. 2). In the stratosphere, the polar night jet was extraordinarily strong in 1975-76, but very weak in 1976-77, when a polar circulation reversal resulted from intense sudden warming.
(6) Twelve-month running averages of tropospheric zonal kinetic energy indicate an apparent quasibiennial cycle, with maximum energy in mid-winter 76-77, the value exceeding that of 75-76 by about 14% (Fig. 5).
(7) Monthly RMS amplitudes of zonal waves 1-4 in the two winters (Fig. 8) show a large increase in tropospheric wave 2 activity from one winter the the next. Wave 2 appears to have grown partly at the expense of wave 3.
(8) Northward eddy heat transport was much greater in winter 76-77 (Fig. 4).

(9) Such features in SST as the large east-west scale of the negative anomaly in the Pacific in late 1976 (in contrast to a more fractured anomaly field in 1975) and the encroaching warm anomaly in the eastern Pacific from September to December 1976, together with the phase characteristics of tropospheric wave 2, suggest a coupling between the atmospheric circulation and the SST field.

(10) The extraordinary polar anticyclone that developed in January 1977, is considered, in combination with a wave 3 contribution in lower latitude, to account for the most severe cold-air advection to lower latitudes during the winter.

---

*Note: Figures 1 and 2 were previously presented at an IAGAP/IAMAP conference (Seattle, August 22 - September 4, 1977). Details of the structure of the polar anticyclone of January 1977 were described at a meeting of the AGU (Washington, DC) in June 1977. The stratospheric-tropospheric warming of December-January 1976-77 was described in GRL, vol. 4, no. 4, April 1977.

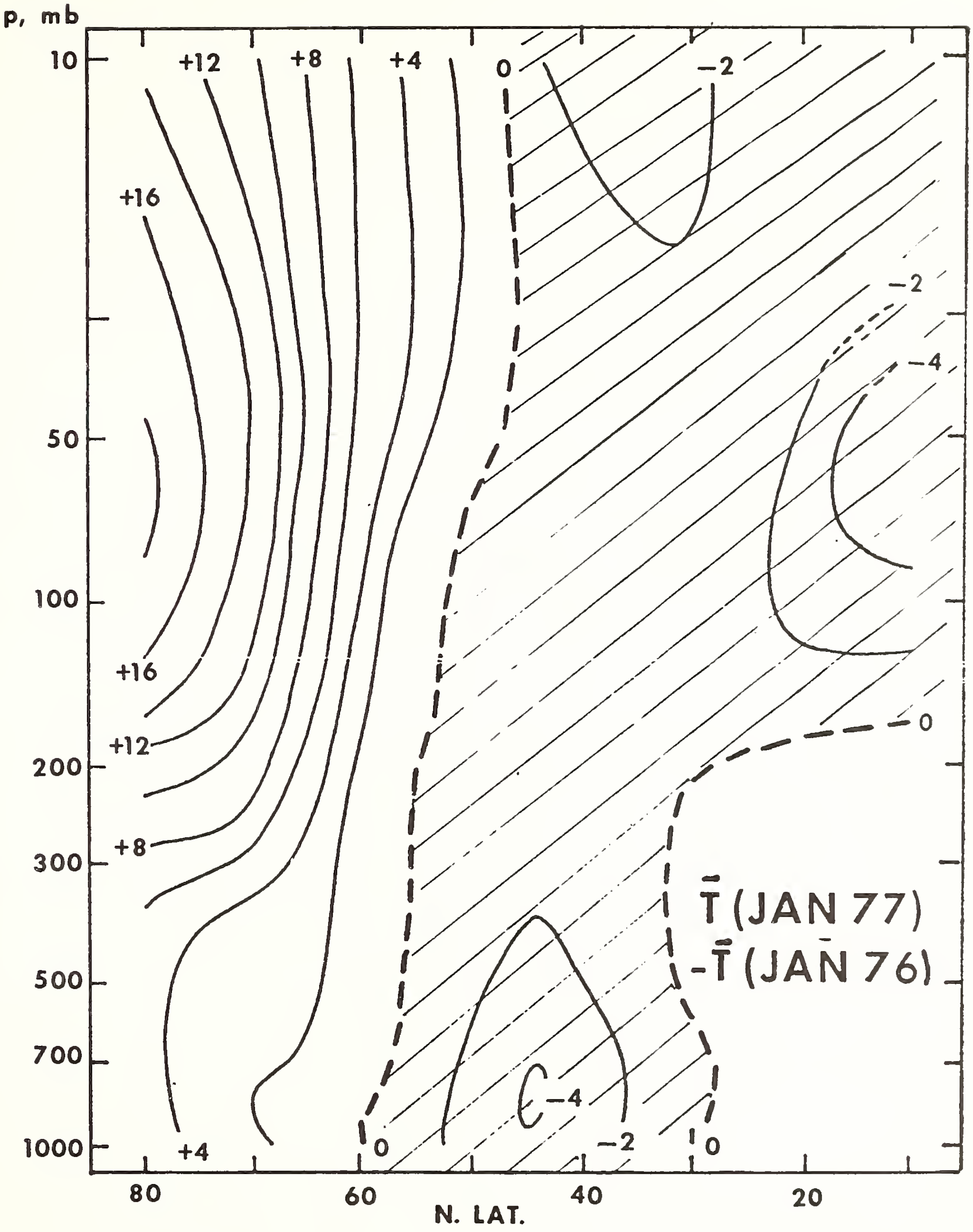

Fig. 1. Difference in zonal mean temperature (January 1977 minus January 1976), deg C. (Figs. 1-5 were constructed from monthly mean values.)

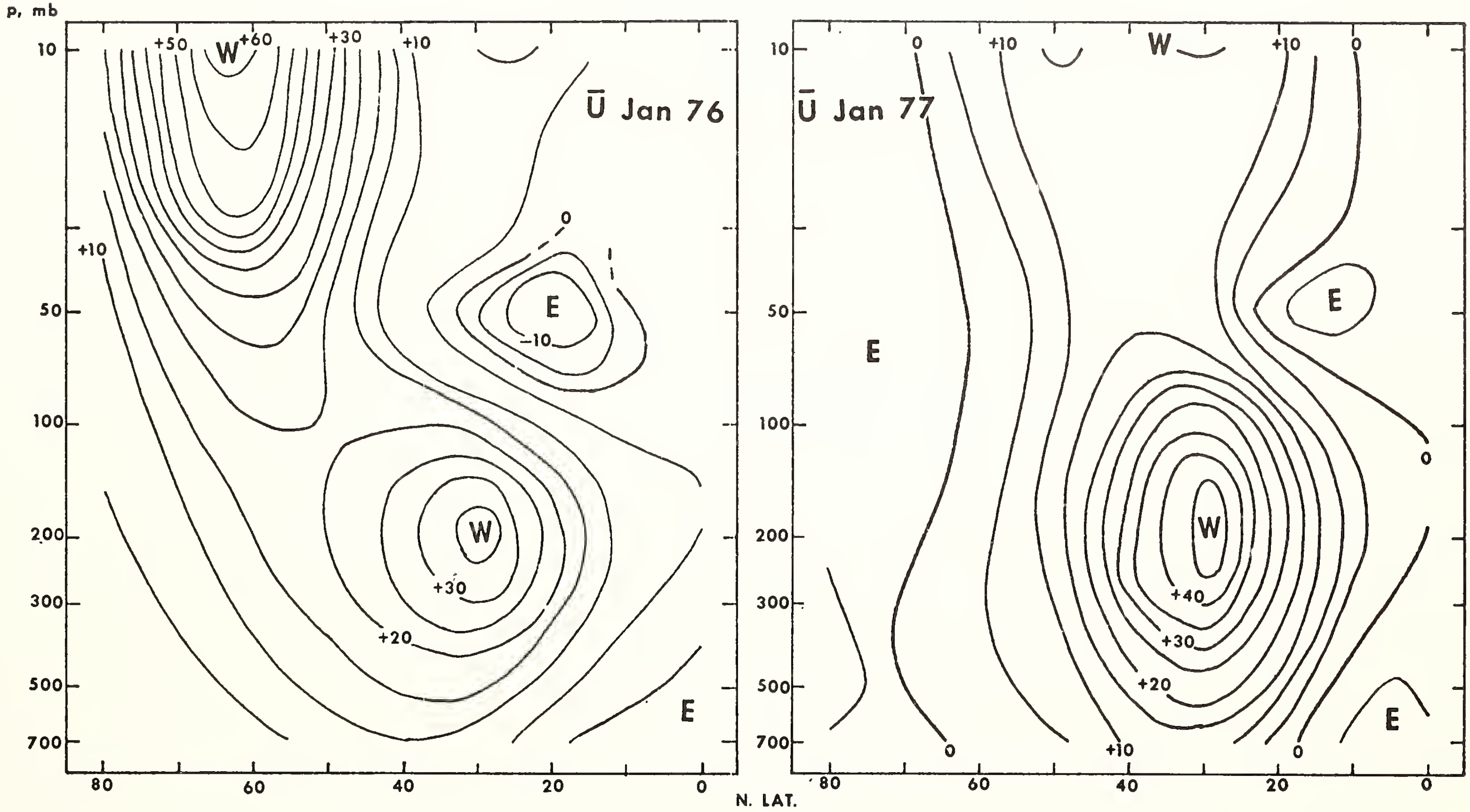

Fig. 2. Mean zonal wind, m s^{-1}, for January 1976 (left) and January 1977 (right).

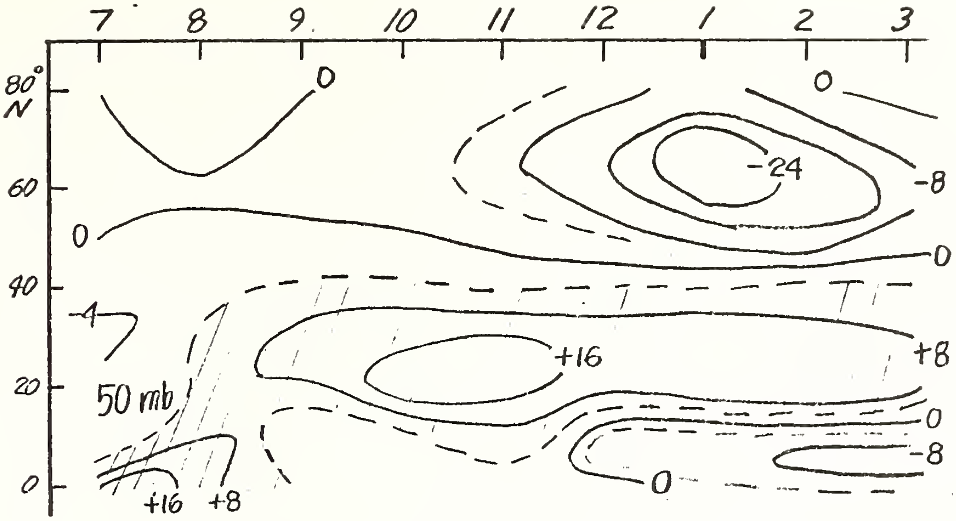

Fig. 3. Difference in mean zonal wind at 500, 200, and 50 mb from 1975-76 to 1976-77.

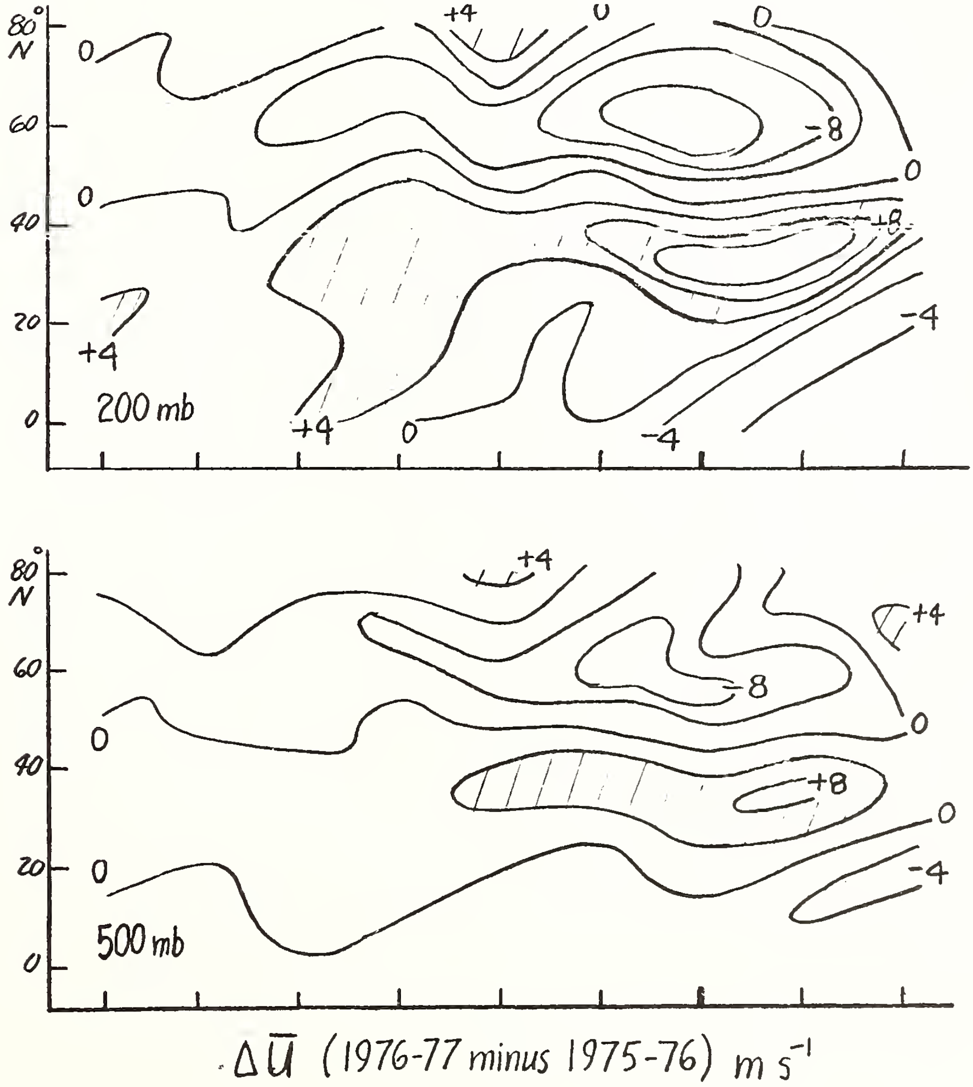

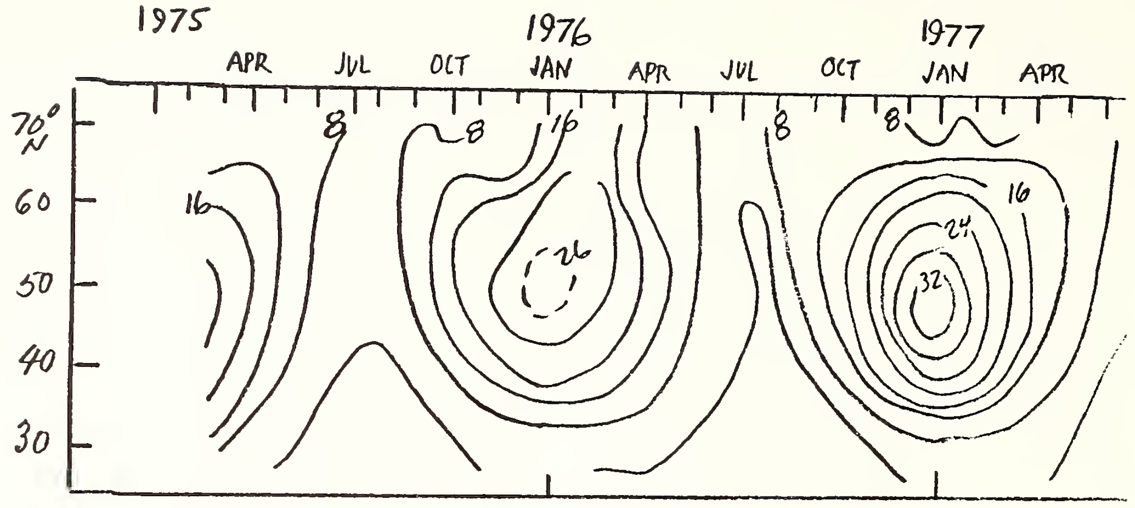

$\overline{v^*T^*}$, 850 mb, m s⁻¹ deg

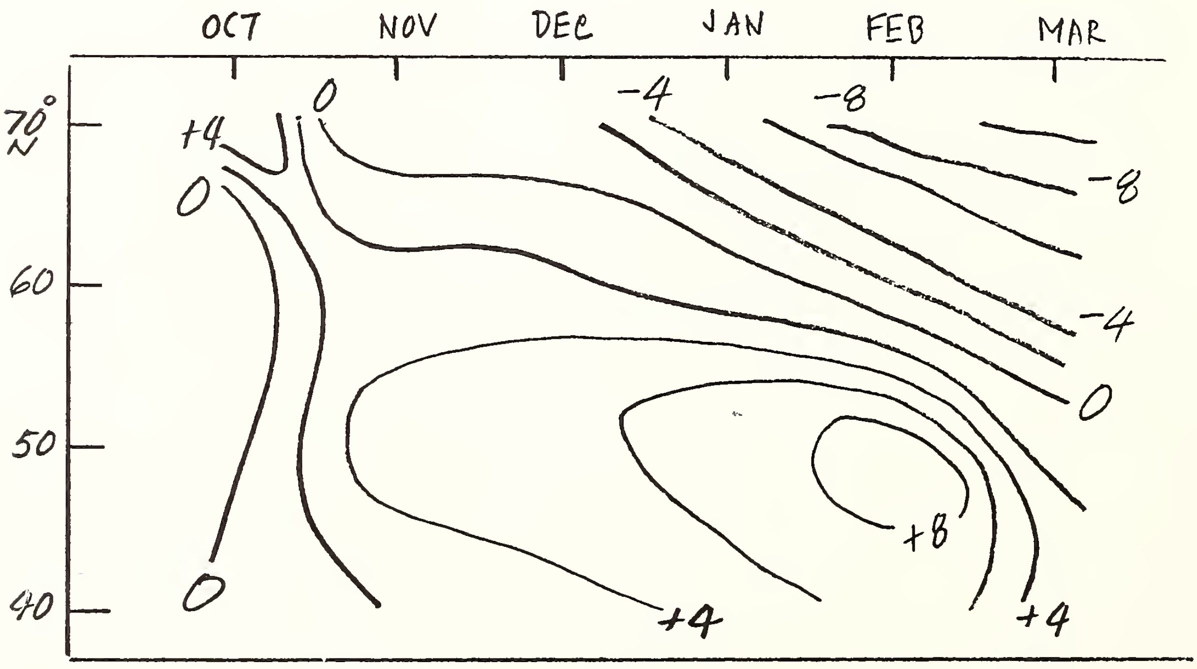

$\Delta\ \overline{V^*T^*}$, 850 mb (1976-77 minus 1975-76)

Fig. 4. Meridional eddy heat transport 1975-77, 850 mb (upper diagram) and difference from 1975-76 to 1976-77 (lower).

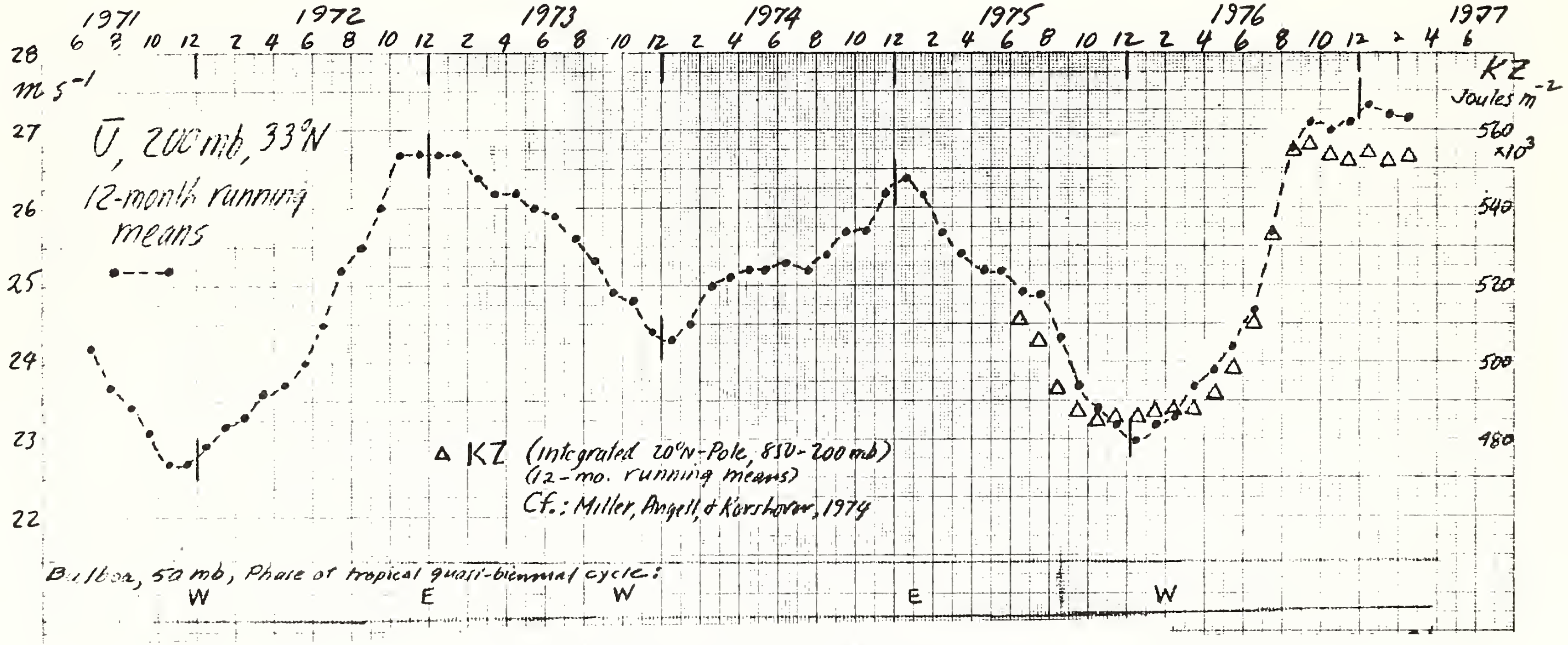

Fig. 5. Twelve-month running means of tropospheric zonal kinetic energy (triangles, 1975-77), suggesting 2-3 year cycle of type described by Miller, Angell, and Korshover (1974); and means of 200 mb mean zonal flow, 33°N (dots, 1971-77), indicating biennial cycle.

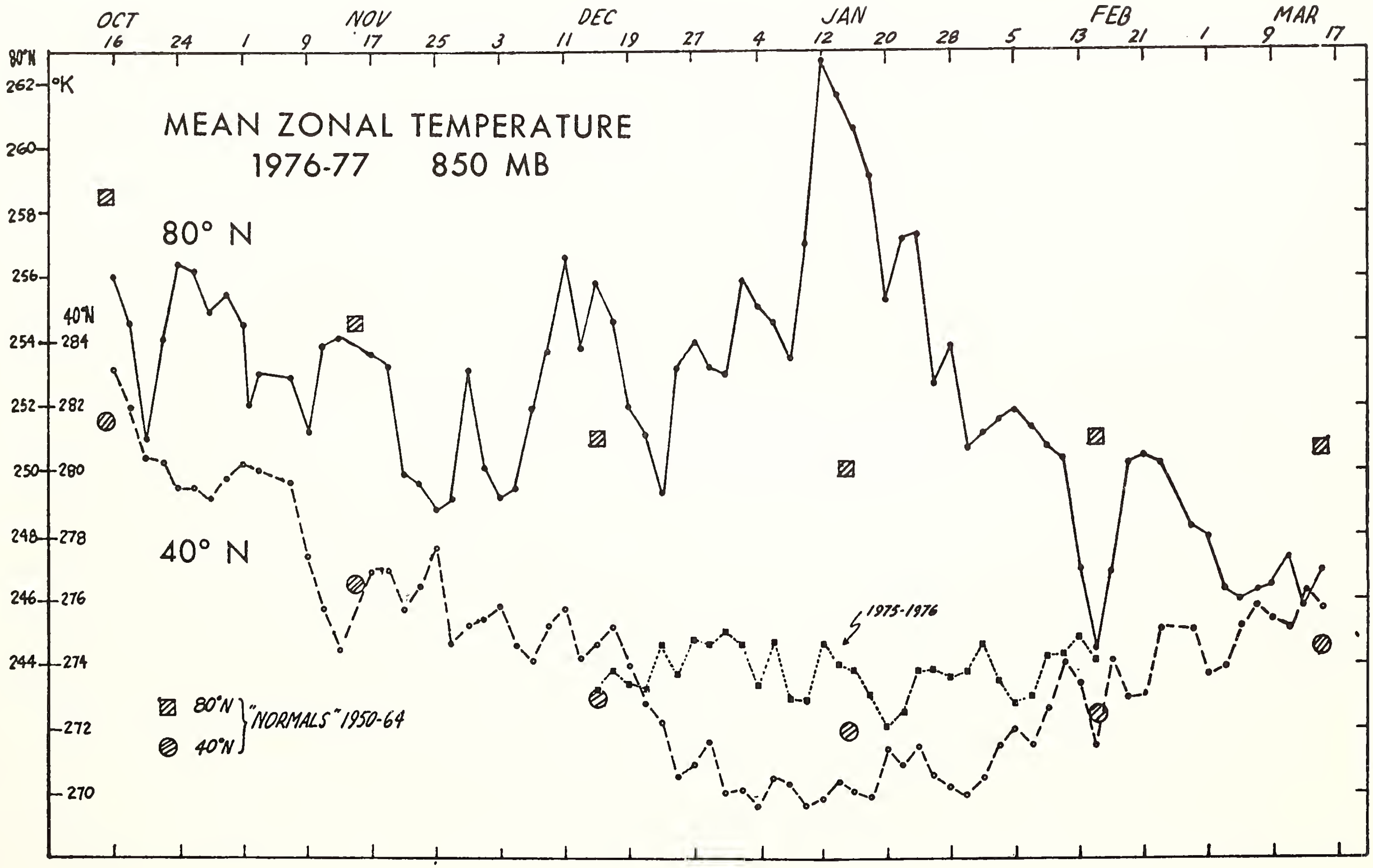

Fig. 6. Mean zonal temperatures, 850 mb, for 80 and 40°N, 1976-77. Compare with monthly normals.

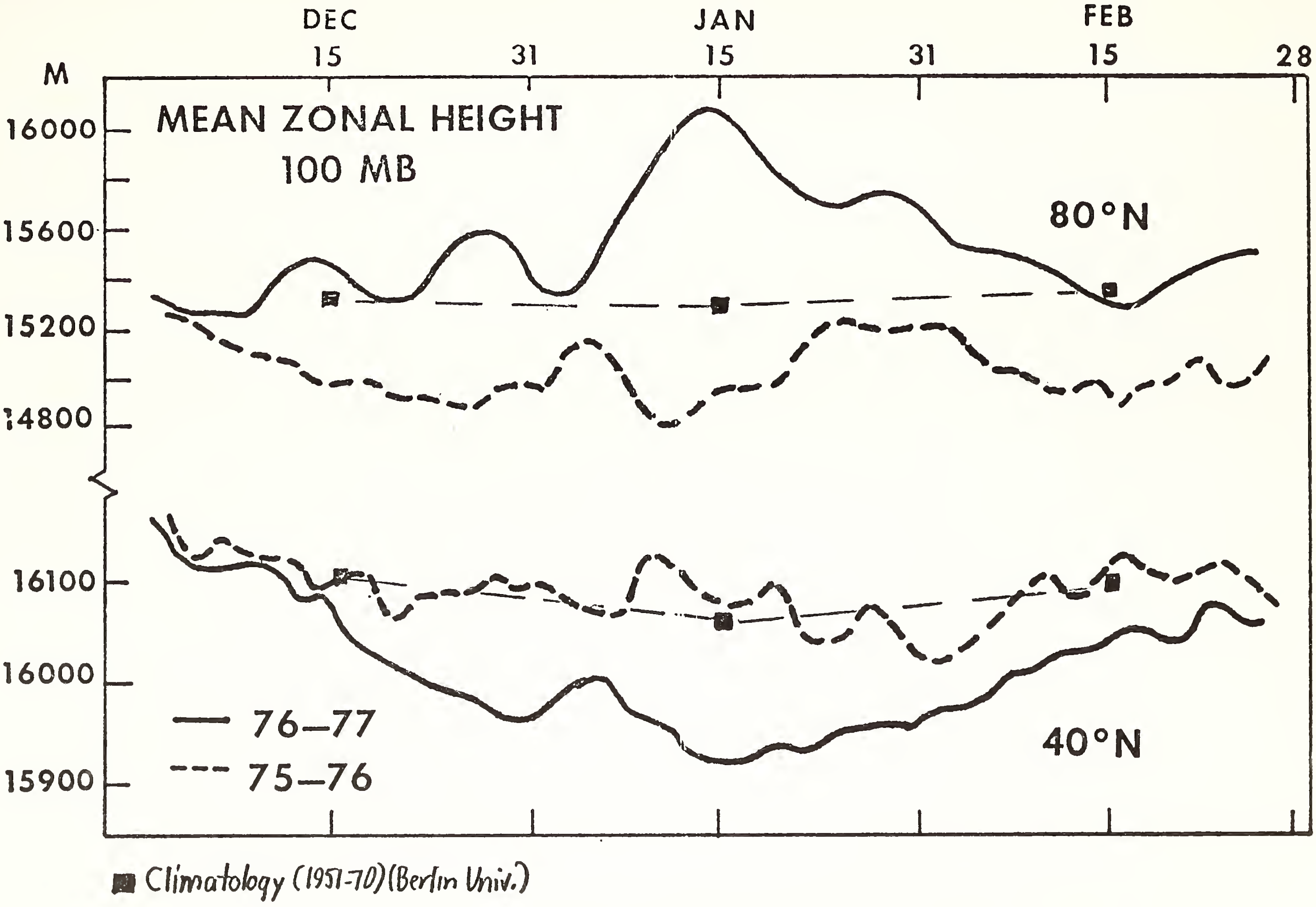

Fig. 7. Mean zonal heights of 100-mb surface in 1976-77 (solid lines) and 1975-76. For December 21-February 19, correlation between heights at 80 and 40°N is -0.88 (1976-77), -0.75 (1975-76).

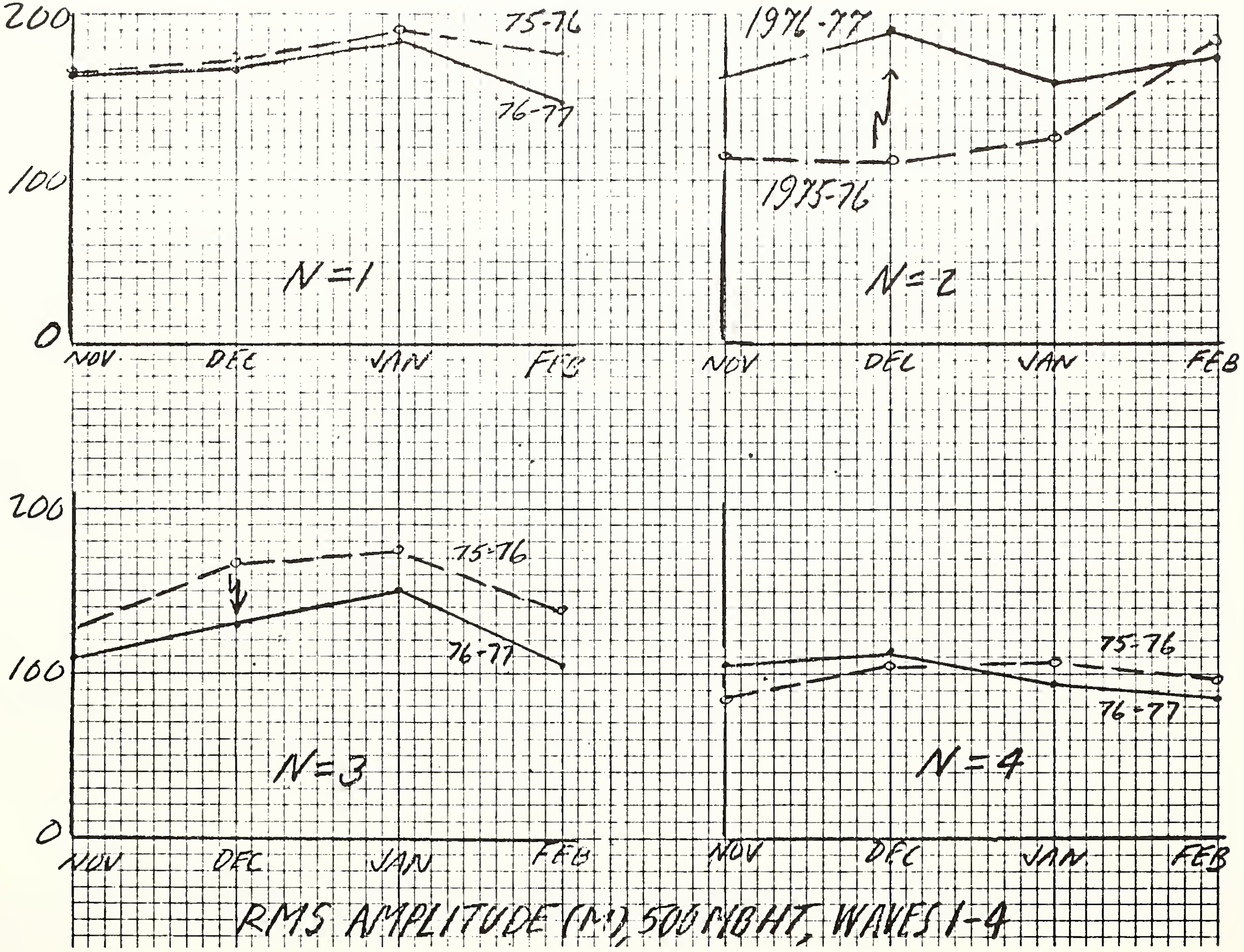

Fig. 8. Monthly RMS amplitudes of waves 1-4, 1975-76 and 1976-77 (based on bi-daily maximum amplitude at any latitude).

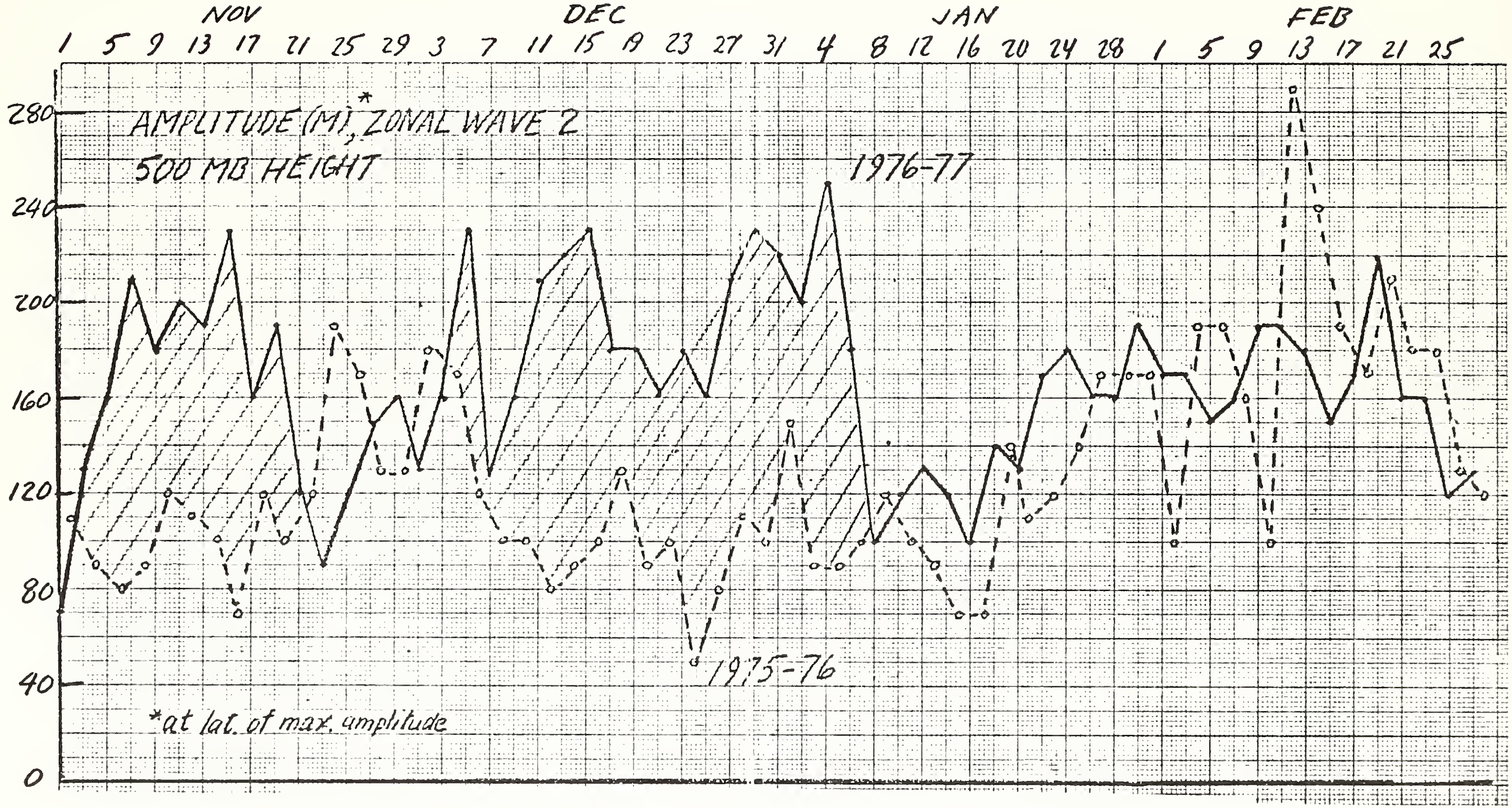

Fig. 9. Bi-daily maximum amplitude at any latitude for waves 1 and 2. Note sustained excesses of wave 2 November 3-21 and December 4-January 7 in 1976-77 versus 1975-76.

STRATOSPHERIC SUDDEN WARMING AND JANUARY 1977 WEATHER

J.P. McGuirk
Dept. of Meteorology
Texas A&M

Specific tropospheric flow patterns are associated with the occurrence of major stratospheric disturbances and sudden warmings (SSW). Because of this association, the flow patterns prevalent about and over the United States last January and February were not all that unusual; the conditions observed may be simply one of the more severe realizations of SSW. This paper makes no statement of exact cause and effect mechanism relating tropospheric and stratospheric flows, but suggests only that one exists.

Almost every winter between 1955 and the present has been marked with at least one major stratospheric disturbance. The tropospheric circulation anomalies during these events, based on a partial analysis of 18 years of data can be summarized as follows:

i) Tropospheric energy (principally zonal available potential energy) decreases (Table I) for an extended period of time (an average of 45% of the annual cycle amplitude for a period of at least a month).

ii) Midlatitude tropospheric temperatures decrease by 1-4°K. The major cooling occurs over continental areas which experience monthly temperature depressions averaging 1.5 standard deviations at the surface (figs. 1 and 8 and Table II).

iii) An anomalous blocking ridge developes over the Aleutian Islands at 500 mb (+120 m average height anomaly at 500 mb for 12 events; fig. 2). Occasionally this ridge appears months before a stratospheric disturbance is detected at 10 mb.

iv) Intensified northward eddy heat flux warms the Arctic fig. 1 and 3, and Table III) by 5-10°K.

v) The intensification of the long wave ridges, at least during 1963, led to a domination of the heat flux by the long waves with only small changes in the cyclone-scale flux.

Although less clear, the momentum balance of the troposphere becomes modified during the stratospheric disturbance. Data from only four years were available to justify these statements (January 1963, 1964-65 1969-70 and 1970-71):

vi) The zonal jet at 30°N and 250 mb intensifies slightly (fig. 4).

vii) During the stronger disturbances, upper midlatitude winds decrease. Following the stratospheric disturbance, average easterlies occasionally appear throughout the troposphere at 50-60°N. This effect results partly from the strong easterly jet appearing over continents (for example, 100+

knots over northeastern Canada at 500 mb in fig. 5), and partly from the lower stratosphere's mimicking upper stratospheric sudden warming. (For example, during the 1971 disturbance, the 100-200 mb layer experienced a reversal of the meridional temperature gradient and a considerable weakening of the average thermal wind.)

January 1977 experienced one of the strongest SSW on record (fig. 6). Oceanic ridges swept across the pole alternately from the Pacific and Atlantic. Records from throughout the 1976-77 winter season indicate that weather effects were being driven, in large part, by phenomena other than ones beginning only in late December 1976. Nevertheless, it is also apparent that a strong similarity exists between the January 1977 circulation and circulations accompanying other SSW (fig. 5). The extremely cold air normally appearing over east central Canada led to large intense polar outbreaks which were able to leave almost the entire U.S. in freezing weather (fig. 7).

An analysis of monthly mean surface temperatures (MMT) at 28 stations across the U.S. following four stratospheric disturbance periods (SSW in January 1963 and 1977 and February 1958, and a major stratospheric disturbance in January 1971) is shown in fig. 8, and Table II. The MMT of these four periods were compared with climatological values from an independent 15 year sample. To the right of the solid line in fig. 8 anomalies at 15 out of 18 stations were found to be lower than climatology with a confidence exceeding 90%. (It is noted that with a sample of only four events confidence must be viewed circumspectly.) The average negative anomaly for the four months at these 18 stations was 1.3 standard deviations. To the left of the line, the average of the absolute value of the anomalies of MMT exceeded one standard deviation at 7 out of 10 locations. The conclusion is that during SSW cold air is advected into the midwest and east, and, depending on the exact position of the Pacific ridge, either very warm or very cold air becomes established over the west. This phenomenon persists for at least thirty days.

Although there may be several causes for the anomalies occurring during the 1976-77 winter, the manner in which the January severity manifested itself suggests that at least the January anomalies are associated with SSW.

TABLE I Tropospheric energy changes occurring during stratospheric disturbances and sudden warming events.

SEASON	ΔA_Z	ΔA_E	ΔK_Z	ΔK_E	ΔE	DATES	MAJOR SSW
63-64	-10.84	-1.06	+ 1.07	+ .91	- 9.92	1/8 - 1/13	no
64-65	- 8.93	+3.16	+ 1.16	+6.26	+ 1.65	12/30- 1/16	no
65-66	- 7.77	- .85	+ 1.23	- .74	- 8.13	2/15- 2/23	no
66-67	-12.53	+3.04	+ .61	+3.95	- 4.93	11/25-12/1	no
67-68	-11.21	-2.14	+ 3.08	+3.81	- 6.46	1/1 - 1/14	yes
68-69	-13.82	+1.65	- 2.53	+5.82	- 8.88	12/20- 1/4	yes
69-70	- 8.10	+ .67	+ 1.56	+ .11	- 5.76	2/11- 3/1	yes
70-71	-16.71	+ .75	- 2.50	+2.47	-15.99	12/30- 2/2	no
71-72	-13.70	- .54	- 1.41	+ .52	-15.13	1/10- 2/3	yes
9-Year Ave.	-11.51	+ .52	+ .25	+2.57	- 8.17	15 days	
Major SSW Ave.	-12.71	+ .33	- .95	+2.55	-10.78	20 days	
Ave. Annual Cycle Amplitude	27	7	13	6	---	---	

TABLE II

Mean monthly temperature anomalies for 28 stations during four SSW periods

	4 event average	February 1958	January 1963	January 1971	January 1977
Negative Anomalies					
Number of stations	21	17	24	16	25
Percentage	74%	61%	86%	59%	90%
Average Negative Anomaly	1.5σ	1.5σ	1.6σ	$.75\sigma$	1.85σ
Average Positive Anomaly	1.0σ	1.3σ	---	1.0σ	---

TABLE III Comparison of tropospheric heating by various mechanisms for the atmosphere north of 75°N. (Jan. 1971)

MECHANISM	TOTAL HEATING	SOURCE
Average January Poleward Flux of Total Energy	34.5°C	Oort (1971)
Long Wave Radiation from Stratosphere	3.9°C	Ramanathan (1977)
Geostrophic Eddy Heat Flux Anomaly	5.1°C	
Observed Polar 10-Day Temperature Increase	7.0°C	McGuirk (1977a)

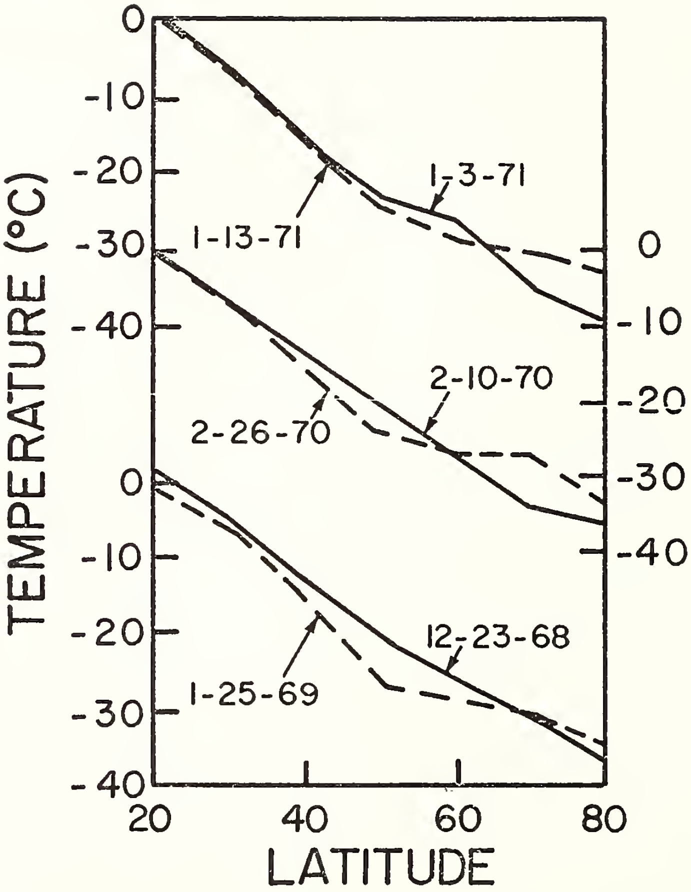

Fig. 1 Profiles of zonally averaged temperatures for the layer 1000-300 mb before and during three periods of strong stratospheric disturbance.

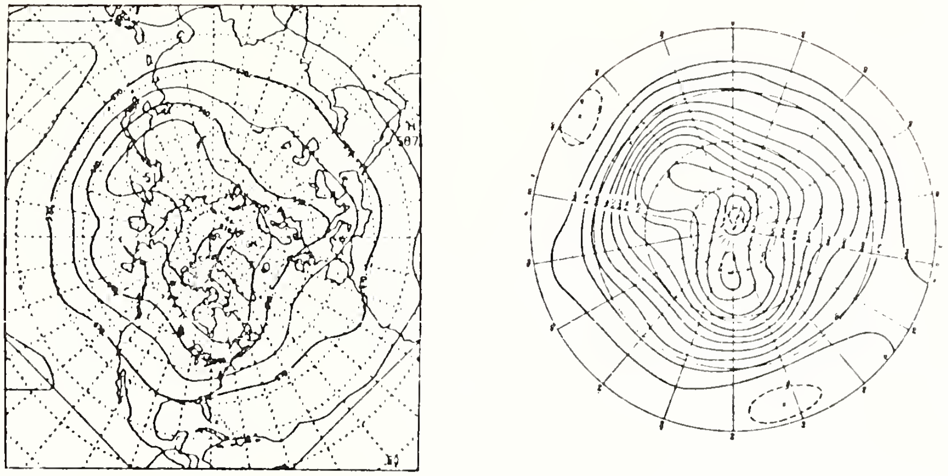

Fig. 2 Mean 500 mb height field (contour interval= 150 m) for twelve days during major stratospheric disturbances (left); climatological mean 500 mb height field (contour interval = 80 m) (right). Note the 120 m height anomaly over Alaska and south of the Bering Strait.

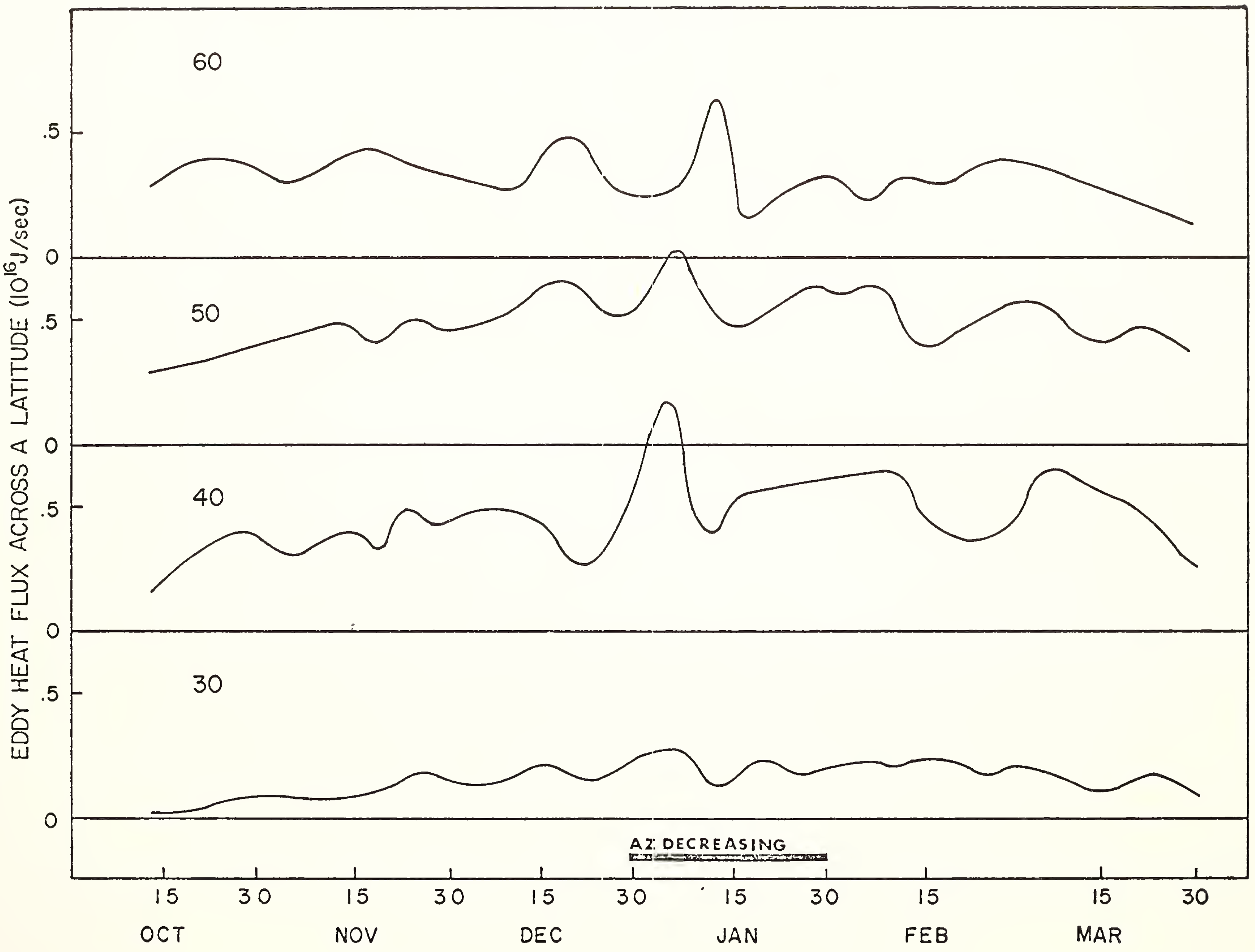

Fig. 3 Total tropospheric geostrophic eddy heat flux across four latitudes for the 1970-71 winter season. The peaks in early January correspond to the period of disturbed stratosphere.

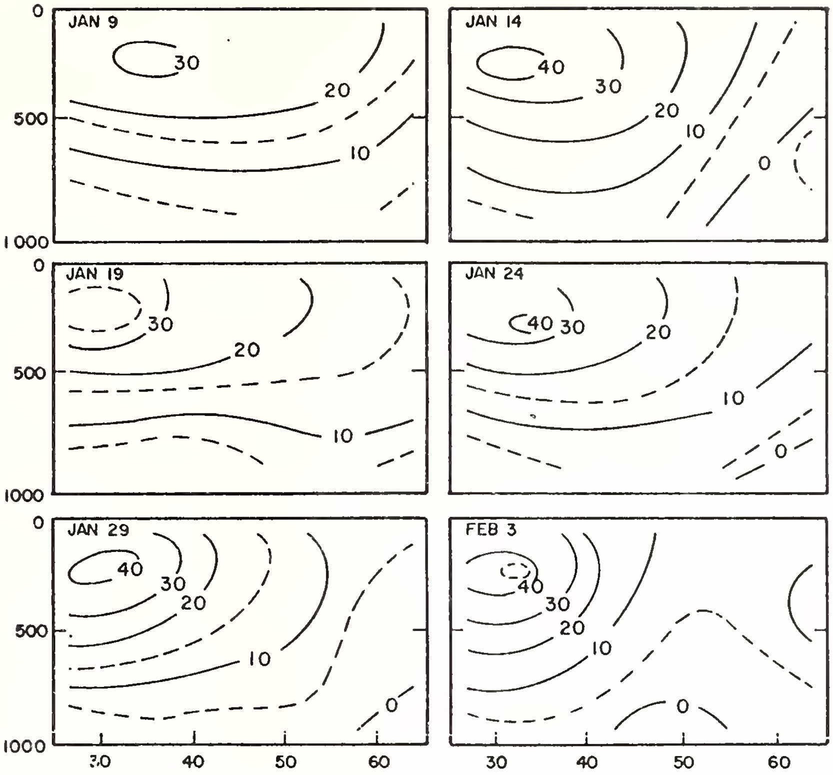

Fig. 4 Meridional cross sections of the geostrophic zonal wind during the 1971 stratospheric disturbance period.

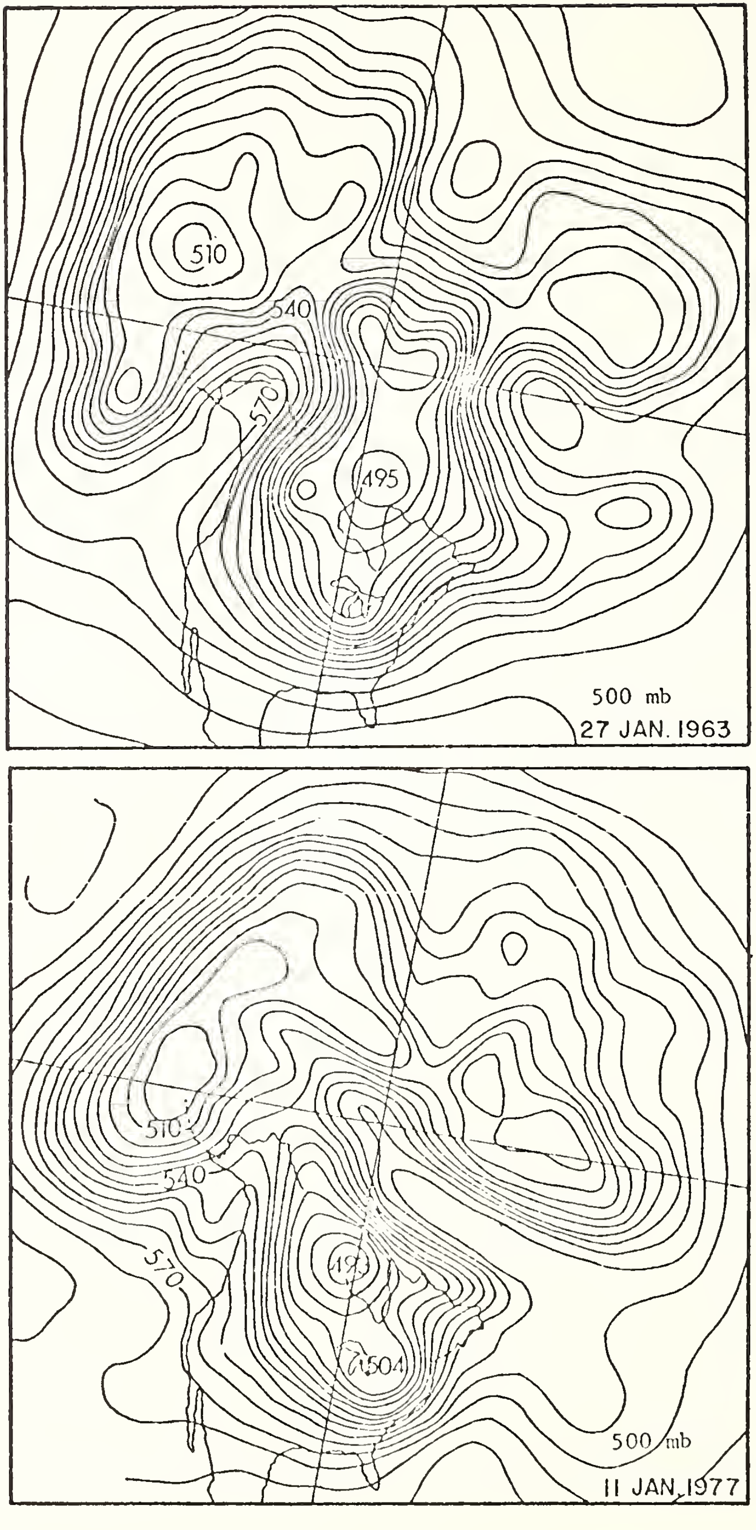

Fig. 5 500 mb height fields (contour interval = 60 meters) during two stratospheric sudden warming events.

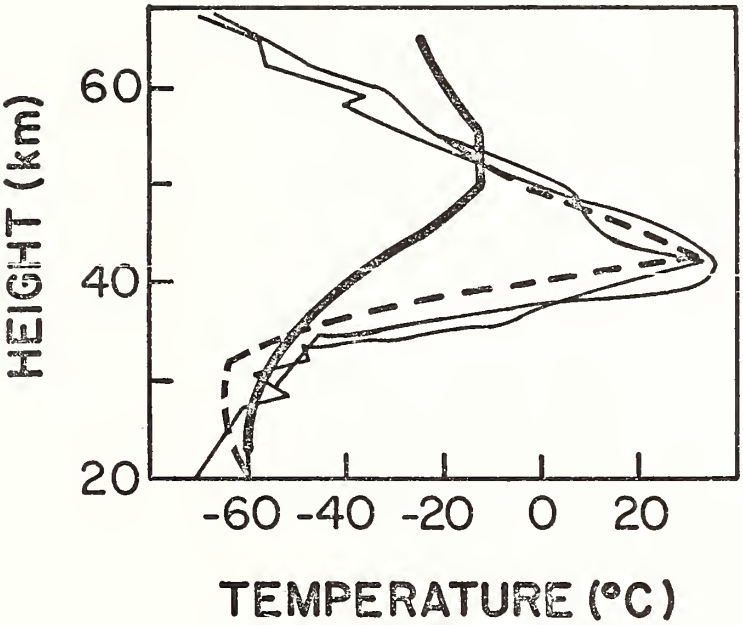

Fig. 6 Stratospheric temperature soundings over Thule (light solid lines) and Churchill (dashed line) during the first week of January 1977, and the January climatological mean (heavy line).

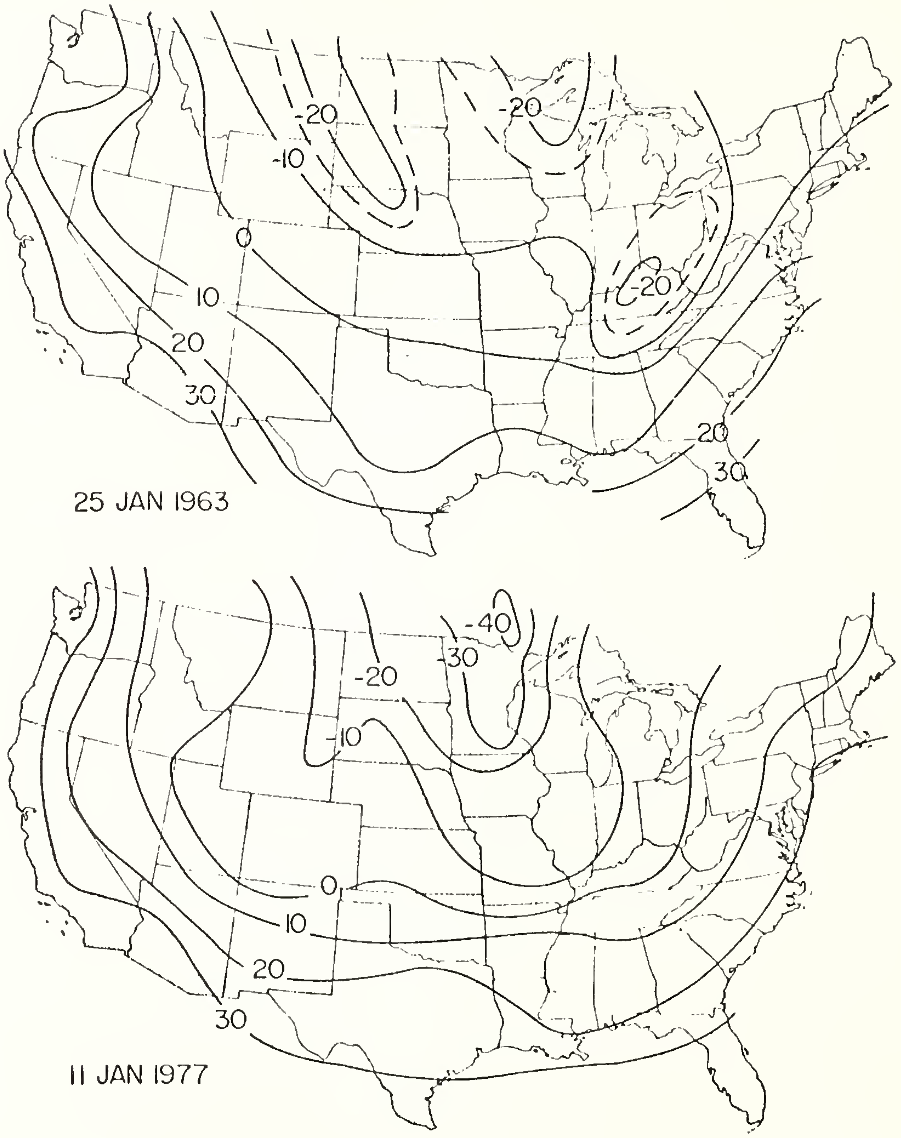

Fig. 7 Surface night time minimum isotherms (in °F) for two days during strong SSW periods.

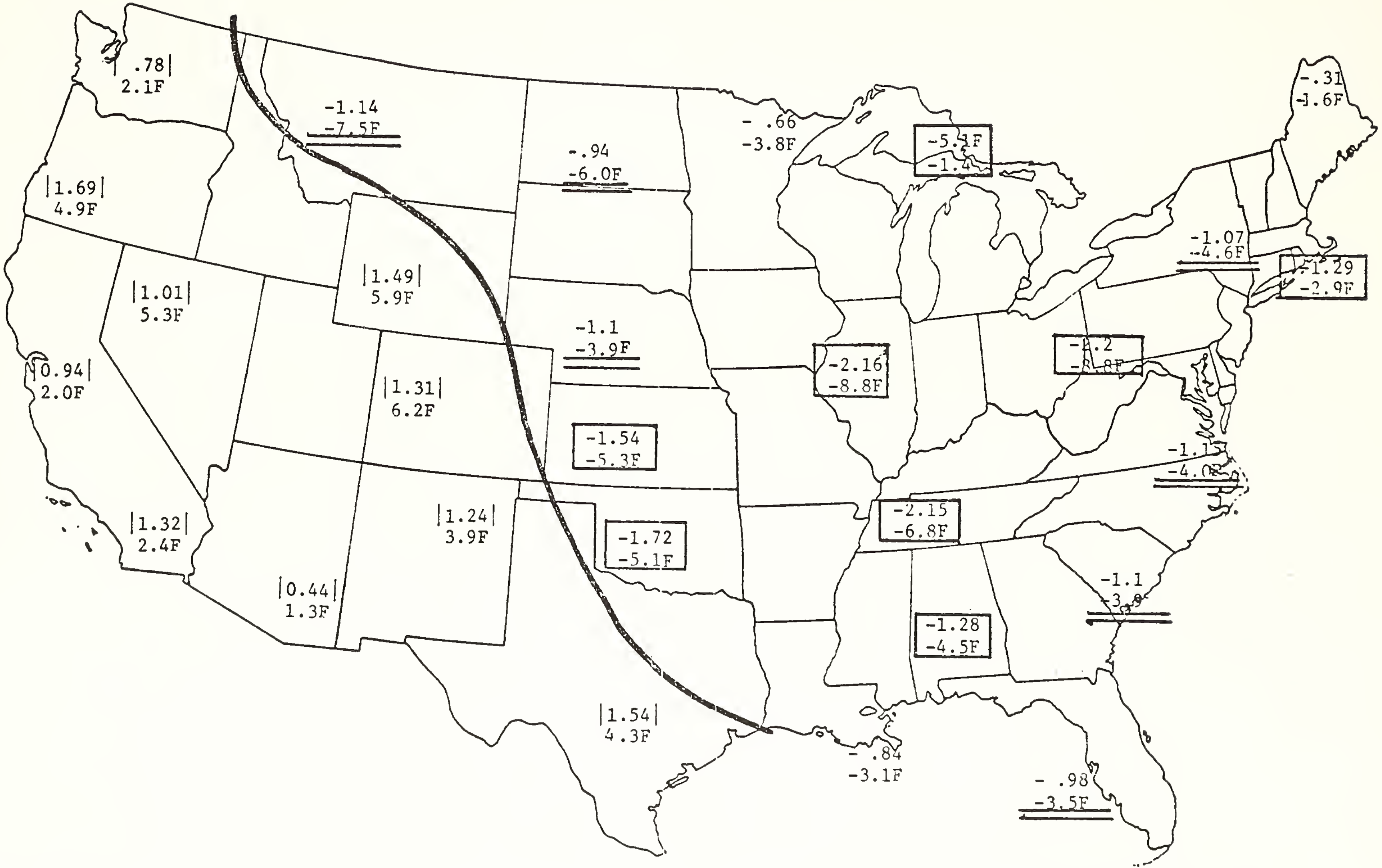

Fig.8 Average mean monthly temperatures (bottom numbers, in Fahrenheit), and climate anomalies (top numbers, in units of standard deviations) for four SSW periods. To the right of the heavy line, arithmetic averaging was used; to the left of the heavy line, an average of absolute deviations was used. Boxed quantities differ from climatology with a confidence exceeding 99%; underlined quantities, with a conficence exceeding 90%.

The Satellite Snowcover Record: Status, Trends, and Relationships

by

Michael Matson
NOAA/National Environmental Satellite Service

Recently the NOAA/NESS 11-year satellite-derived continental winter snowcover record was expanded to include all of the non-winter months. The data set, in the form of monthly mean snowcover maps and their corresponding areal snowcover values, is now complete for all months from November 1966 through September 1977 with the exception of December 1967 and January 1968. The completion of the snowcover data base will (a) facilitate the updating of continental snowcover extent on a monthly basis, and (b) establish an initial climatological data base for monitoring Northern Hemisphere snowcover variability.

From the snowcover data a 12-month running mean of monthly mean snowcover was determined for North America, Eurasia, and the Northern Hemisphere (figure 1). The plot shows a very slight 11-year increase in North American snowcover extent. Eurasia and the Northern Hemisphere, however, had two large increases in snowcover extent; one from 1971-72, and the second from 1976-77. An overall increasing trend in snowcover extent is also evident for both of these areas.

A graphical analysis of the North American and Eurasian 1976-77 winter snowcover extent values and how they compare with the past ten winters of the satellite snowcover record is shown in figure 2. The North American January 1977 snowcover was the highest for North America of the 11-year satellite record. The record January snowcover blanketed 65% of North America and by coincidence, 65% of the contiguous United States. In the Northeast and Midwest the snowline for January was 500 to 600 km south of the 10-year satellite-derived mean snowline (figure 3). There was a deficit of snowcover, however, in the western states.

Figure 2 also shows that Eurasia experienced its second consecutive year of increasing snowcover extent with the winter of 1976-77 being the third highest of the 11-year satellite record. January 1977 was also an 11-year record high Eurasian snowcover extent with 49% of the land mass snow-covered. Most of this increase occurred in Europe and Central Asia.

Even though January 1977 was approximately two standard deviations greater than the average snowcover extent in North America (see Table 1), the other winter months (i.e., December, February, and March) were within the expected standard deviation for these months. It would appear that the record-setting North American January snowcover was the result of an unusual combination of oceanological and meteorological conditions rather than an indication of global climatic change. Table 1 also shows that December 1976 and January 1977 were unusual snowcover months in Eurasia, whereas February and March were within the expected limits of snowcover extent.

Figure 4 shows the monthly mean snowcover maps for North America and Eurasia during the winter of 1976-77. Items of note are (a) the lack of snowcover in the western United States, (b) the large snowcover extent on both continents in January, and (c) the rapid retreat of the snowline on both continents in February and March.

As first reported by Wiesnet and Matson (1976), several statistical relationships between winter months in Eurasia and the Northern Hemisphere have been derived from the snowcover data base. Figures 5-10 are updates of the relationships. Figure 11 is a graph which shows the results of testing the regression equations of figures 5-10 during the winter of 1976-77. The North American estimates are derived by simple subtraction of the Eurasian estimate of the month desired from the corresponding Northern Hemisphere estimate. The Eurasian and Northern Hemisphere March estimates are derived by subtracting the January measured values plus the February estimates from the January through March estimates.

An additional statistical relationship has been derived involving the Eurasian snowcover data and Arctic sea ice cover data (Sanderson, 1975; Atkins, personal communication, 1977). A comparison of the average Eurasian winter snowcover extent (December-March) with antecedent September Arctic sea ice cover in the 0^0-90^0E quadrant shows an inverse relationship between the two data sets (figure 12). Figure 13 is the regression analysis of the relationship. The snowcover data in figures 12 and 13 have been corrected to correspond to a true surface area instead of the usual correction corresponding to an equal area projection. All of the snowcover data (as in figure 1) is now in the process of being formatted to represent true surface area.

References

Sanderson, R.M., 1975: Changes in the area of Arctic sea ice 1966 to 1974, The Meteorological Magazine, 104, 313-323.

Wiesnet, D.R., and M. Matson, 1976: A possible forecasting technique for winter snowcover in the Northern Hemisphere and Eurasia, Monthly Weather Review, 104, 828-835.

TABLE 1

Nine and Ten-Year Averages of Monthly Winter Continental Snow Cover and Comparison with 1976-77 Winter Snow Cover

Continent	Month	Number or data points	Average ($\times 10^6$ km^2)	Standard deviation ($\times 10^6$ km^2)	1976-77 Snow Cover ($\times 10^6$ km^2)
Eurasia	December	9	20.0	1.9	22.4
Eurasia	January	9	23.0	2.0	26.5
Eurasia	February	10	23.7	3.0	25.6
Eurasia	March	10	19.8	2.3	19.3
North America	December	9	13.7	1.0	14.1
North America	January	9	14.8	.5	15.8
North America	February	10	14.4	.5	14.4
North America	March	10	13.1	1.0	12.8

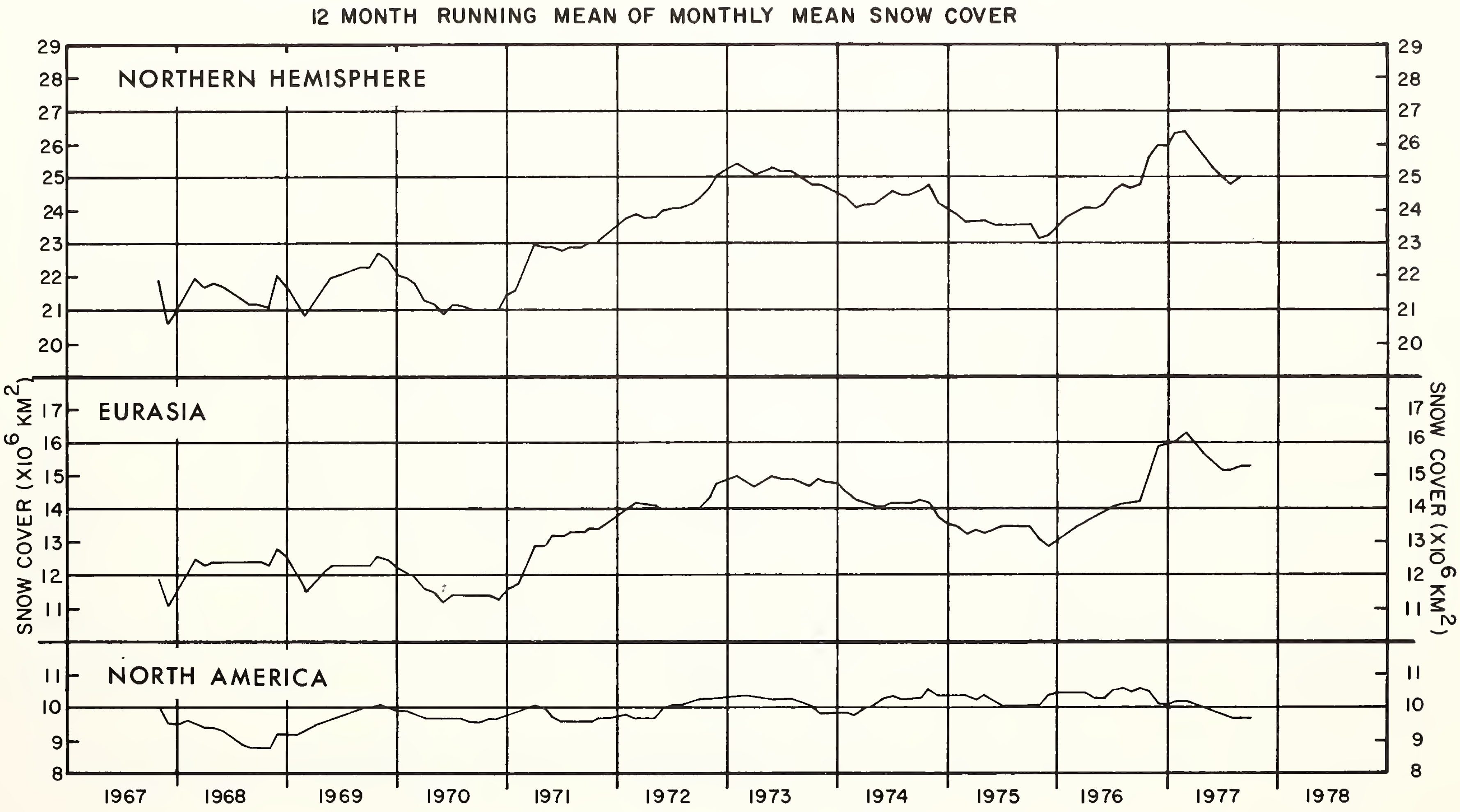

Fig. 1. 12-month running mean of monthly mean snowcover for North America, Eurasia, and the Northern Hemisphere for the period 1966-1977.

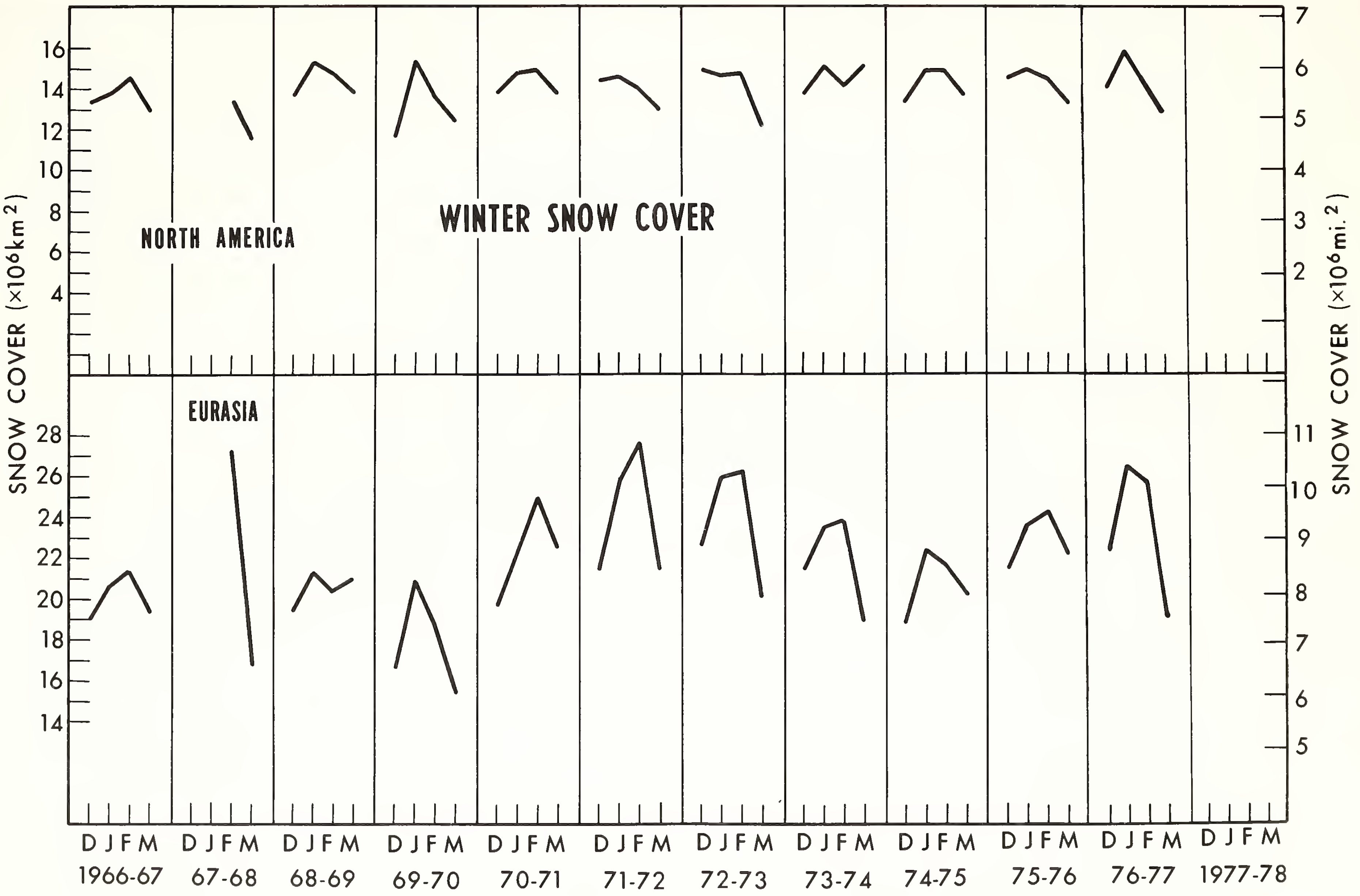

Fig. 2. Monthly mean winter snowcover of North America and Eurasia for the period 1966-1977.

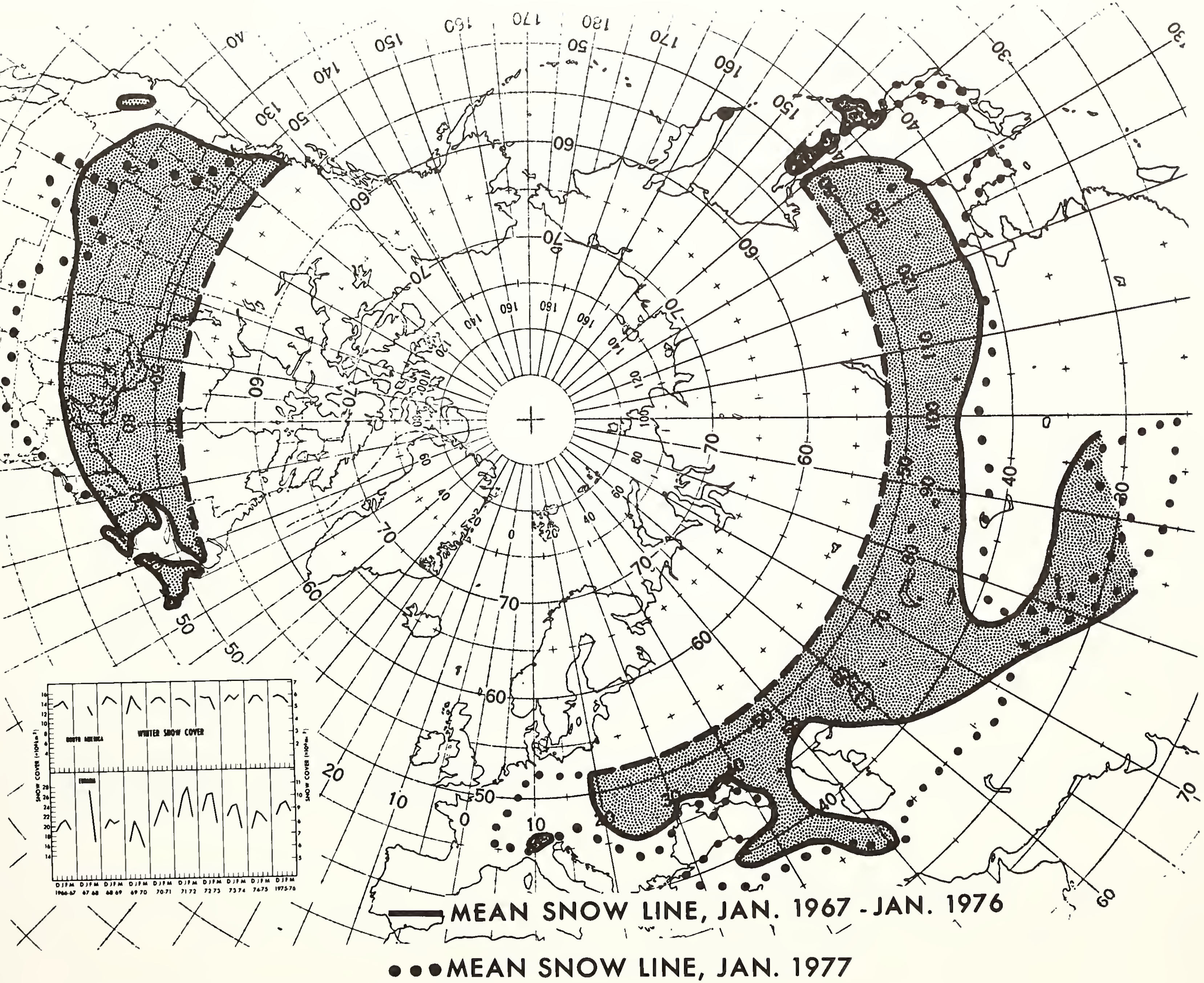

Fig. 3. Comparison of the satellite-derived mean snowline for January 1977 and the 10-year satellite-derived mean snowline.

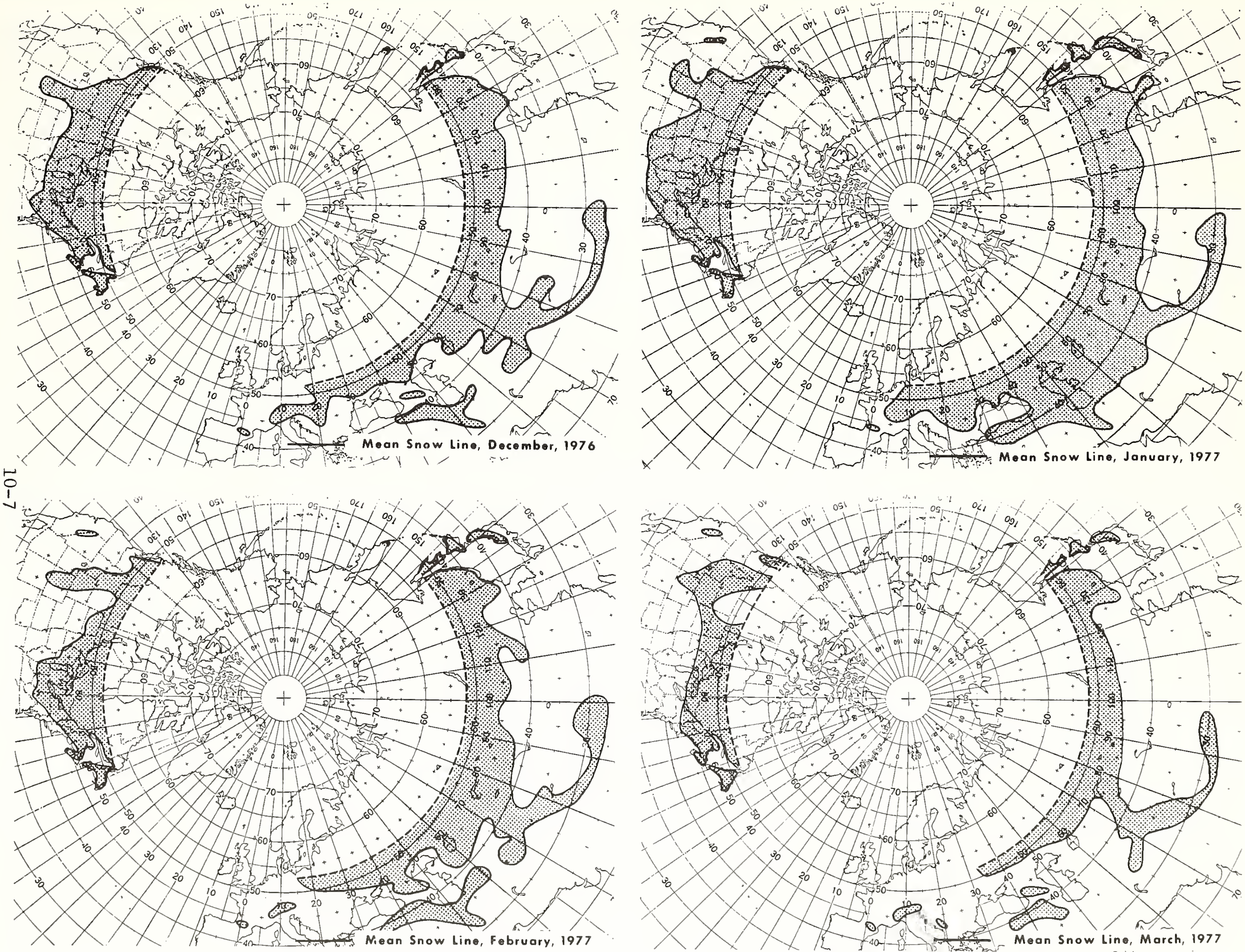
Mean Snow Line, December, 1976
Mean Snow Line, January, 1977
Mean Snow Line, February, 1977
Mean Snow Line, March, 1977

Fig. 4. Monthly mean snowcover maps of North America and Eurasia for December 1976, January 1977, February 1977, and March 1977.

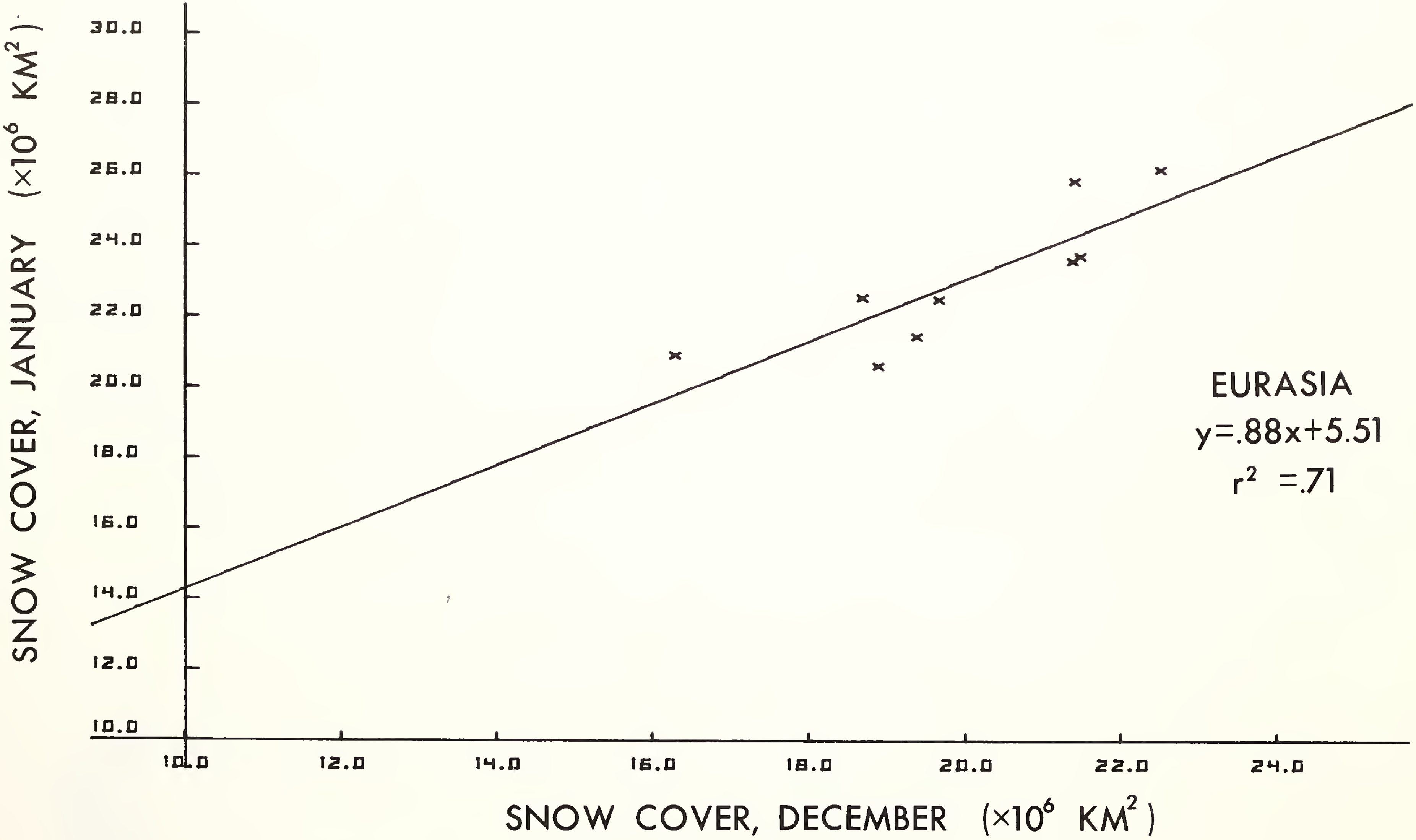

Fig. 5. Regression analysis of Eurasian January snowcover vs. Eurasian December snowcover.

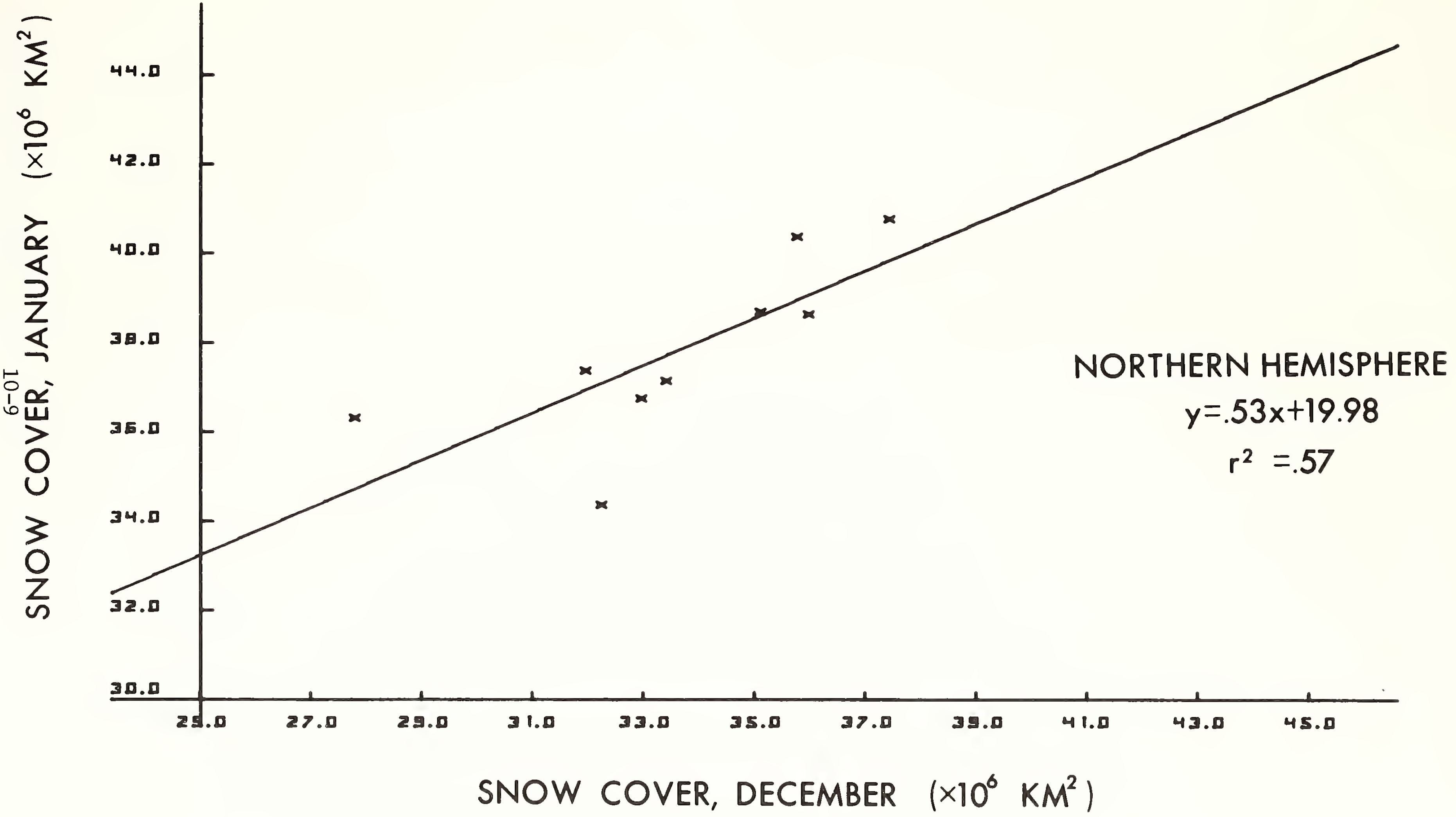

Fig. 6. Regression analysis of Northern Hemisphere January snowcover vs. Northern Hemisphere December snowcover.

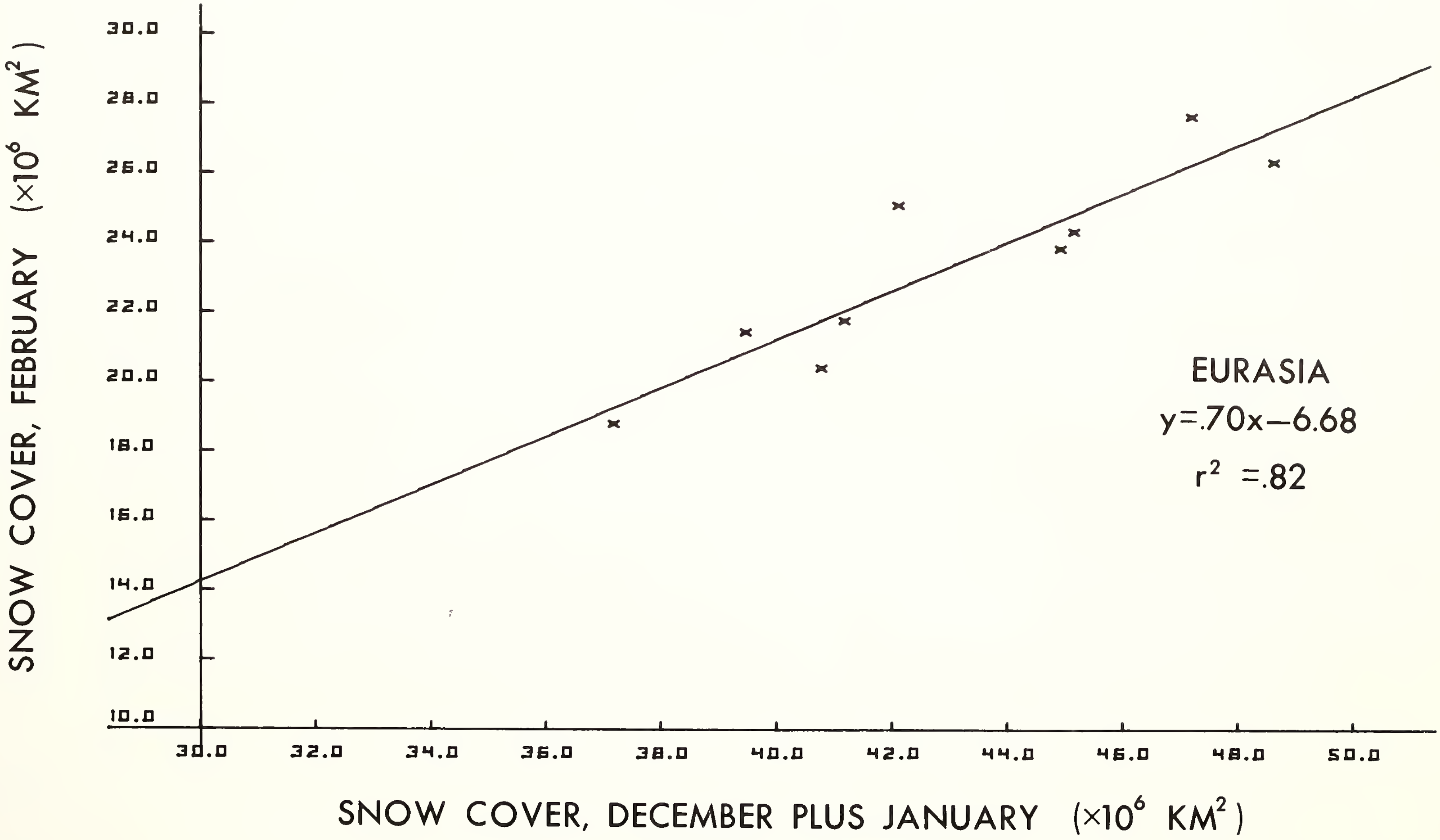

Fig. 7. Regression analysis of Eurasian February snowcover vs. Eurasian December plus January snowcover.

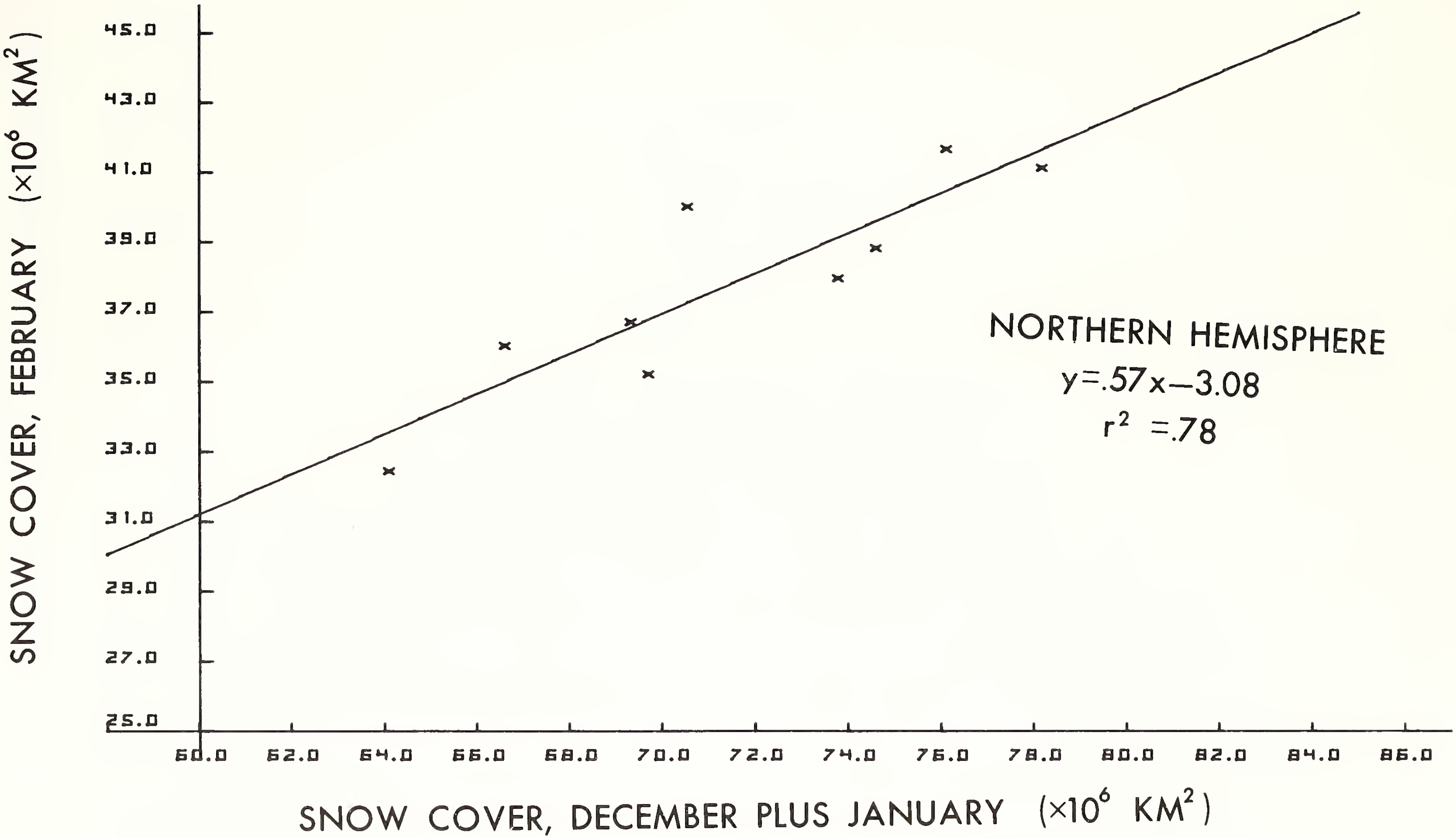

Fig. 8. Regression analysis of Northern Hemisphere February snowcover vs. Northern Hemisphere December plus January snowcover.

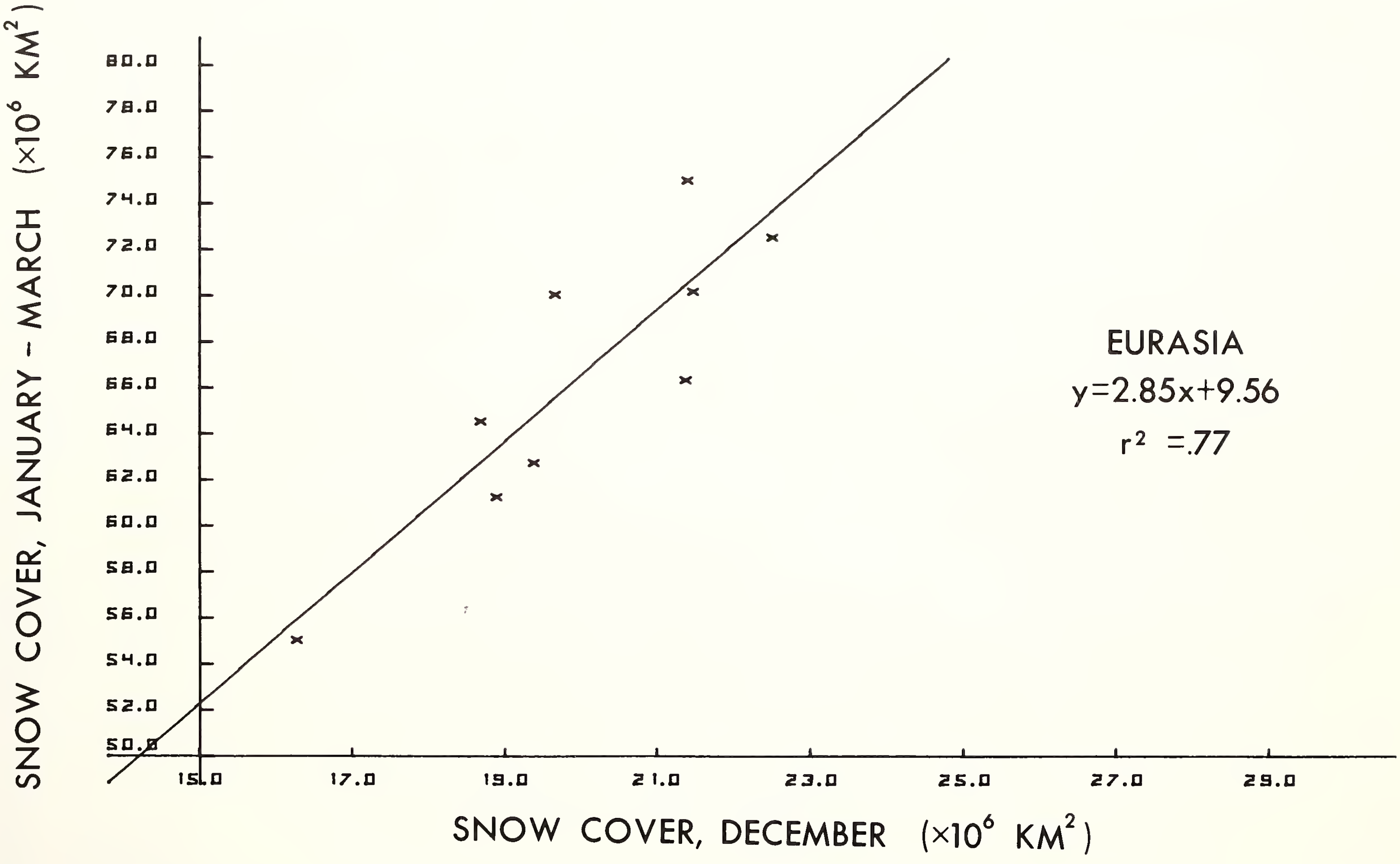

Fig. 9. Regression analysis of Eurasian January through March snowcover vs. Eurasian December snowcover.

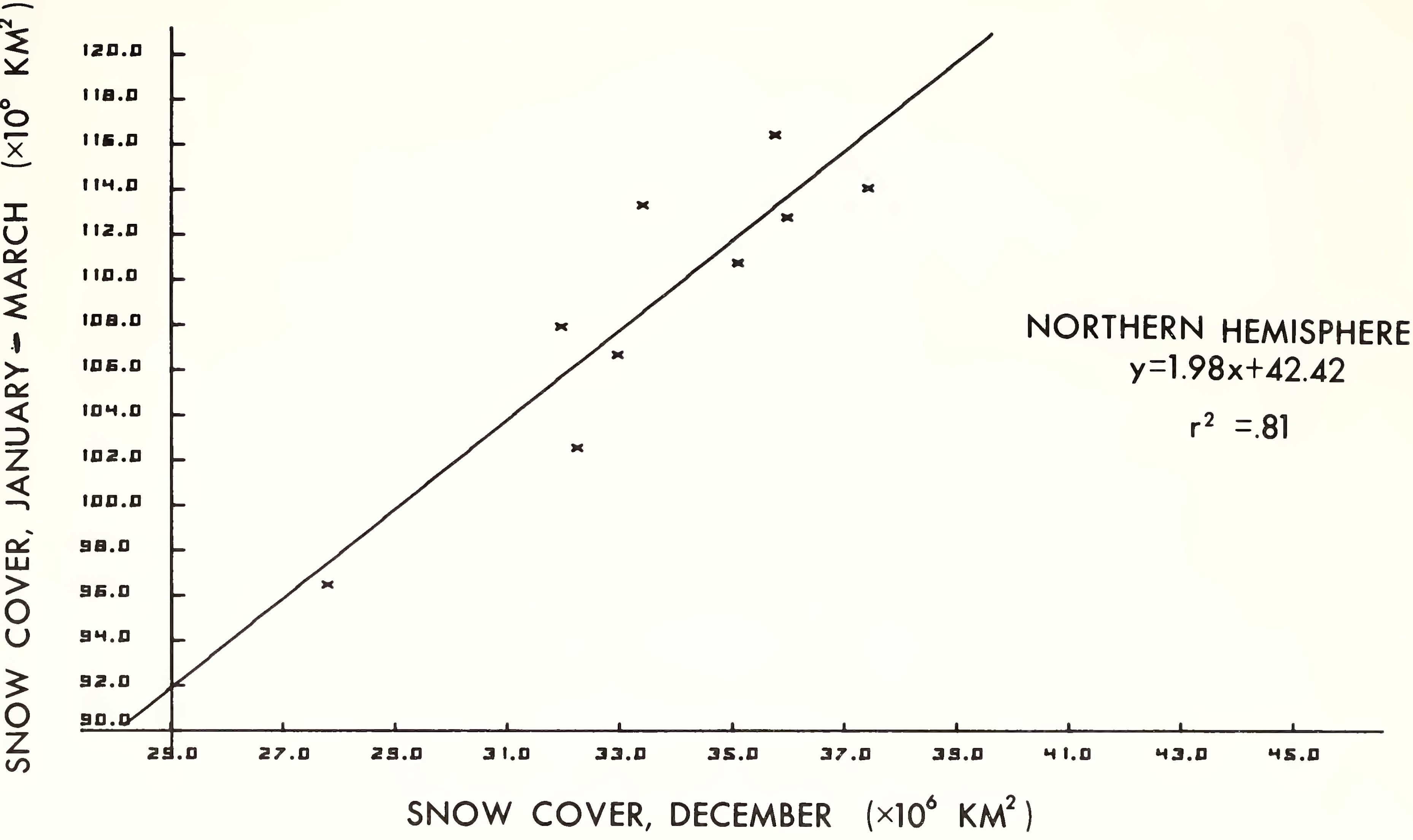

Fig. 10. Regression analysis of Northern Hemisphere January through March snowcover vs. Northern Hemisphere December snowcover.

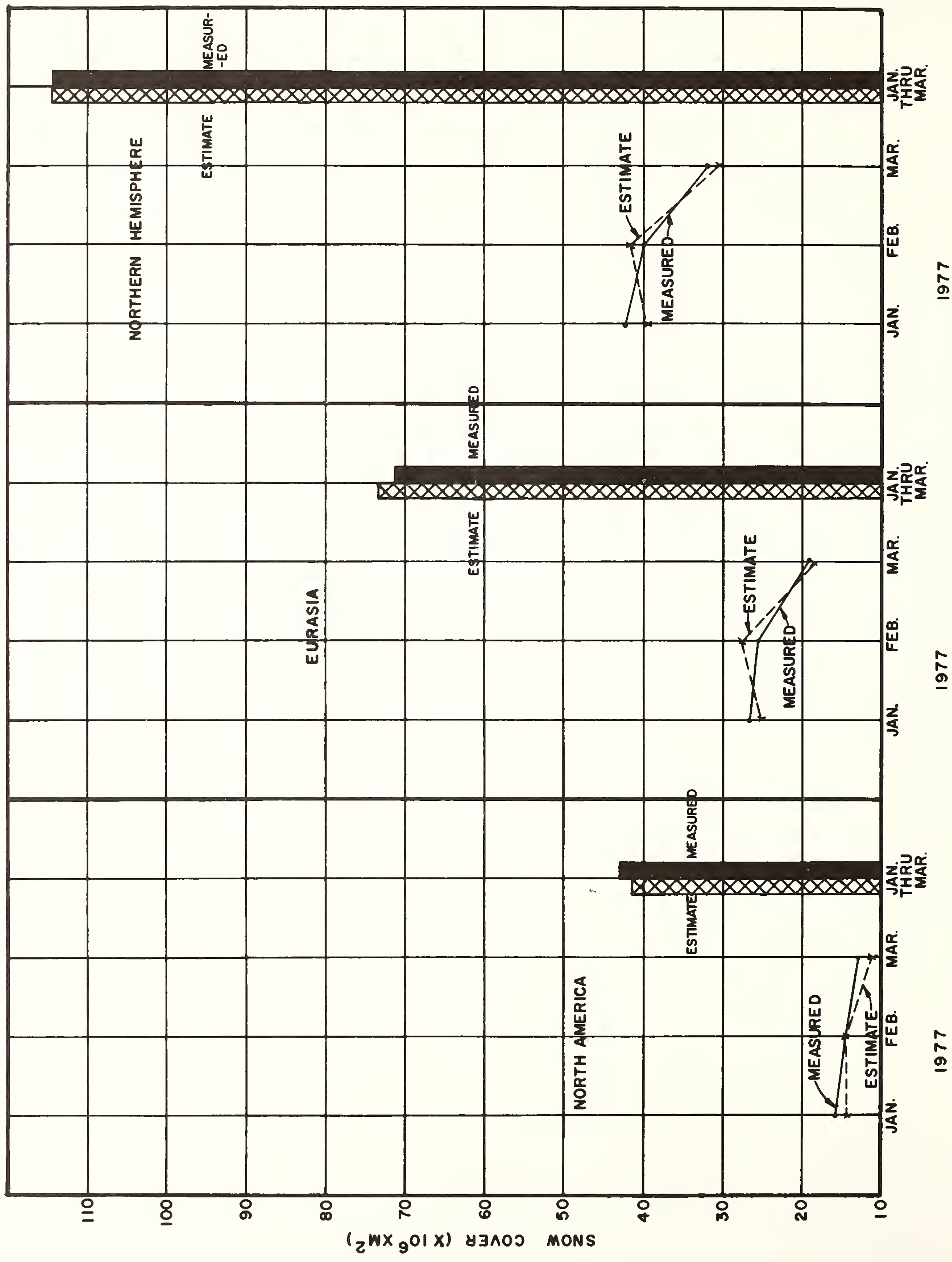

COMPARISON OF WINTER 1977 SNOW COVER ESTIMATES vs. WINTER 1977 SNOW COVER MEASUREMENTS NORTHERN HEMISPHERE

Fig. 11. Winter 1977 snowcover extent estimates vs. winter 1977 snowcover extent measurements.

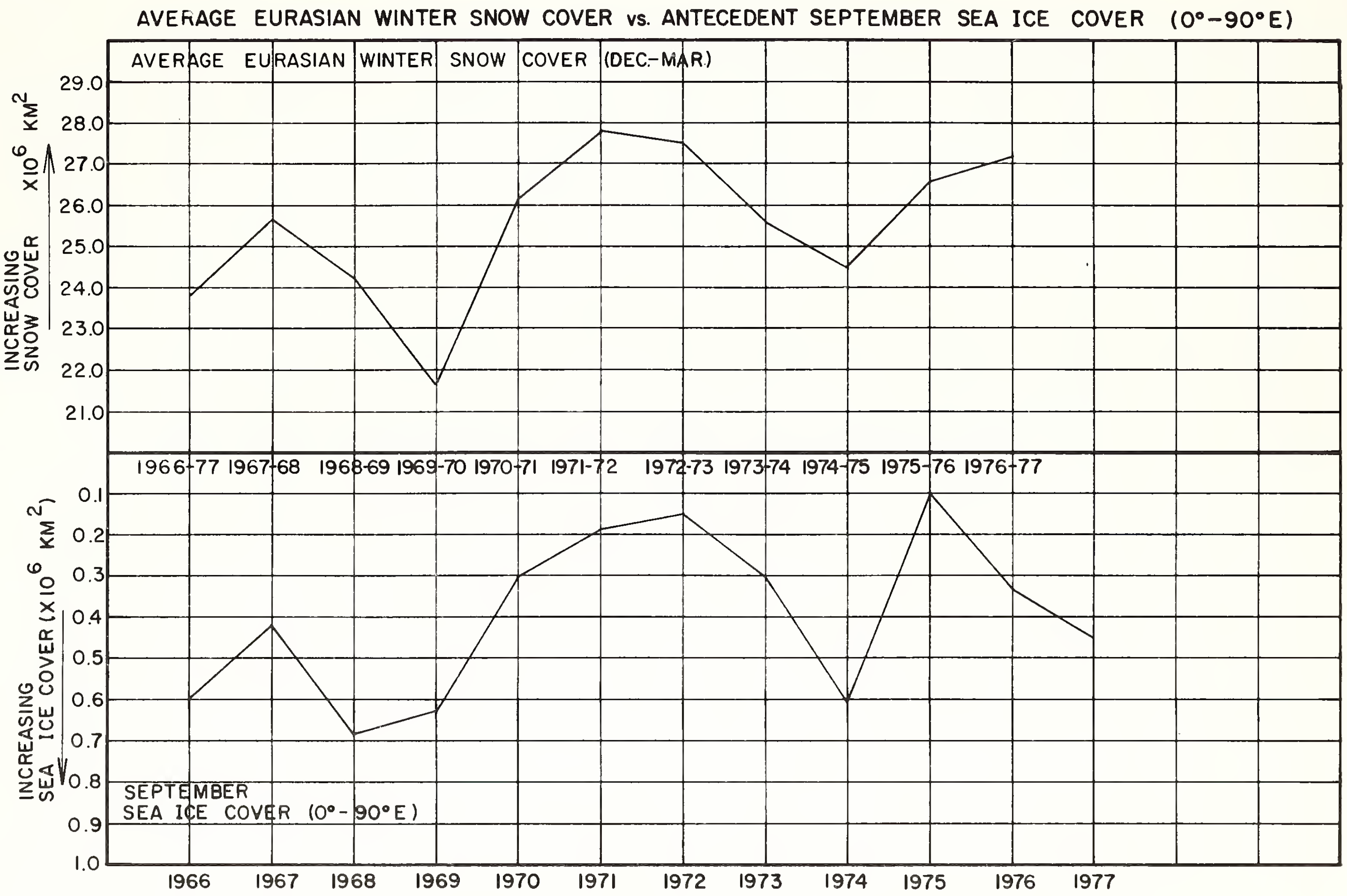

Fig. 12. Comparison of the average Eurasian winter snowcover extent (December-March) and antecedent September Arctic sea ice cover in the 0^{o}-90^{o}E quadrant.

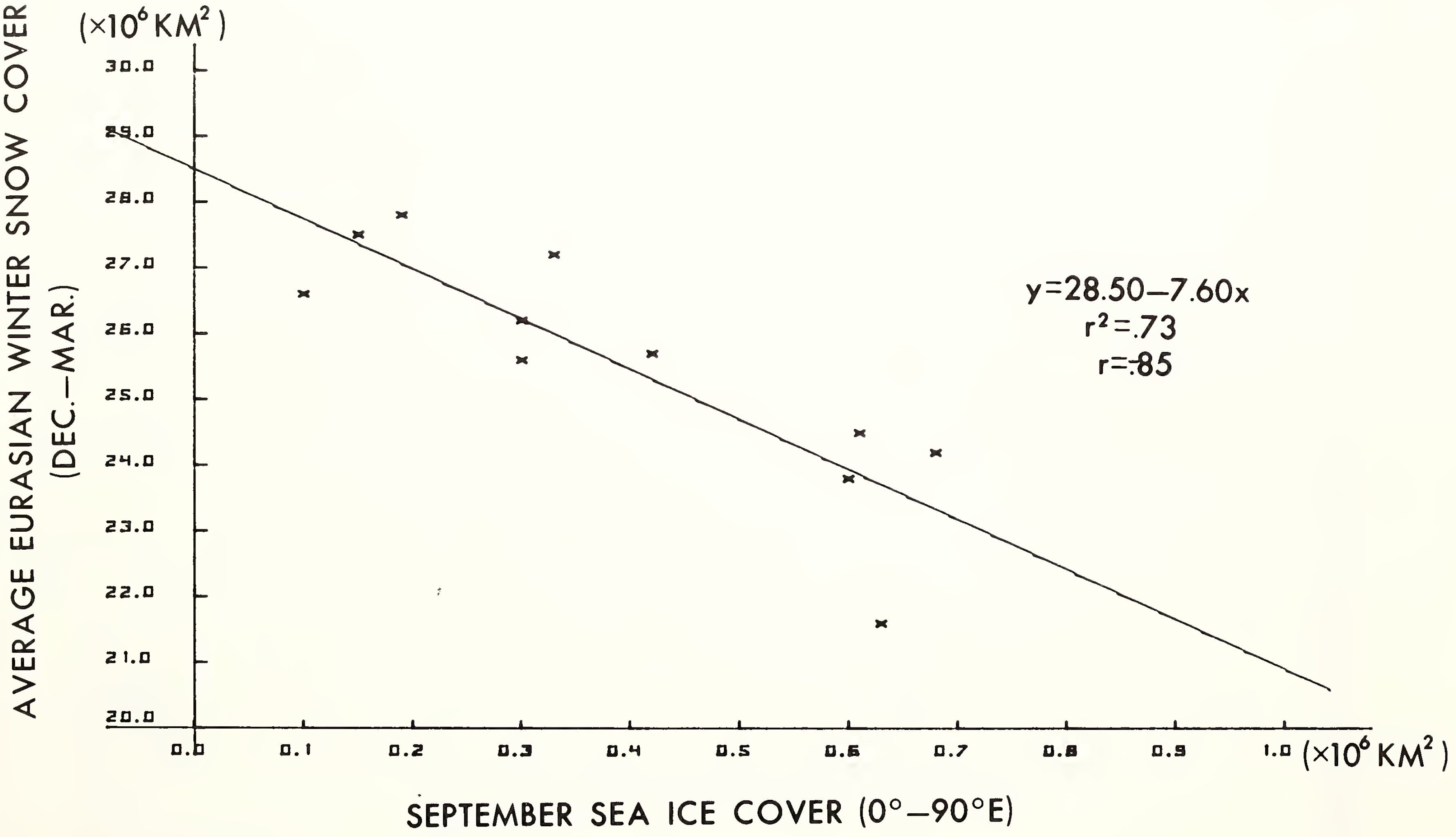

Fig. 13. Regression analysis of average Eurasian winter snowcover extent (December-March) and antecedent September sea ice cover in the 0^o-90^oE quadrant.

Comparison of the last two Winter Season Monthly Zonal Cloud Fractions as Derived from Nimbus-6 ERB Data

Robert J. Curran
Goddard Space Flight Center
Greenbelt, MD 20771

The radiation exchange between the earth, sun and free space is the ultimate driver of the meteorological and oceanographic processes which form the earth's climate. The major constituent of the earth-atmosphere system which moderates the radiation exchanges is atmospheric clouds. The earth's global albedo, which is the ratio of the solar flux reflected from the earth to that incident, is approximately 0.30. Close to one half of this golbal albedo is due to clouds, emphasizing their importance to the energetics of the system.

Regions of the earth with minimal cloud cover for extended periods of time absorb most of the sunlight incident on them and thus act as sources of energy to the system. Similarly, relatively cloud free regions tend to loose much energy by emission of longwave radiation to space. Subtle changes in the temporal and spacial distribution of clouds can strongly effect the magnitude and position of the sources and sinks of radiation energy to the system. To understand the magnitude of the transport processes which distribute radiation energy from the sources to the sinks, measurements of the statistical properties of clouds are necessary.

Satellite imagery such as that from the geosynchronous meteorological satellites demonstrate the strong difference in reflectance between clouds and the clear surface/atmosphere. These reflectance differences are greatest for tropical and mid latitudes where most albedos range between 0.15 and 0.25. Cloud albedos, for many of the cloud masses found in these latitudes, are 0.50 or greater. These differences allow large scale measured albedos to be decomposed into cloud obscured and cloud free fractions. The present study uses albedos derived from measurements made by the Earth Radiation Budget (ERB) instrument on the Nimbus-6 meteorological satellite.

The Nimbus-6 satellite is sun-synchronous and thus observes each latitude at fixed local time. Nimbus-6 was placed in orbit such that all latitudes between 60N and 60S are observed within one hour of local noon. Monthly, zonal determinations of the albedo were gathered from July 1975 to present. The low spectral resolution channels were used to form a data set covering the winter season 75/76 and the winter season 76/77. The monthly zonal values are given in graphical form in figures 1.

To separate cloud contributions from the measured data it is necessary to form a model of the expected cloud free albedo distribution. A model was formed by taking into account the latitude distributions of land and water, the monthly extent of ice and snow cover and the solar zenith angle dependent effects of the cloudfree atmosphere.

The water surface albedo varies with solar zenith angle in accordance with the data of Kondratyev. Ice and snow cover data were gathered from the Nimbus-6 Electronically Scanning Microwave Radiometer (ESMR) and from minimum albedo products from the NOAA Scanning Radiometer. Figure 2 shows representative monthly zonal cloud free albedos as derived from the present model. Comparison of the modeled cloud free albedos with those measured by Nimbus-6 ERB then results in zonal cloud fractions.

Calculations of the zonal cloud fractions for each of the fall-winter-spring seasons of the last two years are shown graphically in Figures 3 and 4. The two major features identifiable in both figures are the southern hemisphere maximum at approximately 65° south latitude and the variable northern hemisphere maximum which is roughly situated in the northern mid to high latitudes. The positions and seasonal variation in the southern hemisphere maximum agree with the data of Van Loon.

Table 1 gives the monthly zonal albedo differences between the winter of 75/76 and that of 76/77. A graphical version of this table is displayed in Figure 5. Because the same instrument is being used to collect the data and because the satellite orbit is sunsynchronous and thus reproducible from year to year this data set is ideal for differential studies as comparisons between adjacent years. The large albedo differences evident in January is suspect and thought to be an artifact of the January 1977 data processing. Therefore, for much of the comparisons January will be excluded. Figure 5 shows substantial albedo increases in the northern hemisphere for the months September through December. These increases in albedo are ascribed to increase cloud fraction by use of the cloud free model.

Table 2 lists the differences in cloud fraction between the two years. The data of Table 2 are displayed graphically in Figure 6.

The differences in cloud fraction amplify the albedo differences noted in Figure 5. Large increases in cloud fraction may be noted in the fall and early winter of 76/77. These increases are followed by decreases in northern hemisphere low latitude cloud fractions in the late winter and early spring.

The decreases in low latitude cloud fractions are defensible because of the lack of large enough surface albedo changes. However, between 40° and 50° latitude changes in cloud cover may be partially explained in terms of changes in the position of the ice/snow boundary between the two years. Efforts are proceeding to assess the impact of these contributions. The magnitude of the albedo differences at 40° to 50°N are greater than that expected from snow cover alone and must be, at least partially the result of changes in cloud cover.

References

Kondrat'ev, K. (editor), "Radiation Characteristics of the Atmosphere and the Earth's Surface, "Amerind Publishing C. Pvt. LTD., New Delhi (1973)

Van Loon, H., 1972: Cloudiness and precipitation in the southern hemisphere. *Meteor. Monogr.* , 13, Chapter 6.

Table 1

ALBEDO DATA OF 76/77 MINUS ALBEDO DATA OF 75/76

LAT	*SEP*	*OCT*	*NOV*	*DEC*	*JAN*	*FEB*	*MAR*	*APR*
¯87.50		¯0.01	0.01	0.00	¯0.05	0.02	0.03	
¯82.50		¯0.01	0.01	0.01	¯0.04	0.02	0.04	
¯77.50	0.02	0.00	0.01	0.01	¯0.03	0.03	0.03	
¯72.50	0.02	0.01	0.02	0.01	¯0.02	0.03	0.02	¯0.01
¯67.50	0.02	0.01	0.02	0.01	¯0.03	0.04	0.03	¯0.01
¯62.50	0.02	0.01	0.03	0.01	¯0.06	0.03	0.02	0.00
¯57.50	0.02	0.01	0.02	0.01	¯0.08	0.02	0.01	0.00
¯52.50	0.00	0.00	0.01	0.01	¯0.09	0.02	0.01	0.00
¯47.50	0.00	0.00	0.02	0.02	¯0.09	0.01	0.01	0.00
¯42.50	0.00	0.01	0.02	0.02	¯0.08	0.00	0.01	0.00
¯37.50	¯0.01	0.01	0.02	0.02	¯0.06	0.00	0.01	0.00
¯32.50	¯0.01	0.00	0.02	0.01	¯0.04	0.00	0.01	¯0.01
¯27.50	¯0.02	0.00	0.01	¯0.01	¯0.02	¯0.01	0.00	¯0.01
¯22.50	¯0.01	0.00	0.00	¯0.01	¯0.01	¯0.01	0.00	¯0.01
¯17.50	¯0.01	0.00	0.00	¯0.02	0.01	¯0.02	0.00	0.00
¯12.50	¯0.01	0.00	0.00	¯0.01	0.02	¯0.01	0.00	0.01
¯7.50	¯0.01	0.00	0.01	¯0.01	0.03	0.00	0.01	0.01
¯2.50	¯0.01	0.01	0.01	¯0.01	0.04	0.01	0.01	0.01
2.50	¯0.01	0.01	0.01	¯0.01	0.04	0.01	0.01	0.01
7.50	¯0.02	0.01	0.01	¯0.01	0.04	0.01	0.00	0.00
12.50	¯0.01	0.00	0.01	¯0.01	0.02	0.00	0.00	0.00
17.50	0.00	0.00	0.01	¯0.01	0.01	¯0.01	¯0.01	0.00
22.50	0.01	0.01	0.01	¯0.02	0.02	¯0.01	¯0.01	0.00
27.50	0.02	0.02	0.01	¯0.02	0.02	¯0.02	¯0.02	0.00
32.50	0.02	0.03	0.01	¯0.01	0.04	¯0.02	¯0.02	0.00
37.50	0.01	0.04	0.01	0.00	0.05	¯0.01	¯0.01	0.00
42.50	0.01	0.04	0.02	0.02	0.06	0.00	0.00	0.01
47.50	0.01	0.04	0.02	0.04	0.05	0.01	0.00	0.01
52.50	0.01	0.04	0.03	0.04	0.03	0.00	0.01	0.01
57.50	0.01	0.05	0.04	0.04	0.02	¯0.02	0.00	0.02
62.50	¯0.02	0.04	0.04	0.06	0.04	¯0.05	¯0.02	0.01
67.50	¯0.01	0.03	0.01			¯0.10	¯0.04	0.00
72.50	¯0.03	0.02				0.02	0.01	0.00
77.50	¯0.03						0.00	0.00
82.50	¯0.02							0.00
87.50	0.01							0.00

Table 2

ZONAL CLOUD FRACTIONS OF 76/77 *MINUS* 75/76

LAT	*SEP*	*OCT*	*NOV*	*DEC*	*JAN*	*FEB*	*MAR*	*APR*
¯87.50		¯0.02	0.03	0.02	¯0.21	0.06	0.10	
¯82.50		¯0.02	0.04	0.04	¯0.20	0.08	0.13	
¯77.50	0.06	0.00	0.06	0.05	¯0.17	0.12	0.11	
¯72.50	0.07	0.03	0.09	0.05	¯0.10	0.13	0.09	¯0.03
¯67.50	0.07	0.05	0.13	0.04	¯0.08	0.09	0.07	¯0.02
¯62.50	0.07	0.04	0.09	0.02	¯0.14	0.06	0.04	¯0.01
¯57.50	0.04	0.01	0.04	0.02	¯0.16	0.05	0.02	0.00
¯52.50	0.00	¯0.01	0.03	0.02	¯0.20	0.03	0.01	0.00
¯47.50	¯0.01	0.00	0.03	0.04	¯0.21	0.02	0.01	0.00
¯42.50	¯0.01	0.01	0.04	0.05	¯0.18	0.01	0.02	0.00
¯37.50	¯0.01	0.01	0.04	0.04	¯0.14	0.01	0.01	¯0.01
¯32.50	¯0.03	0.01	0.04	0.02	¯0.09	0.00	0.01	¯0.01
¯27.50	¯0.04	0.01	0.02	¯0.02	¯0.05	¯0.02	0.00	¯0.02
¯22.50	¯0.03	0.00	0.00	¯0.03	¯0.02	¯0.03	¯0.01	¯0.01
¯17.50	¯0.01	¯0.01	¯0.01	¯0.04	0.02	¯0.04	¯0.01	0.00
¯12.50	¯0.02	0.00	0.00	¯0.03	0.05	¯0.03	0.00	0.02
¯7.50	¯0.02	0.01	0.02	¯0.03	0.07	¯0.01	0.02	0.03
¯2.50	¯0.02	0.02	0.02	¯0.02	0.09	0.01	0.03	0.03
2.50	¯0.03	0.03	0.03	¯0.02	0.10	0.02	0.02	0.01
7.50	¯0.04	0.02	0.03	¯0.02	0.09	0.02	0.01	0.00
12.50	¯0.03	0.00	0.03	¯0.02	0.04	0.00	0.00	¯0.01
17.50	¯0.01	0.01	0.03	¯0.03	0.03	¯0.02	¯0.01	0.00
22.50	0.03	0.02	0.02	¯0.04	0.03	¯0.03	¯0.03	0.01
27.50	0.04	0.04	0.02	¯0.04	0.05	¯0.03	¯0.04	0.00
32.50	0.04	0.06	0.01	¯0.02	0.08	¯0.04	¯0.04	0.00
37.50	0.03	0.08	0.02	0.01	0.11	¯0.03	¯0.02	0.00
42.50	0.02	0.08	0.03	0.05	0.14	0.00	0.00	0.01
47.50	0.02	0.09	0.06	0.09	0.13	0.02	0.01	0.02
52.50	0.02	0.10	0.08	0.11	0.08	0.00	0.02	0.04
57.50	0.02	0.11	0.09	0.10	0.06	¯0.07	0.00	0.05
62.50	¯0.03	0.11	0.11	0.16	0.13	¯0.17	¯0.06	0.03
67.50	¯0.03	0.08	0.02			¯0.30	¯0.15	0.01
72.50	¯0.06	0.04				0.05	0.02	0.01
77.50	¯0.09						¯0.01	0.00
82.50	¯0.05							¯0.01
87.50	0.02							0.01

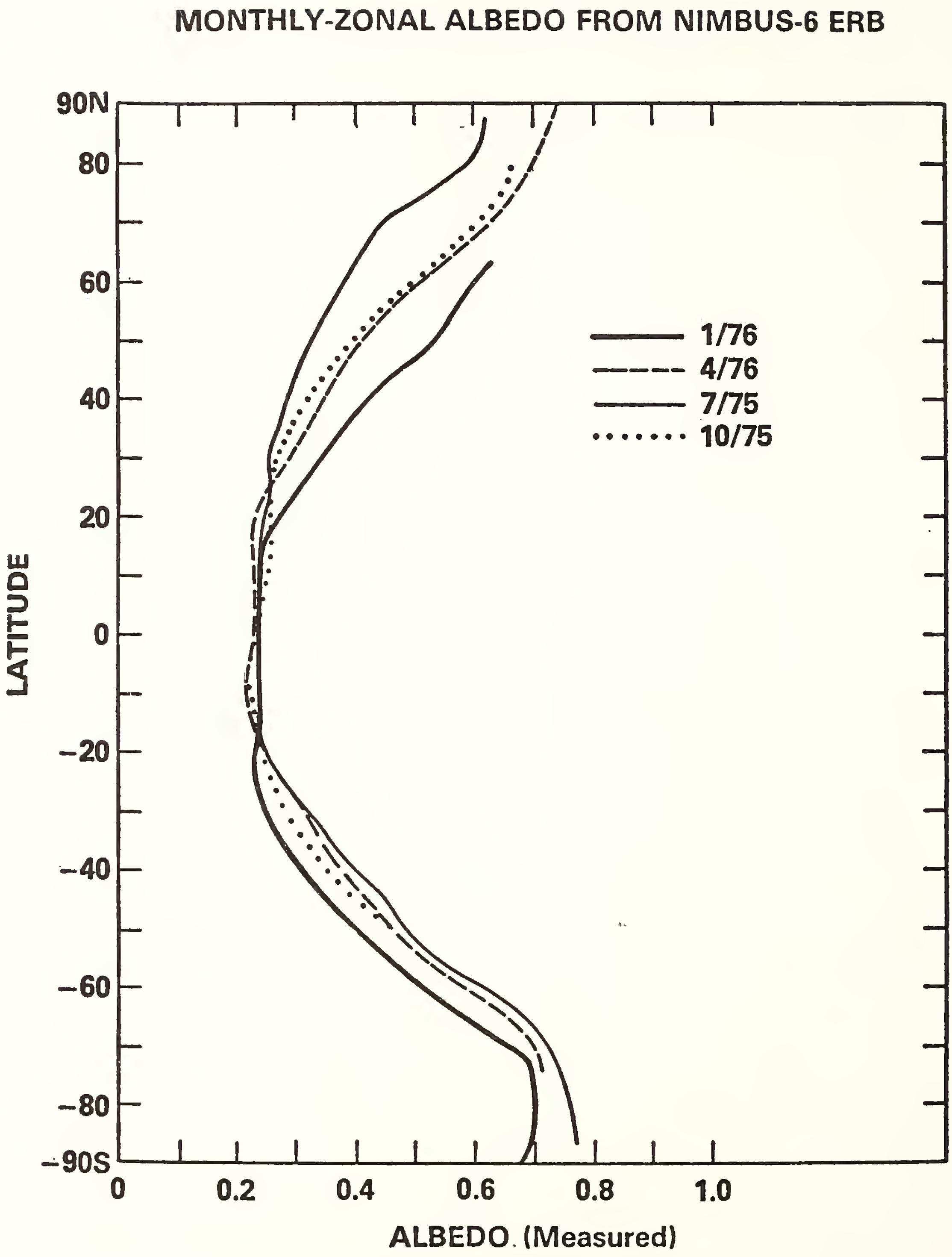

Figure 1 Representative Monthly zonal Albedos from Nimbus-6 ERB for the period 9/75 to 5/76

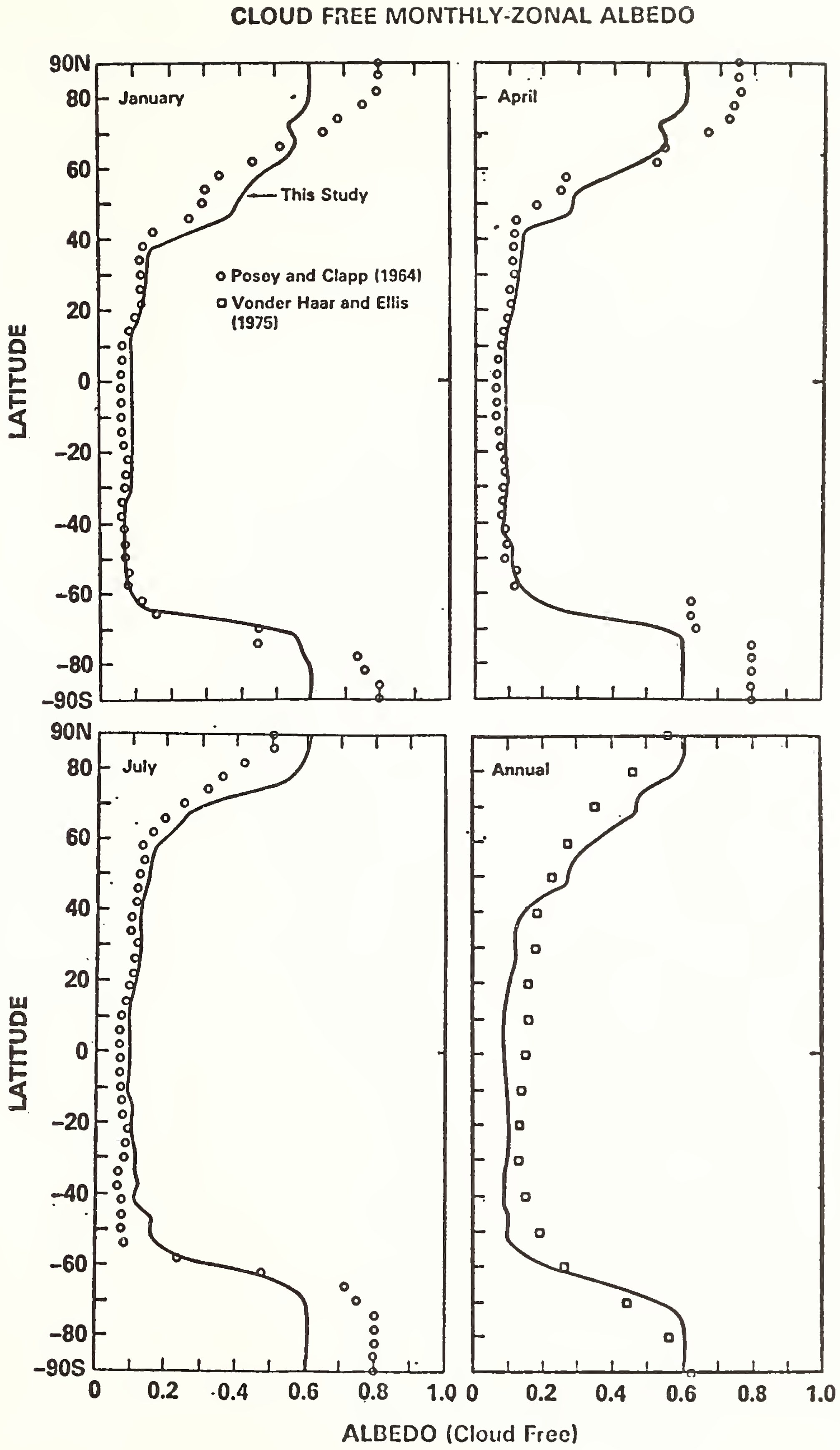

Figure 2 Monthly zonal cloud free albedos calculated from the described model and compared with other determinations

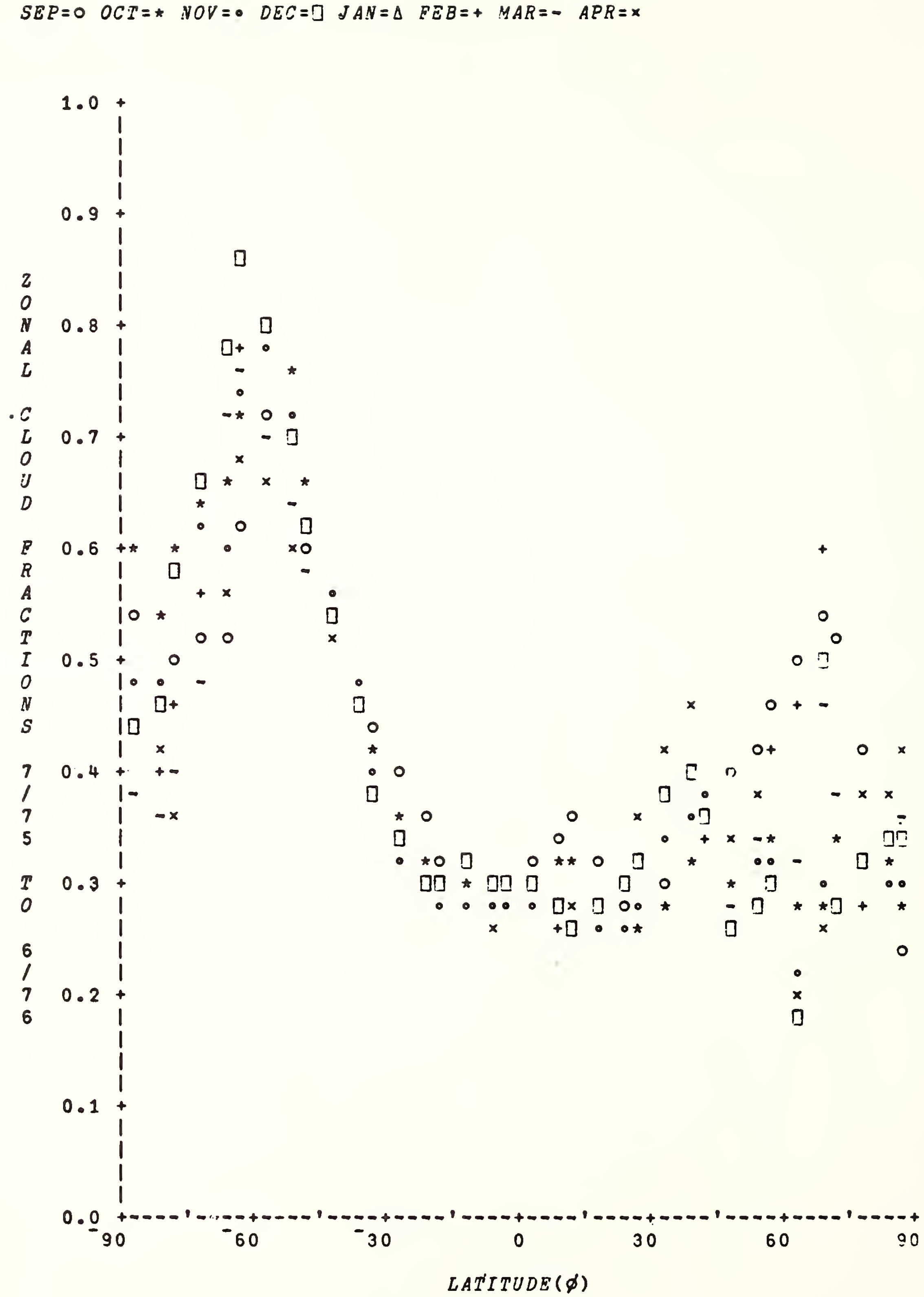

Figure 3 Derived Monthly Zonal cloud fractions for the months September 1975 to April 1976. January 1976 has been excluded from this graph.

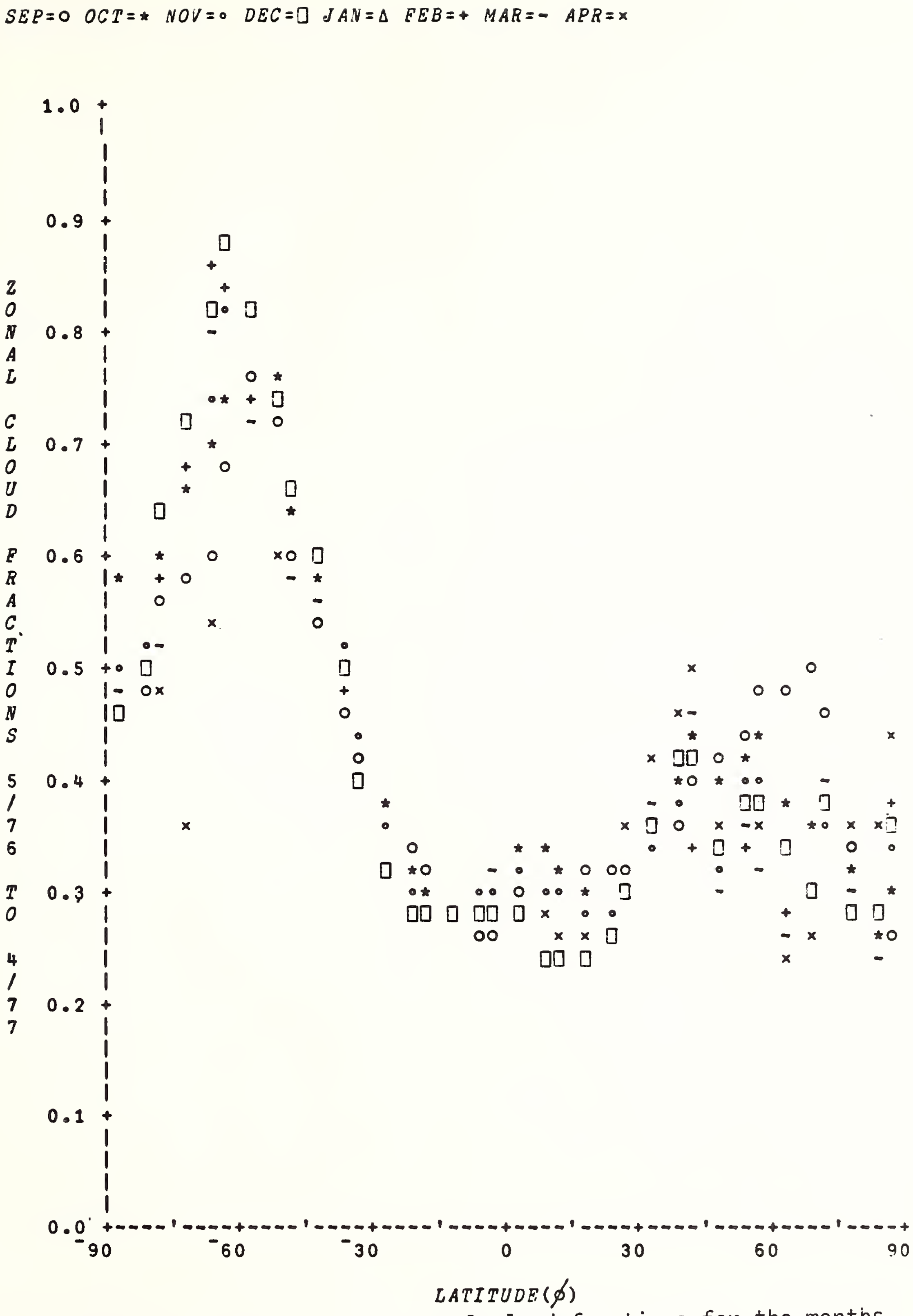

Figure 4. Derived monthly zonal cloud fractions for the months September 1976 to April. January 1977 has been excluded from this graph.

```
SAVED   9.47.58 10/13/77

50  ¯0.1  0.1  60  ¯90  30
```

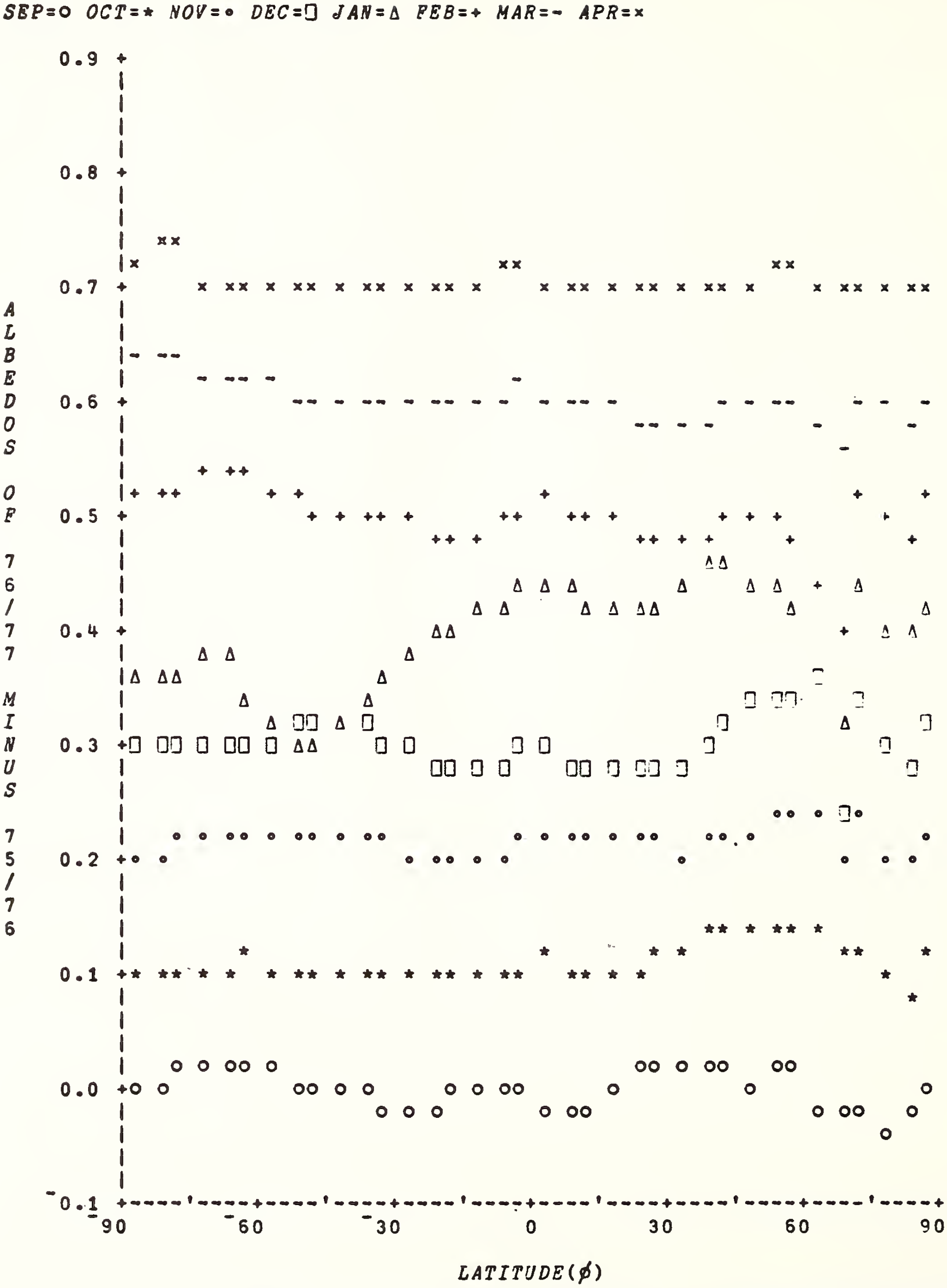

Figure 5. Monthly zonal albedo differences. To separate the monthly values the September value is ploted on the proper ordinate. For each succeeding month the 0.1 has been added to the differences. The January values are assumed to be anomolous.

```
SAVED  13.52.14 10/16/77

50  ¯0.1  0.1  60  ¯90  30
SEP=o OCT=* NOV=∘ DEC=□ JAN=Δ FEB=+ MAR=- APR=×
```

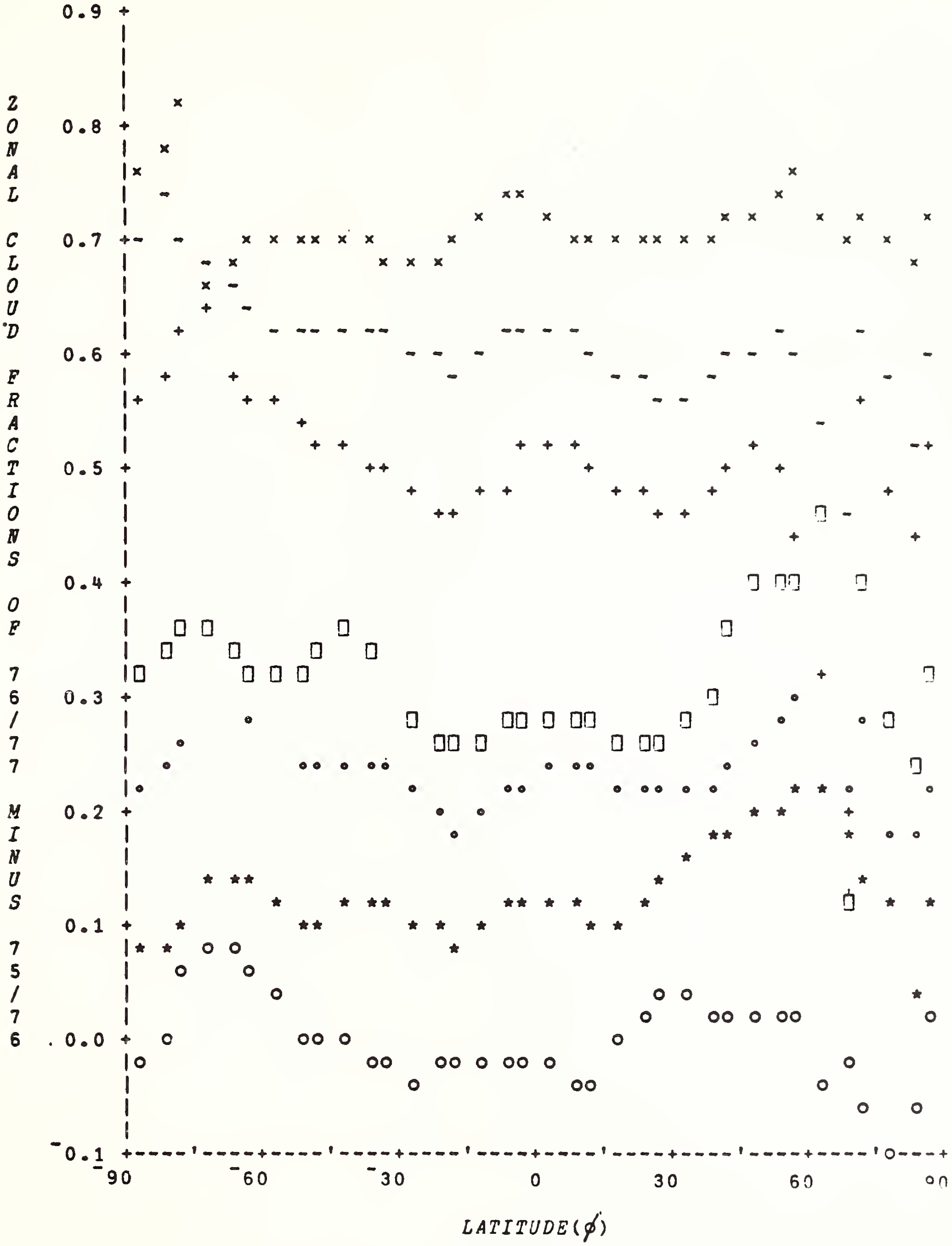

Figure 6. Zonal plots of the differences in monthly cloud fractions. Because the January data is questionable and tends to confuse the plot, it has been deleted from this figure. As in figure 5, months following September have been displaced to permit separation

Multiple Causes of the North American Abnormal Winter 1976-1977

by

Jerome Namias

Scripps Institution of Oceanography
University of California, San Diego
La Jolla, California 92093

The highly abnormal North American winter of 1976-1977, characterized by drought with a strong upper level ridge over the west and severe cold with attendant trough over the east was explained as a result of several synergistic factors:

(1) The quasi-stationary long wave pattern that developed from the North Pacific eastward through North America was in phase with the climatological normal flow pattern, although greatly amplified. This helped "lock in" the anomalous pattern because seasonal forcing did not oppose the factors leading to the abnormal forcing.

(2) The abnormal forcing appears to have been associated with an unprecedented vast area of cold surface water in the antecedent summer which changed to anomalously warm water from the west coast of North America to about 140°W partly as a result of the onset of a changed atmospheric flow pattern when the prevailing winds there blew much more from south to north than usual. This change resulted in reduced sensible and latent heat losses, reduced north to south water mass advection, and reduced upwelling.

(3) The summer to fall atmospheric change, wherein the west coast ridge and east coast trough began to develop, appears to have resulted in part from normal seasonal forcing influences operating on an abnormal wind pattern. In this case a strong trough off the west coast and a drought-producing ridge over the Northern Plains, positioned stably during summer, retrograded to more compatible positions in fall. The detailed mechanics of this change are unclear, but statistical average climatic mid-tropospheric changes from summer to fall suggest the observed evolution.

(4) The enhanced west-east SST zonal gradient over the Pacific introduced increased baroclinicity in the overlying atmosphere, resulting in a zone of frontogenesis, cyclogenesis and increased south to north upper level flow east of 140°W. This flow helped steer storms northward to Alaska rather than allowing them to pursue a normal eastward course, and at the same time produced a barotropic response in the form of a meridionally extensive ridge over the west coast of North America and a trough in the east. These features were manifested by abnormal warmth in Alaska and cold in the eastern half of the United States.

(5) Persistently recurrent Arctic outbreaks displaced the Polar Front far to the south along the gulf coast, and often led to snow far south of normal as well as heavy snows leeward of the Great Lakes. The snow in turn

helped refrigerate the Arctic air in its southward transit, partly through an increased albedo. The snow was therefore not frequently removed from the surface and also was maintained by the frequent Arctic air surges and replenished by storms moving along the south and eastern seaboards.

(6) Because of the enhanced temperature contrast off the eastern seaboard between refrigerated Arctic air and the warm Gulf stream, northeast storms occluded and deepened rapidly, resulting in the "Icelandic low" being displaced to Newfoundland at the surface and to southeastern Canada aloft. This Canadian low seems to have created and maintained the Arctic block which fed back to assist in suppressing the Canadian low.

(7) Many of the above phenomena were clear enough in their evolution so that by November a forecast was made, which while qualitatively correct, did not, nor could not with the present state of the art, predict the degree of severity of the eastern cold or western drought.

If this report stimulates efforts to numerically model the complex chain of synergistic events described, the author would feel that this synoptic study will have been most rewarding.

LEGENDS TO FIGURES

Fig. 1 Observed mean temperature (°F) for the months of Dec. 1976 and January 1977. Shaded areas denote the three categories—below (B), near (N), and above normal (A) whose ranges are determined as terciles from a 30-year climatic record.

Fig. 2 Average winter (December, January and February) mean temperatures at three cities for the winters 1946-47 through 1976-77.

Fig. 3 Mean 700 mb contours for Winter 1976-77 (December, January, and February) labelled in tens of feet.

Fig. 4 Normal winter (December, January, and February) 700 mb contours (labelled in tens of feet) based on the 26-year period, 1947-72.

Fig. 5 January 1977 700 mb contours (solid lines) and isopleths of departure from normal (both labelled in meters). This was the coldest winter month of 1976-77.

Fig. 6 Mean sea level isobars (drawn for 5 mb intervals) for January 1977.

Fig. 7 Standardized 700 mb height departures from normal for Fall, 1976 and January, 1977. Lines are drawn for values of one standard deviation, with maximum central values given by numbers. Note the persistence from the North Pacific through North America.

Fig. 8 Mean monthly North Pacific sea surface temperatures (SST) in °F from 1947 through January 1977. Horizontal broken line gives mean for the 20-year period, 1947-66.

Fig. 9 Summer, 1976 SST anomalies (°F) Lines drawn for each degree F, with core centers numbered. (Shaded areas are in excess of 1°F).

Fig. 10 SST anomalies (°F) for Fall (September, October and November) 1976. (See legend of Fig. 9 for details).

Fig. 11 Winter (December, January, and February) SST anomalies (°F). (See legend of Fig. 9 for details).

Fig. 12 North Pacific Normal (20-year average, solid lines) SST profiles along 40°N for months July 1976 through February 1977. Slant shaded areas are below normal; stippled areas, above.

Fig. 13 Mean 700 mb contours (solid) and departures from normal (broken lines with central values numbered) for summer, (June, July, and August) 1976. Solid lines and centers labelled in tens of feet; isopleths of anomalies drawn for 50 foot intervals.

Fig. 14 Same as Fig. 13 but for Fall (September, October, and November) 1976.

Fig. 15 Normal seasonal changes of 700 mb height (lines drawn for each 50 feet) from summer (June, July, and August) to Fall, (September, October, and November).

Fig. 16 Principal tracks of centers of cyclones at sea level over the North Pacific in January, 1977 (from Mariners Weather Log, 1977).

Fig. 17 Depth of snow on the ground (inches) on January 24, 1977. (From Weather and Crop Bulletin, 1977).

Fig. 18 SST departures from normal (°F) over the tropical Pacific for selected months, showing El Niño conditions which prevailed from Summer, 1976 through Winter, 1976-77, and the demise in March. (From National Marine Fisheries Bulletin, 1976 and 1977).

Fig. 19 Average sea level isobars (solid lines labelled in mb) for seven warmest SST summers (January, February, March) at Puerto Chicama, Peru (El Niños). Differences (broken lines) between these pressures and the mean for the seven coldest periods (anti-El Niños). The later periods were approximately normal. Shading indicates significance at the 5% level. (From Namias, 1976).

Fig. 20 Average sea level isobars (solid, labelled in mb) and departures from normal (broken lines, drawn for each 2 mb) for the 1976-1977 Winter (December, January, and February). Shaded area indicates significance at the 5% level.

Fig. 21 (Lower) Observed anomalies of 700 mb height (lines drawn for each 100 feet) and SST anomalies in °F. Horizontal shading denotes values greater than 1°F above normal. (Upper) Specified anomalies of 700 mb height anomalies from observed SST in lower chart and specified SST anomalies from observed 700 mb anomalies in lower chart.

Fig. 22 Winter teleconnections (cross correlations) between 700 mb height anomaly at 50°N 180° and other areas of the Northern Hemisphere. Isopleths are drawn for each 0.10 and zero correlation line is heavy. Shaded areas exceed correlations of ±0.20. Correlations are based on monthly values of Winters from 1947-75.

Fig. 23 Winter 1976-77 700 mb height anomaly predicted using SST forecast made from initial data of November, 1976 and specification equations relating 700 mb to SST anomalies (see text).

Fig. 24 Predicted and observed temperature and precipitation patterns for Winter, 1976-77 made on December 1, 1976 (see text).

Table I Verification of temperature forecast for Winter, 1976-77 expressed in contingency form (see text for details).

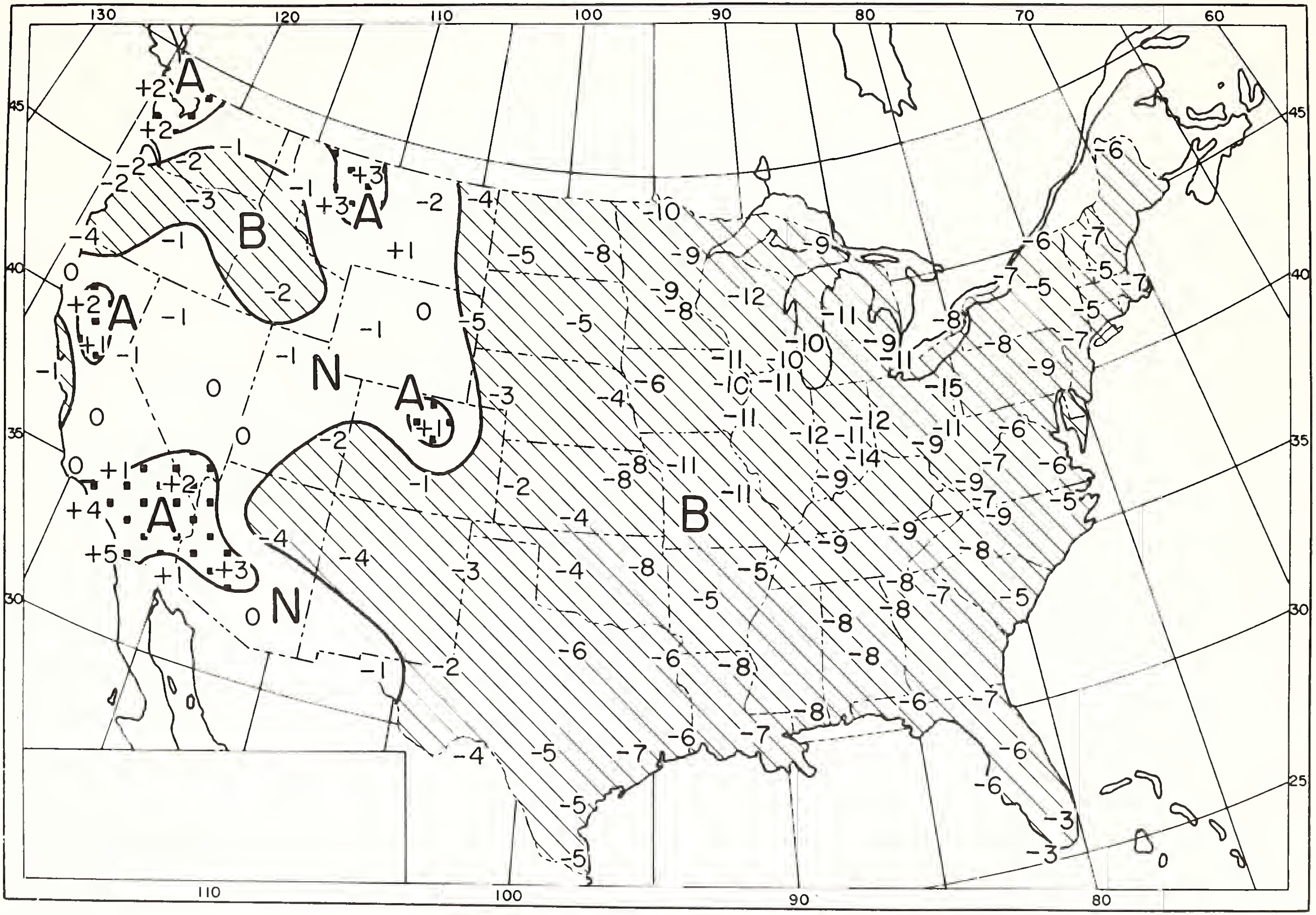

OBSERVED MEAN TEMPERATURE DN DEC. 1, 1976 THROUGH JAN. 31, 1977

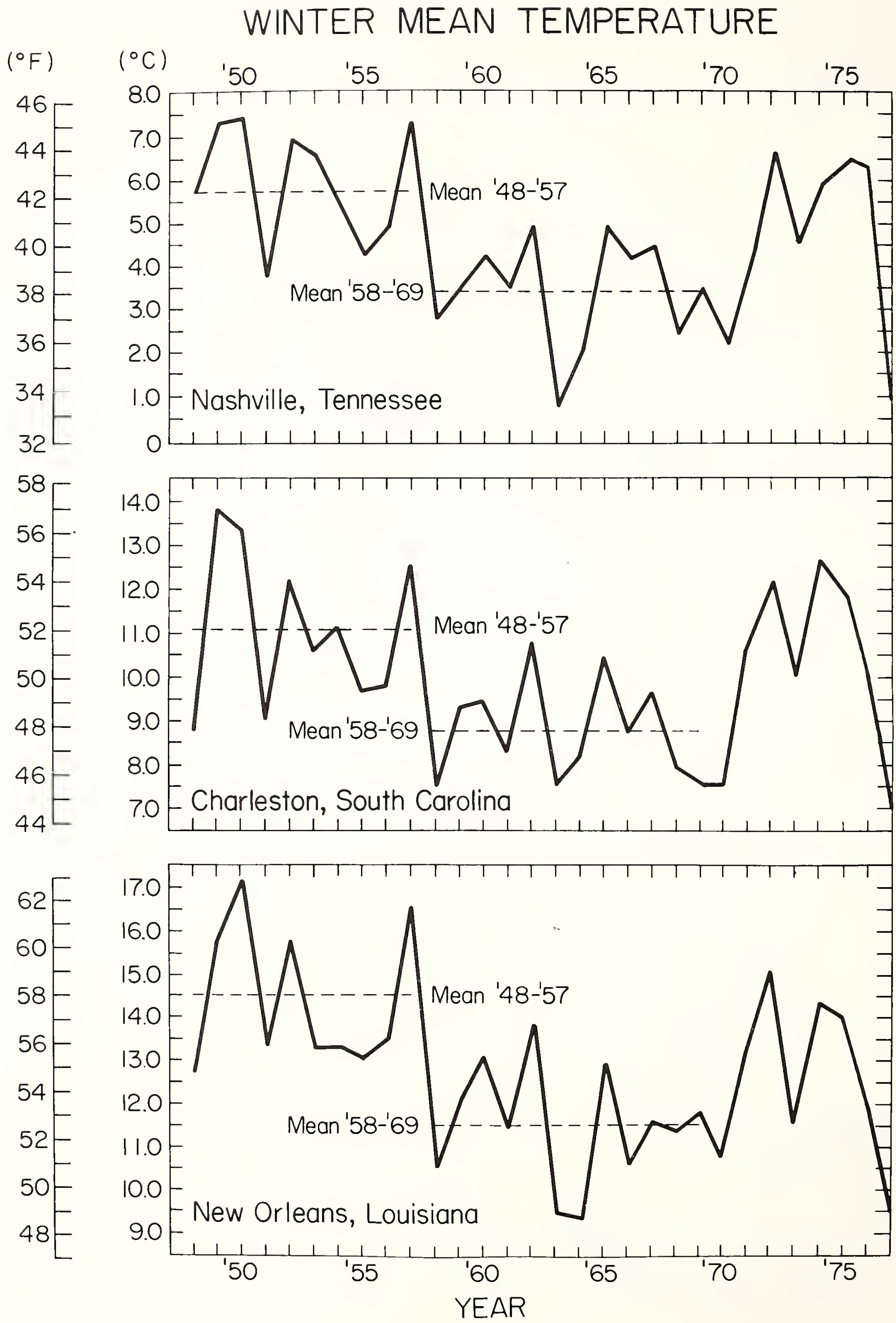

WINTER MEAN TEMPERATURE
(°F)
(°C)
'50
'55
'60
'65
'70
'75
Mean '48-'57
Mean '58-'69
Nashville, Tennessee
46
44
42
40
38
36
34
32
8.0
7.0
6.0
5.0
4.0
3.0
2.0
1.0
0
Charleston, South Carolina
58
56
54
52
50
48
46
44
14.0
13.0
12.0
11.0
10.0
9.0
8.0
7.0
New Orleans, Louisiana
62
60
58
56
54
52
50
48
17.0
16.0
15.0
14.0
13.0
12.0
11.0
10.0
9.0
YEAR

700mb HEIGHT (TENS OF FEET) WINTER 1977

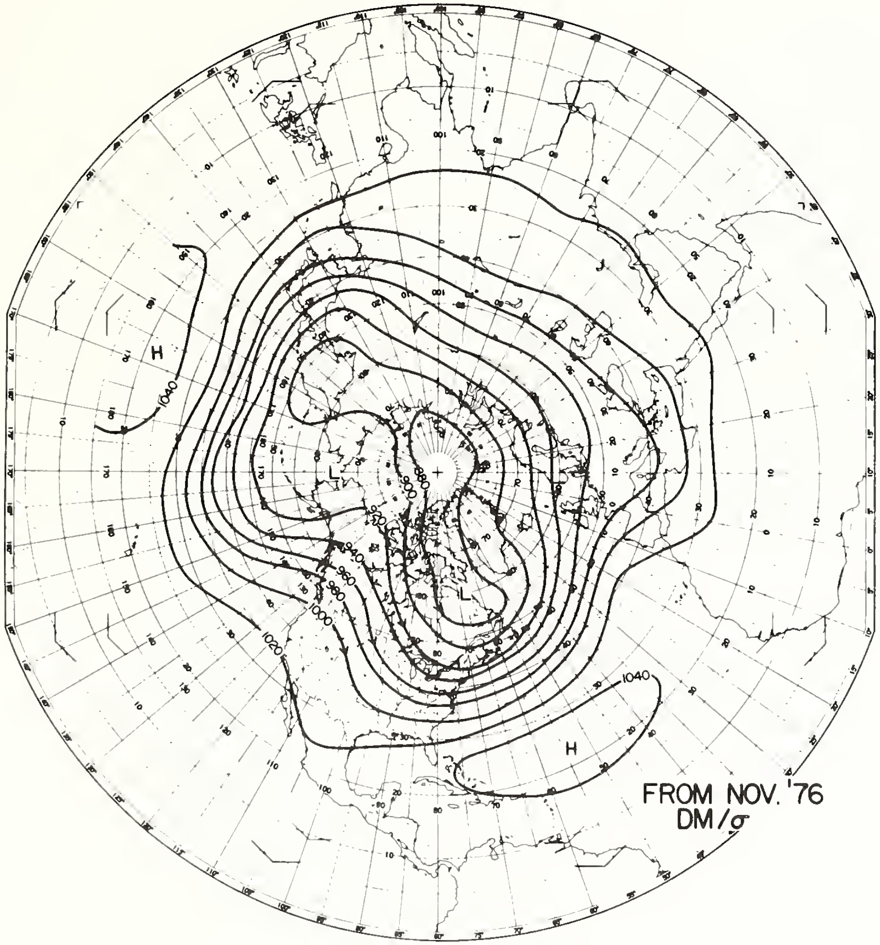

FROM NOV. '76
DM/σ

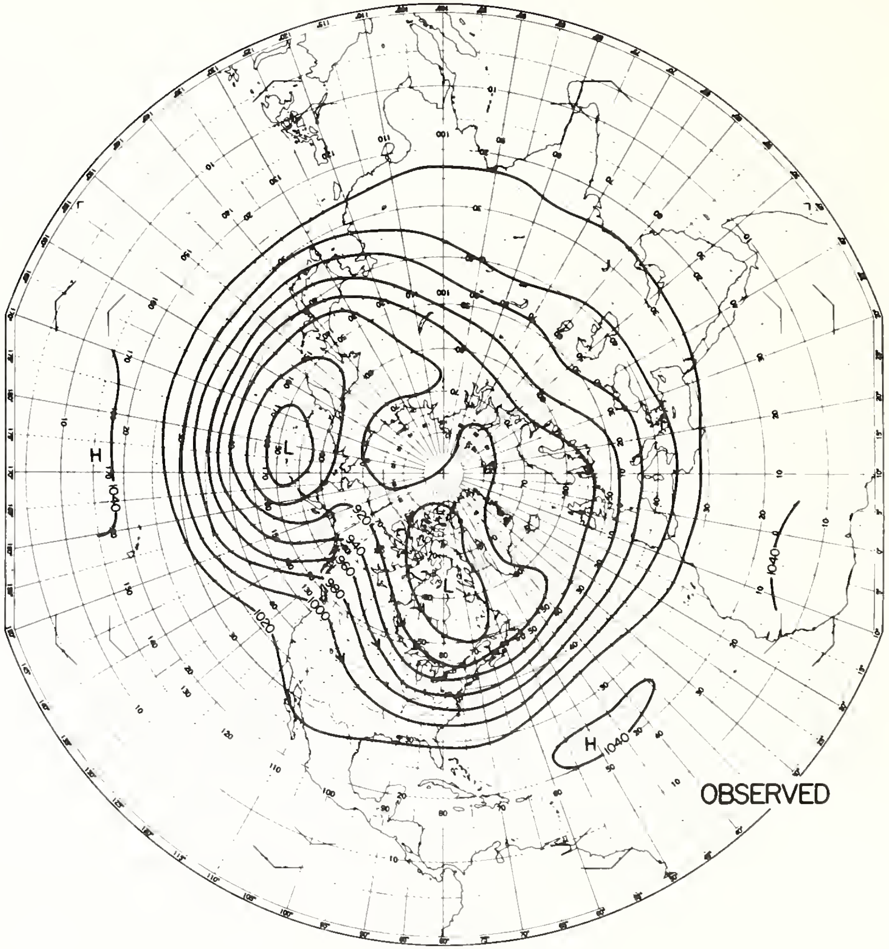

OBSERVED

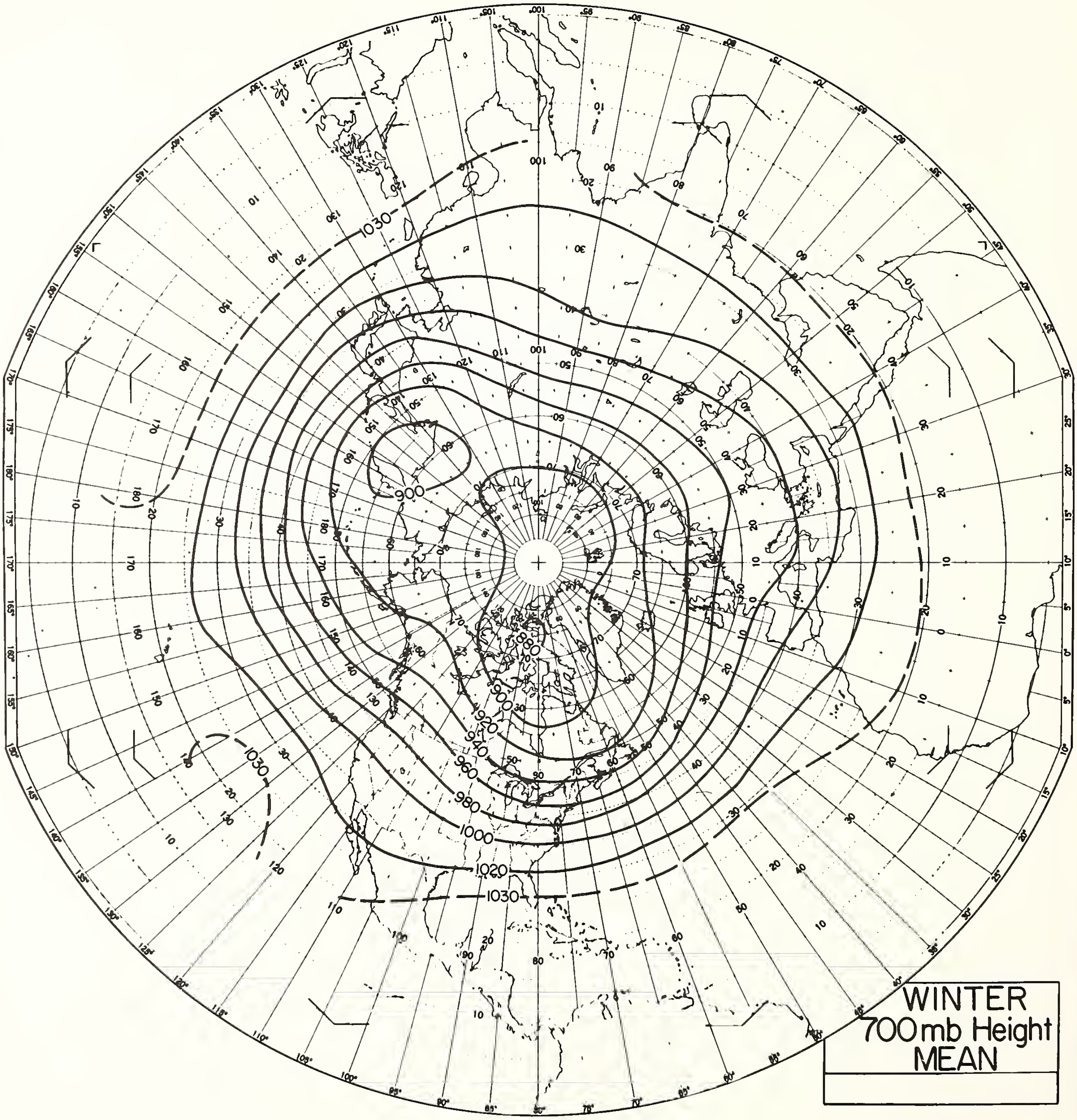

WINTER
700mb Height
MEAN

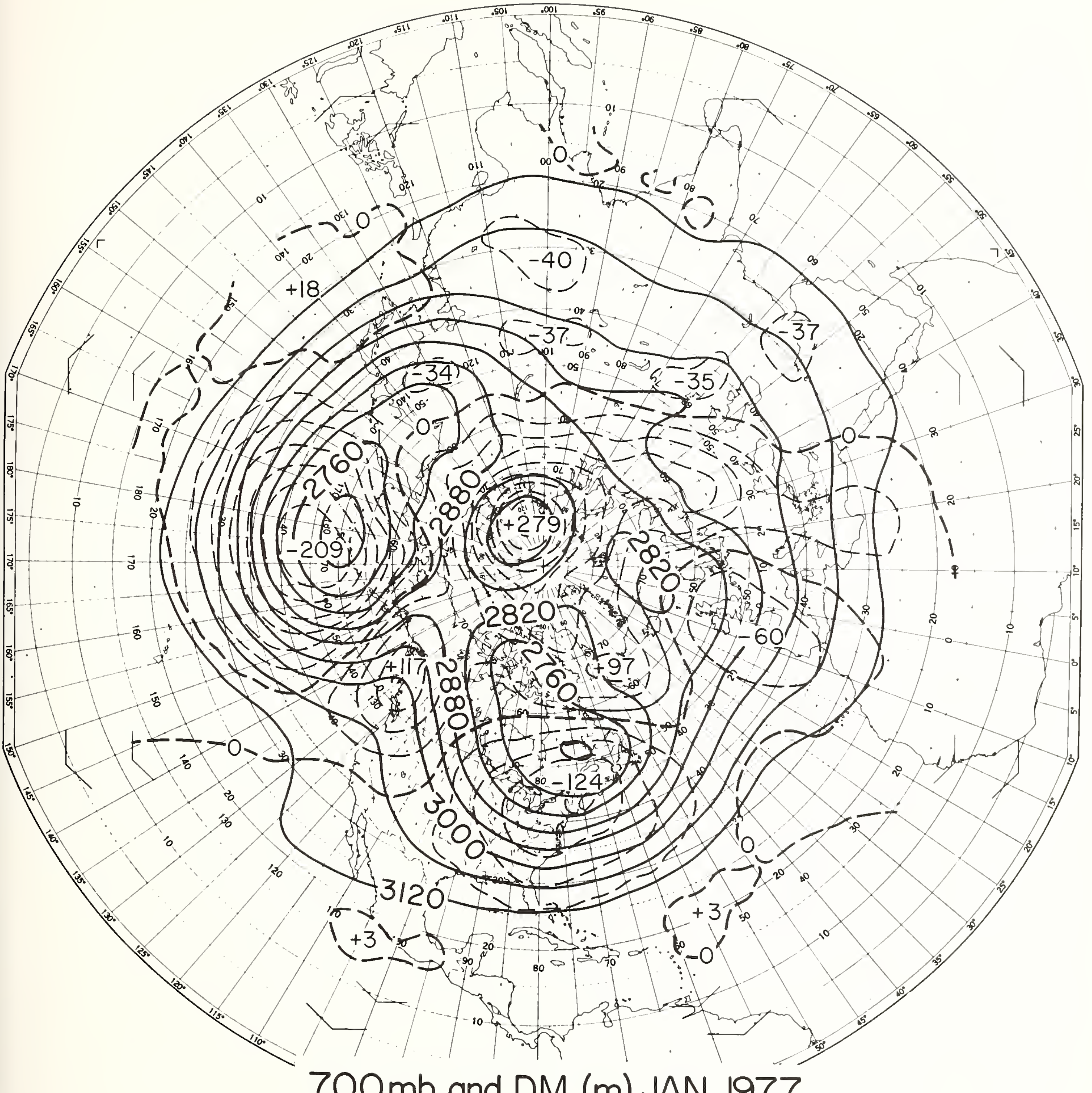

700mb and DM (m) JAN. 1977

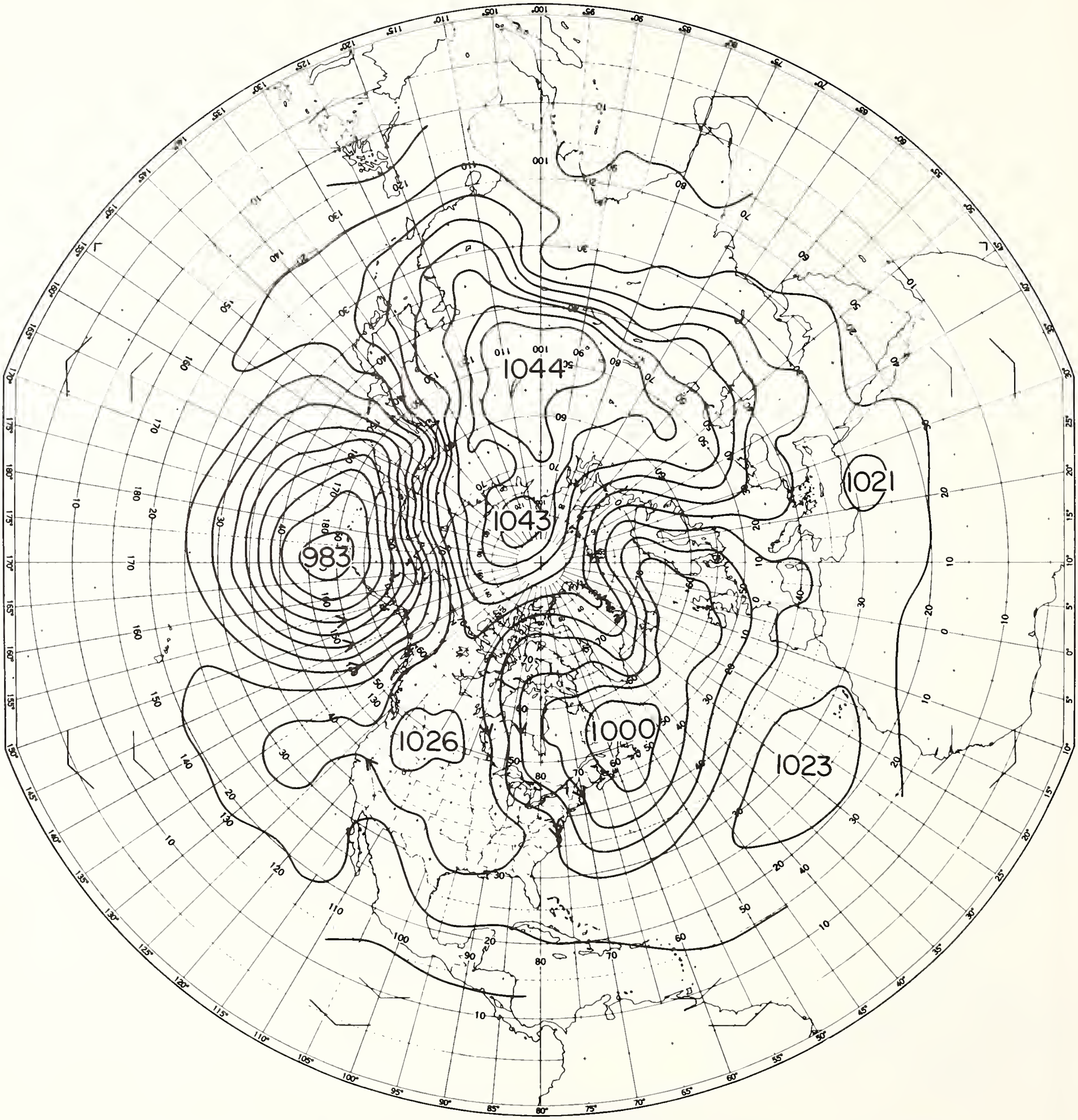

SEA LEVEL ISOBARS JAN. 1977

700 mb HT$_{DM}$/σ

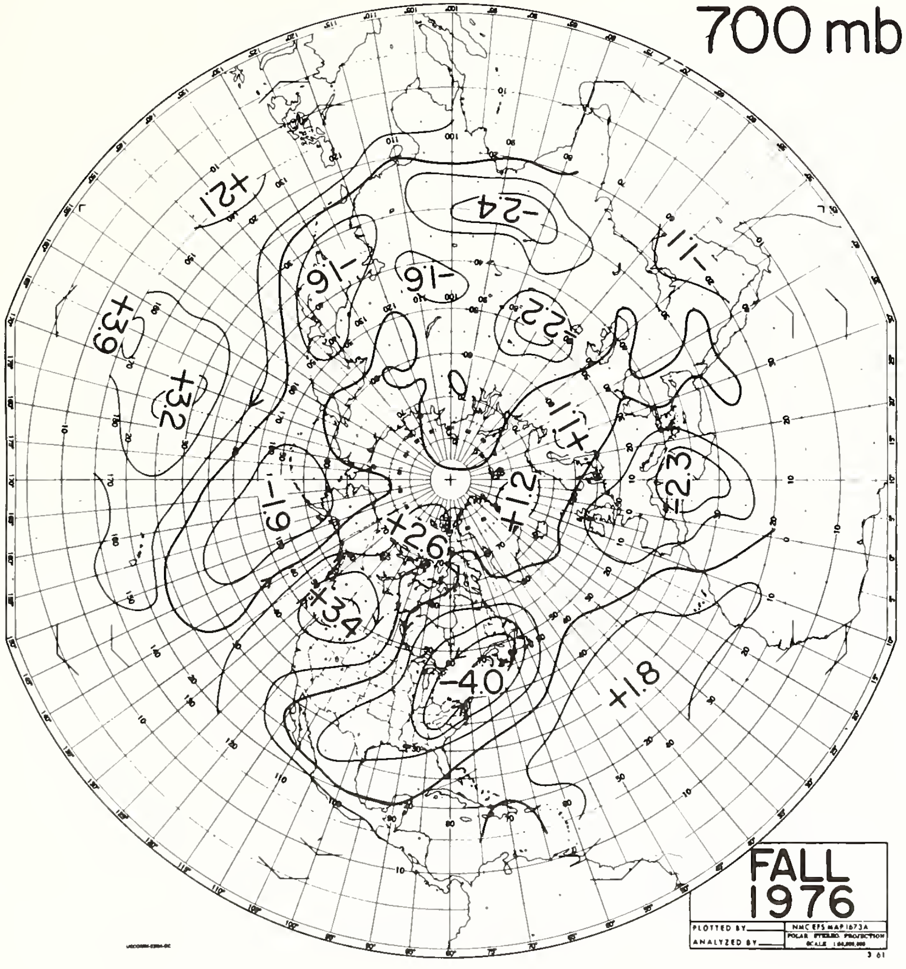
FALL
1976
PLOTTED BY
ANALYZED BY
NMC EFS MAP 1673A
POLAR STEREO PROJECTION
+2.1
-2.4
-1.6
-1.6
-2.2
-1.1
+3.9
+3.2
+1.1
+1.2
-2.3
-1.9
+2.6
+3.4
-4.0
+1.8

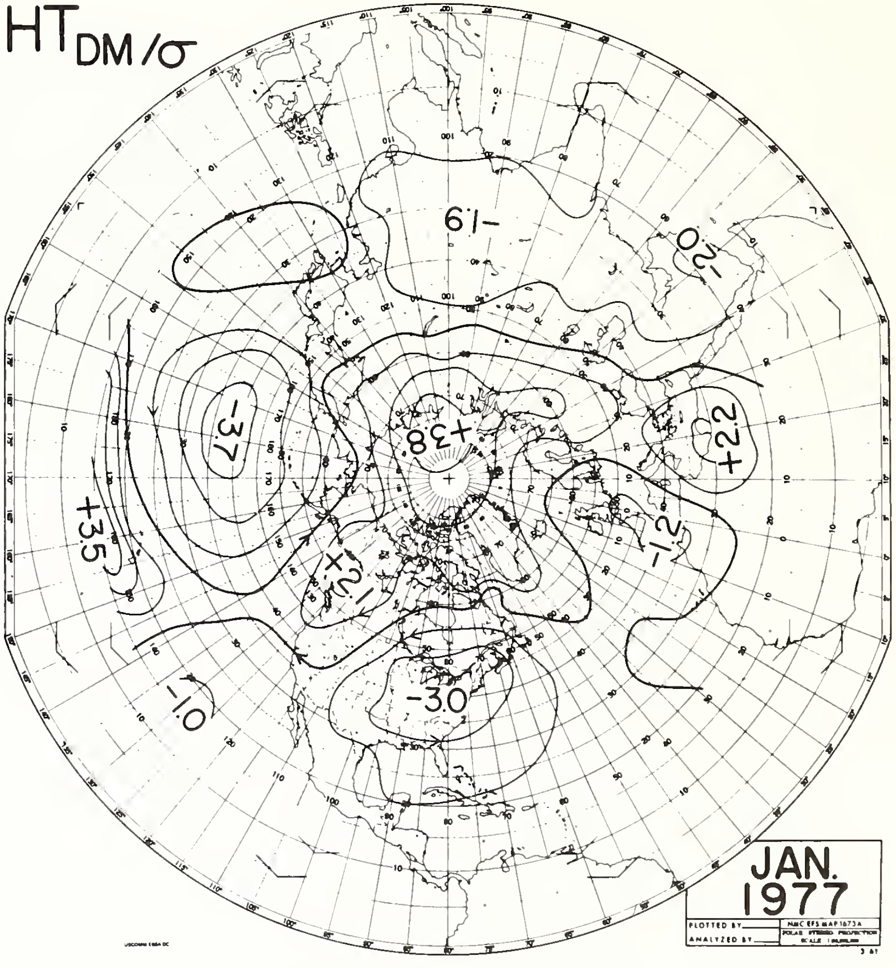
JAN.
1977
PLOTTED BY
ANALYZED BY
NMC EFS MAP 1673A
POLAR STEREO PROJECTION
-1.9
-2.0
-3.7
+3.8
+2.2
+3.5
-1.2
+2.1
-1.0
-3.0

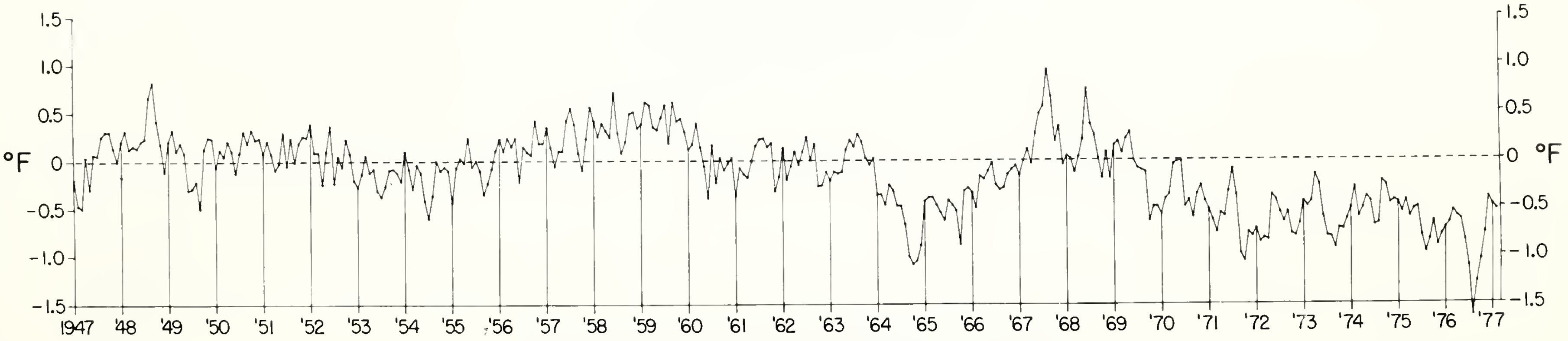

FULL OCEAN WEIGHTED MEANS OF SST_{DM}

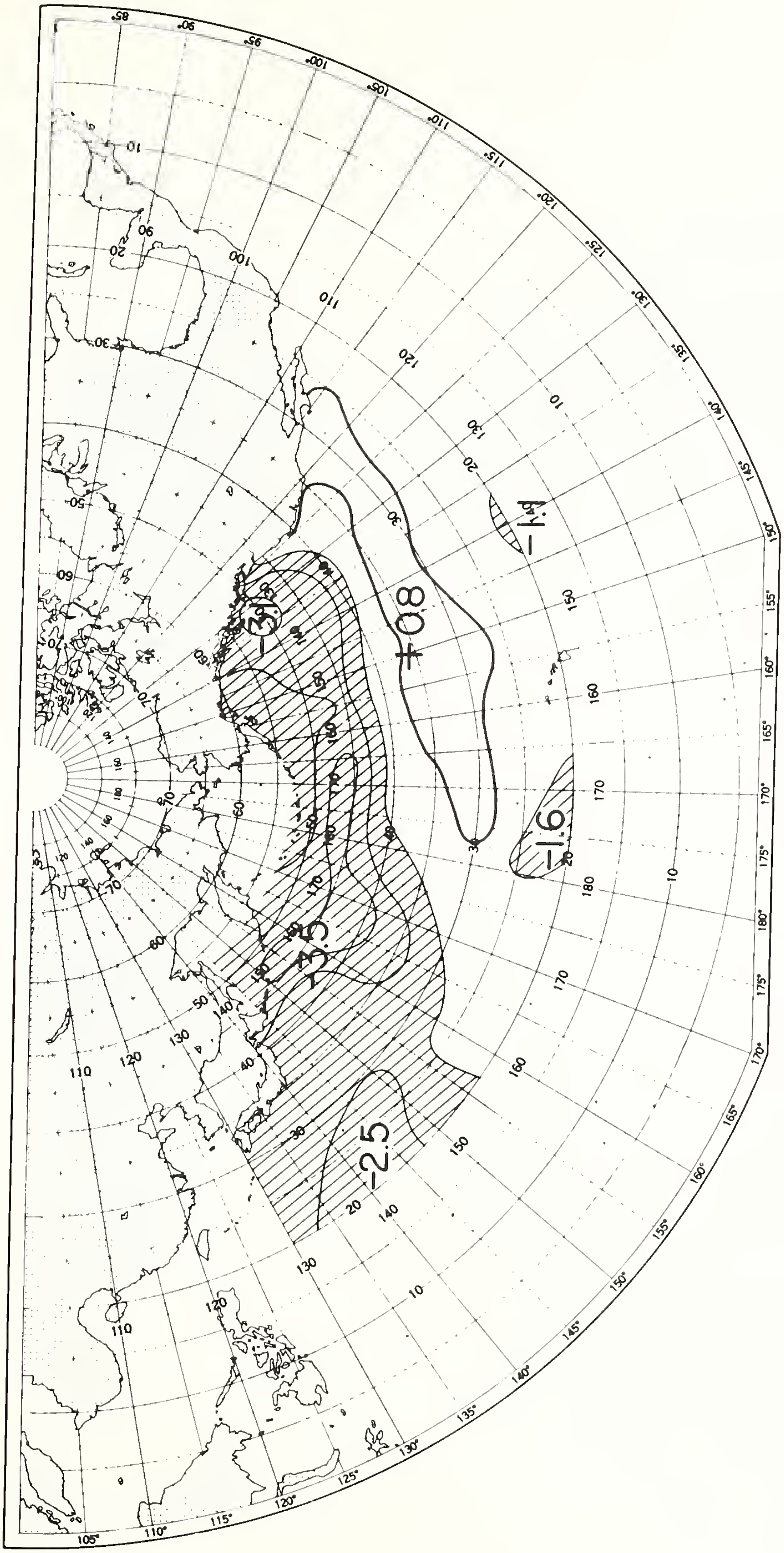

SST$_{DM}$ SUMMER 1976

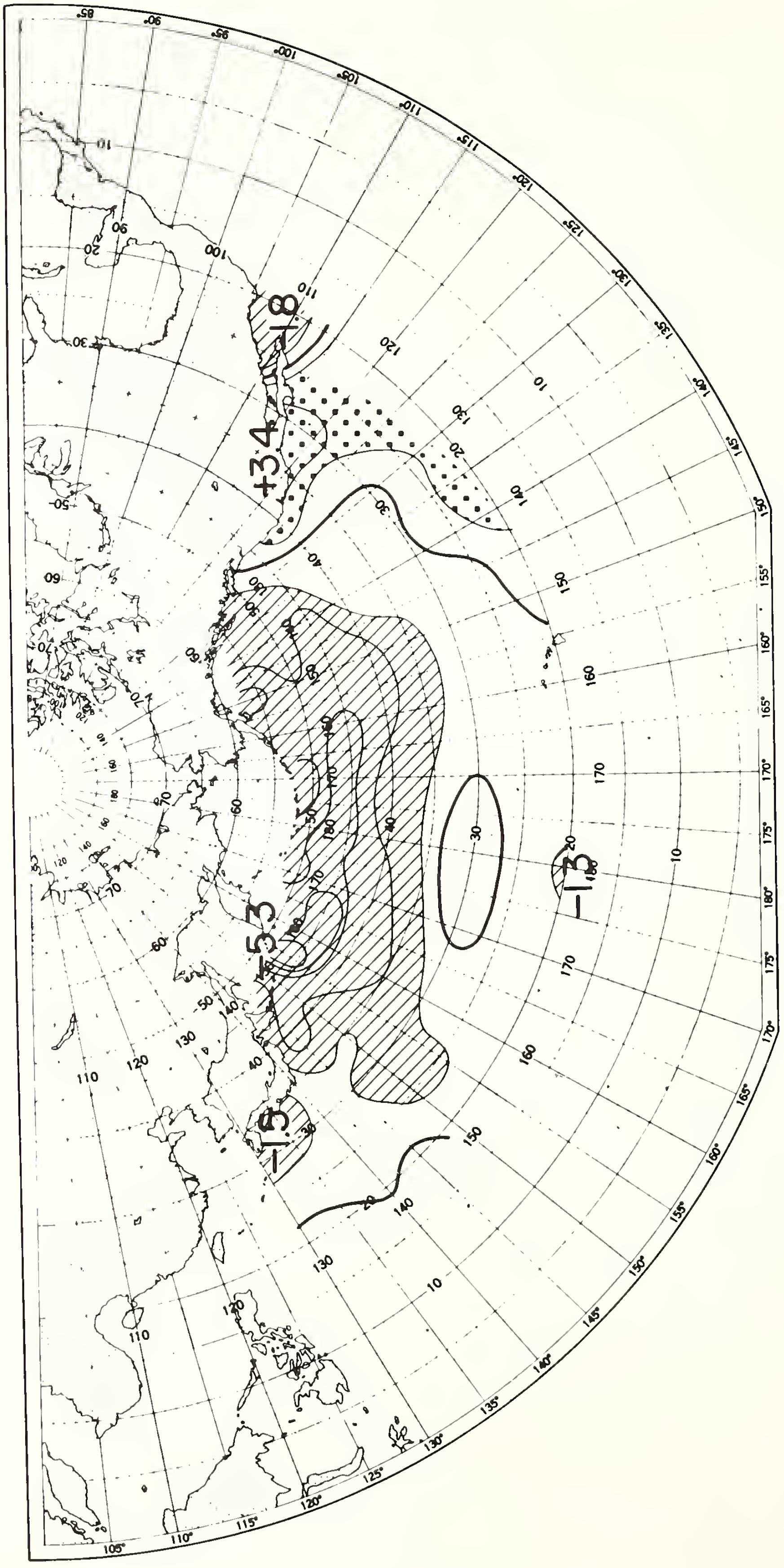

SST$_{DM}$ FALL 1976

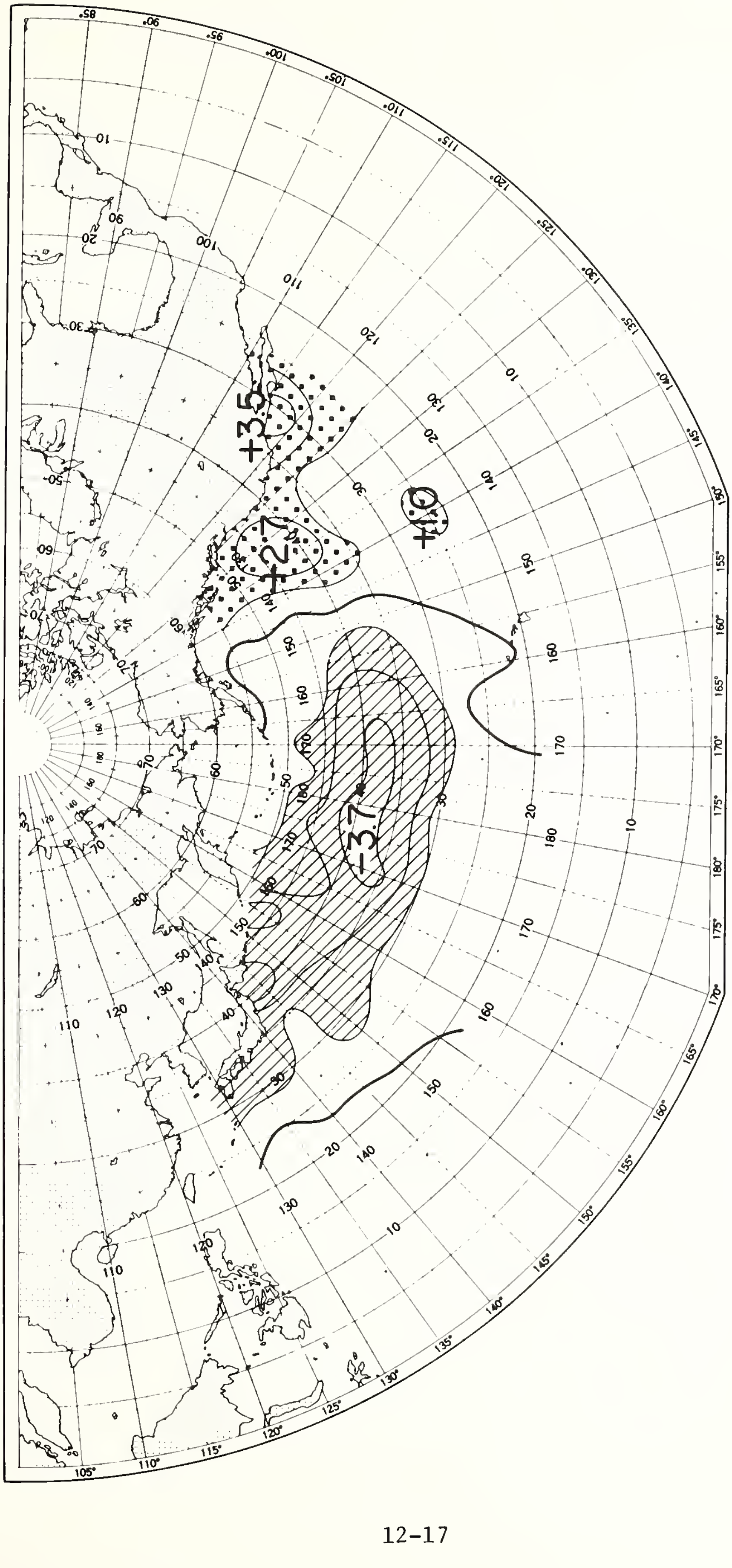

SST$_{DM}$ WINTER 1977

SST 20-YEAR MEAN 40°N (°F)
AND MONTHLY SST, 1976-1977

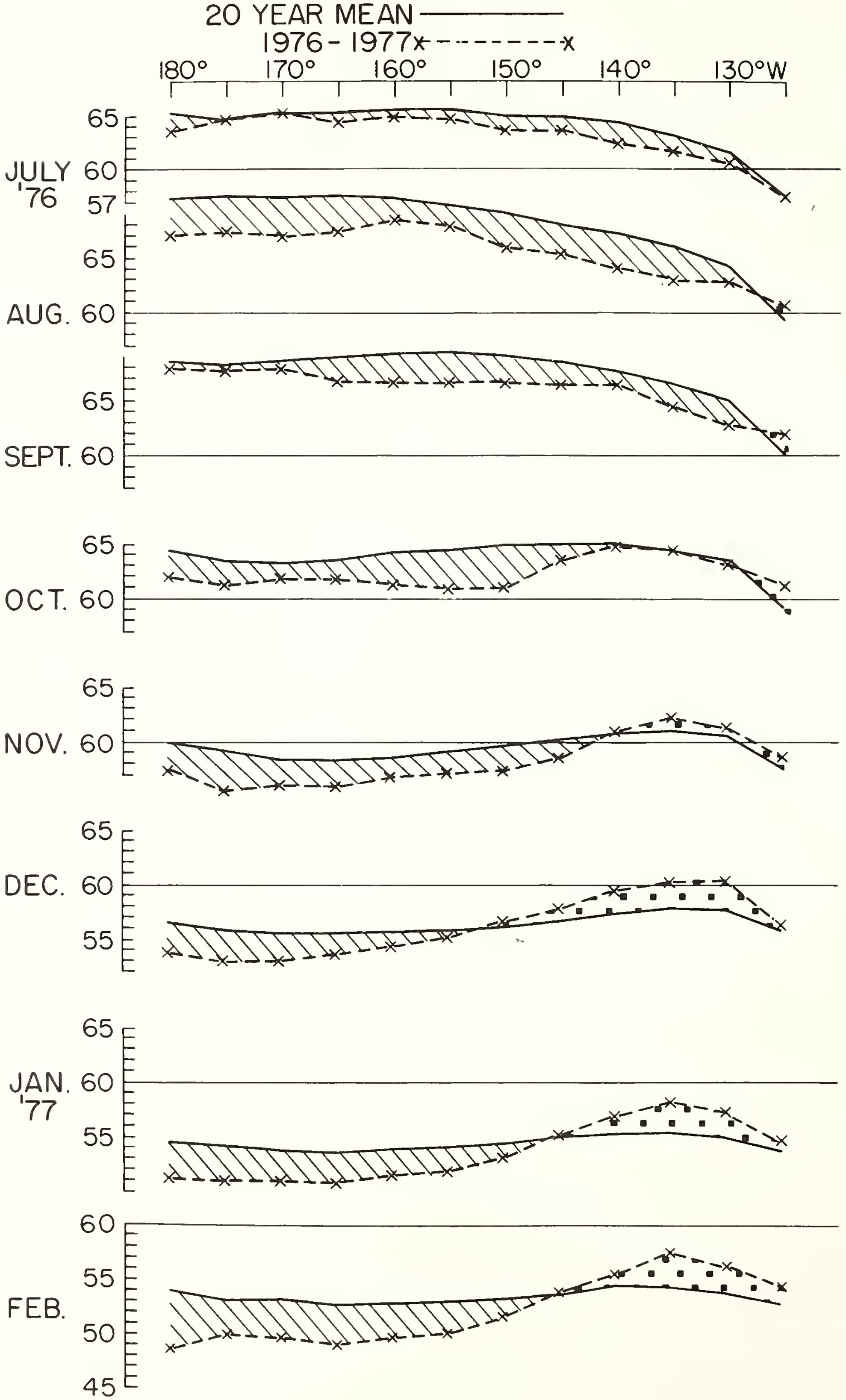

700 mb HEIGHT AND DM

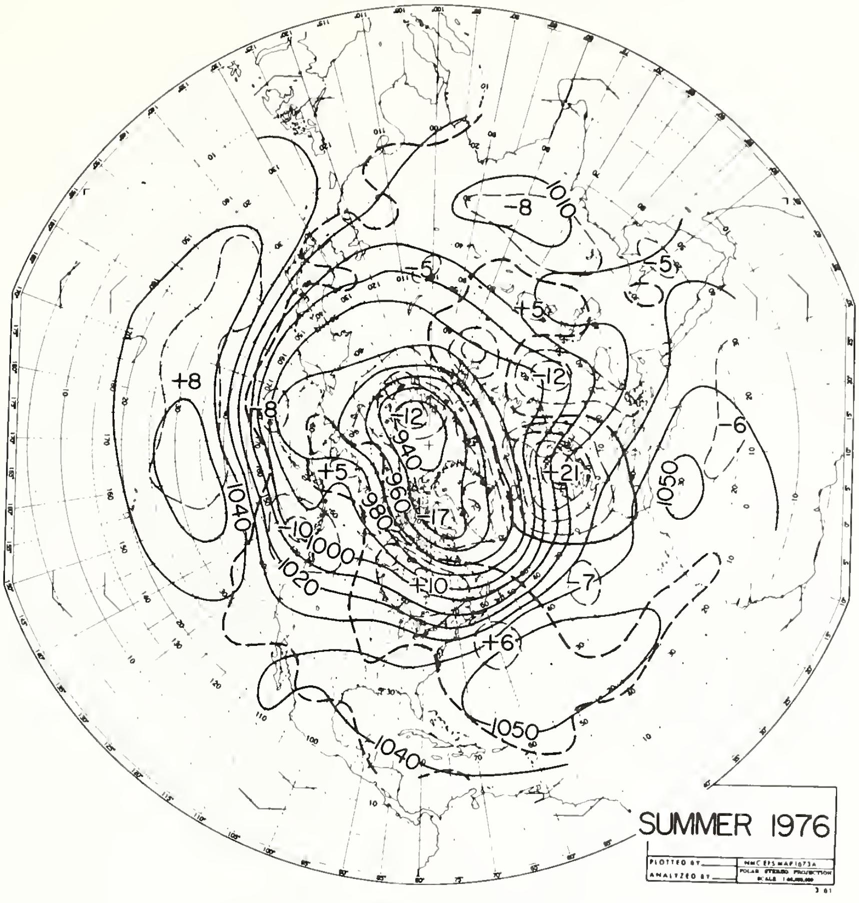

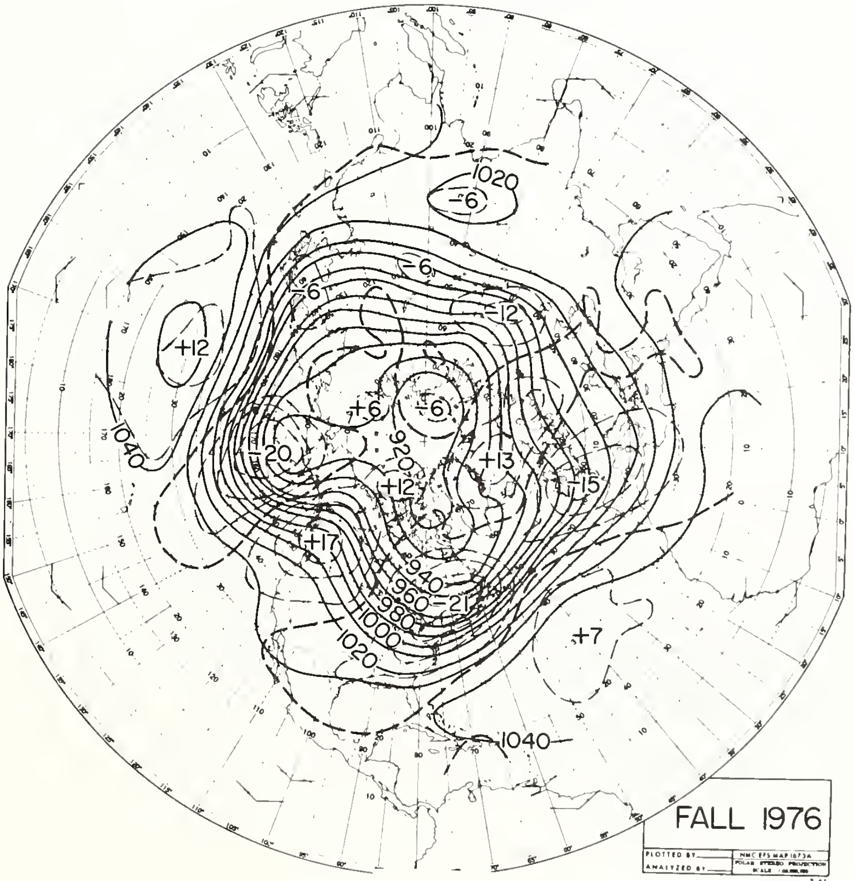

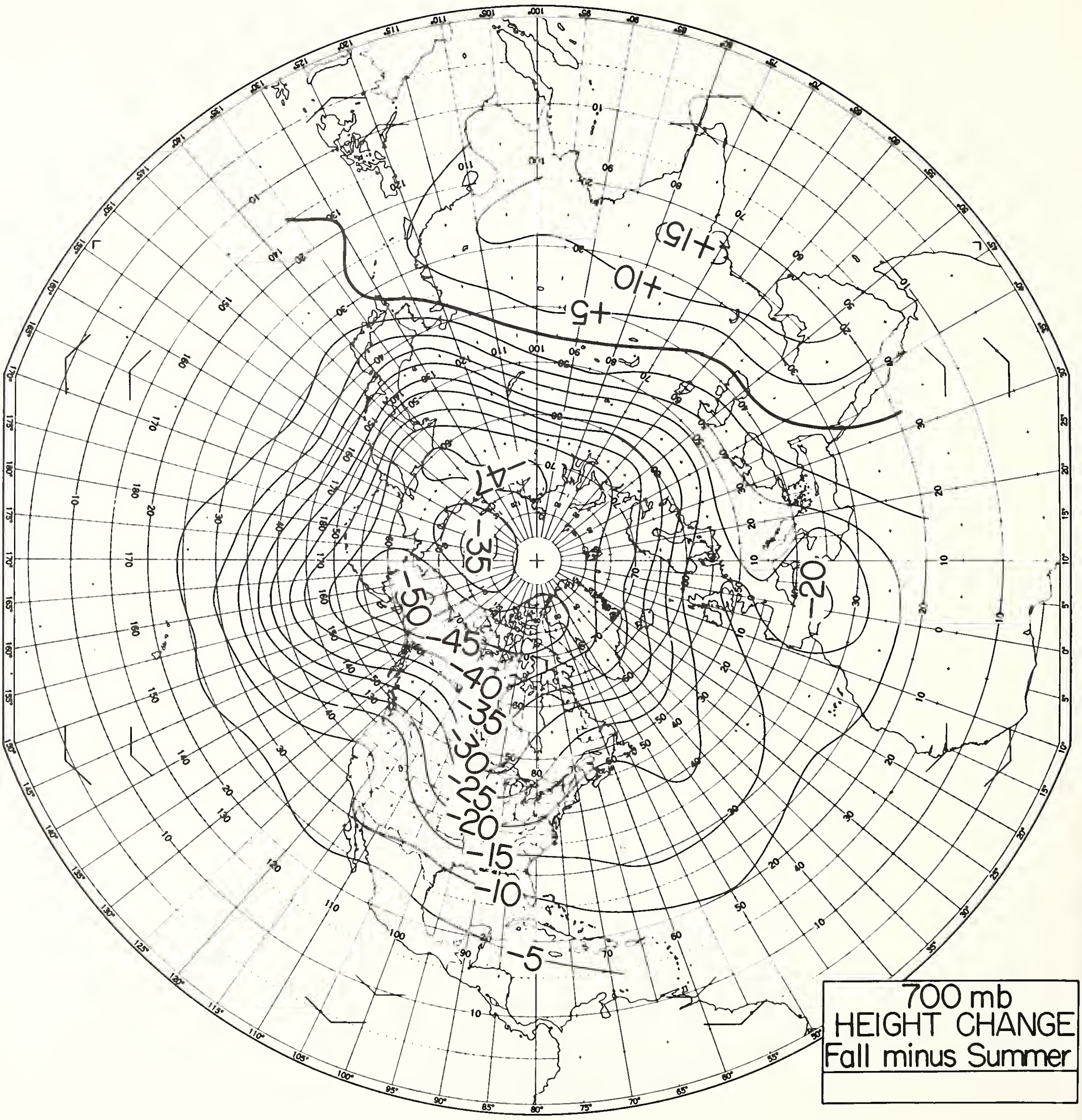

700 mb
HEIGHT CHANGE
Fall minus Summer

Principal Tracks of Centers of Cyclones at Sea Level, North Pacific

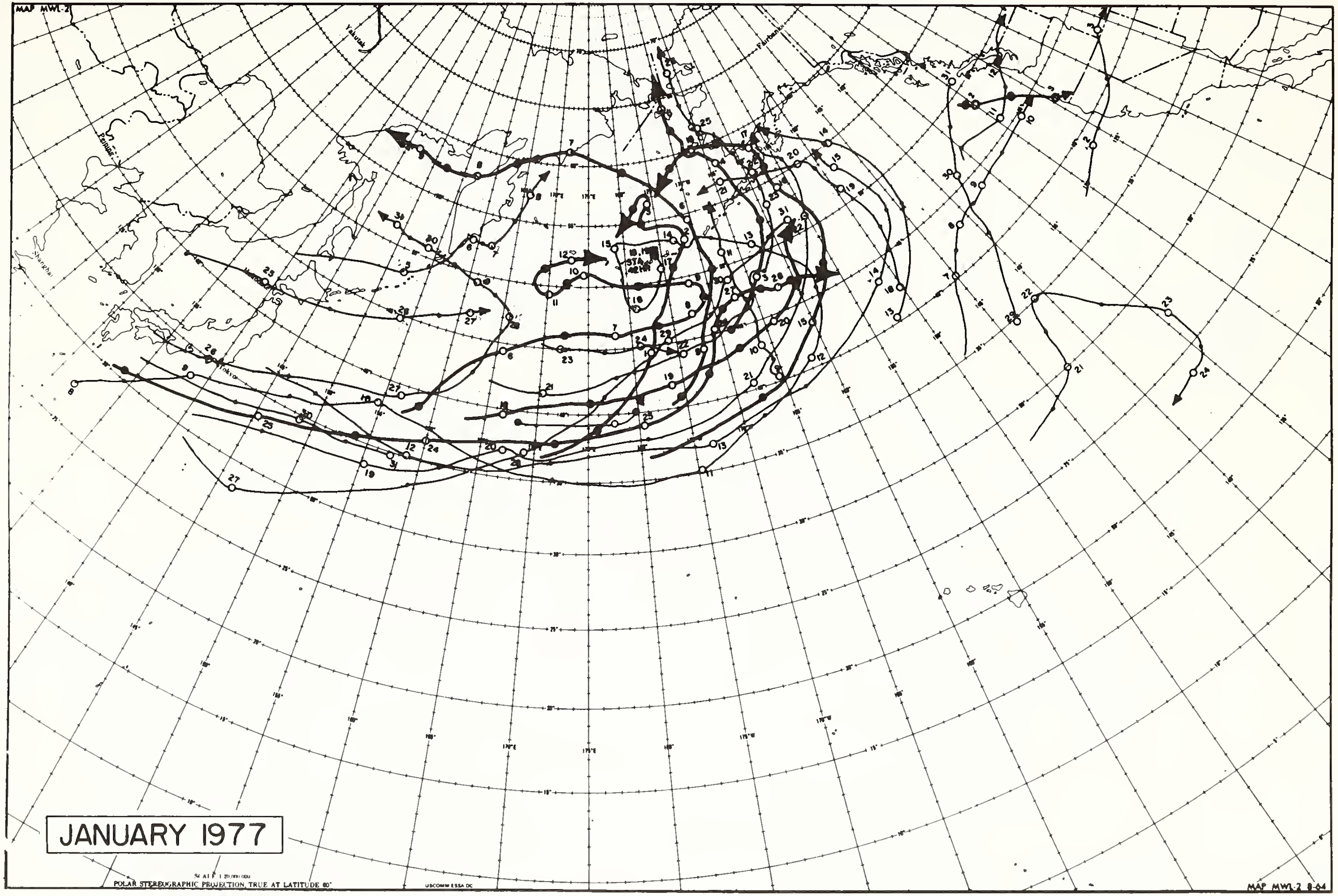

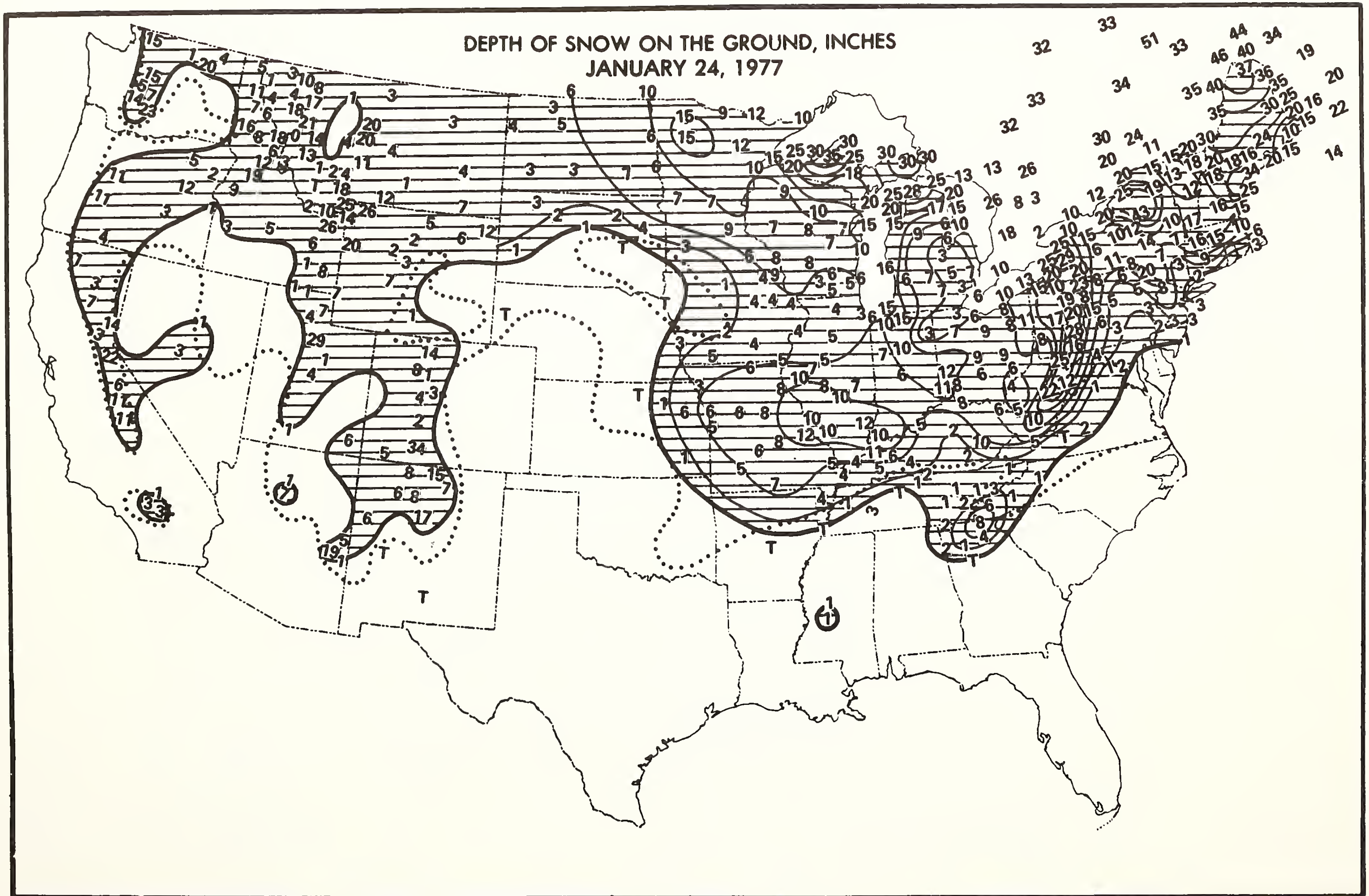

DEPTH OF SNOW ON THE GROUND, INCHES
JANUARY 24, 1977

SST DEPARTURE FROM NORMAL

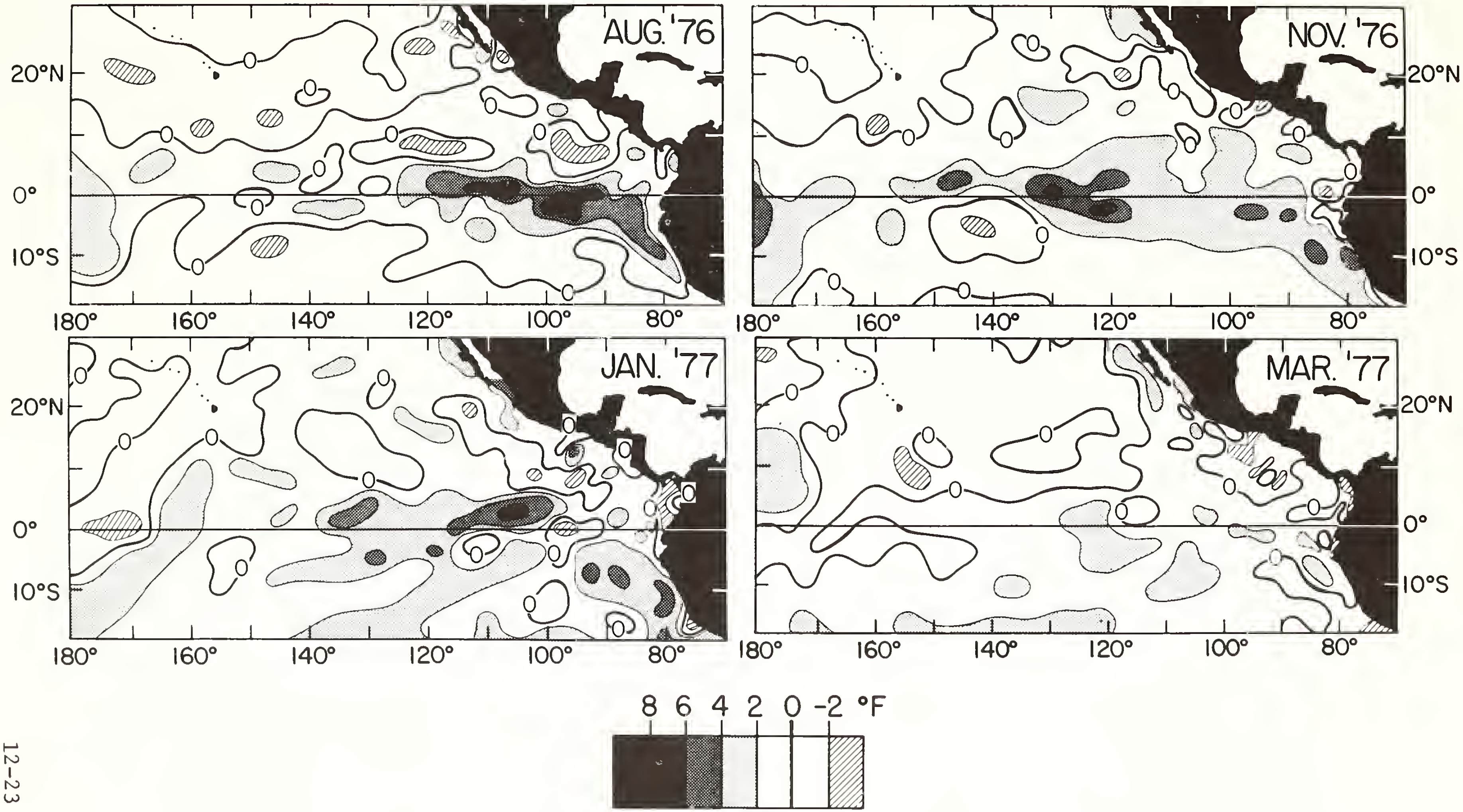

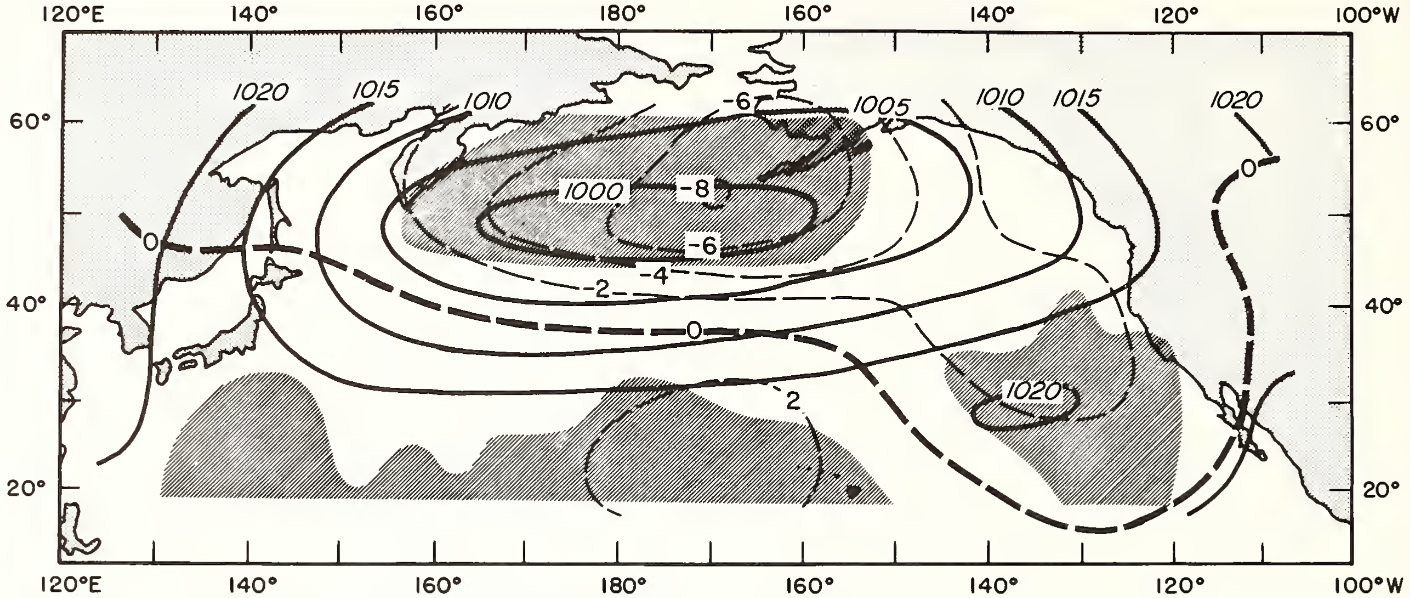

EL NIÑO SLP & DIFFERENCES FROM INVERSE EL NIÑO

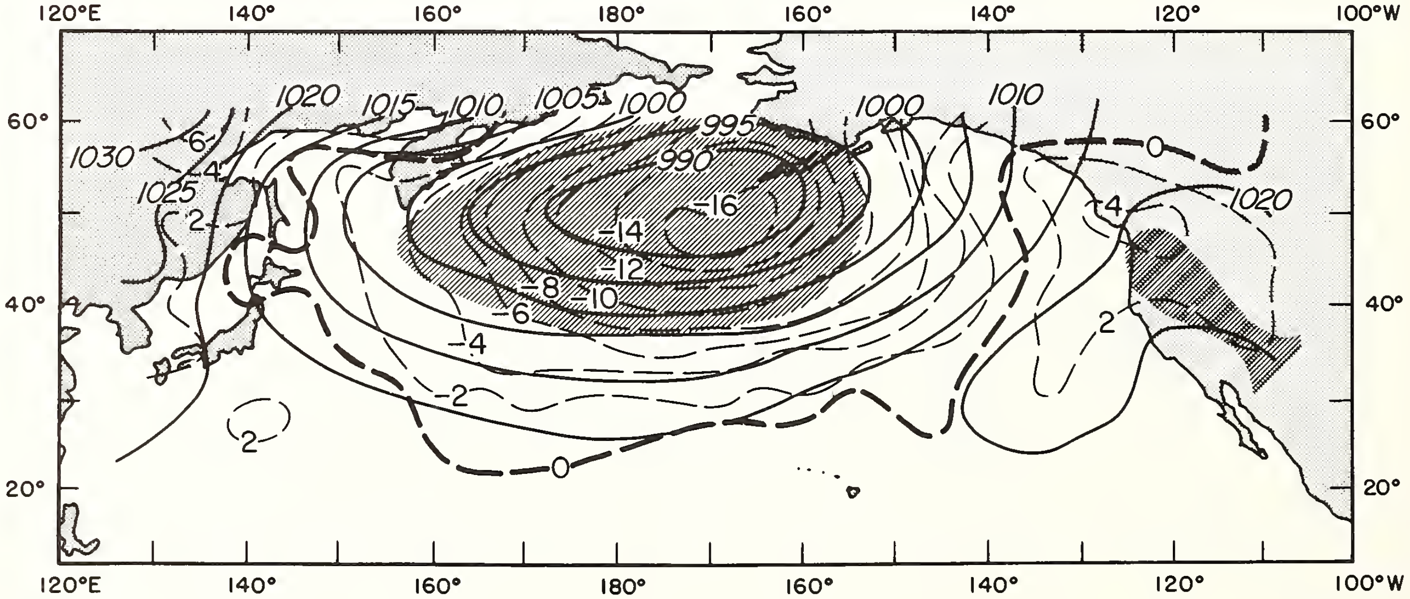

SLP AND DEPARTURE FROM NORMAL, WINTER 1977

WINTER 1976-77

700 mb DM AND SST$_{DM}$

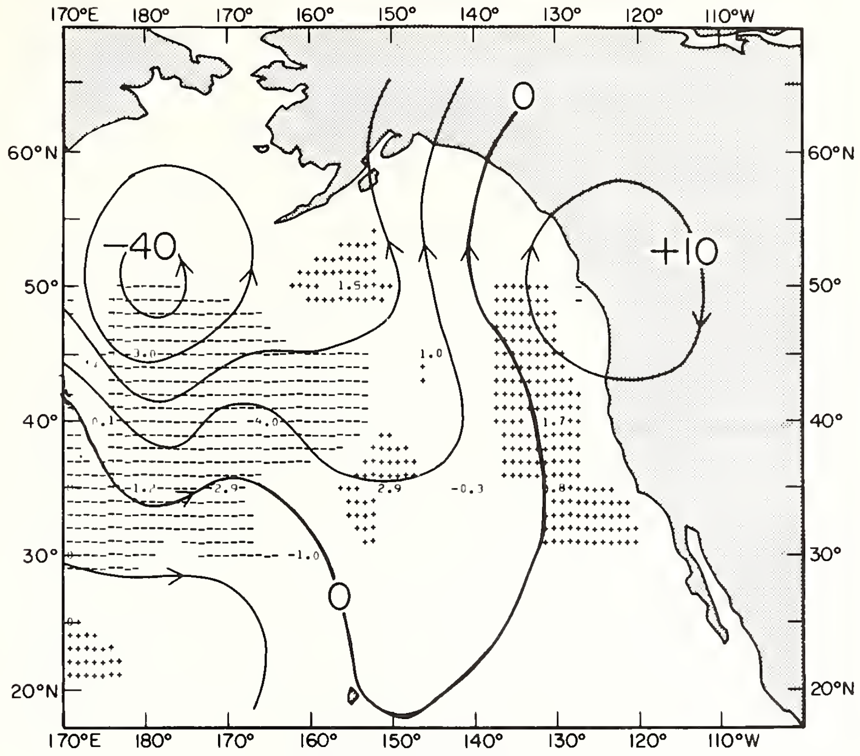

SPECIFIED

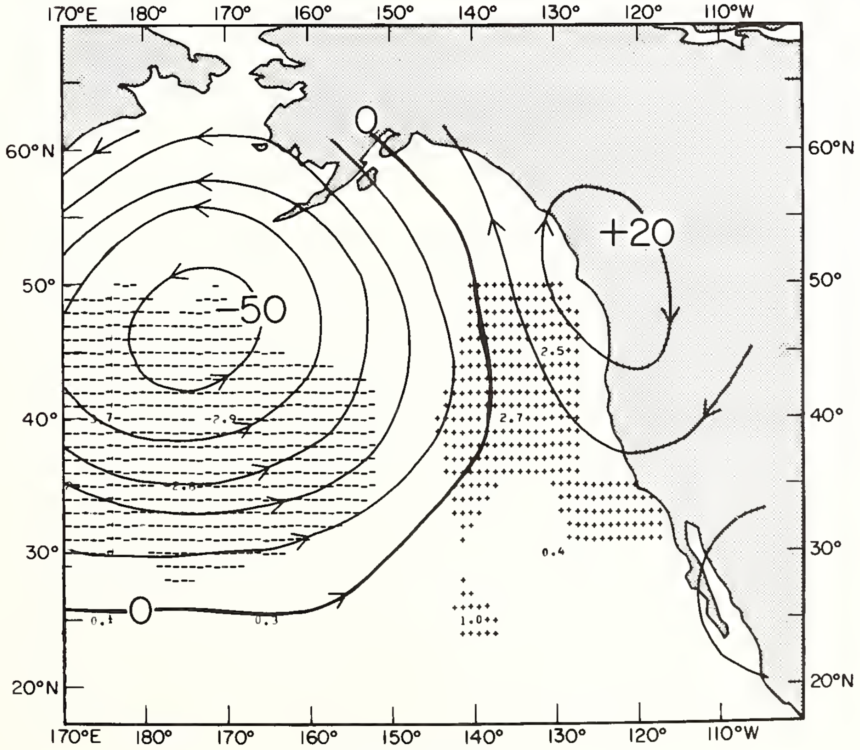

OBSERVED

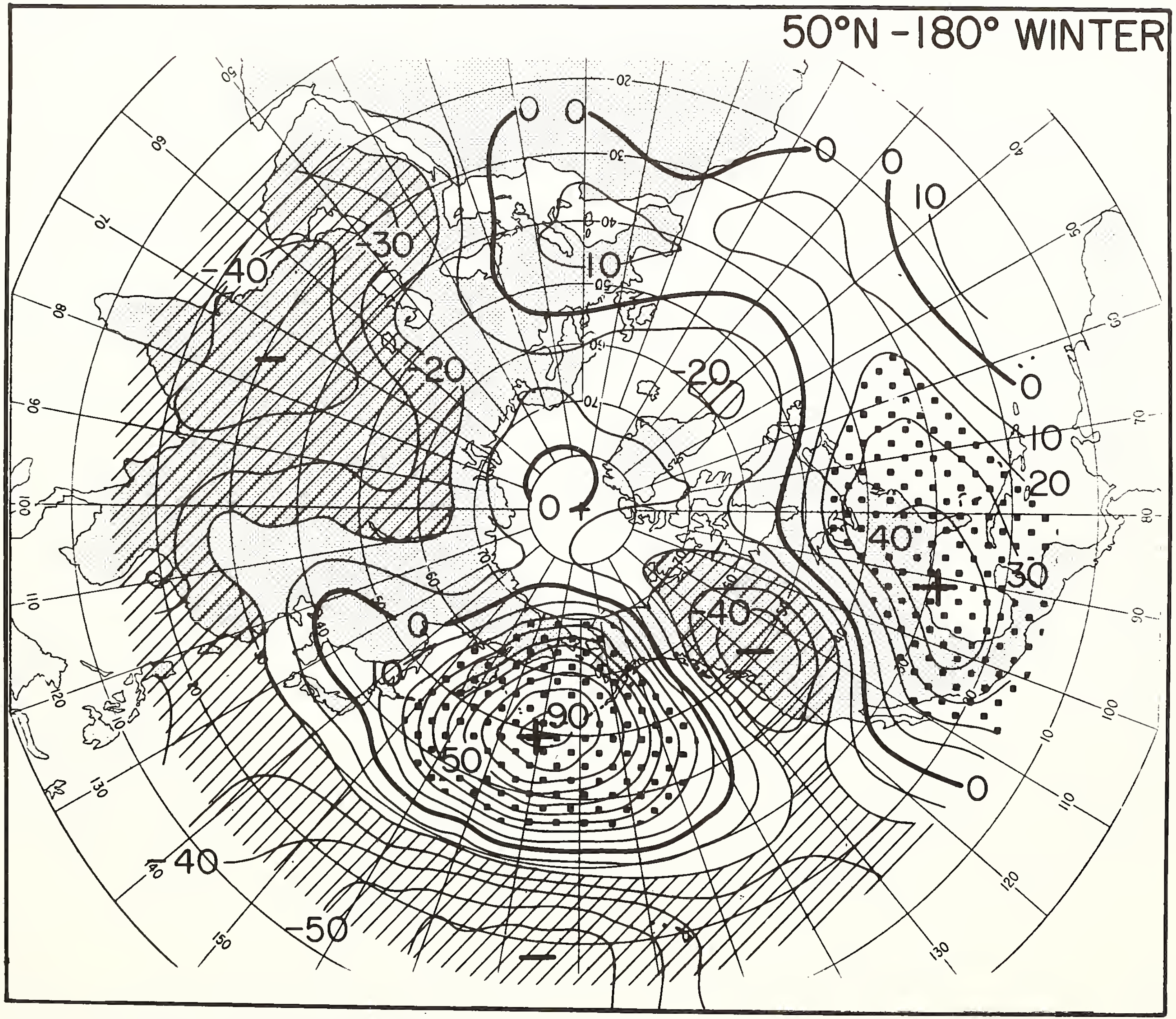

TELECONNECTIONS OF 700 DM

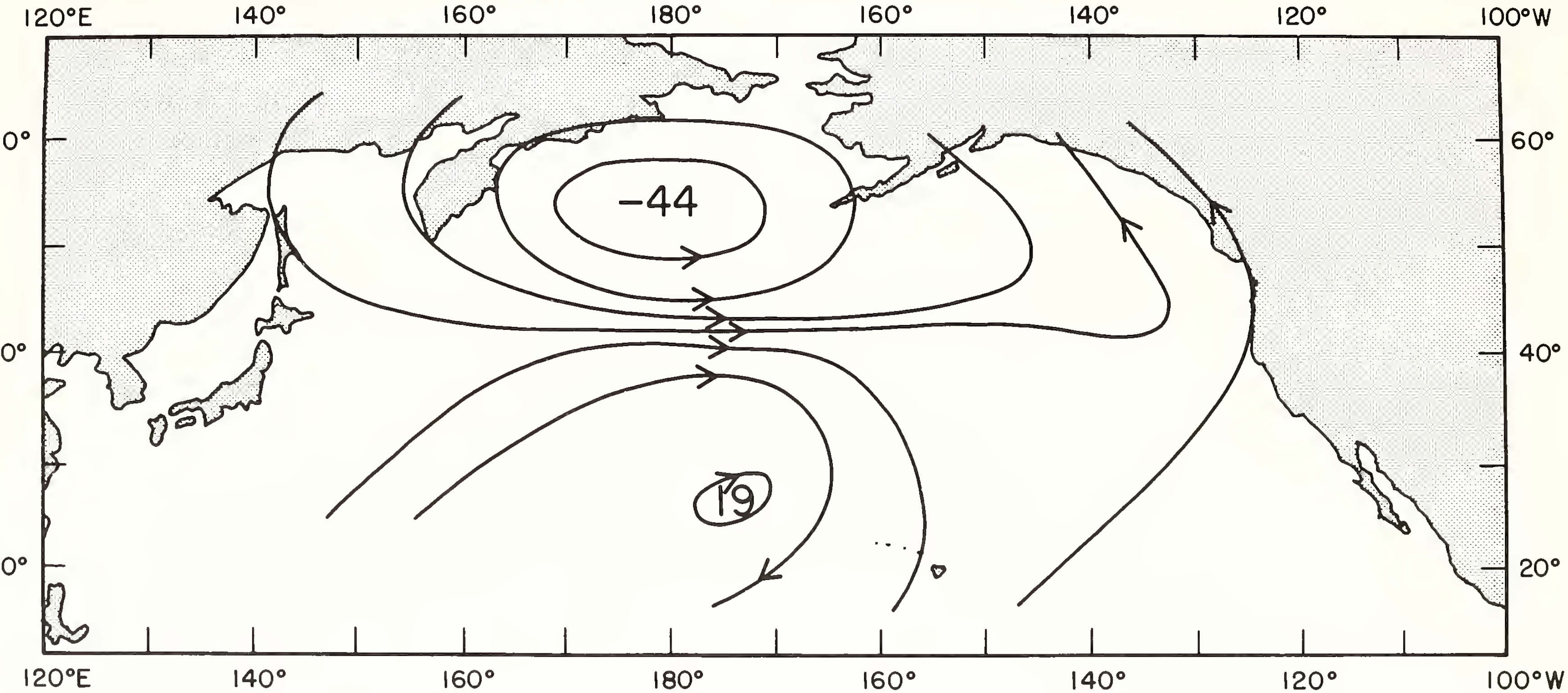

WINTER 1976-77 700mb HEIGHT ANOMALY
PREDICTED FROM ADVECTED NOV. SST

PREDICTED FOR WINTER (DECEMBER, JANUARY, FEBRUARY) 1976-'77

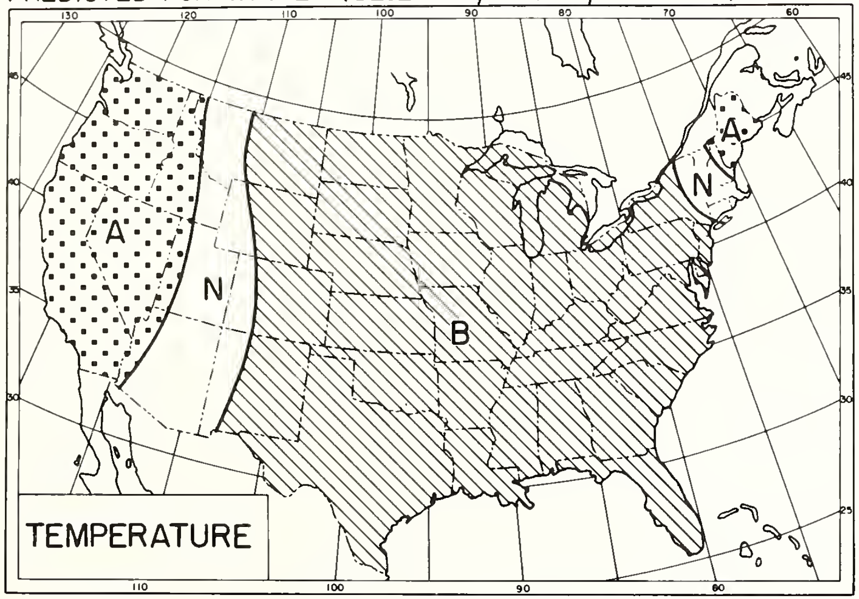

TEMPERATURE

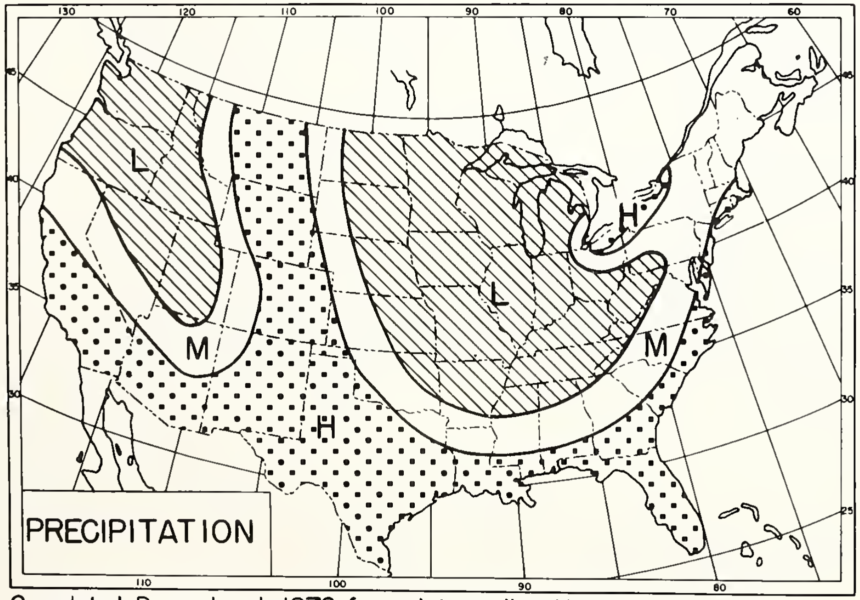

PRECIPITATION

Completed December 1, 1976 from data ending November 23, 1976

OBSERVED FOR WINTER (DECEMBER, JANUARY, FEBRUARY) 1976-'77

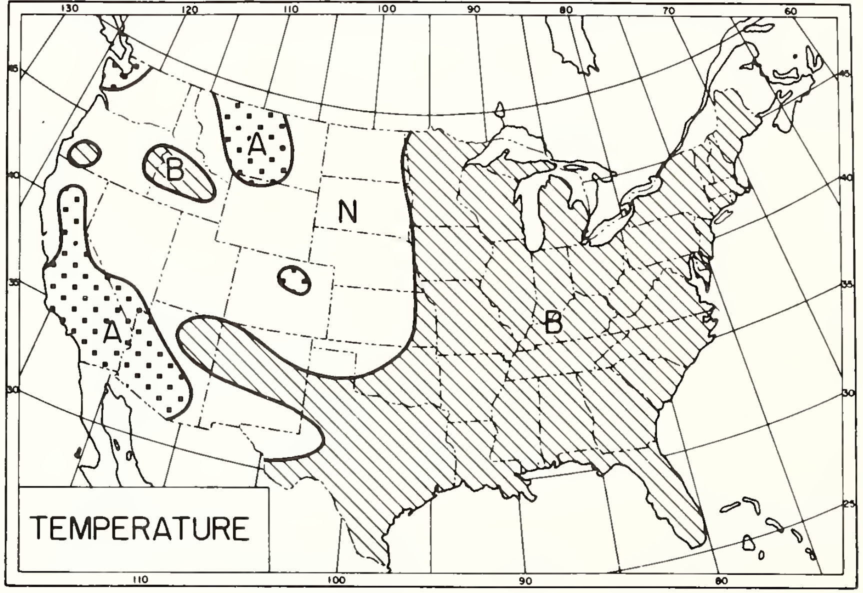

TEMPERATURE

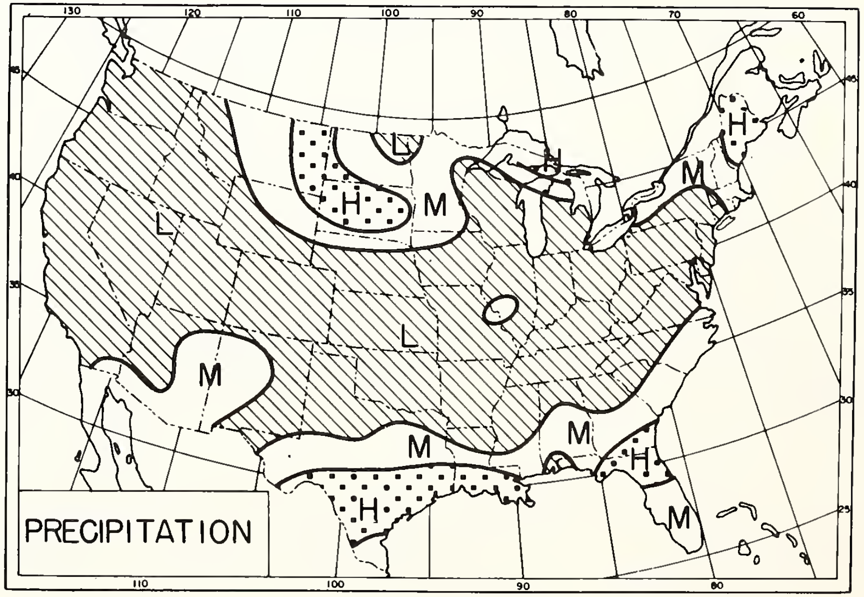

PRECIPITATION

Past Occurrences of Winters Similar to 1976-1977 as Reconstructed from the Tree-Ring Record

by

G. Robert Lofgren and Harold C. Fritts

Laboratory of Tree-Ring Research
University of Arizona
Tucson, Arizona 85721

Trees in stress sites respond to variations in climatic factors including temperature, precipitation, sunshine, and wind, any one of which or all collectively may have limited physiological processes controlling growth. When a number of trees on such stress sites have been sampled, the average width of the annual rings, after having been acccurately dated and the growth trend removed, serves as an integrated measure of all climatic factors which have affected growth, as they have varied throughout the year. Since different species of trees and trees on different sites may respond differently to the same macroclimatic variables, and since the same species may respond differently to the spatial variations in the macroclimate, a wide variety of climatic factors may be calibrated with a given set of tree-ring chronologies. Also, the area covered by the reconstruction of the climatic variable can exceed the area covered by the tree sites because of the spatial continuity of weather systems producing the macroclimate. Hence, significant reconstructions of sea-level pressure anomalies can be made over the North Pacific and North America. Such sea-level pressure anomaly patterns have been obtained from tree-ring data for winter (December through February) from 1602-1962 using multivariate statistics.

The actual sea-level pressure pattern which persisted during much of December, January, and February of 1976-1977 for North America and the north Pacific Ocean was characterized by anomalously low values of greater than 10 mb centered slightly south and west of Dutch Harbor and by anomalously high values of up to nearly two mb along the west coast of North America and extending eastward over the Rocky Mountains.

When this 1976-1977 winter pressure anomaly pattern is correlated with the patterns derived from the modern record since 1899 and with the patterns reconstructed from tree rings during the calibration period, 1899-1962, ten years from each data set are seen to be highly correlated ($r > 0.5$). Seven of the ten years are common to both records (See Fig. 1).

The correlations of the 1976-1977 pressure anomaly pattern with yearly reconstructed pressure patterns from 1600 to 1899 show that winters like the last one appear to occur frequently for certain time periods and then almost disappear for other time periods. Winters similar to this last one have occurred during the eighteenth and nineteenth centuries at frequencies comparable to its occurrence during the twentieth century but have occurred over two times more frequently during the seventeenth century. During the 40-year period from 1615-1655, its occurrence was reconstructed to be over four times more frequent than during the twentieth century. Reconstructions of winter temperature and precipitation for 1615-1655 also show anomalies similar to the winter of 1976-1977, thus helping to confirm that such conditions did occur at that time.

The correlations plotted as a function of time show that the occurrences of winters like 1976-1977 are not random through time. There is a tendency for such winters to occur rather frequently for several decades and then to disappear for a number of decades. Counts were made of all cases of correlations greater than 0.5. The period with the highest count was from 1615-1655 averaging about six out of every ten years. During the period 1800 to 1830 winters similar to this last winter were reconstructed over 40% of the time. This would suggest that it might be possible to enter a climatic regime like one of these periods in which we could encounter a three to fourfold increase in frequency of winters very similar to this last one. However, the average expected frequency throughout the 360-year period is about 1¼ (126%) as great as that observed during the period of the modern climatic record.

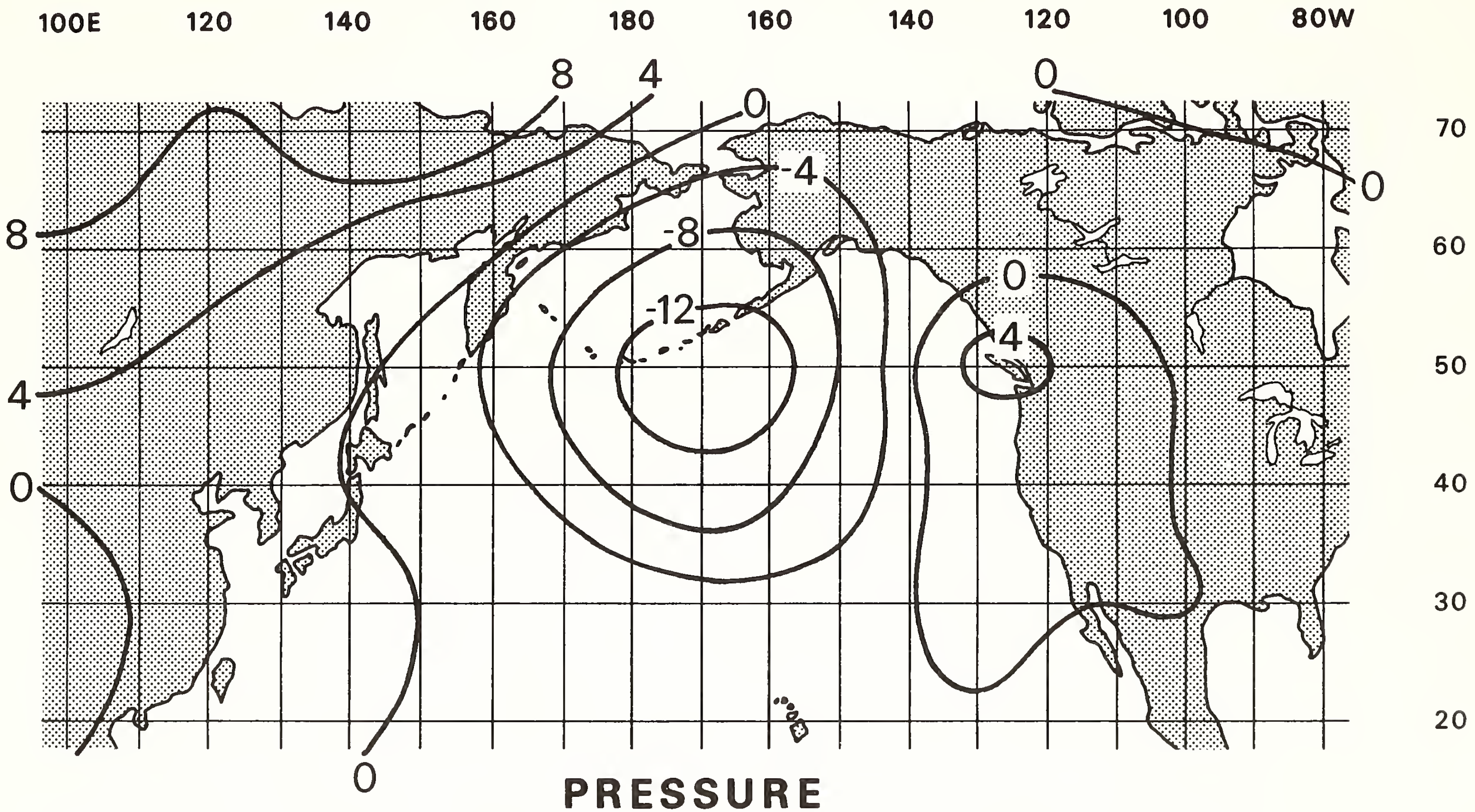

PRESSURE

WINTER 1976-77

CORRELATIONS[1] OF 1976-77 WINTER SEA LEVEL PRESSURE ANOMALIES WITH ACTUAL AND RECONSTRUCTED PRESSURE ANOMALIES 1900-1962

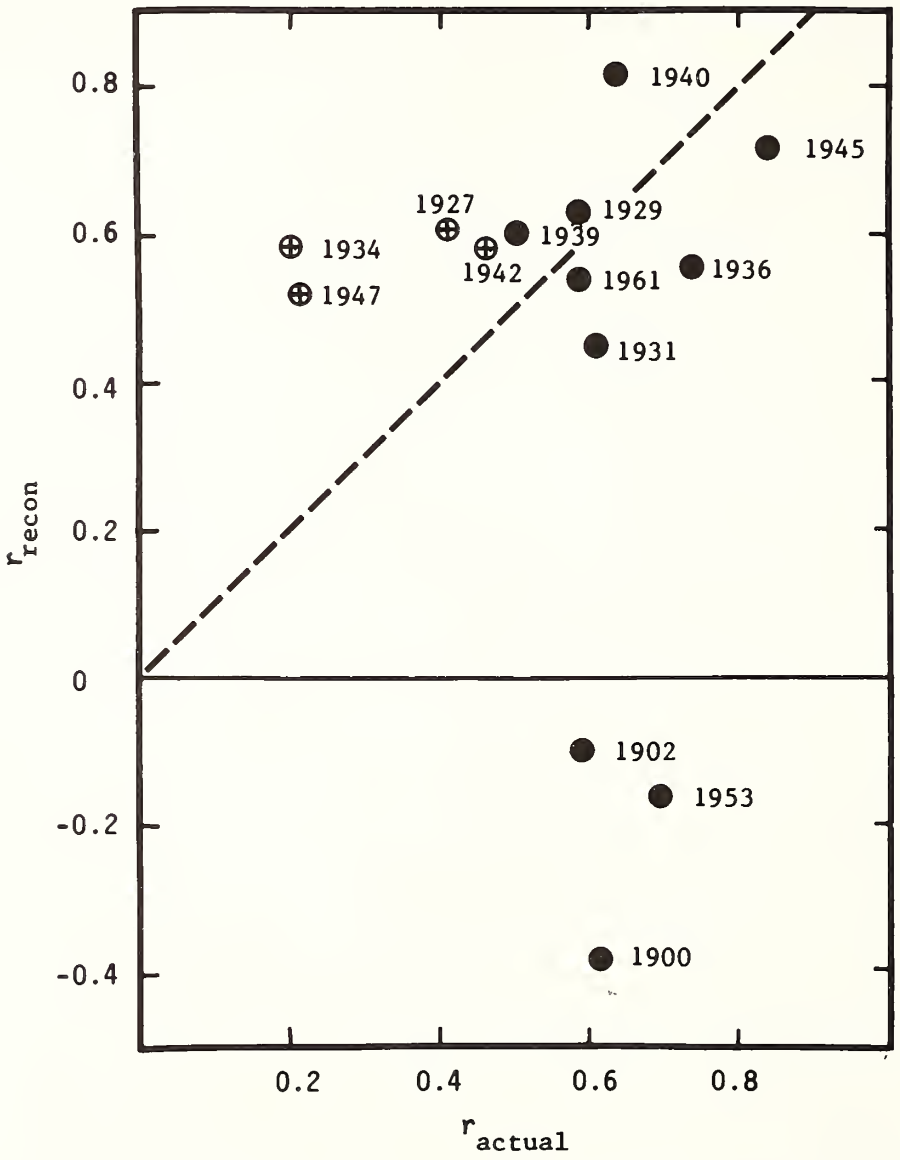

[1] Correlations > 0.5 for at least one of the data sets

● Correlation with actual data > 0.5

⊕ Correlation with reconstructed data > 0.5

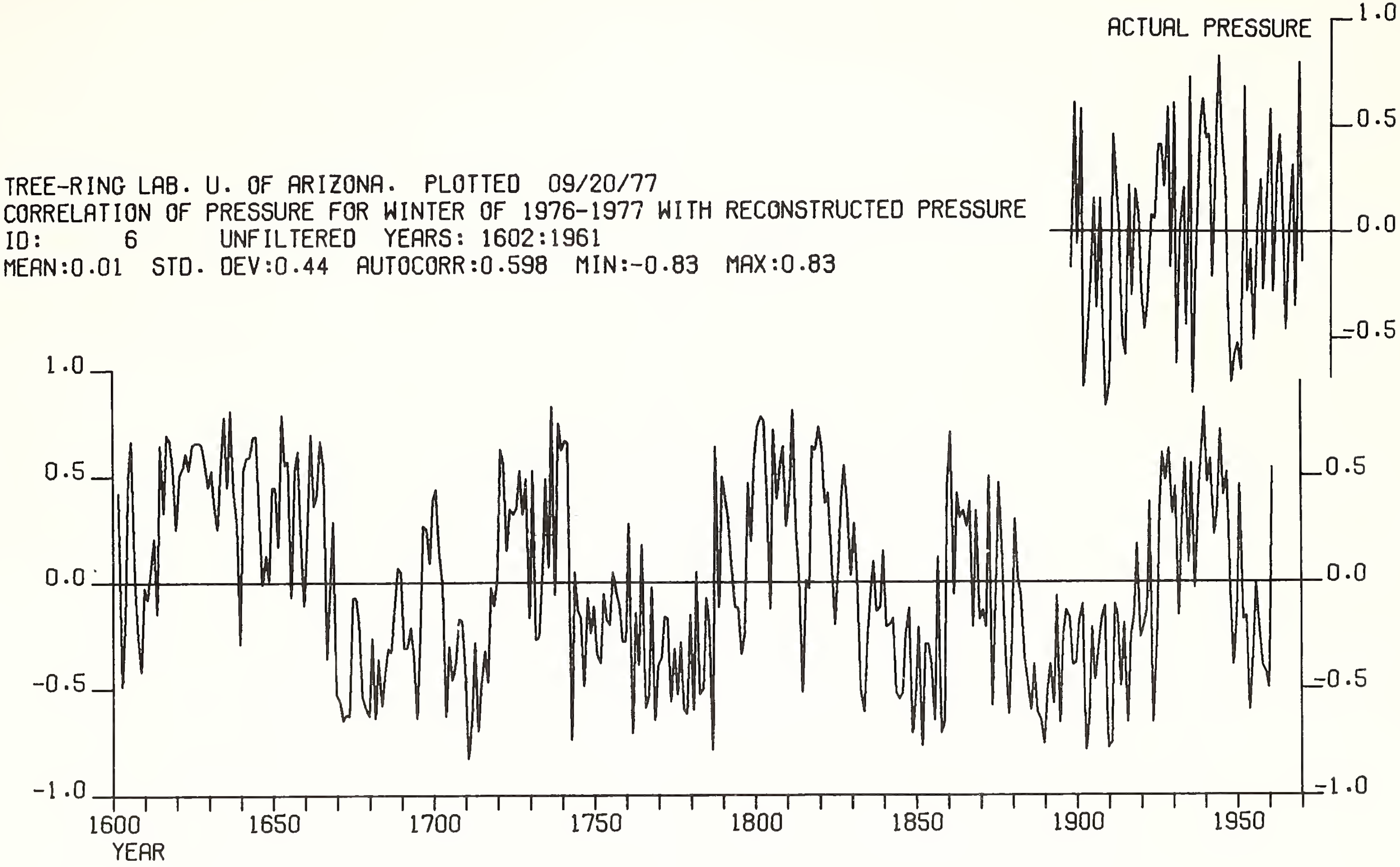

WINTER MODEL BM,IM,IF

TABLE II

Frequency of Reconstructed Winter Pressure Anomalies Similar to the Pressure Anomalies of Winter, 1976-1977

Interval	Frequency	Percentage of 1901-1961
1901-1961[a]	14.8	100
1801-1900	14.0	95
1701-1800	12.0	81
1602-1700	32.3	218
1615-1655	61.0	412
1602-1961	18.6	126

---

[a] Actual climatic data rather than reconstructed values used for 1901-1961 calibration interval only.

AN ATTEMPT AT ONE-MONTH FORECAST OF THE EVENT 1976/77

K. Miyakoda and the Staff *

Geophysical Fluid Dynamics Laboratory/NOAA
Princeton, New Jersey

---

* Presently, the contributors are C. T. Gordon, W. Stern, W. Bourke, R. Hovanec, and A. Rosati

Abstract

This is a part of the simulation project of the winter event of 1976/77, using general circulation models. The first attempt is a one-month prediction, starting with the initial condition of January 1, 1977. The numerical model used in this study is the "spectral transform" model developed by Gordon and Stern (1974) based on the original barogropic spectral model of Bourke (1972). The model has the horizontal resolution of rhomboidal wavenumber 30 and the vertical levels of 9, where the gridpoints between the equator and a pole is 40 and the zonal wavenumber is 30. It includes the standard features of physics employed in the usual general circulation model, but the cloud feed-back was not incorporated. The sea surface temperatures were the climatological normals processed by U. S. Hydrographic Office, and the sea-ice limit was also the January normal. The initial conditions of soil moisture, snow-deposit, and land-ice limit were taken from the solutions of a climate model (Manabe et al, 1974). The soil moisture and snow-deposit in the subsequent days were predicted within the model. Perhaps the most noteworthy merit of this model is its efficiency in calculation. It takes 28 minutes for one day forecast in contrast to 2 hour with a finite difference global model of the equivalent resolution.

The simulation of the event has turned out not good; of course, it may not be expected with the climatologically normal values for the external parameters. Compared with the observation, the predicted height patterns of geopotential height were not bad until the 10th day of the forecast, but the solution had quickly deteriorated since then.

In the next step, it is being planned to use the real sea surface temperature and the real snow extension for January 1977. At present, two data of sea surface temperature from different sources are checked; one

was the ship data provided by Doug Mclain, National Marine Fisheries, and the other was the satellite sounding provided by NESS. The two data are considerably different, and it does not appear an easy task to amalgamate these data.

Circulation Over the Tropics During 1976-77 as Related to that at Middle Latitudes.

Arthur F. Krueger NOAA, NESS
World Weather Building, Washington, D. C., 20233

In retrospect, hints of impending circulation changes over the tropics appeared a year ago. Some of these were the weakening of the South Pacific anticyclone and tradewind flow as well as a warming of much of the eastern equatorial Pacific. How these changes affected the Northern Hemisphere winter circulation is less clear. In this discussion I would like to describe some of the circulation changes over the tropics and attempt to relate them to contemporary circulation changes over the Northern Hemisphere.

Perhaps the most striking feature of this past winter's circulation was the very strong westerlies and their expansion equatorward. The equatorward shift was accompanied by a parallel shift of the subtropical high pressure belt and a weakening of the tradewinds north and south of the equator (fig. 1). This motion of the subtropical ridgeline may be important since it is believed to separate the baroclinically unstable Rossby regime from the Hadley regime. These changes influenced most of the atmosphere and the pressure-integrated zonal kinetic energy can be seen to have doubled at 30°N during January 1977 (fig. 2a). Stronger westerlies also extended to 15°N latitude. Interestingly, parallel but weaker changes occurred over the Southern Hemisphere so that the tropics were bounded by stronger westerlies from both sides.

Concurrently, the eddy kinetic energy over the tropics (20N - 20S) decreased from the previous year (figure 2b). Largest decreases occurred at the equator and also 5°S. To a large extent this eddy kinetic energy is in the low latitude standing eddies as shown in figure 3. Notice these planetary-scale perturbations over the tropics sandwiched in between the subtropical jet streams of both hemispheres. Probably a substantial part of the eddy kinetic energy was in the "Walker Circulation" during January 1976 (upper). Notice the zonal winds in excess of 30 mps over the equatorial Pacific with easterlies near Indonesia-New Guinea. In contrast, during January 1977 (lower figure), this zonal circulation was weaker and speeds here were now barely 15 mps with a maximum no longer along the equator. Instead velocities increased from the northeast tropical Pacific where a deep trough was located, across Northern Mexico to the strong maximum over the Southeastern United States. This weakening of the high level equatorial flow during January 1977 is better shown by the stream function of the 200 mb anomalous flow (figure 4). The base period chosen here is the six-year mean 1968-74. Notice that it is accompanied by a weakening of the South Pacific high level mid-oceanic trough - this is indicated by the anticyclonic anomalous flow over most of the tropical South Pacific. Just to the northeast, anomalous anticyclonic flow also exists over Central America and the Caribbean. The deep trough off Southern California is clearly indicated as well as the strong westerlies over the southern part of the United States. The abnormal trough appears to have been associated with a more active ITCZ over the Northeast Pacific (lower figure 4) and somewhat warmer ocean temperatures. Winston will describe these changes in tropical cloudiness in more detail, but I might point out that the convection normally located over Indonesia was displaced eastwards along the equator and the South American rainfall was displaced southward.

It is also interesting that equatorial westerlies over the Pacific have undergone a yearly alternation for the last six winters with the even years experiencing stronger westerlies and the odd years weak westerlies (fig. 5). The dimensions of these circulation anomalies are such that their influence extends to higher latitudes of both hemispheres. Over the southern part of the United States, for example, the 200 mb westerlies have appeared to vary inversely with those over the equator (except for 1975).

What physical processes were occurring that established and maintained the 1977 tropical anomalies and what role did they play in maintaining the abnormal Northern Hemisphere circulation? It is tempting to invoke a mechanism such as Bjerknes suggested. Perhaps a stronger mean meridional circulation arising as a consequence of greater condensation heating over the tropics did occur and maintained the westerlies south of normal. However, as is well known, monitoring of the strength of the mean meridional circulation is notoriously difficult - especially from routine analyses. Perhaps we can speculate.

The next figure shows the longwave cooling (fig. 6, left), and the mean temperature (fig. 6, right) or total potential energy (since it is the vertical integral) from the NMC analysis for January 1976 and 1977. During early 1977, the tropics were warmer than during early 1976. While the stratosphere was colder, tropospheric temperatures were as much as 1 1/2°C above. Also, it is interesting that from 10°N to 20°S the tropics were warmer than the mean tropical atmosphere. This contributed to maintaining a stronger low latitude temperature gradient. Note how this gradient was stronger between 20°N and 40°N during 1977. Perhaps warmer sea surface temperatures and a more vigorous moist convective process were responsible. The longwave cooling curves indicate slightly lower outgoing radiation between 12°S and 7°N and suggest more cloudiness and upward motion during January 1977. Conversely, higher radiation values near 10 - 15°N suggest less clouds and more downward motion - in other words an enhanced Hadley circulation. It has been suggested that an equatorward shift of the subtropical ridgeline is also indicative of a stronger Hadley cell (Pittock; QJRMS, July 1973).

While processes over the tropics helped maintain a stronger low latitude temperature gradient it must be noted that the mid-latitude eddy circulation also contributed by lowering the temperatures near 40°N latitude. It is interesting that the atmospheric eddy heat transport calculated from the NMC analysis indicates a stronger heat flux divergence at these latitudes during January 1977 (fig. 7). This heat was transported to near 60°N latitude where nearly 50 Wm^{-2} more than 1976 was received and which nearly balanced the radiative heat loss indicated for these latitudes (fig. 7, left). This is not the case near 40°N where the radiative losses together with that due to the eddy flux divergence amount to 200 Wm^{-2}. This large energy loss must largely be replenished by heat transfer processes from the ocean and it is clearly important that these processes be monitored also.

Mean Zonal Wind
1000 mb (NMC analysis)

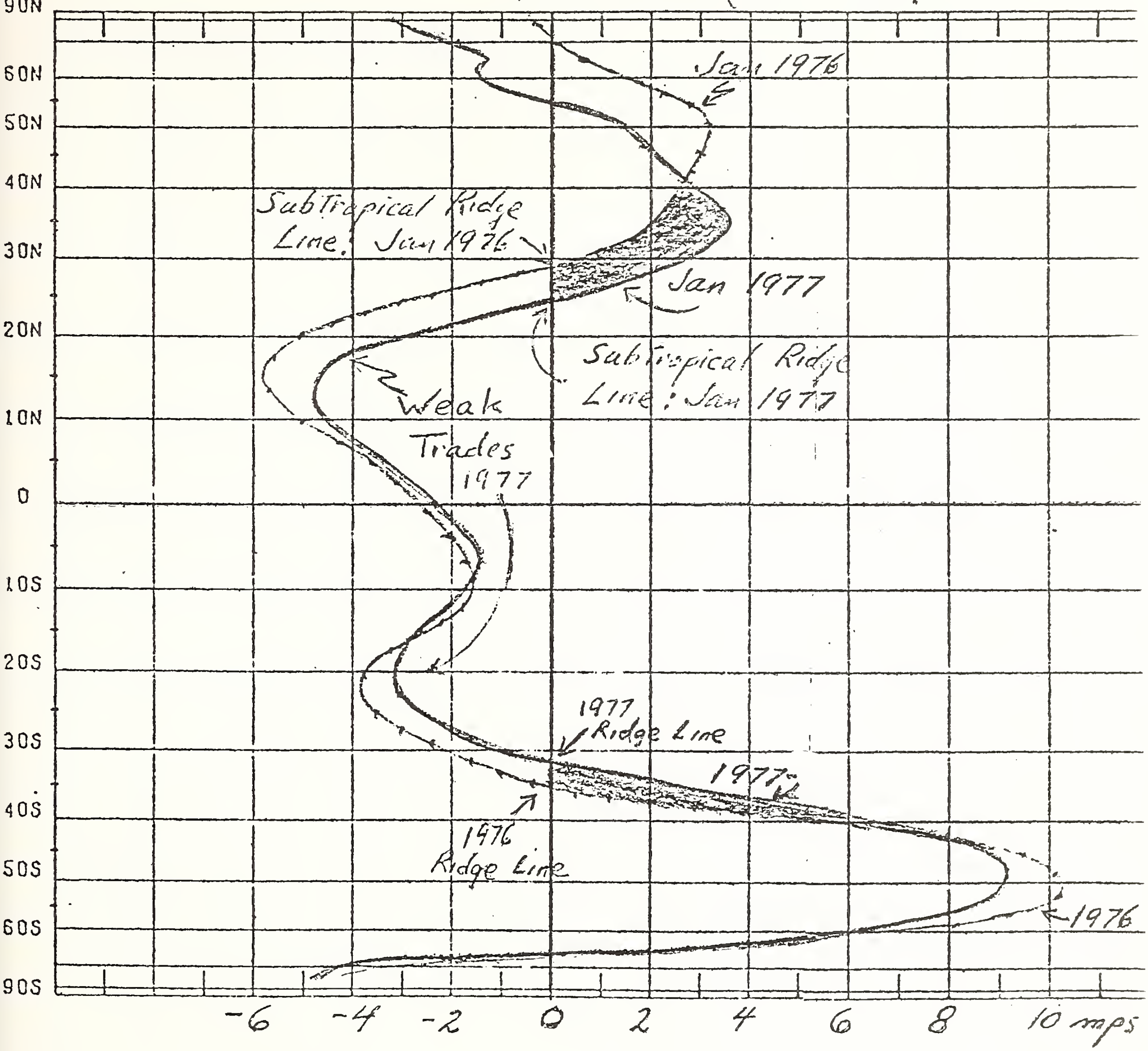

Zonal Kinetic Energy (NMC analysis)

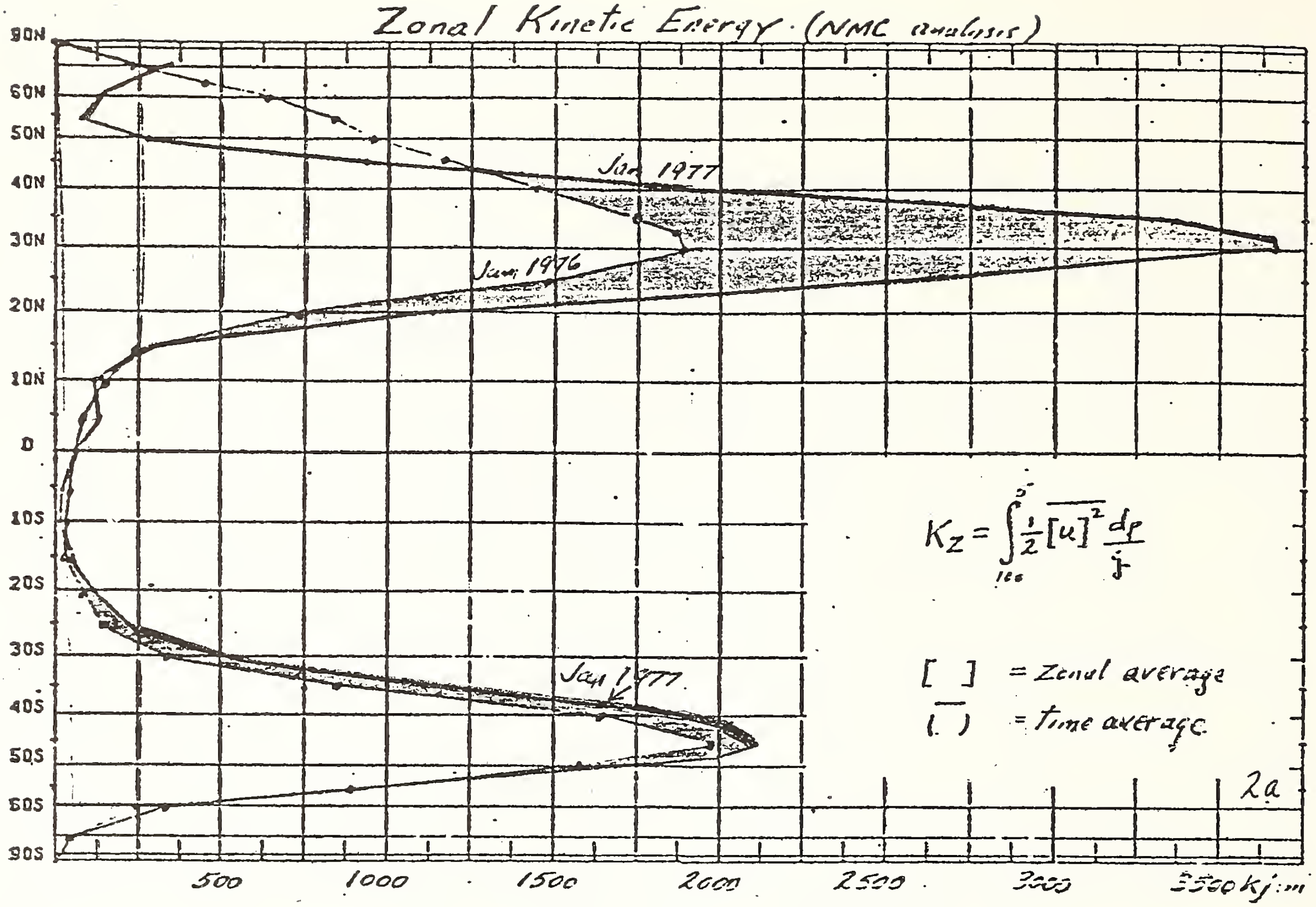

Eddy Kinetic Energy (NMC analysis)

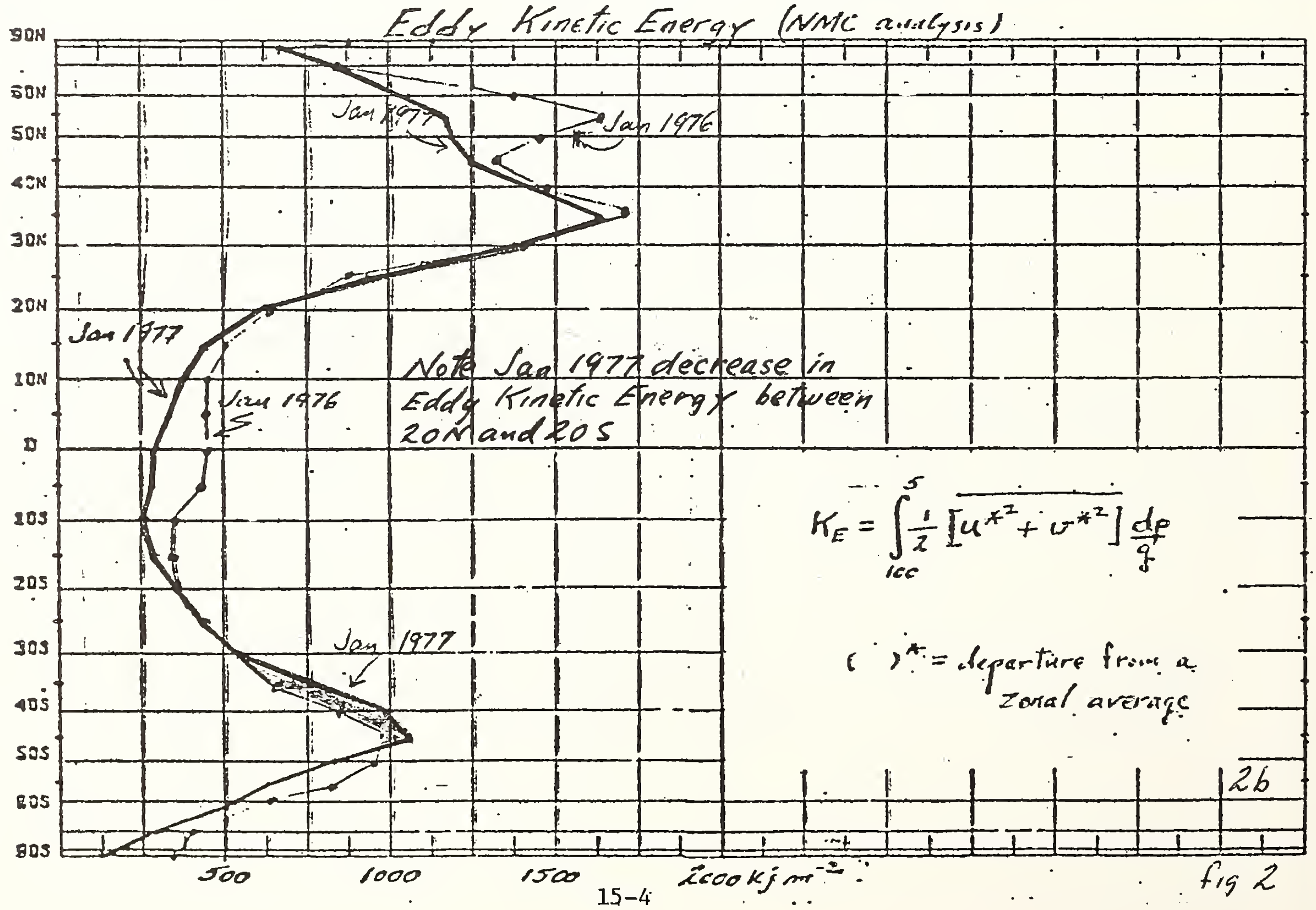

Note Jan 1977 decrease in Eddy Kinetic Energy between 20N and 20S

fig 2

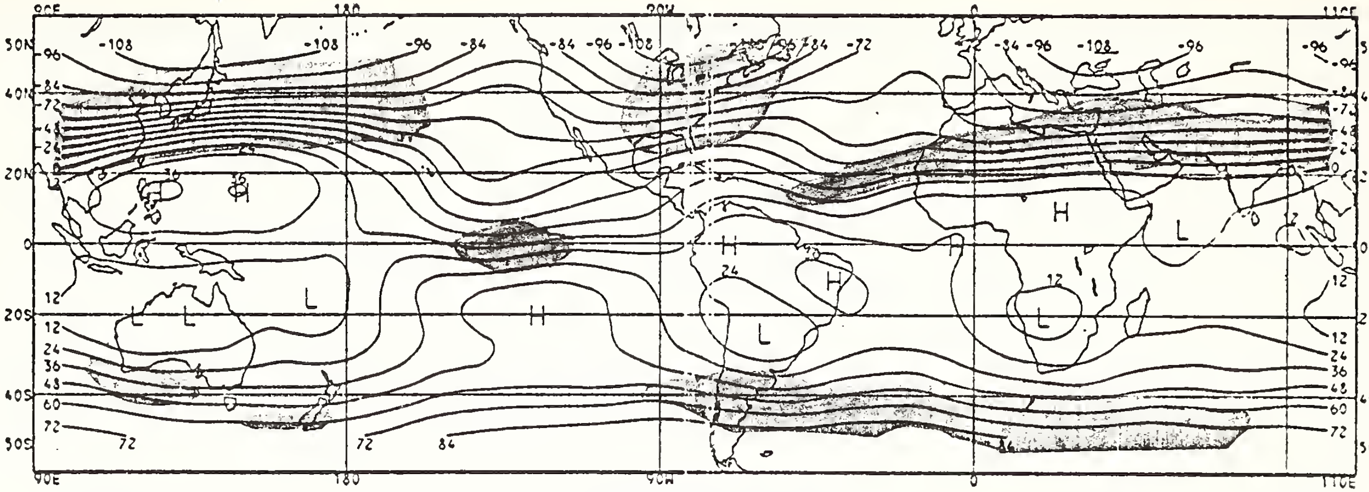

200MB STREAMFUNCTION JANUARY 1976

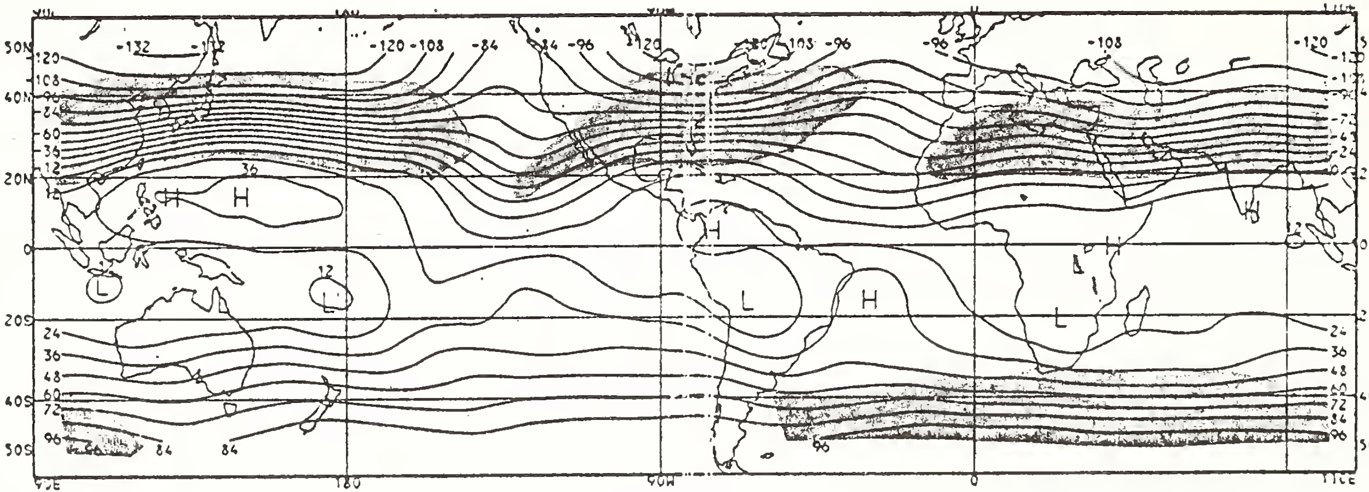

200MB STREAMFUNCTION JANUARY 1977

Winds > 30mps shaded

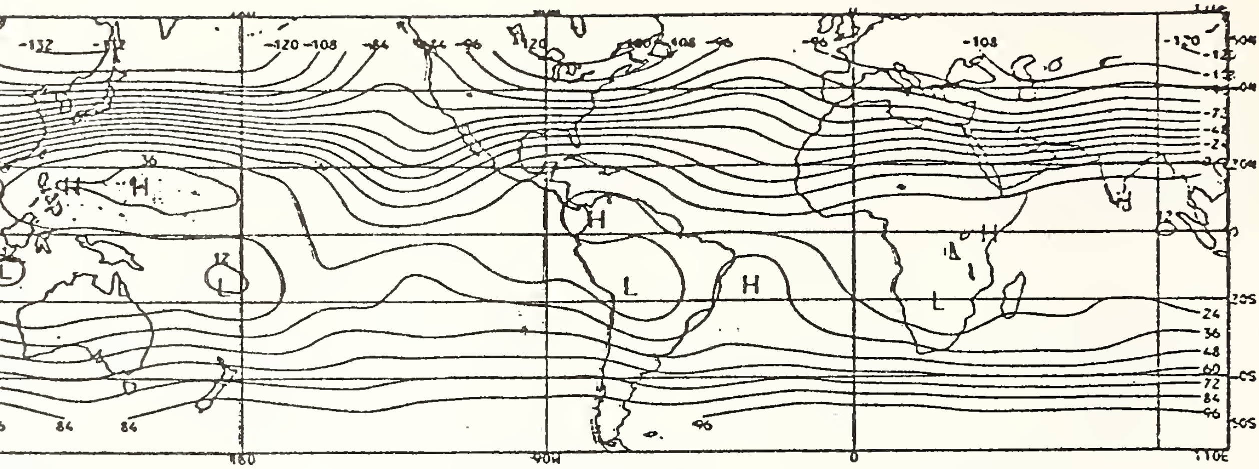

0MB STREAMFUNCTION JANUARY 1977

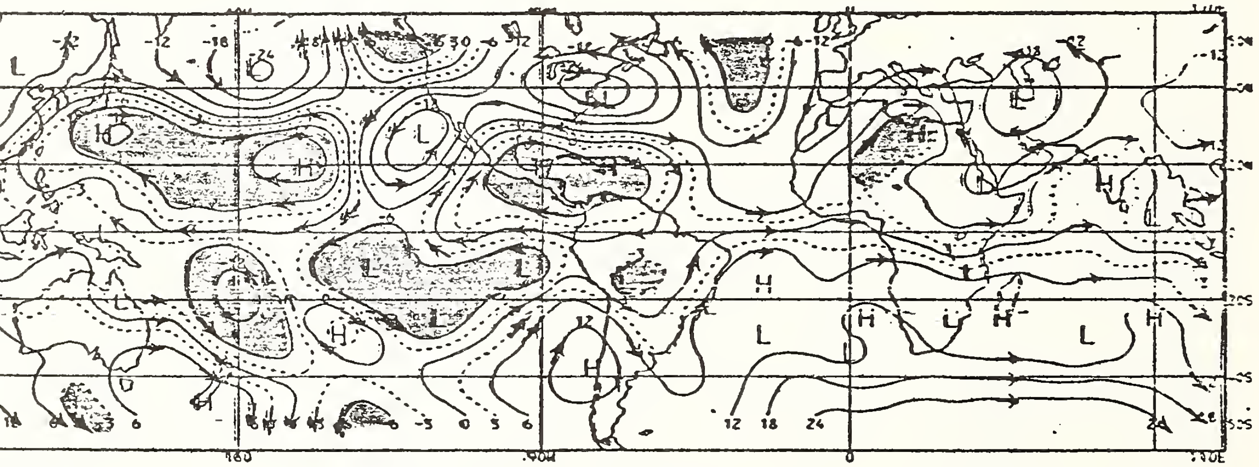

0MB STREAMFUNCTION ANOMALY (6) JANUARY 1977

anticyclonic anomalies shaded

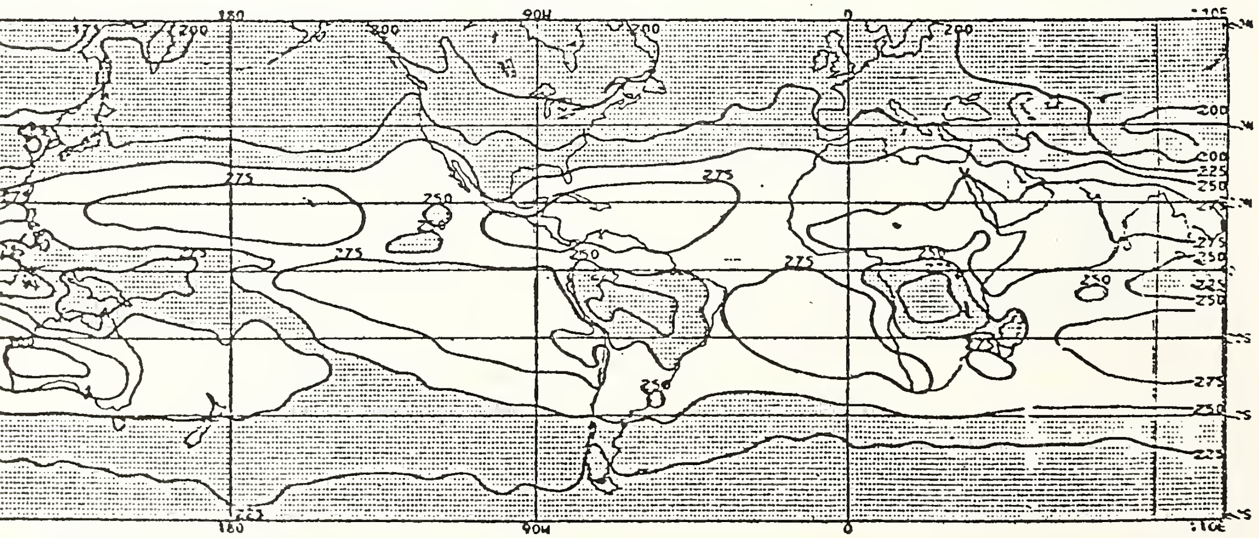

OUTGOING LONGWAVE RADIATION (WM^{-2}) WINTER 1977

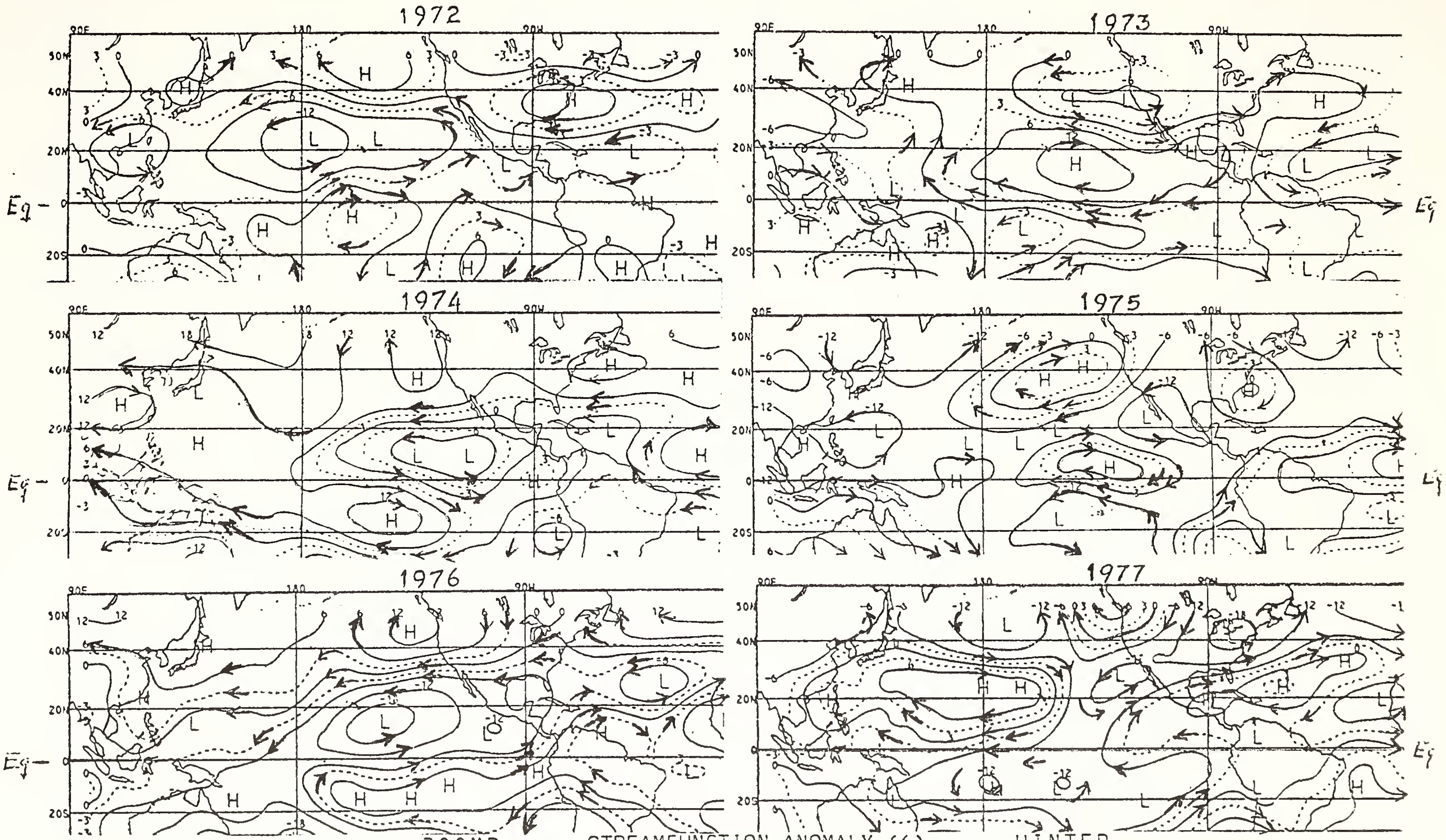

200MB STREAMFUNCTION ANOMALY (6) WINTER

Total Potential Energy (NMC analysis) and Longwave Cooling (NESS-MSL)

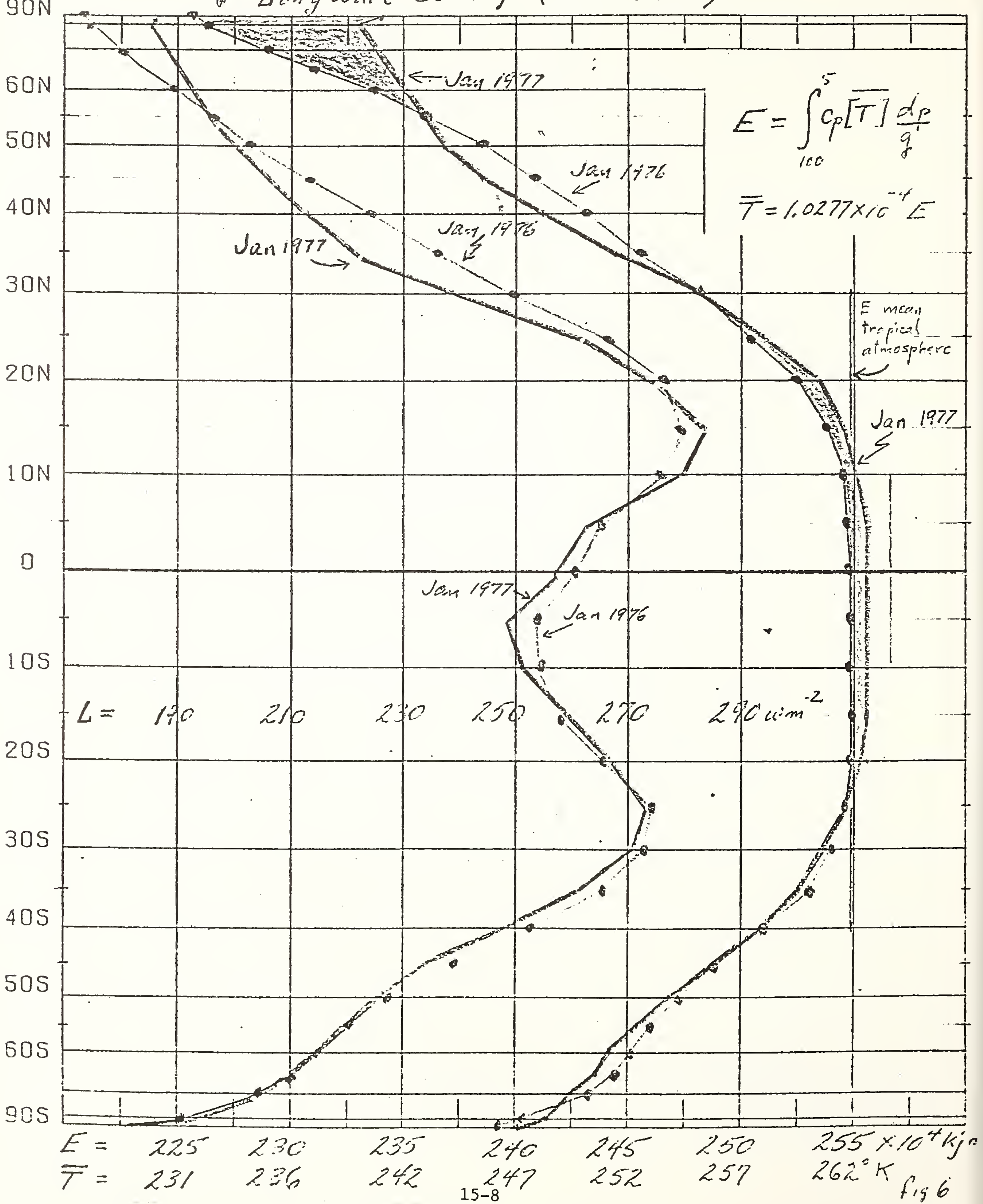

fig 6

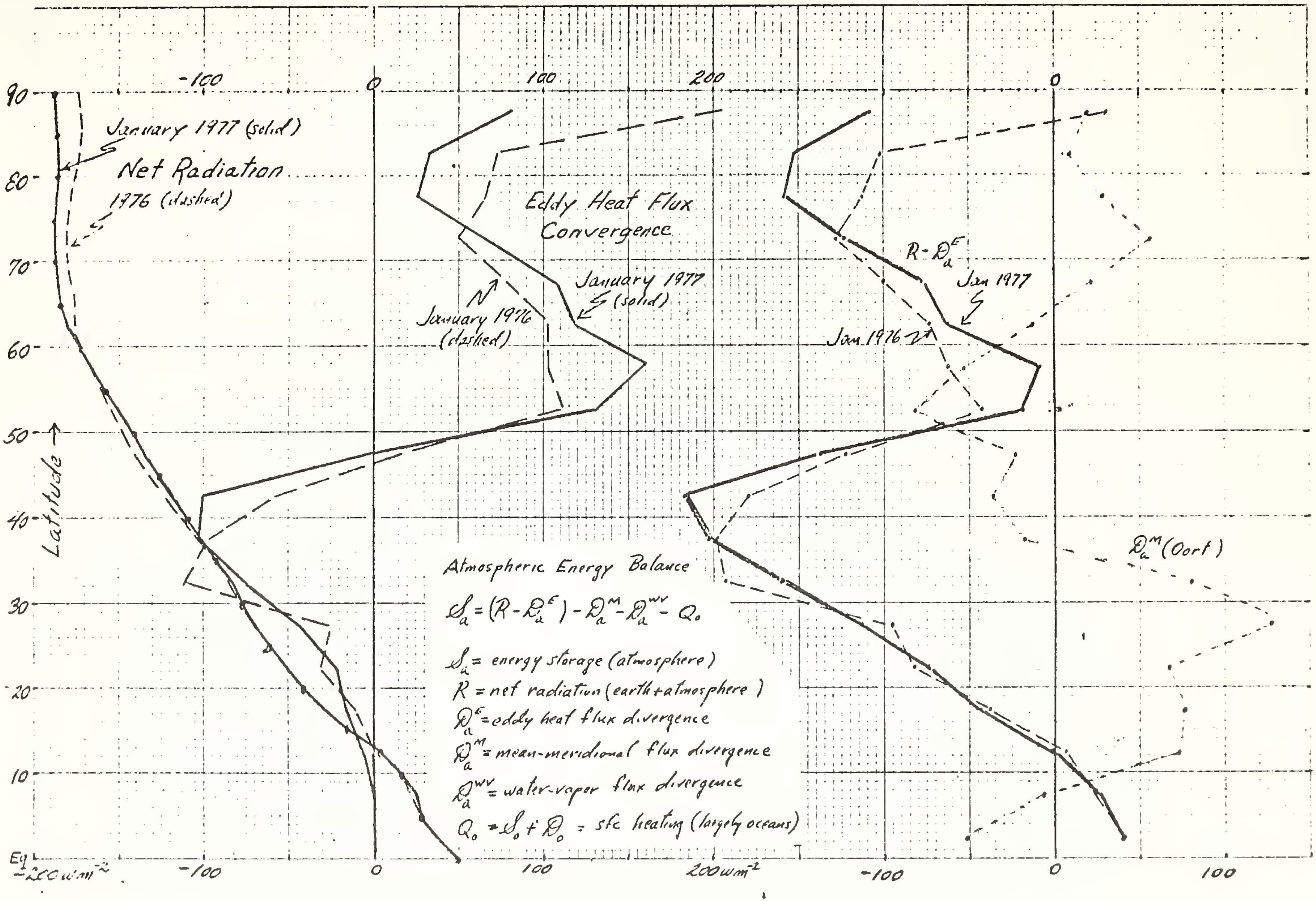
-100
0
100
200
0
90
80
70
60
50
40
30
20
10
Eq
-200 wm^-2
-100
0
100
200 wm^-2
-100
0
100
January 1977 (solid)
Net Radiation
1976 (dashed)
Latitude
Eddy Heat Flux
Convergence
January 1977
(solid)
January 1976
(dashed)
R - D_a^E
Jan 1977
Jan 1976
D_a^M (Oort)
Atmospheric Energy Balance
$S_a = (R - D_a^E) - D_a^M - D_a^{wv} - Q_o$
S_a = energy storage (atmosphere)
R = net radiation (earth + atmosphere)
D_a^E = eddy heat flux divergence
D_a^M = mean-meridional flux divergence
D_a^{wv} = water-vapor flux divergence
$Q_o = S_o + D_o$ = sfc heating (largely oceans)

47 0700

Global Patterns of Earth Radiation Budget Components in 1976-77 as Contrasted with the Preceding Year

Jay S. Winston
NOAA-NESS, Washington, D.C.

Some of the largest changes in outgoing longwave radiation and absorbed solar radiation (albedo) occurred over the equatorial Pacific in 1976-77. These were associated with increased major tropical convection over the central and eastern Pacific from summer* 1976 through spring 1977. Activity decreased by summer 1977 on the north side of the equator, but substantial increases continued to occur on the south side of the equator over the central Pacific.

Noteworthy changes also occurred in absorbed solar radiation over both the eastern Pacific and the North Atlantic Oceans, principally in the subtropics. In general, substantial areas of increased absorbed solar radiation (decreased albedo), due to lesser amounts of cloudiness, occurred in both of these oceans from spring and summer of 1976 until winter of 1976-77. By spring and summer of 1977 lessening amounts of solar radiation were observed as cloudiness began to increase again.

Finally, detailed patterns over North America are presented to illustrate the substantial year-to-year radiation changes observed during the winter of 1976-77 and summers of 1976 and 1977.

Figure Legends

1. Seasonal mean outgoing longwave radiation patterns for the summers, 1976 and 1977. (Values less than 250 W m^{-2} are shaded.) Strong seasonal resemblance of these patterns is apparent. However, substantial differences in pattern may be noted in the central Pacific where a broadened area of less than 250 W m^{-2} is observed along and north of the equator in 1976. In 1977 a much narrower area of less than 250 W m^{-2} is observed there while a more intense minimum occurs south of the equator. Another interesting change is quite apparent over western Europe where values of 250-280 W m^{-2} occurred during the summertime drought of 1976, whereas values less than 250 W m^{-2} prevailed in the more cloudy and wet regime of 1977.

2. Year-to-year differences in seasonal mean outgoing longwave radiation. Upper is the change from summer of 1975 to 1976, lower is change from summer of 1976 to 1977. (Negative changes are shaded, indicating principally increased amounts and/or heights of clouds and to a much lesser degree, lower surface temperatures.) Note the extensive area of decreases in excess of 25 W m^{-2} over the central equatorial Pacific and also the smaller -25 area over the eastern Pacific in the 1976-75 period.

---

*All seasonsare defined relative to the Northern Hemisphere.

Note that most other longitudes near the equator showed increased longwave radiation from 1975 to 1976. The changes from 1976 to 1977 show increases along and north of the equator over the entire central and eastern Pacific. South of the equator, however, a well-defined area of decreases exceeding 25 W m^{-2} occurred. Over western Europe decreases of more than 25 W m^{-2} occurred from 1976 to 1977, but note that only relatively small rises occurred from 1975 to 1976, indicating that the 1975 and 1976 summers there were not substantially different in major cloudiness.

3. Sequence of seasonal year-to-year longwave radiation differences over the Pacific region for five seasons from summer 1976-75 to summer 1977-76. (Note that winter 1976-1975 signifies the winter of 1976-77 minus the winter of 1975-76.) Note the persistence of decreases of outgoing longwave radiation over the central and eastern equatorial Pacific through the winter (1976-1975). By spring (1977-1976), the decreases were virtually all on the south side of the equator. These decreases persisted into the summer (1977-1976) as more substantial increases set in north of the equator.

4. Sequence of seasonal year-to-year albedo differences over the Pacific region for five seasons from summer 1976-75 to summer 1977-76. (Positive changes in albedo are shaded.) Note that over the equatorial Pacific region there is considerable resemblance in the patterns to those of the longwave radiation in Figure 3, with increasing albedo generally coinciding with decreasing longwave radiation. The general southward shift in increased albedo across the equator over the central Pacific from winter to summer is virtually identical with the trend in the zone of decreasing longwave radiation shown in Figure 3.

5. Example of time variations in radiation components over the central equatorial Pacific. Monthly mean values of outgoing longwave radiation and albedo are plotted for the 2 1/2° lat. x 2 1/2° long. grid point centered at 0°, 180°. (The entire record of data starting with June 1974 is shown.) The longwave radiation at this location remained generally high through the 1975-76 period until a sharp drop occurred from May to June 1976. Values then remained substantially below the previous year (and mostly below the year before too) until April 1977. From May 1977 through August 1977 values were again at higher levels that were characteristic of 1974 and 1975. Albedo values show the generally expected inverse relationship to the outgoing longwave radiation; a relationship which is strongest when there are variations in major cloud systems extending into middle and upper portions of the troposphere.

6. Example of time variations in radiation components on southern side of central equatorial Pacific. Monthly mean values of outgoing longwave radiation and albedo are plotted for the grid point centered at 10°S, 160°W. The longwave radiation at this point began to depart substantially from the preceding year by December 1976, and, except for

February 1977, remained well below 1976 through August 1977. Note that the values in June-August 1977 were anomalously low relative to the 3 preceding years. The albedo values again show a generally inverse relationship to the longwave radiation.

7. Sequence of year-to-year differences in seasonal mean absorbed solar radiation over the Pacific sector between 180° and 90°W. In the four seasons at the top, beginning with winter 1975-76 (relative to 1974-75) and through fall 1976 (relative to 1975), increases in absorbed solar radiation predominated between about 5°N and 20°N (up to 30°-35°N in summer and fall) and between 5°S and 20°S. These increases signify decreases in albedo and cloudiness. A very substantial portion of this increased solar radiation reached the ocean surface. Starting in winter 1976-77 (relative to 1975-76) and continuing into summer 1977 (relative to 1976) decreases in absorbed solar radiation became more prevalent, except for the increases over the western portion of the area shown, first between about 5°N and 20°N and then by summer between 0° and 10°N, where major cloudiness decreased markedly relative to summer 1976.

8. Sequence of year-to-year differences in seasonal mean absorbed solar radiation over the North Atlantic. Note the predominance of positive differencesin solar radiation in spring and summer 1976 (relative to 1975) over the region between about 15°N and 40°N. These increases (decreases in albedo and cloudiness) signify a higher input of solar radiation into these latitudes of the Atlantic in these two seasons. By winter 1976-77 (relative to 1975-76) negative differences in absorbed solar radiation began to predominate in these same latitudes, first in the western North Atlantic in winter, then in the southwestern and central portions in spring 1977, and finally over the eastern North Atlantic by summer 1977. These decreases, of course, signify a lower input of solar radiation into these same latitudes (15°N-40°N) of the Atlantic from winter 1976-77 through summer of 1977.

9. Year-to-year differences in seasonal mean outgoing longwave radiation over the North American region for winter 1976-77 relative to winter 1975-76. Especially notable is the well-defined axis of negative differences (more than 10 W m^{-2}) extending from off the west coast of Mexico near 20°N through the Gulf of Mexico into the Atlantic near 35°N. This is indicative of considerable increases of cloudiness in this region which frequently marked the principal active frontal zone during the winter of 1976-77 when cold air masses penetrated far south in North America. Over Mexico and the Pacific this axis was more representative of the increased cloudiness emanating from the eastern tropical Pacific during much of the winter. The increases over much of the Caribbean are related to the dominance of decreased cloudiness in the subtropical anticyclone south of the strong subtropical westerlies near 20°-30°N. The pattern northward of about 40°N is very likely the result of lower surface temperatures in the eastern half of the United States and southern Canada, and higher temperatures and decreased snow cover in the West.

10. Year-to-year differences in absorbed solar radiation over the North American region for winter 1976-77 relative to winter 1975-76. Much of the pattern resembles the longwave pattern of Fig. 9 and, in the subtropical latitudes, essentially for the same reasons: increased subtropical cloudiness from the eastern Pacific off Mexico, through the Gulf of Mexico, and into the Atlantic; and decreased cloudiness in the Caribbean under the subtropical anticyclone. Between 120° and 135°W from about 20°N to 45°N the increases over the ocean and immediate coastal regions are related to a general decrease in cloudiness (especially low cloudiness from 20°-40°N). Inland over the Great Basin, Rocky Mountain, and Plains region the decrease is the result of decreased snow cover as well as smaller amounts of clouds under the dominance of the persistent dry, anticyclonic regime of winter 1976-77.

11. Year-to-year differences in outgoing longwave radiation over the North American region for summer 1977 relative to summer 1976. The extensive negative differences over much of southern Canada and throughout much of the central and southwestern United States are indicative of considerable increases in major cloudiness during this summer. Note the pronounced connection of these negative differences southwestward toward the tropical eastern Pacific. Only areas in the northwest United States, western Canada, and along the southeast and south coasts of the United States had positive differences (decreased cloudiness).

12. Year-to-year differences in absorbed solar radiation over the North American region for summer 1977 relative to summer 1976. The general pattern resembles the longwave pattern except that the differences are considerably larger in magnitude since differences in reflectivity due to increased cloudiness are acting on the large amounts of available solar energy in summer. The more complex pattern over the eastern Pacific is due to variations in the low cloud patterns. Note particularly the decreased solar radiation west of Southern California and Baja California.

13. Year-to-year differences in absorbed solar radiation over the North American region for summer 1976 relative to summer 1975. In general the pattern is very nearly the reverse of the 1977 pattern in Fig. 12. Of particular note are the reversals over the upper Midwest, over the Pacific Northwest and western Canada, and off the coast of Southern California and Baja California. The latter change indicates considerable decreases in low cloudiness from summer 1975 to 1976, while Fig. 12 indicates a return to a more cloudy regime in summer 1977. The bulk of these changes in absorbed solar radiation over the Pacific affect the ocean surface.

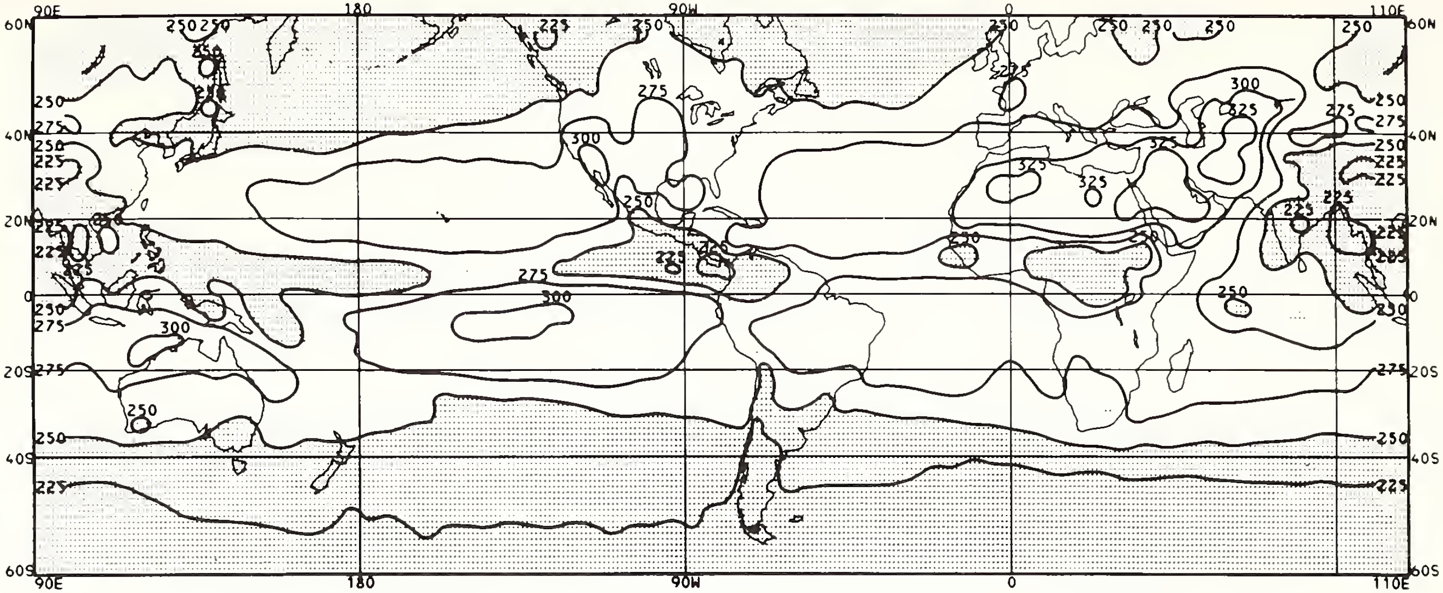

OUTGOING LONGWAVE RADIATION (WM^{-2}) SUMMER 1976

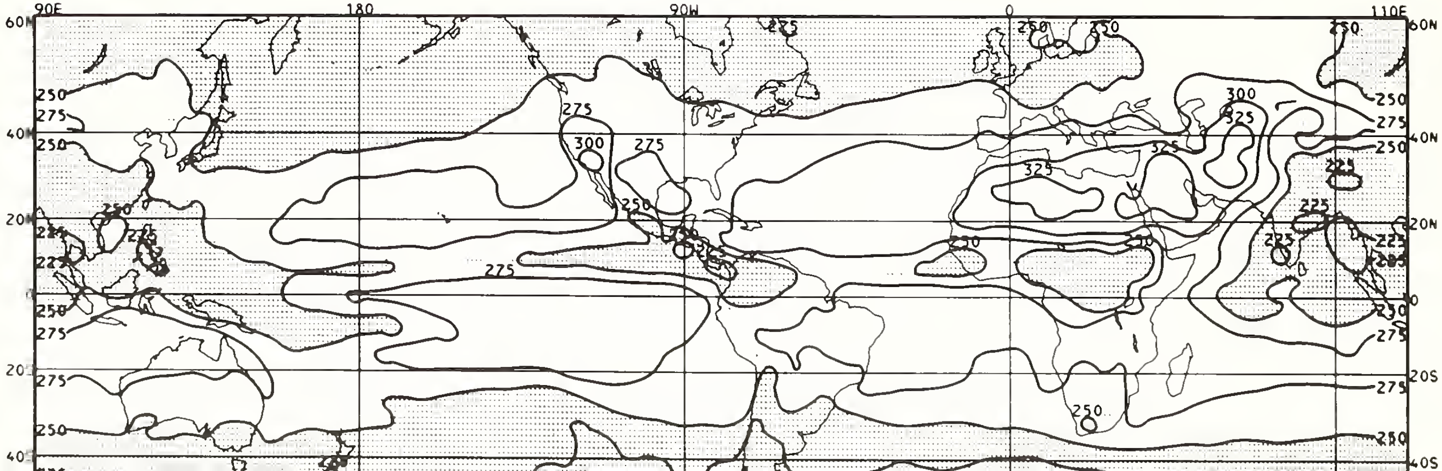

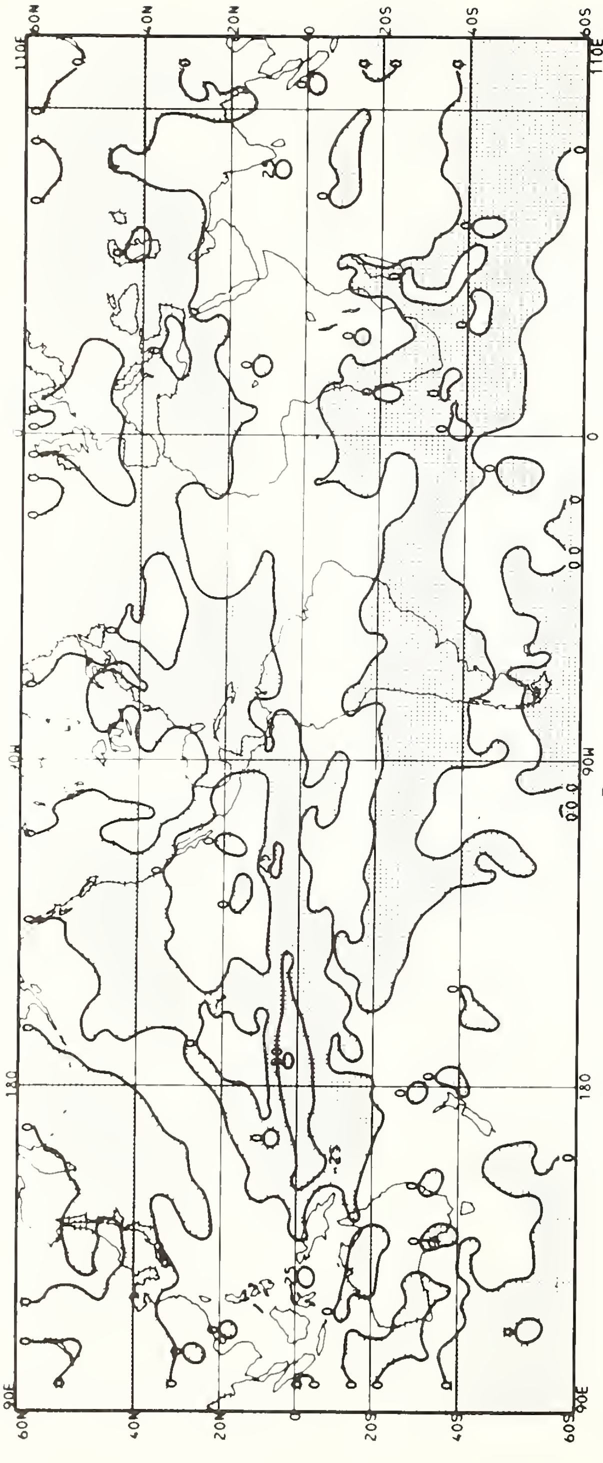

OUTGOING LONGWAVE RADIATION (WM^{-2}) DIFFERENCE SUMMER 1976-1975

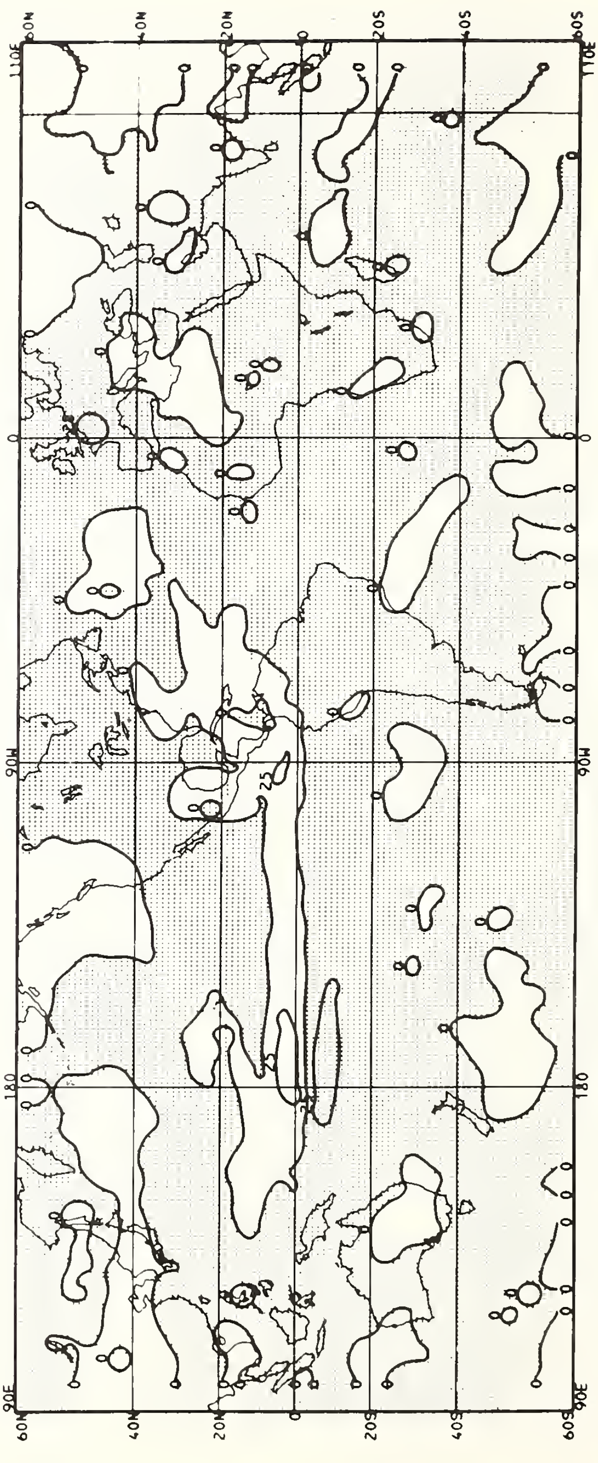

OUTGOING LONGWAVE RADIATION (WM^{-2}) DIFFERENCE SUMMER 1977-1976

OUTGOING LONGWAVE RADIATION (WM^{-2}) DIFFERENCE

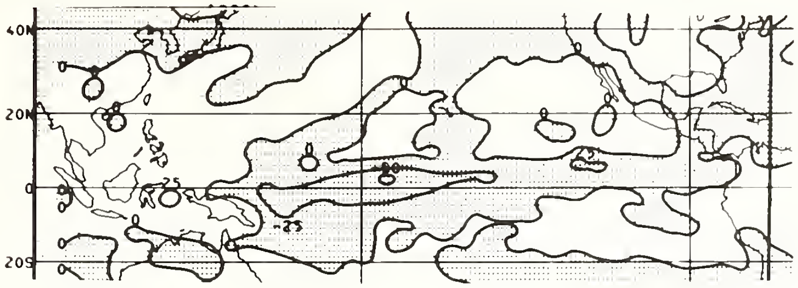

SUMMER 1976-1975

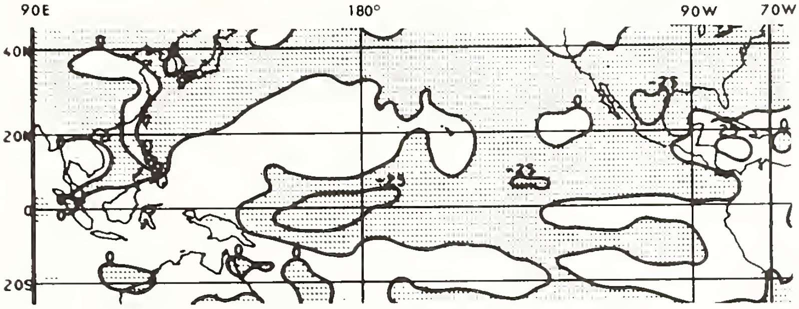

FALL 1976-1975

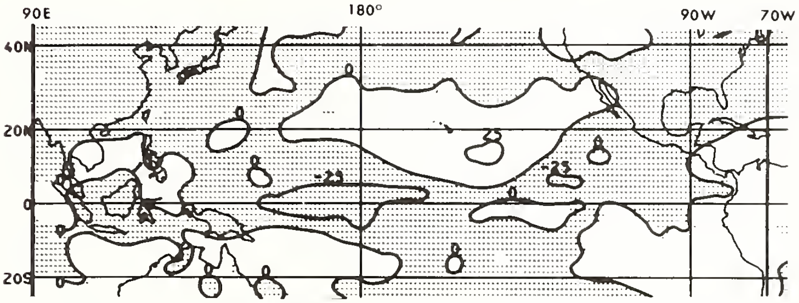

WINTER 1976-1975

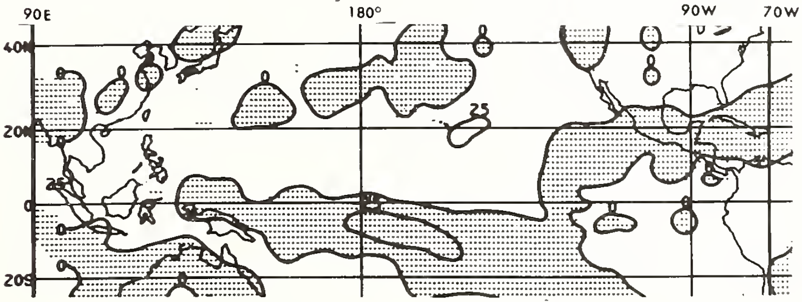

SPRING 1977-1976

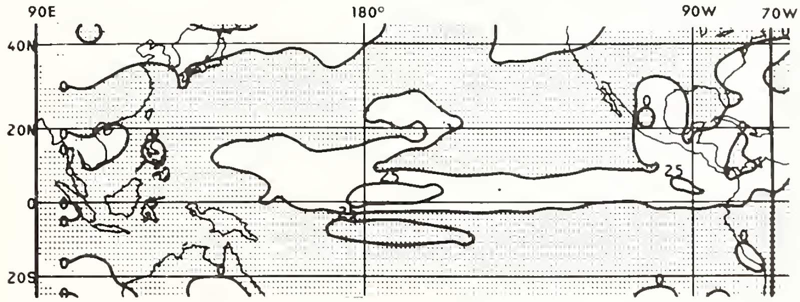

SUMMER 1977-1976

ALBEDO (%) DIFFERENCE

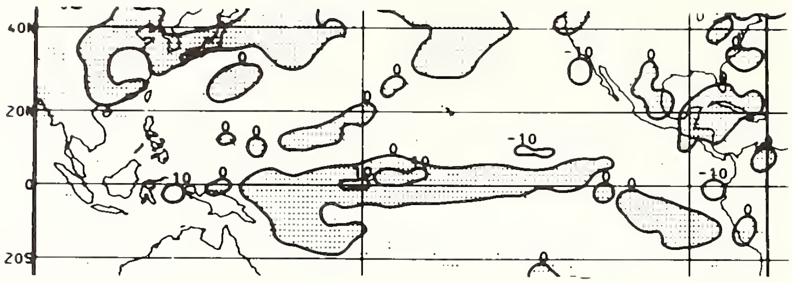

SUMMER 1976-1975

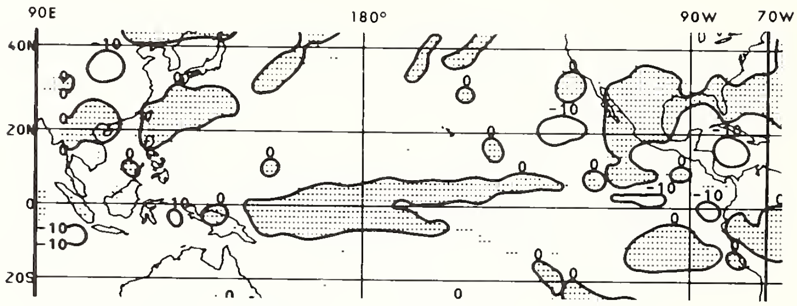

FALL 1976-1975

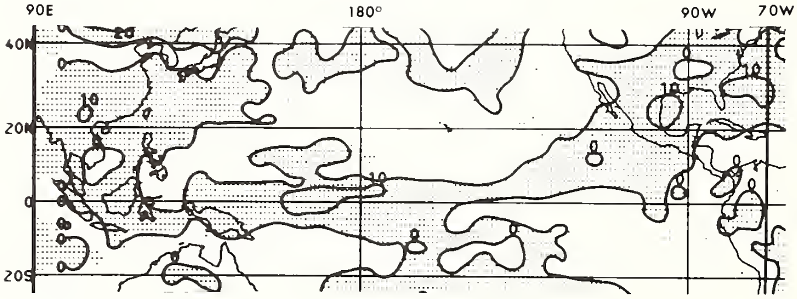

WINTER 1976-1975

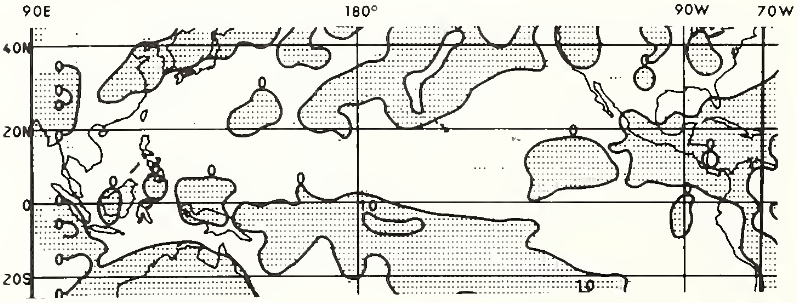

SPRING 1977-1976

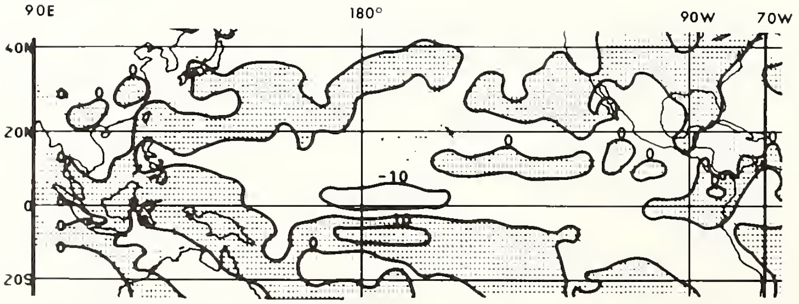

SUMMER 1977-1976

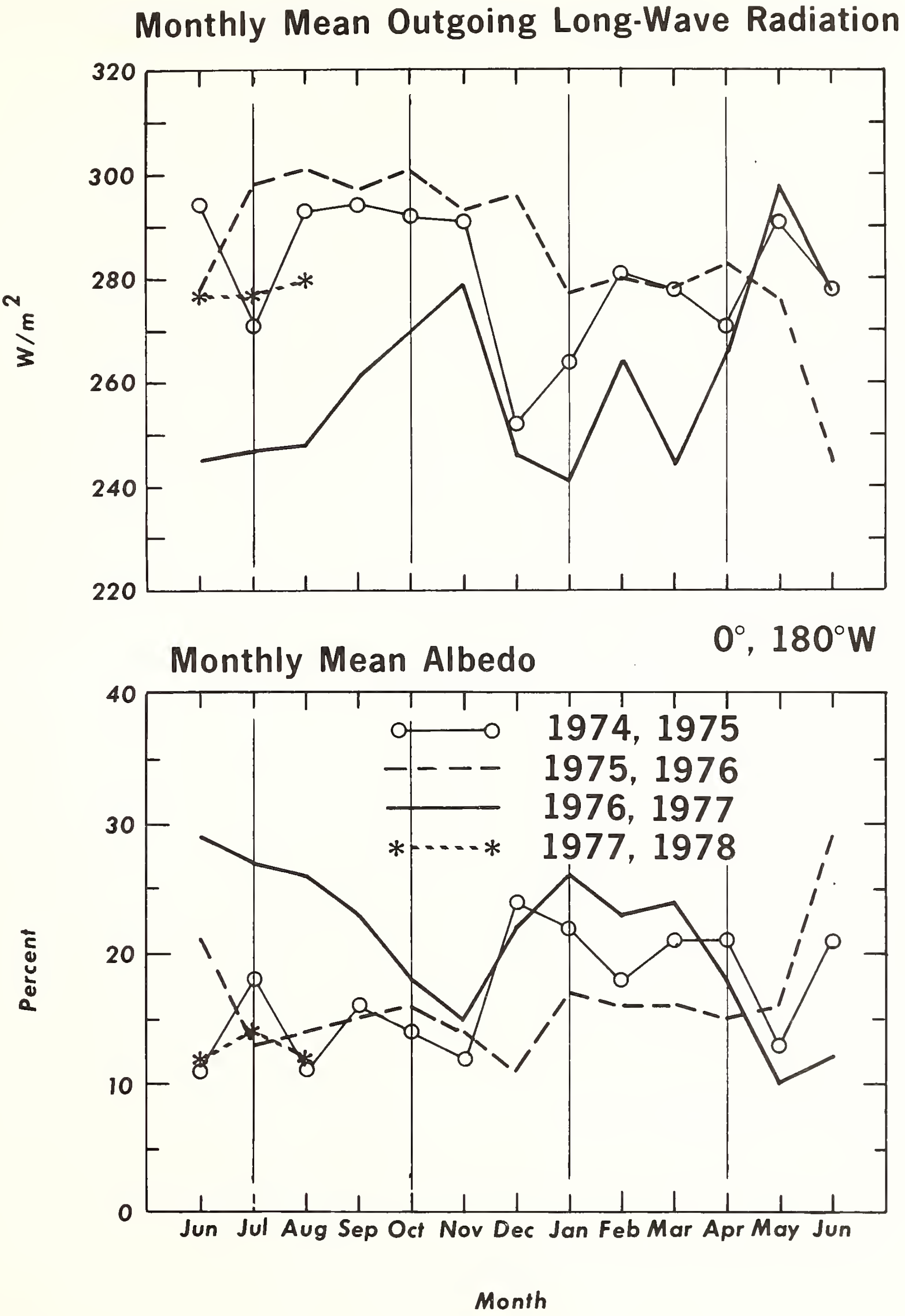

Monthly Mean Outgoing Long-Wave Radiation

Monthly Mean Albedo

0°, 180°W

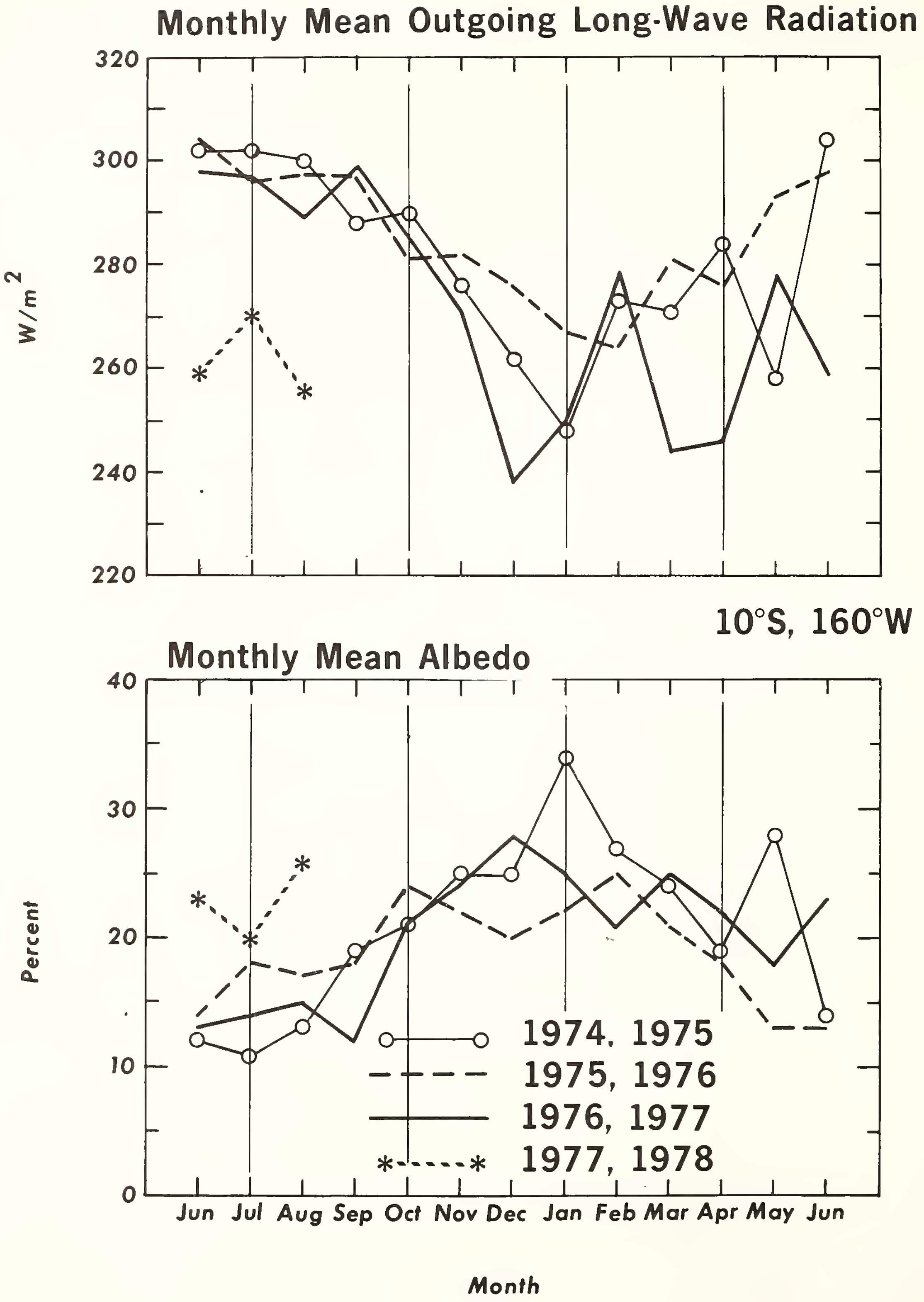
Monthly Mean Outgoing Long-Wave Radiation

10°S, 160°W

Monthly Mean Albedo

ABSORBED SOLAR RADIATION (WM^{-2}) DIFFERENCE

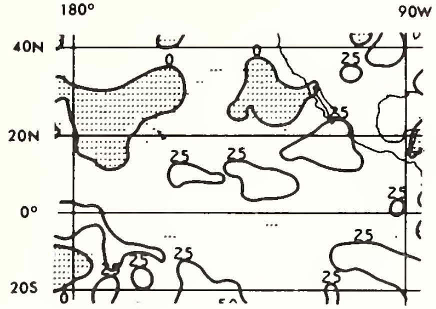

WINTER 1975-1974

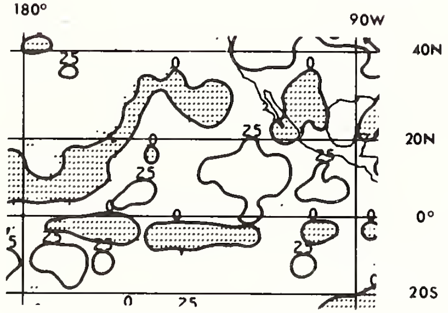

SPRING 1976-1975

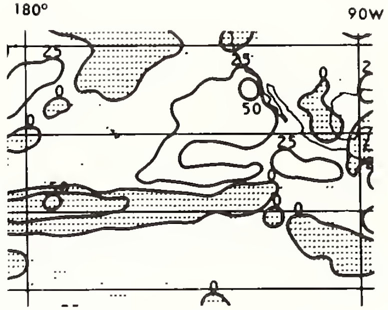

SUMMER 1976-1975

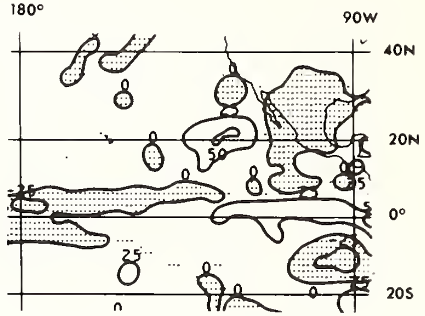

FALL 1976-1975

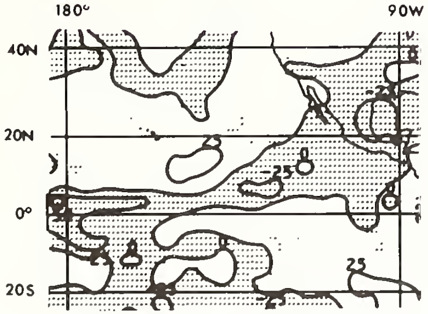

WINTER 1976-1975

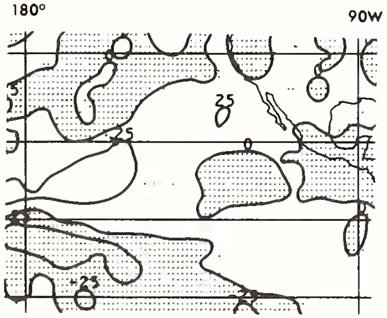

SPRING 1977-1976

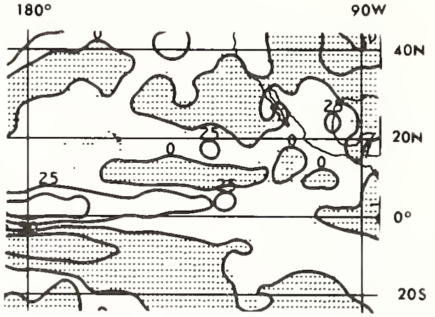

SUMMER 1977-1976

ABSORBED SOLAR RADIATION (WM^{-2}) DIFFERENCE

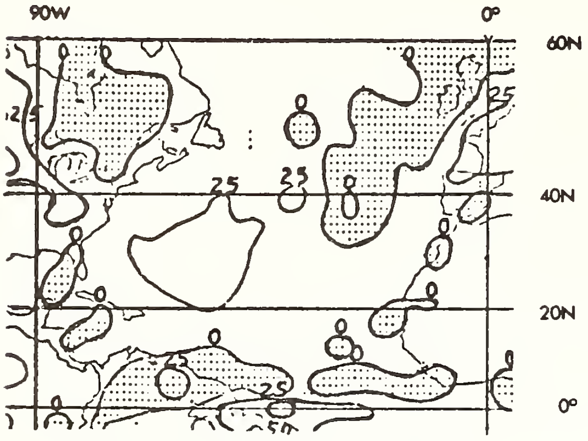

SPRING 1976-1975

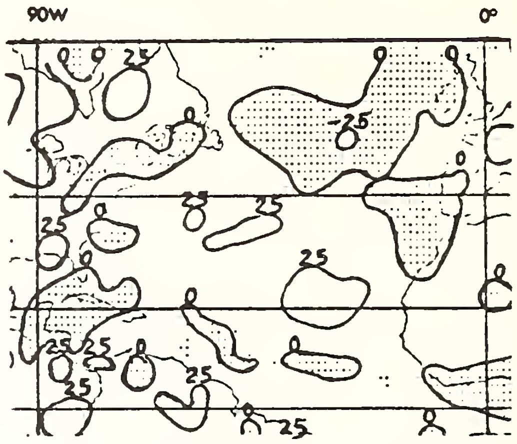

SUMMER 1976-1975

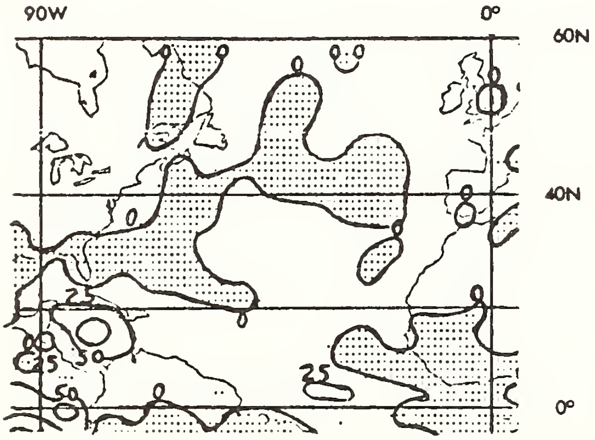

FALL 1976-1975

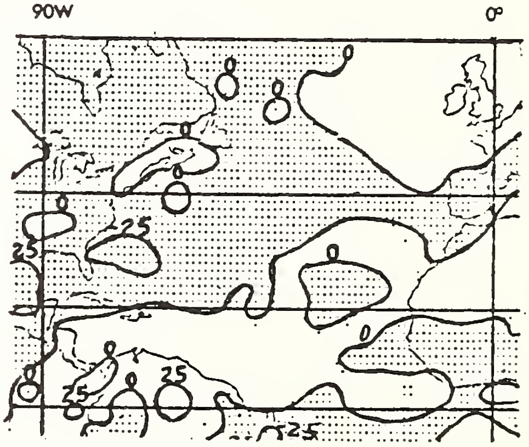

WINTER 1976-1975

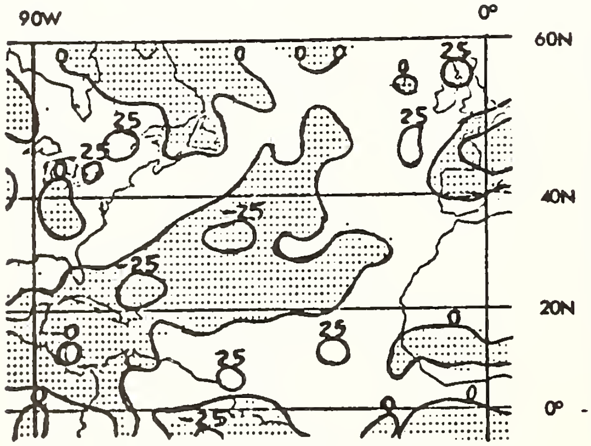

SPRING 1977-1976

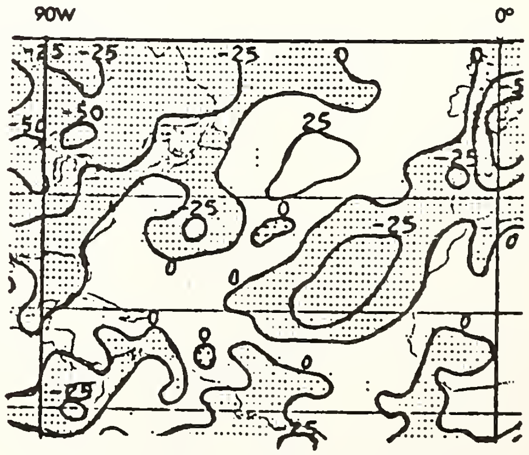

SUMMER 1977-1976

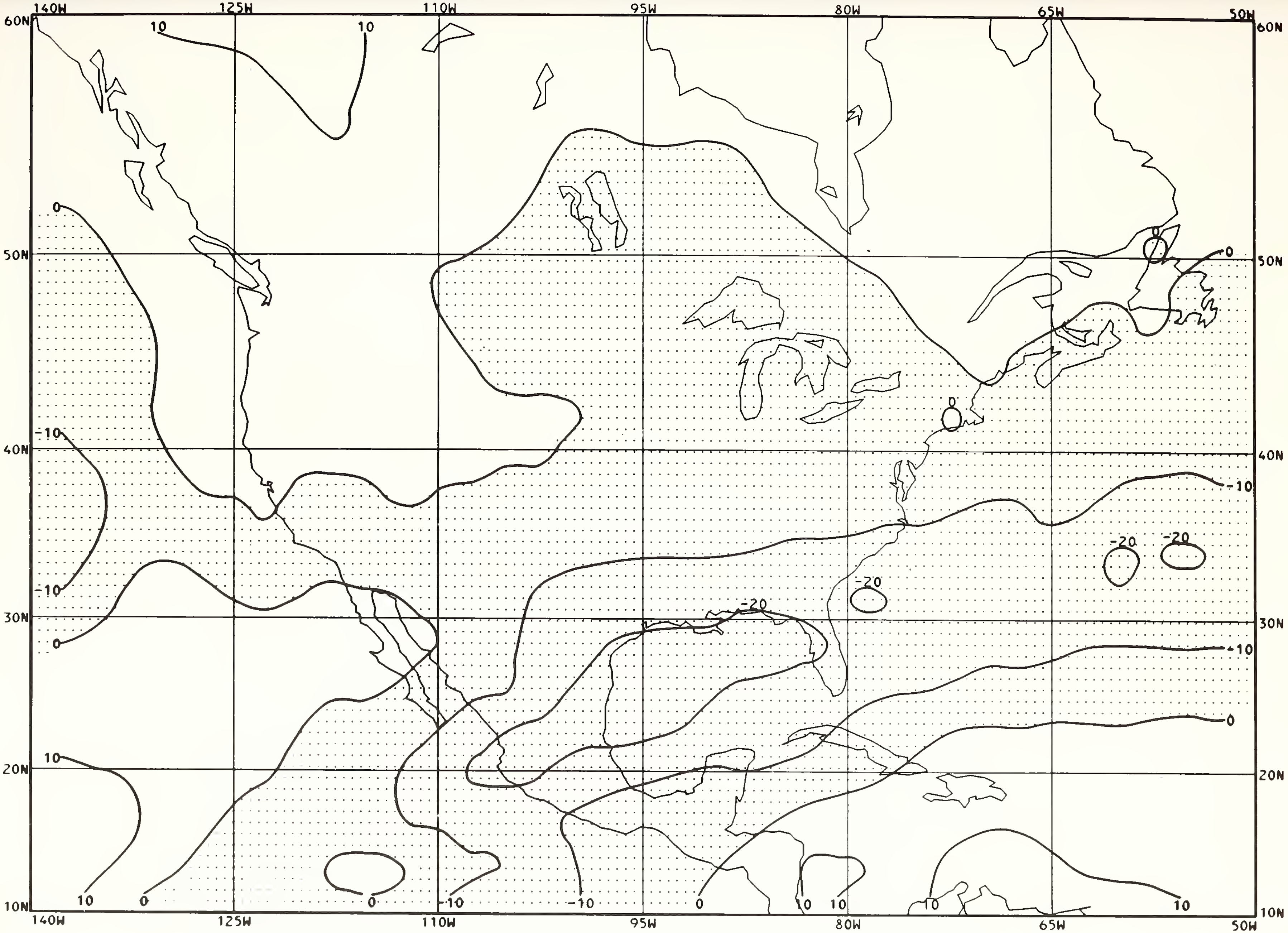

OUTGOING LONGWAVE RADIATION (WM^{-2})
DIFFERENCE WINTER 1976-1975

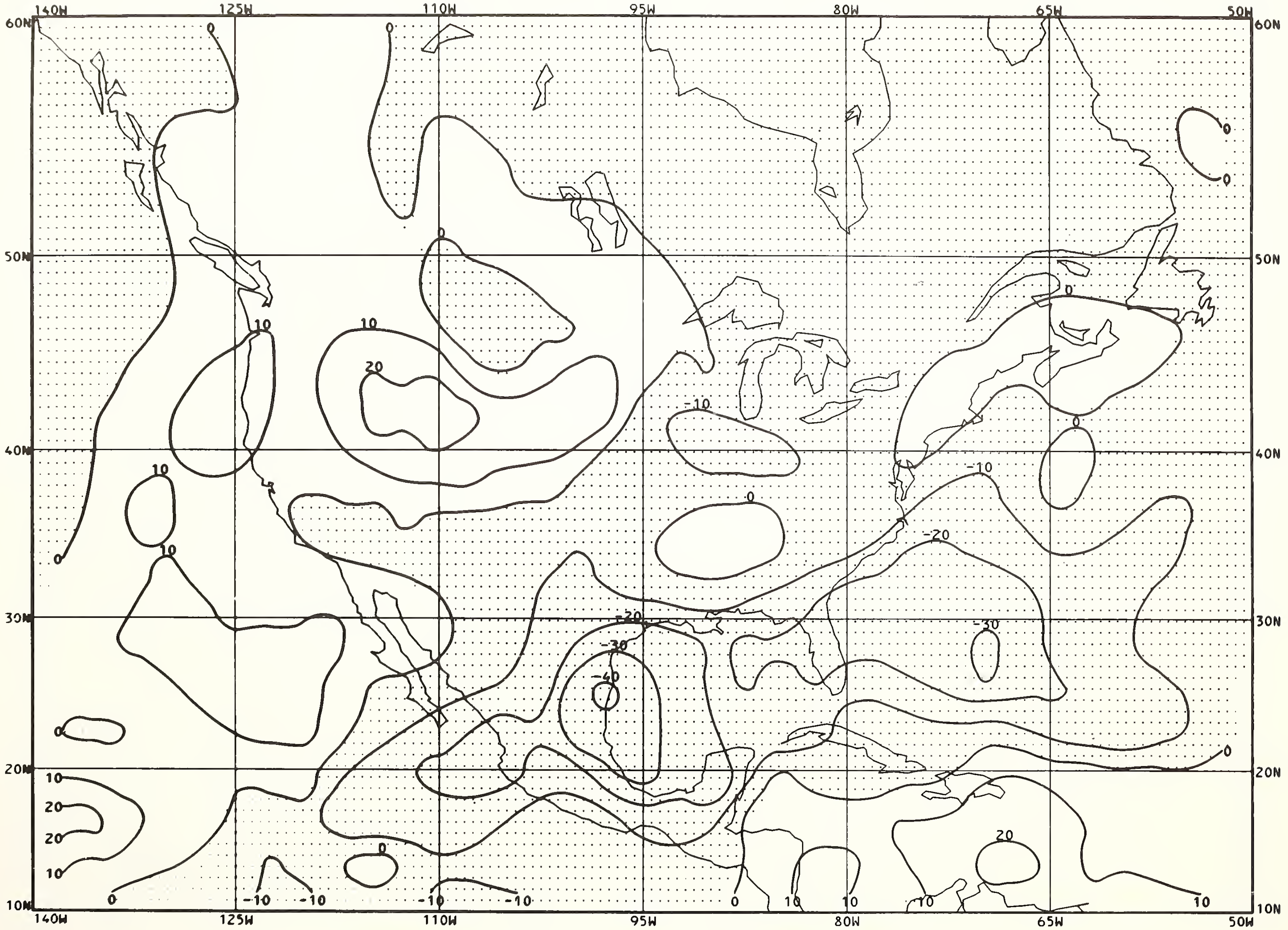

ABSORBED SOLAR RADIATION (WM^{-2})
DIFFERENCE WINTER 1976-1975

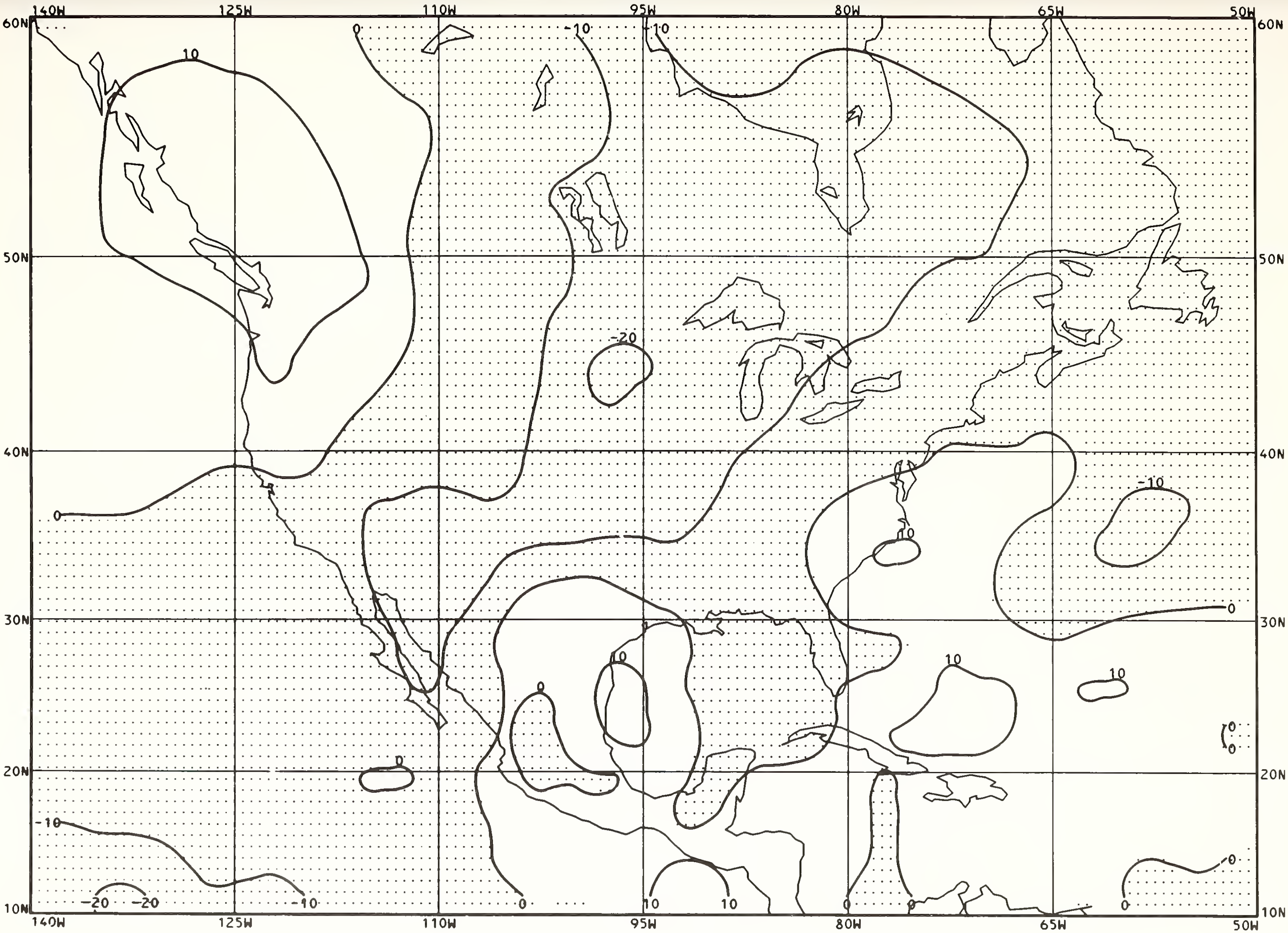

OUTGOING LONGWAVE RADIATION (WM^{-2})
DIFFERENCE SUMMER 1977-1976

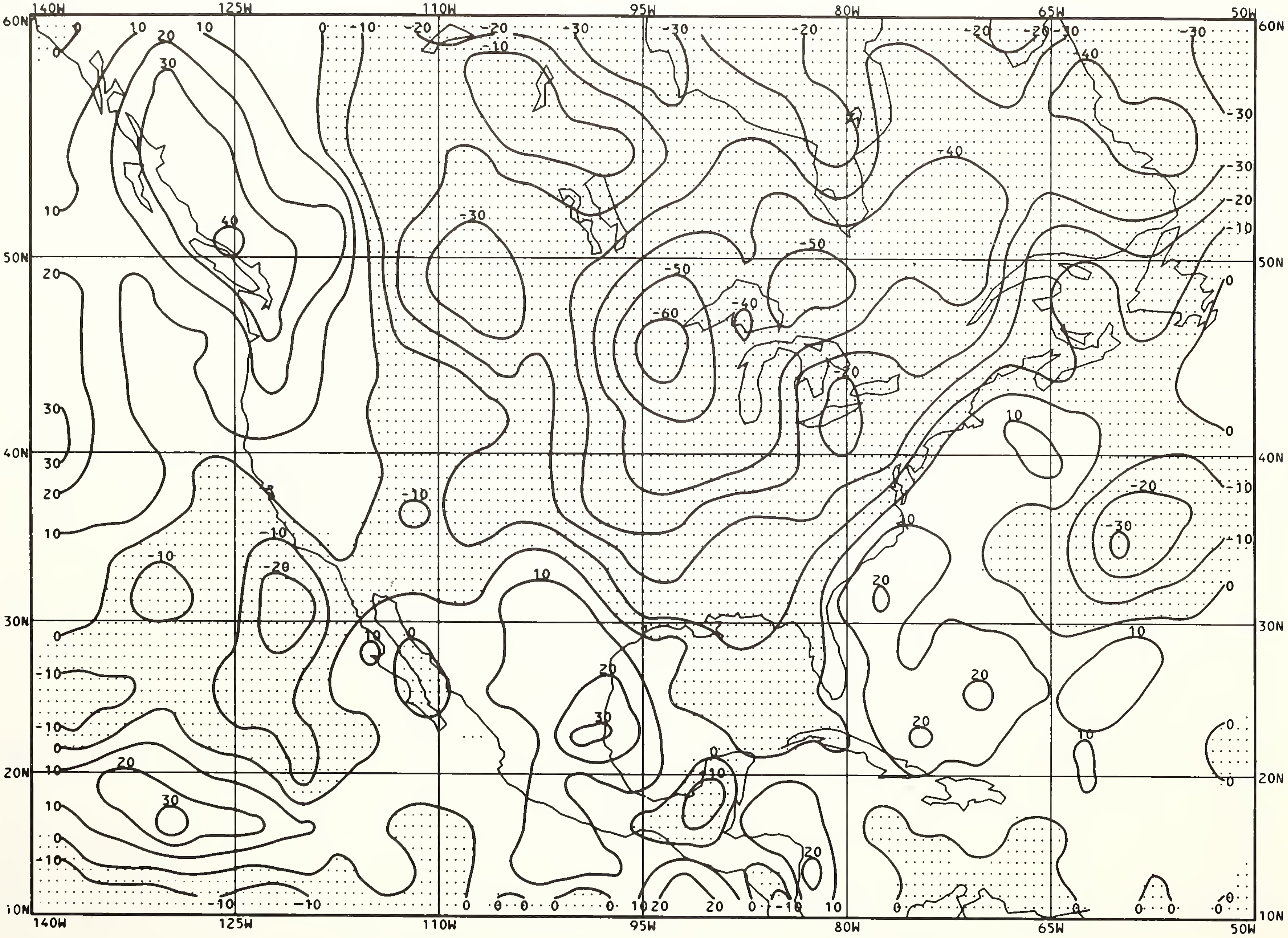

ABSORBED SOLAR RADIATION (WM-2)
DIFFERENCE SUMMER 1977-1976

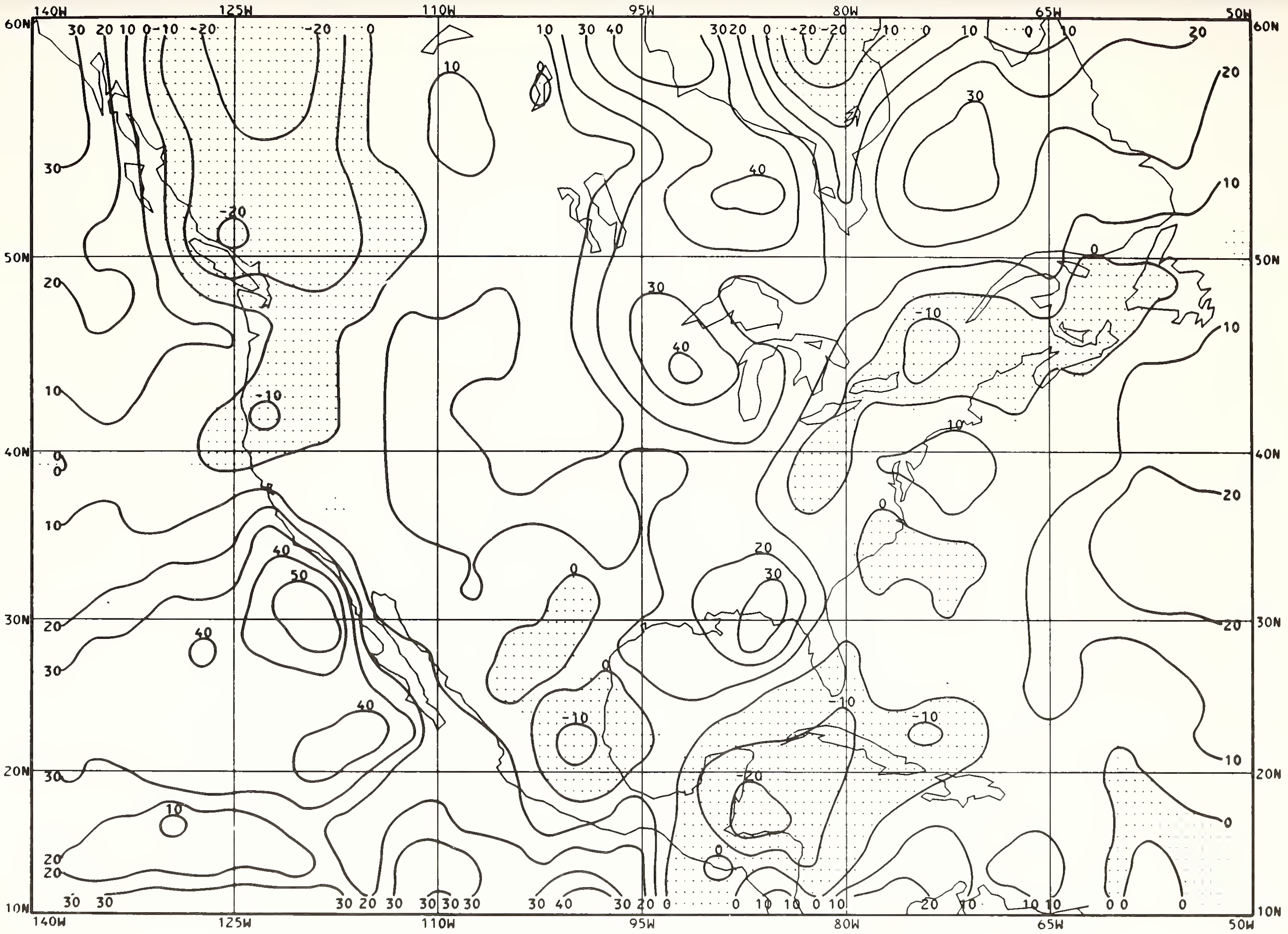

ABSORBED SOLAR RADIATION (WM^{-2})
DIFFERENCE SUMMER 1976-1975

COMMENTS ON ALBEDO OF DESERTS AND DROUGHT*

G. L. Potter
H. W. Ellsaesser

Some recent speculation as to the cause of the drought in the Sahel region at the southern margin of the Sahara desert has attributed the cause to overgrazing and subsequent albedo increase. Otterman [1975] suggested that the local effect of denudation and albedo increase was decreased precipitation due to "thermal depression," i.e. the inverse of a "thermal mountain" which enhances precipitation by inducing convection. Charney [1975] proposed that increased surface albedo over a desert (i.e., on a large scale) leads to a net radiative heat loss in the free atmosphere and that the resulting horizontal temperature gradients induce a frictionally controlled circulation with subsidence tending to restore hydrostatic equilibrium with adjacent areas. Charney et al. [1975] used the GISS GCM to test this hypothesis. Their experiment confirmed a reduction in precipitation following the increased albedo. Ellsaesser, et al. [1976] repeated the experiment using a 2-D zonal atmospheric model to compare with Charney and found similar results. Some confusion has surfaced and several questions as to the validity of the numerical experiments in general have been raised by Idso [1977], Jackson and Idso [1975] and Ripley [1976]. The confusion stems from at least two sources:

(1) A failure to distinguish between the small scale "thermal depression" of Otterman [1975] in which the vertical convection is controlled primarily by the surface temperatures and Charney's [1975] large scale radiationally induced subsidence which can continue in spite of the greater surface temperature of the desert; in fact, it is part of the cause of the greater surface temperature over the desert, and

(2) The effect of evapotranspiration. Charney [1975] and the experiments by Charney et al. [1975] and Ellsaesser et al. [1976] left this effect unconsidered but Otterman and Idso and co-workers could not leave it unconsidered since they were attempting to explain measurements from the real world.

The numerical experiments by Charney, et al. [1975] and Ellsaesser, et al. [1976] were devoid of an evaporating vegetation canopy, therefore the higher albedo surface was similar to volcanic ashfall or "painting" the desert surface. The interesting feature of these experiments is that they shed some light on the effect of large dry, high albedo surfaces in the subtropical latitudes. They show that the deserts reject large amounts of heat

---

*Work performed under the auspices of the United States Department of Energy, under Contract No. W-7405-Eng-48.

Submitted to the Climate Diagnostics Workshop October 18-20, 1977, Scripps Institution of Oceanography, La Jolla, CA.

i.e., the high desert albedo reflects up to 35% of the incoming solar radiation directly and the dry atmosphere allows the infrared radiation to escape to space quite freely. Also the cooler tropospheric column which develops over the desert as a result of this rejection of heat to space, leads to subsidence and adiabatic warming in the lower troposphere. This in turn leads to an even warmer temperature at the desert surface than is found over vegetated surfaces. Because of the large horizontal scale this does not lead to cumulus type convection but rather amplifies the loss of outgoing long wave radiation. The resulting net radiation balance [Charney 1975] is low or even negative over various deserts of the subtropical latitudes. The deserts in a global sense act as a radiative heat sink and not as a heat source, with the effect of "air conditioning" (i.e., cooling) the non-desert portion of the planet.

REFERENCES

1. Charney, J. G., 1975, "Dynamics of deserts and drought in the Sahel," Quart. Jour. Roy. Meteor. Soc., 101, pp 193-202.

2. Charney, J. G., P. H. Stone and W. J. Quirk, 1975, "Drought in the Sahara: A biogeophysical feedback mechanism," Science, 187, pp 434-435.

3. Ellsaesser, H. W., M. C. MacCracken, G. L. Potter and F. M. Luther, 1976, "An additional model test of positive feedback from high desert albedo," Quart. Jour. Roy. Meteor. Soc., 102, pp 655-666.

4. Idso, S. B., 1977, "A note on some recently proposed mechanisms of genisis of deserts," Quart. Jour. Roy. Meteor. Soc., 103, pp 369-370.

5. Jackson, R. D. and S. B. Idso, 1975, "Surface albedo and desertification," Science, 189, pp 1012-1013.

6. Ripley, E. A., 1976, "Drought in the Sahara: Insufficient biogeophysical feedback?," Science, 191, p 100.

The Total Ozone Variation and Atmospheric General Circulation*

Mao-Fou Wu
Systems and Applied Sciences Corporation
6811 Kenilworth Avenue, Suite 610
Riverdale, Maryland 20804

The influence of global air circulation on the distribution of atmospheric ozone has been noted for more than two decades. We believe that year-to-year variations in total ozone are related to year-to-year variations in atmospheric general circulation. Based on this thought, a joint effort to analyze long-term worldwide ozone data along with certain meteorological parameters has begun by the author and Professor R. E. Newell of MIT. Here, two sample maps are presented for general discussions. Figure 1 shows the total ozone departure over the northern hemisphere from long-term mean for February 1976. The data used in the analysis are based on Ozone Data for the World, published since 1957. It is found that the isolines in Figure 1 bear resemblance to those of 1000 - 700 mb thickness deviation from 30-year mean presented by R. R. Dickson during 1976 NOAA Workshop Meeting. To give a visual feeling, the sector of ozone map over the United States is enlarged and shown in Figure 2. Superimposed in this figure are the contour lines of the surface temperature departure from 30-year mean for a comparison.

---

* This research was supported by the Atmospheric Research Section, National Science Foundation, NSF Grant No. ATM76-21039.

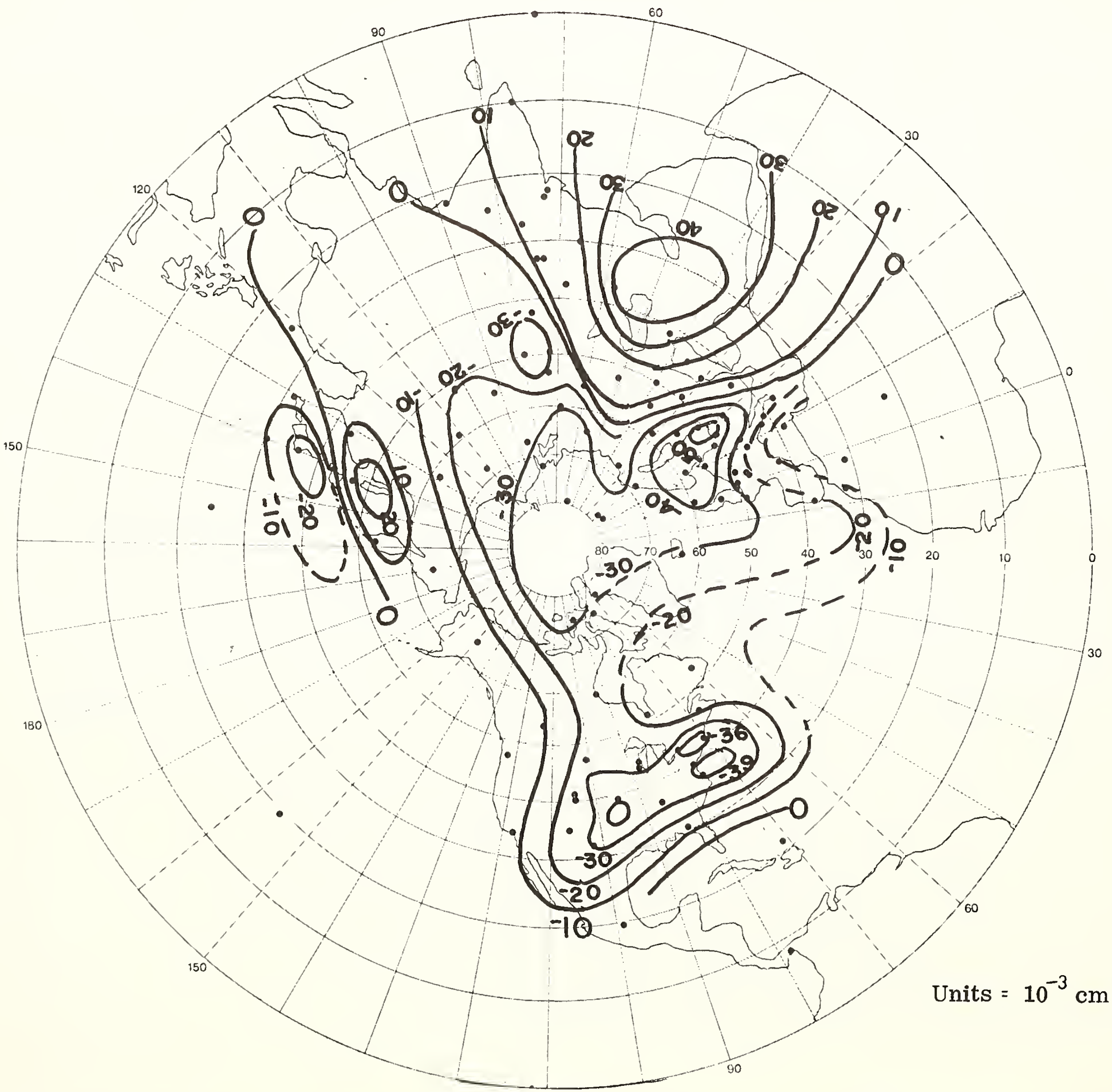

Units = 10^{-3} cm STP

Fig. 1 - Total Ozone Departure from Long-term Mean for February 1976

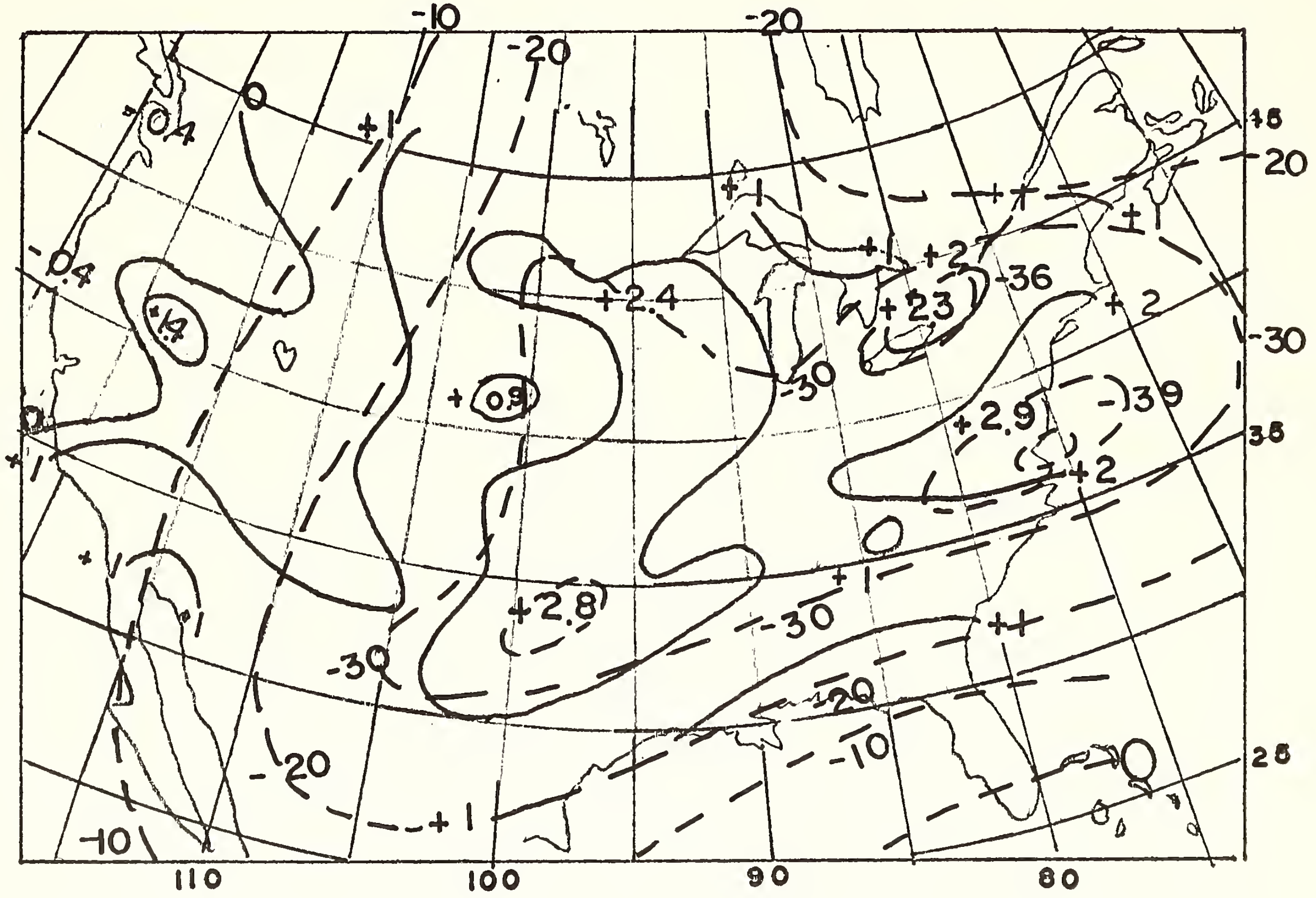

Fig. 2 - Dashed line: Total ozone departure from long-term mean for February 1976 (Units = 10^{-3} cm STP)
Solid line: Standardized surface temperature departure from 30-year mean for February 1976 (after R. R. Dickson)

Monthly Mean Satellite-Derived Sea Surface Temperatures

by A.E. Strong

SUMMARY

During 1976 several changes in the procedures used to obtain sea surface temperatures from NOAA Scanning Radiometer measurements now enable a more credible observation. Using data from conventional sources (viz., NMFS) in the North Pacific Ocean for purposes of comparison, satellite retrievals averaged over a month and subtracted from NMFS normals provide temperature anomaly fields with standard errors of estimate between ±0.4 and ±0.6^{o}C. The anomaly fields show a large negative anomaly that developed over the North Pacific last fall and reached its peak in February. Relatively cool water also prevailed in the South Pacific and South Atlantic last February. Another pool of anomalously cool water appears to be developing in the same area late in the summer of 1977.

FIGURE CAPTIONS

1. Oct. 76 Sea surface temperature anomaly, North Pacific (NMFS normal)
2. Jan. 77 Sea surface temperature anomaly, North Pacific (NMFS normal)
3. Apr. 77 Sea surface temperature anomaly, North Pacific (NMFS normal)
4. Aug. 77 Sea surface temperature anomaly, North Pacific (NMFS normal)

5. Feb. 77 minus Feb. 76, mean sea surface temperature, North and South Pacific

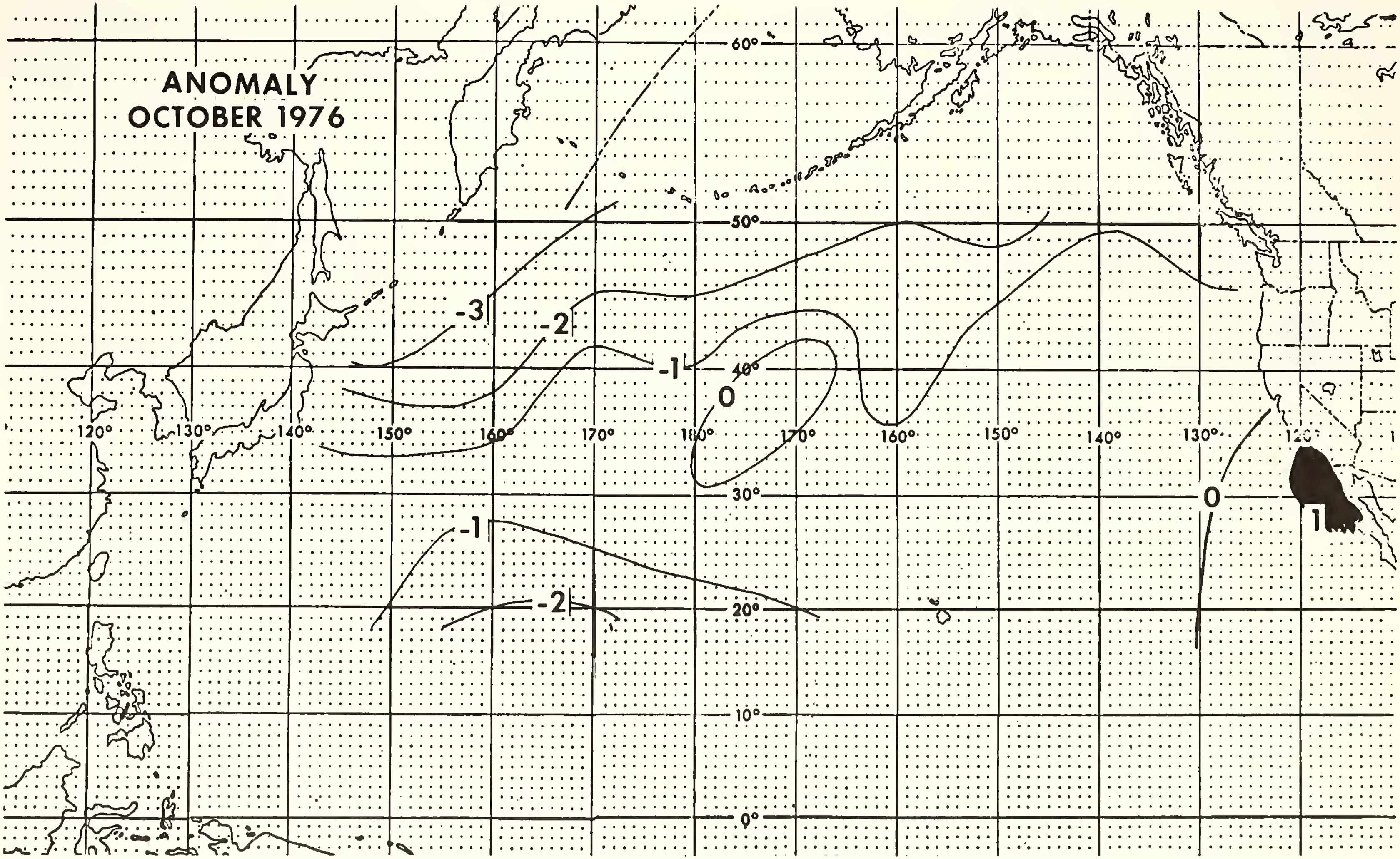

ANOMALY
OCTOBER 1976

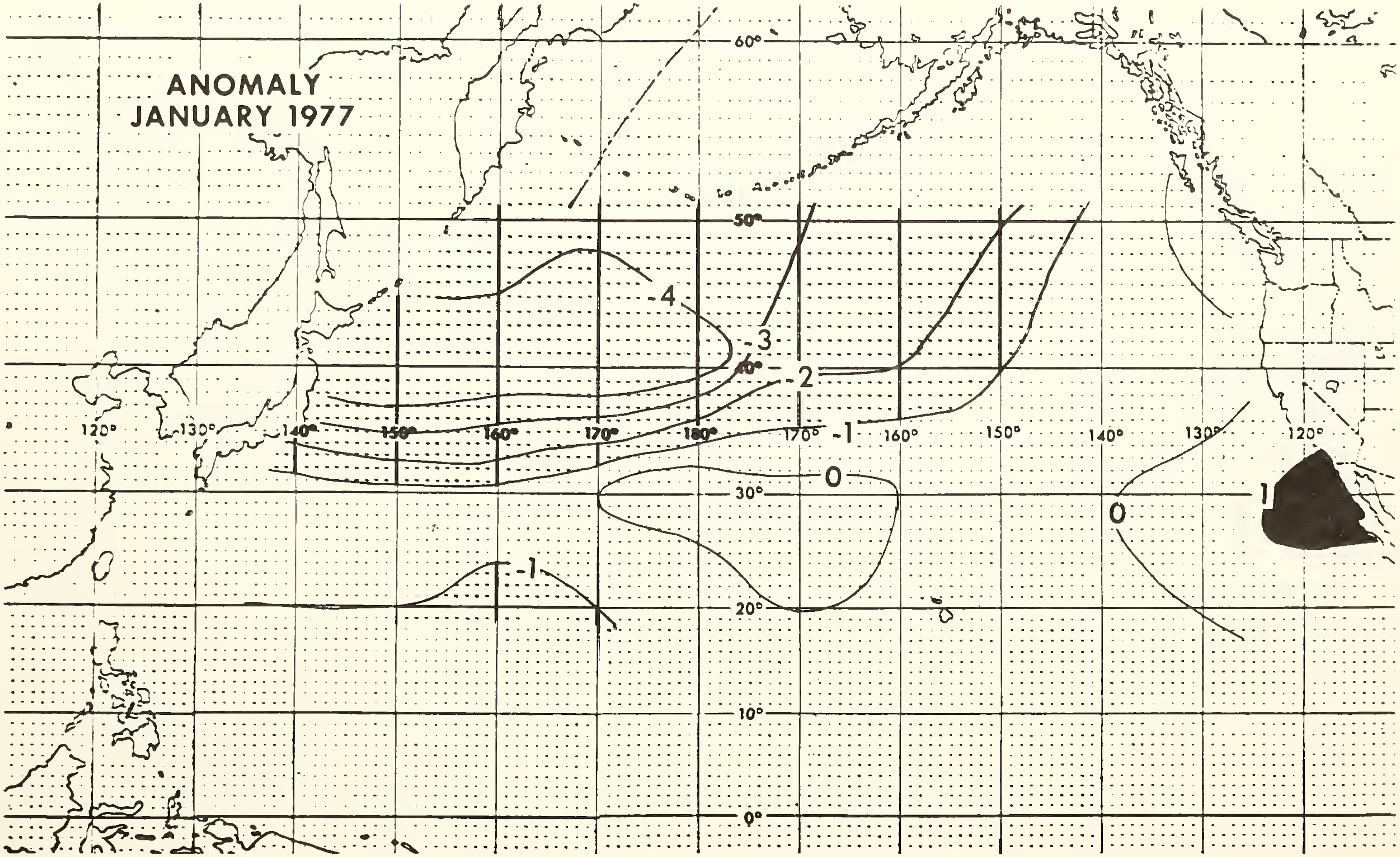

ANOMALY
JANUARY 1977

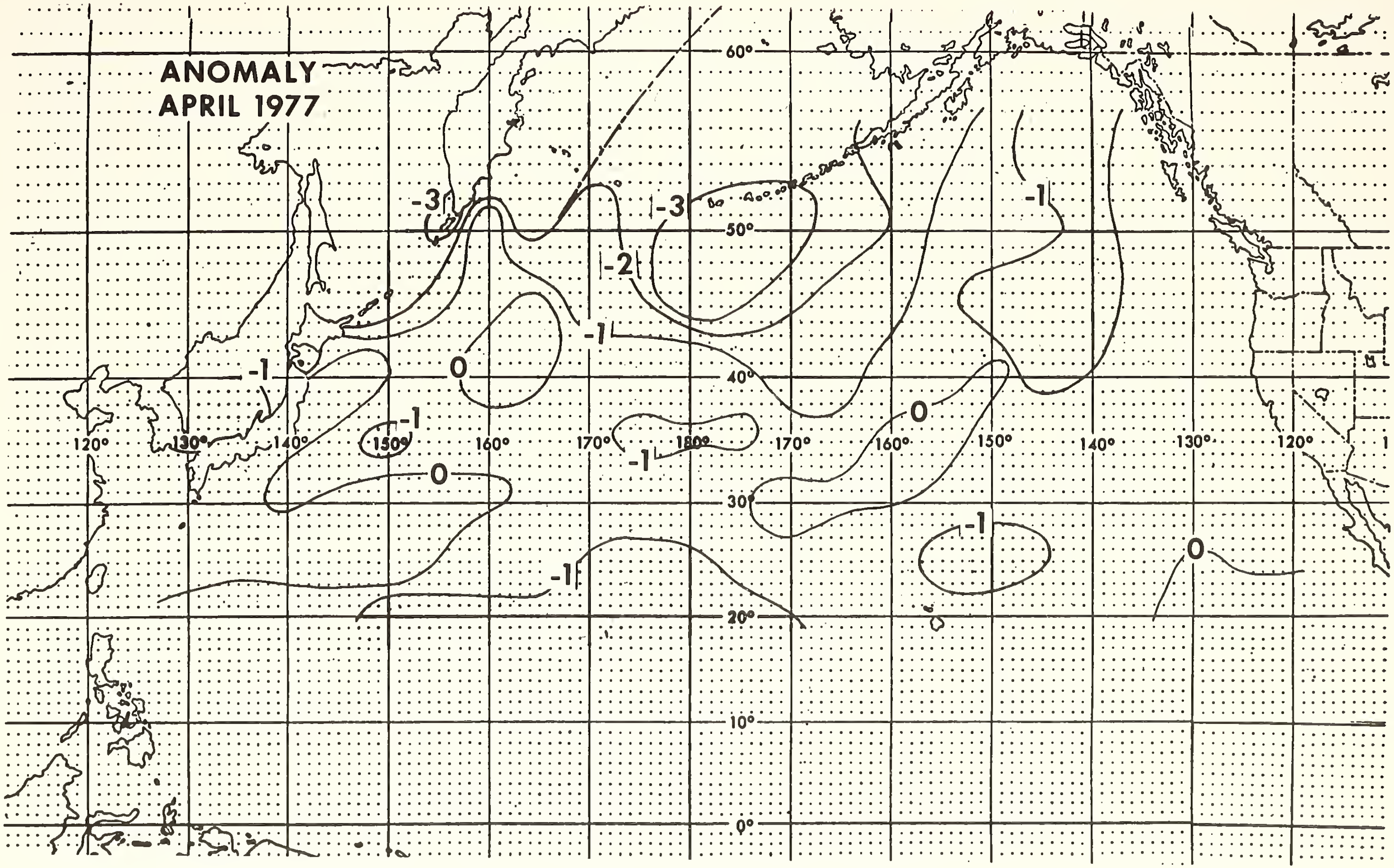
ANOMALY
APRIL 1977
60°
50°
40°
30°
20°
10°
0°
120°
130°
140°
150°
160°
170°
180°
170°
160°
150°
140°
130°
120°
-3
-3
-2
-1
-1
-1
-1
-1
-1
-1
0
0
0
0

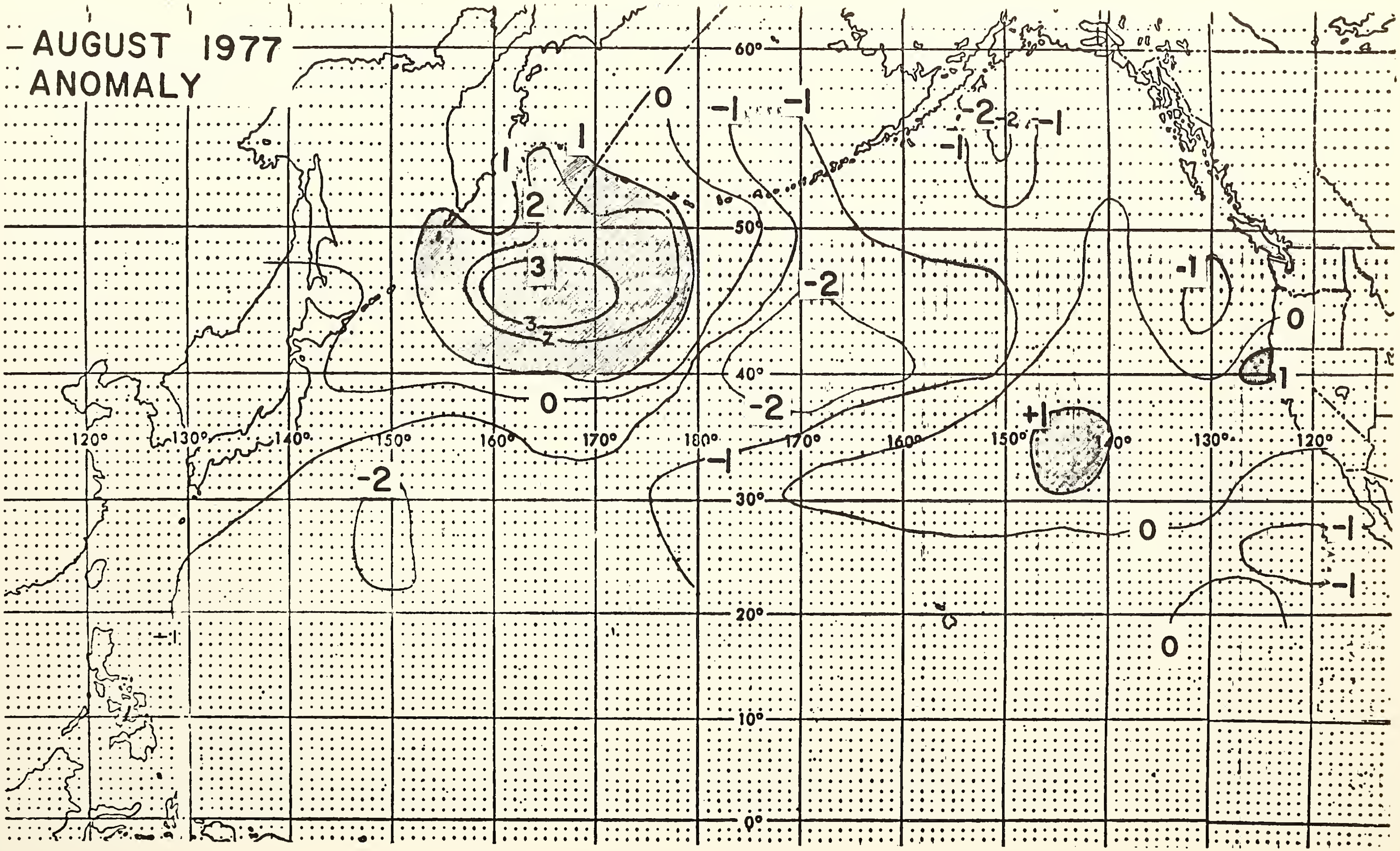
AUGUST 1977
ANOMALY
60°
50°
40°
30°
20°
10°
0°
120°
130°
140°
150°
160°
170°
180°
170°
160°
150°
140°
130°
120°
0
-1
-1
-2
2
-1
-1
1
1
2
3
3
2
0
-2
-2
-1
-2
+1
-1
0
1
0
-1
-1
0

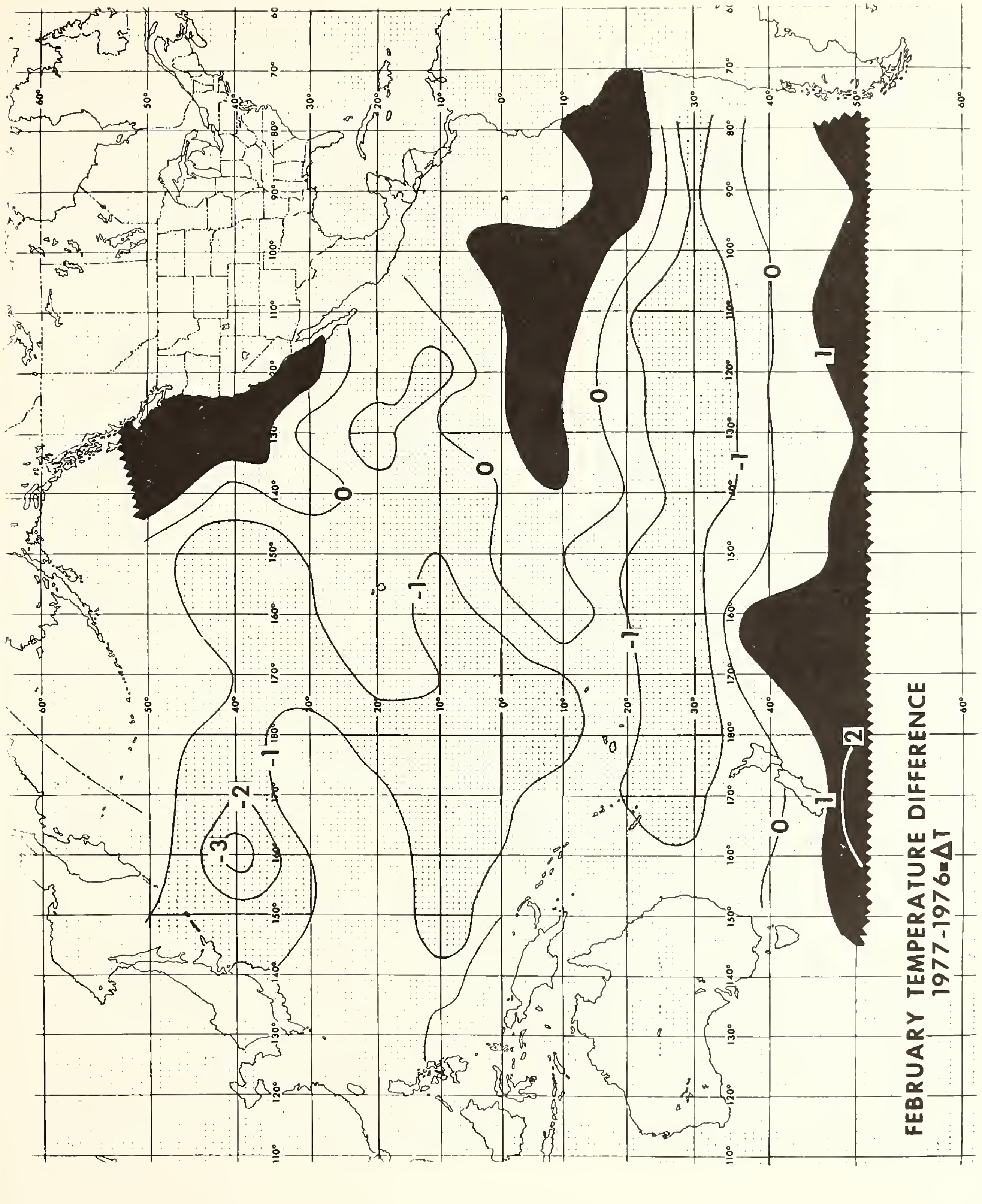

FEBRUARY TEMPERATURE DIFFERENCE
1977-1976=ΔT

THE EL NIÑO OF 1976-77 IN THE SOUTHEAST PACIFIC

by

Forrest R. Miller

Inter-American Tropical Tuna Commission

The National Marine Fisheries Service and the Inter-American Tropical Tuna Commission (IATTC) in La Jolla conduct research in fishery-oceanography to obtain input for fishery management studies, and for developing improved procedures to established fish catch quotas. In the eastern tropical Pacific, quotas on yellowfin tunas, for example, are established by the IATTC each year to prevent over-fishing and maintain the maximum sustainable yield of yellowfin for future fishing seasons in the tropics.

Sea surface temperatures (SST) and the anomalies of SST's provide useful diagnostic aids for monitoring changes in various fisheries from season to season and year to year. Sea surface temperatures are reported by most ships; and SST's are fairly conservative ocean properties. During some fishing seasons, SST's are abnormally cold over much of the eastern tropical Pacific and the migratory paths and apparent abundance of tunas and anchovies differ markedly from those of the very warm or El Niño years such as 1957, 1972 and 1976.

There are characteristic SST patterns which occur during warm or El Niño years in the eastern tropical Pacific; and there are other distinguishable SST patterns in cold or anti-El Niño years. The largest differences between cold and warm years usually shows up from July through December.

Figure 1A is a SST analysis for December 1971 and represents a cold tropical year, and Figure 1B is a SST analysis for December 1972-an El Niño year. The principal differences between cold and warm Decembers are found along the equator and the coasts of Ecuador and Peru where SST's range from 70°F (21°C) to 61°F (16°C) along the coast in Dec. 1971 and where SST's range from 78°F (26°C) to 64°F (18°C) along the coast in Dec. 1972. In addition the area of the eastern tropical Pacific occupied by waters with surface temperature warmer than 80°F (26.7°C) was considerably greater in Dec. 1972 than in Dec. 1971.

The El Niño of 1976 or abnormal warming in the eastern tropical Pacific had its initial beginnings in the northern spring of 1975 when SST's along the equator from the Galapagos Islands to Ecuador and south to central Peru increased to 4°F (2°C) above normal. However, from the southern mid-winter 1975 to March 1976, SST's returned to near or slightly below normal.

During May 1976 along the equator from 5°N to 10°S and east of 110°W extensive warming occurred. In Figure 2 the (hatched) positive SST anomalies east of 90°W were typical for a developing El Niño. After May the warmer off-shore water moved in to the coast where stations in Peru from 5°S to 12°S were reporting SST's 2°F (1°C) to 4°F (2°C) above normal. Some coastal stations near Lima, Peru, as early as April 1976, were reporting SST anomalies greater than in any April since 1972. Coastal regions south of 10°S continued to experience below normal SST's.

From June through August SST's were 2°F (1°C) to 6°F (3°C) above normal along the equator east of 120°W and along the coasts of Ecuador and Peru for the 4th consecutive month (Figure 3). The areas covered by positive SST anomalies greater than 2°F were greater in August than in any previous month of 1976.

During October (Figure 4) the area covered by SST's greater than 2°F (1°C) above normal expanded westward to at least 180°. From September to October there was a poleward and westward expansion of positive SST anomalies especially in the southern hemisphere from the equator to 15°S. During most El Niño years SST's at coastal stations return toward normal in October. This occurred at the coast in 1976 also but to a lesser extent than during the October of 1957 and 1972.

During most of 1976 the SST patterns resembled most closely those of 1965 which experienced an El Niño of moderate intensity. By December 1976 the positive anomalies had expanded farther poleward east of 140°W than in previous months. However, west of 140°W SST's were returning to near normal in the equatorial area with some negative anomalies appearing.

By February 1977 only scattered areas of above normal SST's remained as vestiges of the 1976 El Niño. After February along the equator and along the coasts of Ecuador and Peru SST's rapidly returned to normal or below; but in the southern hemisphere positive SST anomalies remained in the tropics and subtropic until mid 1977.

The atmospheric circulation over the south Pacific plays an important role in maintaining or diminishing wind-induced ocean mixing and/or upwelling. Figure 7 represents two types of surface pressure patterns in July 1972 which were typical of most El Niño years. For periods of 7 to 14 days the south Pacific high pressure center in July 1972 dominated the circulation and the southeast trades were steady and strong (Figure 7A). In contrast, there were other periods of 10 to 15 days when low pressure centers and weather fronts displaced the subtropical high pressure center and the southeast trades were diminished (Figure 7B). During these periods the fronts usually moved closer to the equator than during anti-El Niño years.

Weekly averaged pressure differences between the coast of Peru at 16°S and 30°S, 90°W when compared to the long term mean gradient provided a rough index of the strength of the southeast trade winds off the coast of South America of 15°S.

Figure 8 (bottom) shows that beginning in late April 1976 pressures began to fall off the coast of South America. Thereafter, in May, July and October pressure gradients were far below normal. During the same period SST's along the coast of Peru averaged 1°C (2°F) to 2°C (4°F) above normal (Figure 8, top). A similar pattern of events apparently took place during the El Niño of 1965 as is shown by the positive temperature anomalies (dashed line, Figure 8, top). After February 1977 the surface pressure gradient increased to above normal and have remained normal or above. Coastal SST's also changed to near or slightly below normal after February 1977.

Components of the 700 mb winds, obtained from the National Weather Service (NMC) upper air analyses, provided additional diagnostic aids for monitoring the strength of the circulation over the southeast Pacific. During 1976 there were large departures from a 4 year mean of the 700 mb wind speed (KTS), U and V components of the wind at 33°S, 90°W. During the El Niño of 1976 from about May to December the zonal westerlies decreased to below the 4 year mean and the meridional wind components increased in magnitude with frequent directional changes appearing. The same pattern of events occurred during the 1972 El Niño (dashed line Figure 9). Closer to the equator (21°S, 90°W) the 700 mb wind components revealed the same sequence of events (Figure 10) with more directional changes in the V component at 21°S than at 33°S. A westward shift in the subtropical high pressure system, as revealed in Figure 8, 9 and 10, occurred frequently during the 1976 El Niño and it also occurred in 1972.

Sea temperatures, preferably from the surface to the top of the thermocline, provide accurate and easy-to-measure diagnostic aids to study climatic changes in the atmosphere as well as in the world's fisheries. High resolution infrared and visual satellite data provide additional data about changes in the ocean temperatures, especially in sparse (ship) data regions. Because fish catch records for many fisheries are fairly consistent and accurate for a longer period than detailed sea temperatures, it may be of value in climate diagnostics research to examine various world fisheries for clues to climatic changes. Perhaps the most useful data would come from countries with long fishing histories along the west coasts of continents. Contemporary climatic studies could draw upon world fishery records which have been compiled.

FIGURE 1. Sea surface temperature analyses for December 1971 (A) and December 1972 (B) based on monthly mean temperatures from ships averaged by 1° quadrangles.

FIGURE 2. Monthly sea surface temperature anomalies (deviations from the 1947-1968 means) for May 1976 in intervals of ± 2°F. Shaded areas indicate below normal and hatched areas are more than 2°F above normal.

FIGURE 3. Same as Figure 2 except anomalies are for August 1976.

FIGURE 4. Same as Figure 2 except anomalies are for October 1976.

FIGURE 5. Same as Figure 2 except anomalies are for December 1976.

FIGURE 6. Same as Figure 2 except anomalies are for February 1976.

FIGURE 7. Sea surface pressure and weather from analyses prepared by the National Weather Service, Washington, D.C. for July 3, 1972 (A) and July 27, 1972 (B). Heavy line from coast of Peru (16°S) to 30°S, 90°W indicates end points for obtaining data for pressure gradient index.

FIGURE 8. Annual variations in sea surface pressure gradient between the coast of Peru and 30°S, 90°W (bottom) during 1976-77. Heavy line represents the long-term mean pressure gradient, and the open and hatched areas above and below the mean curve are weekly-averaged departures of pressure gradient. Annual departures of sea surface temperatures from normal for Chimbote and Lima (Callao), Peru (Top) were composited to show above normal (hatched) and below normal temperatures. The dashed curve shows the annual departure of SST for the same stations in 1965-67. Dotted lines show weekly variation of SST in 1976.

FIGURE 9. Annual variation (1976-77) of the mean wind speed, U and V components of wind at 700 mb for 33°S, 90°W based on National Weather Service (NMC) stream function analyses. Data were extracted daily and averaged weekly.

FIGURE 10. Same as Figure 9 except data are for 21°S, 90°W.

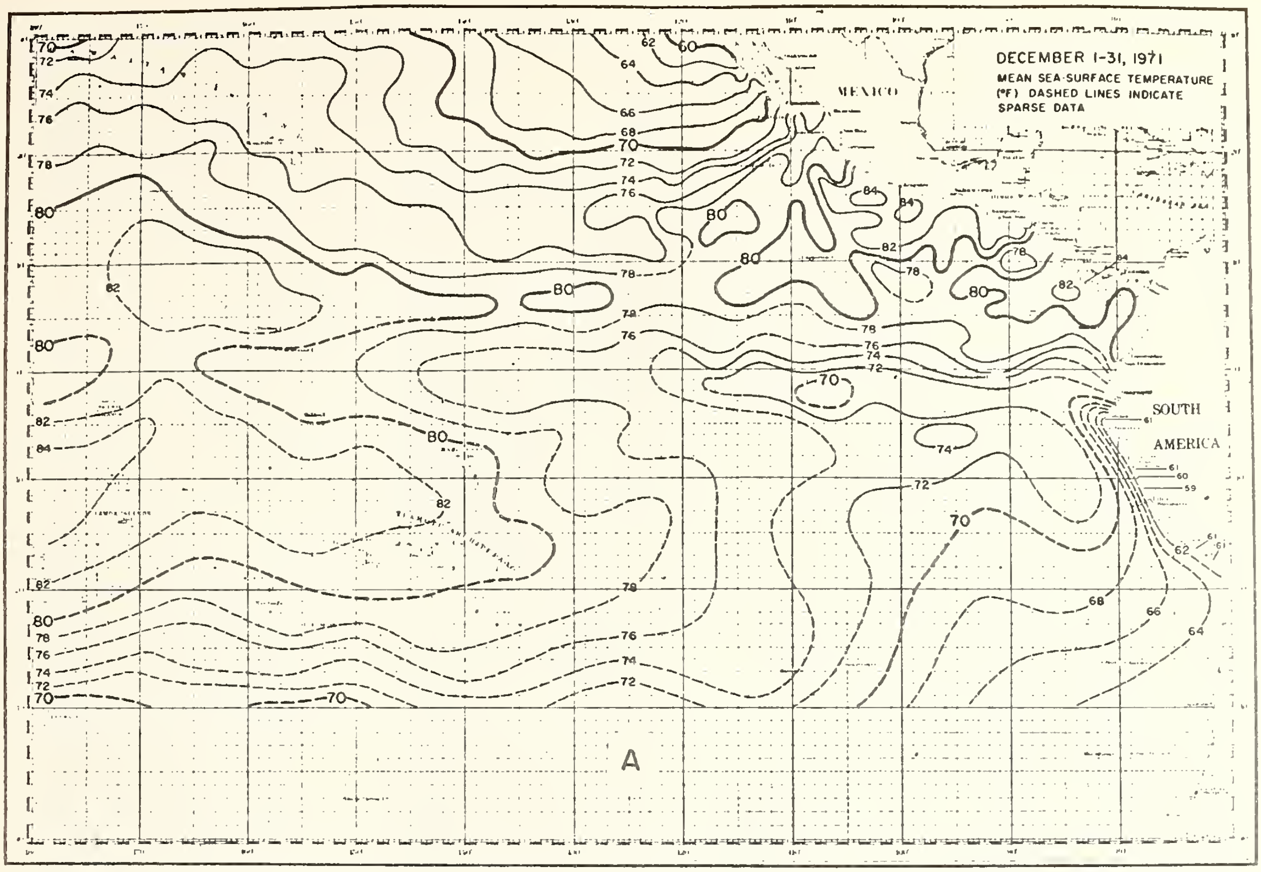

DECEMBER 1-31, 1971

MEAN SEA-SURFACE TEMPERATURE (°F) DASHED LINES INDICATE SPARSE DATA

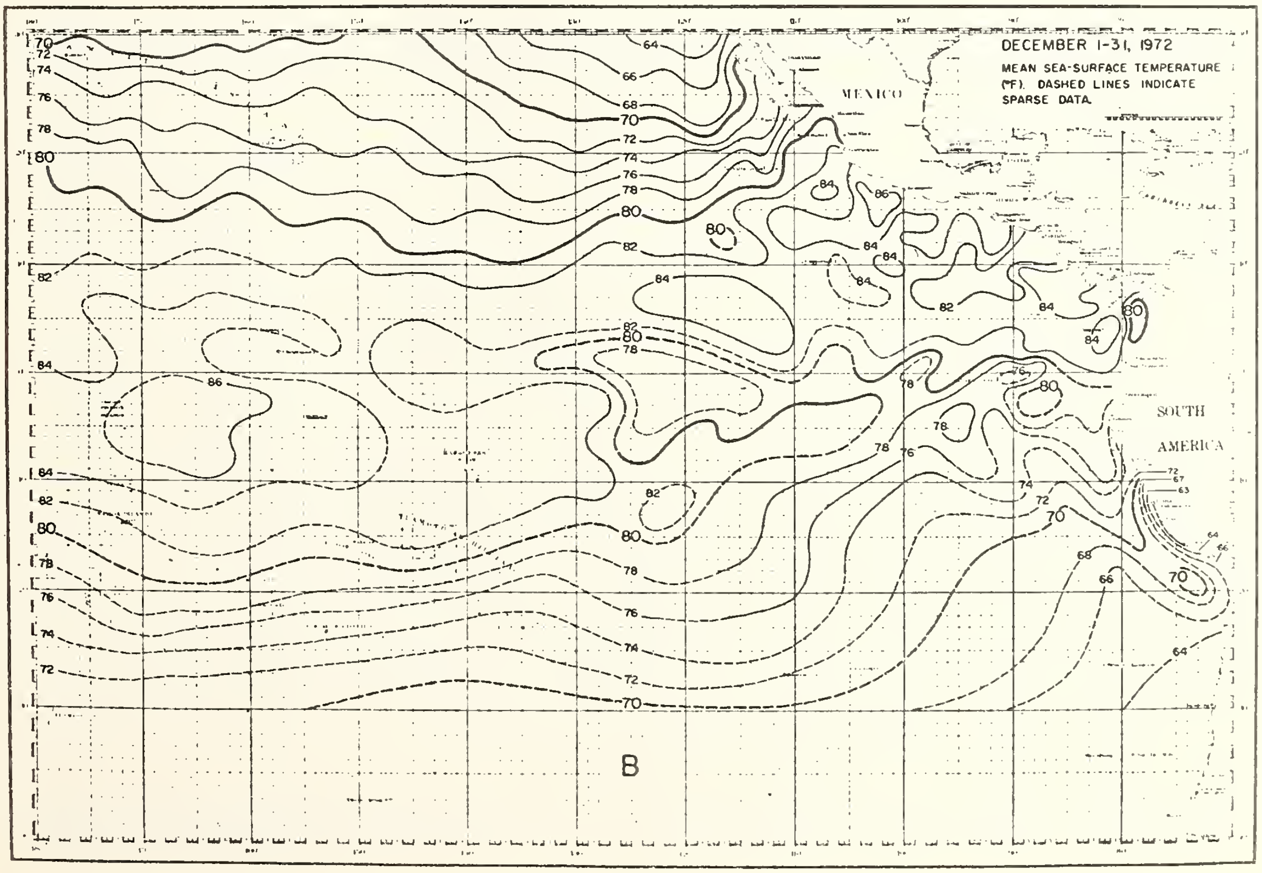

DECEMBER 1-31, 1972

MEAN SEA-SURFACE TEMPERATURE (°F). DASHED LINES INDICATE SPARSE DATA.

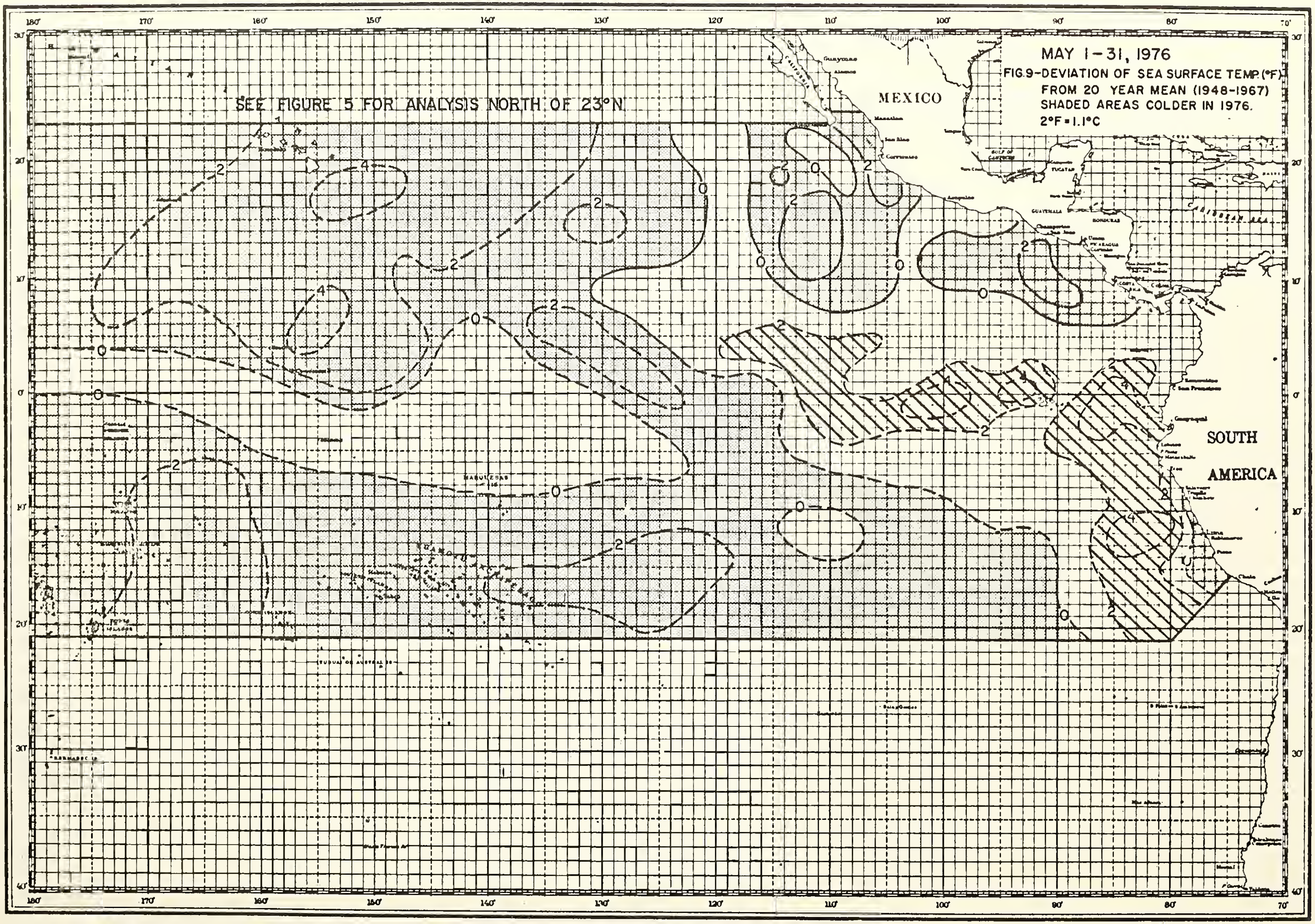

MAY 1-31, 1976

FIG.9-DEVIATION OF SEA SURFACE TEMP.(°F) FROM 20 YEAR MEAN (1948-1967) SHADED AREAS COLDER IN 1976. 2°F = 1.1°C

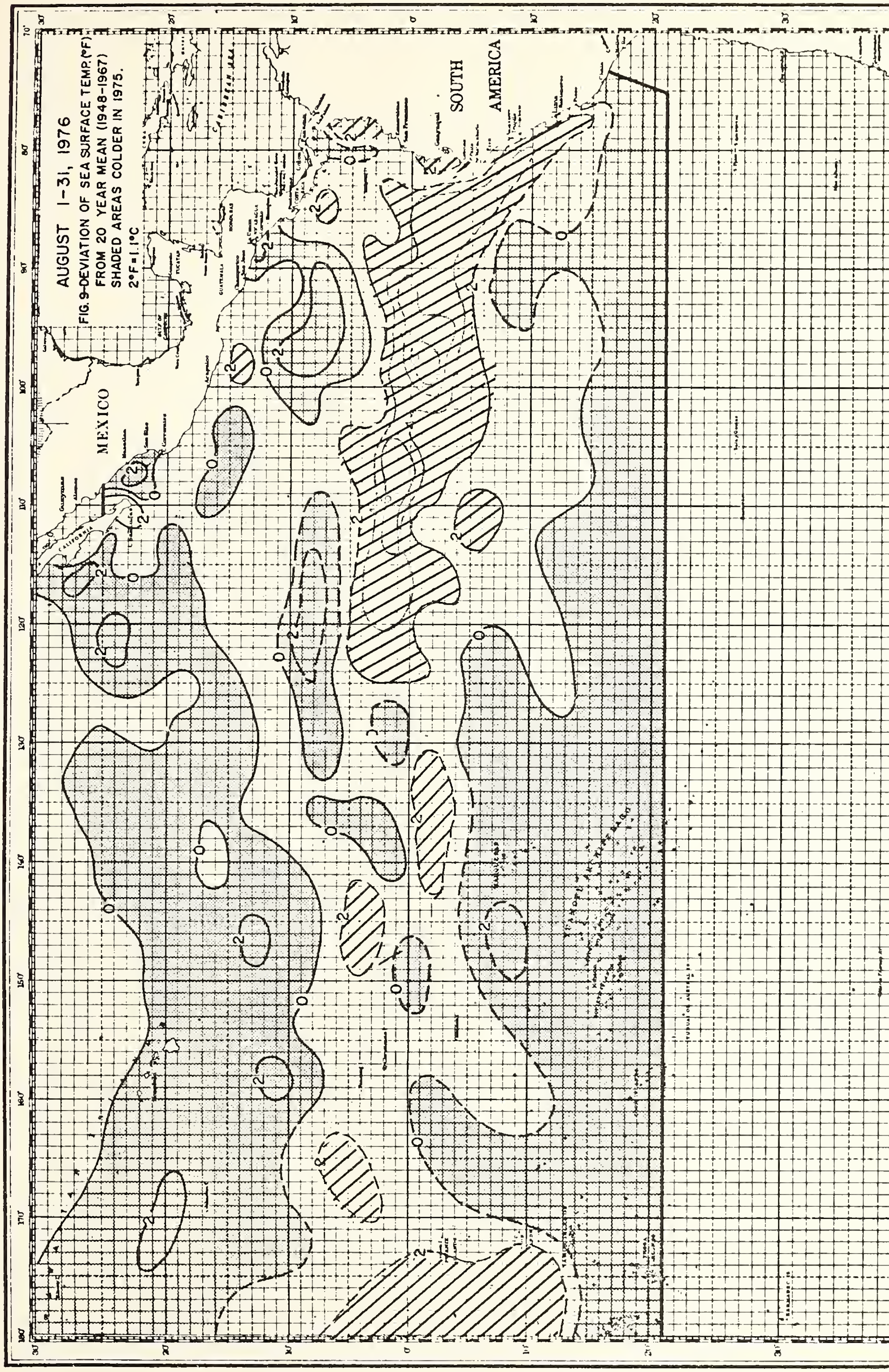

AUGUST 1-31, 1976

FIG. 9-DEVIATION OF SEA SURFACE TEMP. (°F) FROM 20 YEAR MEAN (1948-1967) SHADED AREAS COLDER IN 1975.

2°F = 1.1°C

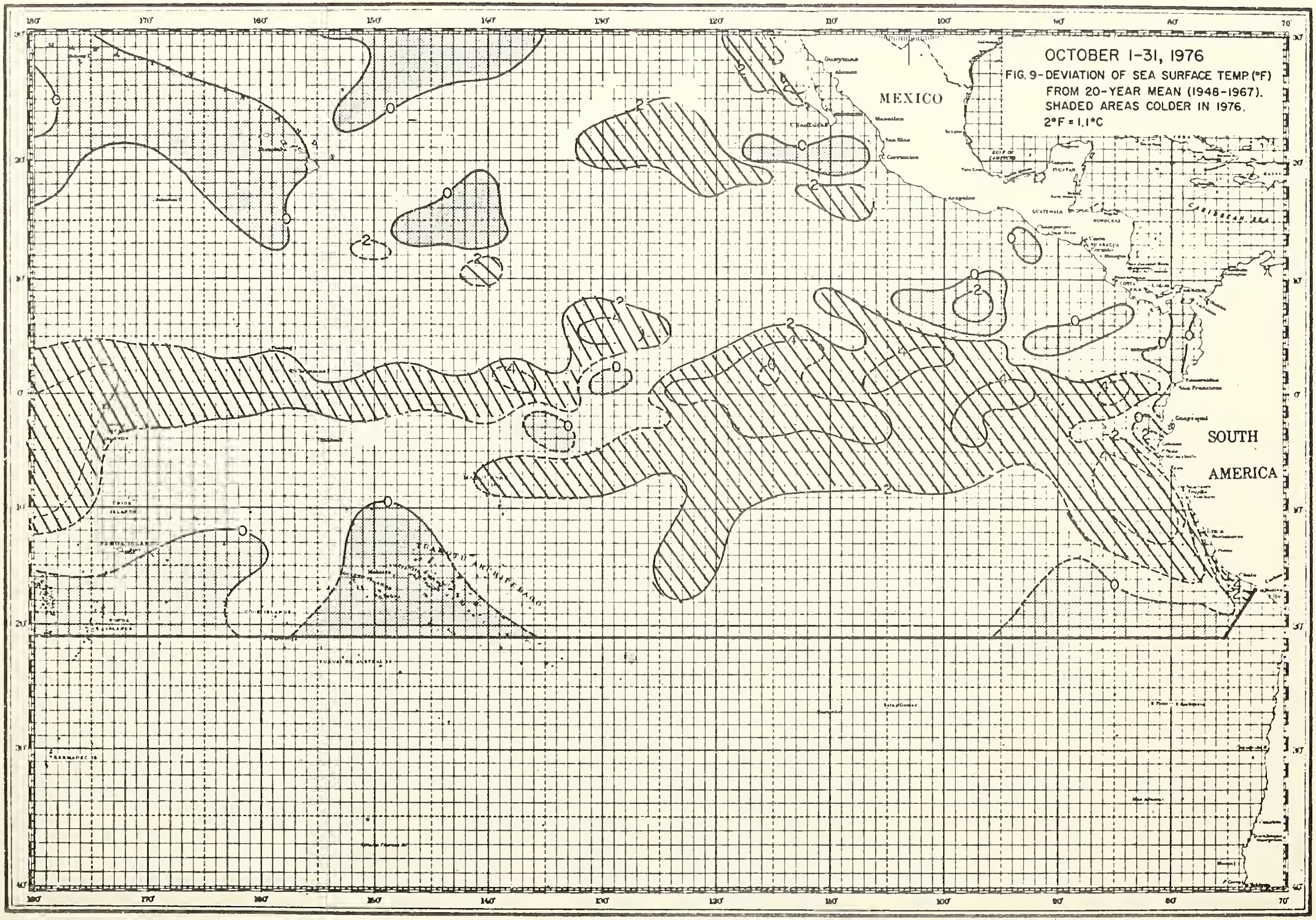

OCTOBER 1-31, 1976

FIG. 9-DEVIATION OF SEA SURFACE TEMP. (°F) FROM 20-YEAR MEAN (1948-1967). SHADED AREAS COLDER IN 1976.

2°F = 1.1°C

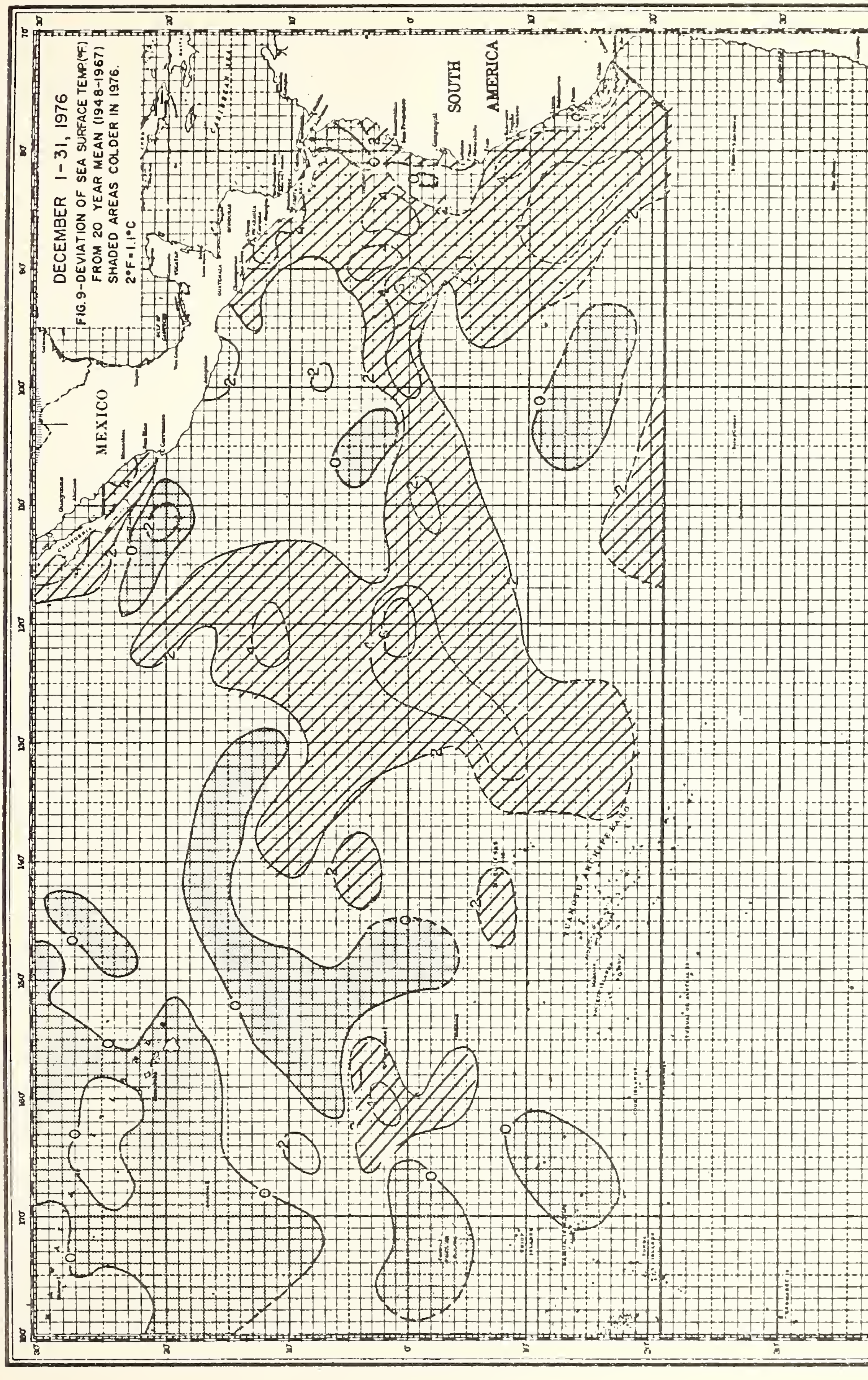

DECEMBER 1-31, 1976

FIG. 9-DEVIATION OF SEA SURFACE TEMP.(°F.) FROM 20 YEAR MEAN (1948-1967) SHADED AREAS COLDER IN 1976.

2°F = 1.1°C

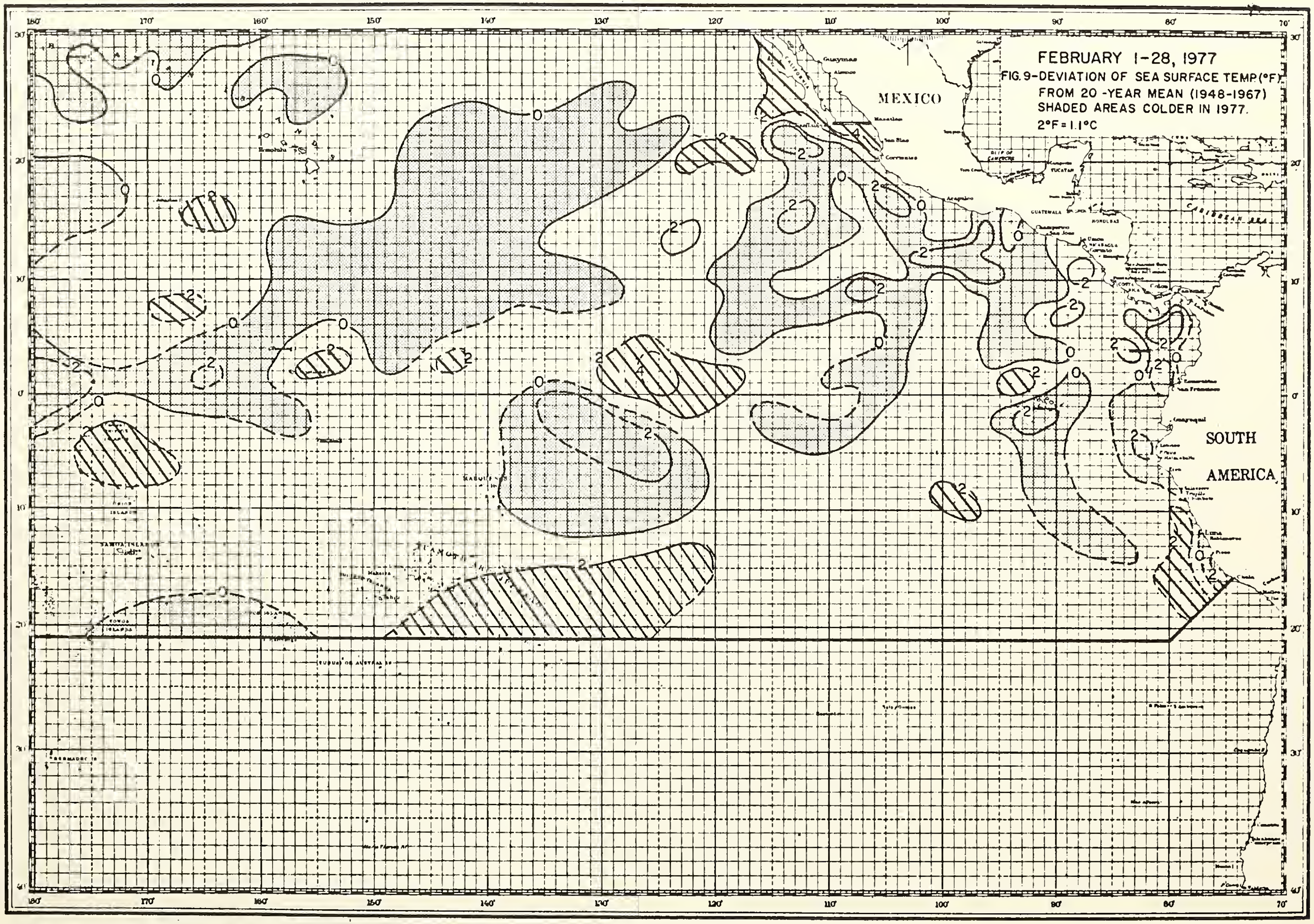

FEBRUARY 1-28, 1977

FIG. 9-DEVIATION OF SEA SURFACE TEMP.(°F) FROM 20-YEAR MEAN (1948-1967) SHADED AREAS COLDER IN 1977. 2°F = 1.1°C

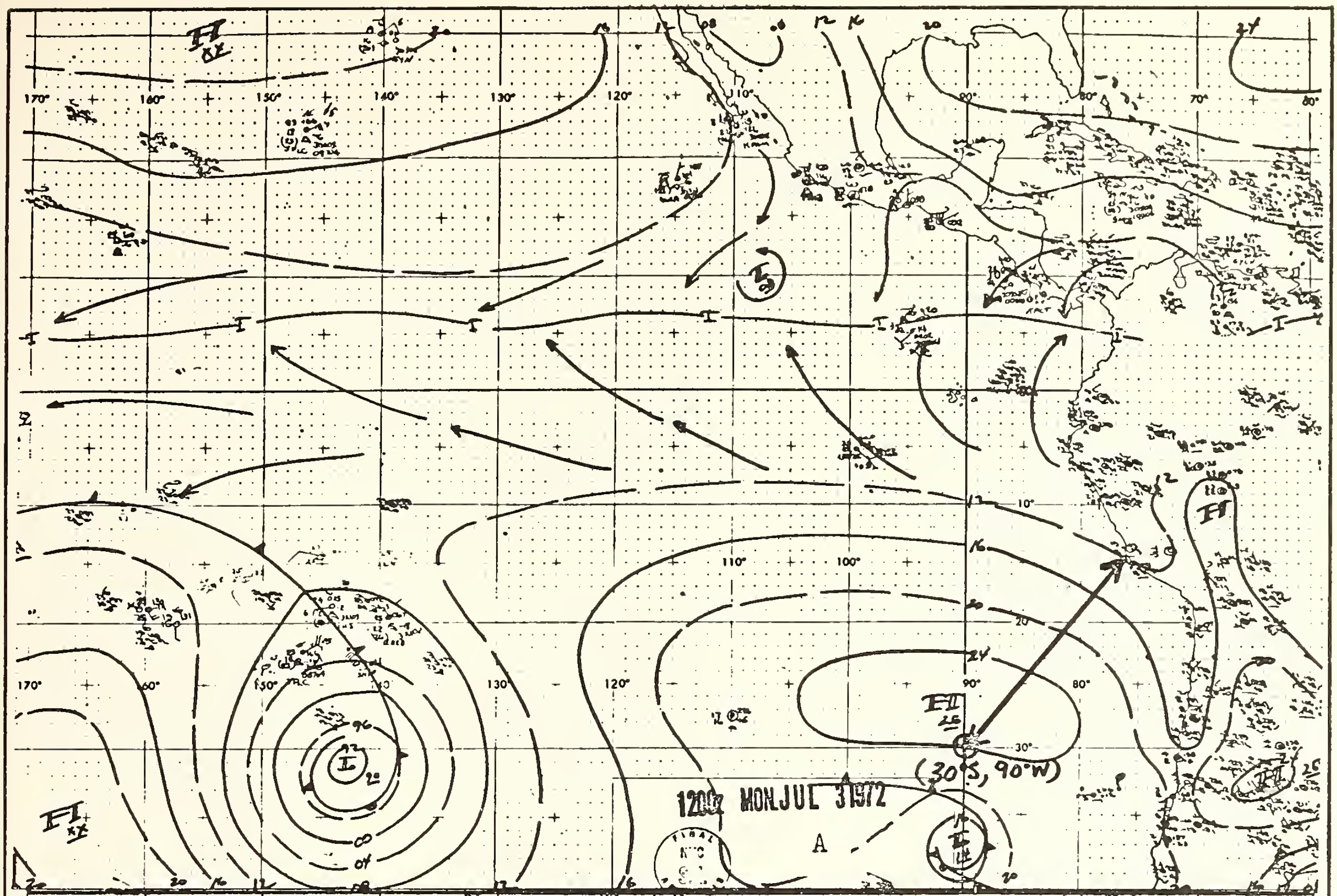
1200Z MONJUL 31 1972
(30°S, 90°W)
A

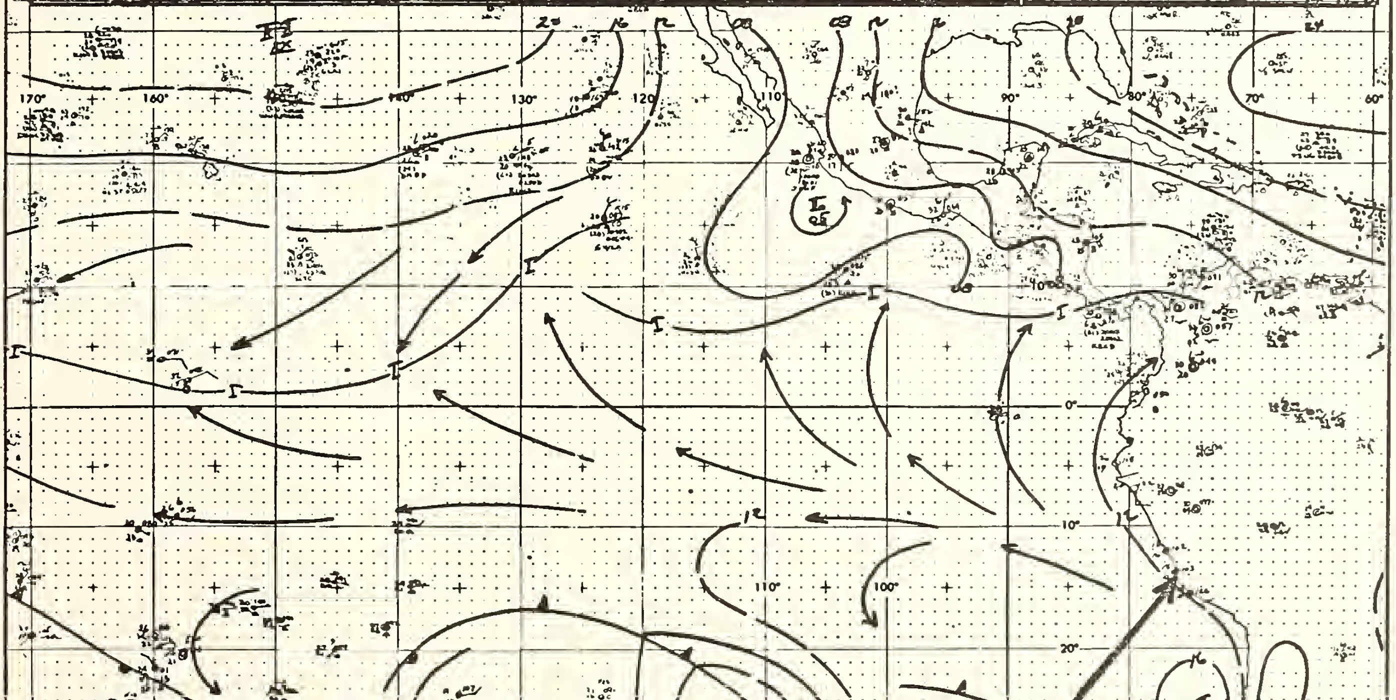
0000Z THU JUL 27 1972
30°S, 90°W
B

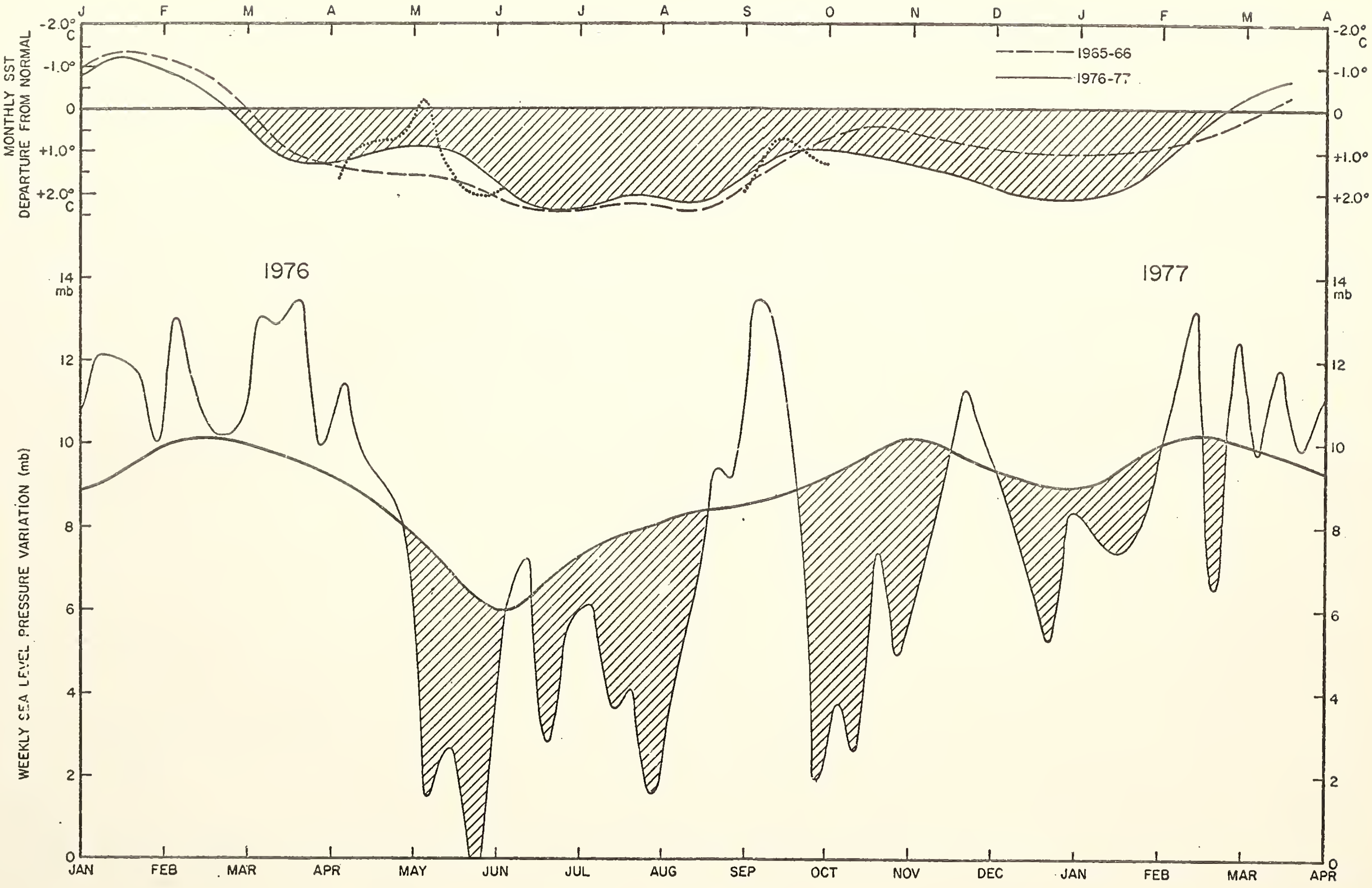
J
F
M
A
M
J
J
A
S
O
N
D
J
F
M
A
-2.0° C
-1.0°
0
+1.0°
+2.0° C
MONTHLY SST DEPARTURE FROM NORMAL
1965-66
1976-77
1976
1977
14 mb
12
10
8
6
4
2
0
WEEKLY SEA LEVEL PRESSURE VARIATION (mb)
JAN
FEB
MAR
APR
MAY
JUN
JUL
AUG
SEP
OCT
NOV
DEC
JAN
FEB
MAR
APR

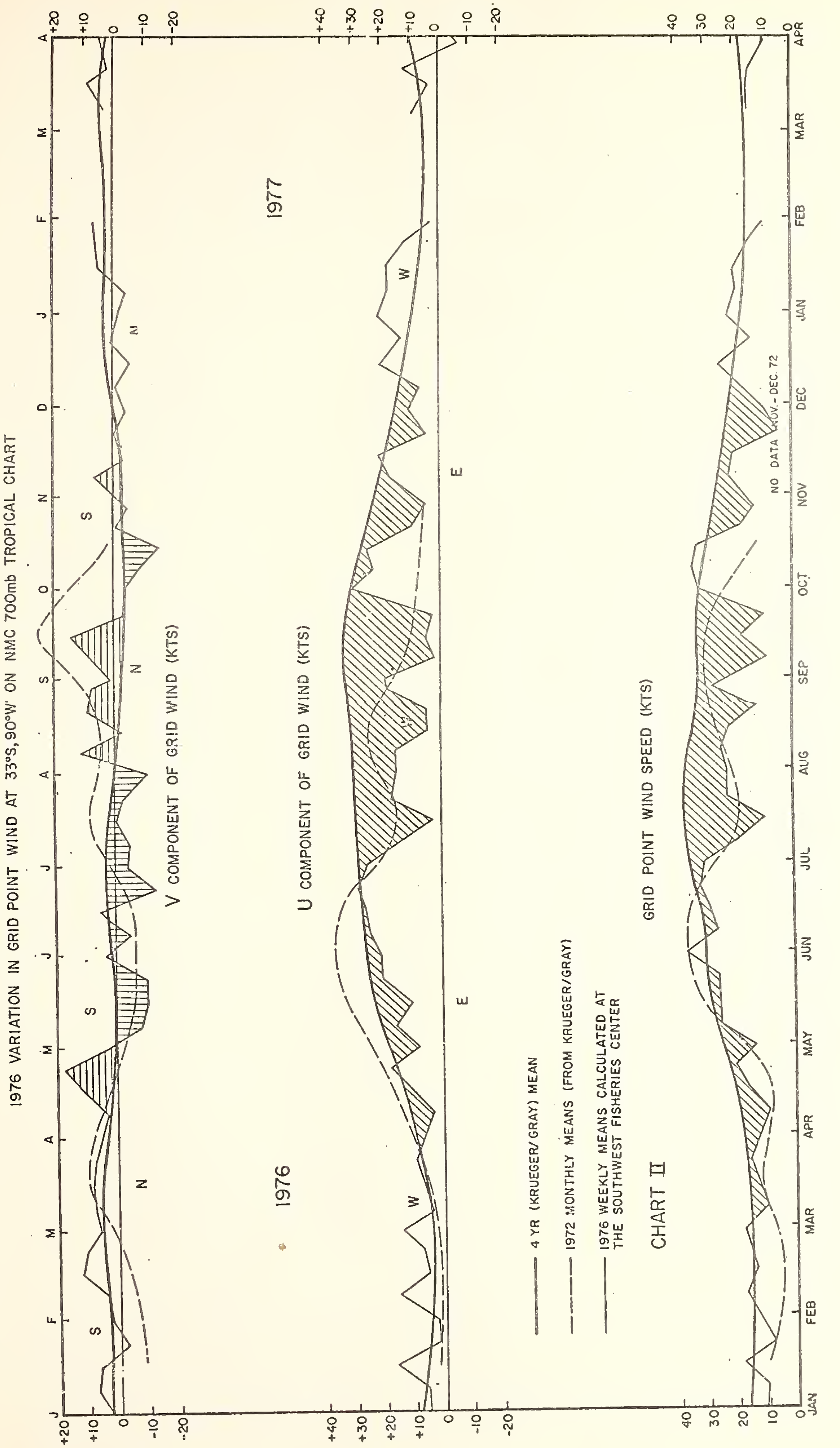

1976 VARIATION IN GRID POINT WIND AT 33°S, 90°W ON NMC 700mb TROPICAL CHART

CHART II

1976 VARIATION IN GRID POINT WIND AT 21°S, 90°W ON NMC 700mb TROPICAL CHART

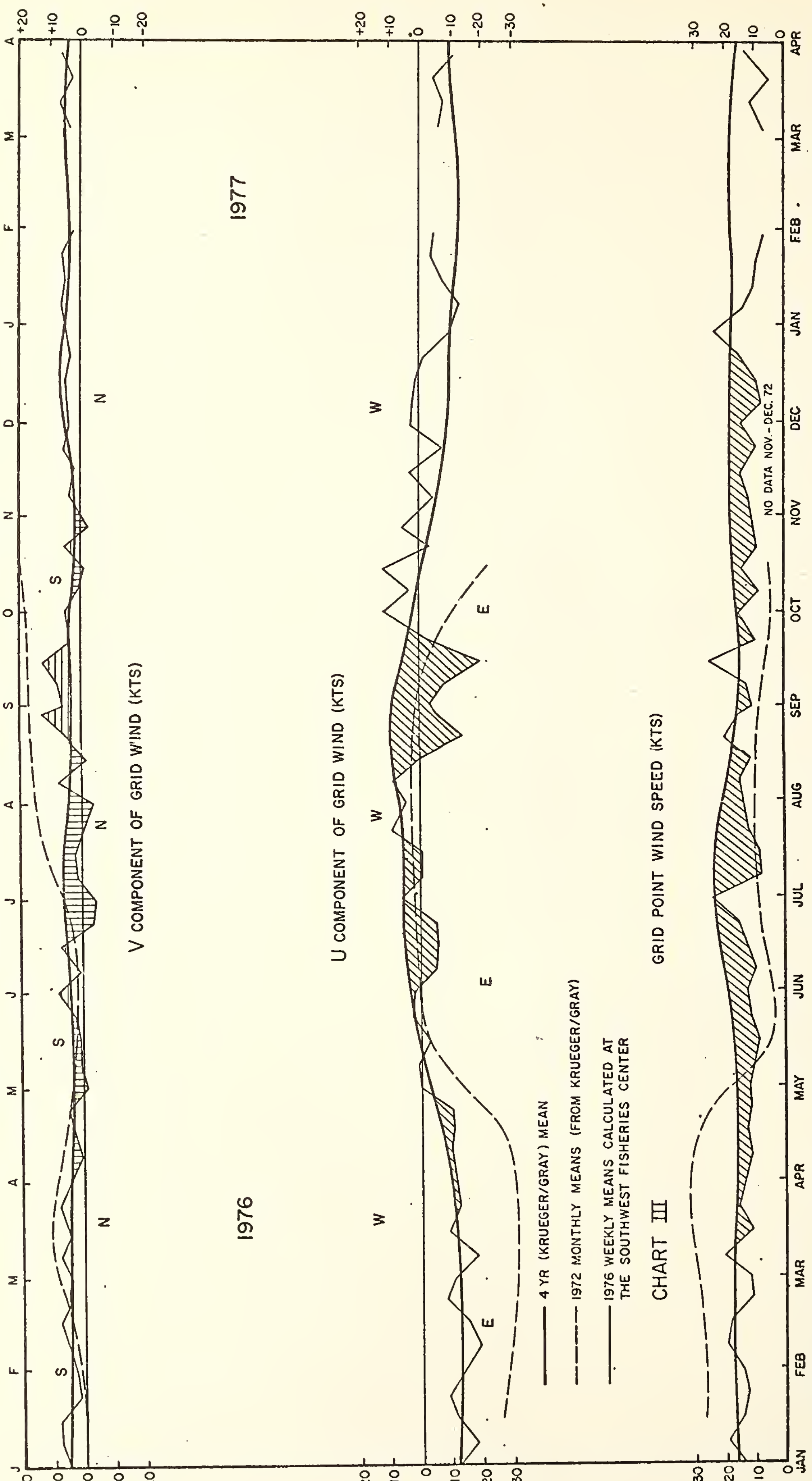

CHART III

Diagnosis of the 1976-77 El Niño

William H. Quinn
School of Oceanography, Oregon State University

The prediction for and preliminary findings pertaining to this event were discussed at last year's workshop. Here the analysis is carried further considering the additional year of evidence. Fig. 1 shows the location of sites referred to in this discussion.

Fig. 2 shows the expected deep 1976 relaxation troughs following the late 1975 pre-event peaks in the triple 6-month running mean plots of Southern Oscillation (S.O.) index anomalies. Fig. 3 shows a similarly filtered plot of the Ship N-Darwin index anomalies compared to the Rapa-Darwin plot. Fig. 4 shows the result of applying the same filter to the Tarawa rainfall anomalies and compares it to the Rapa-Darwin plot. As usual the rainfall peak lags behind the pressure trough. Tarawa rainfall April 1976-March 1977 was 3,791 mm; about double the average annual amount. Also, as one might expect, the Monthly Climatic Data for the world shows that an east monsoon drought affected Indonesia in 1976.

Fig. 5 shows how the Easter-Darwin index anomaly trend relates to sea surface temperature (SST) anomaly trends for Marsden Square (MS) quadrants 10(1) and 10(3) when the triple 6-month running mean filter is applied. MS 10(1) is next to the equator, and when the circulation is strong (S.O. index is high) it shows lower SST's due to the advection of cooler Peru Current water into the area and/or equatorial upwelling; when the circulation is weak (index is low), SST's rise as they did in the case of the 1976 El Niño. MS 10(3) SST's reflect changes in an area affected by the north equatorial countercurrent transport; and, as usual, there is a significant lag in the thermal peak in this area, when compared to the index trough and MS 10(1) SST peak. The 3-month running mean plots of the Easter-Darwin index anomalies and the MS 10(1) SST anomalies (Fig. 6) show the variations in more detail.

Three-month running mean plots of SST for Talara, Puerto Chicama, Chimbote, Don Martin and La Punta (Fig. 7) show what took place along the Peruvian coast and how the 1976-77 event compares to the strong 1972-73 El Niño. Figs. 8 and 9 show how the sea level pressure and air temperature changes relate to the SST fluctuations over this same period at Talara and Chimbote respectively. Based on all evidence it appears that the 1976-77 event was a moderate El Niño.

The forecast for the 1976 event called for it to resemble the 1965 El Niño, and in many respects it did. However, the 1976 event set in a little later (1-2 months) in the year and the anomalous effects held over a little further into 1977 than they did into 1966. Fig. 10 shows the two-stage nature of these two developments as they were represented in the S.O. index anomaly trends. In each case a very weak event (1963 and 1975) preceded the moderate El Niños. Fig. 11 shows the contrasting single stage developments that led up to the strong 1957-58 and 1972-73 El Niños.

The Peruvian anchoveta fishery catch declined from a high of over 12 million tons (about 1/5 the total world catch for all fish) in 1970 to about 2 million tons in 1973 (Fig. 12). Although over-fishing in 1970-71 may have contributed heavily to this decrease in anchoveta catch, the strong El Niño of 1972-73 was undoubtedly also a major cause for this precipitous decline. However, the 1975 catch was still only about 25% of the record 1970 catch, the 1976 catch remained low, and so far it appears that the 1977 catch will continue to be low, indicating the later unfavorable environmental conditions (in lesser degree) have probably contributed to a delay in recuperation of the fishery.

In reply to an April 1977 request for a forecast for this Peruvian fishery region in support of a planned joint Canadian-Peruvian study late 1977-early 1978, the following was provided: "Although the South Pacific subtropical high pressures have continued to be unusually low, I expect to see a rise in the interannual trend of the pressure index later this year. In other words I don't expect to see El Niño type activity in the 1977-78 season, and if anything would expect coastal temperatures to be below normal by that time." At this time I see no reason for a change in this outlook which was issued in late April 1977.

It is my opinion that the more persistent interannual changes (of a radical nature) in large-scale weather conditions over various parts of the globe will tie in with either the El Niño or anti-El Niño extremes (as depicted in the S.O. index anomaly trends) quite consistently. It's fortunate that the initial onset of the El Niño symptom, which is signaled by the pre-event index peak, frequently occurs early in the chain of events that affect a large part of the global tropics. Hence, if we can predict it, the associated activity that generally follows, such as the abnormally heavy central and western equatorial Pacific precipitation and east monsoon drought over Indonesia, can also be included in the prediction. Also, variations in the energy contributed to the heat source region over the western-most equatorial Pacific and Indonesia, as a result of the circulation changes related to the El Niño and anti-El Niño extremes, can be expected and can have even further reaching effects on global climate.

Support by the NSF Climate Dynamics, and IDOE (NORPAX) programs is gratefully acknowledged.

Note: In the figures the annual cycle is largely eliminated from the data by subtracting out long-term average monthly values. The 3-month running mean filter is applied to the resulting anomalies for study of the more immediate trends. Application of the triple 6-month running mean (involves three successive passes of the 6-month running mean over the involved data) filter provides a clearer picture of the extended interannual trend.

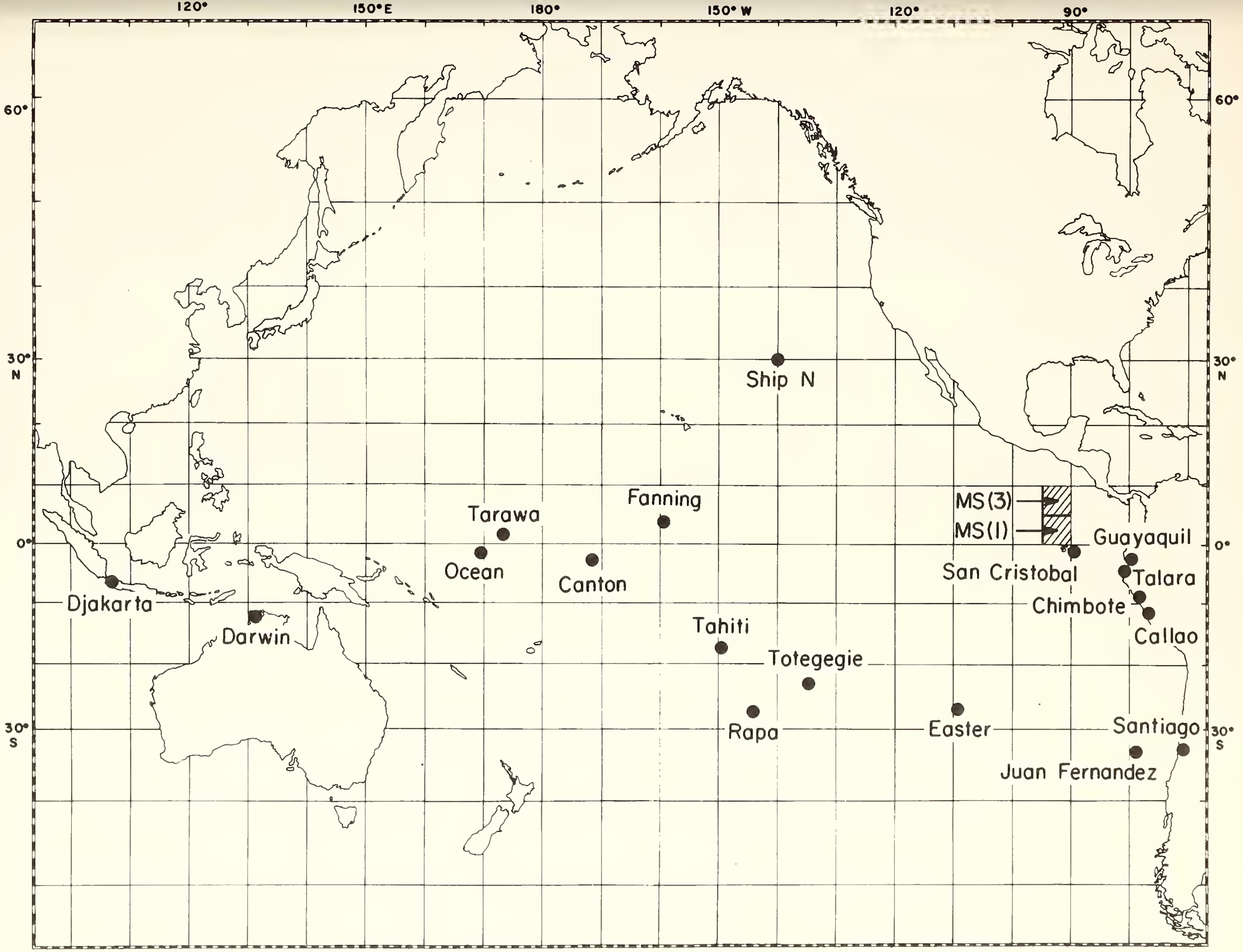

Fig. 1. Locator chart for referenced sites and Marsden square (MS) quadrants 10(1) and 10(3).

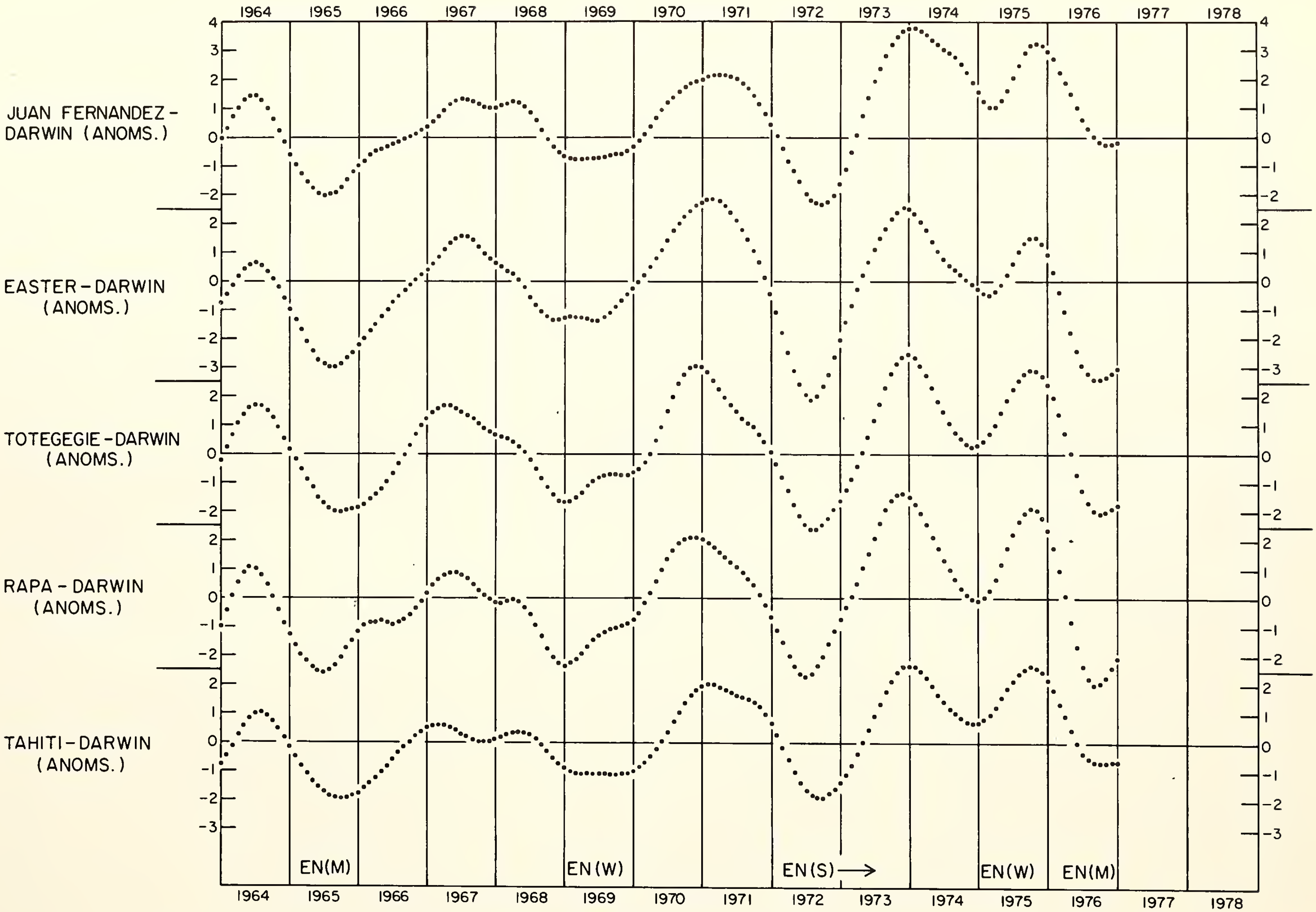

Fig. 2. Triple 6-month running mean plots of anomalies of the difference in sea level atmospheric pressure (mb) between Juan Fernandez I. and Darwin, Australia, between Easter I. and Darwin, between Totegegie and Darwin, between Rapa and Darwin, and between Tahiti and Darwin for 1964-76. El Niño type events (EN) are indicated as strong (S), moderate (M), and weak or very weak (W) in intensity.

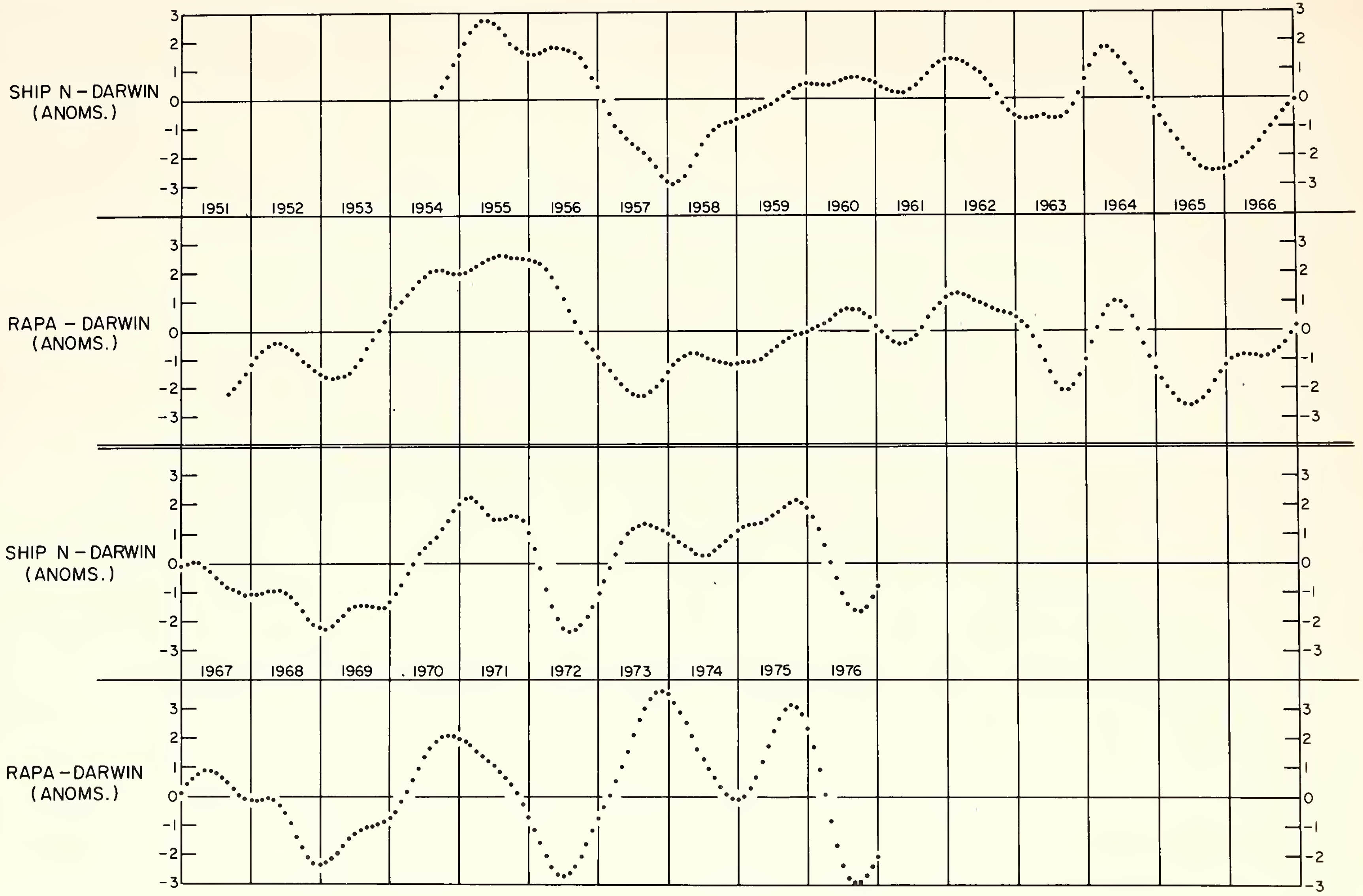

Fig. 3. Triple 6-month running mean plots of anomalies of the difference in sea level atmospheric pressure (mb) between Ship N and Darwin, Australia, and between Rapa and Darwin for 1951-76. (Data for the former Ship N location are now computed from surface synoptic analyses.)

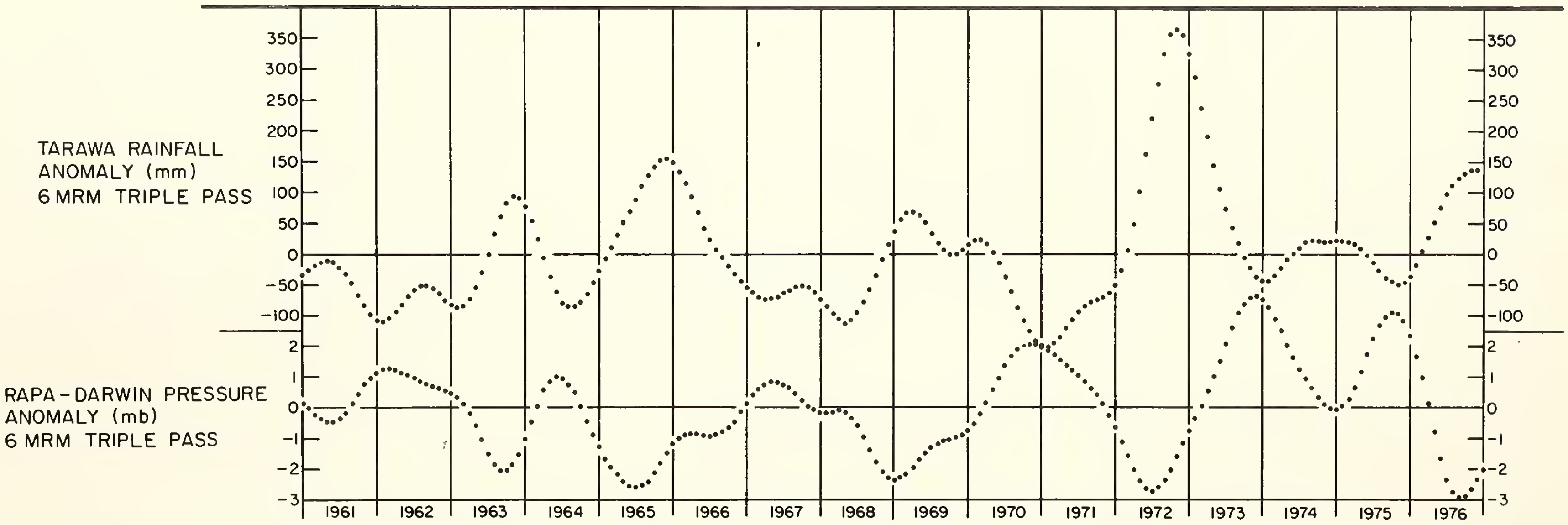

Fig. 4. Triple 6-month running mean plot of anomalies of the difference in sea level atmospheric pressure (mb) between Rapa and Darwin, Australia compared to a similarly filtered plot of Tarawa rainfall anomalies (mm) for 1961-76.

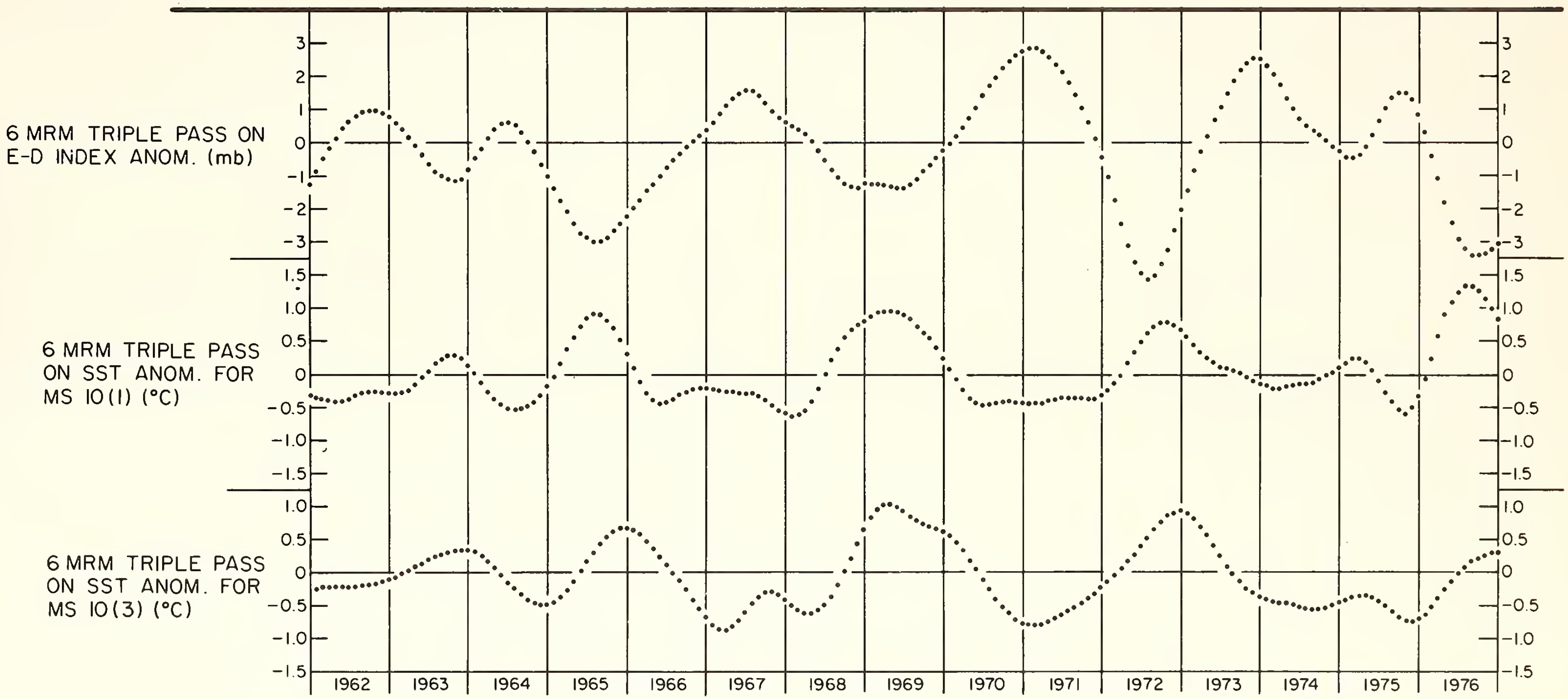

Fig. 5. Triple 6-month running mean plot of anomalies of the difference in sea level atmospheric pressure (mb) between Easter I. and Darwin, Australia compared to similarly filtered plots of sea surface temperature anomalies (°C) for Marsden square quadrants 10(1) and 10(3) for 1962-76.

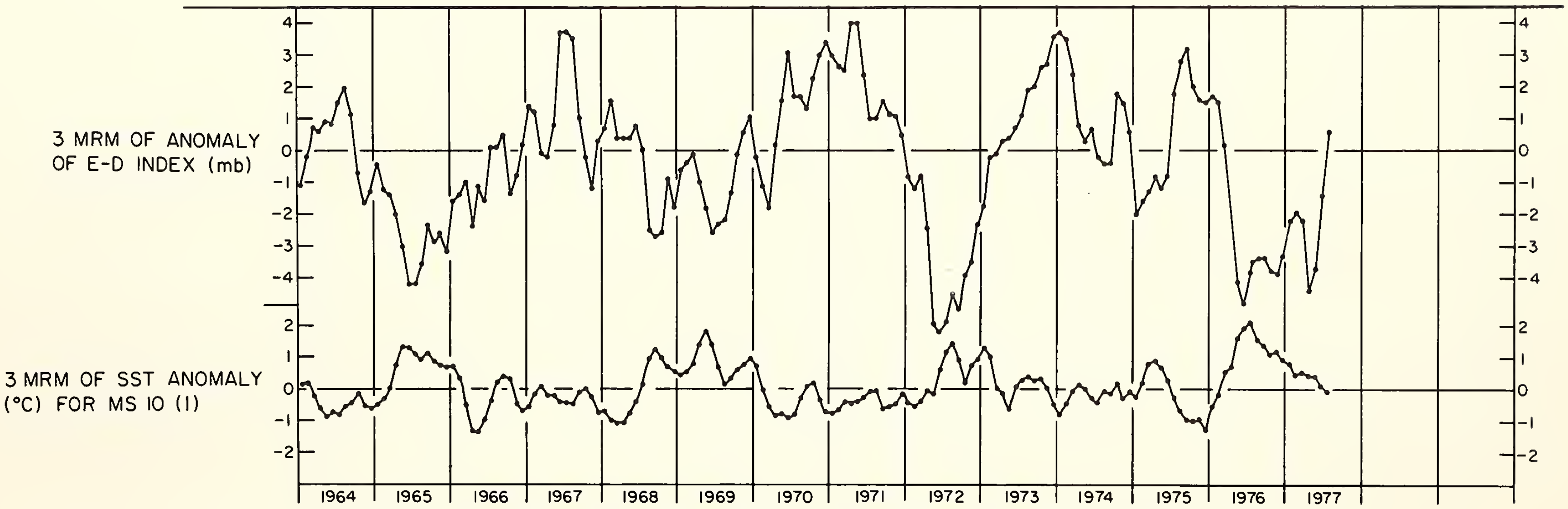

Fig. 6. Three-month running mean plot of anomalies of the difference in sea level atmospheric pressure (mb) between Easter I. and Darwin, Australia compared to a similarly filtered plot of sea surface temperature anomalies (°C) for Marsden square quadrant 10(1) for 1964-76.

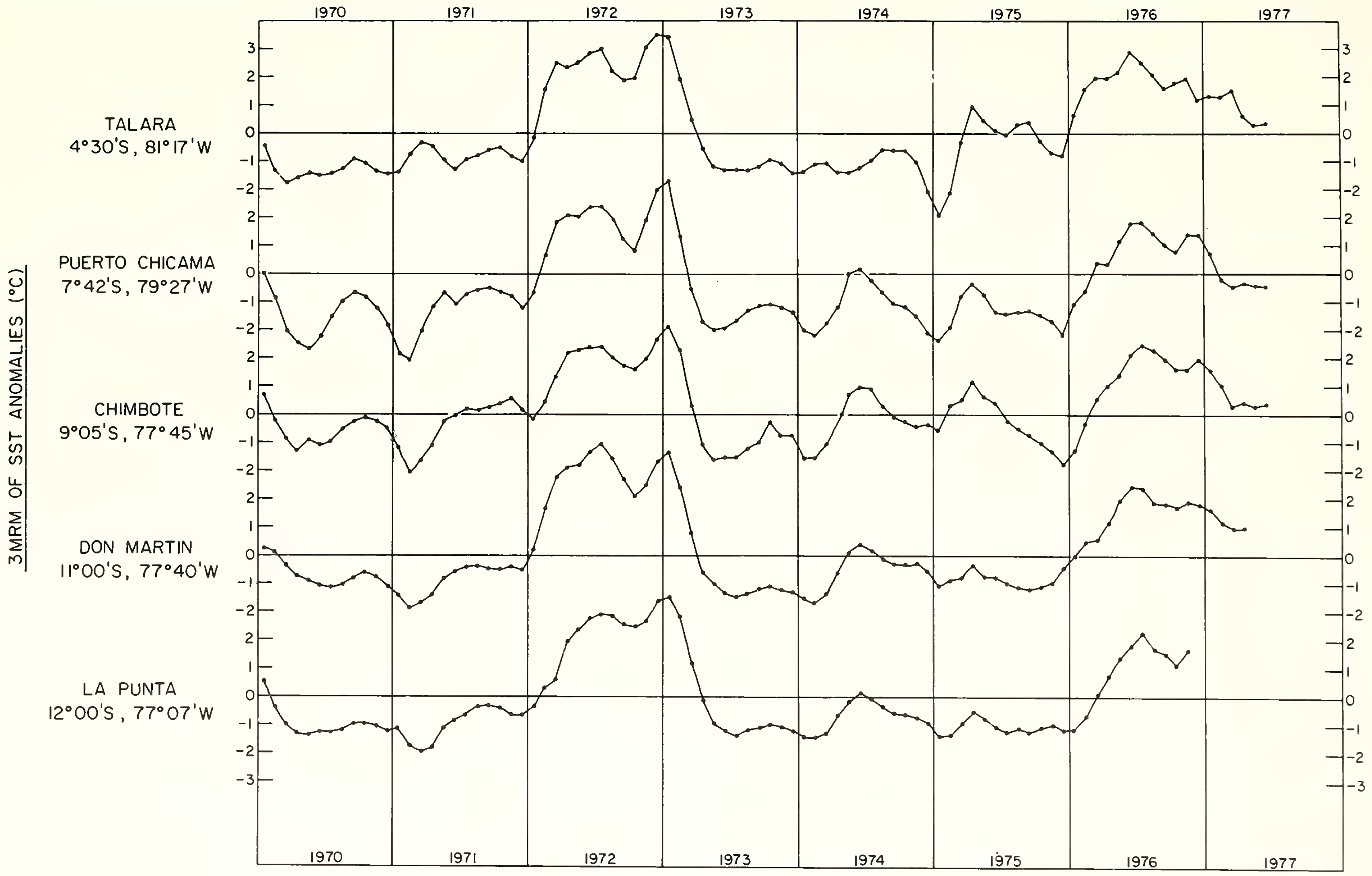

Fig. 7. Three-month running mean plots of sea surface temperature (SST) anomalies for Talara, Puerto Chicama, Chimbote, Don Martin, and La Punta (all are located along the Peruvian coast) for 1970-77.

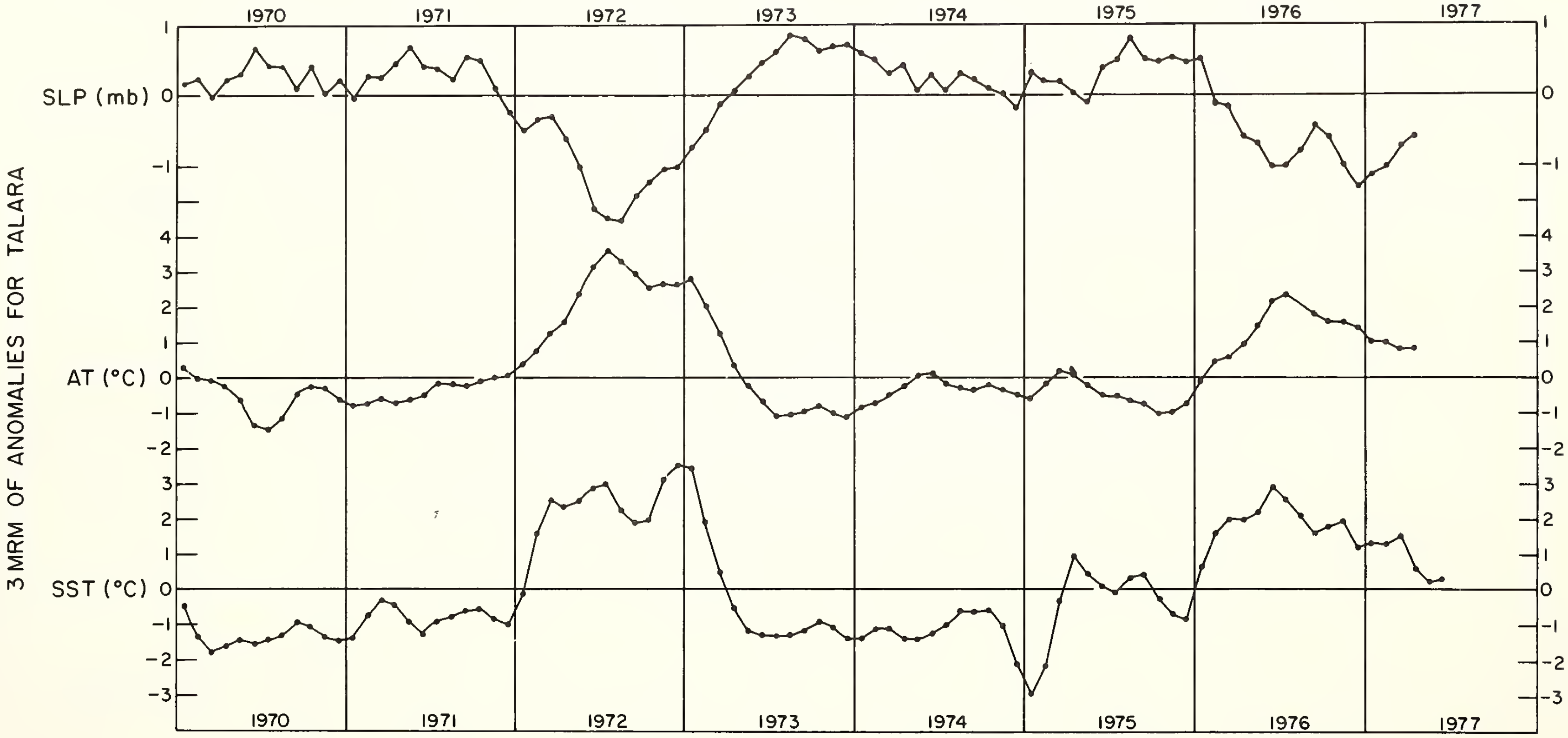

Fig. 8. Three-month running mean plots of sea level atmospheric pressure (SLP) anomalies (mb), air temperature (AT) anomalies (°C), and sea surface temperature (SST) anomalies (°C) for Talara for 1970-77.

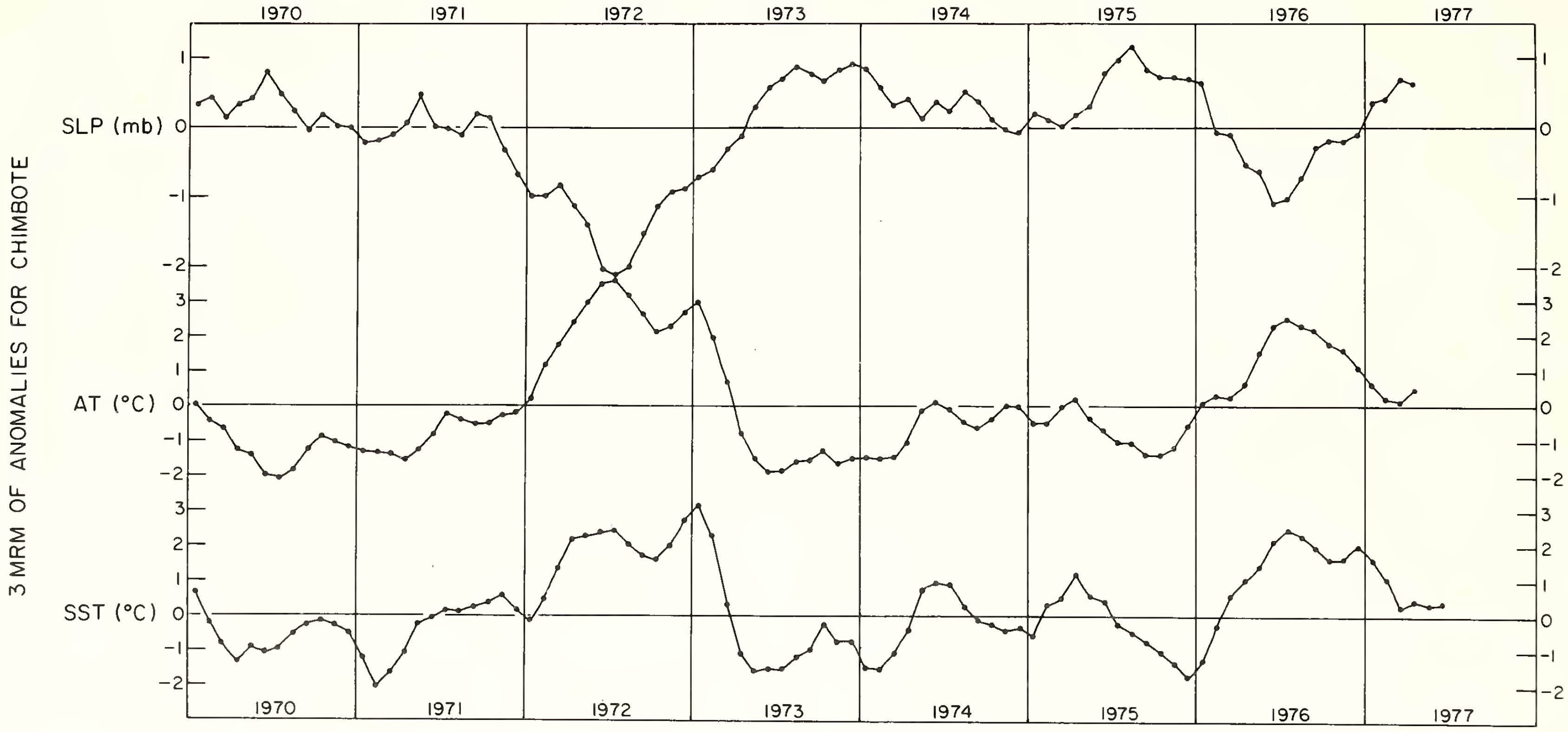

Fig. 9. Three-month running mean plots of sea level atmospheric pressure (SLP) anomalies (mb), air temperature (AT) anomalies (°C), and sea surface temperature (SST) anomalies (°C) for Chimbote for 1970-77.

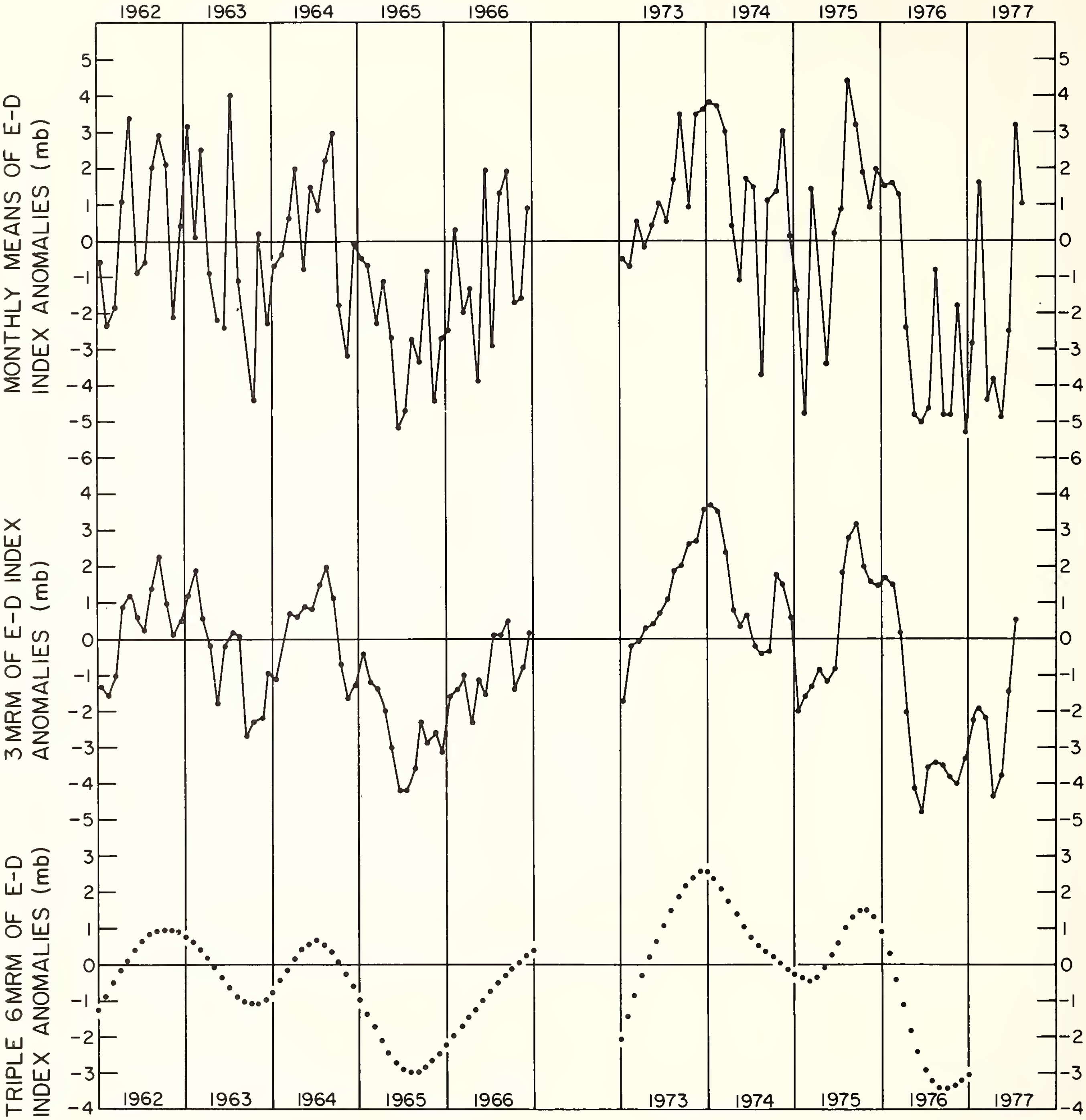

Fig. 10. Monthly mean, 3-month running mean, and triple 6-month running mean plots of anomalies of the difference in sea level atmospheric pressure (mb) between Easter I. and Darwin, Australia for 1962-66 and 1973-77.

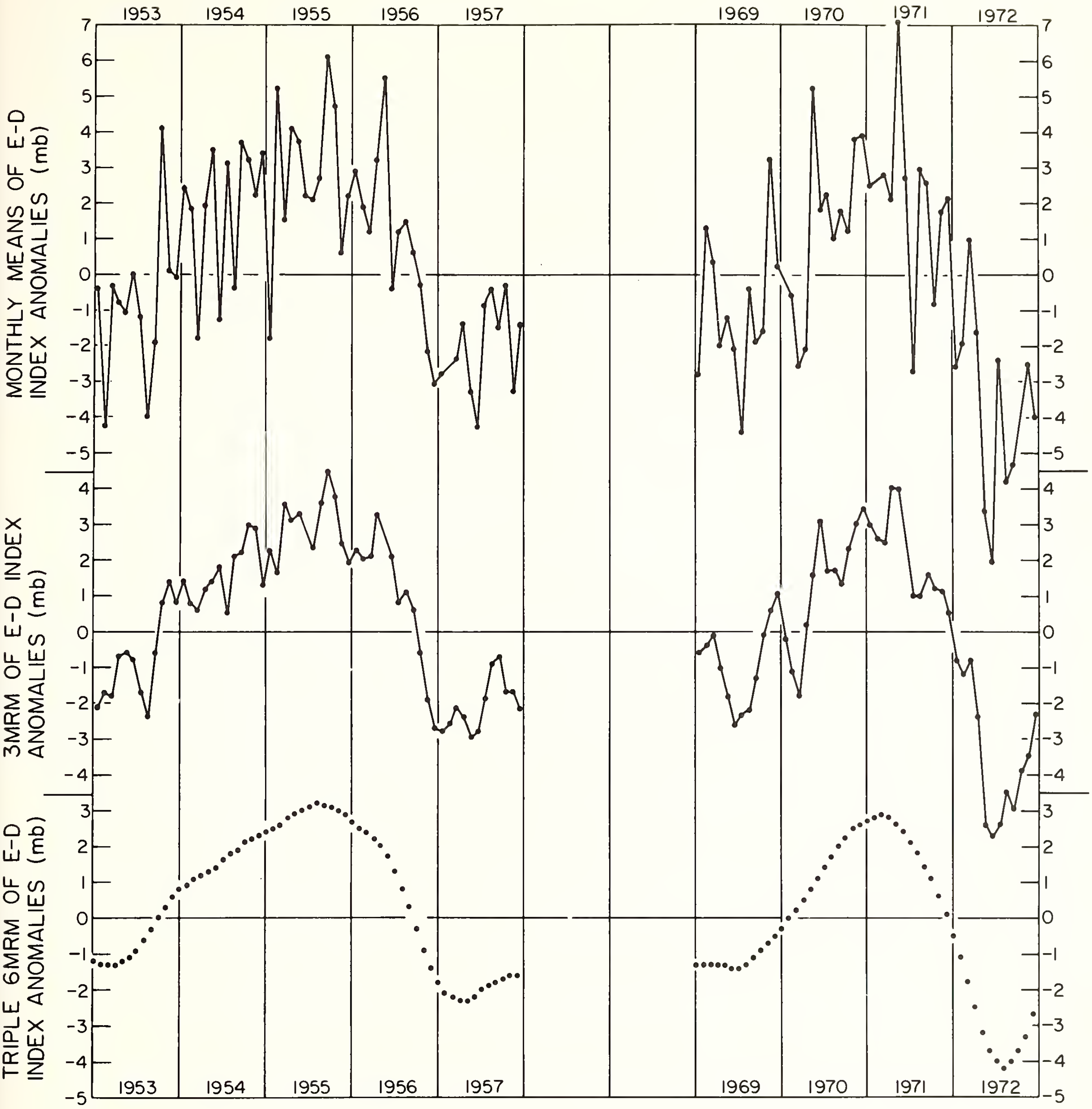

Fig. 11. Monthly mean, 3-month running mean, and triple 6-month running mean plots of anomalies of the difference in sea level atmospheric pressure (mb) between Easter I. and Darwin, Australia for 1953-57 and 1969-72.

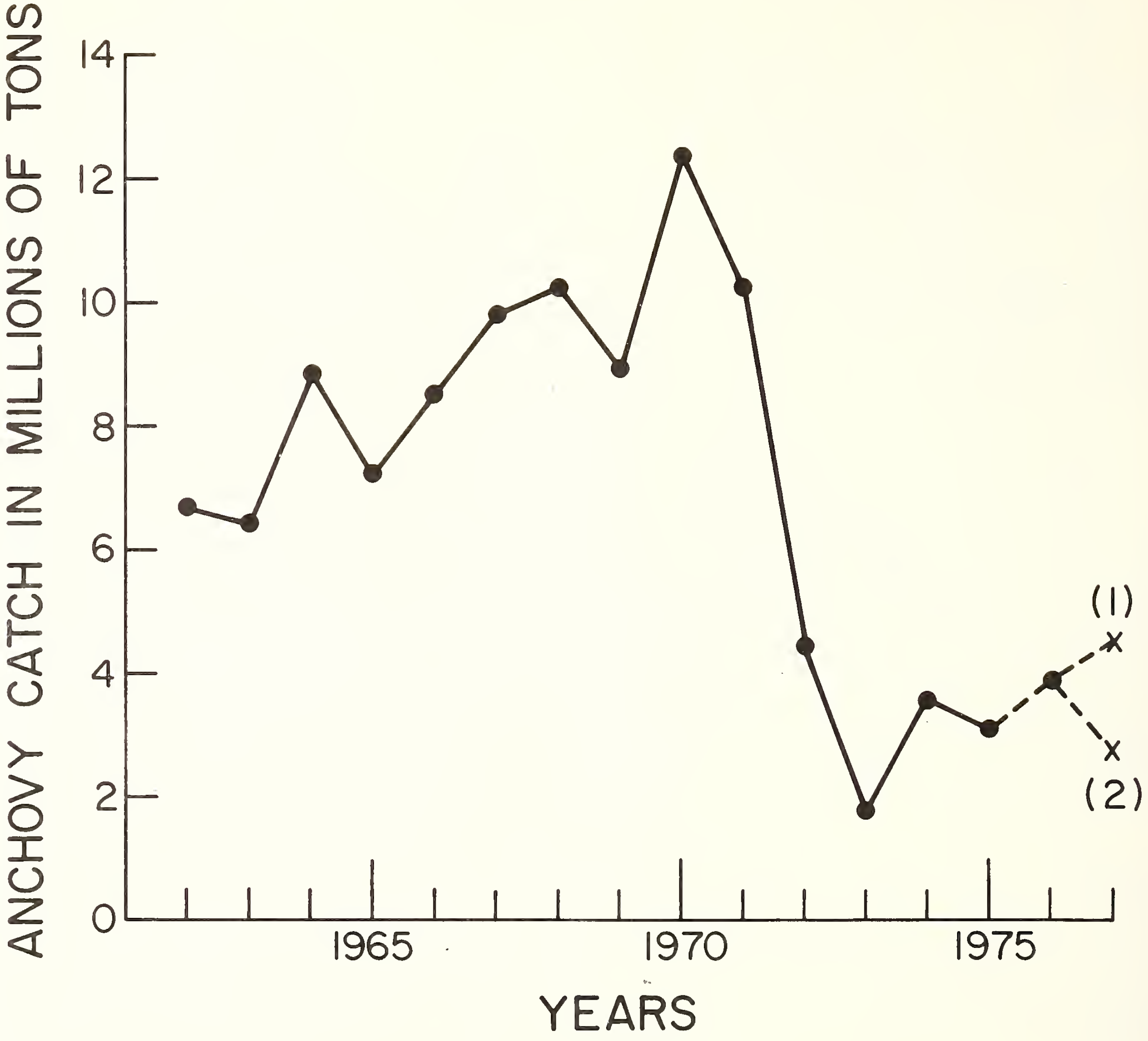

Fig. 12. The Peruvian anchovy catch for the period 1962-76 as obtained from Industrial Fishery Products Market Review and Outlook (NOAA, June 1977). The 1976 figure is a preliminary value. The 1977 forecasts are: (1) by the Peruvian Government, (2) by the U.S. Agricultural Attache in Lima.

RESPONSE OF NORTH ATLANTIC TO ANOMALOUS ATMOSPHERIC FORCES IN SPRING 1977.

by E.B. Kraus, A. Leetmaa, C. Rooth; Cooperative Institute for Marine and Atmospheric Studies, Miami, Florida.

The anticyclonic current system of the subtropics surrounds a thick lens-shaped body of warm water. For example, the east-west temperature cross section along 36°N published by Fuglister (1960) shows how the 15° isotherm slopes down from a depth of less than 200m in the eastern Atlantic to a depth of more than 700m between 48° and 70°W. It rises again steeply to the surface across the Gulf Stream immediately east of Cape Hatteras. The north-south section along the 50°W meridian shows in a similar way a gradual downward slope of the 15° isotherm from a depth of less than 200m in the equatorial region to a maximum depth between 34° and 38°N and a rapid rise back to the surface through the frontal zone of the N. Atlantic current between 38° and 40°N.

The stability of the thermocline effectively isolates the subtropical warm water lens from below. Stability ought to prevent also the influence of air-sea interactions to reach the lower cooler part of the warm water mass directly. These regions can be modified, however, by mixing across the frontal zone and by air-sea interactions in the boundary regions of the gyre where the thermocline becomes shallow or reaches the surface. The effects can then be distributed from there into the interior through mixing within layers of constant potential density.

A substantial portion of the water in the N. Atlantic gyre can be found in a wedge-shaped volume between the 17° and 19° isothermal surfaces. The thick end of the wedge abuts the Gulf Stream front. There, and in the northern Sargasso Sea, it reaches, during late winter, from the surface to a depth of several hundred meters. The wedge tapers out southward into the tropical thermocline.

The so-called 18^{o} water within this wedge appears to be formed primarily by evaporation and sensible heat flux from the surface of the northern Sargasso Sea during winter. It is known from numerous studies and atlases (Budyko, 1963; Bunker and Worthington, 1976) that this is an area of maximum oceanic heat loss to the atmosphere. The resulting penetrating convection not only supplies heat to the air but it also transports heat down to some depths where it becomes available for the generation of kinetic energy.

During recent years, winters have been relatively mild and the production of 18^{o} water appeared to be decreasing. However, the winter of 1976-1977 along the eastern seaboard was notably severe. In April 1977, one of us (A. Leetmaa) conducted a shipboard survey of the northwestern Sargasso Sea to assess the effects of this severe cooling on the ocean. The results have been described (Science, 1977). Newly formed, well-mixed layers of 18^{o} water as deep as 550m were observed. The main thermocline south of the Gulf Stream was also 100 to 150m deeper than in the preceding years. This is shown in Fig. 1, which gives the depths contours of the 15^{o} isothermal surface as observed during the period March 28 to April 15, 1977. The track of the NOAA research vessel "Researcher", which carried out the survey, is marked by straight connected lines. The insert in Fig. 1 gives the composite of the contour lines for the preceding few years.

It can be seen that the main thermocline south of the Gulf Stream was about 100 - 150m deeper during 1977 than in the preceding years. This deepening was probably caused, partly at least, by local surface cooling and penetrating convection during outbreaks of cold air in the preceding exceptionally cold winter. However, this may not have been the only cause; pressure anomalies, as published, for example, in the Monthly Weather Review, show that spring 1977 was characterized by anomalously low pressures in the area of Newfoundland and the Gulf of St. Lawrence. The pressure was anomalously high in the Bermuda region, but again less than normal further south in the Caribbean and subtropic latitudes. Associated with this pressure configuration were anomalously strong southwesterly winds in the latitude of New England and Nova Scotia. The area shown in Fig. 1 was south of this region of maximum westerlies and was therefore affected by an unusually strong anticyclonic wind stress curl. As a result, it was exposed to Ekman layer convergence and this might have contributed, in addition to winter cooling, to the exceptional depth of the thermocline.

About simultaneously with the observational program of the R.V. "Researcher" in the northern part of the gyre, another cruise was carried out in April 1977 by the U. of Miami's R.V. "Gilliss" in the southern branch of the gyre. In the region of the "Gilliss" cruise, along 24°N, conditions are characterized usually by a tongue of salty water which is produced by evaporation in the central region of the gyre. The saline maximum is overlaid by relatively fresh water which spreads northward and westward from the region of the rainfall maximum in the ITCZ. These conditions are illustrated by Fig. 2 which is reproduced here from Worthington's (1976) monograph. Although the Atlantic cruise which is shown in this figure took place in the fall in a direction normal to that of the course of the "Gilliss", the climatic conditions in these two cases are not too different. The chief scientist on the "Gilliss" cruise was also one of the present authors (C. Rooth) and the results obtained then will be presented in a note to Geophysical Research News. Fig. 3 shown here represents a preliminary result.

With anomalously high pressures north of 30°N and low pressures south of 20°N, the region of the "Gilliss" cruise was exposed to an increased cyclonic wind stress curl. A resulting Ekman divergence tends to bring cold water from the thermocline below to the surface. This is well evidenced by Fig. 3. The lower part of the figure shows that the salinity maximum which in Fig. 2 is about 100m below the surface, is brought at several places (Stations 8, 11 and 14) right up to the surface; at these places the surface salinity becomes equal to the salinity maximum. The same locations are characterized also by anomalously low surface temperatures, as indicated by the upper part of the figure. The occurrence of relatively cold water at the surface - which is confirmed also by satellite observation - may have contributed to the very late start of the 1977 hurricane season in the North Atlantic. It might be recalled in this context that a cooling of the sea surface from 25.5^0 to 25.0^0 C represents a decrease of about 1.6^0 C in the equivalent potential temperature which may well affect significantly the kinetic energy generation by rising surface air.

The climatic effect of the thermocline deepening in the northern part of the gyre is more subtle, but in may also be possibly longer-lasting. The large convective cooling of the winter 1977 as well as the surface convergence discussed above, must have produced a decrease in potential vorticity in the thick layer of 18^0 water immediately below. Through the geostrophic relationship, the deficit in potential vorticity and the corresponding increase in anticyclonic vorticity should have been associated with an increased Gulf Stream transport in that region. The effect on the integrated heat transport is less certain. The northward transport of warm water in the surface layers may well have been decreased. Below, in the region of the 18^0 water, it was increased. At still greater depths the deeper location of the thermocline and the resulting increase of potential vorticity there should have been associated, again, with decreased anticyclonic vorticity and decreased transport. The net effect of these various processes cannot be known without further analysis which we hope to carry out in the near future.

Though the mechanical effects are not known in detail, the quoted data do indicate that the anomalous atmospheric conditions of the spring 1977 produced significant and deep-reaching changes in the structure and in the mass transport of the gyre. It takes about 3 or 4 years for the water to move south from the frontal region along the northern boundary of the gyre to the tropics where the thermocline comes again close to the surface. Potential vorticity tends to be conserved during this circuit. It is conceivable, therefore, that the anomalous input of potential vorticity in the northern Sargasso Sea during spring 1977 could have continuing dynamic and thermodynamic effects over several years.

REFERENCES

Budyko, M.I., 1963: Atlas of the heat balance of the world. Mezhd. Geofiz. Komitet Prezidiume Akad. Nauk USSR.

Bunker, A.F. and Worthington, L.V., 1976: Energy exchange charts of the North Atlantic Ocean. Bull. Amer. Met. Soc., 57, No. 6, 670-678.

Fuglister, F.C., 1960: Atlantic ocean atlas of temperature and salinity profiles and data from the International Geophysical year of 1957-1958. The Woods Hole Oceanographic Institution Atlas Series, Vol. 1, Woods Hole, Massachusetts.

Leetmaa, A., 1977: Effects of the winter of 1976-1977 on the northwestern Sargasso Sea. Science, 198, 188-189.

Worthington, L.W., 1976: On the North Atlantic circulation. The Johns Hopkins Oceanographic Studies, No. 6, The Johns Hopkins University Press, Baltimore, 110 pp.

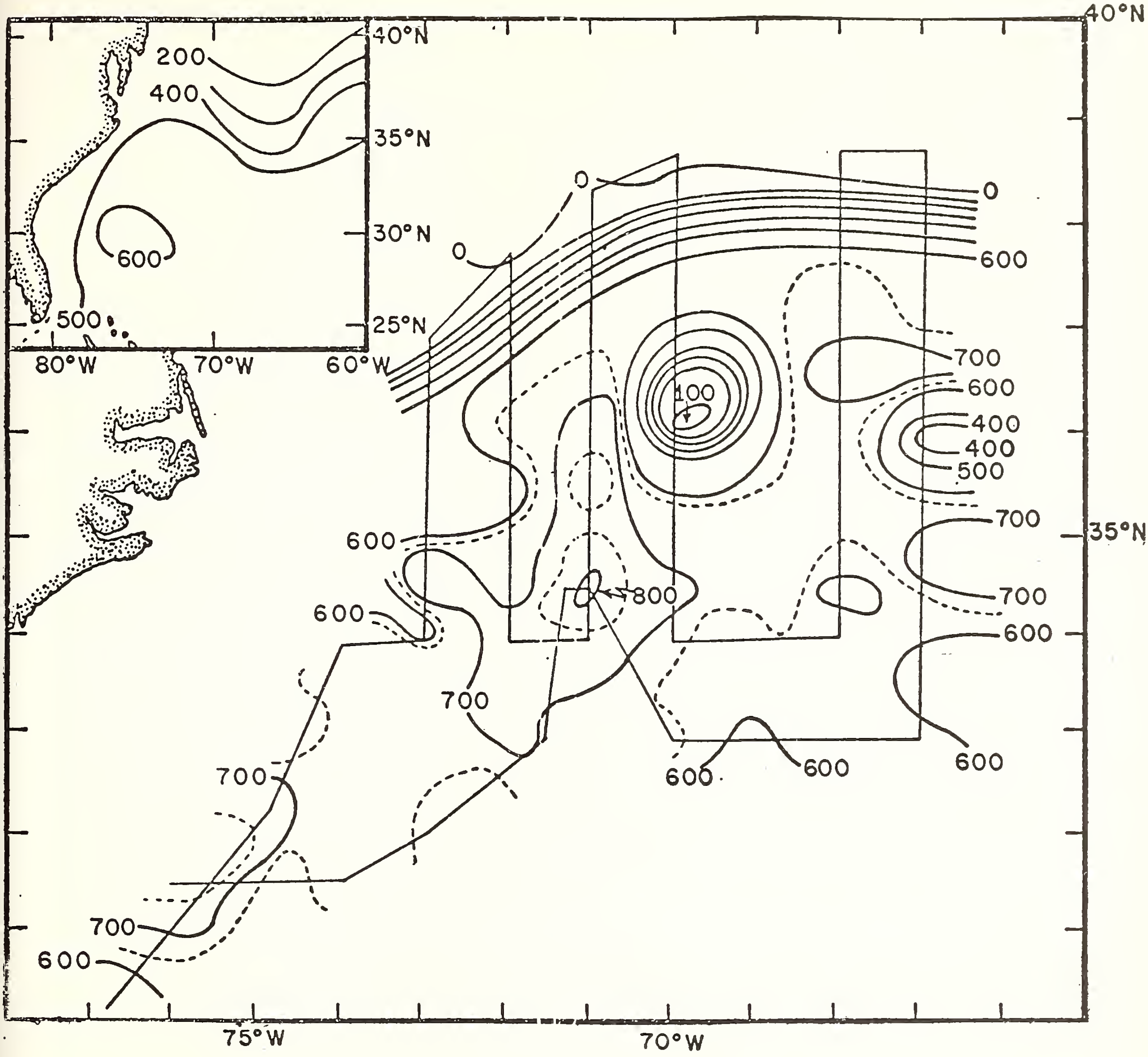

FIGURE 1

Depth in meters of 15^0 isotherm during March/April 1977. (The insert represents composite depth observations during preceding years.) (From A. Leetmaa, 1977.)

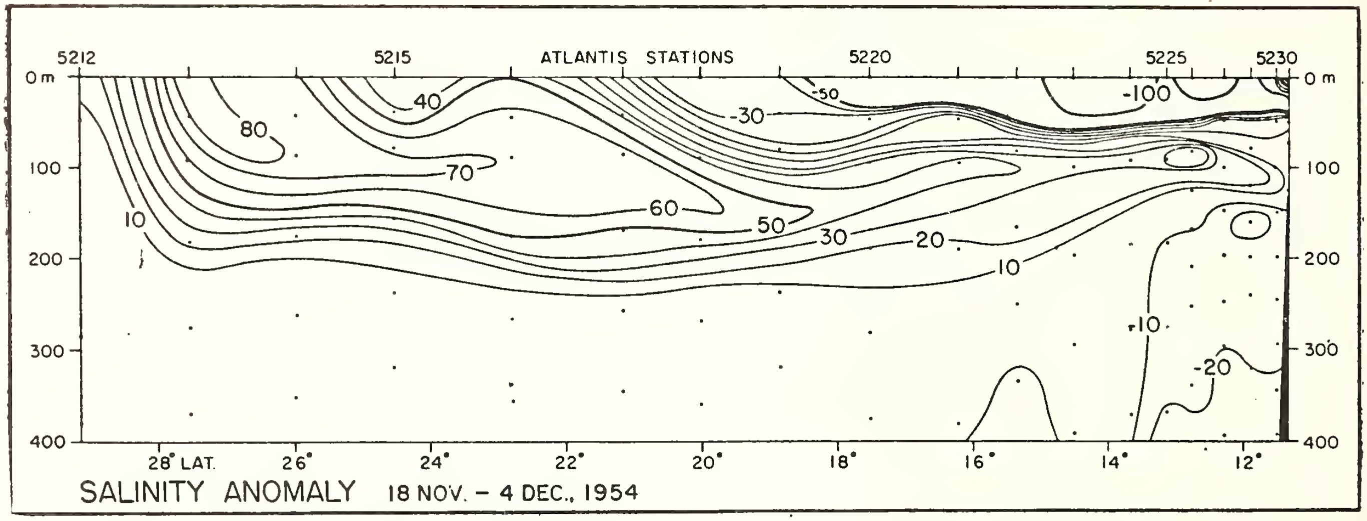

FIGURE 2

Salinity anomaly, parts per 100,000, (top) in November-December 1954 in western N. Atlantic (from Worthington, 1976).

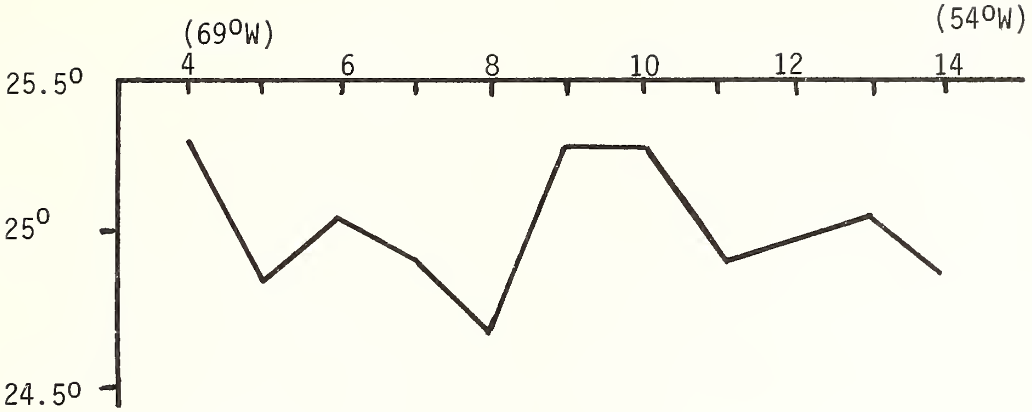

Surface Temperature

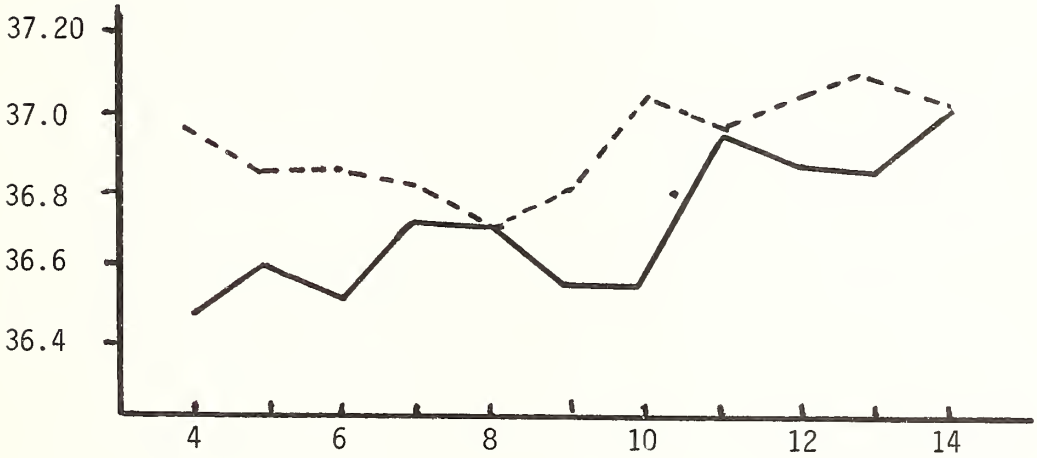

Salinity (in parts per thousand) at surface (———) and at level of salinity maximum (-----).

FIGURE 3

Preliminary data section along 24°N from 69°W to 54°W. (Observed during the R.V. "Gilliss" cruise # 7703 April 1977.)

Fluctuations Of Sea Surface Temperature and Density at Coastal Stations During 1976.

Douglas R. McLain
NMFS Pacific Environmental Group
Monterey, CA

Sea surface temperature (SST) and density measurements have been made routinely at many tide guages and other coastal stations for many years. Although the data suffer from various problems such as gaps in coverage or inadequate exposure to open ocean conditions, careful selection of stations allows the data to be used as an inexpensive monitor ofclimatic fluctuations in nearshore waters. This report summarizes monthly mean SST and density fluctuations for both 1976 and a long term mean for three coasts of North America. The data are contoured in a common manner for each coast to flag unusual climatic events and to allow comparison of fluctuations between coasts.

This report is a refinement for 1976 of similar data presented by J. Goulet Jr. in the 1975 Status of Environment Report. Goulet's plots were for the years 1974 and 1975 only as longterm historical data were not available in a computer compatable format. During 1976 J. Goulet Jr. and E. Haynes of the NMFS Central Office developed a computer tape of all available historical monthly mean temperature, density and sea level data compiled from National Ocean Survey (NOS) tide guage stations. The NOS Tides Branch provided update punch cards of monthly mean data which along with certain Canadian data were merged with the historical tape for preparation of this report. Data for the Canadian stations were provided by Dr. L. Giovando (pers. comm.). The computer tape is now maintained by the National Oceanographic Data Center and is available to interested users from NODC.

Presented in this report are plots of long term means for the period 1948 to 1975 and anomalies from the mean for 1976 of SST and density at selected stations along the following coasts of North America:

a) West Coast - Imperial Beach, CA to Adak, AK.
b) East Coast - Key West, FL to Eastport, ME.
c) Gulf Coast - Key West, FL to Padre Island, TX.

The 1948-75 reference period used in this report is a different period than the 1948-67 period used for other Status of Environment Report data sets such as maps of SST anomaly (McLain, 1977). This change was necessary to develop means for certain stations which were established only in the last decade.

The stations used in this report are shown in Figure 1. The stations chosen where those which had the best combination of desirable characteristics: availability of data, exposure to open ocean conditions, long data record, and uniform spacing with distance along a coast. The ideal combination seldom existed and consequently many of the stations used were in estuaries, had gaps in coverage or are at uneven distance intervals along the coast. For example, data coverage is poor in Oregon and Washington as all stations are subject to river runoff (as at Neah Bay near the mouth of the Strait of Juan de Fuca). Good coverage was available from British Columbia light houses which have long complete data records available from open, exposed locations.

The data are plotted as contoured isograms of longterm mean and anomaly by month and station position along the coast. The plots were made on an electrostatic plotter at Fleet Numerical Weather Central in Monterey, CA. Temperature data are presented in degrees Celcius and density data are in sigma t units.

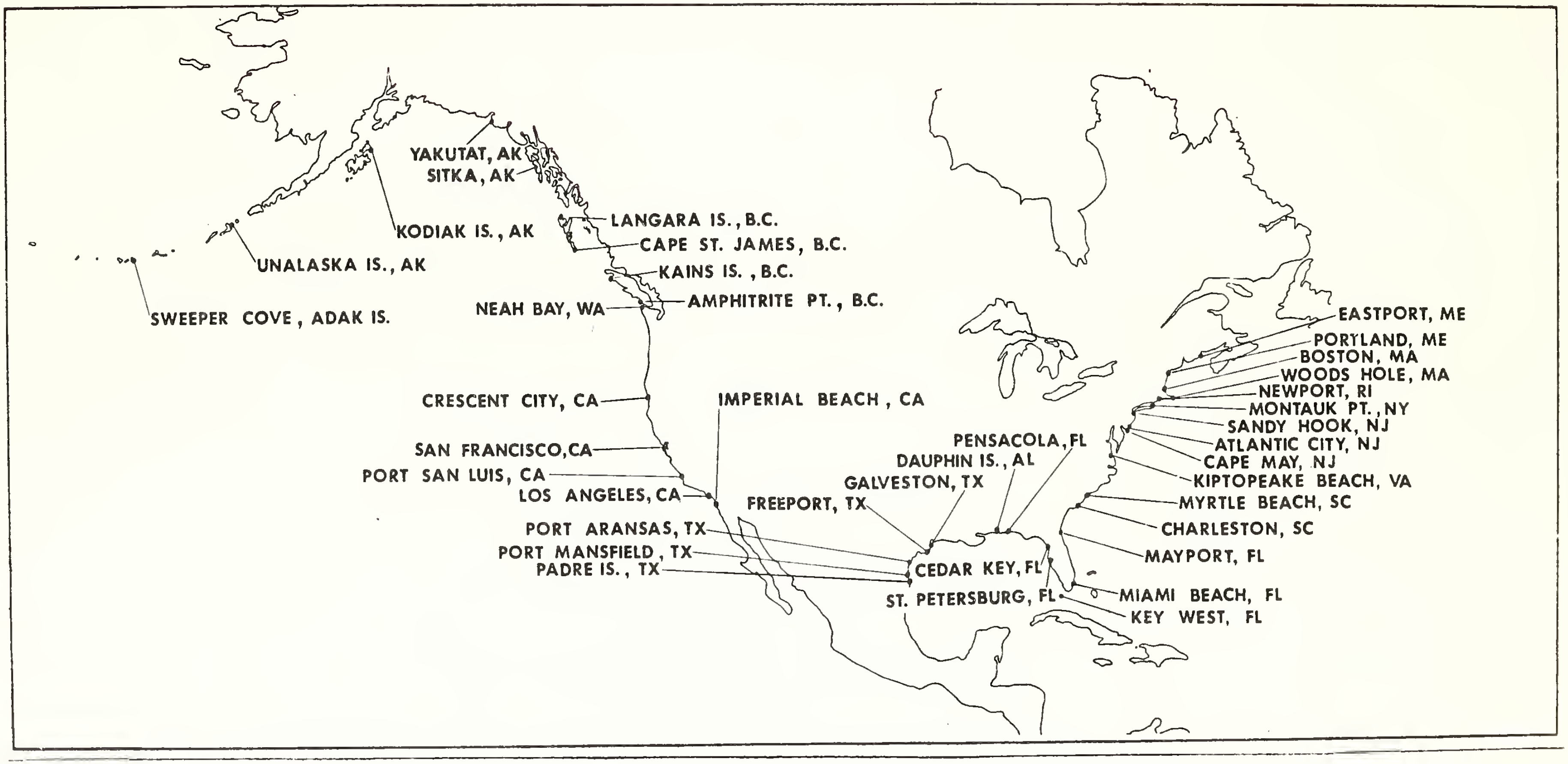

Figure 1. Location of Coastal Stations.

WEST COAST SST

The longterm monthly mean SST at stations along the West Coast of North America (Figure 2) have minimum values in January and February and maximum values in July or August. Minimum winter temperature occurred at Kodiak, AK, while maximum summer temperature occurred at Los Angeles, CA. The winter minima occur earlier (in January) at the southern stations (California to southern British Columbia) than at the northern stations where minimum values occurr in February. Summer maxima occur in August at all stations along the coast except at Neah Bay, WA where the maximum occurs in July.

Bakun, McLain, and Mayo (1974) described the long term mean distribution of SST from ships in 1° squares of longitude and latitude adjacent to the west coast of the United States. Their data show that offshore SST minima and maxima occur about one month later than at the coastal stations. This may result from more rapid warming in spring and cooling in fall in shallower coastal waters. The summer maximum temperatures offshore reported by Bakun et al. (1974) are similar to those at the coastal stations but winter minimum temperatures are about 1°C lower at the coastal stations. This depression of coastal temperatures may result from shallowness and lower heat capacity of the water column at the coastal stations as compared to offshore areas.

Both Figure 2 and the figure of Bakun et al. (1974) show a horizontal trend to the isotherms between Port San Luis and Los Angeles, LA. This "flattening" of the isotherms is an indication of change of ocean water masses at Point Conception between the cold California Current water to the north and the warmer water of the Southern California Bight to the south.

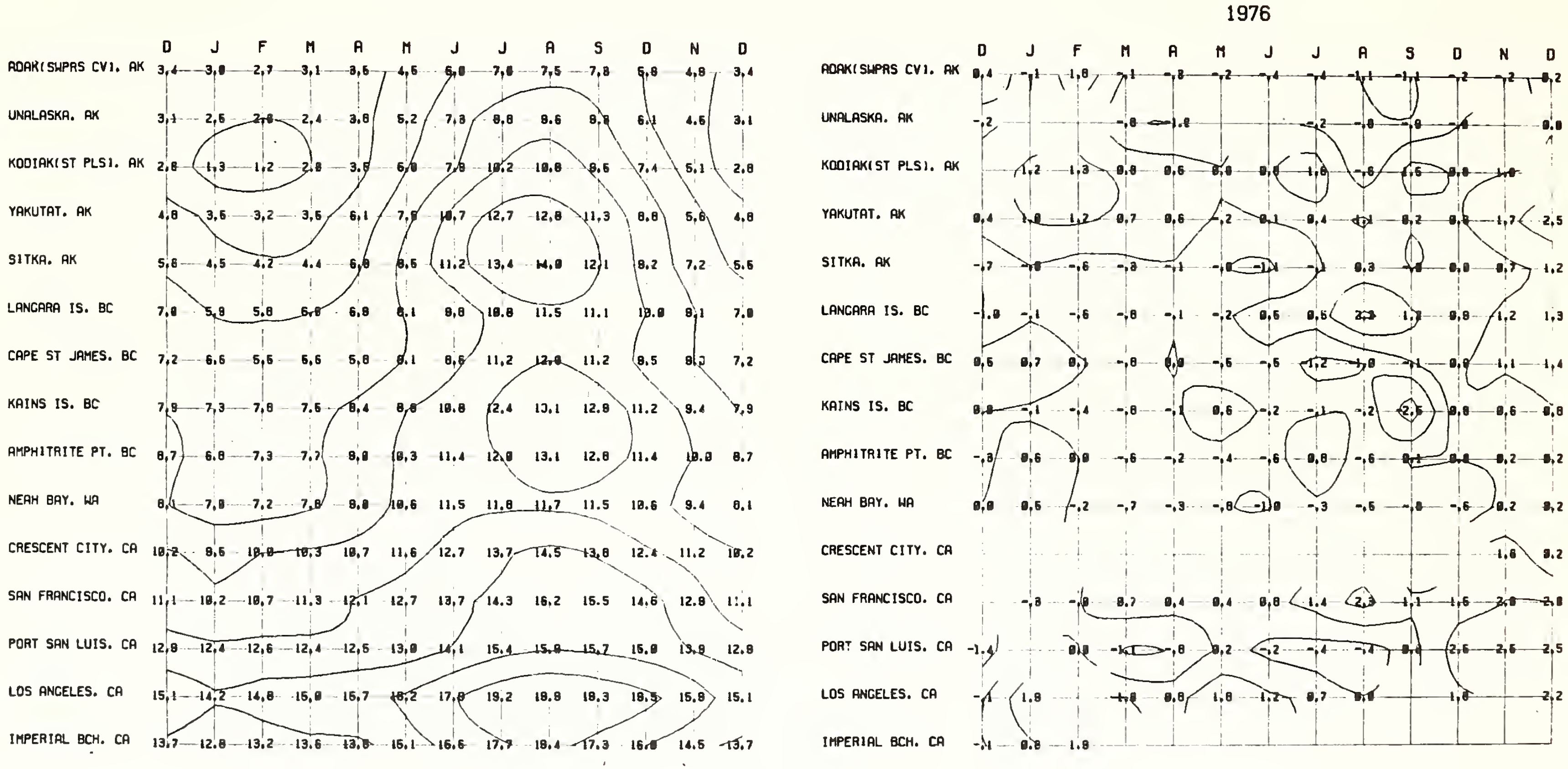

Figure 2. Longterm mean for 1948-75 (left) and anomalies for 1976 from mean (right) of sea surface temperature in degrees Celsius along West Coast. Contour intervals 2.0°C for mean and 1.0°C for anomalies.

During 1976 the anomalies of SST at coastal stations were rather noisy and the only major trend was the presence of cooler than average water along the coast during spring and summer from Sitka, AK south to California. During summer, first in southeastern Alaska and later farther south, the anomalously cool water was replaced by warmer than normal water which reached maximum anomalies of +2.5°C at Yakutat, AK and Southern California in November and December.

The SST charts presented monthly in Fishing Information show general negative anomalies of SST along the coast during 1976 until July when positive anomalies first impinging against the Oregon and southern California coasts. Positive anomalies spread during summer and fall and occurred along the entire coast in November and December, in agreement with the coastal station data.

WEST COAST DENSITY

The long term mean distribution of density along the west coast of North America (Figure 3) shows that minimum densities occur off much of the West Coast in February probably in response to winter rains.. In Alaska, however, minimum densities occur in June or July due to snow and glacial melt.

During 1976 observations of density were spotty but showed positive anomalies over most of the coast most of the year. Large positive anomalies of density off San Francisco and Crescent City, CA were associated with drought conditions existing over California most of the year. The low densities at Kodiak in August and September were apparently in response to local precipitation.

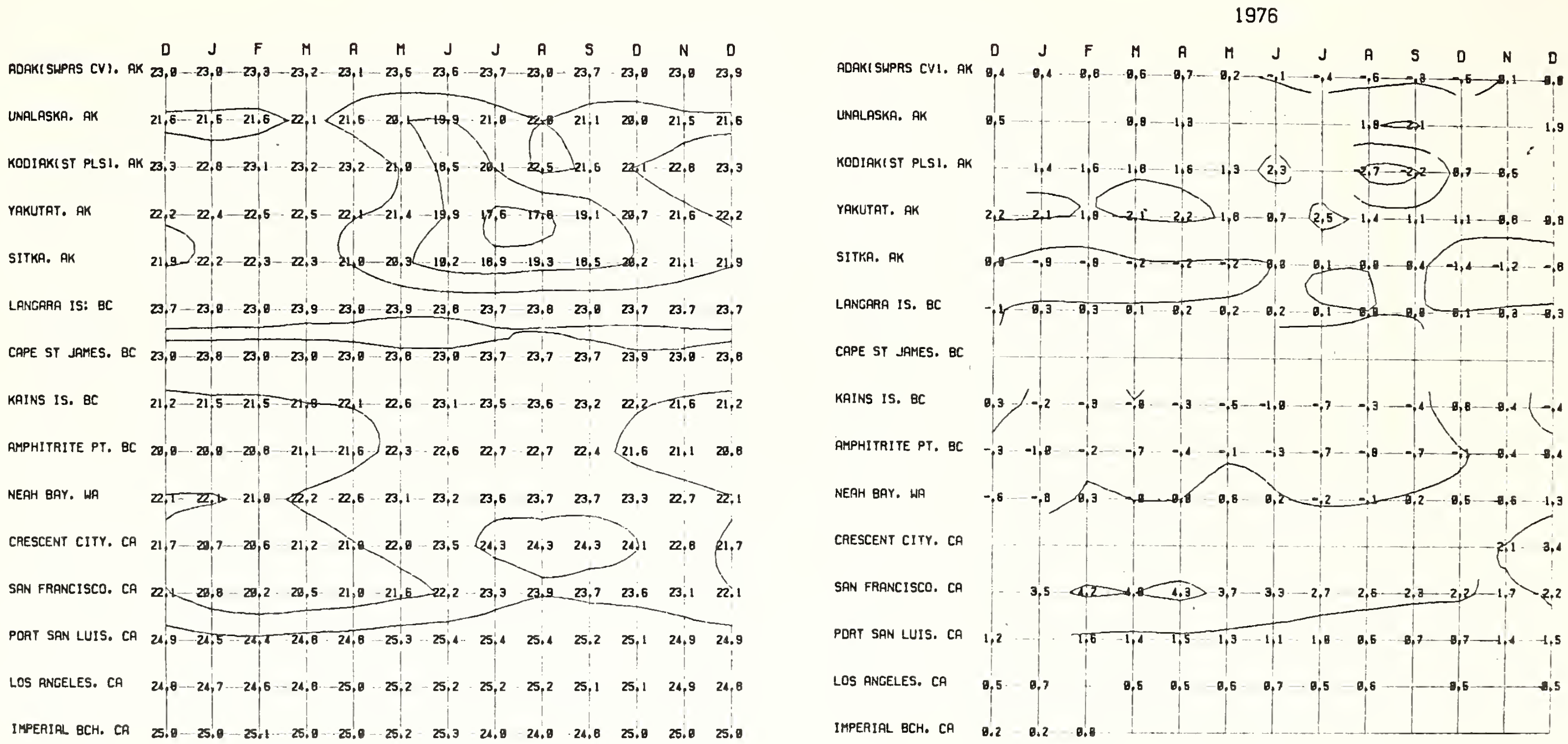

Figure 3. Longterm mean for 1948-75 (left) and anomalies for 1976 from mean (right) of density in sigma t units along West Coast. Contour intervals 2 units for mean and anomalies.

EAST COAST SST

The longterm mean SST at stations along the East coast (Figure 4) show minimum temperatures at all stations in January to March and maximum temperatures in July to September. As was seen on the West Coast, the peaks are earlier (January and July-August) at the southern stations and later (February-March and August-September) at the northern stations. Minimum winter temperatures of 0.6°C occurred in February at Portland, ME. and maximum summer temperatures of 30.7°C occurred at Key West, FL. in August.

Two regions of rapid change of SST with distance along the coast can be seen in Figure 4. These regions are between Kiptopeake Beach, VA and Myrtle Beach, FL and between Mayport, FL and Miami Beach, FL. As the case at Point Conception on the West Coast, these regions are associated with changes in ocean circulation and occur at Cape Hatteras and Cape Canveral respectively. Unlike Point Conception, however, where the greatest SST change between adjacent stations occurred in summer (4.0°C change in August), the greatest changes is SST between stations on the East Coast in winter or spring (8.2°C change in January at Cape Canveral and 5.7°C in April at Cape Hatteras).

During 1976 sampling at the stations was incomplete and many values were missing. In January anomalies of SST were negative along the entire coast as were air temperatures over most of the Eastern U.S. (Wagner, 1977). Anomalous warming occurred in February and by March SST's were above normal along the coast (up to 2.6°C above normal at Charleston, SC). This warming was also mentioned by Taubensee (1976a). During the summer months anomalies were positive at Montauk Pt., NY

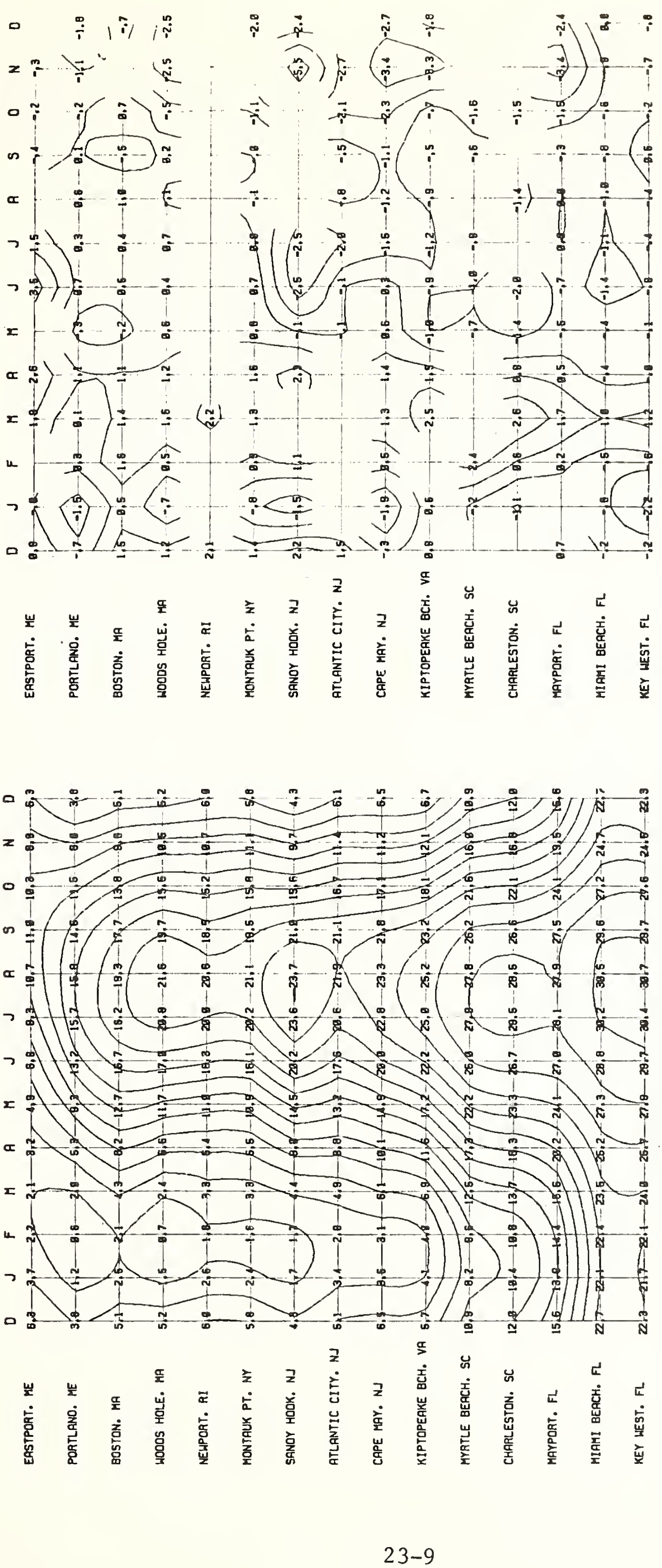

Figure 4. Longterm mean for 1948-75 (left) and anomalies for 1976 from mean (right) of sea surface temperature in degrees Celsius along East Coast. Contour intervals 2.0°C for mean and 1.0°C for anomalies.

and to the north but were negative to the south. SST's were generally below normal during the fall and became extremely cold in November as the unusually cold winter of 1976-77 began. An extreme negative anomaly of $-5.5^{\circ}C$ was observed at Sandy Hook, NJ in November.

Chamberlain and Armstrong (1977) summarized air temperature data along the East Coast to show the development of the winter of 1976-77 when strong northerly winds occurred over much of the eastern United States. Their data, from National Weather Service weather stations for the period July 1976 to January 1977, indicated that anomalies of air temperatures in the fall of 1976 were most negative during November over most of the coast. This is in agreement with the SST data. In neither the air temperature nor the SST data did large negative anomalies occur as far south at Miami or Key West, FL. Dickson (1977c) also shows that southern Florida air temperatures were not unusually cold in November. The strong negative anomalies of SST in November were caused by a combination of effects of strong winds of cold, dry air from the north and northwest. Such effects included heat loss by the water, strengthened southerly flowing coastal currents, and possibly upwelling. Evidently such effects were not effective at Miami and Key West where SST's are more associated with Gulf Stream advection processes.

EAST COAST DENSITY

The long term mean density data on the East Coast (Figure 5) show that many of the stations are affected by river runoff. The effects of runoff are particularly evident at Boston, MA, Sandy Hook, NJ,

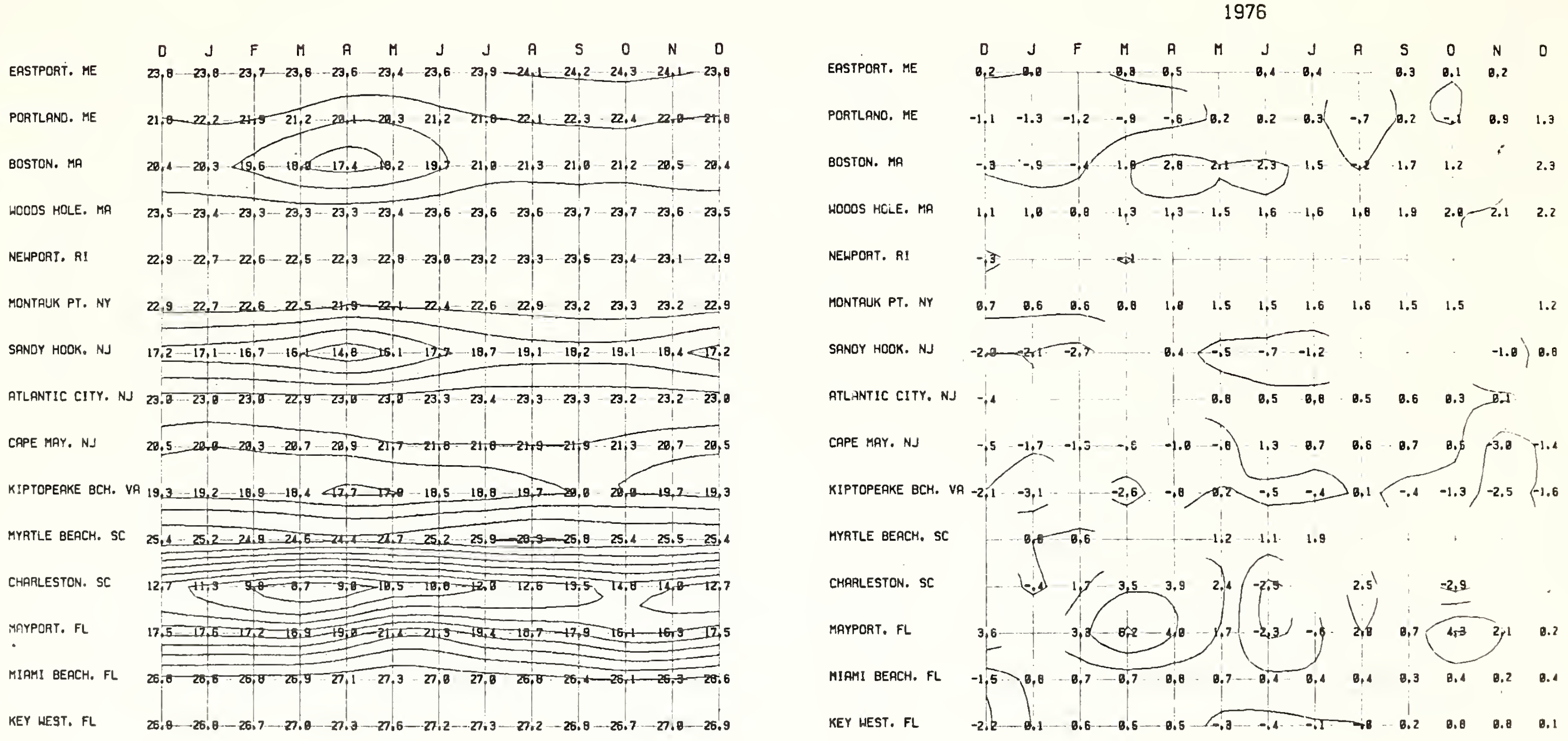

Figure 5. Longterm mean for 1948-75 (left) and anomalies for 1976 from mean (right) of density in sigma t units along East Coast. Contour intervals 2 units for mean and anomalies.

Kiptopeake Beach, VA, and Charleston, SC where closed contours enclose regions of minimum water density. Minimum density water occurs at the northern stations in March to May while at the southern stations it occurs in January to April. This delay in occurrence of minimum density at the northern stations results from retarded snowmelt and river run-off in spring in the North relative to winter precipitation in the south. The timing of maximum water density similarly is delayed to the north as maximum density generally occurs in May to September at the southern stations and during September or October at the northern stations.

During 1976 density observations were frequently missing and what observations that are available do not have large coherence from station to station or month to month. A region of coherent positive anomalies occurred from Montaut Pt., NY and north over most of the year, with the obvious exception of Boston, MA and Portland, ME during January to March. Anomalous density at Woods Hole, MA and Montauk Pt., NY increased rather steadily during the year.

Large and variable anomalies occurred at Charleston, SC and Mayport, FL and resulted from fluctuations of river runoff near these stations. For example, the positive anomalies of density at these stations in February to May were associated with drought during February and March (Dickson, 1976b and Taubensee, 1976a). Similarly the negative density anomaly at these stations in June was associated with higher than normal precipitation in the area (Dickson, 1976b and Taubensee, 1976b).

GULF COAST SST

The longterm mean of SST at all stations along the northern coast of the Gulf of Mexico (Figure 6) show minimum values in January and

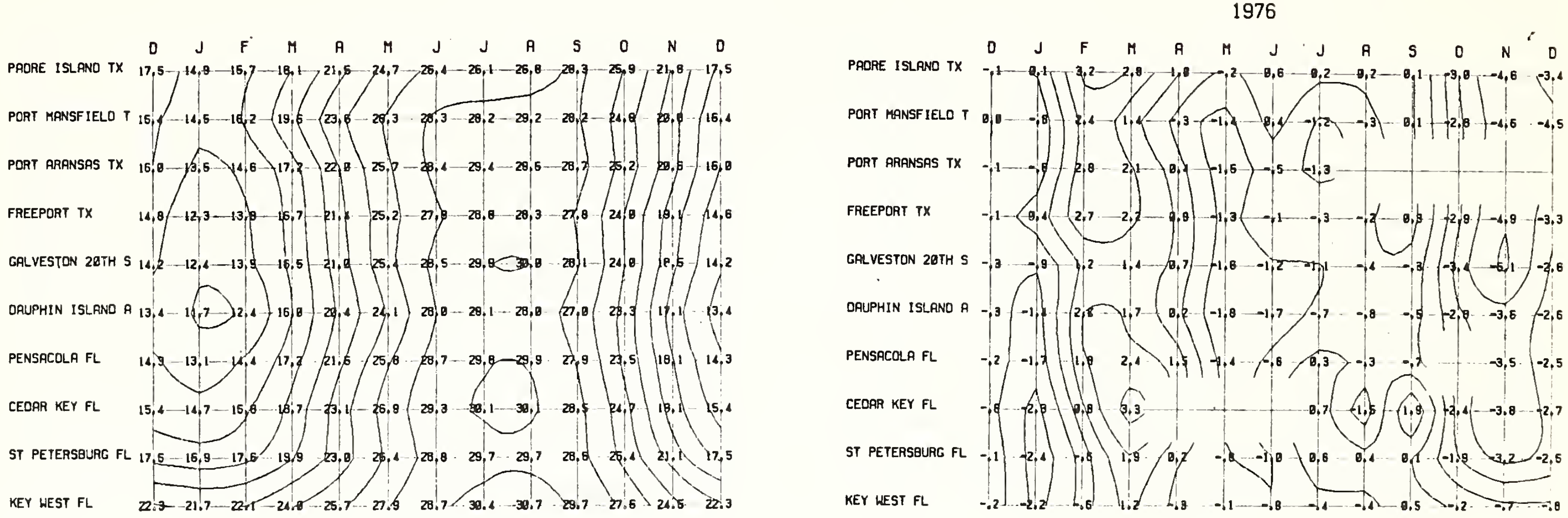

Figure 6. Longterm mean for 1948-75 (left) and anomalies for 1976 from mean (right) of sea surface temperature in degrees Celsius along the Gulf Coast. Contour intervals 2.0°C for mean and 1.0° for anomalies.

maximum values in July or August. Minimum winter temperatures occurred at the most northern and estuarine station Dauphin Island, AL, and maximum summer temperatures occurred at the most southern and open ocean station, Key West, FL.

During 1976 observations of SST at Gulf Coast stations were fairly complete and showed good coherence in space and time. A similar pattern of anomalies of SST occurred as that observed at East Coast stations from New Jersey to Florida. SST was anomalously cold at all Gulf Coast stations during December 1975 and January 1976 with greatest anomalies in Florida. Anomalous warming began in February in Texas and SST anomalies peaked in March at Cedar Key, FL. Anomalous cooling then occurred over most of the area for the remainder of the year, peaking in the large negative anomalies of November over most of the coast. The negative anomalies in November were less than 1°C in magnitude only at Key West, FL. The greatest negative anomaly (-5.1°C) was at Galveston, TX. Chamberlain and Armstrong (1977) included Gulf of Mexico data in their summary of air temperatures during late 1976 and also found greatest negative anomalies at Galveston, TX during November.

GULF COAST DENSITY

Long term mean water density (Figure 7) ranged from almost fresh water in January at Dauphin Island in Mobile Bay, AL to open ocean conditions at Key West, FL. The months of minimum and maximum densities were variable and reflected variations in timing of local river runoffs. Minimum densities occurr in January to June and maximum densities in June to November.

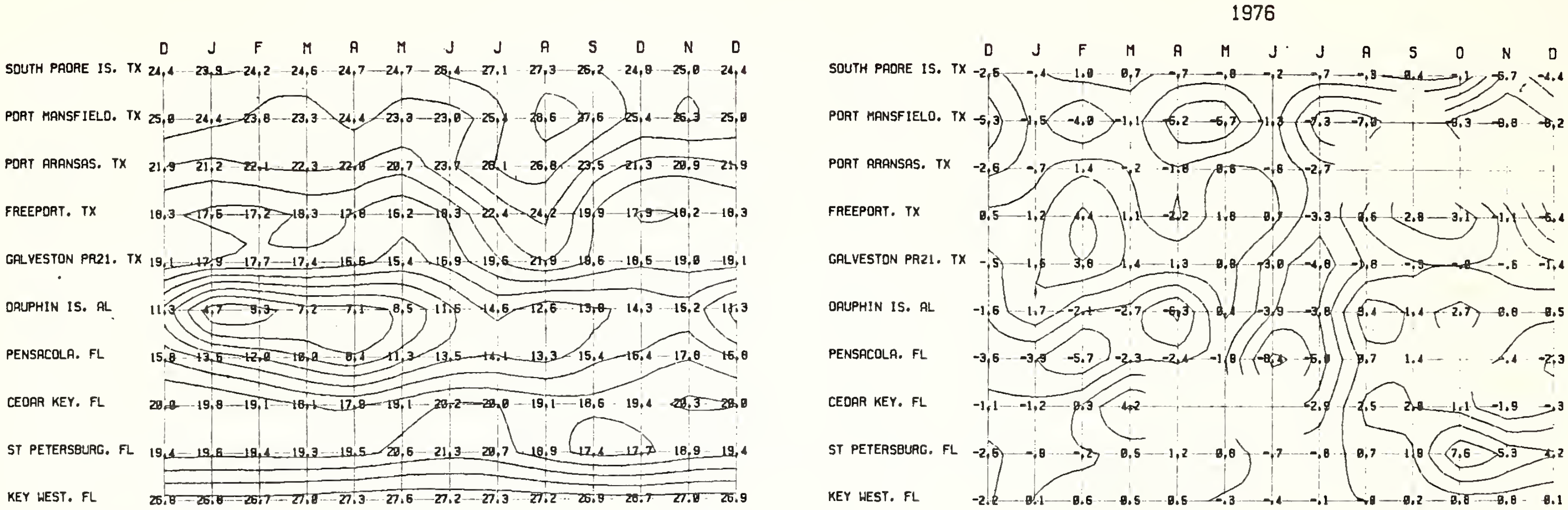

Figure 7. Longterm mean for 1948-75 (left) and anomalies fcr 1976 from mean (right) of density in sigma t units along Gulf Coast. Contour intervals 2 units for mean and anomalies.

Anomalies of density in 1976 were variable and were apparently related to local fluctuations of precipitation and runoff. Negative anomalies of density were observed almost all year at south Texas stations. Positive anomalies occurred during August to October from Dauphins Is., AL to Key West, FL and into December at South Florida stations.

SUMMARY

Although the coastal station data are noisy and have frequent gaps in coverage, the data show large scale coherences between stations. These coherences are in general caused by climatic fluctuations that affect long stretches of coastline. An extreme example of such a climatic change are the strong northerly winds over much of the Eastern United States during November 1976. These winds created negative anomalies of SST at coastal stations of at least -1.0°C in magnitude from Portland, ME to Mayport, FL and from St. Petersburg, FL to Padre Island, TX. Extreme anomalies of -5.5°C were observed at Sandy Hook, NJ and -5.1°C at Galveston, TX in November.

LITERATURE CITED

Bakun, A., D.R. McLain, and F.V. Mayo. 1974. The Annual Mean Cycle of Coastal Upwelling off Western North America as Observed from Surface Measurements. Fish Bulletin. 72(3), pp. 843-844.

Chamberlain, J.L., and R.S. Armstrong. 1977. Data on Cold Weather Conditions Along the Atlantic and Gulf Coasts During the Fall and Winter of 1976-77. Unpublished ms. NMFS Atlantic Environmental Group, Narragansett, RI.

Dickson, R.R. 1976a. Weather and Circulation of February 1976. Monthly Weather Review. 104(5), 660-665.

Dickson, R.R. 1976b. Weather and Circulation of May 1976. Monthly Weather Review. 104(8), 1084-1089.

Dickson, R.R. 1977c. Weather and Circulation of November 1976. Monthly Weather Review. 105(2), 239-244.

McLain, D.R. 1977. Sea Surface Temperature Anomalies. In: Status of Environment Report - 1976. J. Goulet and E. Haynes, Eds. National Marine Fisheries Service, Washington, D.C.

Taubensee, R.E. 1976a. Weather and Circulation of March 1976. Monthly Weather Review. 104(6), 809-814.

Taubensee, R.E. 1976b. Weather and Circulation of June 1976. Monthly Weather Review. 104(9), 1200-1205.

Wagner, A.J. 1977. Weather and Circulation of January 1976. Monthly Weather Review. 104(4), 491-498.

Presentation for NOAA Climate Diagnostics
Workshop, Oct. 18-20, 1977, LaJolla, California

Present Status of Climate Data in Oceanography

Sydney Levitus NOAA/ERL/GFDL

All available historical temperature, salinity, density, and oxygen data from the National Oceanographic Data Center have been used to construct global analyses of these parameters. The analyses are computed on a one-degree latitude-longitude grid from the ocean surface to a depth of 5000 meters at NODC standard levels. Depending on the amount of available data for each parameter the analyses have been performed for annual, seasonal, and monthly periods. The data are not synoptic and the analyses must be interpreted accordingly as a delineation of permanent and semi-permanent features in the fields. A description of the data and objective analysis scheme used is given by Levitus and Oort (1977).

The analyses are being used for computation of quantities of climatic importance such as oceanic heat storage (Oort and Vonder Haar, 1976; Ellis, Vonder Haar, Levitus and Oort, 1977).

References

Ellis, J. S., T. H. Vonder Haar, S. Levitus, and A. H. Oort, "The Annual Variation in the Global Heat Balance of the Earth"; J. Geophys. Res., in press.

Levitus, S. and A. Oort, "Global Analysis of Oceanographic Data"; Bulletin of the American Meteorological Society, in press.

Oort, A. and T. H. Vonder Haar, "On the Observed Annual Cycle in the Ocean-Atmosphere Heat Balance Over the Northern Hemisphere; J. Phys. Oceanogr., 6, 781-800, 1976.

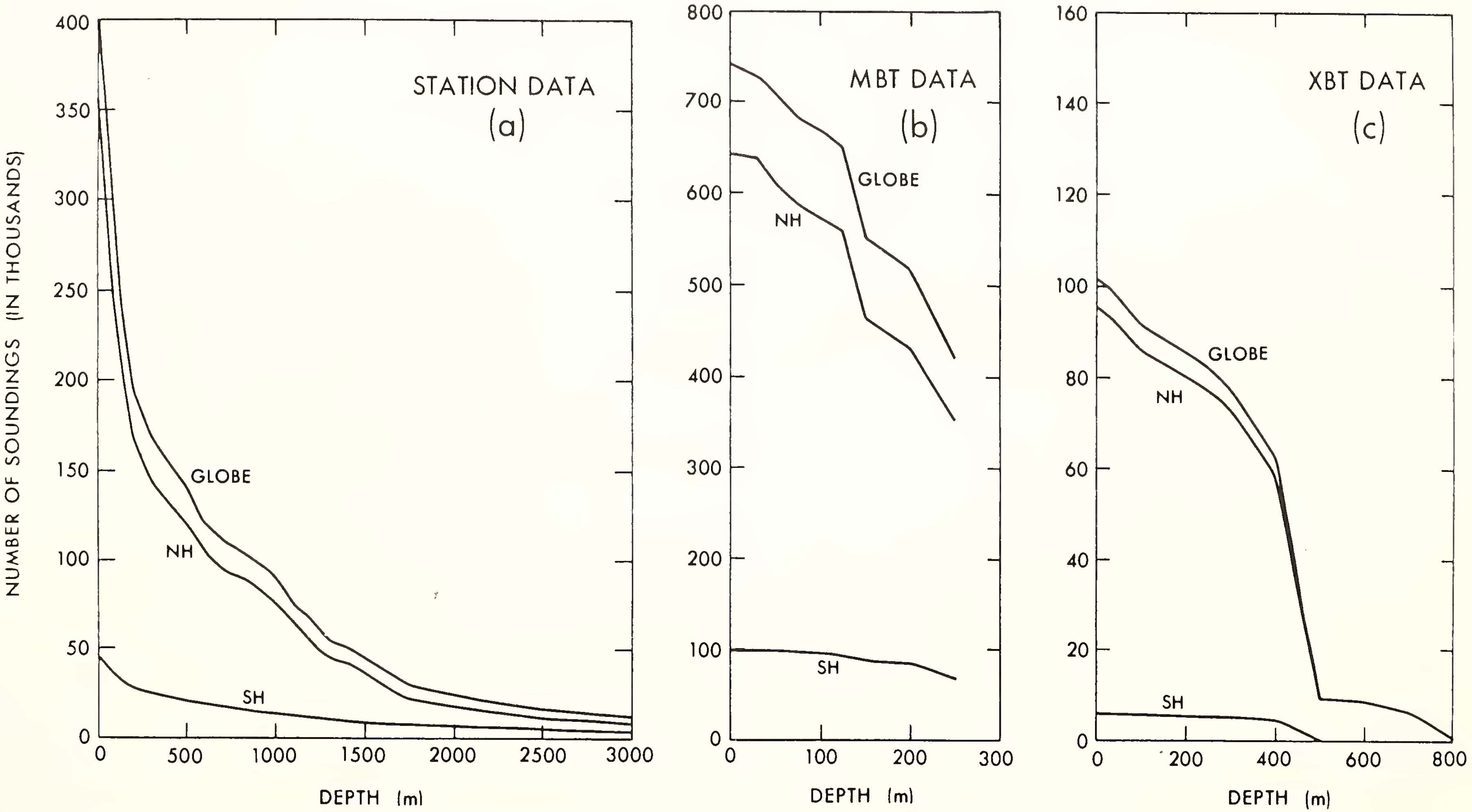

Fig. 1a. Distribution of Station Data temperature observations as a function of depth.

1b. Distribution of MBT observations as a function of depth.

1c. Distribution of XBT observations as a function of depth.

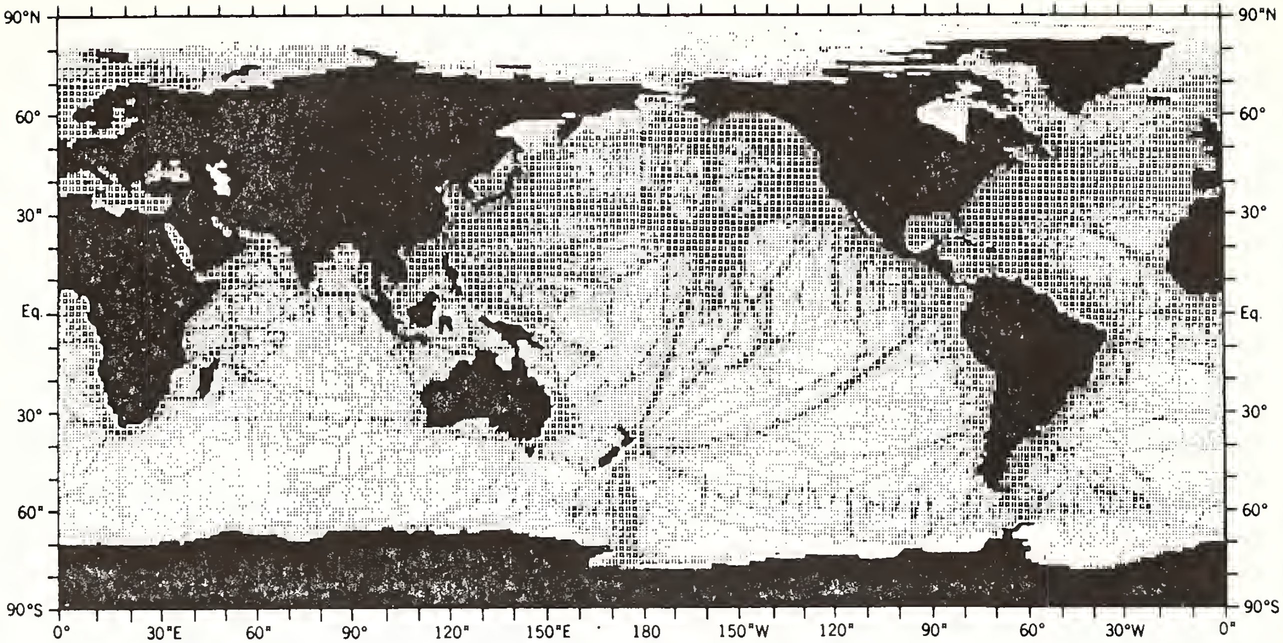

Fig. 2 Sea surface distribution of one-degree squares containing observations from the merged data set consisting of all Station data, MBT and XBT temperature observations for the annual period. A small dot indicates a square containing one to nine observations and a large dot indicates ten or more observations.

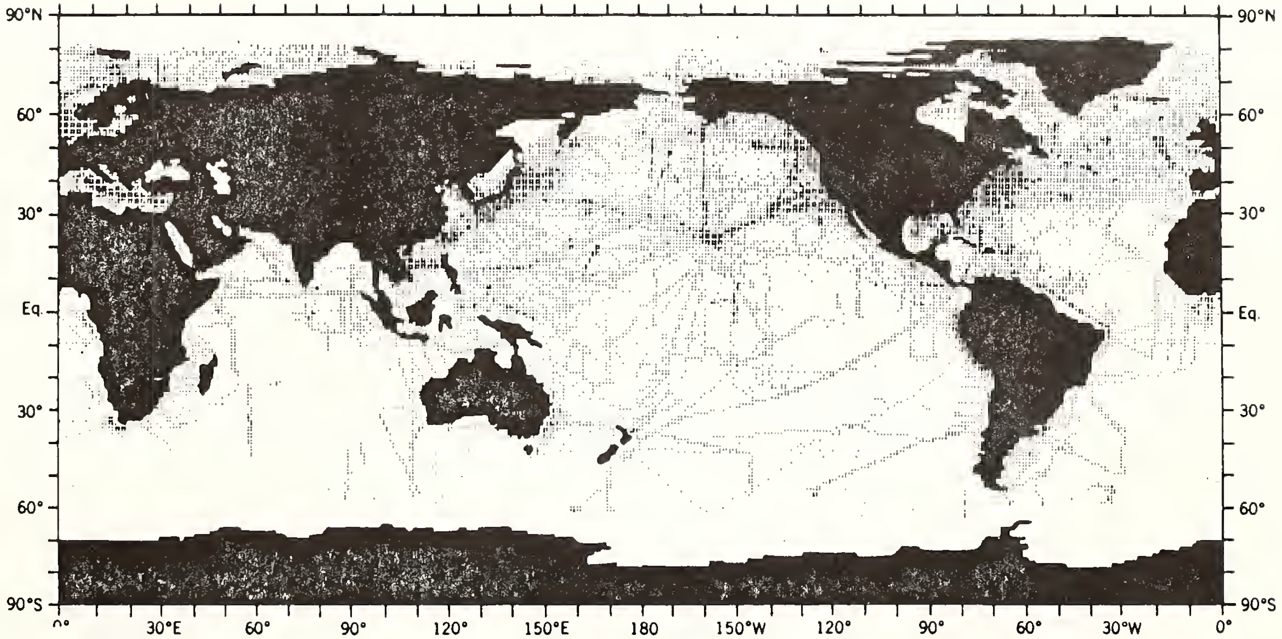

Fig. 3 Sea surface distribution of one-degree squares containing temperature observations from the merged temperature data set for the month of September. A small dot indicates a one-degree square containing from one to four observations and a large dot indicates five or more observations.

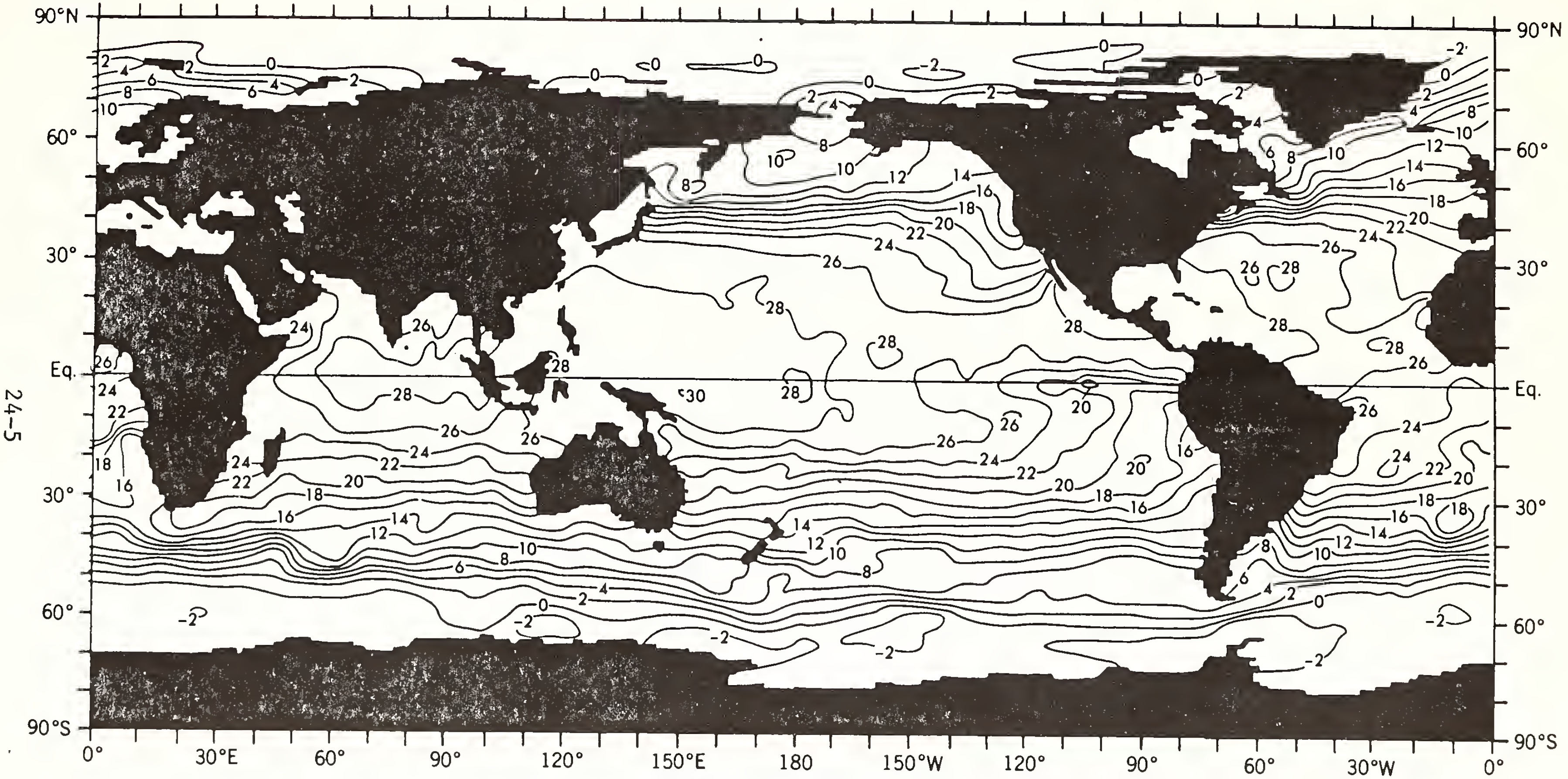

Fig. 4 Sea surface temperature analysis for the month of September (°C).

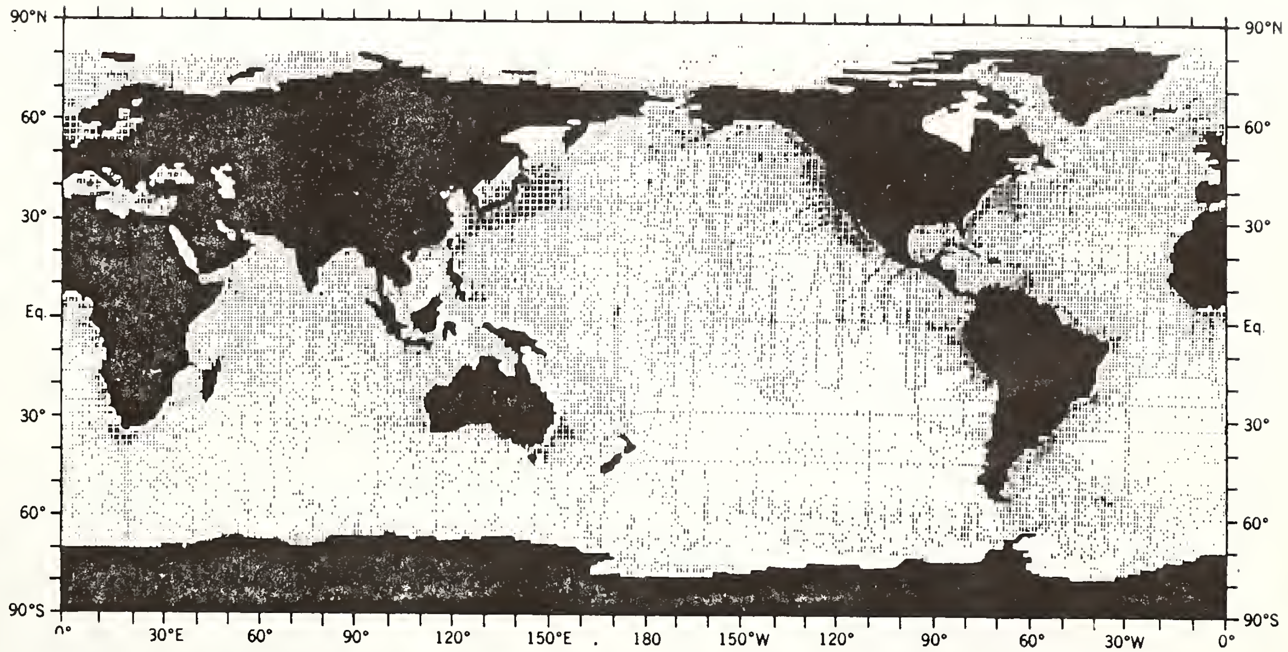

Fig. 5 Sea surface distribution of one-degree squares containing dissolved oxygen observations for the annual period. A small dot indicates a square containing one to nine observations and a large dot indicates ten or more observations.

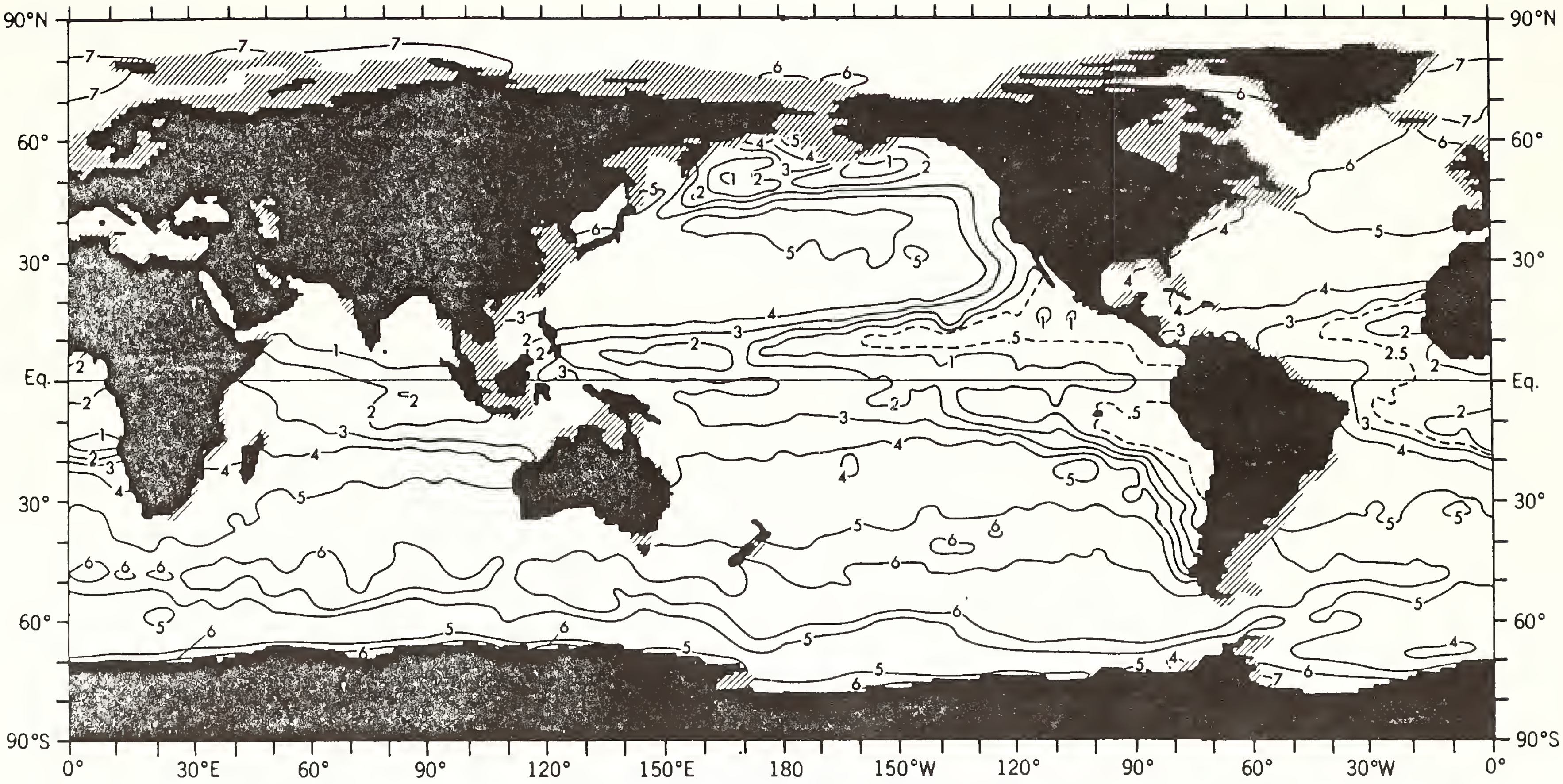

Fig. 6 . Dissolved oxygen analysis at the 250m level for the annual period (ml/l).

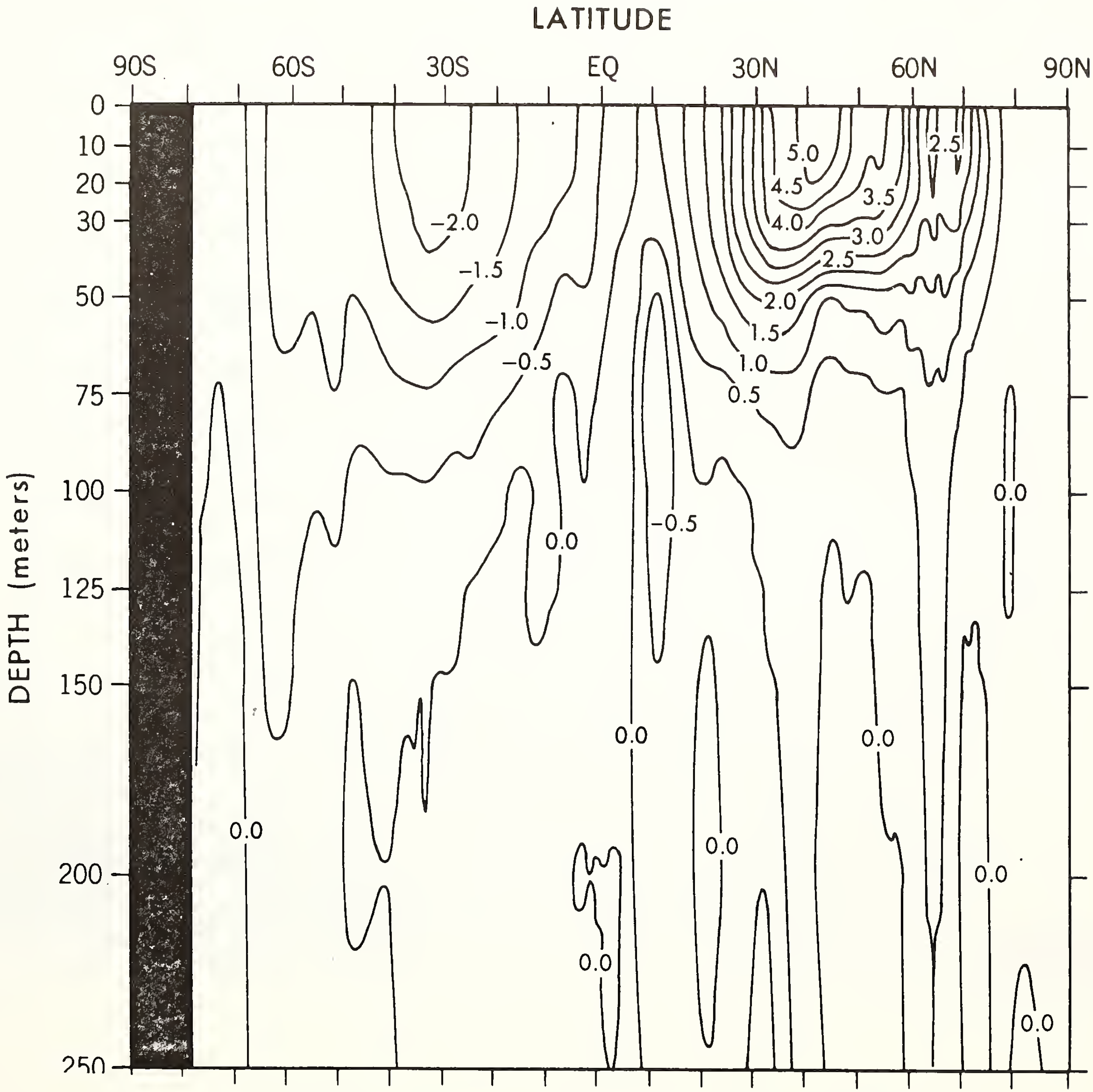

Fig. 7 Zonally averaged cross section of the September minus annual temperature difference field (°C).

RELATIONSHIP BETWEEN MONSOON ACTIVITY OVER SOUTHEAST ASIA AND THE CHANGES IN UPPER FLOWS OVER THE EQUATORIAL PACIFIC

Takio Murakami
University of Hawaii

As shown in Fig. 1, rainfall along the west coast of India increases steadily during the transition from premonsoon to monsoon season. There is a marked interannual difference in how and when the monsoon starts. The normal onset date at Bombay is around 5 June. In 1970 and 1971, monsoon rain increased sharply in late May (earlier than normal). In 1972, however, the advance of the monsoon was delayed by 10 to 15 days. The delayed onset and early withdrawal of the monsoon from India (about a week to 10 days earlier than the normal date of withdrawal) led to droughts in many parts of India. In contrast, monsoon rain was above normal in 1970. Interannual rainfall changes in summer were also substantial in other regions. Table 1 demonstrates this. Four regions were selected near south Japan, the Philippines, New Guinea, and the western North Pacific. The area-averaged summer (June-August) rainfall was computed using monthly mean data, published in "Monthly Climatic Data for the World," ESSA. The stations used for this computation are as follows:

South Japan: 10 stations; Osaka (35°N, 136°E), Hiroshima (34°N, 132°E), Izuhara (34°N, 129°E), Fukuoka (34°N, 130°E), Oita (33°N, 132°E), Nagasaki (33°N, 130°E). Kagoshima (32°N, 131°E), Miyazaki (32°N, 131°E), Ashizuri (33°N, 133°E), Naze (28°N, 130°E).

Philippines: 5 stations; Basco (20°N, 122°E), Aparri (18°N, 122°E), Dagupan (16°N, 120°E), Manila (15°N, 121°E), Legaspi (13°N, 124°E).

New Guinea: 3 stations; Madang (5°S, 146°E), Lae (7°S, 147°E), Port Moresby (9°S, 147°E).

Western Pacific: 6 stations; Kwajalein (9°N, 168°E), Majuro (7°N, 171°E), Truk (7°N, 152°E), Ponape (7°N, 158°E), Tarawa (1°N, 173°E), Taguac (14°N, 145°E).

In Table 1, it is evident that during summer 1972, rainfall was well above normal over south Japan, the Philippines, and the western North Pacific. On the contrary, rainfall was much below normal near New Guinea where severe droughts occurred. Such abnormal rainfall patterns are well reflected in the fields of 200 mb divergence. Fig. 2 shows the distribution of 200 mb divergence computed from NMC data for two contrasting years; 1970 and 1972. During 1970 summer, upper divergence near India is above average as expected. In 1972, small divergence near India and even convergence around New Guinea contrasted strong upper divergence near Japan, the Philippines, and the equatorial North Pacific. The intense 1972 El Niño was fully established in March and reached a peak in December. Rainfall was above normal in the equatorial central Pacific, while a negative rainfall anomaly was found near New Guinea.

Fig. 3 (top) shows the 200 mb $<\psi>$-isopleths for summer 1972. A weak Tibetan high was accompanied by a deep trough over the North Pacific with extremely strong westerlies to its south. Considerable changes in location and intensity of the 200 mb anticyclone were observed between 1970-72 summers. The intensities, as measured by the $<\psi>$ value at the anticyclone center, are as follows: 3.5 at 30°N, 50°E in 1970; 3.3 at 30°N, 70°E in 1971; and 2.5 at 27°N, 90°E in 1972, in the units of 10^7 m^2 s^{-1}. In this case, and perhaps in general, the upper anticyclone shifts to the east, during a weak monsoon year, from its usual position. In Fig. 3 (top), note a well established ridge system extending eastward along about 10°N from the Philippines to the equatorial central Pacific, congruent with above average upper divergence over that region (Fig. 2, bottom).

Anomalous features in 200 mb $<\chi>$ for 1972 summer are depicted in Fig. 3 (bottom). The primary $<\chi>$ minimum center was located near its normal position around 17°N, 120°E. Little change was observed in the location of the primary $<\chi>$ minimum center from one year to the other. This is in marked contrast to considerable location changes in the primary $<\psi>$ maximum center. During the active monsoon year of 1970, there existed a large phase difference (∿ 70° longitude) between the primary $<\psi>$ maximum and $<\chi>$ minimum centers. During the weak monsoon year of 1972, a secondary $<\chi>$ minimum center was encountered around 10°N, 160°E (Fig. 3, bottom). This is a part of the prominent upper divergent outflows occurring over an extensive region from the Philippines to the western and central Pacific (refer also to Fig. 2 , bottom). Thus, the net large-scale negative $<\chi>$ regions appear to shift eastwards as well as equatorwards during a weak monsoon year, accompanied by a weakening and eastward displacement of the upper anticyclone over the Indian region. During summer 1972, there also exists a vertical circulation anomaly of two cells along the equator whose anomalous rising branches cover the central Pacific region and whose anomalous sinking branches reduce the rainfall to the west and east. The same conclusion was made in an earlier work of Krueger and Winston (1974).

Fig. 4 (top) shows the differences in 200 mb $<u>$ along 19.6°N between the summers of 1970-72. Interestingly, easterlies in 1972 are much weaker (2 to 4 m s^{-1}) than usual over an extensive zone between about 30°E and 150°E. In contrast, extremely strong westerlies are encountered over the North Pacific, reaching 22 m s^{-1} at 165°W. Along 5°N (Fig. 4 , bottom), on the other hand, easterly anomalies are encountered over the equatorial Pacific between about

130°E and 150°W during summer 1972. These features are undoubtedly associated with the unusual development of a ridge system around 10°N and an exceptionally deep trough poleward of about 15°N, over the North Pacific in 1972 summer (Fig. 3, top). Based on a primitive equation model, Murakami (1974) attempted to examine whether changes in monsoon rains over Southeast Asia were related in any way to those in the upper circulation over the equatorial Pacific Ocean. By prescribing a hypothetical heating (cooling) anomaly over Southeast Asia, he found a pronounced westerly (easterly) response occurring in the upper troposphere over the equatorial central Pacific.

REFERENCES

Krueger, A. F., and J. S. Winston, 1974: A comparison of the flow over the tropics during two contrasting circulation regimes. J. Atmos. Sci., 31, 358-370.

Murakami, T., 1974: Atmospheric response to heat sources during July. Dept. of Meteorology, U. of Hawaii, UHMET 74-04.

Table 1. Summer rainfall over south Japan, the Philippines, New Guinea and the western North Pacific for individual year in 1970-72, in units of mm. Also shown is the three year summer mean rainfall over each of the selected regions. See text for further information.

	1970	1971	1972	Ave.
South Japan	902	869	1083	951
Philippines	915	867	1881	1221
New Guinea	737	653	431	607
Western Pacific	724	995	1139	953

FIGURES

Fig. 1. Daily rainfall (cm day^{-1}) along the west coast (Konkan, Coastal Mysore and Kerala) of the Indian Peninsula during the summers of 1970-72, extracted from the Monsoon Rainfall Summary--Supplement to the Indian Daily Weather Report, India Meteorological Department. Full lines are for the long-term average (normal) rainfall.

Fig. 2. 200 mb summer mean divergence in 1970 (top) and 1972 (bottom), in units of 10^{-6} s^{-1}. Interval 1 unit. Hatching indicates horizontal divergence.

Fig. 3, top: Mean 200 mb streamfunction, $\langle\psi\rangle$, for 1972 summer, in units of 10^7 m^2 s^{-1}. Interval 1 unit. Arrows indicate the direction of the non-divergent winds. Also shown by dots are the locations of season mean anticyclones during the summers of 1970-71. Bottom: As in the top except for 1972 summer mean velocity potential, $\langle\chi\rangle$, in units of 10^6 m^2 s^{-1}. Interval 1 unit. Regions of negative $\langle\chi\rangle$ are shaded. Arrows indicate the direction of divergent winds.

Fig. 4. Meridional distributions of summer mean zonal component of winds, $\langle u\rangle$, at 200 mb between 20°E and 115°W along 19.6°N (top) and 5.0°N (bottom) for 1970-72.

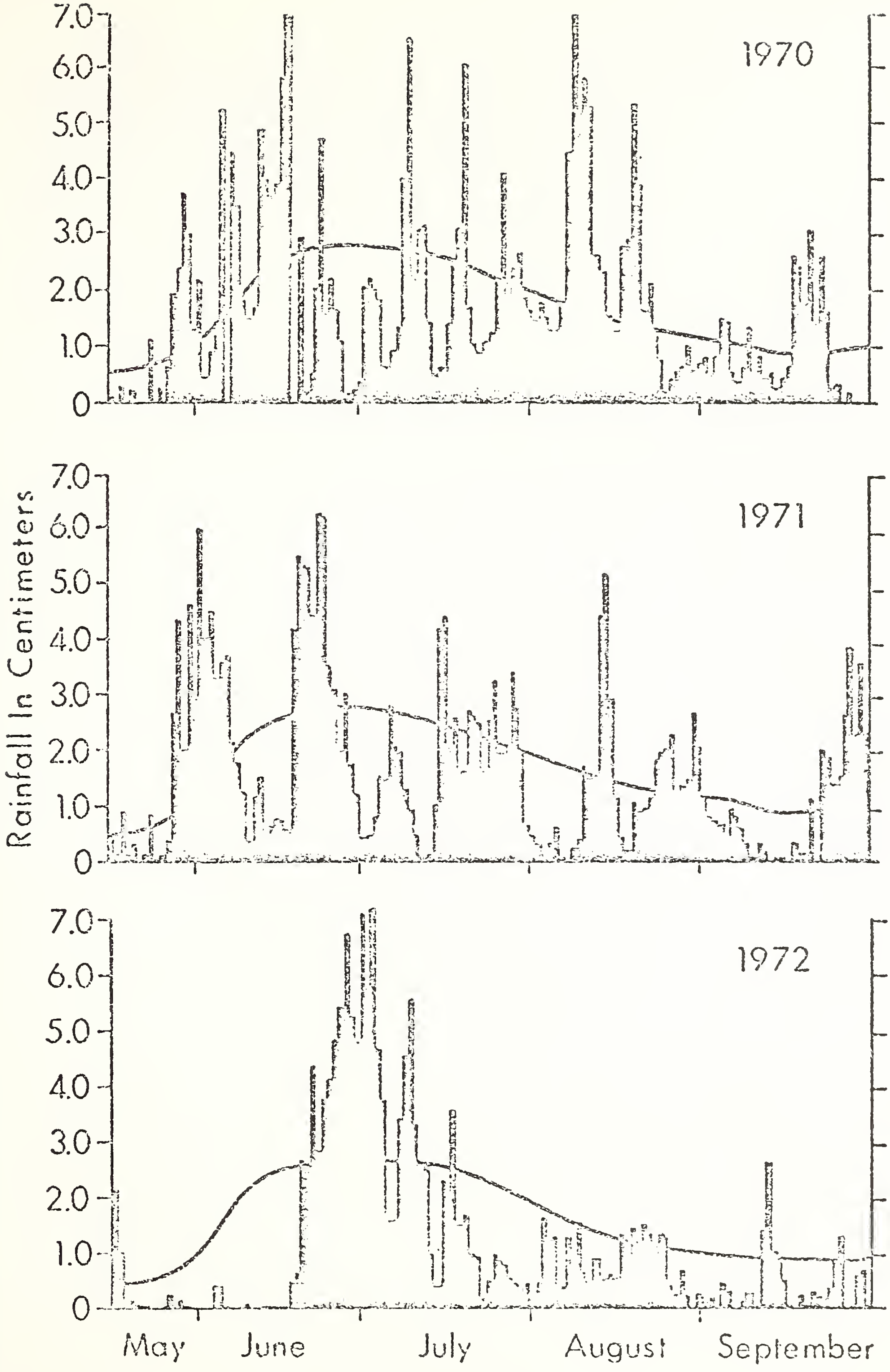
Rainfall In Centimeters
7.0
6.0
5.0
4.0
3.0
2.0
1.0
0
1970
1971
1972
May
June
July
August
September

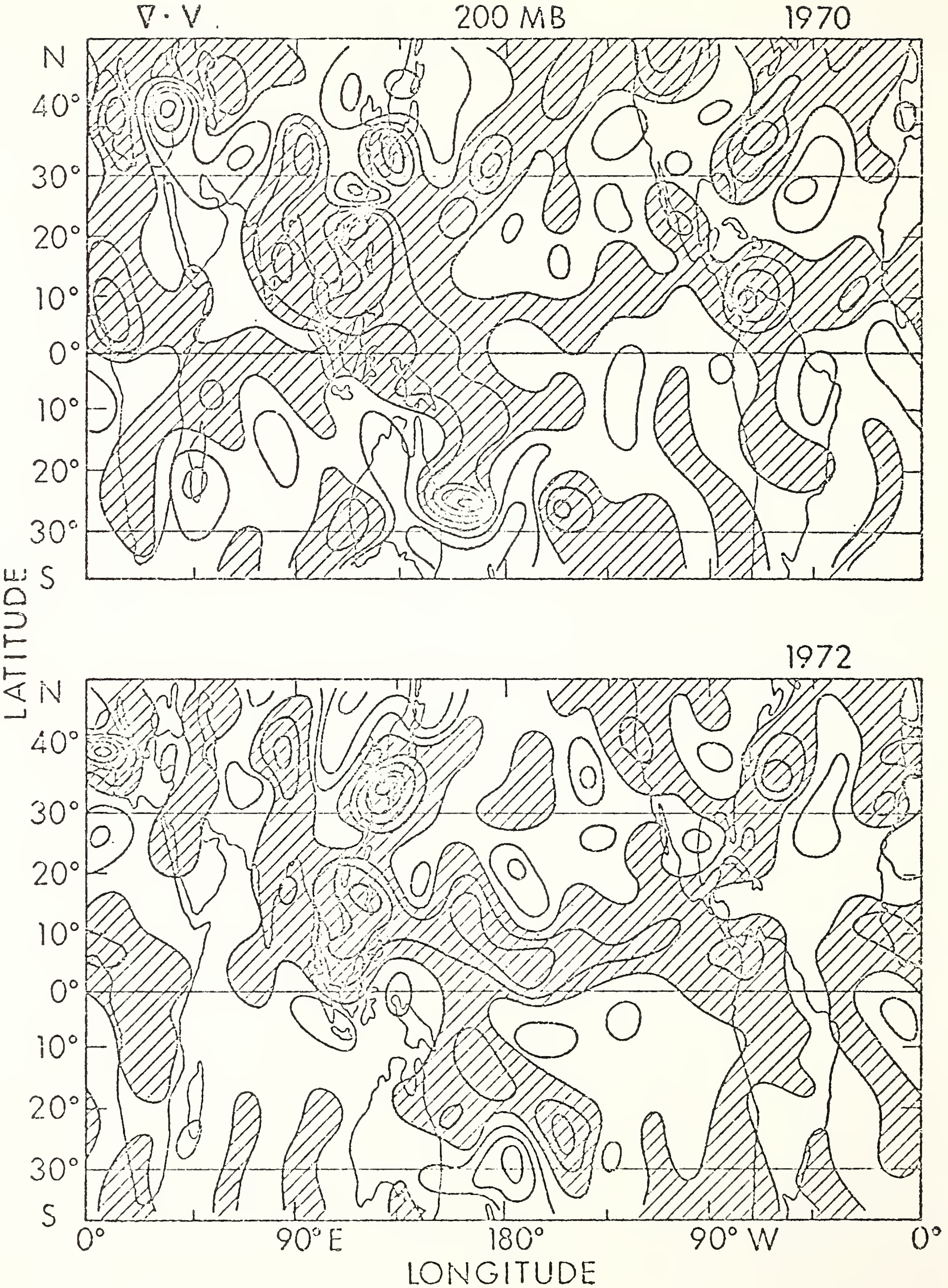
∇ · V
200 MB
1970
1972
N
40°
30°
20°
10°
0°
10°
20°
30°
S
LATITUDE
0°
90° E
180°
90° W
0°
LONGITUDE

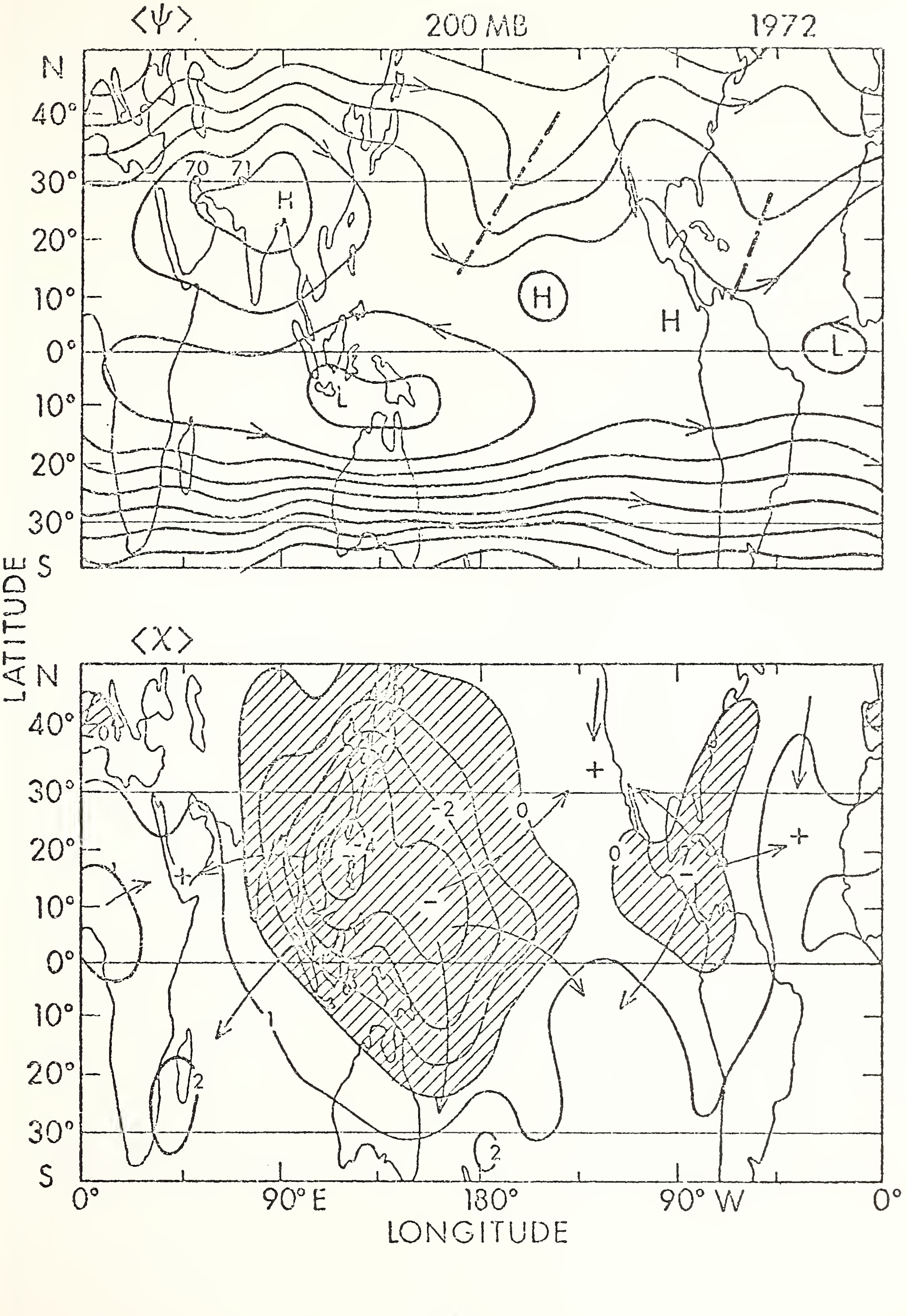
⟨ψ⟩
200 MB
1972
N
40°
30°
20°
10°
0°
10°
20°
30°
S
70
71
H
H
H
L
L
LATITUDE
⟨χ⟩
N
40°
30°
20°
10°
0°
10°
20°
30°
S
20
+
-2
-4
0
-
+
0
-
+
1
2
2
0°
90° E
180°
90° W
0°
LONGITUDE

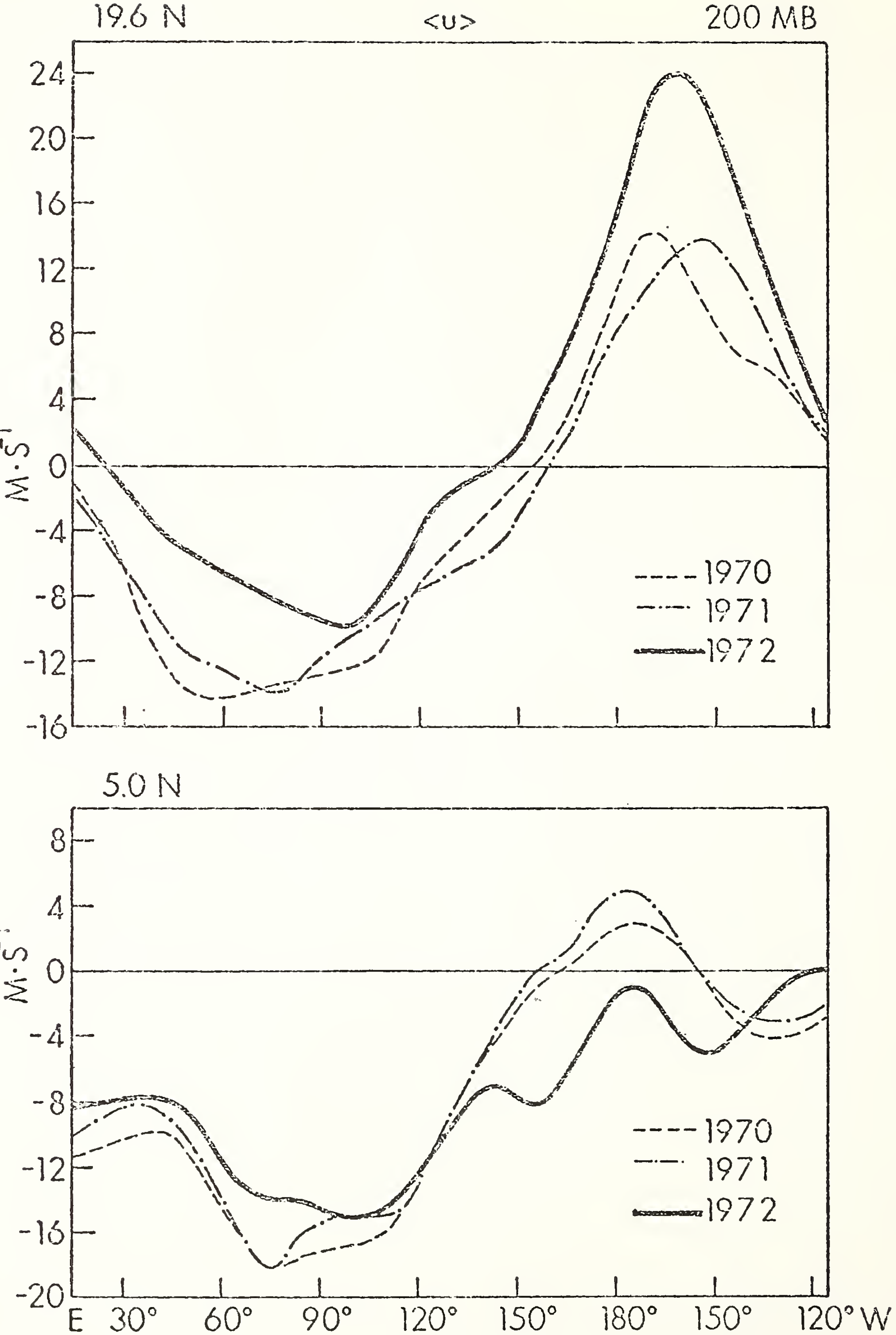
19.6 N
<u>
200 MB
24
20
16
12
8
4
0
-4
-8
-12
-16
M·S⁻¹
1970
1971
1972
5.0 N
8
4
0
-4
-8
-12
-16
-20
M·S⁻¹
1970
1971
1972
E 30°
60°
90°
120°
150°
180°
150°
120° W
LONGITUDE

Teleconnections at Middle and High Latitudes in Winter

Harry van Loon
National Center for Atmospheric Research

Jeffery Rogers
University of Colorado

There is a well known tendency for winter temperatures to be low over northern Europe when they are high over Greenland and the Canadian Arctic, and conversely. Well defined pressure anomalies over most of the Northern Hemisphere are associated with this regional seesaw in temperature, and these pressure anomalies are so distributed that the pressure in the region of the Icelandic Low is negatively correlated with the pressure over the North Pacific Ocean and over the area south of 50°N in the North Atlantic Ocean, Mediterranean, and Middle East, but positively correlated with the pressure over the Rocky Mountains. The scope of the seesaw is thus not limited to the higher latitudes in the Atlantic Ocean, but it encompasses the domains of both the North Pacific Oscillation and the North Atlantic Oscillation.

The intrahemispheric variations in pressure in the seesaw and the associated regional variations in air temperature anomaly indicate that opposite changes in temperature tend to occur in different regions on the scale of the pressure anomalies in the seesaw.

Correlation coefficients between grid points of sea level pressure during the seesaw are statistically significant and confirm the relationship between the North Atlantic and Pacific pressure fields. A periodicity of about 2.2 to 2.5 years in the pressure cospectra primarily contributes to these coefficients. Correlation coefficients between temperatures at stations are not so high nor so statistically significant as those of pressure but a quasi-biennial variation largely accounts for them too.

The composite patterns of pressure anomalies in the seesaw are almost identical to the first eigenvector in the monthly mean pressure but the standard deviations of pressure anomalies in individual seesaw months are as large as the standard deviations of monthly means in general. Since 1840 the seesaw, as defined by temperatures in Scandinavia and Greenland, occurred in more than 40% of the winter months and the occurrences are seemingly not randomly distributed in time. They happened such that one anomaly would prevail over the other for several decades. For this reason the circulation anomalies in the seesaw come to play an important part in deciding the level of regional mean temperatures in winter and thus in deciding the long-term temperature trends. These regional temperature trends are then closely associated with changes in frequency of atmospheric circulation types, and it is therefore unlikely that the trends are caused directly by changes in insolation or in atmospheric constituents and aerosols.

During long periods of the winter of 1976/1977 the pressure anomalies of the seesaw had the largest share of the anomaly pattern, and the temperature anomalies over North America and Europe were then distributed according to the temperature anomaly pattern of the seesaw.

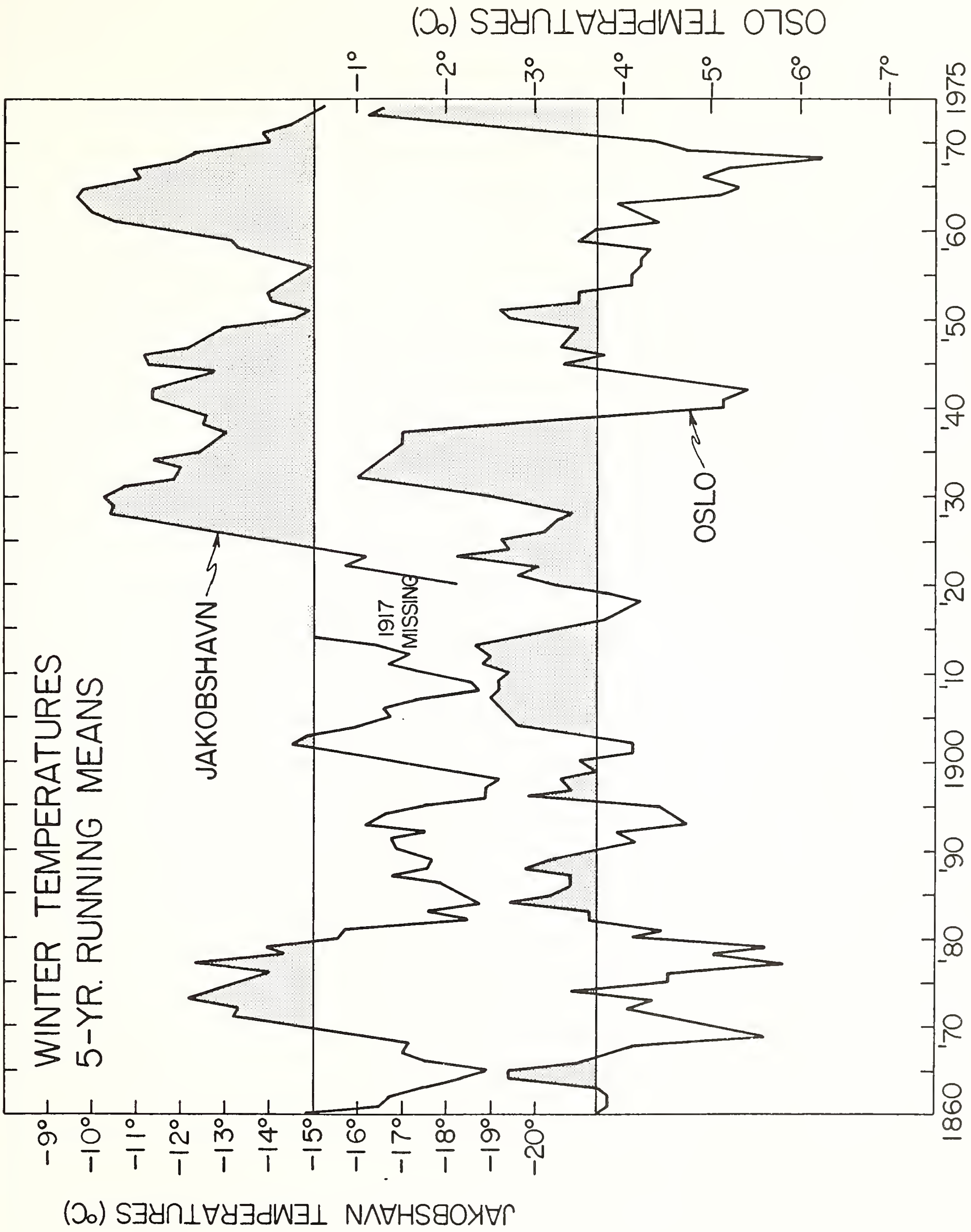

Five-year running means of winter temperature at Jakobshavn and Oslo (°C).

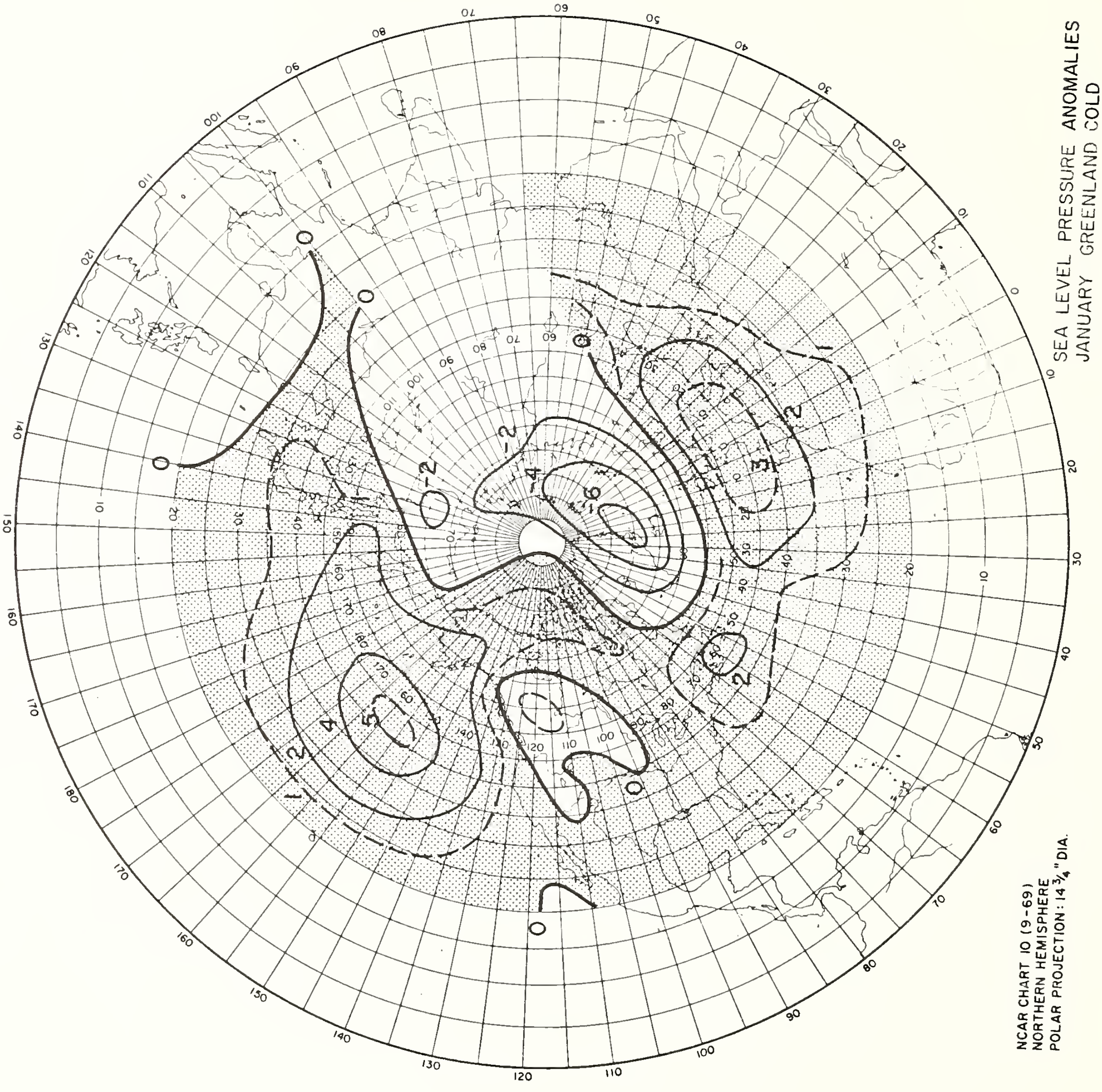

Figure 1. Sea level pressure anomalies (mb) in January when the temperature at Jakobshavn was below and at Oslo above the mean, and the temperature anomalies were ≥ 4°C apart.

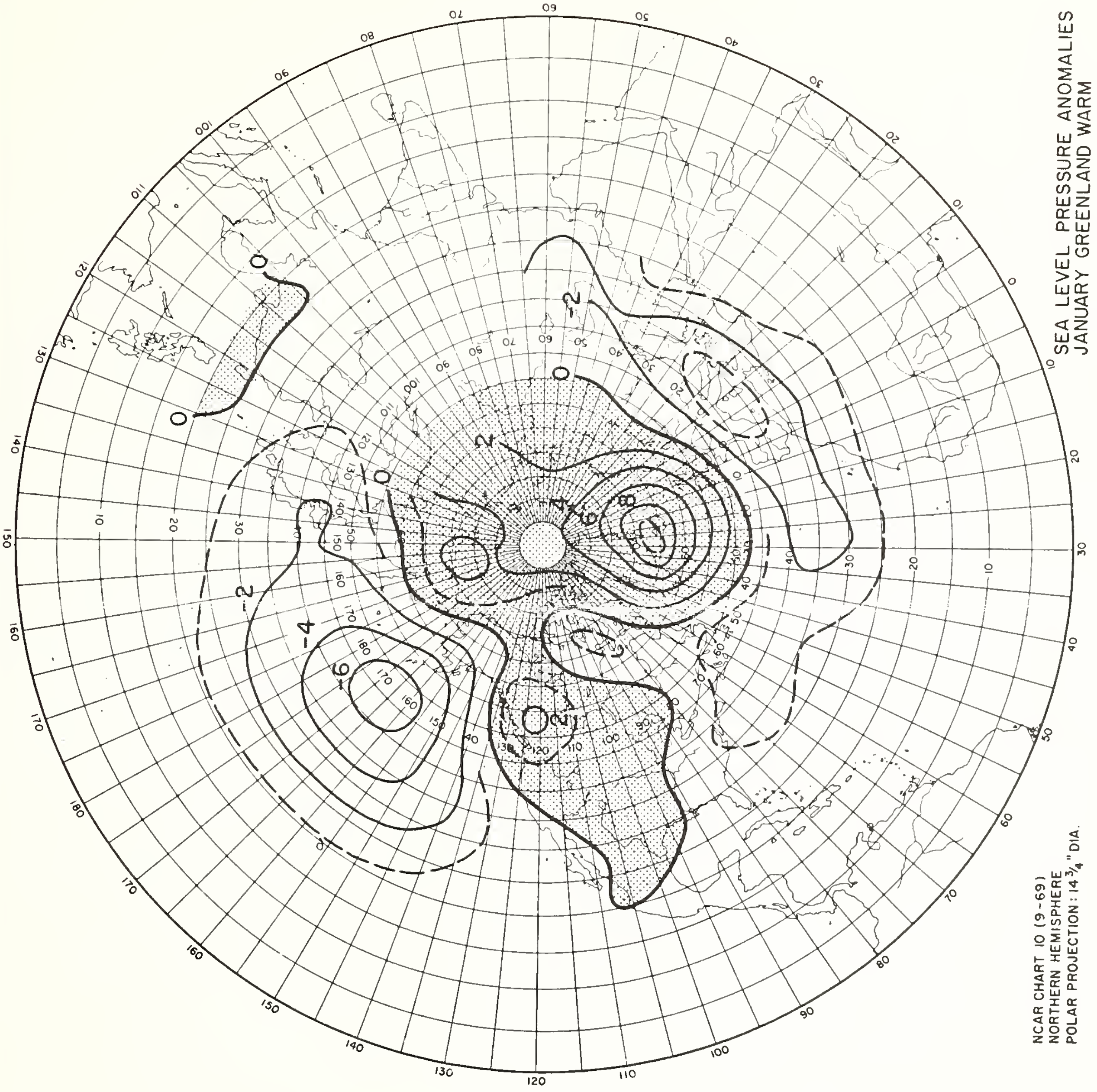

Figure 2. The same as Figure 1 but for temperature above the mean at Jakobshavn and below the mean at Oslo.

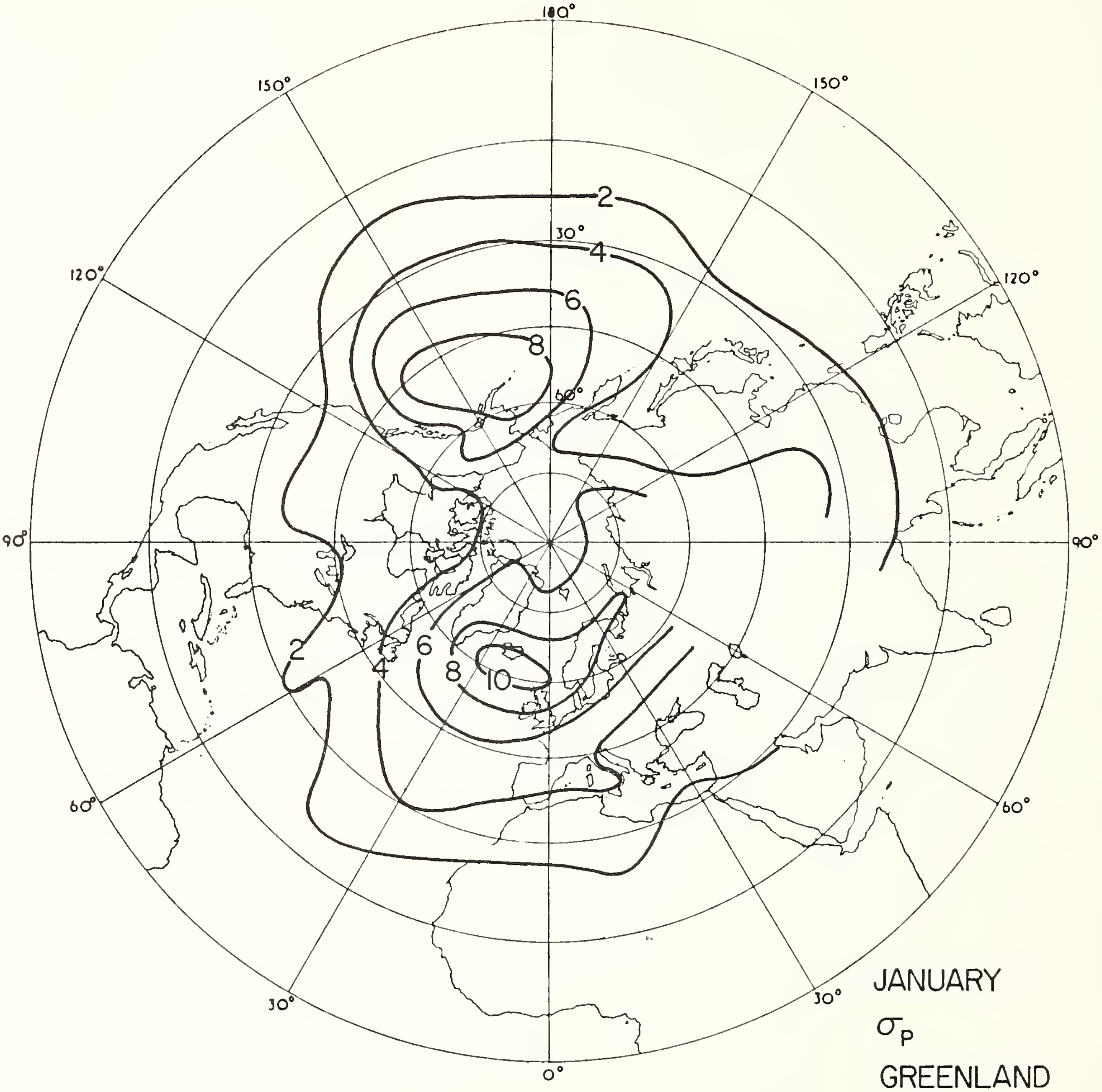

The standard deviation (mb) from the 77-yr. mean pressure of the years when Jakobshavn was above and Oslo below the mean. January.

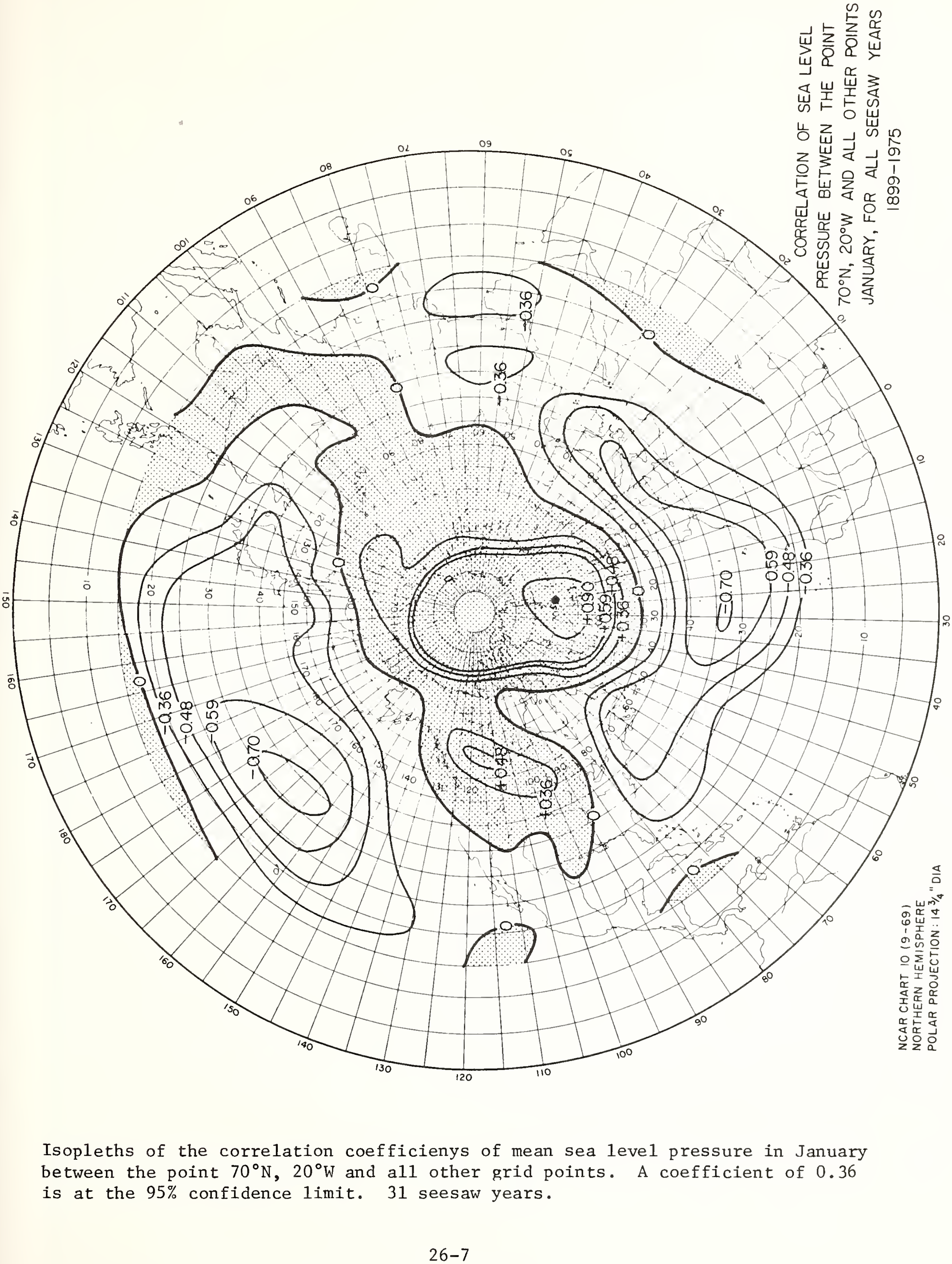

Isopleths of the correlation coefficienys of mean sea level pressure in January between the point 70°N, 20°W and all other grid points. A coefficient of 0.36 is at the 95% confidence limit. 31 seesaw years.

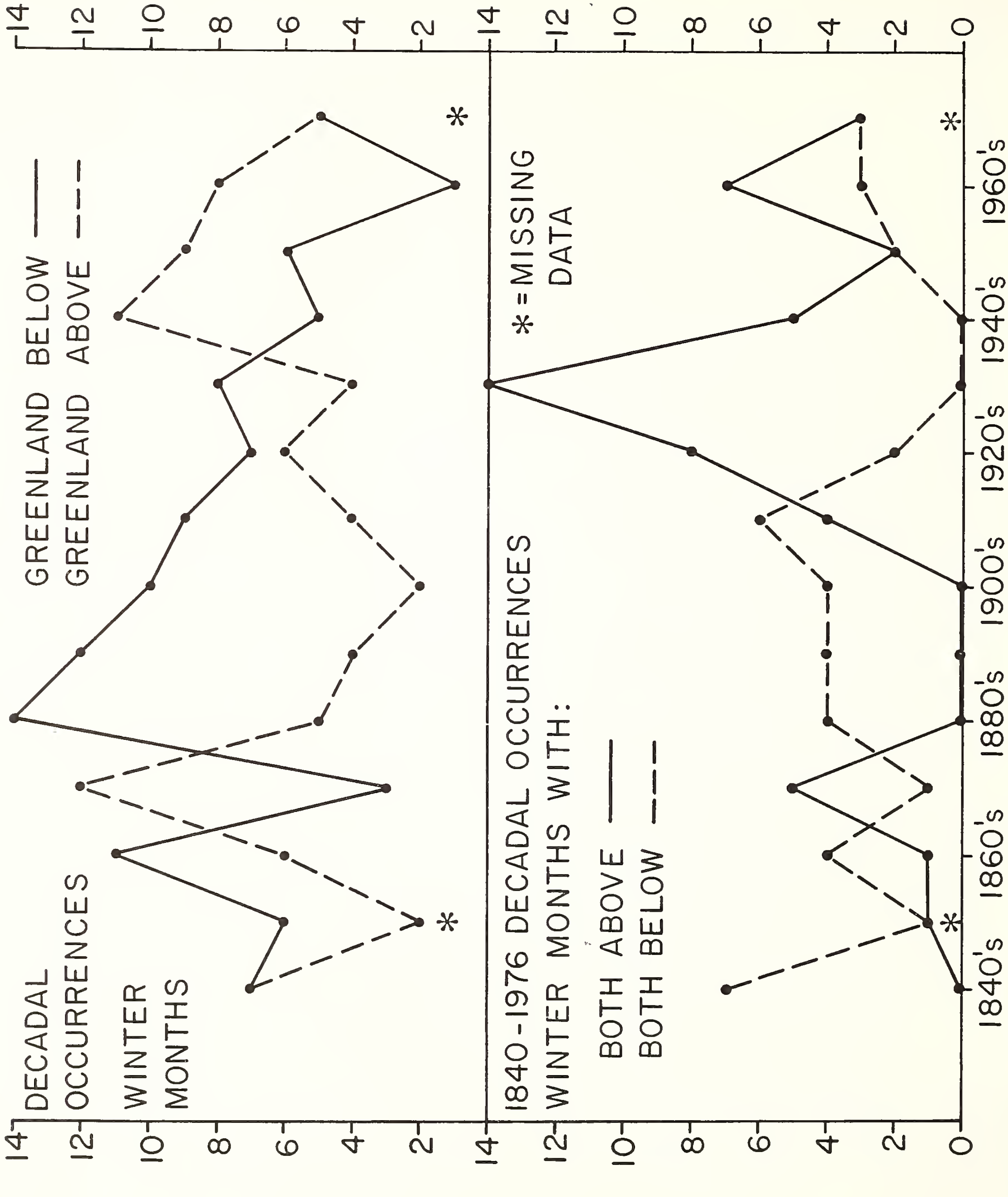

The number of cases per decade of the four temperature categories in winter (DJF) Asterisks denote incomplete decade.

On Modes of Tropical Circulation and Climate Anomalies

by

Stefan Hastenrath
University of Wisconsin

Principal component analysis of sea level pressure (SLP) over the tropical Atlantic and Eastern Pacific during 1942-71 identifies four preferred spatial patterns. These are found to be connected with extreme climatic events in key tropical regions. The first eigenvector pattern accounting for 43 percent of the variance, is characterized by inverse SLP anomalies over the Pacific and Atlantic, respectively, with particularly large amplitudes over the Southern oceans. This pattern is significantly correlated with sea surface temperature off the Ecuador/Peru coast, and a weaker correlation of opposite sign exists with rainfall in Northeast Brazil. The second eigenvector (26 percent of variance) represents SLP variations of the same sign in the entire map area, but with smallest values in the Equatorial Atlantic. This pattern is also significantly correlated with sea temperature off Ecuador/Peru, whereas weaker correlations of the opposite sign are found with rainfall in the Central American-Caribbean region and Subsaharan West Africa. The third eigenvector (14 percent of variance) shows a strongest SLP variation over the Eastern South Pacific, and is again correlated with Ecuador/Peru sea temperature. The fourth eigenvector (10 percent of variance) is dominated by inverse pressure variations in the North and South Atlantic, and has significant correlations of opposite sign with rainfall in the Central American-Caribbean region and Northeast Brazil, respectively; a weak correlation with Ecuador/Peru sea temperature has a sign opposite to that with Northeast Brazil rainfall. The principal component analysis complements our earlier approach to mechanisms of extreme climatic events in the tropical Americas and Africa.

Power Spectral Analysis of the Dominant Empirical Orthogonal Functions of Pacific SST and Global Free Air Temperatures

Bryan C. Weare

Department of Land, Air and Water Resources

University of California

Davis, California 95616

Power spectral and cross-spectral analyses have been carried out on the time coefficients of empirical orthogonal functions of anomalies of Pacific SST and global free air temperatures at the 850, 500, 300, 200 and 100 mb levels. The empirical orthogonal function analysis produces linear functions which explain the largest fraction of the variance. The SST functions are based on monthly departures from long-term monthly means at 160 points north of 20°S for the period 1949-1973(Weare, et al., 1976). The air temperature functions are based upon departures for 150 stations throughout the globe for the period 1958-1974. All spectra and cross-spectra were calculated with the time coefficients of these functions for the 200 months, May, 1958 through December, 1974. All series had linear trends removed.

Several important points are:

1) As previously discussed in Weare, et al., the dominant function of Pacific SST closely resembles the space and time variations associated with the so-called El Niño and its inverse. This function explains 23% of the variance of Pacific SST.

2) The most important functions at 850, 500, 300, 200, and 100 mb explain 6.8, 7.8, 7.0, 9.2, and 11.1 of the variance of their respective fields. The spatial patterns of the dominant functions at 500, 300 and 200 mb all have large regions of coherence in the tropics and subtropics. The 500 mb functions suggest a possible variation in wavenumber of the standing wave in the Northern Hemisphere midlatitudes.

3) The time coefficients of the dominant functions of Pacific SST (PNS_1), and normalized temperature departures at the 500 ($T500_1$), 300 ($T300_1$) and 200 mb ($T200_1$) levels have very strong spectral peaks at periods of 3.3 years explaining between 18.5 and 35 percent of the variance. Much smaller significant peaks probably have periods of 5 - 8 months.

4) The time coefficients of the dominant function of un-normalized temperature departures at the 500 mb level have a much "whiter" spectrum than those of the normalized departures.

5) Cross spectra between the series of the dominant SST function and those of the normalized temperature deviations at 500, 300 and 200 mb all show squared coherence greater than 0.78. The dominant period is between 2.2 and 6.7 years. The SST coefficients lead the air temperature coefficients by an average of 2.0 months where the uncertainty at the 95% confidence level is ±.2 months.

6) No "biennial" peak is apparent in the first or second most important functions of the normalized departures at any of the levels investigated.

Weare, B.C., A.R. Navato and R. E. Newell, 1976: "Empirical orthogonal analysis of Pacific sea surface temperatures." J. of Phys. Ocean., 6, 671-678.

Figure Legends

1. Most important empirical orthogonal function (EOF) of Pacific sea surface temperatures (PNS_1) and its corresponding time coefficients. Longer tics are January of the respective years.
2. The most important EOF of global 500 mb temperature ($T500_1$) as in 1.
3. Power spectra of time series of PNS_1.
4. Power spectra of time series of $T500_1$.
5. Power spectra of time series of $T200_1$.
6. Power spectra of time series of un-normalized $T500_1$.
7. Coherency square between the time series of PNS_1 and $T500_1$.
8. Coherency square between the time series of PNS_1 and $T200_1$.

Fig. 1

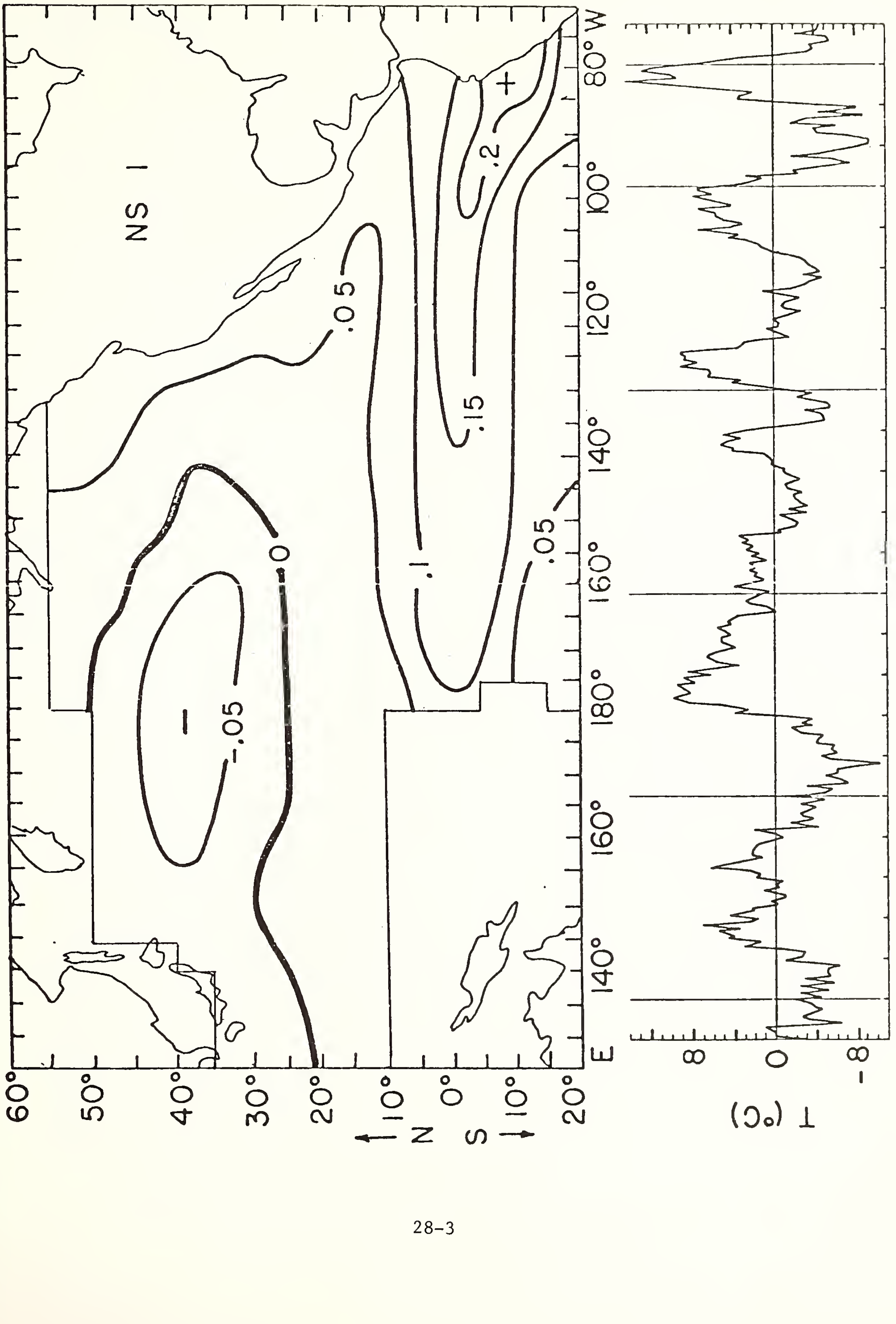
NS I
.05
.15
.2
+
.1
0
-.05
-
.05
60°
50°
40°
30°
20°
10°
0°
10°
20°
N
S
E
W
140°
160°
180°
160°
140°
120°
100°
80°
T (°C)
8
0
-8
1950
1955
1960
1965
1970
1973

Fig. 2

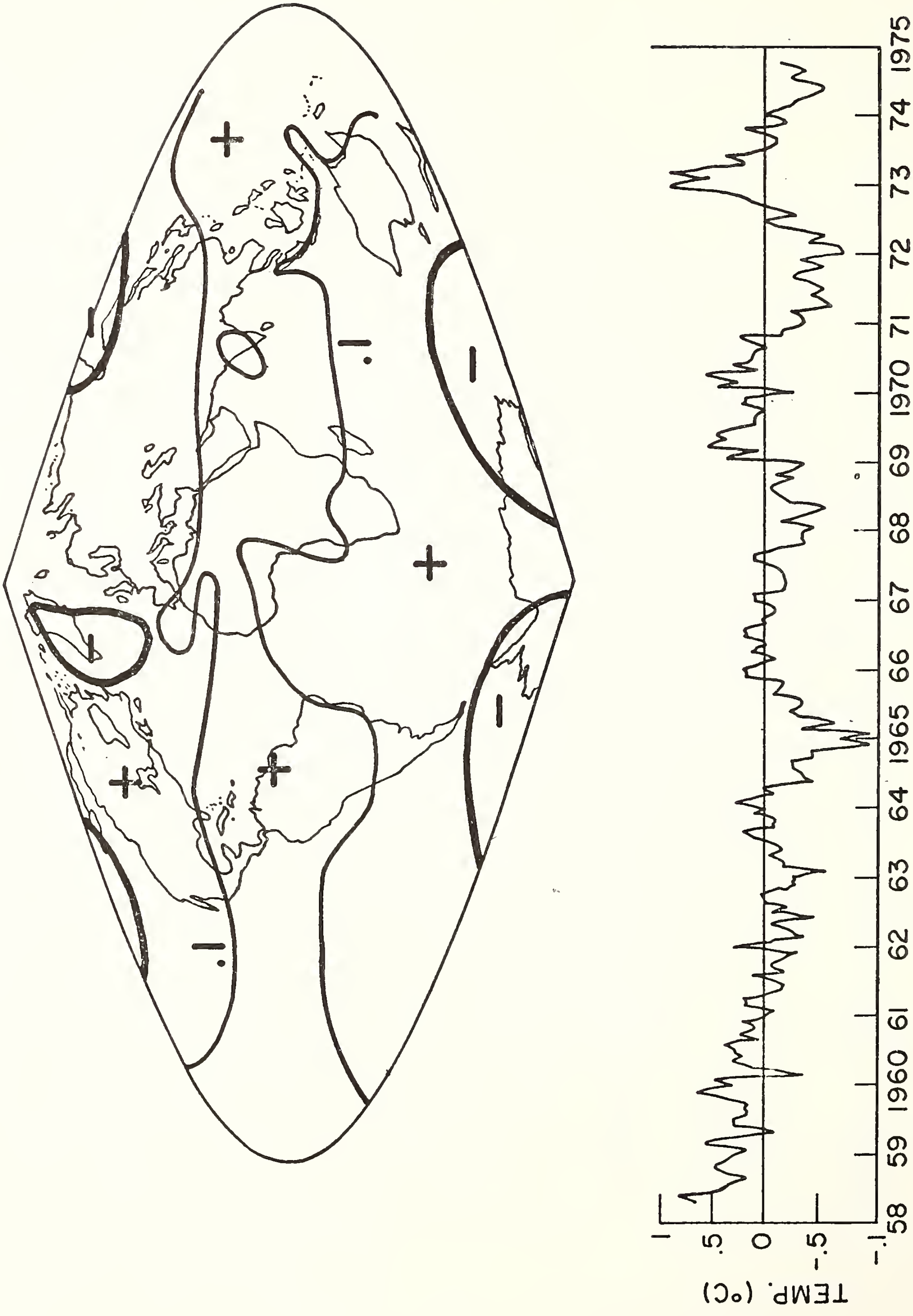
+
-
TEMP. (°C)
1
.5
0
-.5
-1
58
59
1960
61
62
63
64
1965
66
67
68
69
1970
71
72
73
74
1975

Fig. 3

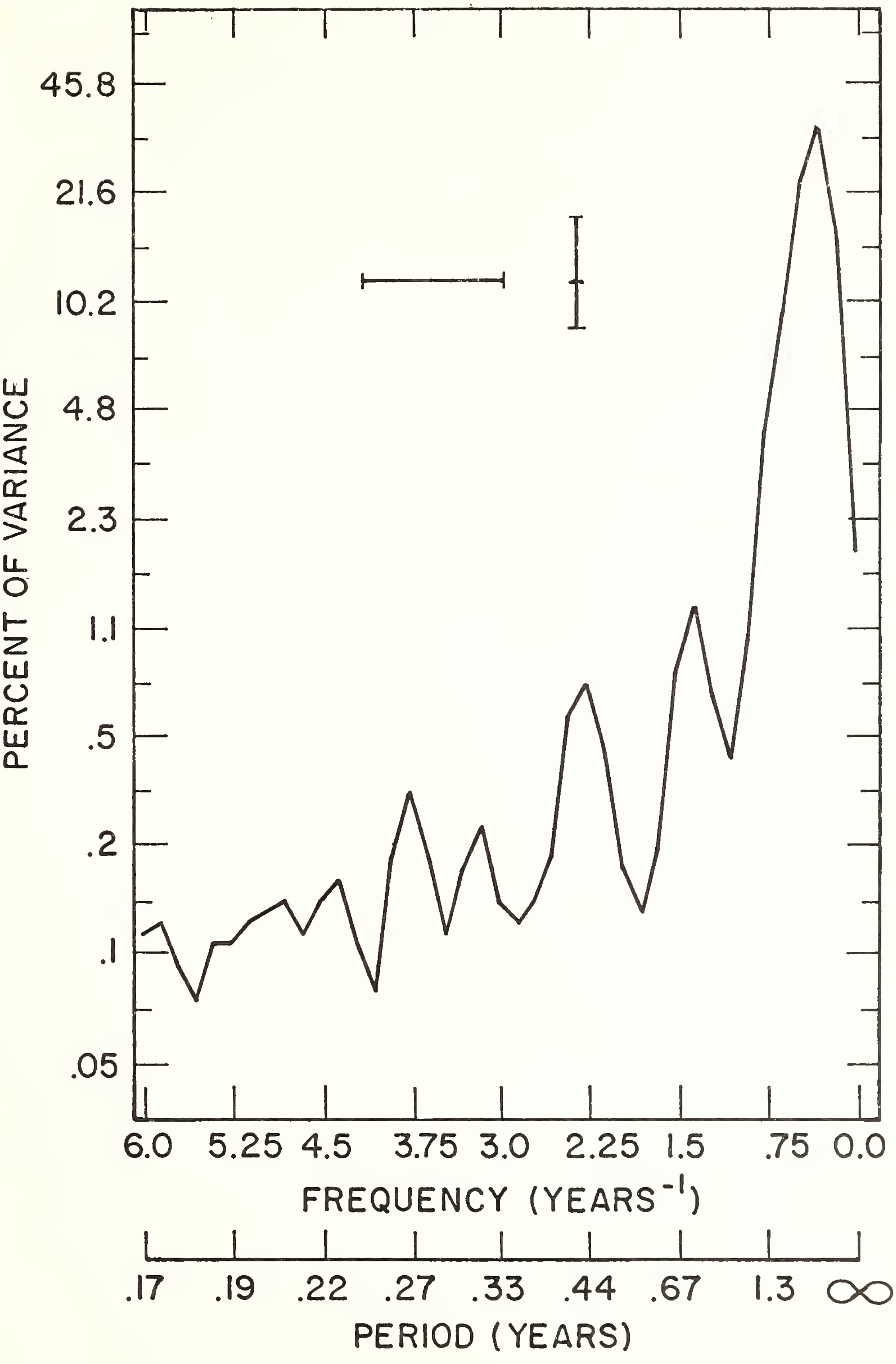

PNS$_1$

PERCENT OF VARIANCE
45.8
21.6
10.2
4.8
2.3
1.1
.5
.2
.1
.05
6.0
5.25
4.5
3.75
3.0
2.25
1.5
.75
0.0
FREQUENCY (YEARS^{-1})
.17
.19
.22
.27
.33
.44
.67
1.3
∞
PERIOD (YEARS)

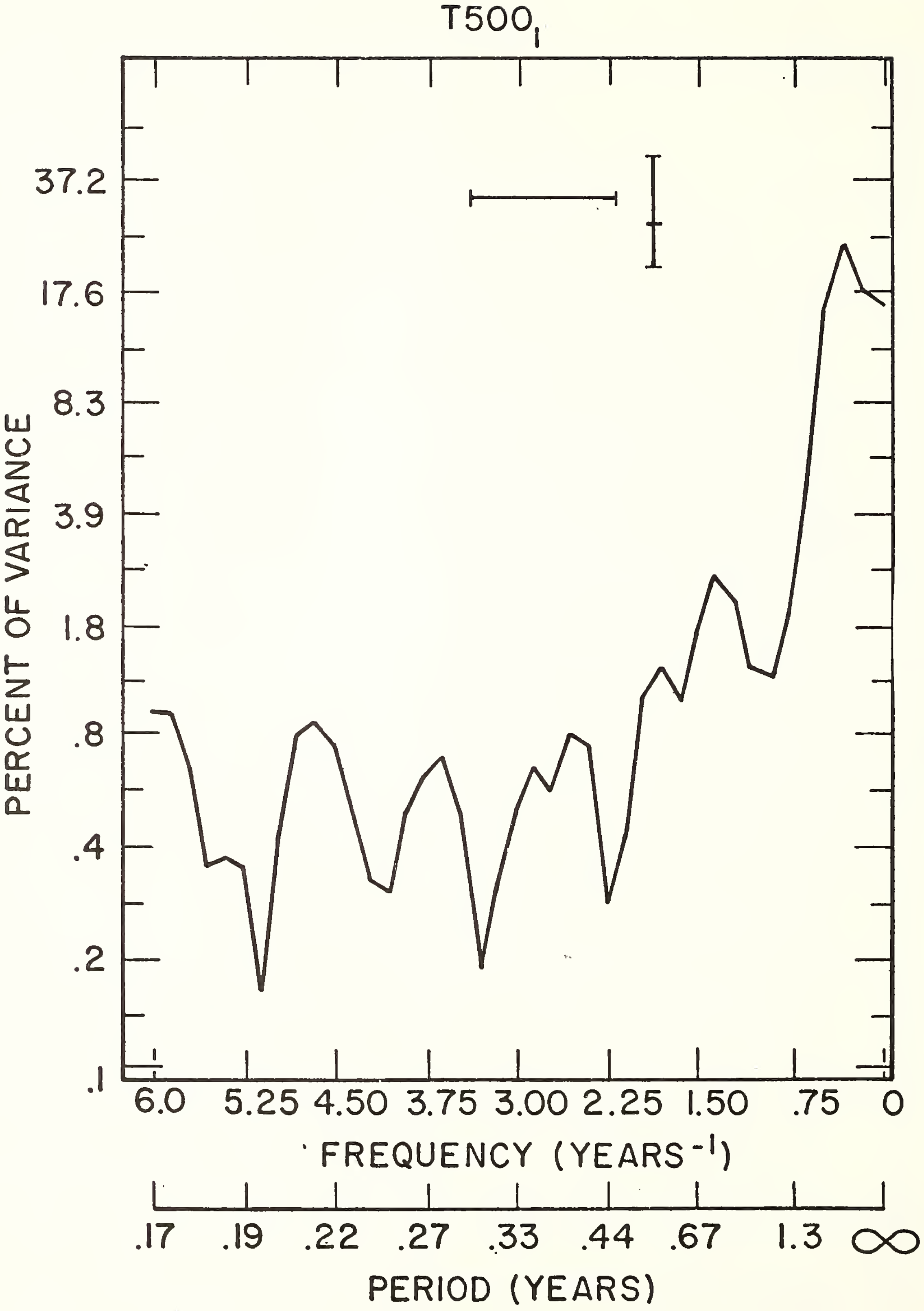
T500$_1$
37.2
17.6
8.3
3.9
1.8
.8
.4
.2
.1
PERCENT OF VARIANCE
6.0
5.25
4.50
3.75
3.00
2.25
1.50
.75
0
FREQUENCY (YEARS^{-1})
.17
.19
.22
.27
.33
.44
.67
1.3
∞
PERIOD (YEARS)

Fig. 5

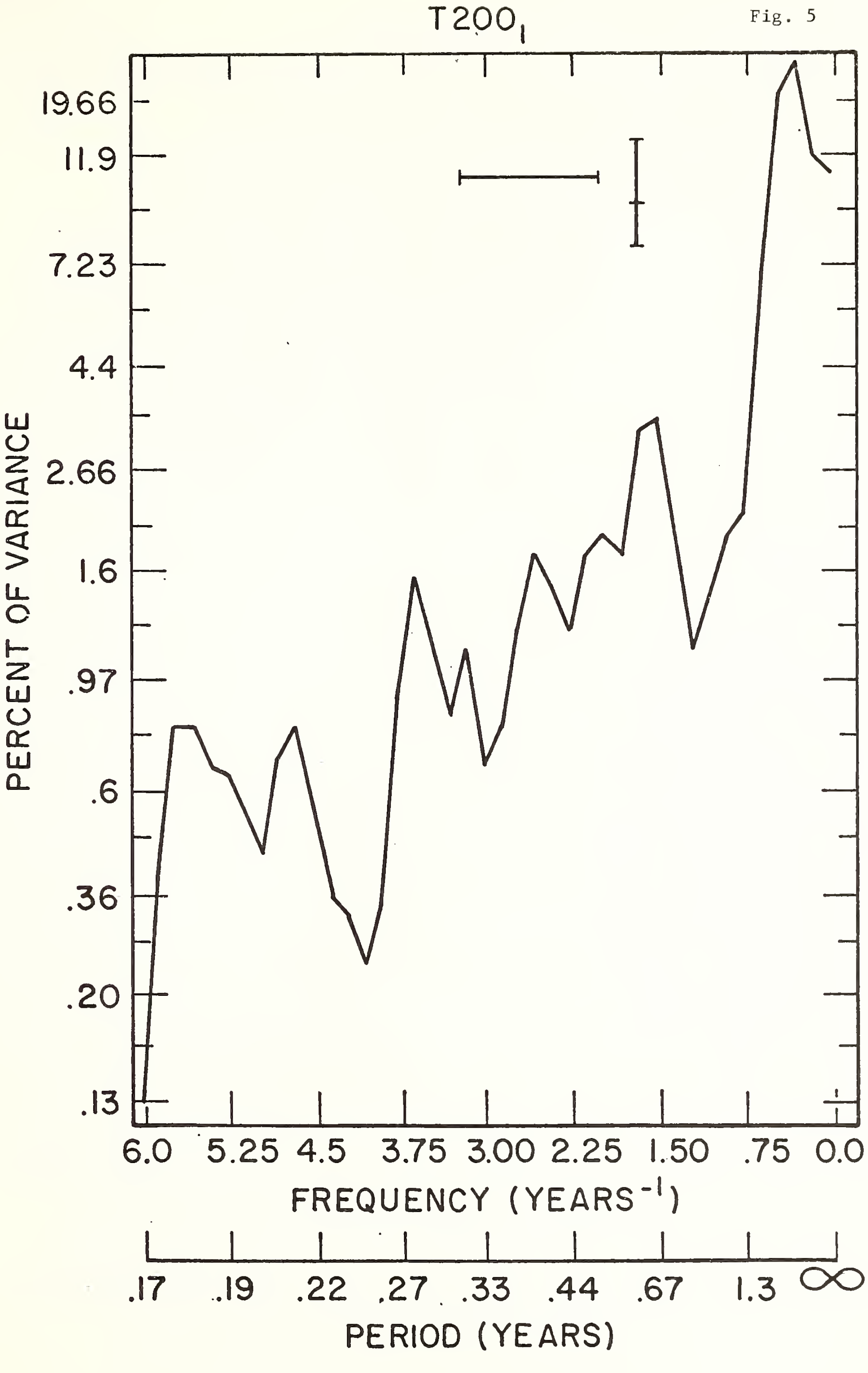
T200₁
19.66
11.9
7.23
4.4
2.66
1.6
.97
.6
.36
.20
.13
PERCENT OF VARIANCE
6.0
5.25
4.5
3.75
3.00
2.25
1.50
.75
0.0
FREQUENCY (YEARS⁻¹)
.17
.19
.22
.27
.33
.44
.67
1.3
∞
PERIOD (YEARS)

Fig. 6

$T500_1$

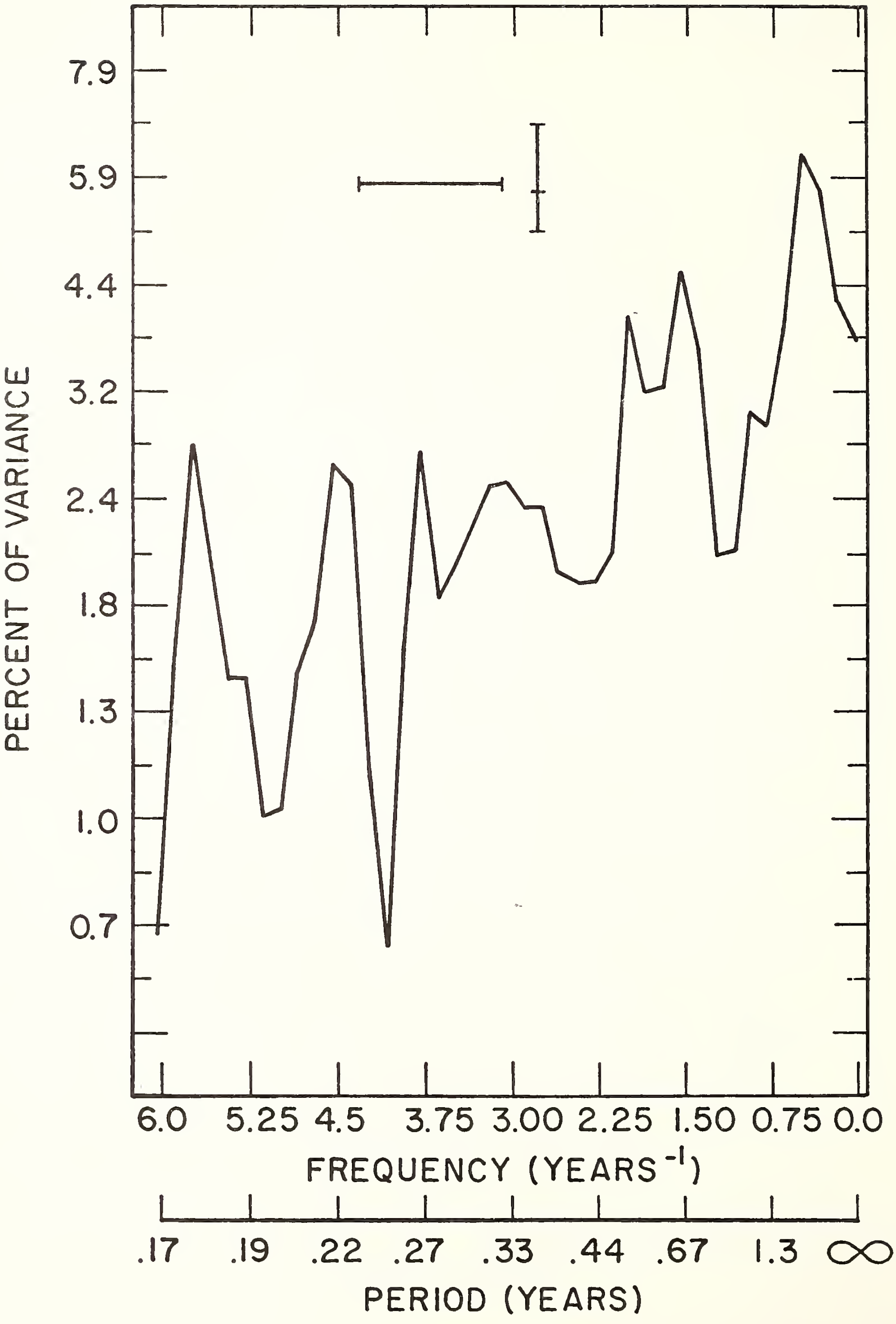
7.9
5.9
4.4
3.2
2.4
1.8
1.3
1.0
0.7
PERCENT OF VARIANCE
6.0
5.25
4.5
3.75
3.00
2.25
1.50
0.75
0.0
FREQUENCY (YEARS^{-1})
.17
.19
.22
.27
.33
.44
.67
1.3
∞
PERIOD (YEARS)

Fig. 7

PNS_1 vs $T500_1$

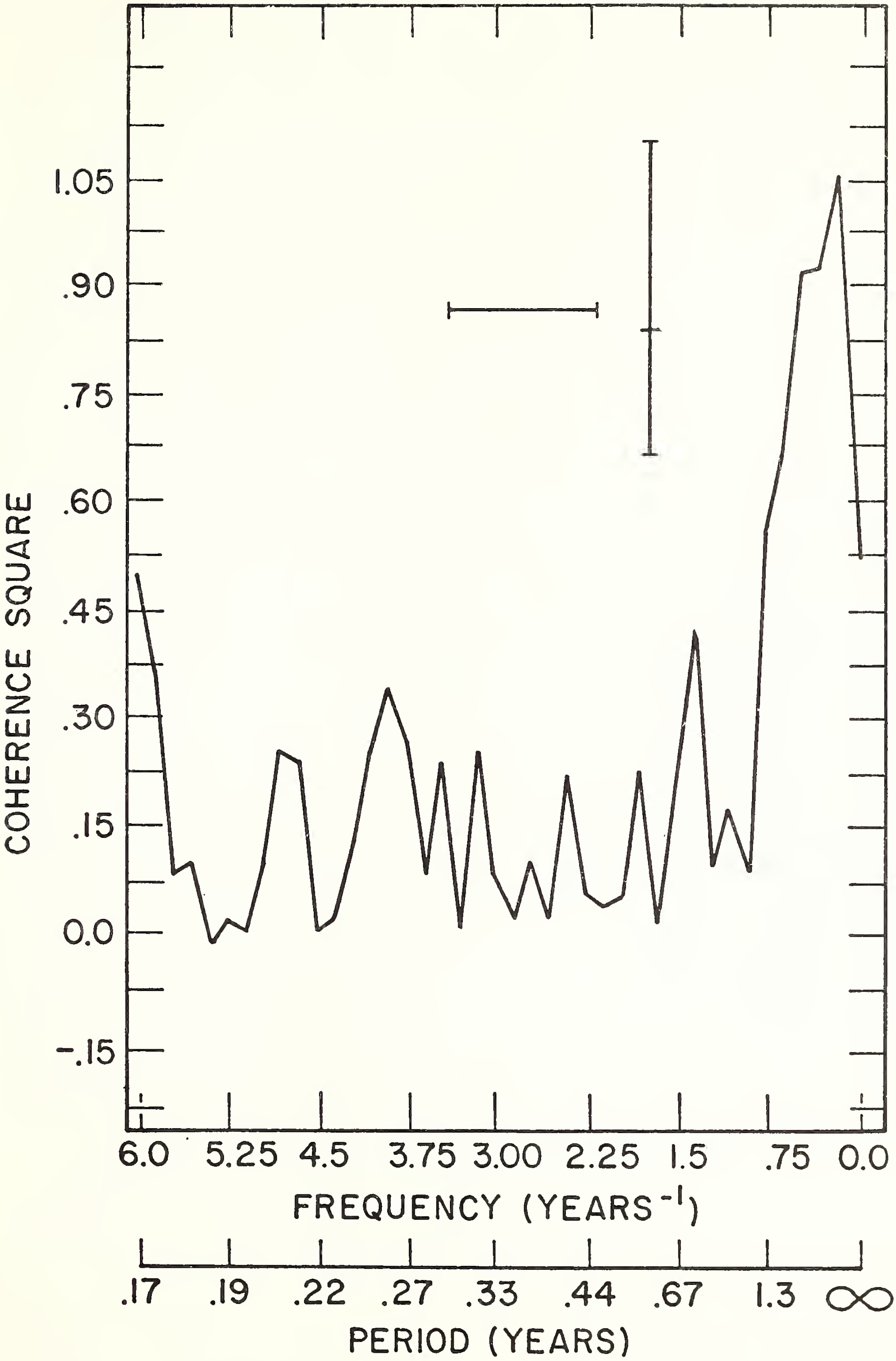

Fig. 8

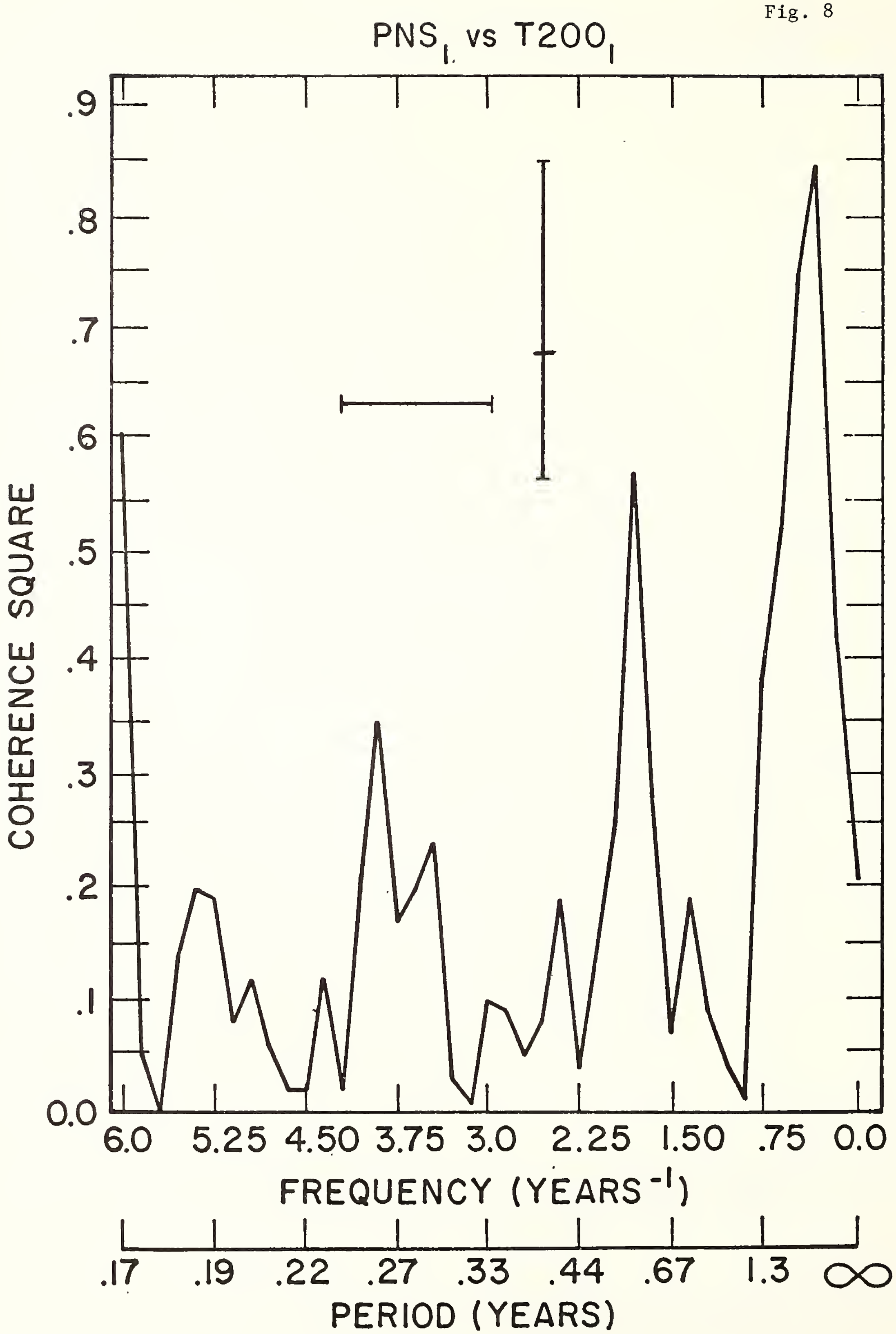
PNS$_1$ vs T200$_1$
COHERENCE SQUARE
.9
.8
.7
.6
.5
.4
.3
.2
.1
0.0
6.0
5.25
4.50
3.75
3.0
2.25
1.50
.75
0.0
FREQUENCY (YEARS^{-1})
.17
.19
.22
.27
.33
.44
.67
1.3
∞
PERIOD (YEARS)

Principal Component Analysis of U.S. Surface Temperature Data

E. M. Rasmusson, P. Arkin and J. Jalickee

Center for Experiment Design and Data Analysis
Environmental Data Service
National Oceanic and Atmospheric Administration
Washington, D.C.

A principal component analysis of surface temperatures has been performed using mean monthly values from the 344 climate divisions which cover the 48 contiguous United States. The data cover the 45 year period 1931-1975.

After subtracting the mean seasonal trend i.e. the mean monthly values from the data, the first 5 components were computed for the following fields:

(1) Mean monthly data from the entire period of 540 months.

(2) Normalized mean monthly data from the entire period.

(3) Mean monthly data for the winter months January-February (90 months).

(4) Mean monthly data for the summer months July-August.

A statistical summary of the results for the first 5 components is given in the following table.

PRINCIPAL COMPONENT ANALYSIS
MEAN MONTHLY TEMPERATURE (U.S.) 1931-1975
(SEASONAL CYCLE REMOVED)

Field	Variance (°F^2)	Explained Variance (Per Cent) 1	2	3	4	5
ALL MONTHS	11.3	47.1	23.8(71.5)	8.9(80.4)	4.5(84.9)	2.5(87.4)
ALL MONTHS (NORMALIZED)	1.0	45.2	20.8(66.0)	10.0(76.0)	5.3(81.3)	3.3(84.6)
WINTER (JAN-FEB)	22.4	45.4	29.2(74.6)	9.5(84.1)	3.8(87.9)	2.5(90.4)
SUMMER (JUL-AUG)	4.5	48.5	14.9(63.4)	10.4(73.8)	5.9(79.7)	3.5(83.2)

The following are the main points of interest.

1. The first three components explain from 74-84% of the total variance. In the case of the total data set this represents a reduction in the total number of data points required to describe the fields from 185,760 to 2655.

2. The variance during the winter months is approximately 5 times the value during the summer months.

3. For a given number of components, the explained variance is highest in winter.

Maps of the principal components and the associated amplitude time series will be published at a later date. The following are the most significent features of the analyses.

1. The first principal component, which explains 45-50% of the variance, shows maximum values over the eastern half of the country. Values over the western portions of the nation are smaller and of opposite phase. A similar pattern is found in all the analyses, although the main features of the summer field are displaced westward relative to those computed for the winter months. The first component reflects the major long-term temperature trends. These low frequency variations are often quite different for the summer and winter months. For the year as a whole, the temperatures over most of the country were highest during the 30's and 40's, with decreasing temperatures during the 50's and early 60's, and an apparent turn toward higher temperatures in the early 70's.

2. The second component, which explained 15-30% of the variance exhibited a maximum in the vicinity of Montana. Variations of opposite phase which are found over the eastern and southeastern states, are most pronounced during summer when a second maximum of opposite sign from that over Montana is centered over the lower Mississippi Valley.

3. The pattern of the third component, which explains around 10% of the variance changes significantly from summer, to winter. This component exhibits a strong north-south variation, as opposed to the first two components, which primarily represented east-west variations. Perhaps the most striking feature of the analyses is found in the time series of amplitude coefficients, which shows no long term trends, but exhibits a remarkably strong quasi-biennial oscillation during most of th 45 year period, particularly when normalized data are analyzed. For example, there are 15 similar and pronounced oscillations in the time series between the maxima of April 1942 and April 1973, giving an average period of 2.2 years. Many of the maxima and minima can also be identified as individual extrema in the coefficient time series for the first and second components. Spectral analysis of these time series, which have not as yet been performed, should shed further light on this subject.

USE OF EMPIRICAL ORTHOGONAL FUNCTIONS IN DIAGNOSING AND PREDICTING CLIMATE FLUCTUATIONS

R. W. Preisendorfer
Pacific Marine Environmental Laboratory
Seattle, Washington 98105

Figure 1 gives the basic algorithms for generating EOF's (principal components). Of particular importance is the exact representation of the original data via the EOF's $X_i(x)$ and their amplitudes $A_i(t)$. The all-important variance-carrying property of the eigenvalues of $\Phi(x,x')$ is shown on the last line. The current uses and problems of EOF's are shown in Figure 2. The workshop discussion concentrated on the problems. Under certain simple conditions, EOF's are the eigenmotions of simple conservative linear systems (Figs 3, 4), a result which may be proved rigorously. However when the systems are no longer conservative, linear or simple, this property no longer holds. Figures 5, 6 illustrate a property of EOF's which may not be widely observed or accounted for: when sample sizes are less than the number of points considered, some of the eigenvalues become zero. Rules were given for determining the number of statistically non degenerate eigenvalues. A well known example of the exponential fall-off of eigenvalues with index for cases of large p is shown in Figure 7. The phenomenon can be reproduced by Monte Carlo experiments with random time series (Fig 8), and can in principal be understood from the general probability theory of the eigenvalues (Fig 9) and deductions therefrom (Fig 10). On the whole, however, questions concerning the statistical significance of EOF results are best explored using Monte Carlo experiments, some results of which are summarized in Figures 11, 12, 13, 14. These results can be applied to determine the stopping rule – i.e., the method of deciding how many of Φ's eigenvalues are not due to chance fluctuations (Fig 15).

Work continues on extension of these results.

Figure 1

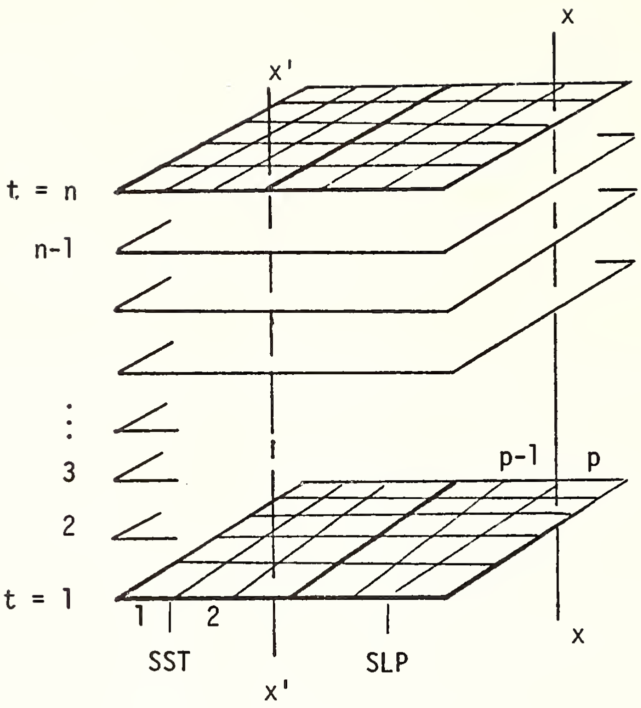

EMPIRICAL ORTHOGONAL REPRESENTATION OF THE DATA SET F(t,x)

where t = 1, 2, ..., n and x = 1, 2, ..., p.

Form covariance matrix

$$\Phi(x,x') \equiv (n-1)^{-1} \sum_{t=1}^{n} F(t,x)F(t,x')$$

The ith eigenvector of $\Phi(x,x')$ going with ith eigenvalue λ_i is:

$$X_i = (X_i(1), X_i(2), \ldots, X_i(p))$$

Then writing

$$\text{'}A_i(t)\text{' for } \sum_{x=1}^{p} F(t,x)X_i(x)$$

we have

$$\boxed{F(t,x) = \sum_{i=1}^{p} A_i(t)X_i(x)}$$

Generally: $\sum_{x=1}^{p} X_i(x)X_j(x) = \delta_{ij}$ $\qquad (n-1)^{-1} \sum_{t=1}^{n} A_i(t)A_j(t) = \lambda_i\delta_{ij}$

and

$$(n-1)^{-1} \sum_{t=1}^{n} \sum_{x=1}^{p} F^2(t,x) = \sum_{i=1}^{p} \lambda_i$$

Figure 2

USES OF EOF'S:

A) COMPACTION OF LARGE DATA SETS (VIA DIMENSIONAL REDUCTION)

B) INDICATORS OF COMMON CAUSAL RELATIONS

C) DATA FILTERING

D) DATA INTERPOLATION } IN REDUCED DIMENSIONAL FORM

E) DATA EXTRAPOLATION

PROBLEMS OF EOF'S:

A) PHYSICAL INTERPRETATIONS, IF ANY

B) TWO RECURRENT PHENOMENA (DEGENERACY AND EXPONENTIALITY)

C) TESTS FOR STATISTICAL SIGNIFICANCE

D) SEPARATION OF SIGNAL FROM NOISE

Figure 3

EMPIRICAL EIGENVECTORS ARE EIGENMOTIONS OF CONSERVATIVE LINEAR PHYSICAL SYSTEMS

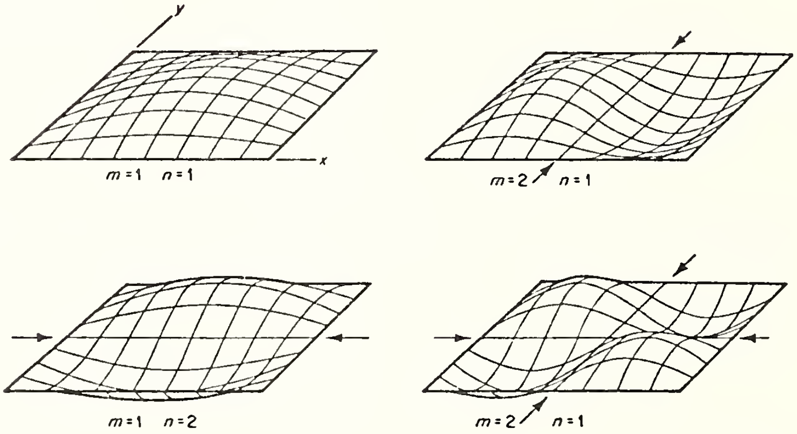

Shapes of the first four normal modes of a rectangular membrane. Arrows point to the nodal lines.

Figure 4

THE $\Phi\ (x,x')$ MATRIX FORMED FROM THE FOLLOWING MOTION WILL YIELD A SORTING OUT OF EIGENMOTIONS X AND THEIR RELATIVE WEIGHTS λ.

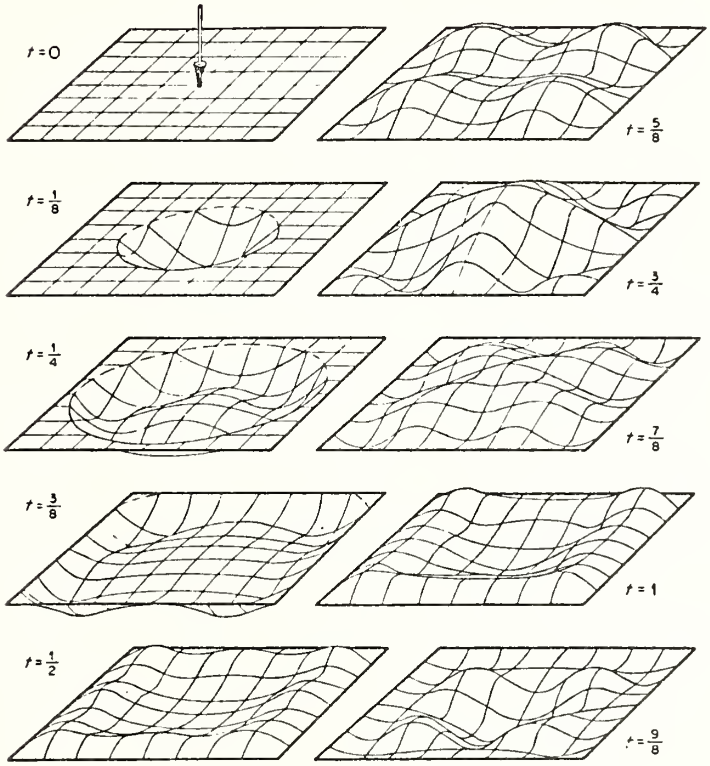

SUCCESSIVE SHAPES OF A RECTANGULAR MEMBRANE STRUCK AT ITS CENTER. TIMES ARE GIVEN IN TERMS OF FRACTIONS OF THE FUNDAMENTAL PERIOD OF VIBRATION.

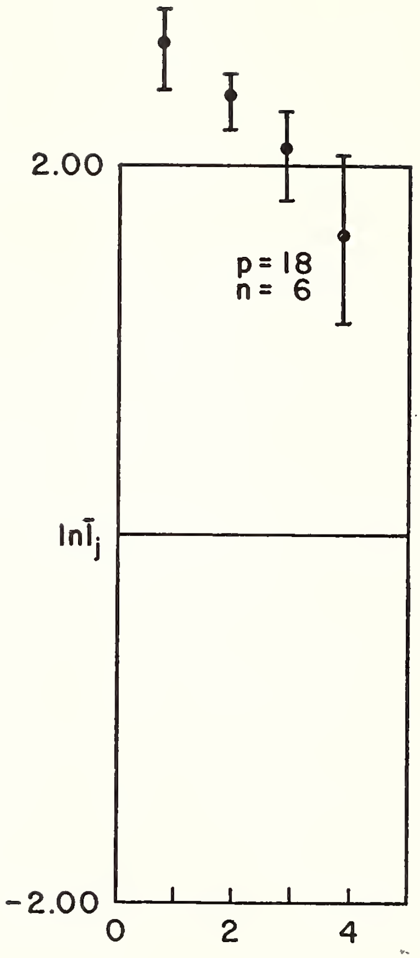

FOR P = 18 DATA POINTS AND SAMPLE SIZE N = 6 THERE ARE NOT 18 NONZERO AVERAGE EIGENVALUES, BUT ONLY FOUR, AS FOUND IN THIS MONTE CARLO EXPERIMENT OF 100 REALIZATIONS.

Figure 6

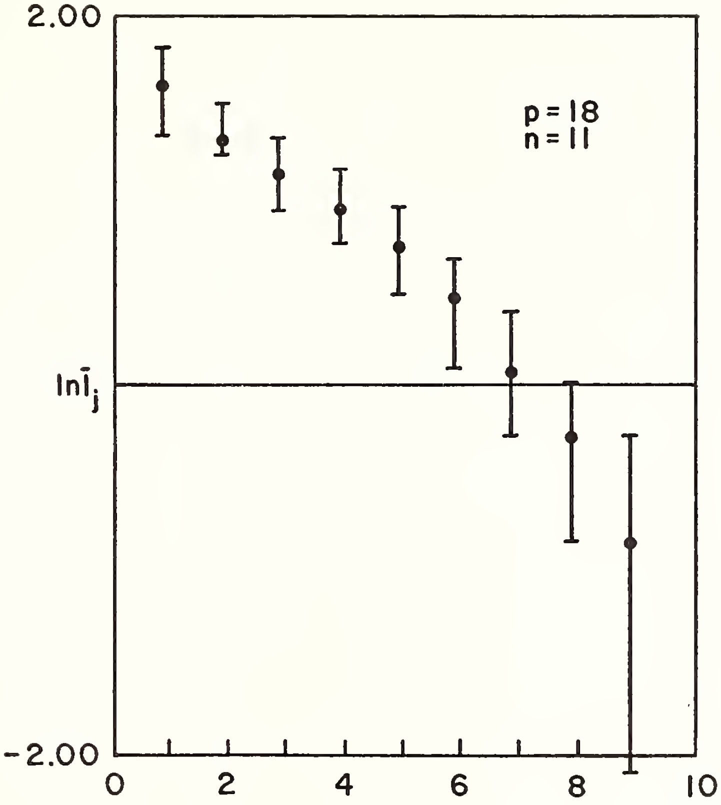

INDICATING DEGENERACY OF EIGENVALUES WHEN $n < p + 3$. GENERALLY THERE WILL BE $n - 3$ NON DEGENERATE MOST PROBABLE EIGENVALUES.

Figure 7

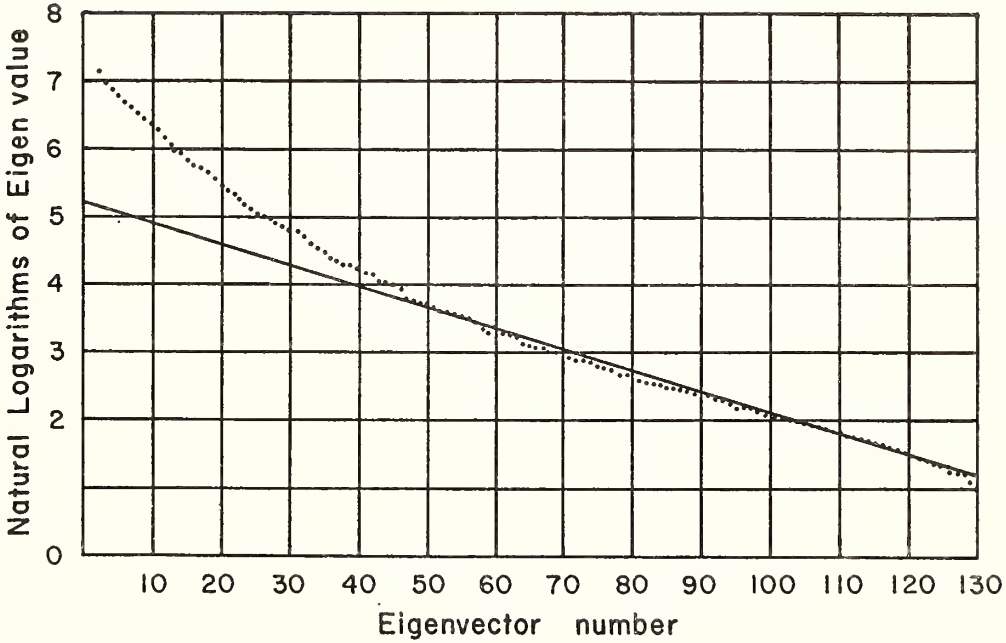

SHOWING EXPONENTIAL DECAY OF EIGENVALUES FOR LARGE P.

(FROM CRADDOCK & FLOOD, 1969).

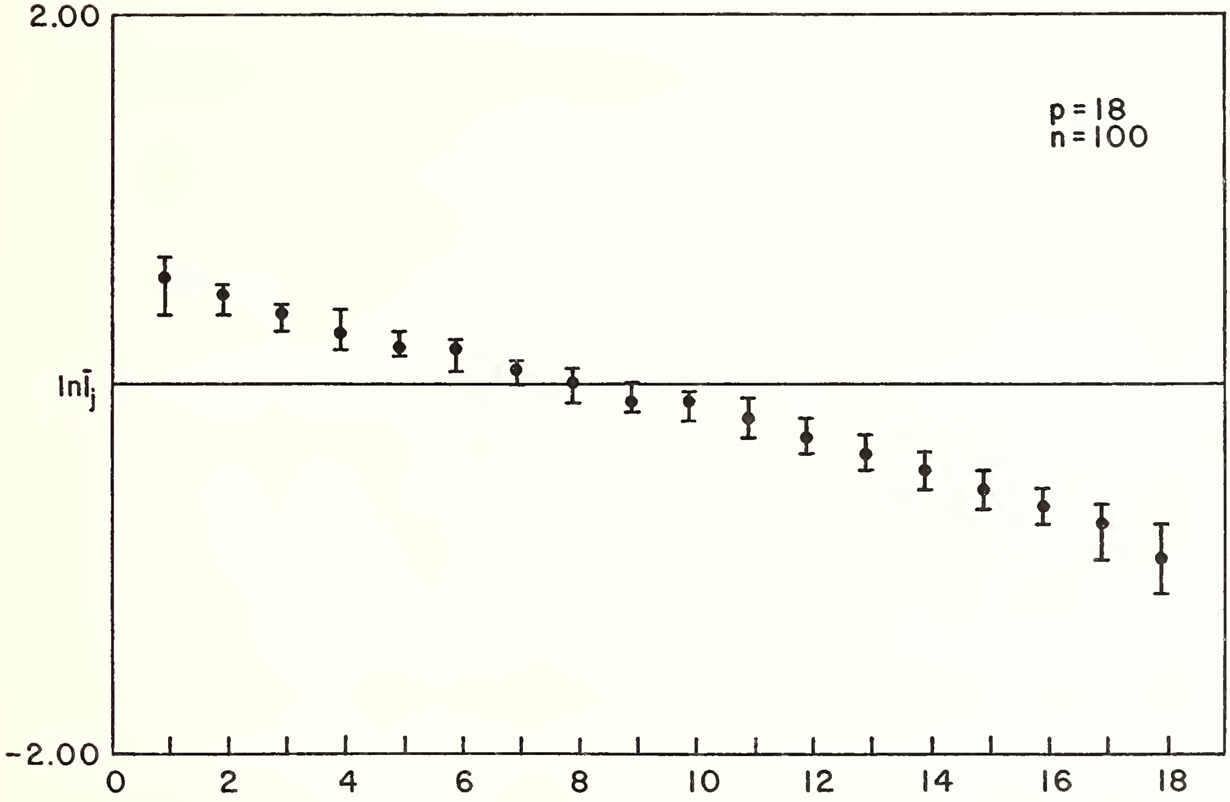

MONTE CARLO VERIFICATION OF EXPONENTIAL DECAY OF EIGENVALUES (100 REALIZATIONS).

Figure 9

CLASSICAL THEORY OF EIGENVALUES OF A RANDOM COVARIANCE MATRIX

is based on the formula for the joint probability density function of the eigenvalues λ_i:

$$p(\lambda_1, \lambda_2, \ldots, \lambda_p) = \frac{\pi^{\frac{1}{2}^{2}} \left[\prod_{i=1}^{p} \lambda_i^{\alpha} \right] \exp \left\{ -\frac{1}{2} \sum_{i=1}^{p} \lambda_i \right\} \prod_{i<j} (\lambda_i - \lambda_j)}{2^{\frac{1}{2}p(n-1)} \prod_{i=1}^{p} \left\{ \Gamma\left(\frac{n-i}{2}\right) \Gamma\left(\frac{p+1-i}{2}\right) \right\}}$$

with $\alpha = \frac{1}{2}(n - p - 2)$.

Only approximate formulas for various statistical tests of the λ_i exist, and are inadequate for ranges of n and p found in meteorology and oceanography.

Consequently we must generally resort to Monte Carlo experiments to determine the statistics of the λ_i. There are some exceptions, as in the case of the most probable eigenvalues deduced from the above formula.

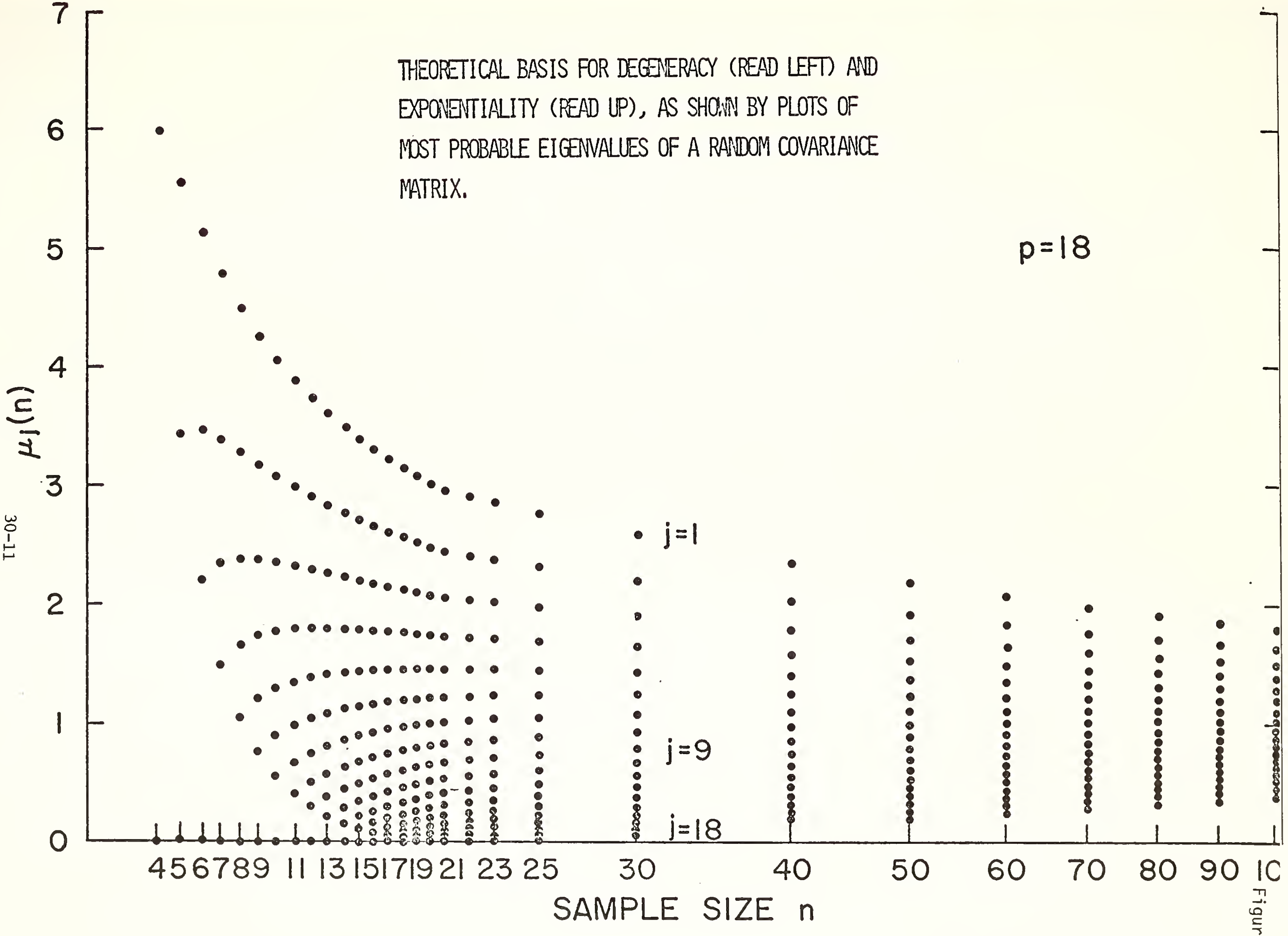

THEORETICAL BASIS FOR DEGENERACY (READ LEFT) AND EXPONENTIALITY (READ UP), AS SHOWN BY PLOTS OF MOST PROBABLE EIGENVALUES OF A RANDOM COVARIANCE MATRIX.

Figure 10

Figure 11

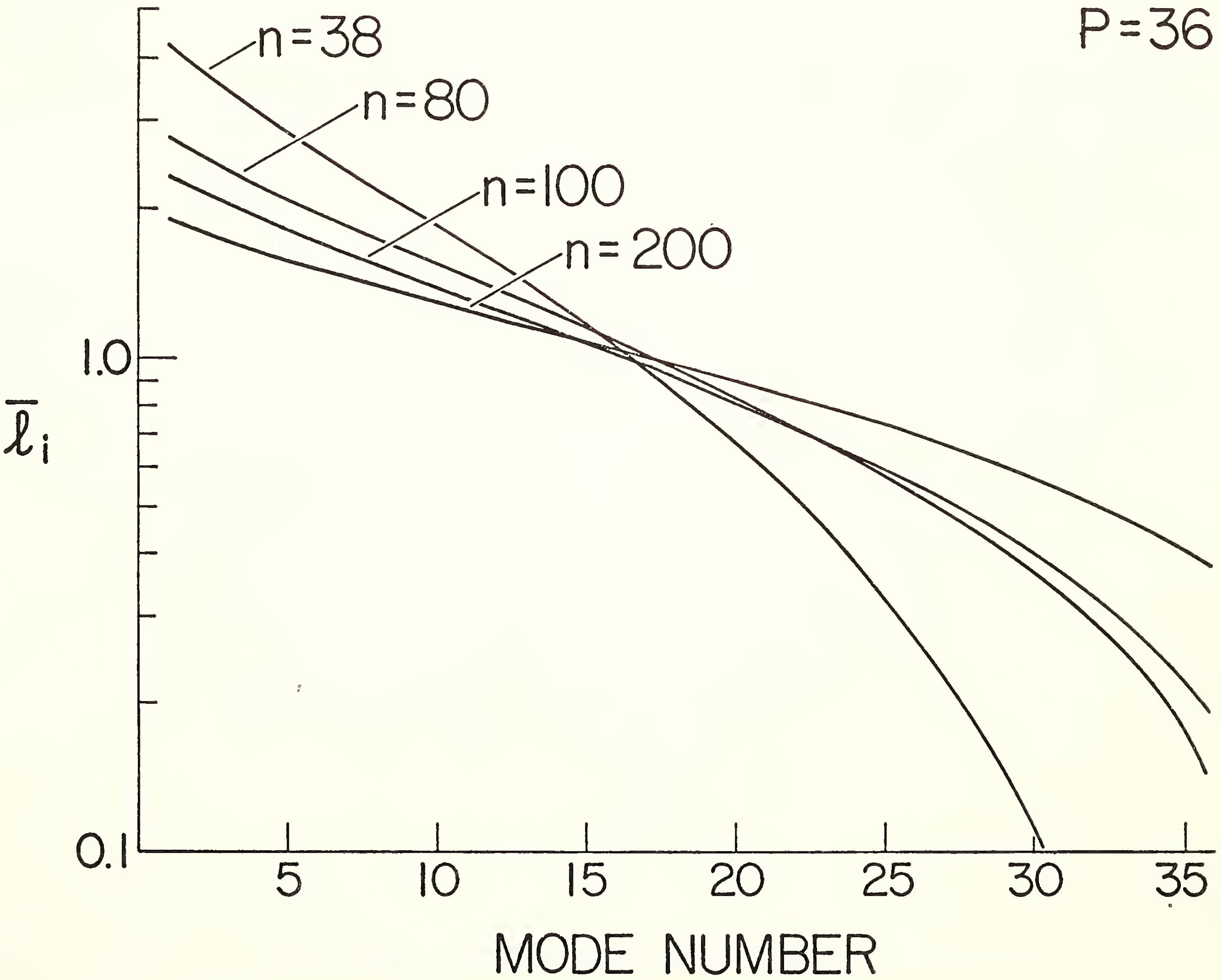

MEAN EIGENVALUES OF A RANDOM COVARIANCE MATRIX. FROM 100 REALIZATIONS OF A MONTE CARLO EXPERIMENT.

Figure 12

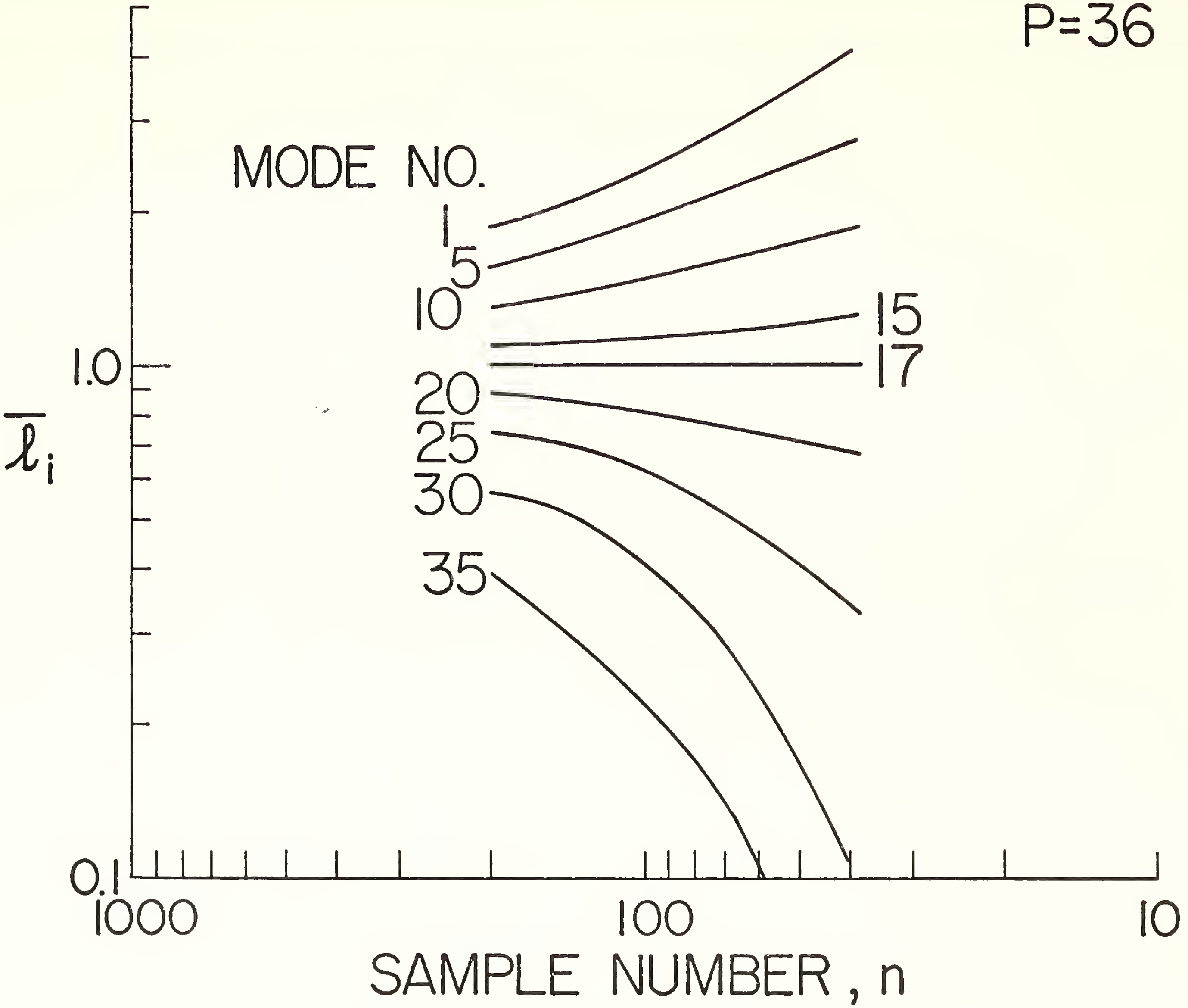

MEAN EIGENVALUES OF A RANDOM COVARIANCE MATRIX. FROM 100 REALIZATIONS OF A MONTE CARLO EXPERIMENT.

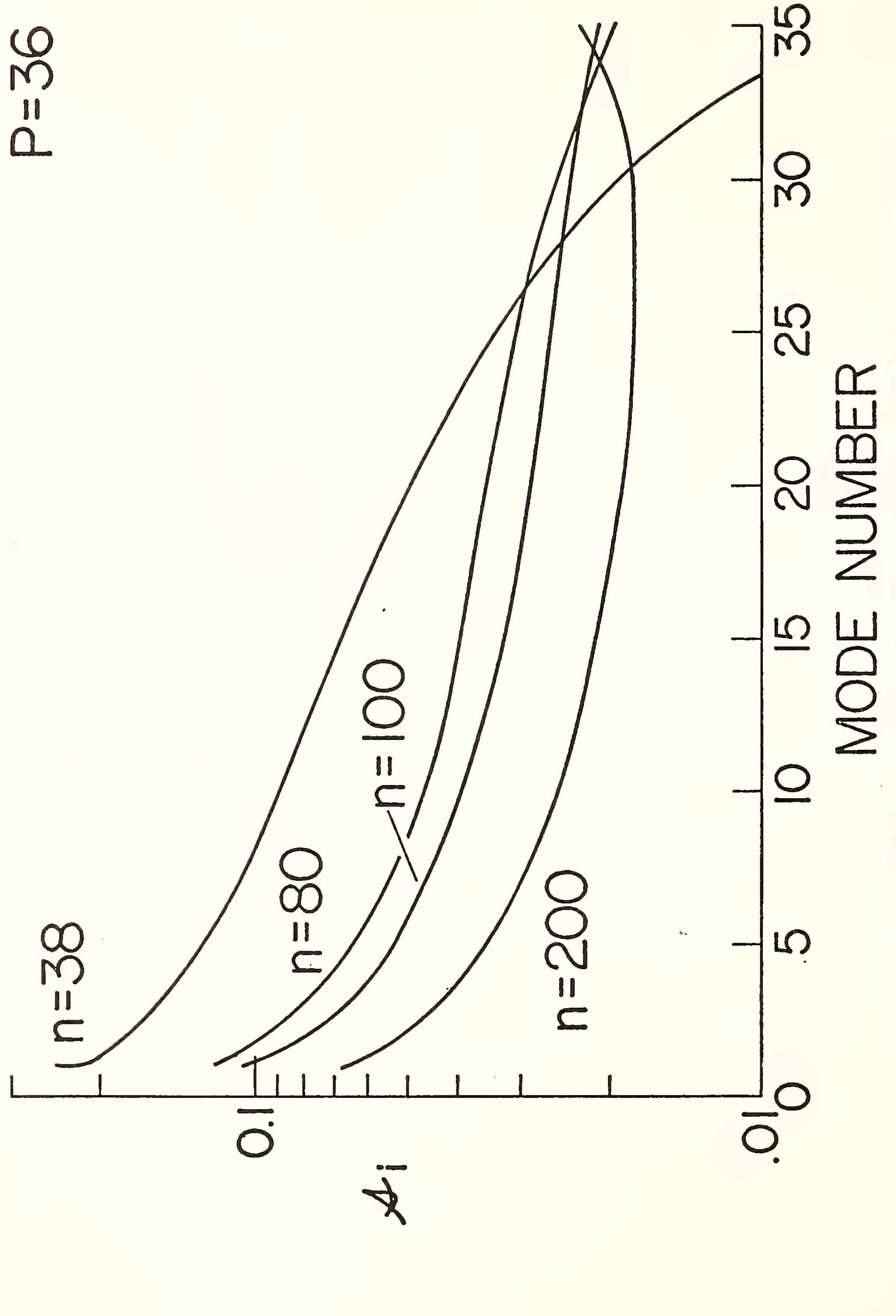

STANDARD DEVIATIONS OF THE MEAN EIGENVALUES OF A RANDOM COVARIANCE MATRIX. FROM 100 REALIZATIONS OF A MONTE CARLO EXPERIMENT.

Figure 14

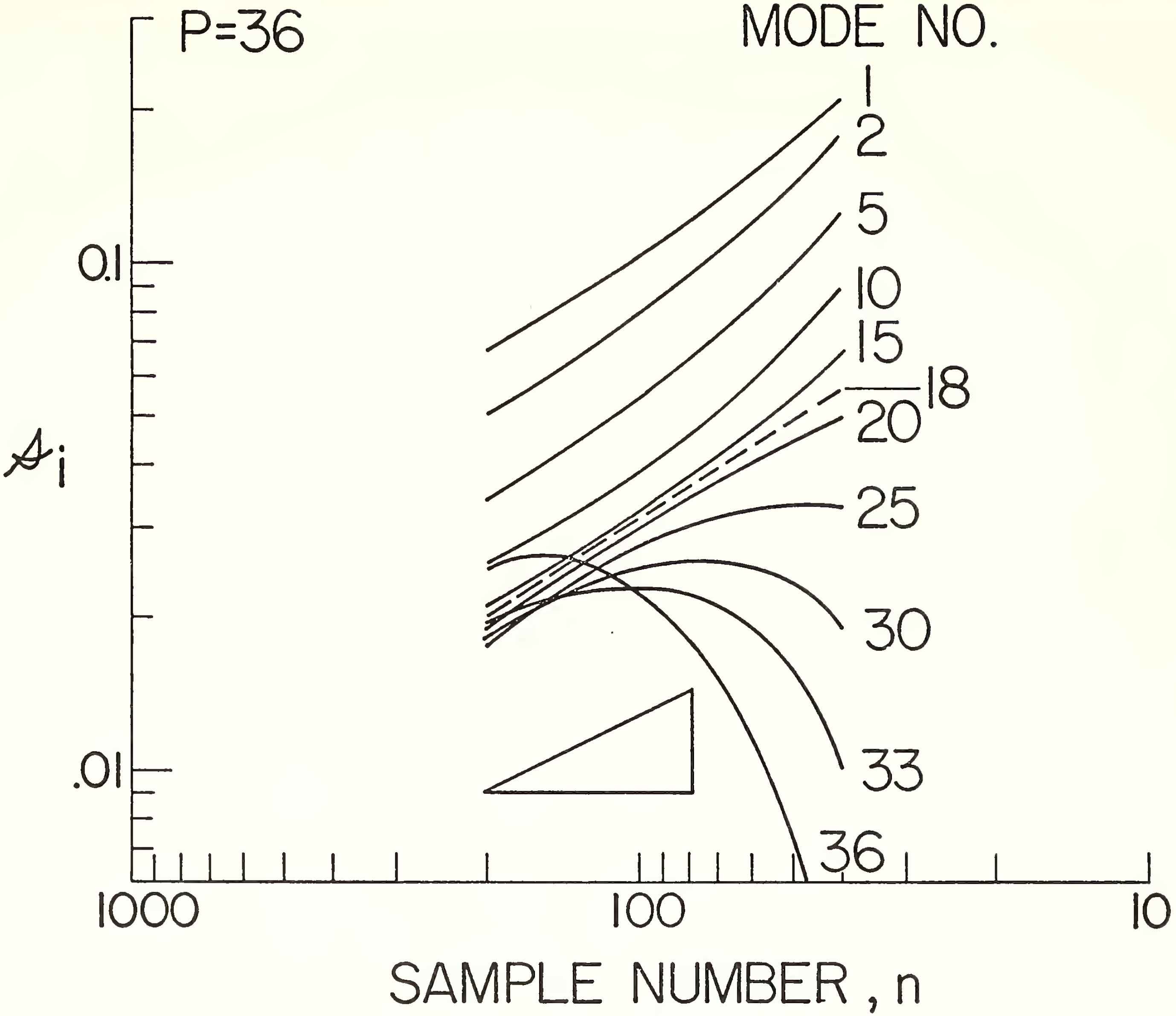

STANDARD DEVIATIONS OF THE MEAN EIGENVALUES OF A RANDOM COVARIANCE MATRIX.

FROM 100 REALIZATIONS OF A MONTE CARLO EXPERIMENT.

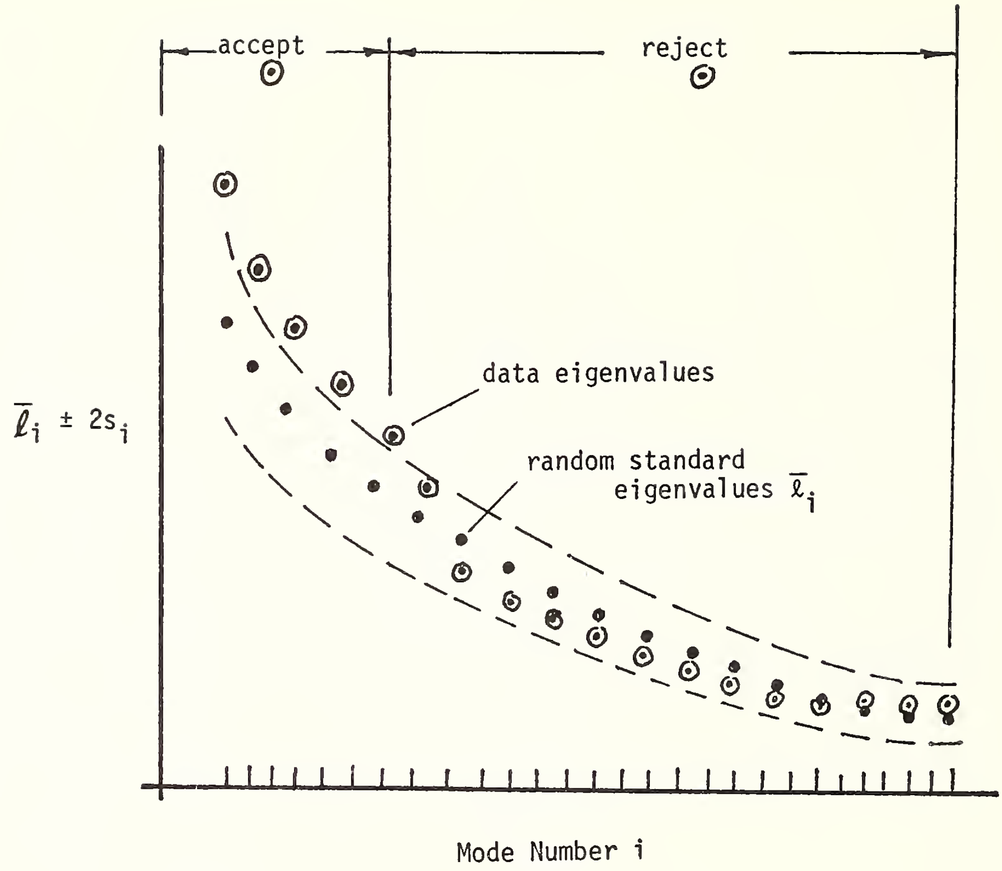

EXAMPLE OF A STOPPING RULE FOR EIGENVALUES OF AN EOF ANALYSIS. BASED ON MONTE CARLO EXPERIMENTS FOR P = 18. FIRST FOUR DATA EIGENVALUES ACCEPTED AS SIGNIFICANT ON 95% LEVEL RELATIVE TO RANDOM EIGENVALUES OF SAME P AND SAMPLE SIZE N.

APPLICABILITY OF ANALOG METHODS TO DIAGNOSIS OF CLIMATE FLUCTUATIONS

by

T. P. Barnett

Consider the first eigenvector (property) of a climate state vector computed for winter seasons only. This map shows contemporaneous relations existing between the anomalies of 700 mb height, thickness, sea-surface temperature and rainfall. This particular pattern is intriguing from a number of points of view. For instance, the relations between 700 mb height and sea-surface temperature over the Pacific region have been oft described by Namias. He has also invoked Rossby wave dynamics to conclude that subsequent "teleconnections" will be associated with these climatic perturbations in the Pacific; namely the occurrence of, say, an unusual low pressure in the Pacific will result in amplification of the high pressure ridge over the west coast of North America and subsequent lower-than-normal pressure (and temperature) over the southeastern U.S. In fact, this is exactly the pattern observed in the figure. In addition we see that there is a definite perturbation in the rainfall field that accompanies these temperature/pressure fluctuations. Quite apart from Namias, Van Loon has discussed the existence of a "seesaw" affect resulting in oscillations of pressure and temperature between Greenland and the European continent. Van Loon has also gone on to show that these variations are related to the "North Atlantic oscillation" as first described by Walker. We now see that both of the descriptions offered by the above authors fit into a single pattern of climatic variability. That is, the above discussions must be considered in a single context since the variability they described occurs simultaneously.

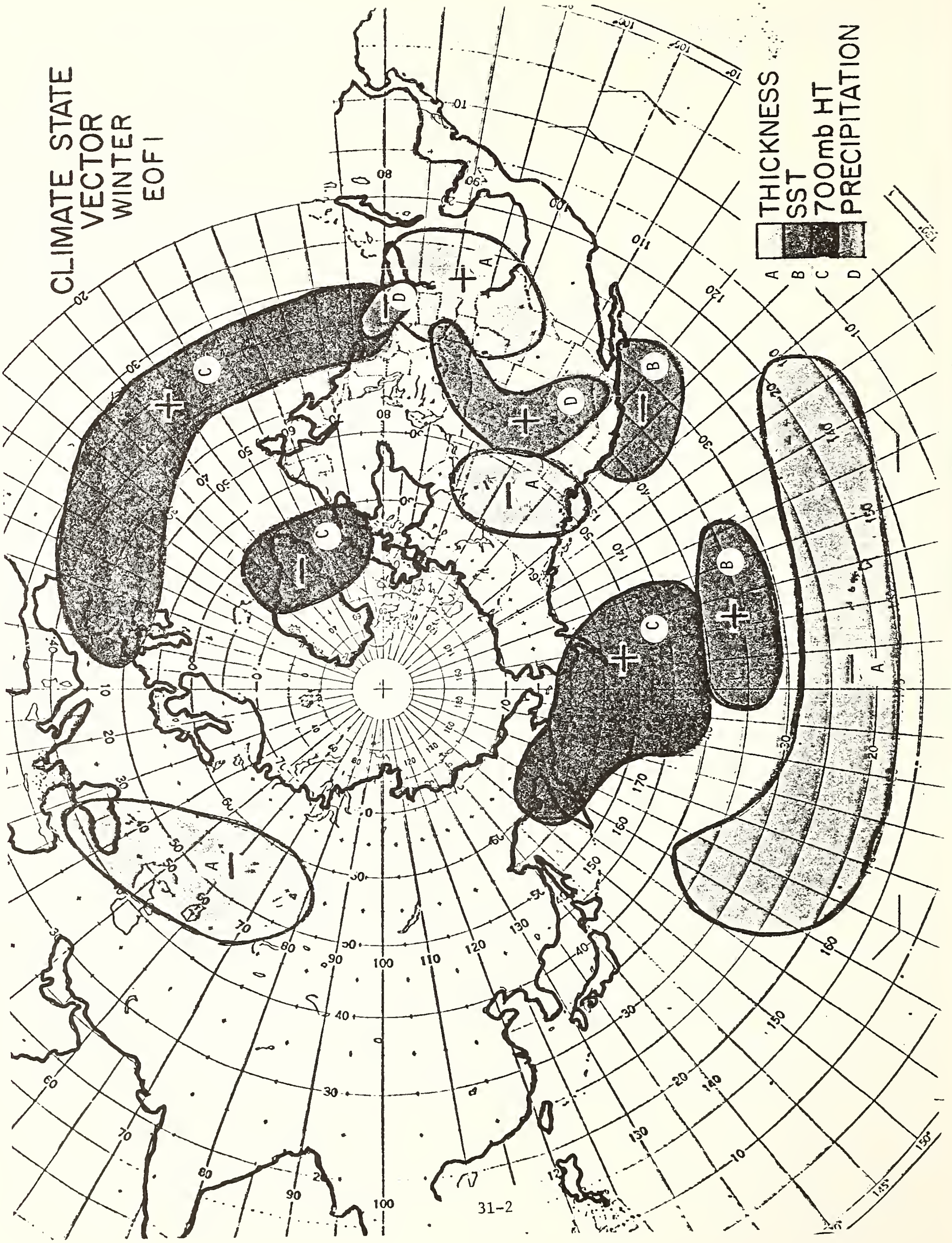
CLIMATE STATE
VECTOR
WINTER
EOF I
A THICKNESS
B SST
C 700mb HT
D PRECIPITATION

Objective Winter Temperature Predictions

Robert P. Harnack
Cook College
Rutgers - The State University of New Jersey
New Brunswick, N.J. 08903

Various statistical methods have been employed in order to make objective mean winter temperature predictions for the eastern and central U.S. based on physical-statistical relationships proposed in the literature. The purpose has been to test the reliability of some of the predictors deemed important in the context of seasonal temperature prediction by using the available climatic data base.

The most recent work in this regard involves the use of area averaged winter temperatures as the predictand, principal components of sea surface temperature and 700 mb height fields as the predictors, and multiple linear regression as the statistical method relating the predictors to predictand.

Fig. 1 describes the data reduction of the November SST and northern hemisphere 700 mb height fields accomplished by the use of principal component analysis. Fig. 2 gives the groupings of the predictor types used in the various screening runs. In addition to the principal components, a southern oscillation index as defined by P.B. Wright was also used as a predictor variable.

Fig. 3 summarizes winter temperature category verifications (below normal, near normal, above normal) based on winter temperature forecasts for each of nine areas east of the Rocky Mountains for five recent winters (45 forecasts in total) obtained by applying the regression equations which were derived using data from the previous 23 years (1949-71). The table has been divided into four sections: the top most portion gives verifications for category forecasts made for winter periods ranging in length from December only to the four-month period composed of December to March; the second portion gives verifications for only the December-February period using selected subsets of the total number of predictors; the third portion gives verifications for December-February forecasts based on persistence and climatology; and the last portion gives comparable verification statistics for subjective forecasts made by the Long Range Prediction Group.

The major points inferred from comparing verification statistics in the table are:

1. The forecasts improved as the length of winter period increased. The December only prediction model showed no skill compared to an assumed random chance mean percentage correct of 33 percent.

2. Forecasts made using SST only showed good skill while forecasts made using circulation only and reduced number of components showed no skill.

3. Persistence forecasts for the five most recent winters were superior to other methods, however, when the persistence method was applied to the full 46 year sample the verification statistics indicate only slight skill. The same conclusion can be made for the climatological contingency method.

4. Verification of the Long Range Prediction Group forecasts, made to conform to the geographical areas used here and 3 group temperature categories, showed only slight skill in terms of correct category forecast but rarely was in error by more than one category.

Figures 4 through 13 show the category forecast and observed maps for the winters of 1975-76 and 1976-77. These show that the SST prediction model was the best at discriminating between the mild winter of 1975-76 and the cold winter of 1976-77.

Figure 14 lists the predictors and their frequency of selection in the regression runs for predictors selected in the first 3 steps of the equations derived for the December-February winter period. Maximum possible frequency of selection is 9. For the all predictors regression this listing indicates that circulation and SST predictors were of comparable importance.

The following figures show diagnostic work done for investigating the possible physical links between some of the selected predictors and winter temperatures in the eastern U.S. The predictors selected for investigation here are FHTN7 (figures 13-17), FP2 (figures 18-22), and SOASO (figures 23-28). Figure captions explain the meaning of the analyzed data. The following major points may be summarized from this diagnostic work and related figures:

1. The predictor, FHTN7, represents primarily a meridional circulation pattern of the November 700 mb heights (figure 16) with wavelength of about 80° longitude. This predictor has a positive correlation with winter temperatures in the eastern U.S. (figure 15) so the statistical relationship shown indicates that this predictor represents a persistence circulation feature (see figures 17-19).

2. The predictor, FP2, represents primarily an oscillation in the November Pacific SST field centered at about 40 N, 155 W (see figures 21-23). The positive correlations seen in figure 20 can be explained by reference to figure 24, which indicates that low FP2 values (enhanced SST gradients in latitude band 40-50 N) tends to precede a deepened winter Aleutian low system. Sympathetic tendencies are seen downstream over North America with lower heights in eastern North America relating to low FP2 values.

3. The predictor, SOASO, which is the southern oscillation index as defined by Wright for the August-October period, takes on a value which is closely related to the Eastern Tropical Pacific SST (correlation coefficient of -.84 between SOASO and FTP1). Given the FTP1 spatial pattern, seen in figure 26, this implies that low SOASO values relate to warmer than normal tropical Pacific SST's and high SOASO values relate to cooler than normal tropical Pacific SST's. The positive correlations seen in figure 25 and the sea level pressure maps shown in figures 27-29 further confirm the Bjerknes hypothesis that warm SST's in the Eastern Tropical Pacific tend to precede winters with a deep Aleutian low and equatorally suppressed westerlies in the Eastern Pacific. Additionally, there is a tendency for colder than normal winter temperatures in the southeastern U.S. with this situation, probably due to downstream circulation response over eastern North America.

It should be pointed out in closing that the Eastern Tropical Pacific SST's were above normal and the central Pacific region deemed important for determining the value of FP2 had below normal SST's during the cold winter of 1976-77.

It appears that useful guidance can be obtained for making winter temperature forecasts based on the use of objective methods and physically plausible statistical relationships.

Fig. 1. Data reduction by principal component analysis used for predictive purposes

Data type & region (all data for Nov.)	Period	No. of variables	No. of components extracted	Cumulative explained variance	Explained variance by component 1	2	3
Eastern Tropical Pacific SST	1949-71	34	5	79.6	51.2	11.0	7.5
Eastern North Pacific SST	1947-71	50	7	82.0	27.9	17.4	10.8
North Atlantic OWS SST	1949-71	7	2	57.0	29.4	27.7	
N. Hemisphere 700 mb Heights	1947-71	95	8	82.4	19.4	15.2	11.5

Fig. 2. Potential predictors used for screening

Predictor model	Predictor types	Variable names		Total number of predictors
Fall circulation and Nov. SST	N.H. 700 mb hts (Nov)	FHTN1-FHTN8		8
	Pacific SST (Nov)	FP1-FP7		7
	Trop. Pacific SST(Nov)	FTP1-FTP5		5
	Atlantic OWS SST (Nov)	FA1-FA2		2
	Southern oscillation (Aug-Oct)	SOASO		1
			Total	23
Nov. SST only	Pacific SST (Nov)	FP1-FP7		7
	Trop. Pacific SST (Nov)	FTP1-FTP5		5
	Atlantic OWS SST (Nov)	FA1-FA2		2
			Total	14
Fall circulation only	N.H. 700 mb hts (Nov)	FHTN1-FHTN8		8
	Southern oscillation (Aug-Oct)	SOASO		1
			Total	9
All predictors - reduced components	N.H. 700 mb hts (Nov)	FHTN1-FHTN6		6
	Pacific SST (Nov)	FP1-FP5		5
	Trop. Pacific SST (Nov)	FTP1-FTP3		3
	Atlantic OWS SST (Nov)	FA1-FA2		2
	Southern oscillation (Aug-Oct)	SOASO		1
			Total	17

Fig. 3. Winter temperature category forecast verifications

Predictor types (method)	No. of predictors	Dependent sample	Independent sample	Forecast period	No. of categories defined	Mean percent correct	Mean percent 2 cat. miss (conditional)	Mean percent correct given obs "extreme"
Fall circulation and Nov. SST (REG)	23	1949-71(23 yrs)	1972-76(5 yrs)	Dec	3	18	29	22
Fall circulation and Nov. SST (REG)	23	1949-71(23 yrs)	1972-76(5 yrs)	Dec-Jan	3	44	27	53
Fall circulation and Nov. SST (REG)	23	1949-71(23 yrs)	1972-76(5 yrs)	Dec-Feb	3	40	17	53
Fall circulation and Nov. SST (REG)	23	1949-71(23 yrs)	1972-76(5 yrs)	Dec-Mar	3	51	13	60
Fall circulation only (REG)	9	1949-71(23 yrs)	1972-76(5 yrs)	Dec-Feb	3	29	27	30
Nov. SST only (REG)	14	1949-71(23 yrs)	1972-76(5 yrs)	Dec-Feb	3	51	26	53
All predictors-reduced components (REG)	17	1949-71(23 yrs)	1972-76(5 yrs)	Dec-Feb	3	22	41	30
Nov. temps (persistence)	1		1972-76(5 yrs)	Dec-Feb	3	58	3	69
Nov. temps (persistence)	1		1931-76(46 yrs)	Dec-Feb	3	40	26	43
Nov. temps (climatological contingency)	1	1931-71(41 yrs)	1972-76(5 yrs)	Dec-Feb	3	42	22	28
Antecedent circulation (NMC-subjective)	?	1947-present	1972-76(5 yrs)	Dec-Feb	3	38	4	40

REG = regression

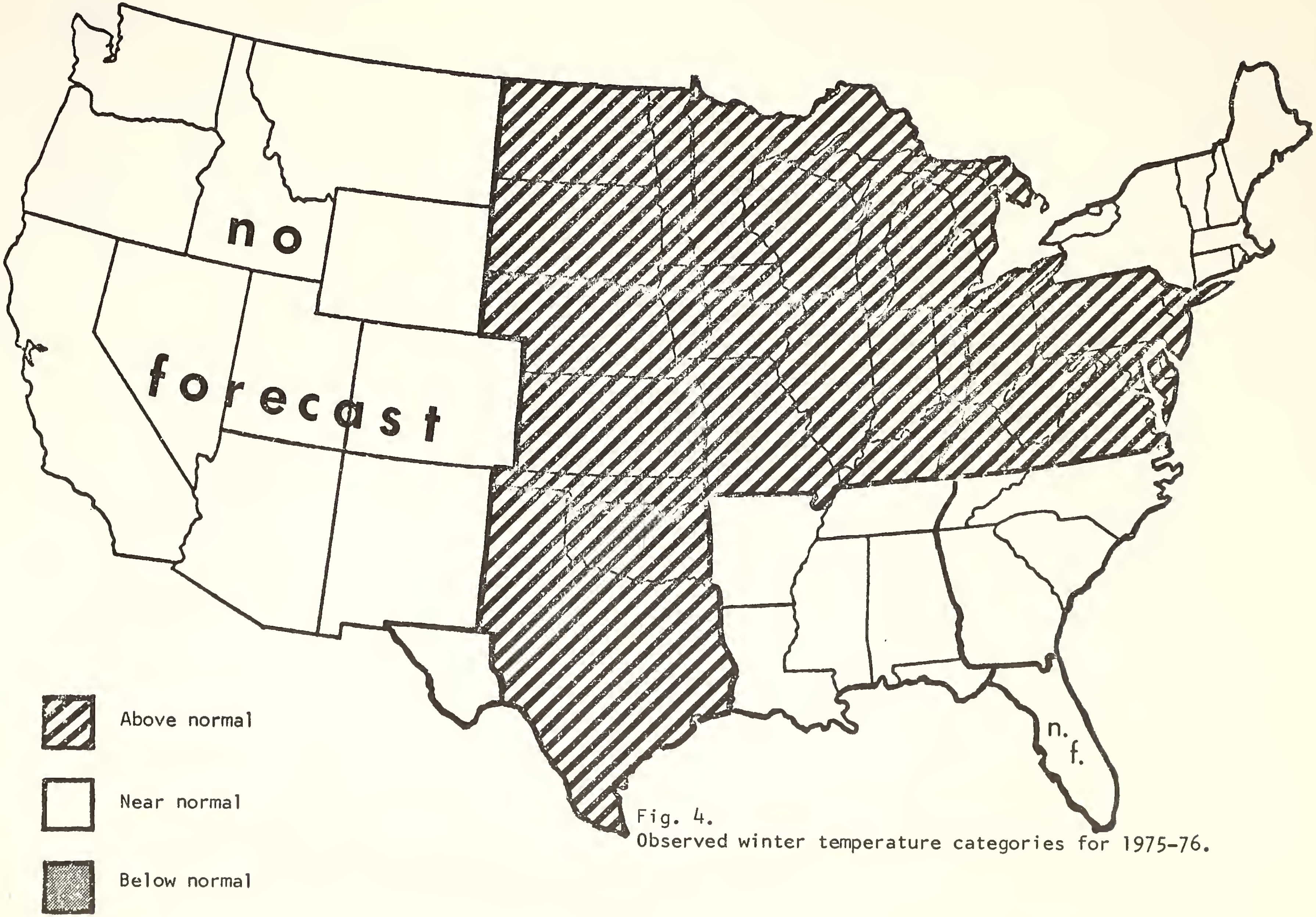

Fig. 4.
Observed winter temperature categories for 1975-76.

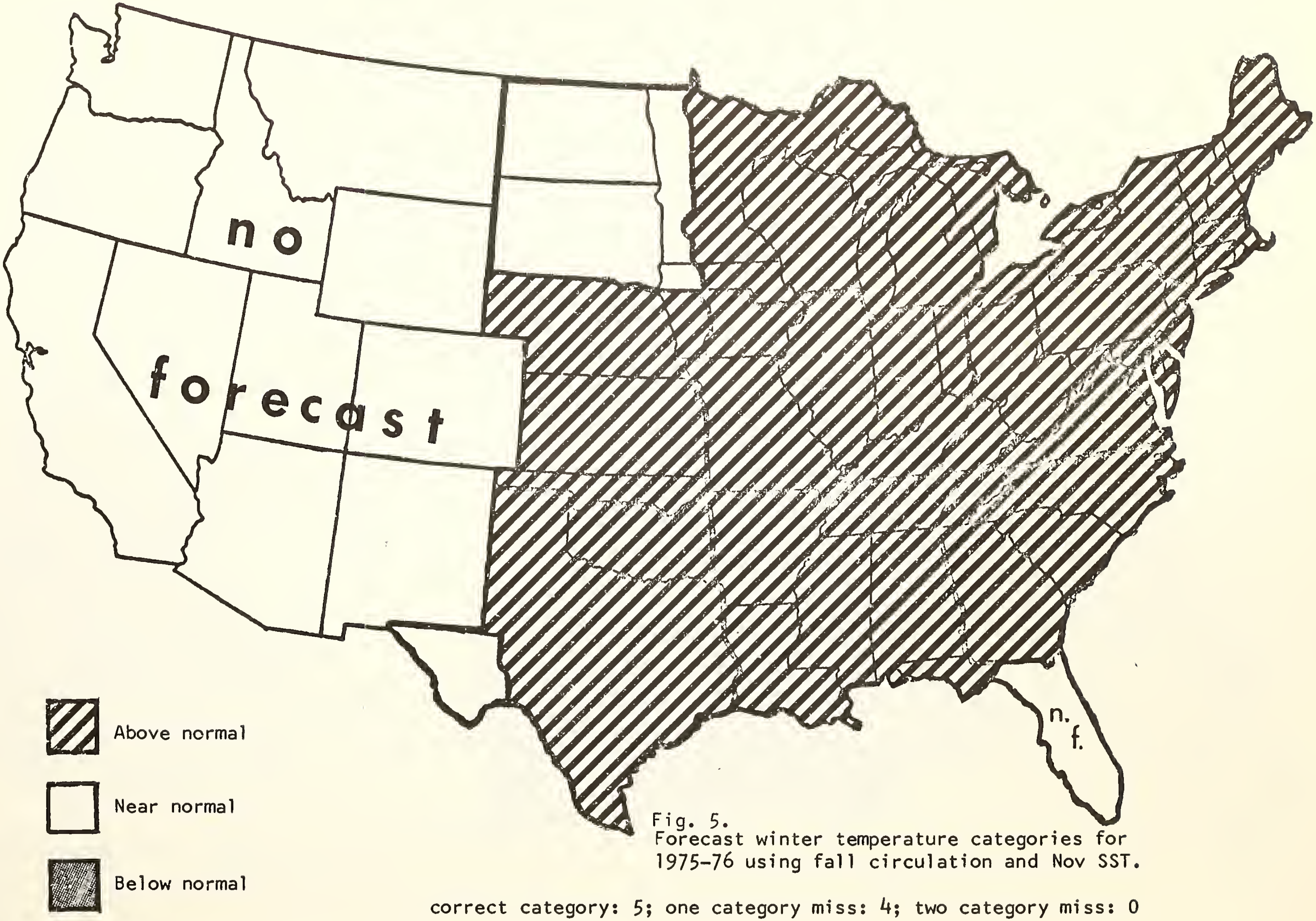

Fig. 5.
Forecast winter temperature categories for 1975-76 using fall circulation and Nov SST.

correct category: 5; one category miss: 4; two category miss: 0

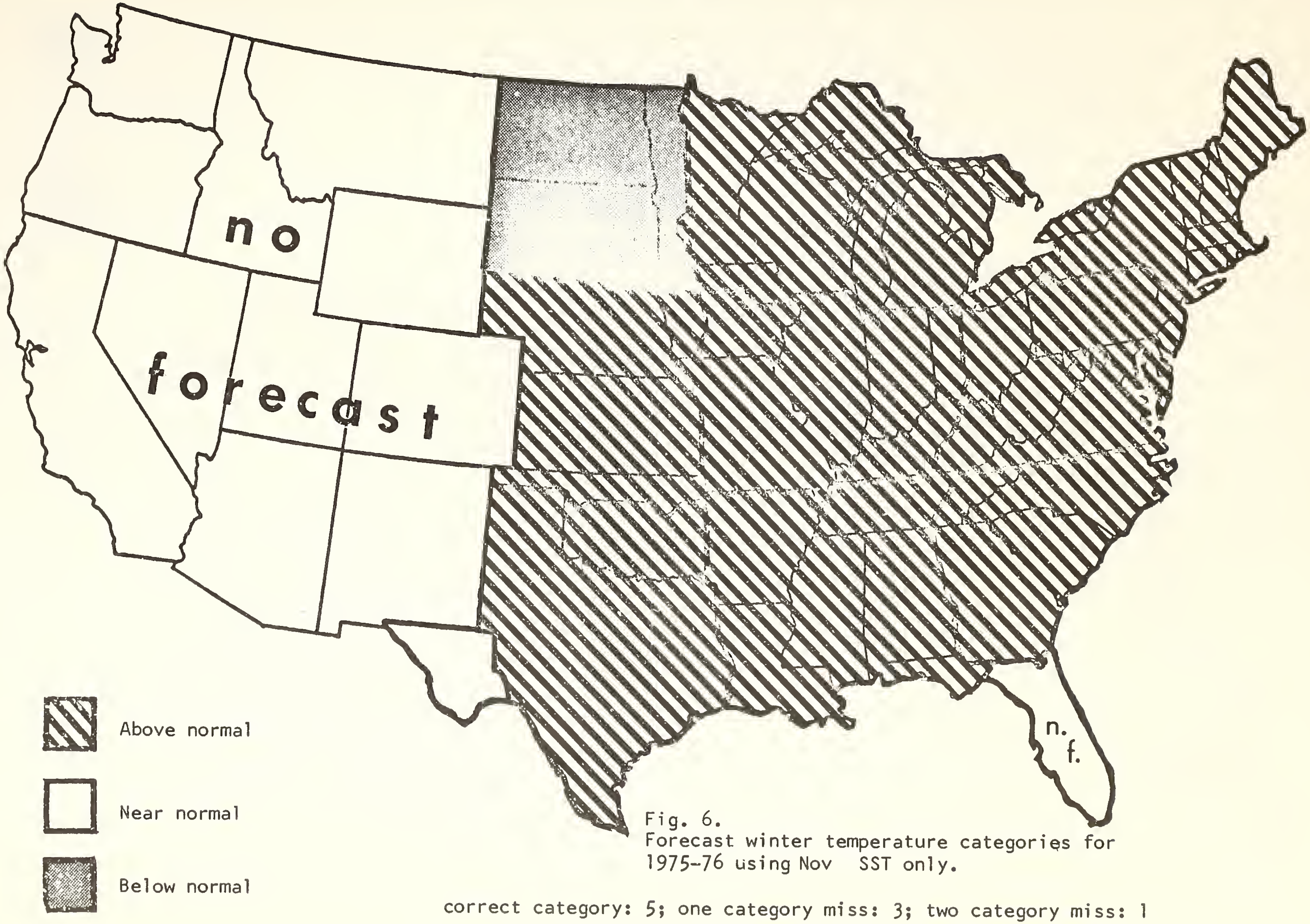

Fig. 6.
Forecast winter temperature categories for 1975-76 using Nov SST only.

correct category: 5; one category miss: 3; two category miss: 1

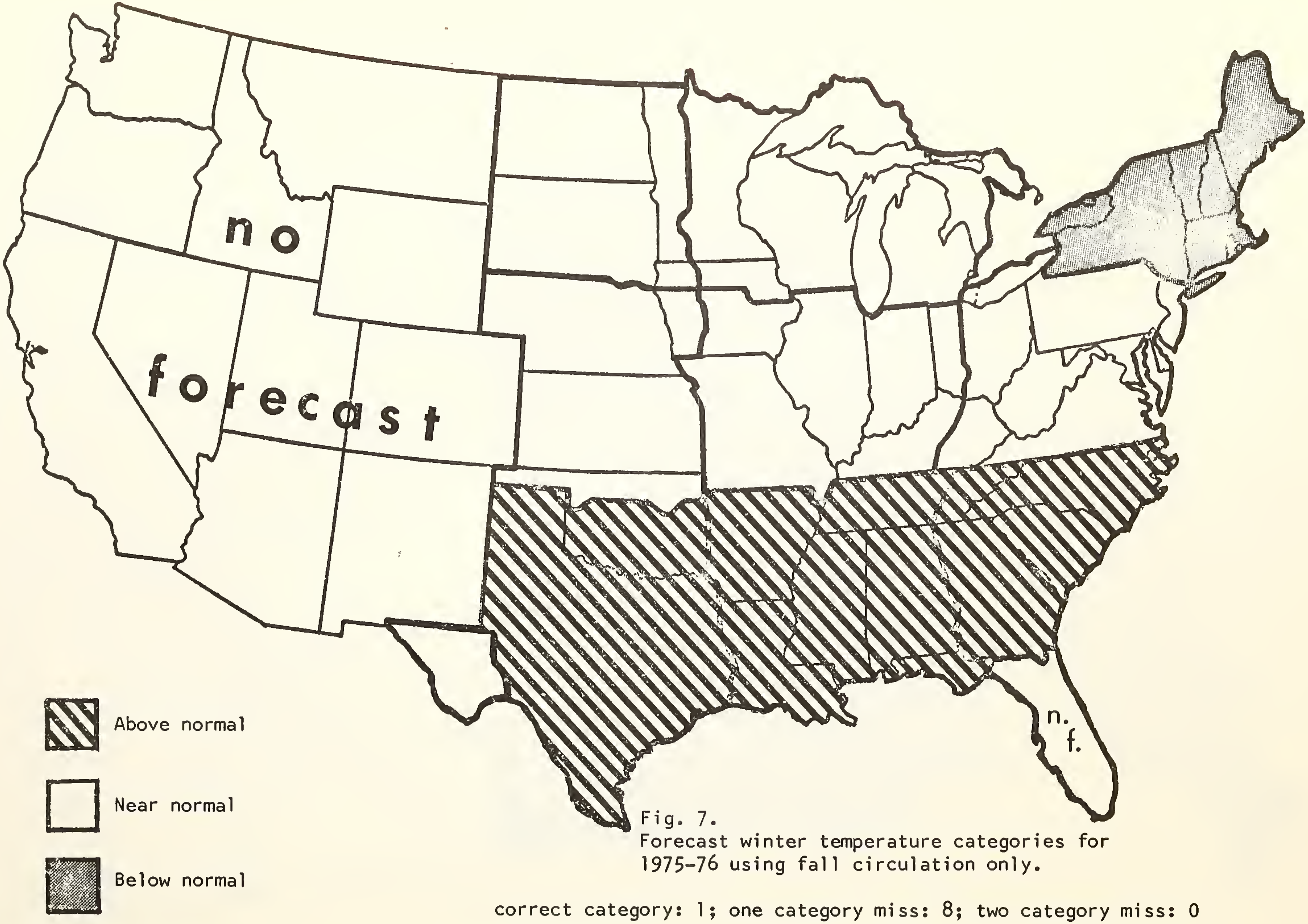

Fig. 7.
Forecast winter temperature categories for 1975-76 using fall circulation only.

correct category: 1; one category miss: 8; two category miss: 0

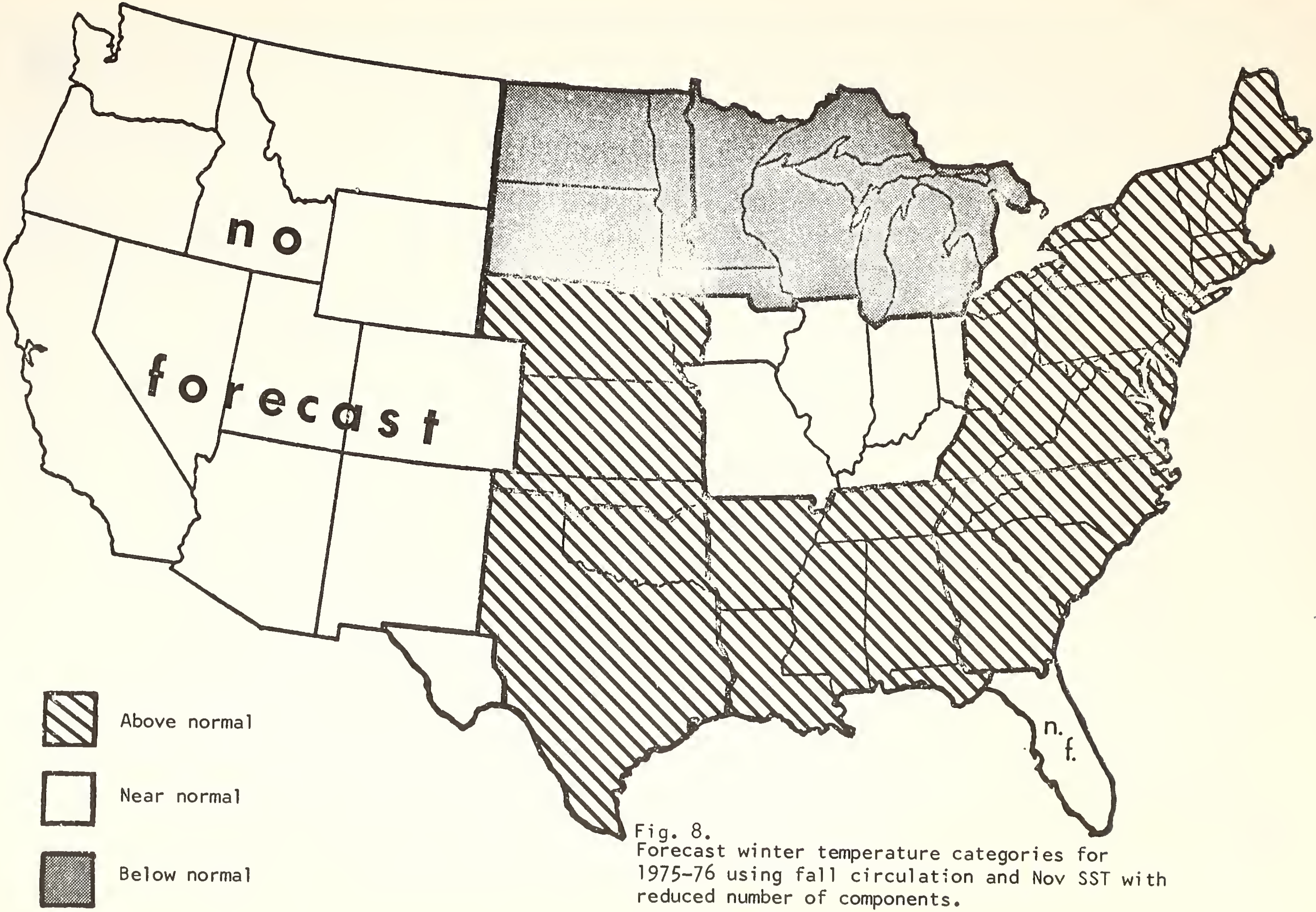

Fig. 8.
Forecast winter temperature categories for 1975-76 using fall circulation and Nov SST with reduced number of components.

correct category: 3; one category miss: 4; two category miss: 2

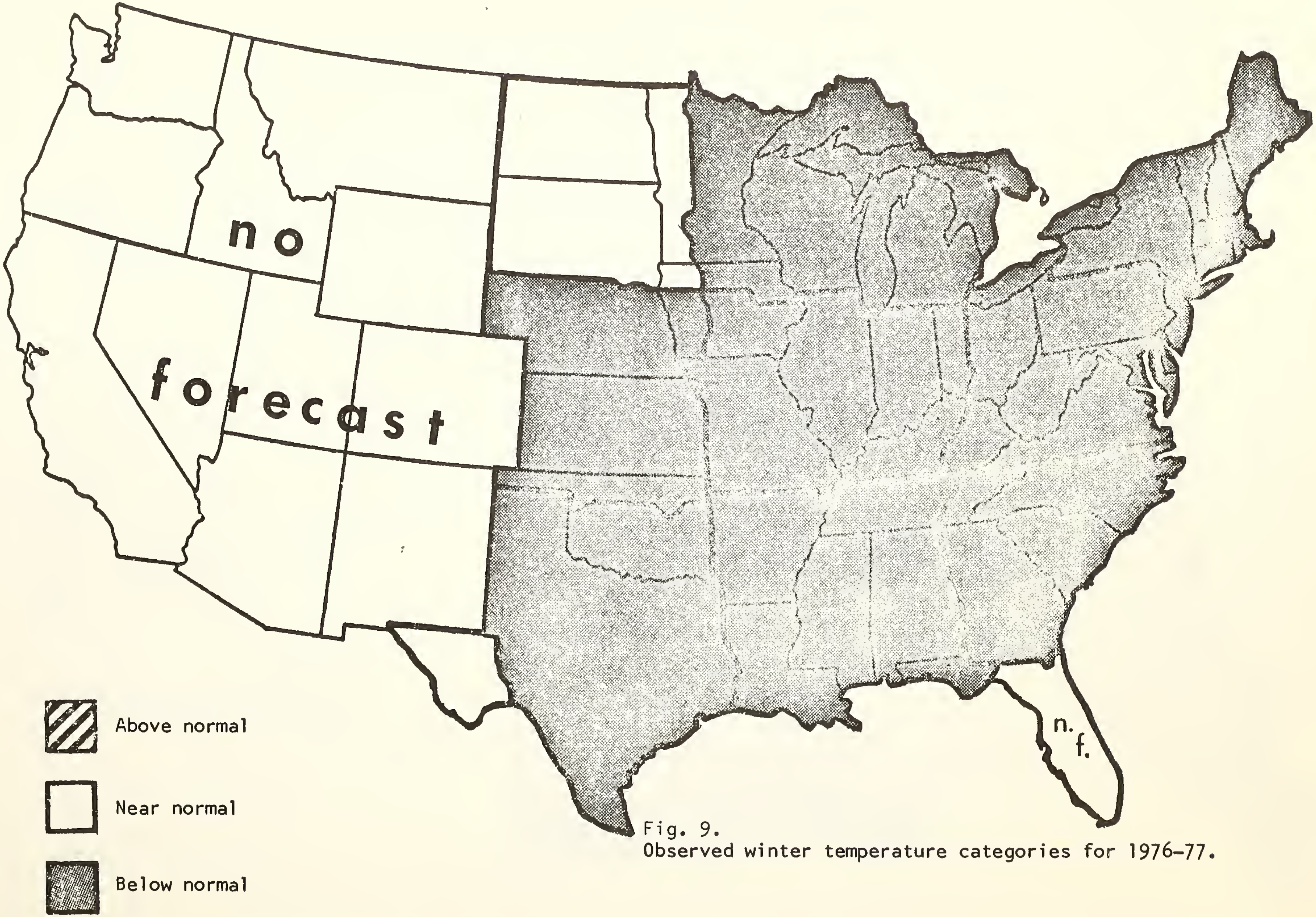

Fig. 9.
Observed winter temperature categories for 1976–77.

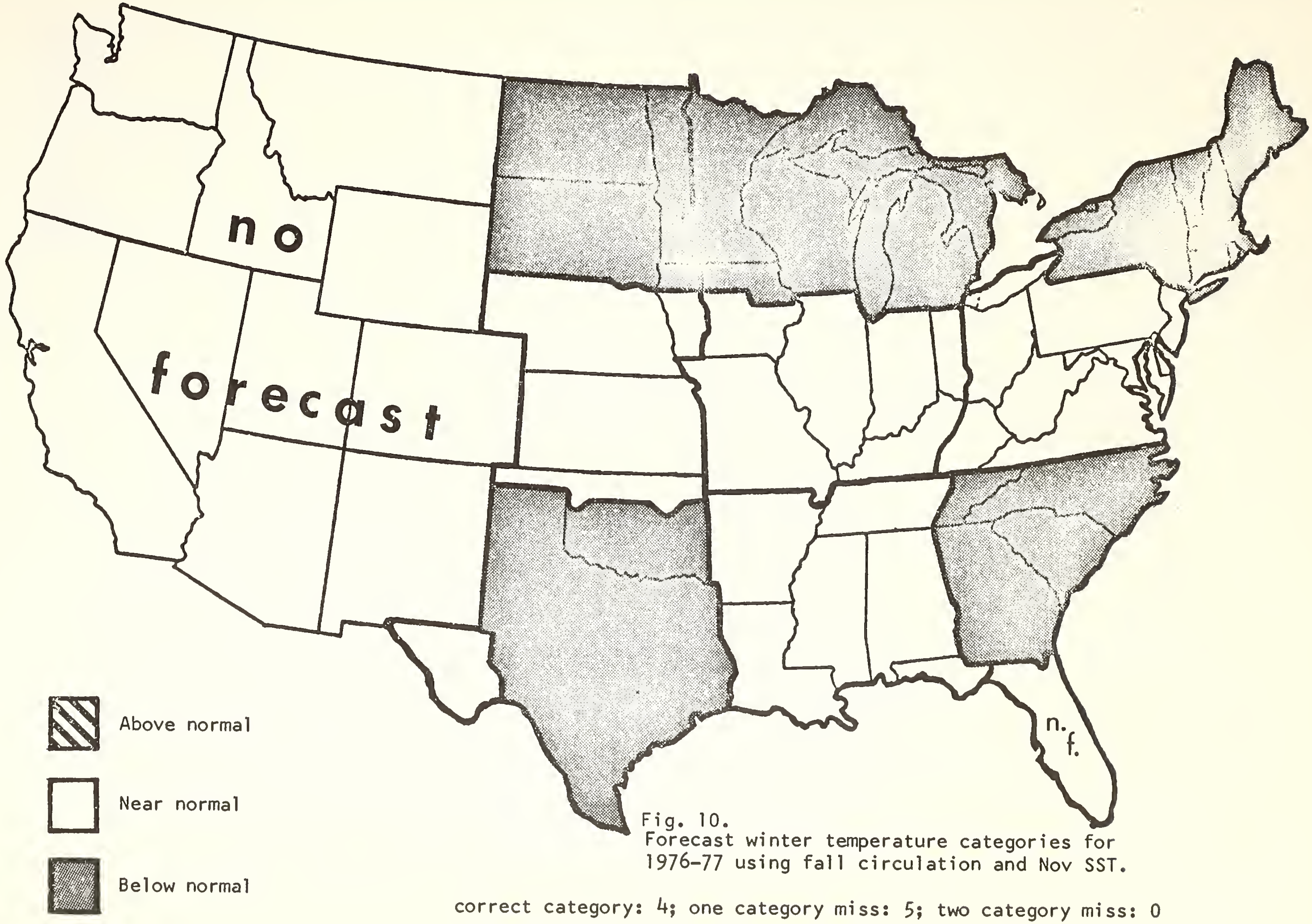

Fig. 10.
Forecast winter temperature categories for 1976-77 using fall circulation and Nov SST.

correct category: 4; one category miss: 5; two category miss: 0

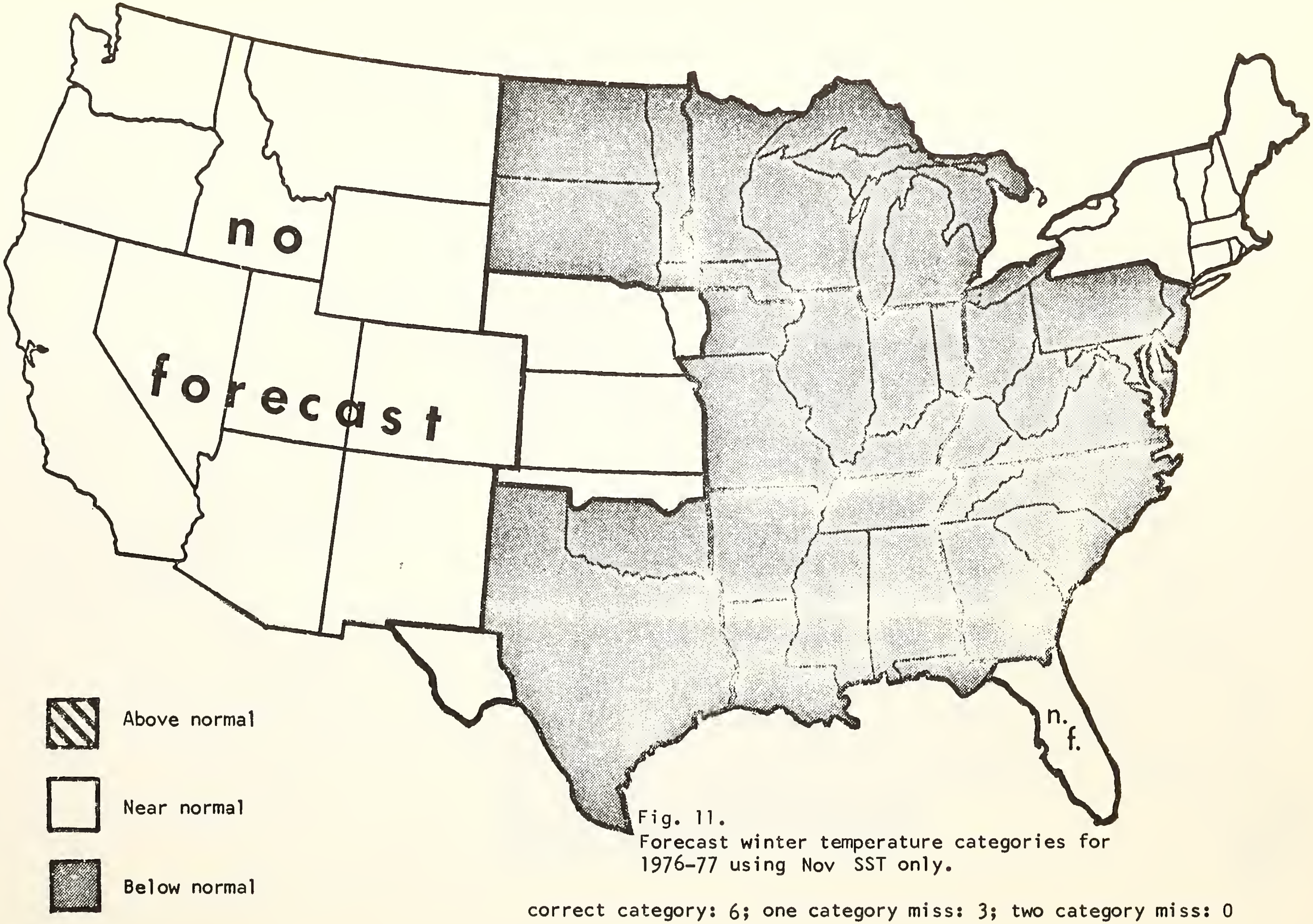

Fig. 11.
Forecast winter temperature categories for 1976-77 using Nov SST only.

correct category: 6; one category miss: 3; two category miss: 0

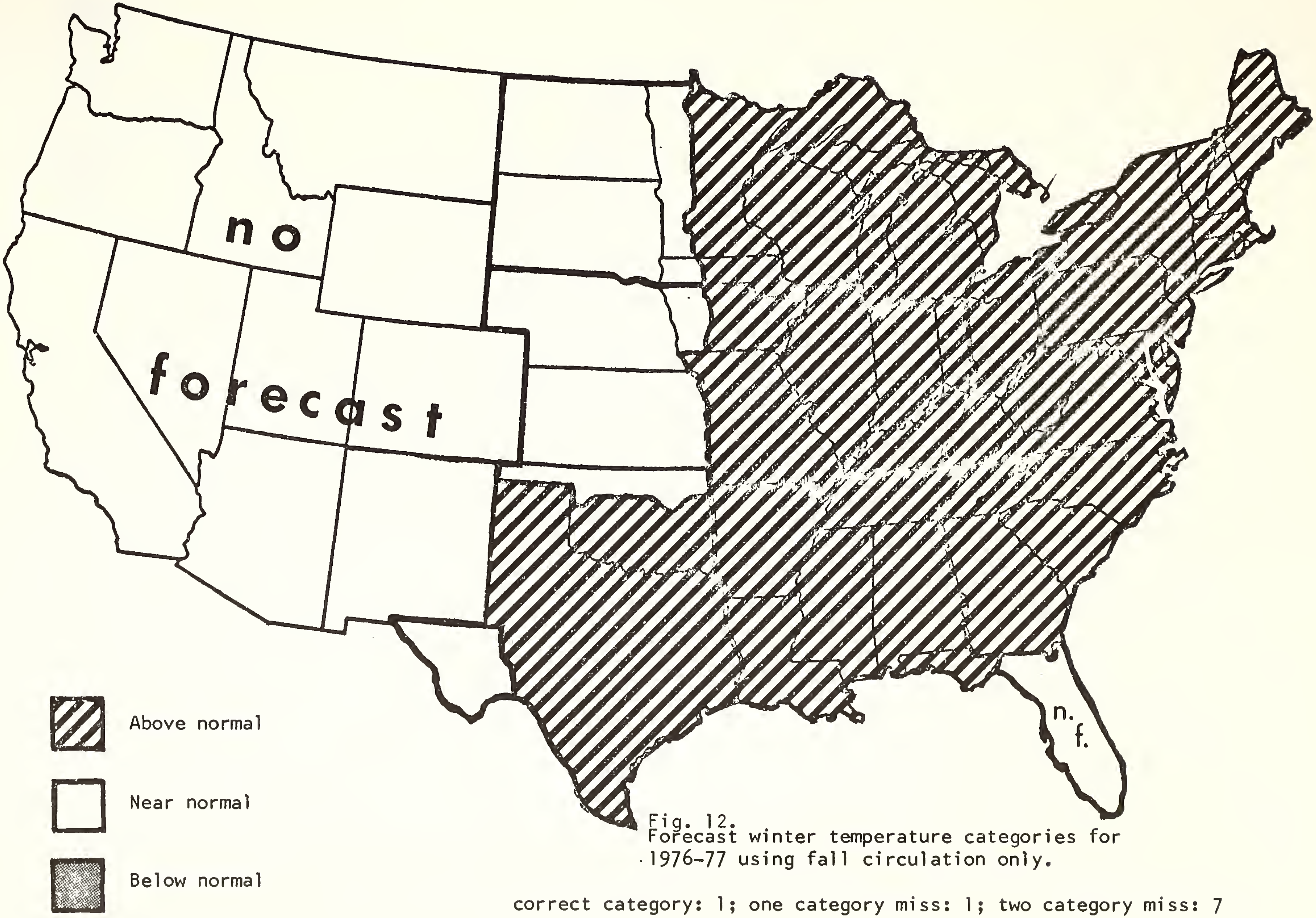

Fig. 12.
Forecast winter temperature categories for 1976-77 using fall circulation only.

correct category: 1; one category miss: 1; two category miss: 7

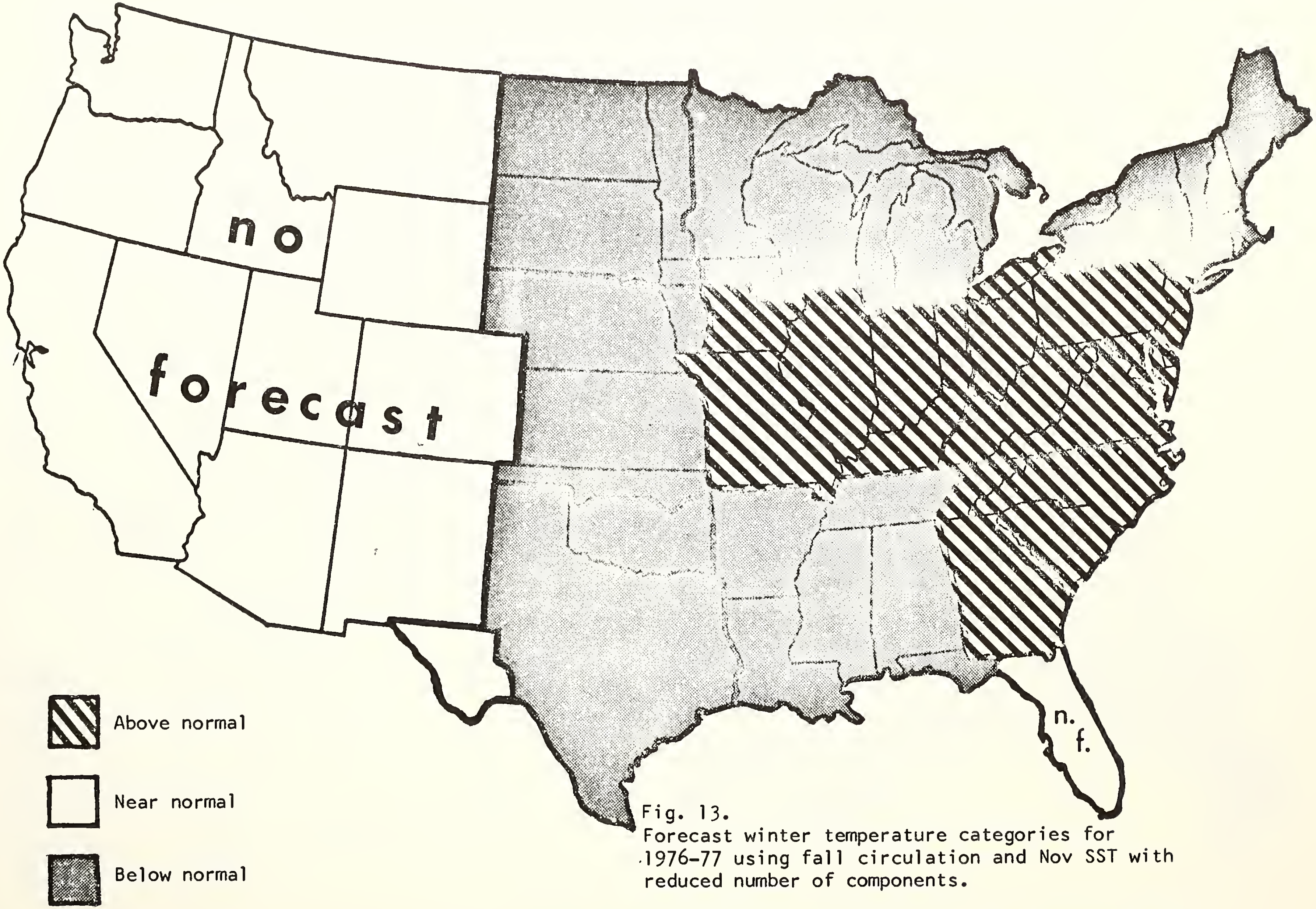

Fig. 13.
Forecast winter temperature categories for 1976-77 using fall circulation and Nov SST with reduced number of components.

correct category: 5; one category miss: 1; two category miss: 3

Fig. 14. List of three most important predictors in regression equations for December-February period

Regression run	Predictors (frequency)
Fall circulation and Nov. SST	FHT7(6), FP2(5), FP3(5), FP7(3), FHT8(3), FHT3(1), FHT4(1), FTP3(1), FTP4(1), FP5(1)
Fall circulation	FHT7(7), FHT4(7), SOASO(4), FHT8(3), FHT2(3), FHT6(2), FHT1(1)
Nov. SST only	FP3(7), FP2(6), FP1(3), FP4(2), FP5(2), FP7(2), FTP1(2), FTP3(2), FTP4(1)

Key: FP = Pacific SST factors (Nov)
FTP = Tropical Pacific SST factors (Nov)
FHT = 700 mb height factors (Nov)
SOASO = Southern oscillation index (Aug.-Oct.)

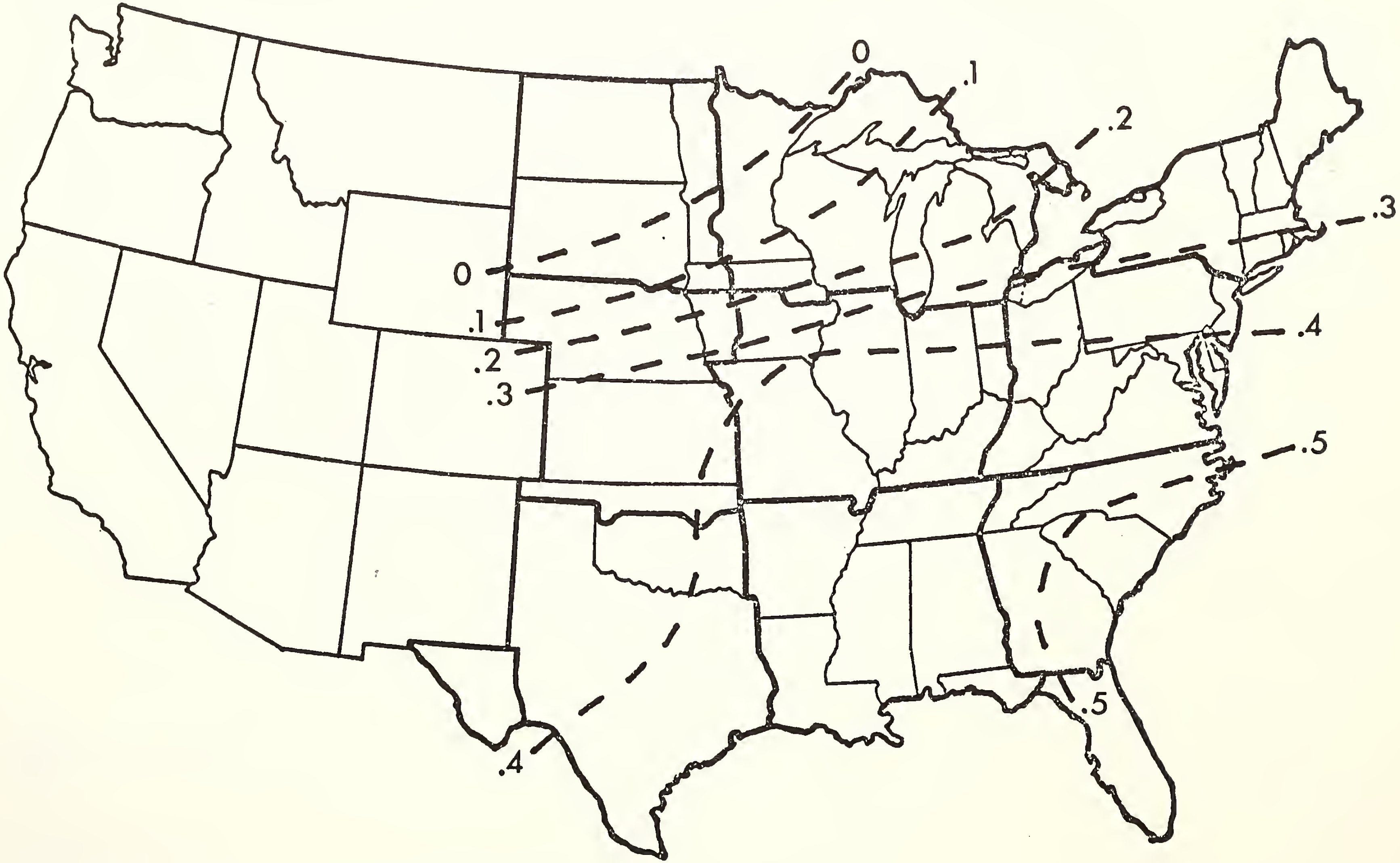

Fig. 15.
Correlation coefficient pattern for the seventh component of the Northern hemisphere 700 mb heights for November (FHTN7) versus the following mean winter (December-February) temperatures for the period 1949-76.

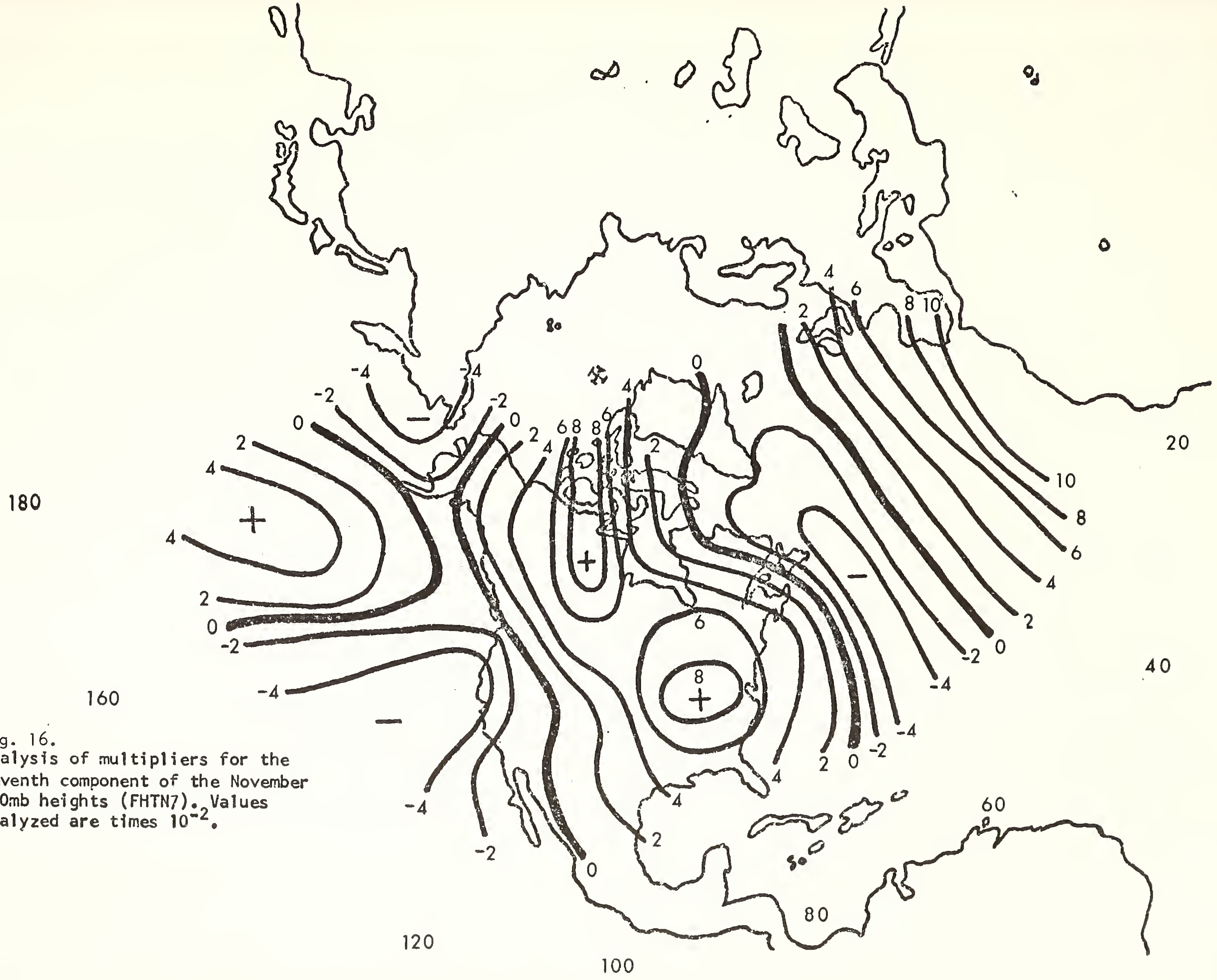

Fig. 16.
Analysis of multipliers for the seventh component of the November 700mb heights (FHTN7). Values analyzed are times 10^{-2}.

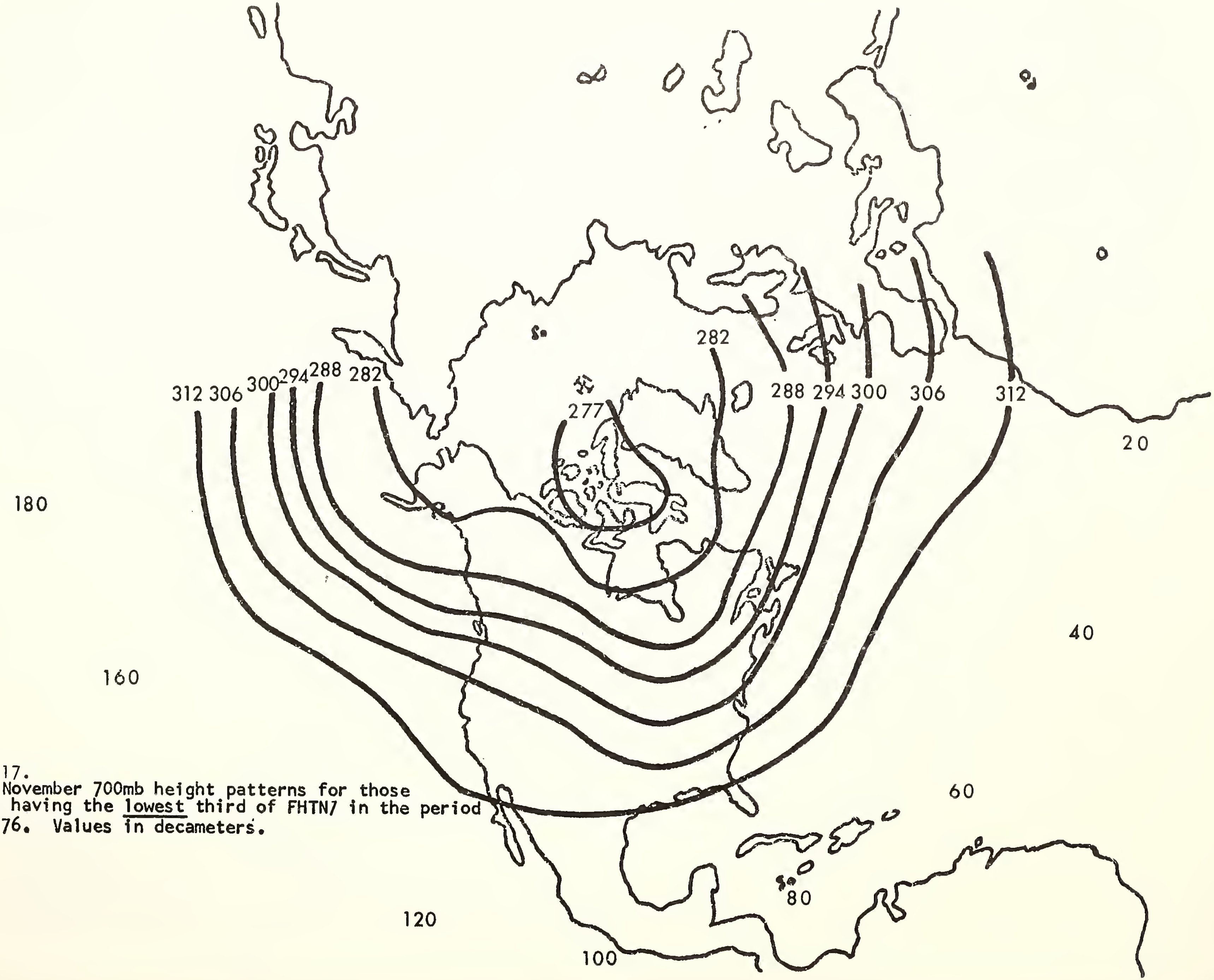

Fig. 17.
Mean November 700mb height patterns for those years having the lowest third of FHTN7 in the period 1949-76. Values in decameters.

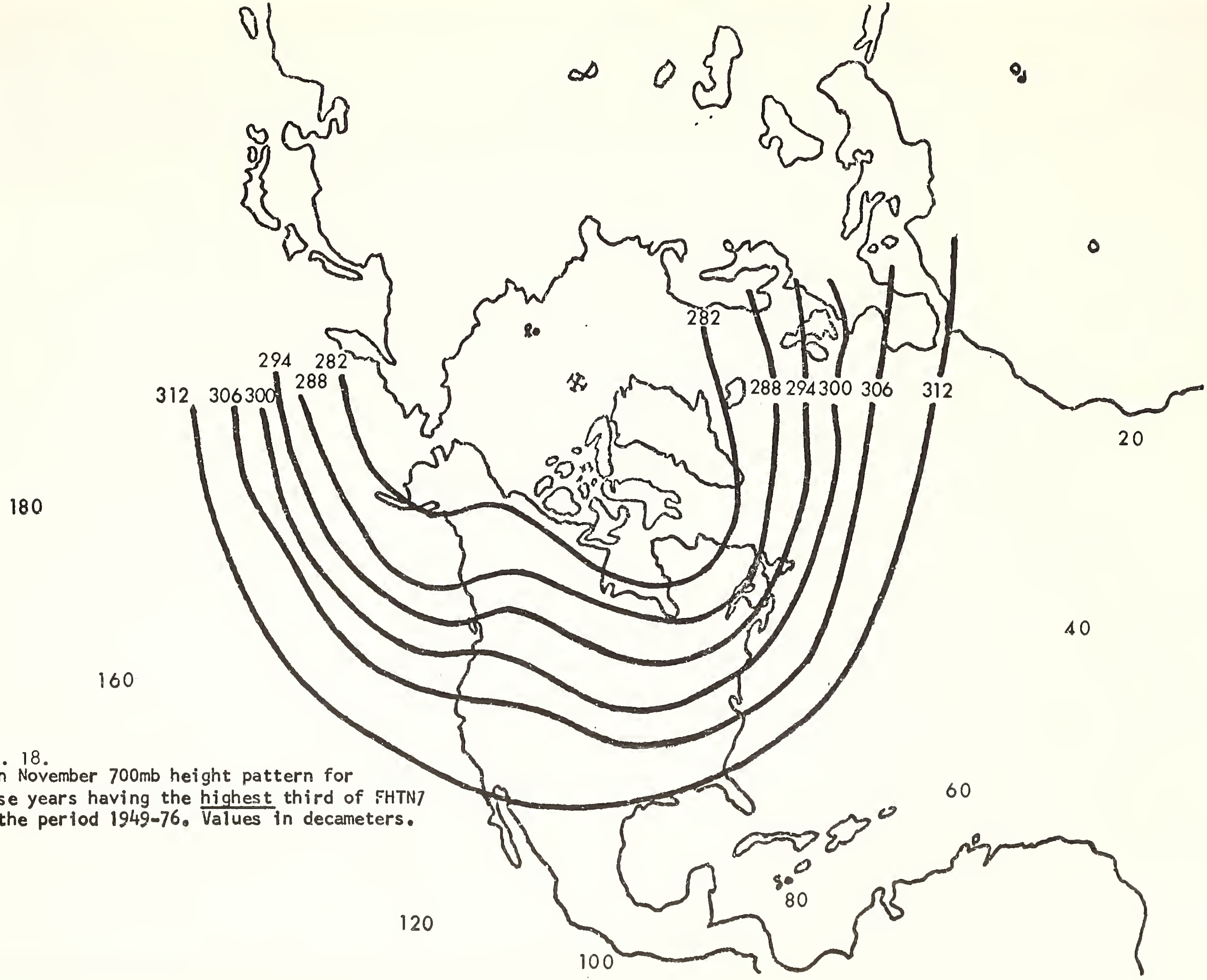

Fig. 18.
Mean November 700mb height pattern for those years having the highest third of FHTN7 in the period 1949-76. Values in decameters.

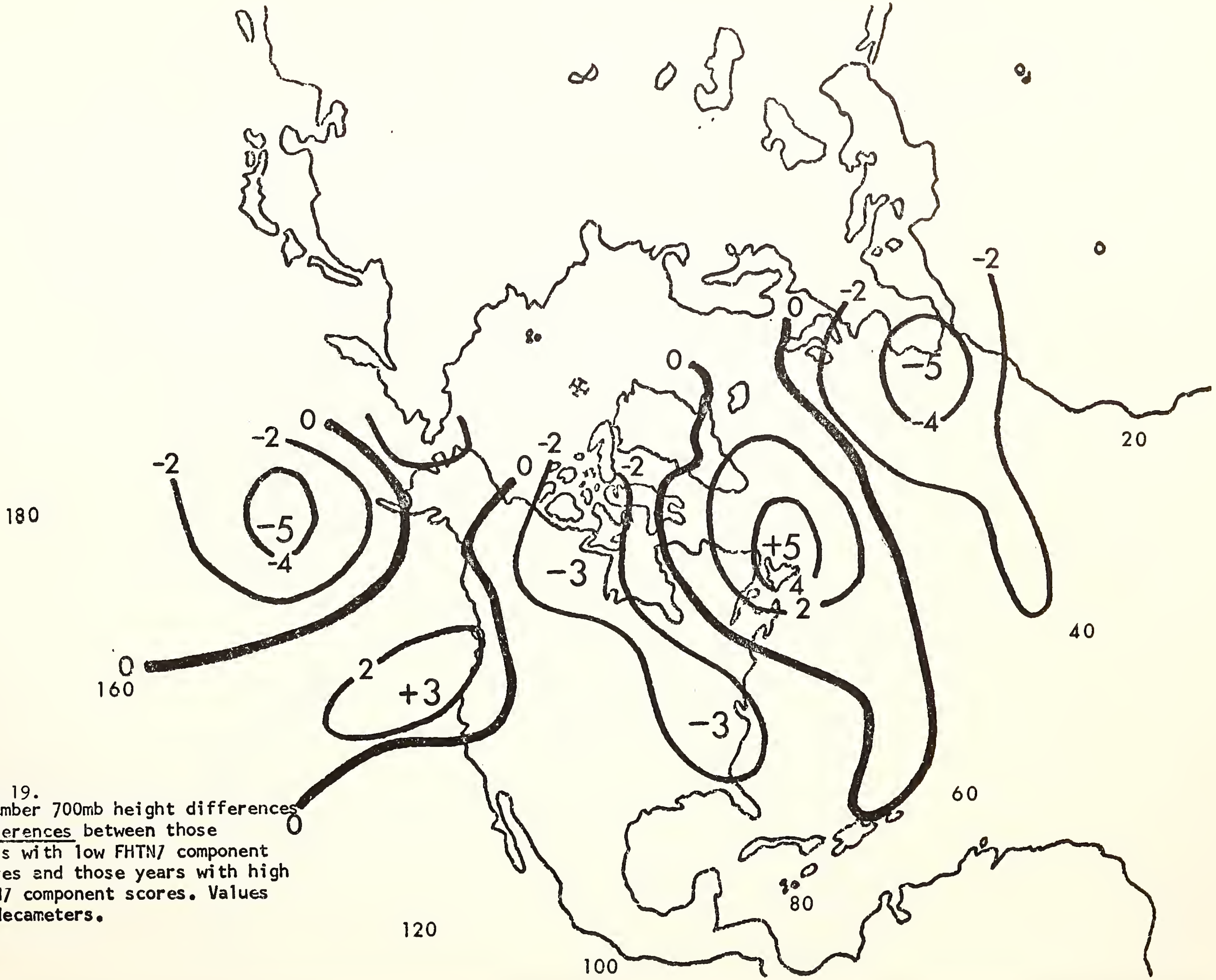

Fig. 19.
November 700mb height differences differences between those years with low FHTN7 component scores and those years with high FHTN7 component scores. Values in decameters.

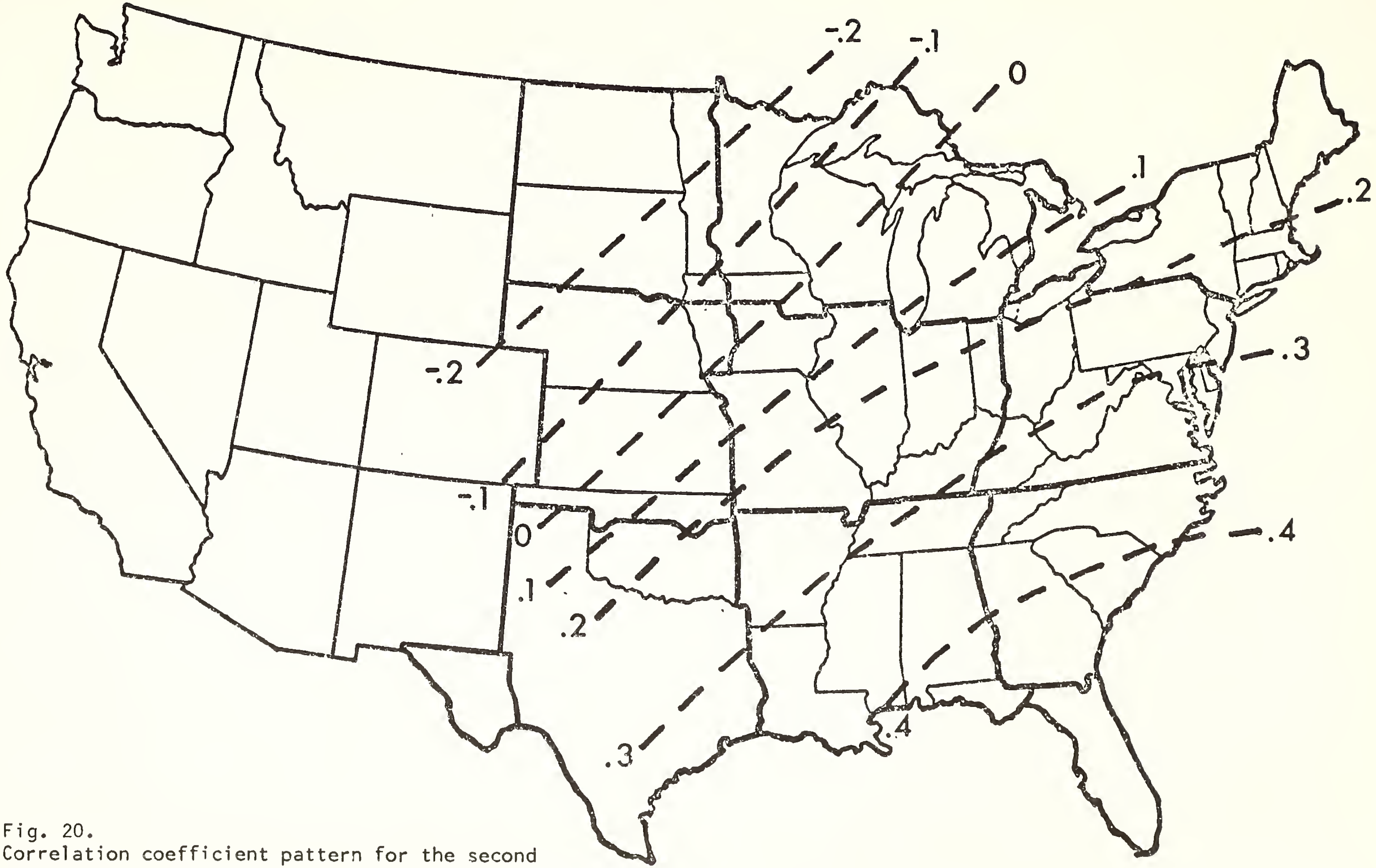

Fig. 20.
Correlation coefficient pattern for the second component of the North Pacific sea surface temperatures for November (FP2) versus the following mean winter (December-February) temperatures for the period 1949-76.

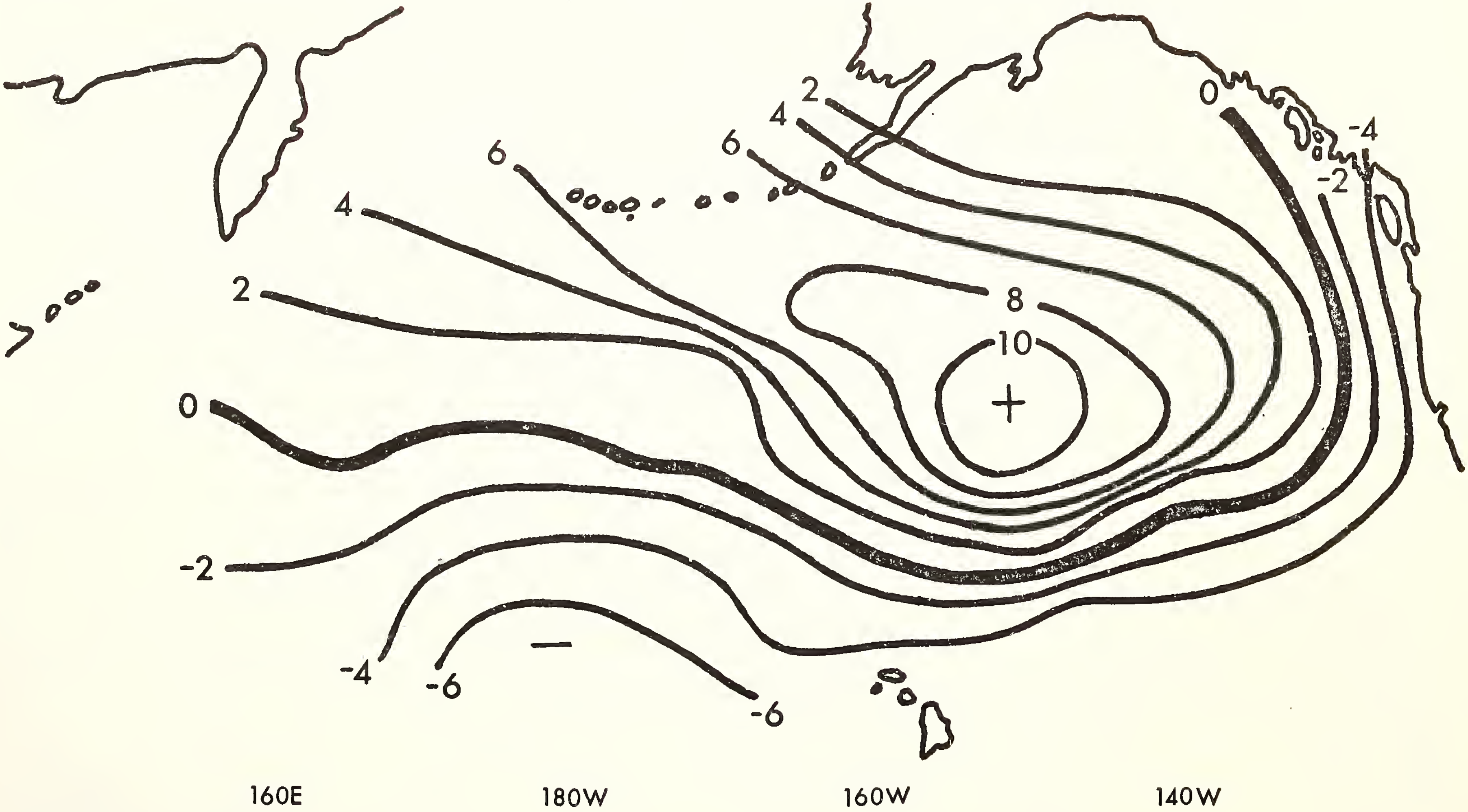

Fig. 21.
Analysis of multipliers for the second component of the North Pacific sea surface temperatures for November (FP2). Values analyzed are times 10^{-2}.

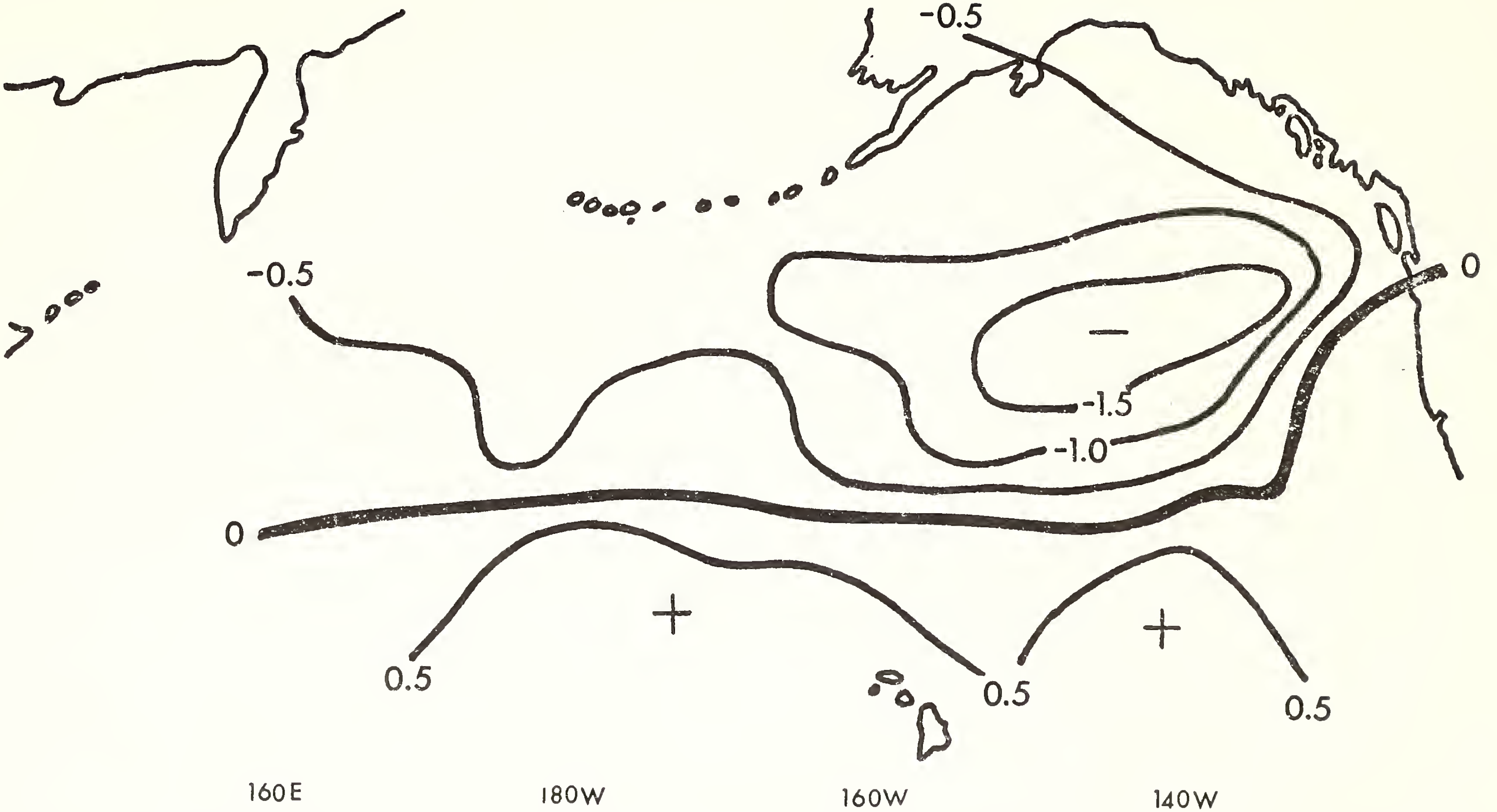

Fig. 22.
Mean sea surface temperature anomalies (°F) for November in the North Pacific for those years in the lowest third of FP2 component scores of the period 1949-76.

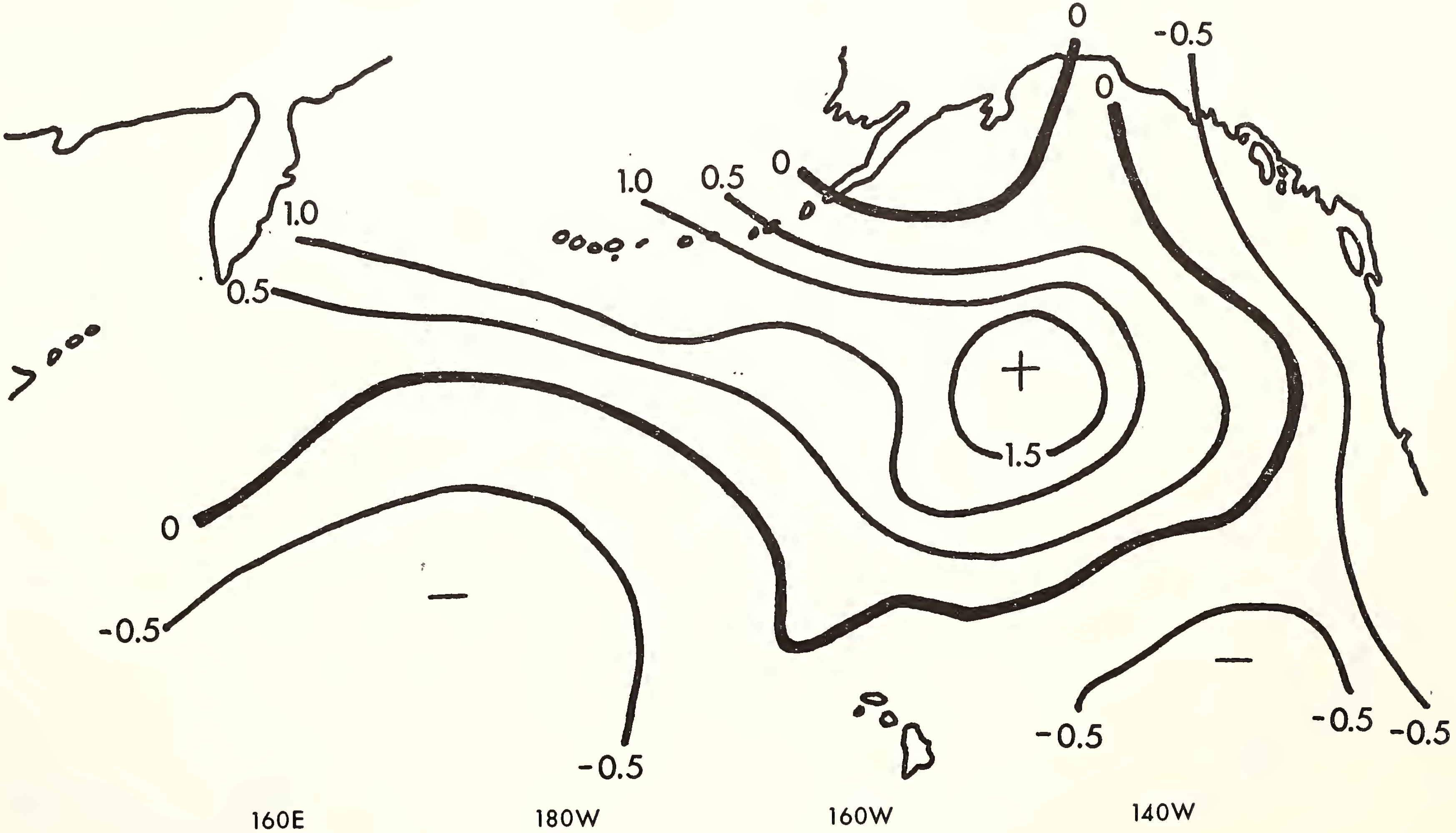

Fig. 23.
Mean sea surface temperature anomalies (°F) for November in the North Pacific for those years in the highest third of FP2 component scores of the period 1949-76.

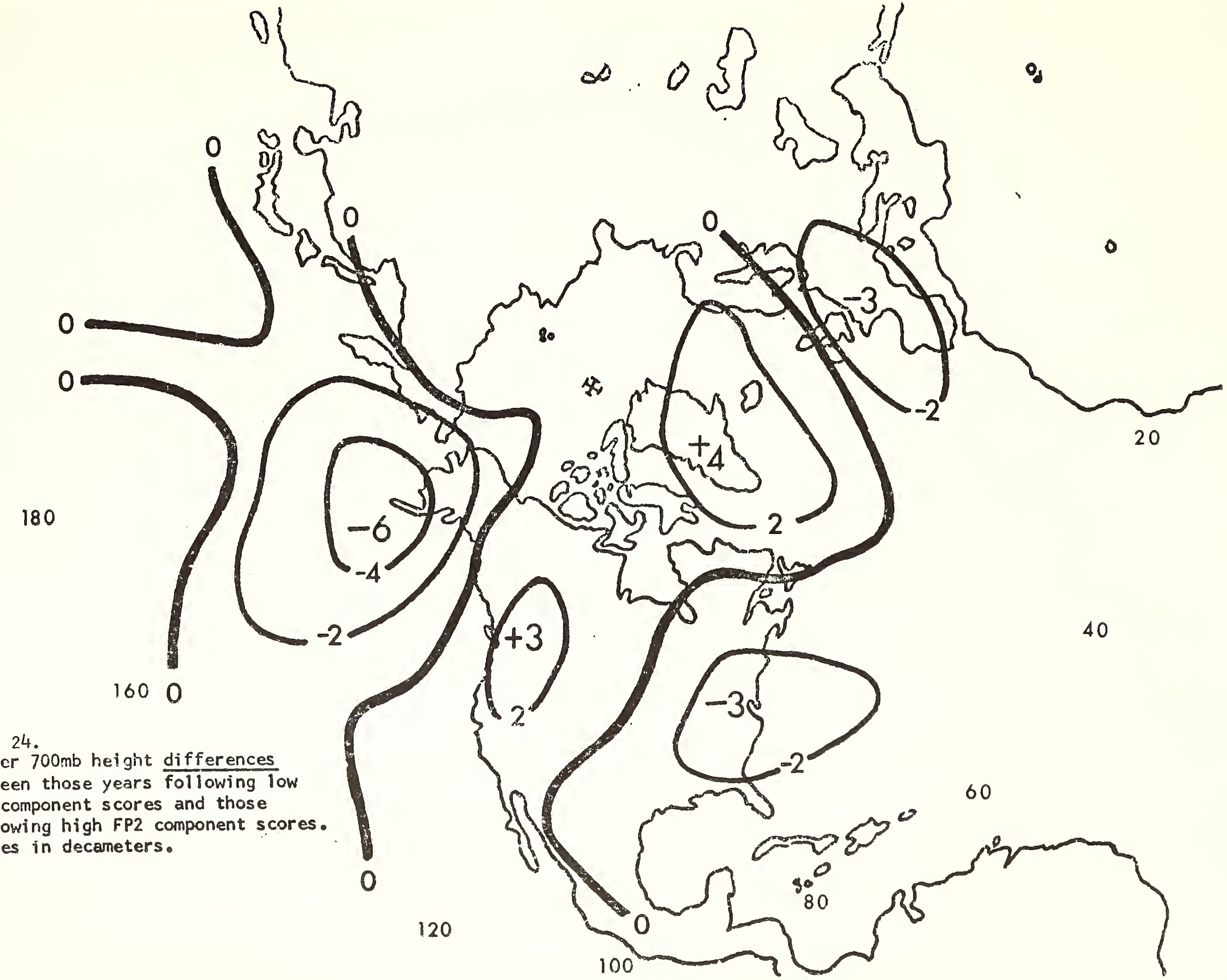

Fig. 24.
Winter 700mb height differences between those years following low FP2 component scores and those following high FP2 component scores. Values in decameters.

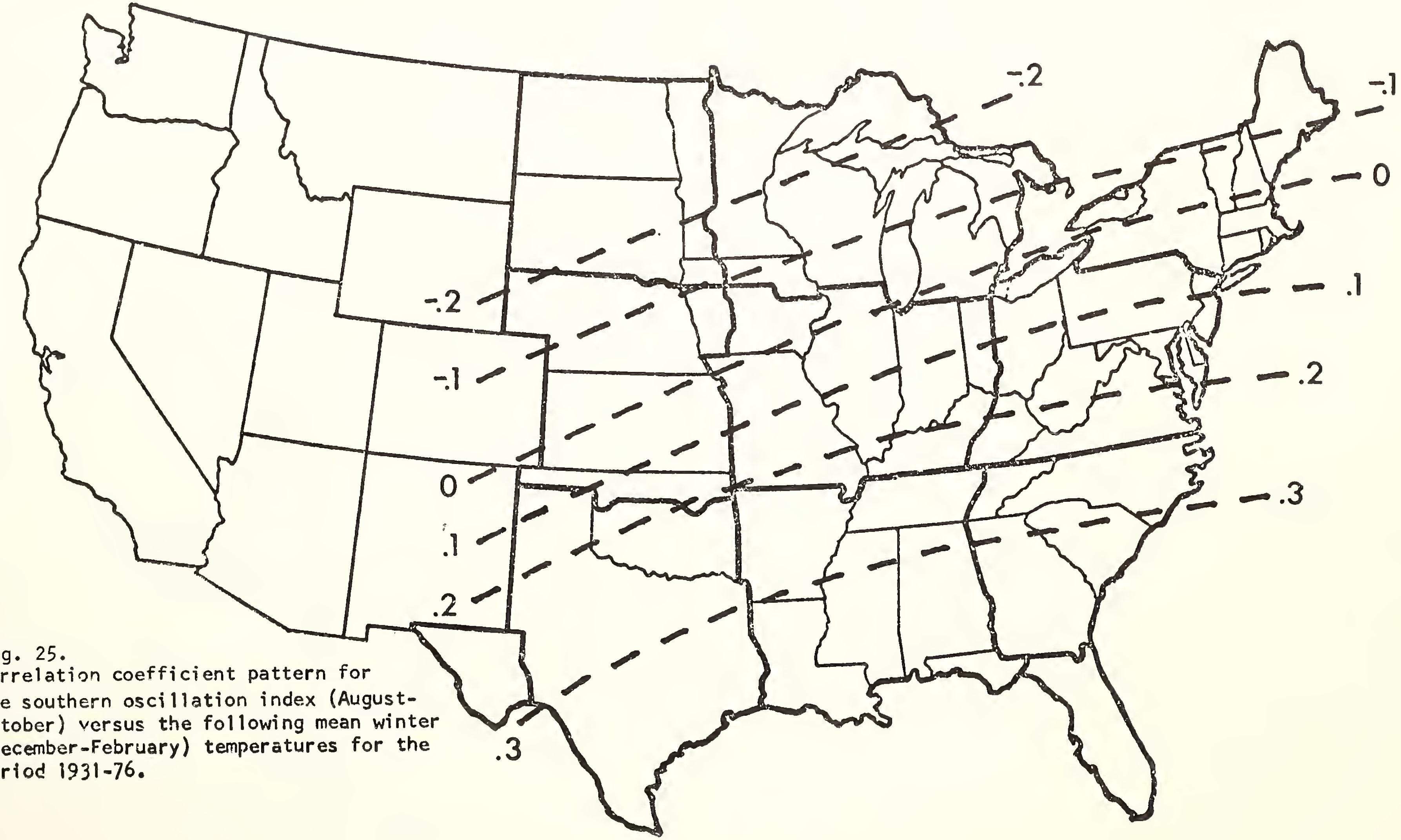

Fig. 25.
Correlation coefficient pattern for the southern oscillation index (August-October) versus the following mean winter (December-February) temperatures for the period 1931-76.

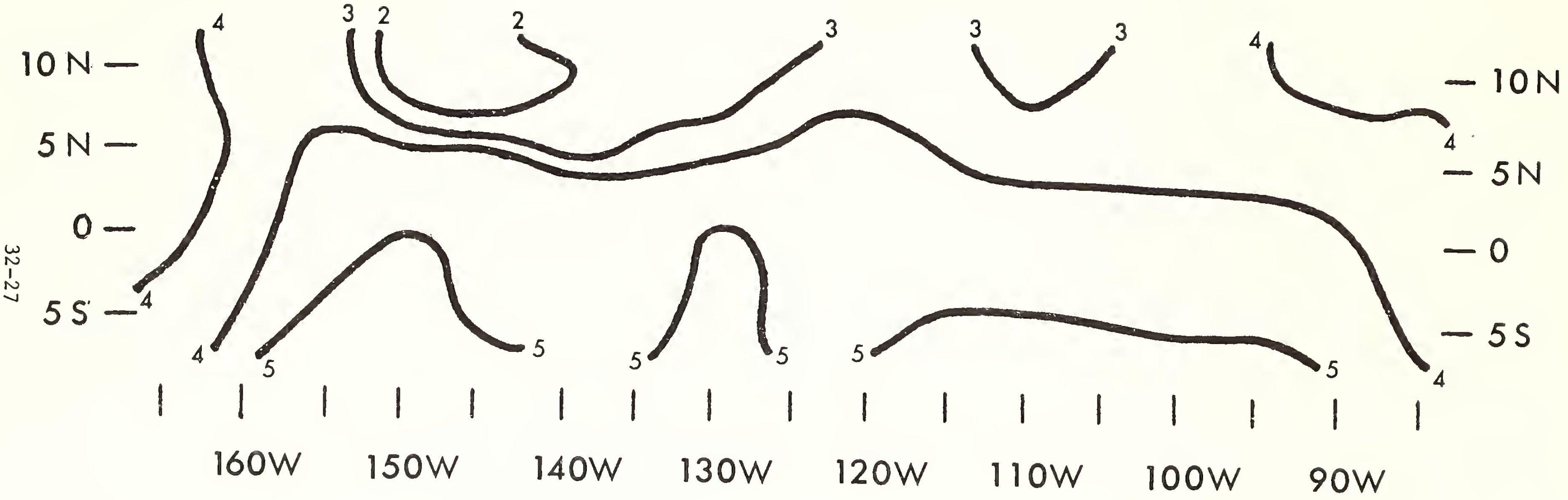

Fig. 26.
Analysis of multipliers for the first component of the Eastern Tropical Pacific sea surface temperatures for November (FTP1). Values analyzed are times 10^{-2}.

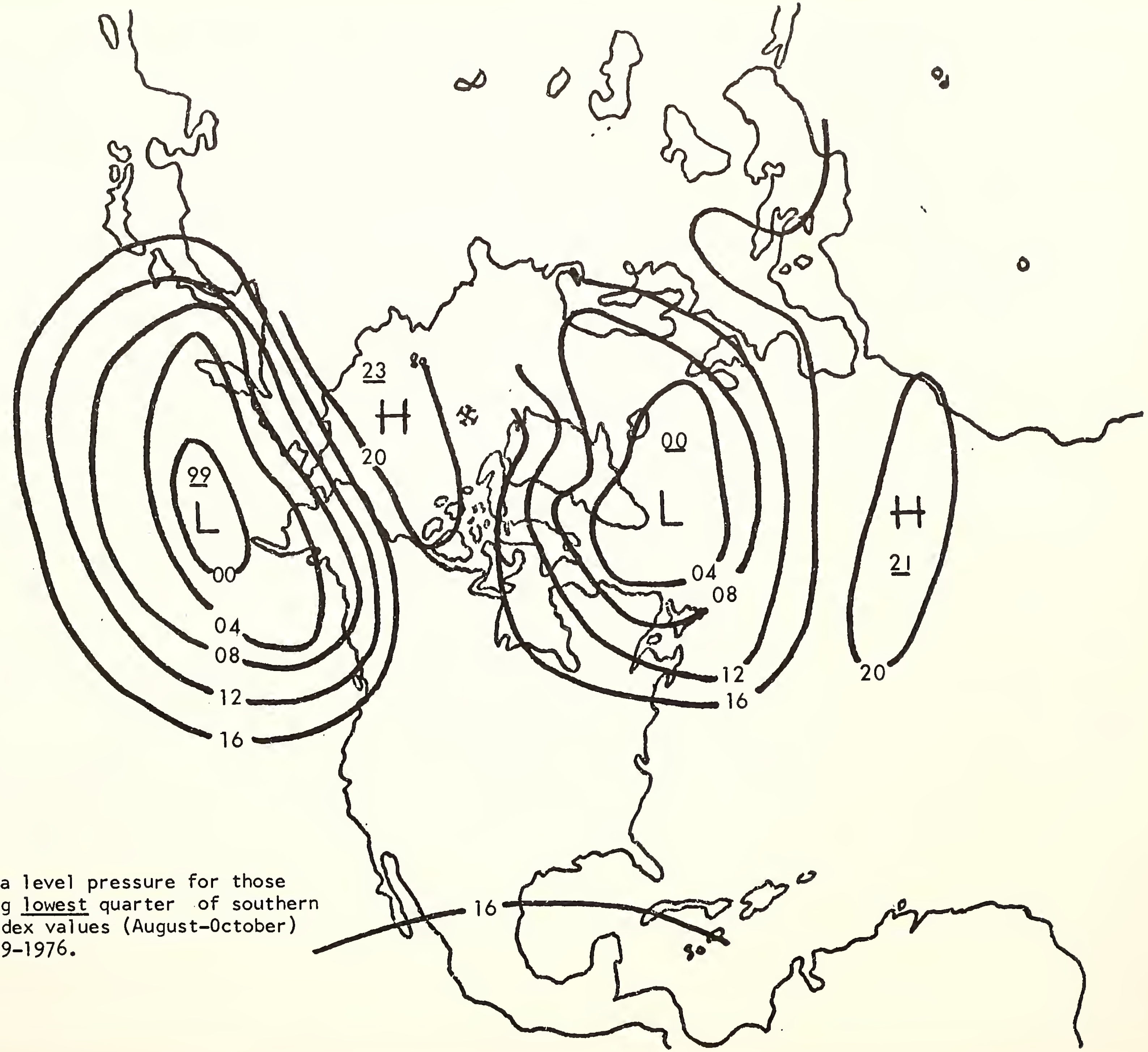

Fig. 27.
Mean winter sea level pressure for those years following lowest quarter of southern oscillation index values (August-October) for period 1899-1976.

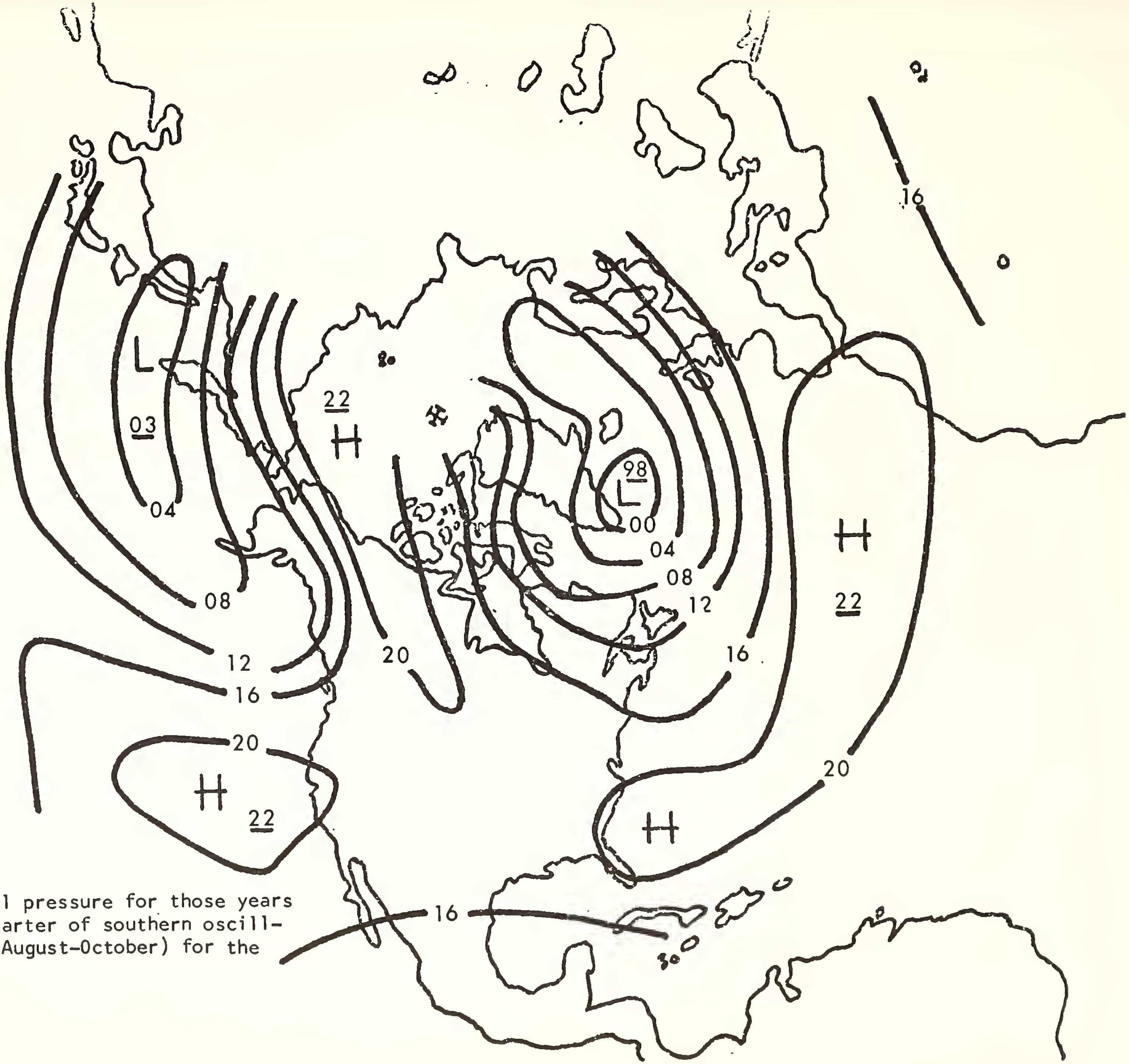

Fig. 28.
Mean winter sea level pressure for those years following highest quarter of southern oscillation index values (August-October) for the period 1899-1976.

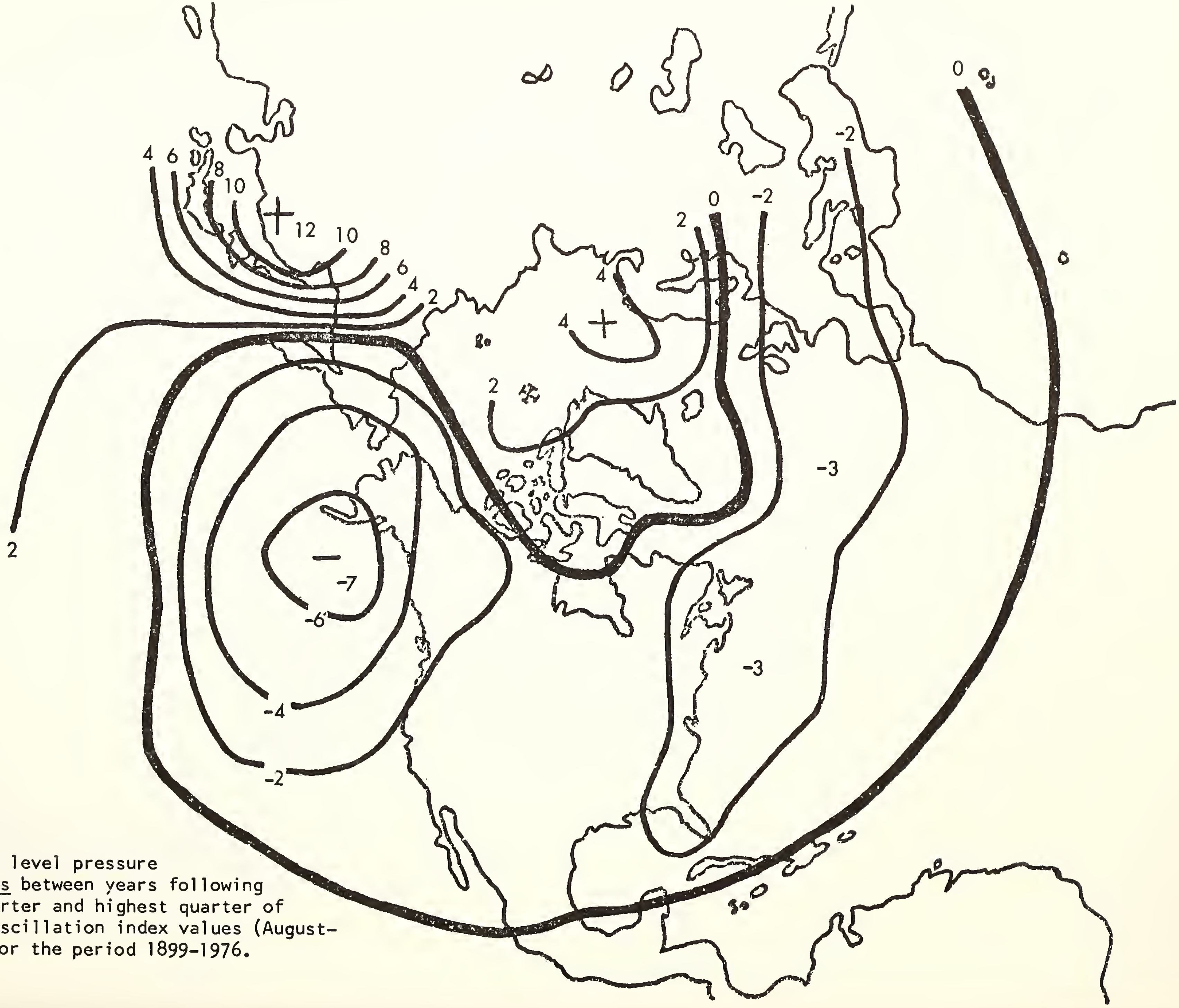

Fig. 29.
Winter sea level pressure differences between years following lowest quarter and highest quarter of southern oscillation index values (August-October) for the period 1899-1976.

An Experimental Climate Forecasting Model and Its Performance

Reid A. Bryson, E.W. Wahl
and T.B. Starr
Center for Climatic Research
University of Wisconsin, Madison, 53706

A model has been constructed on the assumption that climatic variations on the order of decades in length are thermodynamically driven while those on the order of months to a few years (except for the annual variation) are mechanical in origin (such as might be produced by atmospheric tides).

The thermodynamic drive submodel is based on the Bryson-Dittberner one-dimensional hemispheric surface temperature model with volcanic and anthropogenic inputs as control parameters (JAS, Nov. 1976). To this Wahl has added a statistical submodel that converts the five year mean surface temperature and its first two derivatives with time into a pattern of five year mean sea level pressure anomalies. These we call the trend anomalies of pressure.

To the trend anomalies we add the sea level monthly mean pressure anomalies produced by pole tides generated by the Chandler motion of the earth's rotational axis (Bryson and Starr, JAS, Dec. 1977). These calculated Chandler anomalies are added to the trend anomalies based on the calculated likely temperature to obtain the northern hemisphere sea level pressure anomaly prediction for specific months. Tests, with lead times greater than one year, on 20 months of independent data for 1976 and 1977 to date give the correct sign of the pressure anomaly at 180 grid points more than three standard deviations above chance. An example is given in Figures 1-3.

While we have not yet fully tested precipitation forecasts based on the pressure anomaly forecasts, we have developed regression models for precipitation based on calculated hemispheric mean temperature, its derivatives, and the Chandler tide modulation of the local precipitation at stations around the hemisphere. Thus the regression is based on the same parameters as the pressure pattern model. Tests on ten years of independent data for 120 stations in North America have been completed. For five year mean monthly precipitation (for January, April, July, and October) skill scores for above and below median (NOAA criterion) average about 0.21. For individual months the skill scores average about 0.03-0.04. Best results are obtained for July precipitation with the corresponding skill scores being 0.27 for five year July station means and 0.09 for individual July station totals (Table I). Tests on 60 stations in India give similar results, again with July forecasts producing the highest scores (Table II).

Improvements in the volcanic prediction model and the Chandler tide model are currently being sought, and other factors are being tested.

Skill Scores for Predicted Monthly Precipitation Departures from the Median (Two Classes) Using the Mark I Trend Plus Chandler Tide Model on Independent Data

Table I

North America 120 Stations

Month	1st 5 Years	2nd 5 Years	Individual Months
Jan	0.08	0.23	0.00
Apr	0.19	0.26	0.04
Jul	0.26	0.28	0.10
Oct	0.14	0.19	0.01
Overall	0.17	0.24	0.04

Table II

India 60 Stations

Month	1st 5 Years	2nd 5 Years	3rd 5 Years	Individual Months
June	0.14	0.18	0.00	0.17
July	0.45	0.20	0.17	0.02
Aug	0.08	0.14	0.48	0.04
Overall	0.22	0.17	0.25	0.08

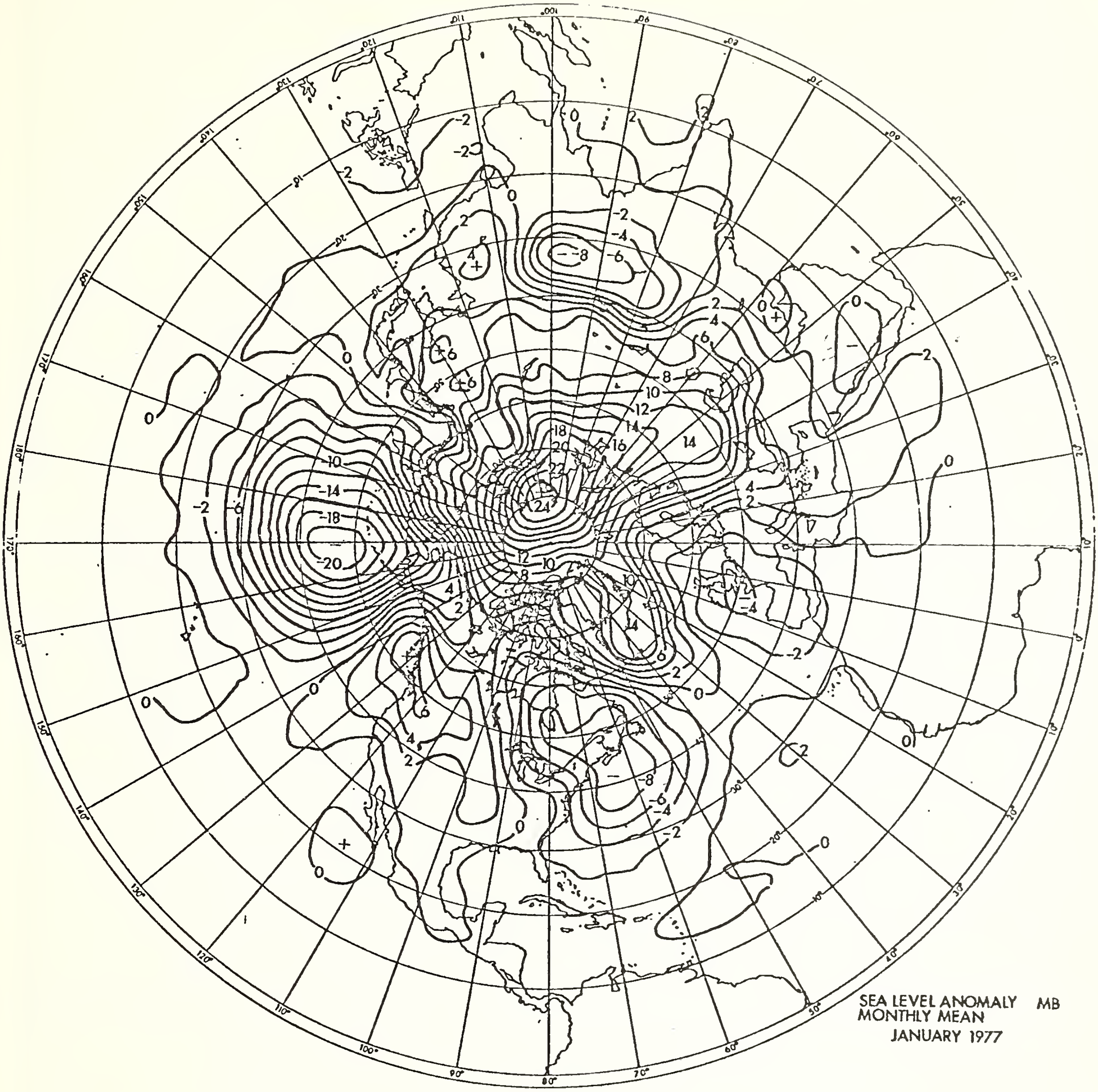

Figure 1. Observed sea level pressure anomaly for January 1977, courtesy NOAA. Anomalies in millibars.

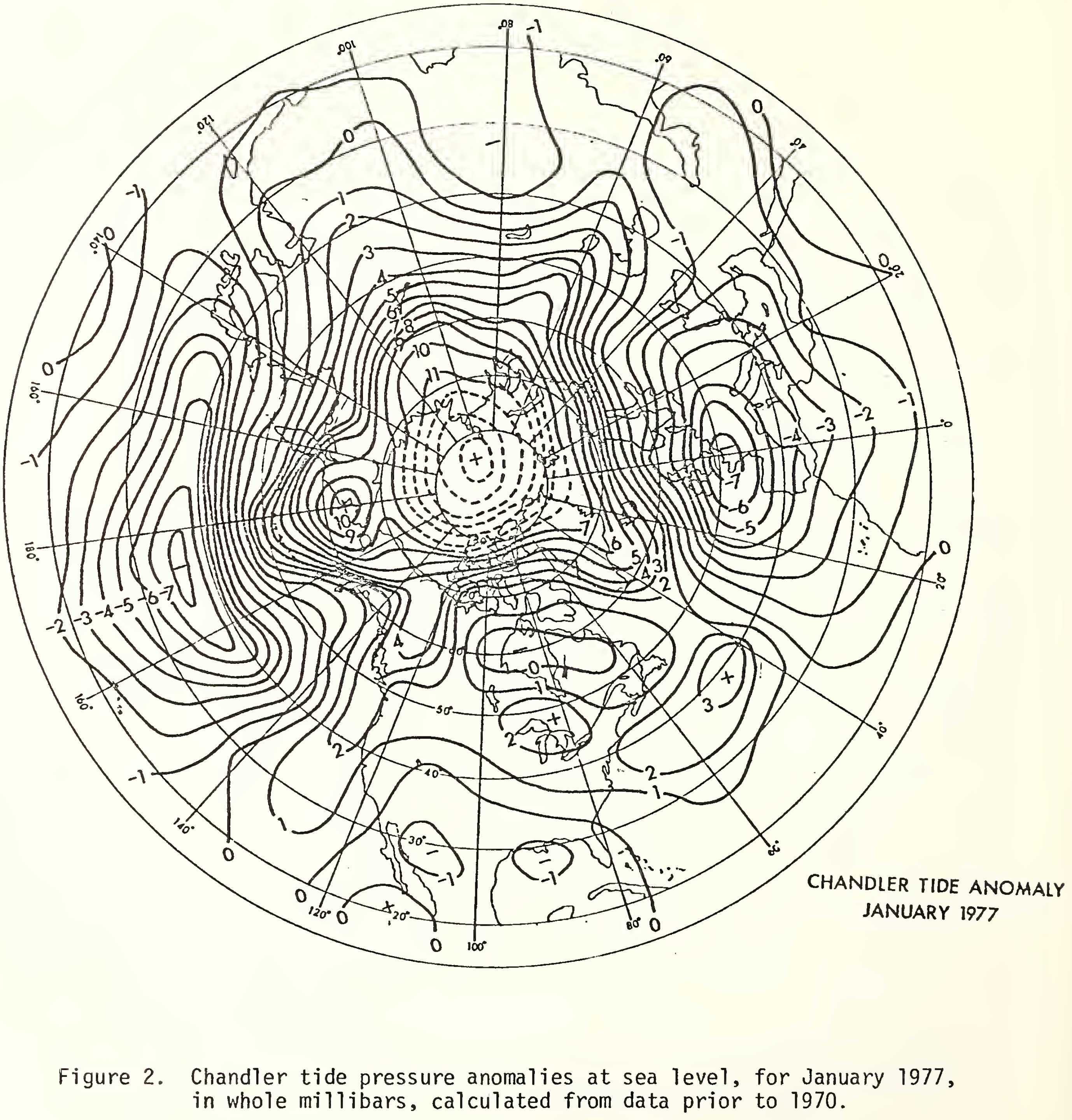

Figure 2. Chandler tide pressure anomalies at sea level, for January 1977, in whole millibars, calculated from data prior to 1970.

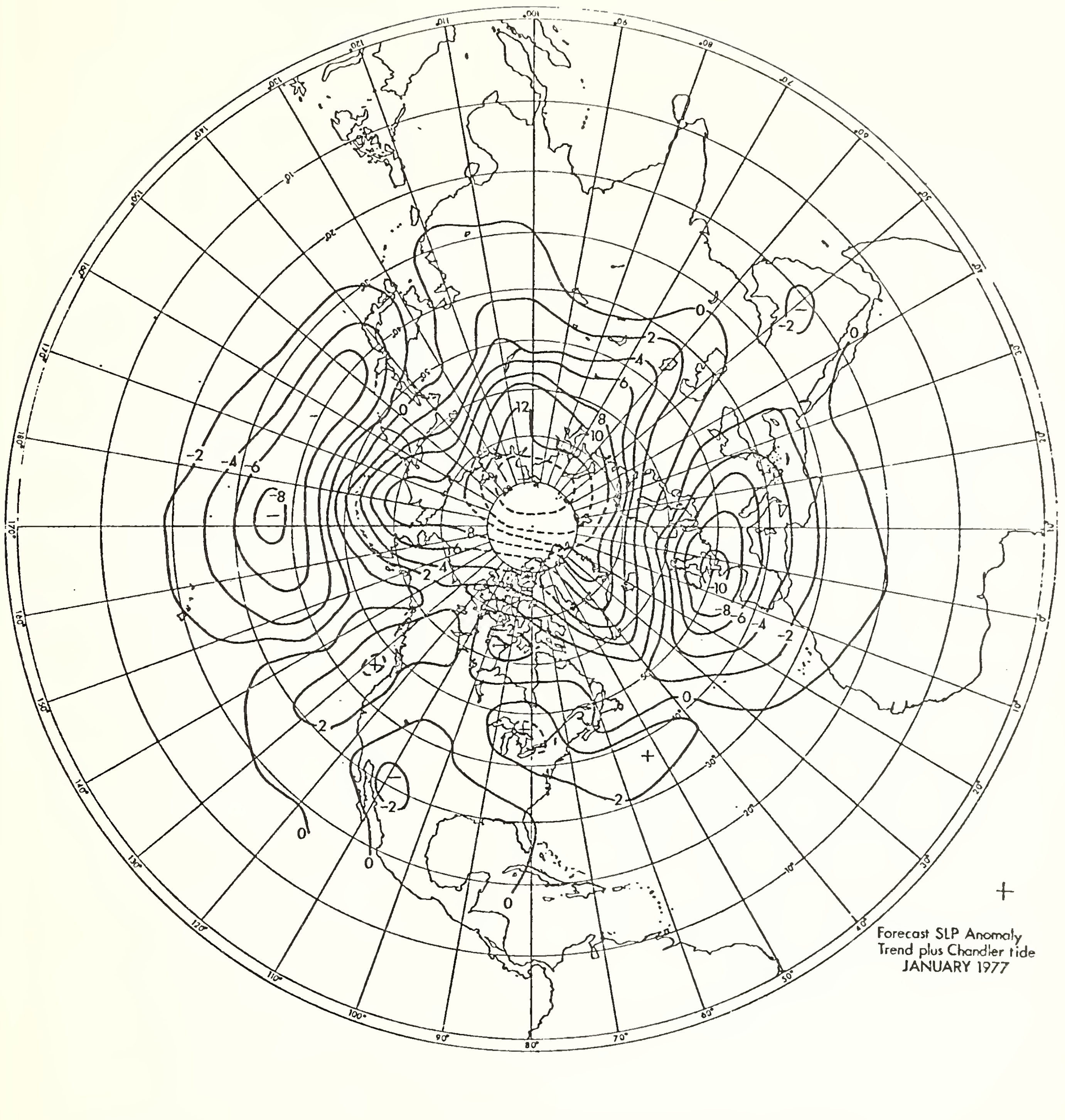

Figure 3. Trend plus Chandler tide calculated sea level pressure anomaly pattern for January 1977, in millibars, based on hemispheric mean temperature data prior to 1975 and Chandler tide data prior to 1970.

COMMENTARY BASED ON: PANEL DISCUSSION ON VERIFICATION OF CLIMATE FORECASTS

John Laurmann

The final session of the climate diagnostics workshop consisted of a colloquium on climate forecast verification problems, headed by a panel made up of J. Namias (chairman), R. Bryson, R. Davis, D. Gilman and R. Preisendorfer. The following account is a synopsis of the statements made by the panel members and the subsequent interactive discussions involving the panel and other workshop participants.

The need for verification

Rising expectations for achievement of significant short term climate forecasting capability together with growing awareness of the vulnerability of various economic sectors of society to severe climatic anomalies has placed particular stress on the need for evaluation of climate forecasting skills. Assessment of forecast model performance is needed both for comparing the merits of existing forecasting schemes, for aiding the researcher in model improvement and for guiding managerial decisions on the development or implementation of particular forecasting techniques.

Careful consideration of verification needs can lead to a better match of forecast capability with user requirements, as well as to the inclusion of evaluative procedures as a standard corollary in the design of climate forecast experiments.

Finally, better verification standards should also serve to inform and guide the potential user as to the capabilities and limitations to be expected from a particular forecasting model.

Verification criteria

The specification of criteria for definition of forecast skill appears to be even more elusive for climate prediction than for weather forecasting, no doubt due in part to the characteristically large probable error of a climate forecast and in part to the wide range of forecast methodologies that are being investigated with a correspondingly wide range of possible uses. We thus find that verification standards and techniques must be geared to the use to which the forecast is put, and it follows that a recommendation for the employment of a particular measure of skill or of a preferred verification technique cannot be made. In such a situation the effort needed in the evaluation of the effectiveness of various forecasting methods is considerable, since it is to be expected that useful techniques will show varying capabilities reflecting different applications. It would thus appear that a multiplicity of skill assessments of a given forecast scheme are needed, each with a different skill measure and verification process, dependent on user objectives.

In addition to the specialized demands in particular applications, forecasts appropriate to broad based user needs may also be useful, again calling for a different set of verification criteria. By contrast, highly specialized evaluative tests, sensitive to a particular facet of a forecasting scheme, may be needed in the research phase of model development.

Varying requirements in using climate forecasts result, not just in concern with different ranges of values of climate variables, but also with their temporal and spatial location and extent. Differing measures on the utility of a forecast relative to margins of error will surely also exist, so that predictions with a large variance may be useful in some applications and not in others. All these features have to be included in an evaluation of forecast effectiveness.

In dealing with the development of wider and more systematic use of measures of climate forecast effectiveness, a number of non-scientific issues appear as major hindrances. Amongst these is an apparent apathy of a sector of the public as to the degree of reliability of a particular forecasting technique or forecaster that it uses, and the problem of the establishment of the credibility of climate forecast skills that have in fact been reputably verified and published. As an aid in dealing with the latter situation, creation of an impartial group of experts, perhaps under the aegis of the National Academy of Sciences, would be desirable; its function would be the assessment of the forecasting skills of particular techniques, having regard to the use for which they are intended, or, at a minimum, the establishment of a set of guidelines for setting up verification procedures.

Verification methodology

As has just been stressed, the ultimate judge of the utility of a climate forecast is its user (whether this be a member of the public or the forecast model developer himself), but in all instances utility must be judged relative to a norm, and although the obvious standard of comparison for a forecast is its realization in nature, this is not always possible, or indeed appropriate. Thus, climate forecasts, because of the long predictive times they involve, inherently suffer from the lack of an adequate data for verification, especially when empirical fitting uses all the available historical observations. Statistical significance may then be difficult to establish, and whenever possible it is preferable to base models on partial historical data, so that hindcasting can be used to aid in model verification.

Alternatives to the direct use of realizations to check a forecast exist. For example, modification of a predictive model's contents, designed to improve performance, may be tested relative to the skill of the original version. An expansion of this concept is the use of a weather forecasting model to establish a climate prediction, this to be used as the standard for verification of a climate forecasting model that is supposedly constructed with the same dynamical contents.

A commonly used reference norm for weather forecasts is a persistence prediction. This is inappropriate for climate forecasting, but it can be amended by adding climatology and even by allowing for the climatology of anomalies. Such a standard could serve as a basic minimum comparator, except that the highly smoothed nature of this norm would mitigate against climate forecasts that were poor for average state prediction yet good for extremes, the latter attribute being the more important for many users. Another reference norm was suggested, the "stochaster". Here the forecast is compared with a suitably designed die-throwing experiment, which results in a stochastic forecast. This concept appears as a useful tool in assessing the significance of various types of categorical forecasting. It extends to climatology the time-honored methods of statistics wherein now null hypotheses concerning the performance of the forecaster are made and tested for acceptance or rejection.

The other basic ingredient in the design of a verification technique is establishment of the measure to be used for skill assessment. Since this should be closely related to the utility of the forecast, user needs should be the main consideration in the selection of an appropriate measure. Thus specific recommendations cannot be made outside the context of particular applications, but there are broadly different types of measures that can be discussed in a more general way.

Long range weather or climate predictions are commonly published in categorical format, which can serve as the basis for skill assessment. Although crude, this type of presentation may in fact be the most useful for some user needs. A modification of this approach is to predict only the extremes, perhaps even on a quantitative basis. Not only are extreme events often of greater importance to a user, but many forecasting methods will perform better in this mode as compared with forecasting around normal conditions; at least this appears to be the situation for predicting cold events (in the Northern Hemisphere) as contrasted to warm.

A more thorough approach, commonly used within the forecast community for assessment of model capability, is the statistical measure of r.m.s. error. This favors the conservative forecaster, who performs well for average state prediction, and hence may not be appropriate for some user needs. Even more elaborate quantitative measures can be devised, based upon complete evaluation of statistical error distribution functions. If possible to obtain, their knowledge can be used to establish any quantitative measure of utility of forecast reliability that is desired, though it may not always be easy for the user to define his needs in this comprehensive a fashion. These statistical measures are especially easy to use and useful when the distribution of the variables is normal, such as is the case for temperature. Non-Gaussian distributions, for example, precipitation or hurricane frequency and other rare event phenomena, are less suitable candidates for this type of analysis.

Another modification of the detailed quantitative approach involves relaxation of the criteria for specification of the spatial or temporal location of an event of interest. For example, some users may be satisfied with knowing that a storm will occur within a particular time period or within a specified geographical location. A forecast that provides such information quite adequately might still perform badly according to an r.m.s. measure of skill based upon grid point comparisons.

A final methodological approach is to ask the designer of the forecast scheme to choose his own measure of skill upon which it is to be evaluated. In this case the user will have to judge whether the criteria thus established correspond to his own needs.

A general characteristic of the impact of the imposition of a particular test measure on forecaster behavior is the tendency to adapt the model to maximize its skill as defined by this measure. If the verification technique is a good one for the user need at hand, such adaptions may serve a useful purpose, but otherwise are not beneficial to effective forecast development. Of the measures listed above, those using probability distributions are least susceptible to this interactive influence.

☆ U. S. GOVERNMENT PRINTING OFFICE : 1978—261-238/445

PENN STATE UNIVERSITY LIBRARIES
A000072022443